SYNTHESIS OF SELECTIVE *N*-HETEROCYCLIC SCAFFOLDS UNDER GREEN CONDITIONS USING ZIRCONIA SUPPORTED BIMETALLIC CATALYSTS

by

V H S SANDEEP BHASKARUNI

Submitted in fulfillment of the academic requirements for the degree of

Doctor of Philosophy in the Department of Chemistry, School of Chemistry & Physics

College of Agriculture, Engineering and Science

University of KwaZulu-Natal

Durban

SEPTEMBER 2019

As the candidate's supervisor, I have approved this thesis for submission

Supervisor: **Prof. S.B. Jonnalagadda** Signed_____ Date: _____

Co-Supervisor: **Prof. Werner E. van Zyl** Signed_____ Date: _____

.....Dedicated to…..

Beloved Peoples President, The Missile man of India

"Bharat Ratna Dr. A.P.J Abdul Kalam"

Where there is righteousness in the heart, there is beauty in the character. When there is beauty in the character, there is harmony in the home. When there is harmony in the home, there is order in the nation. When there is order in the nation, there is peace in the world.

Dr. A. P. J. Abdul Kalam

ABSTRACT

Many natural products and pharmaceuticals with a broad range of biological activities constitute one or other heterocyclic scaffolds. In pursuit of new synthetic methodologies for diverse heterocyclic compounds, the Multicomponent Reaction (MCR) is an advanced strategy to develop and design versatile organic molecules with high atom economy in a short period. Major advantages of MCRs is the reaction takes place in a one-pot strategy with no need for the separation and purification of intermediates. The synthesis of diverse heterocyclic scaffolds using the MCR strategy can be achieved, and is on the increase.

Green Chemistry is an emerging branch of synthetic chemistry, which is to design sustainable synthetic protocols from easily available starting materials and non-corrosive solvents. One fundamental aspect of green chemistry is the reusability of materials and reducing waste. This allows chemists to consider heterogeneous catalysis in reactions because it is easy to separate from the reaction mixture and is reusable. Ease in handling, greater chemo-regio selectivity, and thermal stability are the added advantages of heterogeneous catalysis.

Heterogeneous catalysis using mixed metal oxides is gaining importance due to the tuning of surface properties of materials, i.e., one is able to design the catalyst as per requirement by loading/doping of necessary metals on supports. Among many support materials, zirconia gained prominence due to its higher surface area and amphoteric surface properties, which make it an ideal catalytic support. Having a high surface area is advantageous for a reaction to takes place on the surface, which provides necessary active sites to accelerate the reaction. This research was designed to synthesize various novel core *N*-heterocyclic moieties by using zirconia-supported mixed metal oxide catalysts. During the study, an attempt was made to develop fast reaction protocols to synthesize various pyridine,

pyrimidine and pyrazole derivatives with excellent yields using green solvents and mild conditions. These new protocols demonstrated efficacy and high selectivity under eco-friendly conditions. The following six series of reactions were studied:

1. Synthesis of eleven novel functionalized 1,4-dihydropyridine derivatives by using V_2O_5/ZrO_2 as catalyst for the multicomponent reaction using various aromatic aldehydes, 5,5-dimethyl-1,3-cyclohexanedione, acetoacetanilide and ammonium acetate.

2. A one-pot protocol to synthesize novel functionalized halopyridine derivatives by using RuO_2/ZrO_2 as an efficient reusable catalyst for the condensation of aromatic aldehydes, malononitrile, diethyl acetylene dicarboxylate and 3-chloro-4-fluoroaniline under green conditions.

3. A room-temperature synthesis of 2,4-dihydropyrano[2,3-c]pyrazole-3-carboxylates by the condensation of aromatic aldehydes, malononitrile, hydrazine hydrate and diethyl acetylene-dicarboxylate using Bi_2O_3/ZrO_2 as a cost-effective catalyst with ethanol as a greener solvent.

4. Greener synthesis of indenopyrimidine derivatives by using Ag_2O on ZrO_2 as a recyclable catalyst for the one-pot condensation between an aromatic aldehyde, 1,3-indanedione and guanidinium hydrochloride at room temperature.

5. Synthesis of new 1,4-dihydropyridine derivatives via cyclo-condensation between an aromatic aldehyde, 1,3-cyclohexanedione, acetoacetanilide and ammonium acetate in an one-pot strategy through a green protocol using Fe_2O_3/ZrO_2 as a reusable catalyst at room temperature.

6. A four-component fusion protocol for the synthesis of novel 1,4-dihydropyridine derivatives by the one-pot condensation between substituted aldehydes, ethyl acetoacetate,1,3-cyclohexadione/5,5-dimethyl-1,3-cyclohexanedione and ammonium acetate in ethanol.

All the prepared catalytic materials were characterized by PXRD, TEM, SEM, Pyridine-IR and BET surface area analysis. All the synthesized organic compounds were characterized and confirmed by ^{1}H NMR, ^{15}N NMR, ^{13}C NMR, FT-IR, single-crystal XRD, and HRMS. Advantages offered by these protocols are environmentally-friendly simple procedure, mild conditions and short reaction times with excellent yields.

DECLARATION 1 - PLAGIARISM

I, **V H S Sandeep Bhaskaruni,** declare that

1. The research reported in this thesis, except where otherwise indicated is my original research.

2. This thesis has not been submitted for any degree or examination at any other university.

3. This thesis does not contain other persons' data, pictures, graphs or other information, unless specifically acknowledged as being sourced from other persons.

4. This thesis does not contain other persons' writing, unless specifically acknowledged as being sourced from other researchers. Where other written sources have been quoted, then:

a. Their words have been re-written, but the general information attributed to them has been referenced

b. Where their exact words have been used, then their writing has been placed in italics and inside quotation marks, and referenced.

5. This thesis does not contain text, graphics or tables copied and pasted from the Internet, unless specifically acknowledged, and the source being detailed in the thesis and in the References sections.

Signed: ……

DECLARATION 2-PUBLICATIONS

DETAILS OF CONTRIBUTION TO PUBLICATIONS that form part and/or include research presented in this thesis .

1. **Sandeep V H S Bhaskaruni**, Suresh Maddila, Werner E. van Zyl and Sreekantha B. Jonnalagadda. "V_2O_5/ZrO_2 as an efficient reusable catalyst for the facile, green, one-pot synthesis of novel functionalized 1,4-dihydropyridine derivatives." **Catalysis Today.** 309 (2018) 276–281.

Contributions: I synthesized and characterized all the derivatives under the supervision of Prof. S.B Jonnalagadda (Supervisor) and Prof. Werner E. van Zyl (Co-supervisor), and drafted the article. The supervisors and Dr. S. Maddila (a Postdoctoral fellow working under Prof. Jonnalagadda) facilitated the preparation of the final manuscript. I was the first author, while Prof. Jonnalagadda was corresponding author.

2. **Sandeep V H S Bhaskaruni**, Suresh Maddila, Werner E. van Zyl and Sreekantha B. Jonnalagadda. "RuO_2/ZrO_2 as an efficient reusable catalyst for the facile, green, one-pot synthesis of novel functionalized halopyridine derivatives." **Catalysis Communications.** 100 (2017) 24–28.

Contributions: I synthesized and characterized all the derivatives under the supervision of Prof. S.B Jonnalagadda (Supervisor) and Prof. Werner E. van Zyl (Co-supervisor), and drafted the article. The supervisors and Dr. S. Maddila (a Postdoctoral fellow working under Prof. Jonnalagadda) facilitated the preparation of the final manuscript. I was the first author, while Prof. Jonnalagadda was corresponding author.

3. **Sandeep V H S Bhaskaruni**, Suresh Maddila, Werner E. van Zyl and Sreekantha B. Jonnalagadda. "An efficient and green approach for the synthesis of 2,4-dihydropyrano[2,3-

c]pyrazole-3-carboxylates using Bi_2O_3/ZrO_2 as a reusable catalyst." **RSC Advances.** 8 (2018) 16336-16343.

Contributions: I synthesized and characterized all the derivatives under the supervision of Prof. S.B Jonnalagadda (Supervisor) and Prof. Werner E. van Zyl (Co-supervisor), and drafted the article. The supervisors and Dr. S. Maddila (a Postdoctoral fellow working under Prof. Jonnalagadda) facilitated the preparation of the final manuscript. I was the first author, while Prof. Jonnalagadda was corresponding author.

4. **Sandeep V H S Bhaskaruni**, Suresh Maddila, Werner E. van Zyl and Sreekantha B. Jonnalagadda. "Ag_2O on ZrO_2 as Recyclable Catalyst for Multicomponent Synthesis of Indenopyrimidine Derivatives." **Molecules.** 23 (2018) 1648.

Contributions: I synthesized and characterized all the derivatives under the supervision of Prof. S.B Jonnalagadda (Supervisor) and Prof. Werner E. van Zyl (Co-supervisor), and drafted the article. The supervisors and Dr. S. Maddila (a Postdoctoral fellow working under Prof. Jonnalagadda) facilitated the preparation of the final manuscript. I was the first author, while Prof. Jonnalagadda was corresponding author.

5. **Sandeep V H S Bhaskaruni**, Suresh Maddila, Werner E. van Zyl and Sreekantha B. Jonnalagadda. "A green protocol for the synthesis of new 1,4-dihydropyridine derivatives using Fe_2O_3/ZrO_2 as a reusable catalyst." **Research on Chemical Intermediates.** 45, (2019), 4555–4572.

Contributions: I synthesized and characterized all the derivatives under the supervision of Prof. S.B Jonnalagadda (Supervisor) and Prof. Werner E. van Zyl (Co-supervisor), and drafted the article. The supervisors and Dr. S. Maddila (a Postdoctoral fellow working under Prof. Jonnalagadda) facilitated the preparation of the final manuscript. I was the first author, while Prof. Jonnalagadda was corresponding author.

6. **Sandeep V H S Bhaskaruni**, Suresh Maddila, Werner E. van Zyl and Sreekantha B. Jonnalagadda. "4-Component fusion protocol with NiO/ ZrO_2 as robust recyclable catalyst for novel 1,4-dihydropyridines" **ACS Omega,** *DOI: 10.1021/acsomega.9b02608*

Contributions: I synthesized and characterized all the derivatives under the supervision of Prof. S.B Jonnalagadda (Supervisor) and Prof. Werner E. van Zyl (Co-supervisor), and drafted the article. The supervisors and Dr. S. Maddila (a Postdoctoral fellow working under Prof. Jonnalagadda) facilitated the preparation of the final manuscript. I was the first author, while Prof. Jonnalagadda was corresponding author.

Signed:……

ACKNOWLEDGMENTS

First and foremost, I would like to thank my research advisors, Prof. Sreekantha Babu Jonnalagadda and Prof. Werner E van Zyl for all their guidance and support. Without their inspiration and mentorship, this work would not have been possible. I acknowledge the School of Chemistry and Physics, College of Agriculture Engineering and Science, University of KwaZulu-Natal for providing the platform to do the research.

My sincere thanks to Prof. S.B Jonnalagadda for facilitating my research by providing a bursary from his research funds. It is not easy without any financial assistance.

I would also like to thank Dr. Suresh Maddila and Dr. Surya Narayana Maddila for outstanding help throughout my PhD research. I must thank Dr. S.Rana, Dr. Kranthi Kumar Gangu and Dr. Nagaraju Kerru for their support throughout my research work. I am fortunate to work with many incredible colleagues in my group. I am grateful for their support and friendship.

My wonderful friends, including Dr. Narayana Reddy Palakollu, Ms. Lalitha Gummidi, Dr. Sanjeev Dhawan, Dr. Vashen Moodley, Dr. Michael N Pillay, Dr.Hari Narayana Bandaru, and Ms. Maxime L Pillay who have enriched my experience at UKZN and made it a very rewarding time.

I especially need to thank my best friends Sarath Chandra Behara, Neelendra Bandaru, Gopi Krishna Bachu, Eswara Reddy Medagam, Dhanunjay Ronanki and Jagadeesh reddy Goli for being good listeners whenever I vented my frustrations from time to time.

I would like to thank Dr. Nagaraju Kerru and Ms. Lalitha Gummidi for their unforgettable help towards the development of my skills in organic synthesis and Dr. Viswanadham Balaga for his help with material characterisation during the initial stages of my research. Special thanks to Mr. Dilip Jagjivan, Mr. Gregory Moodley, Mr. Suresh Soodeyal and Mr. Prashan Nandakumar for their support, and always willing to help me during the course of this work. I must thank Mr. S. Zamisa for his help with the single crystal analyse.

I also owe greatly thanks to Mrs. Rukmini Jonnalagadda and Sreeharsha Jonnalagadda for their support during my stay in Durban. I am thankful to these people throughout my life.

I would like to thank my parents Venkata Rambabu Bhaskaruni, Hima Chowdeswari Bhaskaruni and my brother Sai Dileep Bhaskaruni for always being there for me. Your love, your care, your faith gave me strength and encouragement, which is the backbone of my achievements. I am fortunate to have incredible parents whom I look up to as role models, and my amazing cousins Subbarao Nuthalapati, Chakravarthi Nuthalapati and Bhargava Dammavalam for their lovely encouragement towards choosing science as career and who have always believed in me. I am thankful for their love.

Last, but certainly not least, I would like to thank the god Sai Baba, for bountiful blessings.

CONFERENCE PARTICIPATION

1. **V H S Sandeep Bahskaruni**, Suresh Maddila, Werner E. van Zyl and Sreekantha B. Jonnalagadda. "Ag_2O on ZrO_2 as a recyclable catalyst for multicomponent synthesis of indenopyrimidine derivatives". For a Poster presentation at the **College of Agriculture, Engineering and Science Research Day**, 29th November 2016, *Howard College Campus, UKZN*.

2. **V H S Sandeep Bahskaruni**, Suresh Maddila, Werner E. van Zyl and Sreekantha B. Jonnalagadda. "Catalyst-free green synthesis of newly substituted pyrazolo[3,4-b] pyridines in water/ethanol under ultrasound irradiation.". For a Poster presentation at the **College of Agriculture, Engineering and Science Research Day**, 25th October 2017, *Westville Campus, UKZN*.

3. **V H S Sandeep Bahskaruni**, Suresh Maddila, Werner E. van Zyl and Sreekantha B. Jonnalagadda. "A green protocol for the synthesis of new 1,4-dihydropyridine derivatives using Fe_2O_3/ZrO_2 as a reusable catalyst". For a Poster presentation at the **8th IUPAC International Conference on Green Chemistry 2018**, 9-14th September 2018, *Shangri-La Hotel, Bangkok, Thailand*.

4. **V H S Sandeep Bahskaruni**, Suresh Maddila, Werner E. van Zyl and Sreekantha B. Jonnalagadda. "A green protocol for the synthesis of new 1,4-dihydropyridine derivatives using Fe_2O_3/ZrO_2 as a reusable catalyst". For a Poster presentation at the **College of Agriculture, Engineering and Science Research Day**, 25th October 2018, *Westville Campus, UKZN*.

LIST OF ABBREVIATIONS

Abbreviations	Full name
$(Bmim)BF_4$	1-Butyl-3-methylimidazolium tetrafluoroborate
1,4-DHPs	1,4-Dihydropyridines
3-CR	Three component reaction
4-CR	Four component reaction
AcOH	Acetic acid
AMPD	2-Amino-2-methyl-1,3-propanediol
ArH	Aromatic ring proton
BET	Brunauer-Emmett-Teller
Calcd.	Calculated
CNTs	Carbon nanotubes
COSY	Correlated spectroscopy
d	Doublet
DABCO	1,4-Diazabicyclo[2.2.2]octane
DBU	1,8-Diazabicyclo(5.4.0)undec-7-ene
dd	Doublet of doublet
DMF	N,N-Dimethylformamide
DMSO-d_6	Deuterated dimethyl sulfoxide
dt	Doublet of triplet
EDX	Energy-dispersive X-ray
EtOH	Ethanol
FT-IR	Fourier Transform Infrared Spectroscopy
HM	Hydromagnasite
HMBC	Heteronuclear Multiple Bond Coherence
HRMS	High Resolution Mass Spectrometry
HSQC	Heteronuclear Single Quantum Coherence
HTlc	Hydrotalcite
ICP-OES	Inductively Coupled Plasma-Optical Emission Spectroscopy
IPA	Isopropyl alcohol

IUPAC	International Union of Pure and Applied Chemistry
J	Coupling constant
m	Multiplet
M:O	Metal:Oxygen atom ratio
MCRs	Multicomponent Reactions
MeOH	Methanol
MMOs	Mixed metal oxides
MW	Microwave
NPs	Nano particles
RT	Room Temperature
S	Singlet
SEM	Scanning electron microscopy
T	Triplet
TEA	Triethylamine
TEM	Transmission electron microscopy
TFA	Trifluoroacetic acid
THF	Tetrahydrofuran
TLC	Thin-layer chromatography
TMSI	Trimethylsilyl iodide
Tos	Toluenesulfonyl
TsOH	p-Toluenesulfonic acid
OTf	Triflate
AAPTMS	N-(2 amino ethyl)-3-amino propyl trimethoxy silane
m-	Monoclinic
HAp	hydroxyapatite
Ar	Aromatic
LSMO	$La_{0.7}Sr_{0.3}MnO_3$
BPAT	bis(4-pyridylamino) triazine
GO	Graphene oxide
ChCl	Choline chloride
THF	Tetrahydrofuran

MeCN	Acetonitrile
CH_3OH	Methanol
L-His	L-histidine
HAP	Hydroxyapatite
HMS	Hexagonal mesoporous silica
OTf	triflate
PEG-600	Poly(ethylene glycol)
SBA-15	Mesoporous silica
KCC-1	Fibrous nano-silica
^{1}H NMR	Proton Nuclear Magnetic Resonance spectroscopy
^{13}C NMR	Carbon-13 Nuclear Magnetic Resonance spectroscopy
^{15}N NMR	Nitrogen-15 Nuclear Magnetic Resonance spectroscopy
^{19}F NMR	Fluorine-19 nuclear magnetic resonance spectroscopy

LIST OF CONTENTS

Chapter 1

1 INTRODUCTION

1.1 Green Chemistry

Green chemistry can be defined as an emerging science, which is aimed at developing new technologies for environment-friendly protocols by minimizing the usage and production of hazardous materials. The twelve fundamental principles, which make up the concept of Green chemistry are outlined in Figure 1.[1]

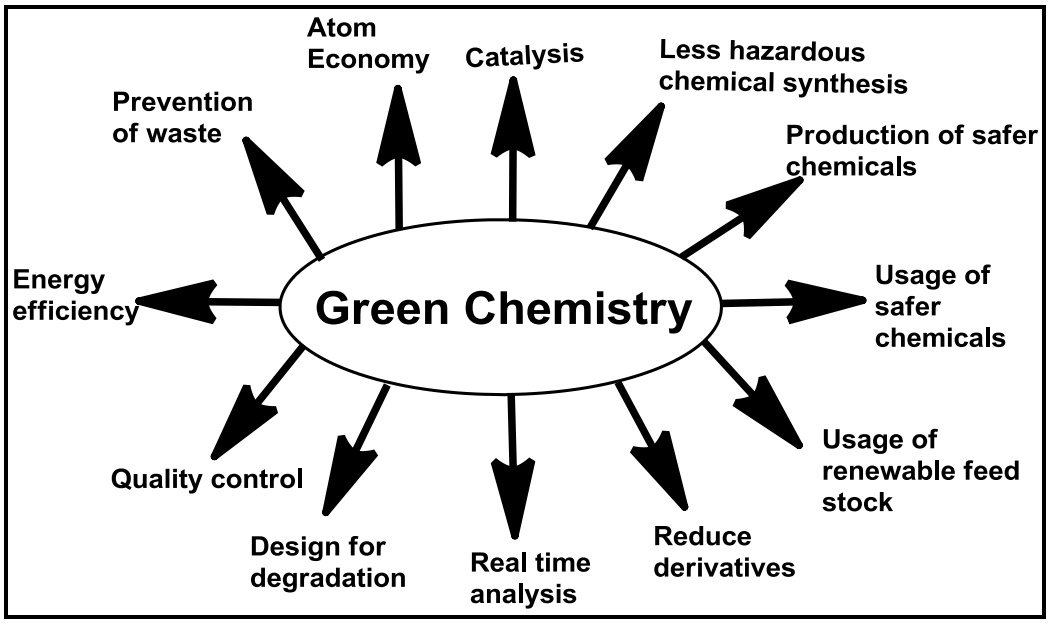

Figure 1: Fundamental principles of Green Chemistry.

Heterogeneous catalysis broadly supports green chemistry and its principles, and offers numerous benefits, which include reusability and higher selectivity as compared to stoichiometric reagents under optimal conditions, easier separation of the heterogeneous catalysts, together with their recyclability major advantages.[2]

1.2 Catalysis

In 1836, Berzelius defined a catalyst "…as a compound, as that which is not consumed in a reaction but alters the rate of that reaction".[3] The two main aims for using a catalyst is to control the rate of a chemical reaction and understand its mechanism.[4] Berzelius and Oswald in 1895 gave the new definition as "a catalyst is a substance that changes the rate of a chemical reaction without itself appearing in the products". On the other hand, in 1976, IUPAC offered the official definition of a catalyst as ''a substance that, being present in small proportions,

increases the rate of attainment of chemical equilibrium without itself undergoing chemical change".[5] It is observed that the main role of a catalyst is to decrease the activation energy of the reactants. Lowering of the activation energy leads to a faster reaction rate.[6]

Catalyzed reactions are very prominent in the industrial sector. From the industrial processes, most fuels and chemicals are obtained by using catalysts.[7] The stoichiometric process utilized in homogeneous catalytic reactions poses many problems, such as difficulty in recovery of catalyst and waste of reagents, which can be overcome by selective catalytic methods.[8] Moreover, catalysis becomes progressively more important in minimization of environmental pollution by minimizing the usage of corrosive reagents.[9] In short, catalysis is valuable for sustainable production and economy and it will be even more important in the future.[10]

1.2.1 Classification of catalysts

Catalysis is classified into three main types. These are:

(i) enzymatic catalysis

(ii) homogeneous catalysis and

(iii) heterogeneous catalysis

The three categories of catalysts are hereafter discussed individually.

1.2.1.1 Enzymatic catalysis

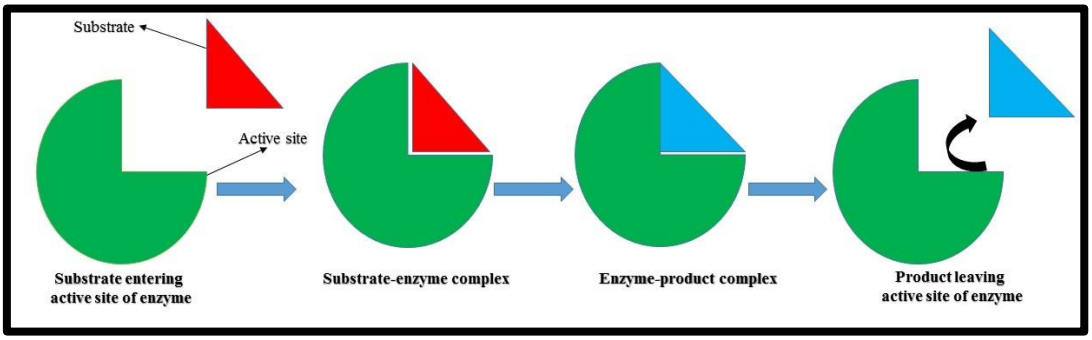

Figure 2: Schematic representation of an enzymatic catalytic reaction.

This type of catalysis mainly deals with enzyme-mediated reactions. It is also a part of homogenous catalysis, where the catalysts are typically targeted enzymes (Figure 2). These enzyme catalysts have excellent regio- and stereoselectivity under room temperature conditions without any side reactions. [11],[12] Having an advantage such as high selectivity, enzymatic

catalysis also has drawbacks such as miscibility in the reaction mixture and difficult to separate, stability with respect to temperature, sensitivity towards strong chemicals and pH resistance which allows a narrow scope of enzymes as a catalyst.[13] Enzymes are stable at room temperature and pressure if the temperature and pressure of the reaction are different there is a loss of catalytic activity, and enzyme production are costly processes which make the protocol expensive.[14]

1.2.1.2 Homogeneous Catalysis

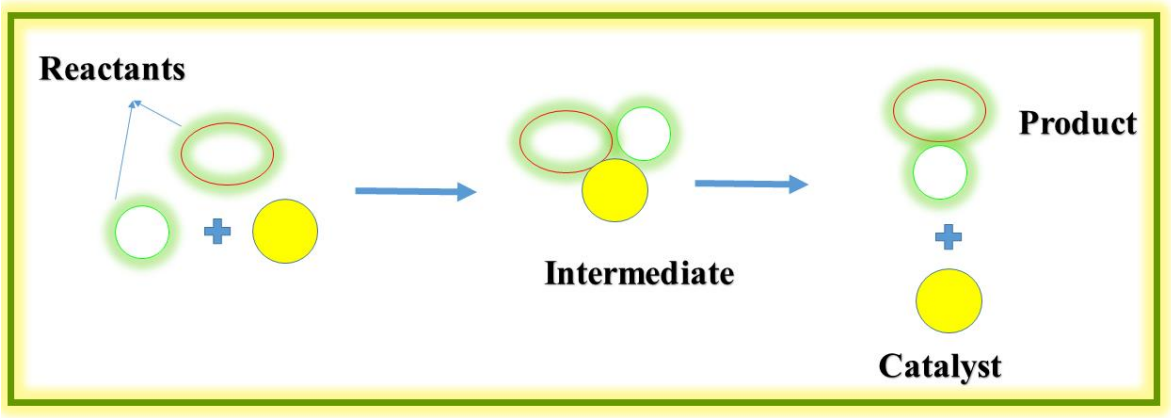

Figure 3: Schematic representation of a homogeneous catalytic reaction.

In homogeneous catalysis, all of the reactants, as well as the catalyst are in the same phase, which is commonly the liquid phase (Figure 3).[15] High activity and selectivity are the main advantages given by homogeneous catalysts, and the main limitations are difficulty with separation of catalyst, the corrosive nature of the materials and the long workup.[16] Homogeneous catalysts, which typically gained importance in industry, are: Wilkinson's catalyst for hydrogenation of alkenes,[17] cobalt and rhodium catalysts for hydroformylation reactions[18] and Ziegler-Natta catalyst for polymerization reactions[19] to mention a few. Despite having high activity and selectivity, homogeneous catalysis suffers from main disadvantages like reusability issues with high-temperature reaction conditions and quenching steps,[20] furthermore by-product formation is another disadvantage which requires further purification steps.[21] Difficult neutralization processes involve corrosive reagents which are harmful to human as well as nature. [12]

1.2.1.3 Heterogeneous catalysis

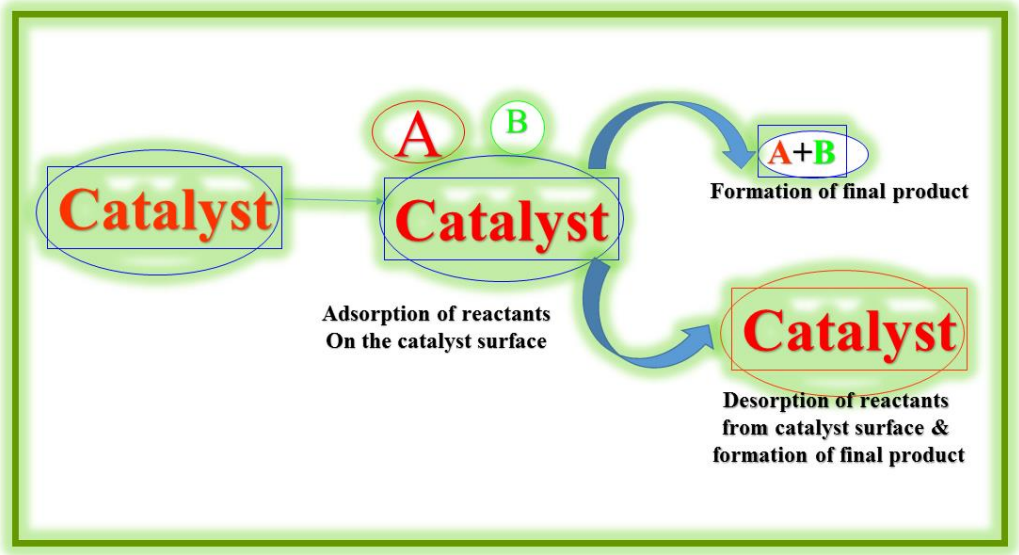

Figure 4: Schematic representation of a heterogeneous catalytic reaction.

Heterogeneous catalysis usually takes place between two different phases i.e. the reactants in one phase and the catalyst is in another phase. In general, the catalyst is in the solid phase and the reactants are in the liquid/gas phase. [12] In these reactions, the reactants are held together on the active sites in the catalyst surface by adsorption, which is a weak physical attraction (Figure 4).[22] Important examples of the utilization of heterogeneous catalysts are: oxidation of ammonia to nitrous oxide by the Ostwald process and the use of alumina-silicates for petroleum cracking reactions.[23] Heterogeneous catalysts have more advantages compared to homogeneous catalysts, with the main advantages being easy separation of the catalyst from the reaction medium due to easy removal by filtration which makes the total recovery of catalyst simple and cost-effective.[24] Thermal stability of the catalyst makes it attractive towards the usage of heterogeneous catalyst in the industrial sector. [25]

The main benefits of heterogeneous catalysis compared to homogeneous and enzymatic catalyst is the well-defined surface active sites and its wide range of applicability towards industrial reactions.[26] The versatile surface active sites can be tuned by loading/doping with other metals or surface functionalization with other ligands makes heterogeneous catalysts a selective way in the synthesis. High surface area and porosity are the added attractive features.[27]

1.3 Multicomponent Reactions (MCRs)

Urea was the first organic molecule that was synthesized in 1828 by Wöhler, and ever since, synthetic chemists all around the world became interested in taking on the challenging task of synthesizing new molecules with progressive and adaptable chemical strutures. [28] This has remained one of the main motivations behind the discovery and invention of new reagents and catalysts which facilitate the design and development of complex scaffolds by the sequence of a number of different reactions.[29] Over the last thirty years, chemists are understanding more and becoming more responsible to develop environmentally adapted protocols for minimizing this harmful impact.[30] As green chemistry started to become more significant, it has allowed chemists to design concise, efficient and convergent protocols.[31] The main objective of green chemistry is the use of alternate and sustainable variations as compared to convergent protocols.[32] Different synthetic strategies, which include environmental considerations as early as possible in the design stage, is where MCRs came into the picture.

MCRs are reactions that occur in a single pot, having more than two starting materials and they typically yield products with the characteristics of the starting materials (Figure 5).[33] In organic synthesis, one-pot reactions are attaining more importance due to its high atom economy. The ideal MCR is one in which all the starting reagents are added together at the start of the reaction, and one in which all of the reactants react in an ideal way under the same reaction conditions.[34] The success of MCR mainly depends on the equilibrium balance, and on the reaction having a suitable sequence of reversible and irreversible steps. High atom economy, high rates of efficiency, mild conditions and the use of green solvents are the factors which validate MCRs as a great tool for sustainable synthetic methodology.[35] The validation and application of MCRs have increased in the medicinal, agrochemical and drug discovery fields, however, there still remain a lot more developments to be made and there are, however, still a lot more eco-friendly issues to be dealt with. [36]

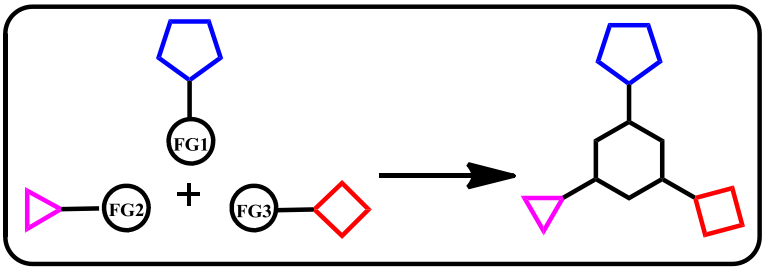

Figure 5: General concept of MCRs.[33]

1.3.1 Various named reactions in MCRs

Based on the reactants and reaction conditions, MCRs are typically classified into the following types. [36]

- Passerini reaction
- Biginelli reaction
- Strecker reaction
- Hantzsch reaction
- Mannich reaction
- Ugi reaction
- Petasis reaction
- Gewald reaction
- van Leusen reaction
- Groebke-Blackburn-Bienayme reaction
- Bucherer-Bergs reaction
- Grieco multicomponent reaction
- Kabachnik-Fields reaction

These reactions each have something different about them, which mainly deals with the reagents used or their reaction conditions. These named MCRs are discussed here.

1.3.1.1 Passerini reaction

Mario Passerini discovered this reaction in 1921.[37] This reaction refers to as α-acyloxycarboxamides synthesis using carbonyl compounds, carboxylic acid, and isocyanide (**Scheme 1**).

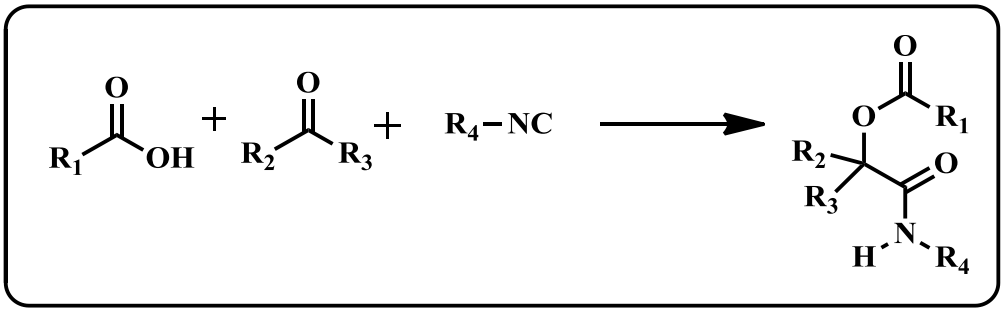

Scheme 1: General scheme for the Passerini reaction.

1.3.1.2 Biginelli reaction

This reaction is mainly used for the synthesis of 3,4-dihydropyrimidin-2(1H)-one derivatives, by reacting an aromatic aldehyde with ethyl acetoacetate and urea as the starting materials (**Scheme 2**). This one-pot procedure was developed in 1891 by Biginelli.[38]

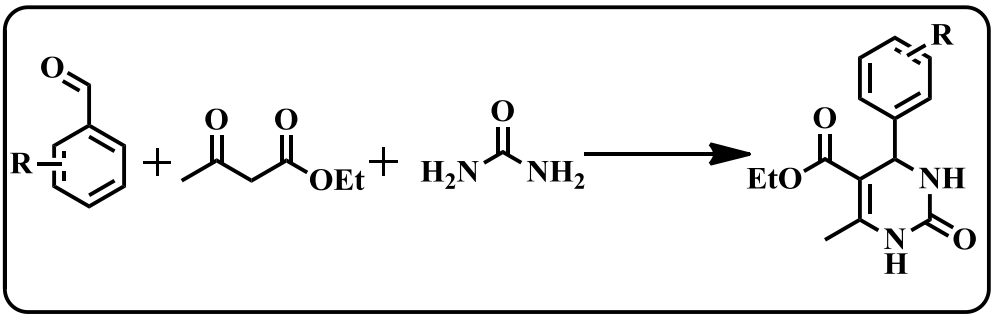

Scheme 2: General scheme for the Biginelli reaction.

1.3.1.3 Strecker reaction

It is a straight-forward synthetic protocol for the formation of α-amino acids. It was first discovered in 1850 (**Scheme 3**). This method involves the reaction between carbonyl compounds with amines and a cyanide source. Generally, an alkaline metal cyanide or hydrogen cyanide is used for this.[39]

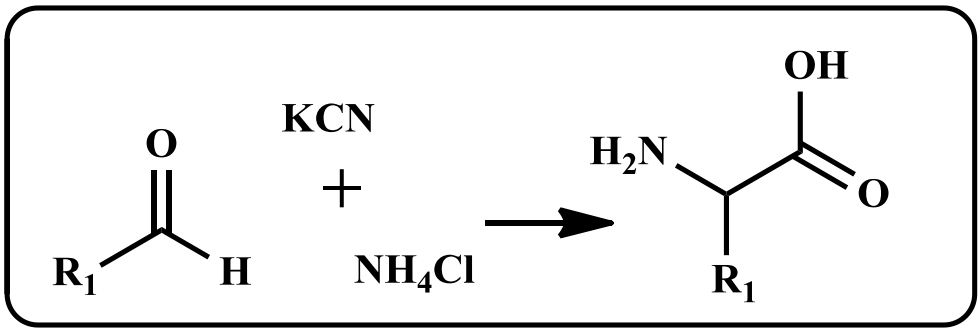

Scheme 3: General scheme for the Strecker reaction.

1.3.1.4 Hantzsch reaction

The Hantzsch reaction was discovered in 1882 by A.R. Hantzsch. The protocol involves a reaction between aldehydes and β-keto ester and ammonia as the nitrogen source (**Scheme 4**). The method has been proven to offer a wide type of symmetrical and unsymmetrical dihydropyridines by using different β-keto esters.[40]

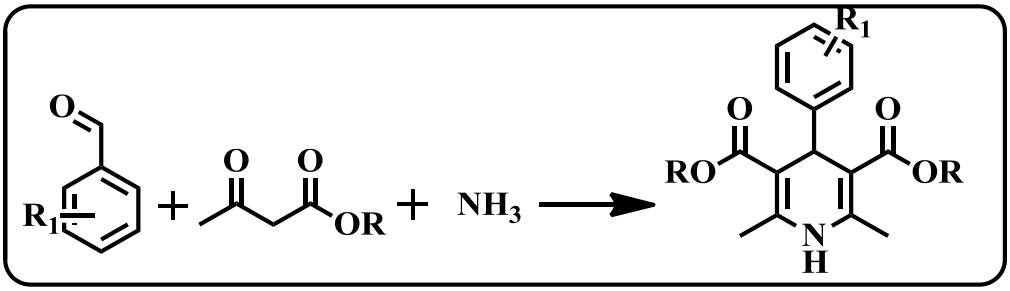

Scheme 4: General scheme for the Hantzsch reaction.

1.3.1.5 Mannich reaction

The Mannich reaction was discovered in 1912 by Carl Mannich. The procedure offers the formation of new C-C and new C-N bonds to afford β-amino-carbonyl compounds (**Scheme 5**). The three-component reaction involves the coupling of an enolizable carbonyl compound together with formaldehyde, which is non-enolizable with an amine (primary or secondary).[41]

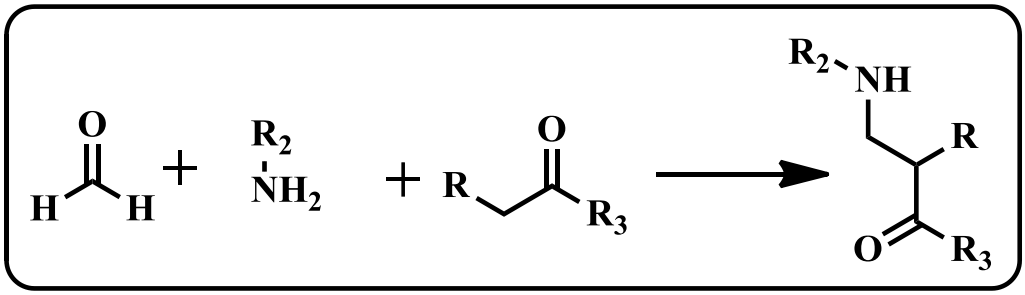

Scheme 5: General scheme for the Mannich reaction.

1.3.1.6 Ugi reaction

This reaction was first reported in 1959 by Ivar K. Ugi.[42] This is a straightforward protocol for the formation of bis-amide derivatives (**Scheme 6**). This procedure is similar to the Passerini reaction but it has an amine as a fourth component in C-C bond formation. This study reported on the reaction between carbonyl compound with amines, an isocyanide and carboxylic acids.

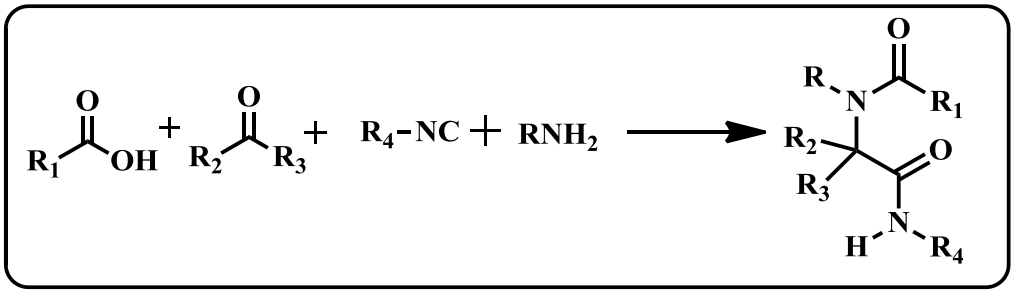

Scheme 6: General scheme for the Ugi reaction.

1.3.1.7 Petasis reaction

This reaction was first reported by Nicos Petasis in 1993, for the synthesis of substituted amines.[43] This was done using an aldehyde, amine and substituted boronic acid as reactants (**Scheme 7**). It is similar to the Michael addition reaction but with a small variation where boronic acid serves as the nucleophile to afford the substituted amines, while in a Michael addition reaction, the product forms through enolates.

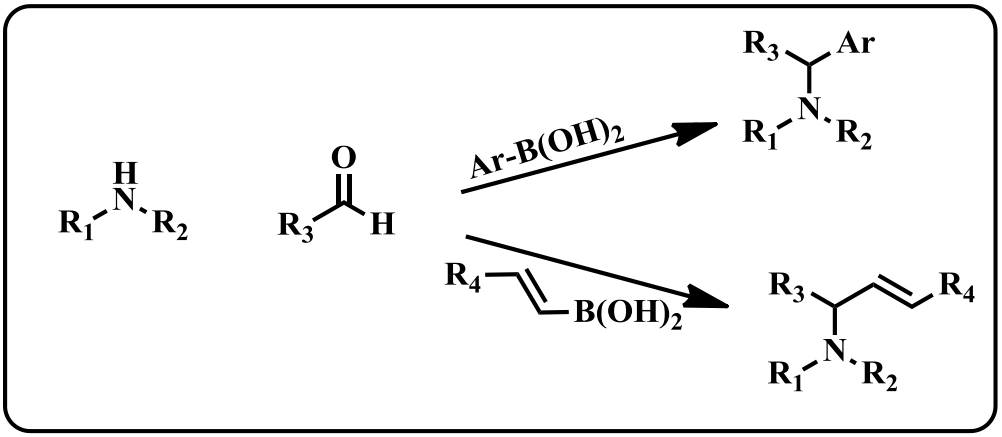

Scheme 7: General scheme for the Petasis reaction.

1.3.1.8 Gewald reaction

The Gewald reaction was first reported in 1966 by K.Gewald.[44] This protocol offers a method to synthesize polysubstituted 2-amino-thiophene derivatives (**Scheme 8**). The product formation involves the one-pot reaction between an aliphatic aldehyde/ketone with an α-cyano ester, in the presence of elemental sulfur.

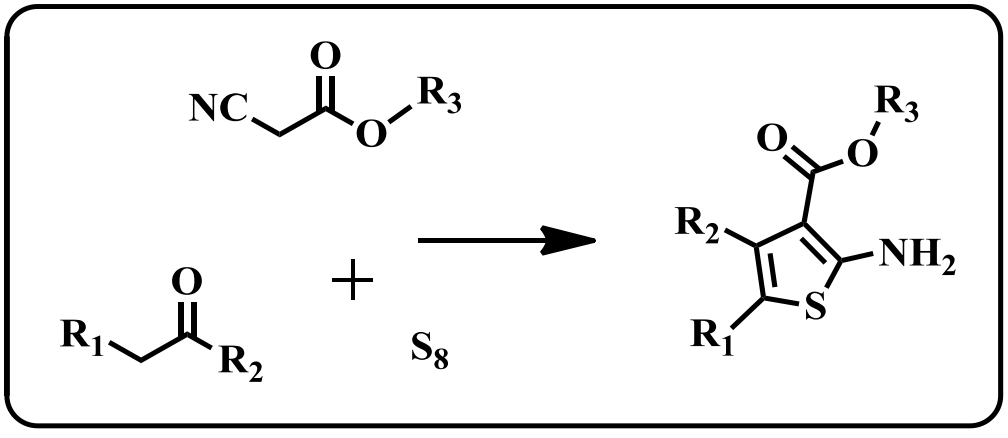

Scheme 8: General scheme for the Gewald reaction.

1.3.1.9 Van Leusen reaction

This protocol was reported by Van Leusen in 1977.[45] The reaction involves a condensation reaction between ketones and toluenesulfonylmethyl isocyanide to yield nitriles (**Scheme 9**). The main advantage of this method is that if the reaction was performed by utilizing an aldehyde as the reactant oxazole then imidazole derivatives are synthesized.

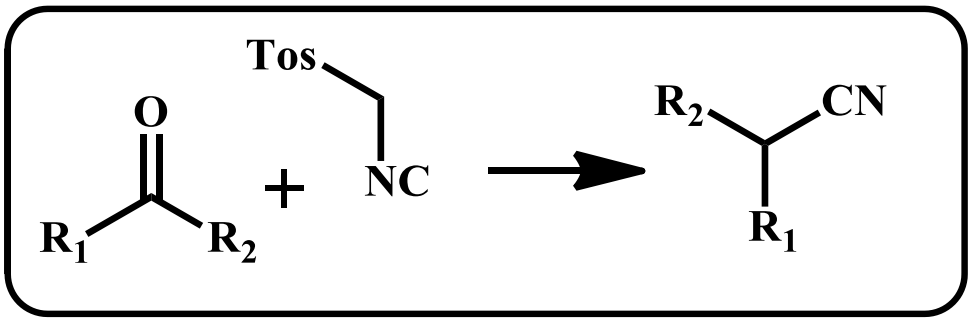

Scheme 9: General scheme for the Van Leusen reaction.

1.3.1.10 Groebke-Blackburn- Bienayme reaction

Theis reaction is a one-pot protocol to synthesize of *N*-bridgehead heterobicyclic derivatives (**Scheme 10**). This protocol involves the reaction between aldehydes, heterocyclic amidines, and isocyanides.[46]

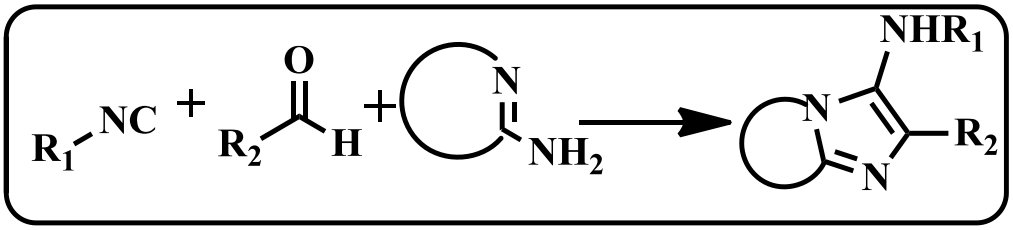

Scheme 10: General scheme for the Groebke-Blackburn- Bienayme reaction.

1.3.1.11 Bucherer-Bergs reaction

This protocol highlights a synthetic route for the formation of hydantoins (**Scheme 11**). The method involves a reaction between cyanohydrin together with ammonium carbonate.[47]

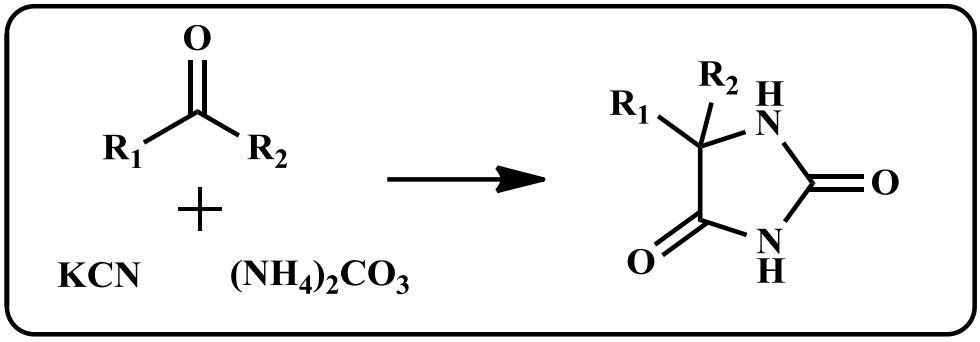

Scheme 11: General scheme for the Bucherer-Bergs reaction.

1.3.1.12 Grieco reaction

This reaction was discovered by Paul Grieco in 1985, for the synthesis of *N*-heterocyclic six-membered rings.[48] This protocol involves a reaction between an aldehyde, aniline and alkenes (**Scheme 12**).

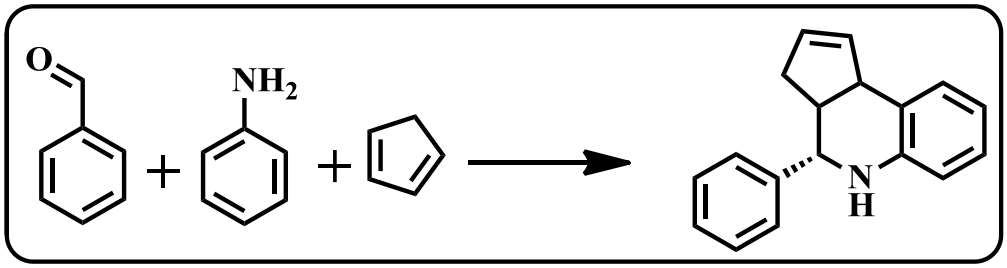

Scheme 12: General scheme for the Grieco reaction.

1.3.1.13 Kabachnik- Fields reaction

This reaction offers a protocol for the synthesis of α-aminophosphonates derivatives by using carbonyl compounds, an amine functionality and dialkyl phosphonate (**Scheme 13**). [49]

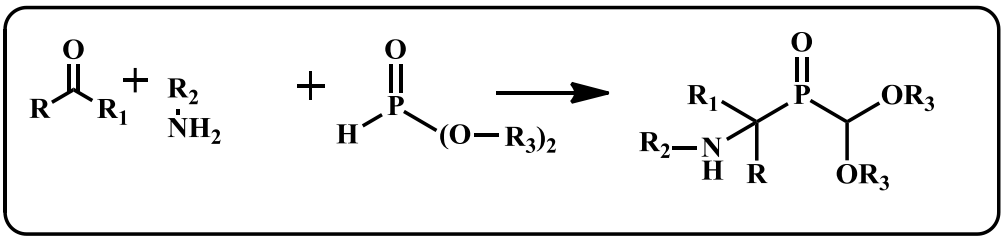

Scheme 13: General scheme for the Kabachnik-Fields reaction.

1.4 Heterocyclic chemistry

Heterocyclic compounds cover a wide area in organic and medicinal chemistry. Heterocyclic scaffolds have a significant number of applications in industries like pharmaceutical, medicinal and agrochemicals. In many alkaloids, heterocycles are the main

active constituents.[50] In heterocyclic molecules, *N*-heterocyclic scaffolds attain great interest because of having versatile pharmaceutical importance. The older methods in the synthesis of *N*- hetero cyclic moieties through the conventional approach is replaced by more sustainable methods through advantageous paths. In *N*-heterocycles, dihydropyridines, pyrazoles, and pyrimidines are the most attractive scaffolds because of their anti-inflammatory,[51] anticancer,[52] and anti-tubercular[53] properties. Other than the medicinal importance, heterocyclic molecules are important in other applications like pesticides and insecticides in the agrochemicals sector,[54] animal products,[55] polymers,[56] dyes[57] and as corrosions inhibitors.[58] In addition to these properties, an attempt has been made to synthesize pyrazoles, pyridines, and pyrimidines scaffolds by one-pot protocol under green conditions.

1.5 Heterogeneous catalysis under green conditions

Heterogeneous catalysis typically involves the reactants and the catalyst in different phases, which is what makes it easier to separate the catalyst from the reaction mixture and products. The chemistry of heterogeneous catalysis involves the diffusion and adsorption of reactants onto the active sites of the surface, followed by the reaction between the charged species of reactants on the surface and, finally, desorption from the surface sites.[59] As the adsorption and desorption occur on the surface area of the material, the catalyst plays a key role by providing catalytic activity.[60] In heterogeneous catalysis, porosity plays a crucial role because generally, as the porosity of catalyst increases, the material obtains a greater surface area. The main advantage of porous materials used as catalysts is that molecules not only interact on the external surface but also within the interior surface of the material, therefore metal oxides with higher surface area and high porosity are extensively studied.[27] It has been found that transition metal oxides are able to form an oxidation-reduction cycle between the higher and lower oxidation states due to them having multiple valence states, moreover, these metal oxides have versatile properties like (a) stoichiometric ratios of metal cations and oxy anions, (b) presence of cationic and anionic vacancies, (c) cations can easily undergo redox reactions, (d) presence of surface acidic and basic sites, and (e) presence of covalent and ionic bonding between metal cations and oxy anions.[25]

Metal oxides are classified into 3 main types based on their pore size.[25] These are:

i. Microporous (pore size is less than 2 nm)
ii. Mesoporous (pore size is 2-50 nm), and
iii. Macroporous (pore size is greater than 50 nm).

1.5.1 Metal oxide catalysts

Traditionally, usage of oxide catalysts are limited to vapour phase reactions in the petrochemical industries, but as of recent times, metal oxide catalysts attain more of their importance in synthetic chemistry.[25] Simple oxides are generally used as solid acids or bases because they have shown activity for some oxidations and reductions. The oxide catalysts are of 2 types, mainly: (i) electrical insulators, and (ii) semiconductors. In insulators, the M:O ratio is stoichiometric due to the cation having a single valence, examples of this category are MgO, Al_2O_3 and SiO_2. These materials are used as solid acids/bases rather than oxidation catalysts, whereas semiconductor oxides are widely used in oxidations, and this is due to their cation's metallic property which creates a site that can easily be cycled between two or more valence states. This can be due to different oxidation states as in Fe_2O_3, V_2O_5, TiO_2 or the interconversion between the positive ion and neutral metal, as is the case with the more easily reduced oxides such as ZnO and CdO. Generally, metal oxides contain metal cations (M^{x+}) and oxy anions (O^{2-}) which cover the surface of the metal oxide. It is commonly found that the size of oxy anions are far larger as compared to M^{x+}, moreover, the surface possesses -OH groups which are anchored at the end of the surface and which act as conjugate acid-base pairs in corresponding oxy anions.

Oxides which are categorized on the basis of their composition fall into two different types, namely:

(i) Simple oxides, which have shown some catalytic activity in certain oxidation reactions. Generally, they are used as solid acids/bases. These simples oxides do have one main disadvantage which is low synthetic importance due to its lower activity, and

(ii) Oxides with two or more metal cations are referred to as mixed metal oxides (MMOs). These are simple oxides which have been modified by loading or doping other metals and this alters its catalytic activity thereby making MMOs more advantages over simple oxides. An in-depth view of the morphology of MMOs shows it to contain two parts, where one is the support and the other is the active material. The support will typically provide mechanical strength, thermal stability and surface area, which is essential for the wide dispersion of the active material and this provides active interactions between the active material and the support, which makes the material an ideal catalyst for transformations. The crystal structure of prepared oxides can be explained on the basis of oxide composition i.e., ABO_3 corresponds to perovskites, ABO_4 corresponds to scheelites, AB_2O_4 corresponds to spinels and $A_3B_2O_8$ are palmeirites. In most of these metal oxides, the surface arrangement is M-OH, M=O and M-O-M types of

bonding. The presence of variable oxidation states in the transition metal oxides has proven its efficiency as effective catalysts towards redox reactions. The efficiency of these catalysts depends on the active material and the support where the higher the surface area of the support, the higher the concentration of active material that will be loaded on the surface so that the active sites can be increased.

The two main factors which are used to choose the catalytic supports are:

(a) The support should be stable throughout the reaction without any loss of its activity under thermal, chemical and work-up process.

(b) High surface-area, where the pore size must be >20Å, which is a typical quality of mesoporous materials, in which reactants can diffuse into the active sites.

For many industrial catalysts, the main requirement to be a catalyst is having thermal and mechanical stability, high surface area and mesoporous texture. These properties fit well with zirconium oxide or zirconia (ZrO_2).

1.6 Importance of zirconium oxide in organic synthesis

Zirconium can exist in various oxidation states, from +I to +IV with different coordination numbers, which range from 4 to 8. The ZrO_2 compound is usually a ceramic oxide, which attained importance in heterogeneous catalysis as a catalyst/support, because of its bifunctional nature. Because of its mechanical and thermal stability, it is popularly known as "Ceramic Steel". Zirconia can exist in three polymorphic forms on the basis of thermal treatment. These are: (a) monoclinic, which is stable <1170 ºC, in which Zr^{X+} cation is 7 coordinate and the O^{2-} anion exists as 3 or 4 coordinated, (b) tetragonal, which exists in between 1170 – 2370 ºC, and (c) cubic, which exists at temperatures >2370 ºC. In both the tetragonal and cubic phases, the cation is 8 coordinated and the anion is 4 coordinated.[61] The chemical inertness makes ZrO_2 an ideal material when compared to other classical supports like Al_2O_3 and SiO_2. The surface of ZrO_2 is covered with Zr^{3+} and Zr^{4+} which are the source of Lewis acidic sites and -OH groups are responsible for the weak Brønsted acid/base sites. Carbon monoxide (CO) adsorption studies reveal that t-ZrO_2 is more acidic as compared to m-ZrO_2. It is observed that the surface area of ZrO_2 is directly affected by calcination temperature and phase, as the temperature increases from 300 to 900 ºC, the surface area of the material decreases while Brønsted acidity increases. This is due to the escape of oxygen from the coordinates.[62] In this study, the surface property was altered by loading the surface of zirconia with other metals, and it is known that if the surface is loaded with basic oxides the acidity

decreases, and vice versa. On the other hand, if the surface is loaded with acidic oxides its acidity increases.

The advantages of utilizing zirconia in catalysis are:

1) Zr has an electronic configuration [Kr] $4d^2 5s^2$. The incomplete d sub-shell electrons can act as an attraction which facilitates the reactants to bind on its surface, thereby making Zr an ideal catalyst.
2) Zr has a high melting point, which permits the studies at high-temperature conditions.
3) The amphoteric nature of the material, which allows for the alteration of the surface properties by using other metals, and
4) The non-toxic, non-corrosive and inexpensive nature makes zirconia an ideal material for these catalytic applications.

Zirconia catalyses many organic reactions, facilitating the formation of C-C and C-X bonds, of which some reactions are detailed.

Diamine functionalized mesoporous zirconia (AAPTMS/m-ZrO_2) as a recyclable catalyst for the formation of new C-C and C-N bonds.[63] In the reaction between the electrophilic carbonyl group of aromatic aldehydes and the compounds having active methylene group i.e, malononitrile and thiazolidine-2,4-dione with ammonium acetate *via* the Knoevenagel-Michael addition pathway, in the presence of ethanol (**Scheme 14**). This protocol gives high yields of the pyridine derivatives up to 95 % in 3.5 h at 70 ° C.

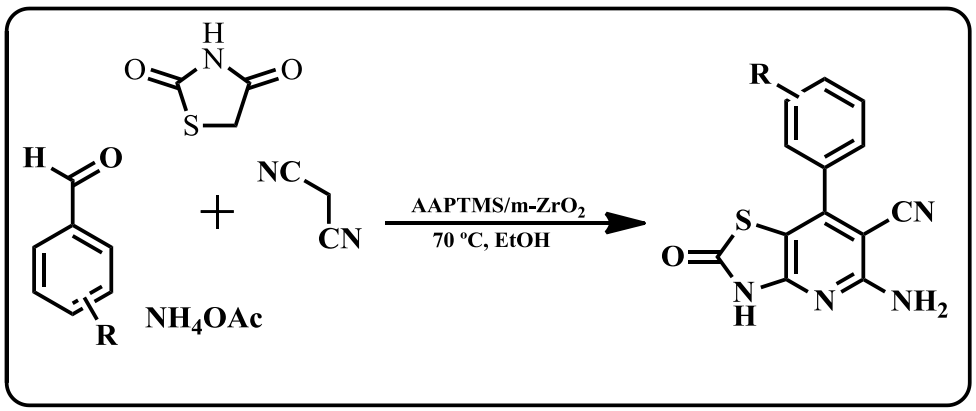

Scheme 14: Synthesis of pyridine derivatives.

CeO_2/ZrO_2 has been used as a catalyst for new C-C and C-N bond formation under milder reaction conditions [64] This protocol involves a reaction between carbonyl groups of an substituted benzaldehyde with ethyl acetoacetate, hydrazine and malononitrile to form novel pyranopyrazole derivatives, and the reaction proceeds in ethanol at room temperature and offers

yields of up to 98 % in 15 min (**Scheme 15**). This method is more advantageous for the preparation of different aromatic pyranopyrazole derivatives.

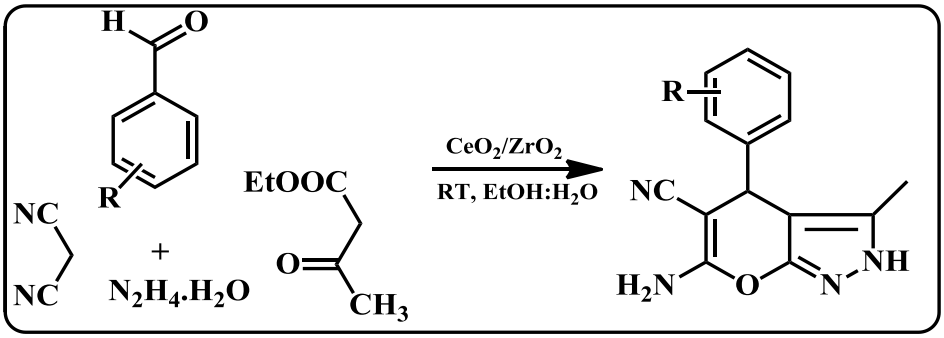

Scheme 15: Synthesis of pyranopyrazole derivatives.

Nano-zirconia-supported sulfonic acid was used for the synthesis of 1,4-dihydropyridine derivatives under solvent-free condition.[65] This protocol offers yields up to 93 % in 1 h (**Scheme 16**). The MCR involves reacting aromatic aldehydes, 1,3- cyclohexadione and ammonium acetate. The Lewis acidic sites activate the carbonyl group, which makes the carbonyl carbon partially positive and thereby allow Knoevenagel condensation-Michael addition type tandem reaction.

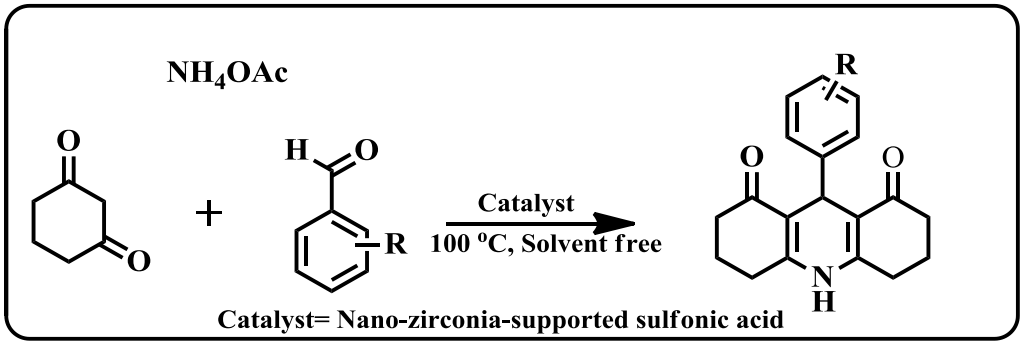

Scheme 16: Synthesis of 1,4-dihydropyridine derivatives.

Another good example is of a Knoevenagel-Michael type reaction between aromatic aldehydes, ethyl acetoacetate, and ammonium acetate by using zirconocene bis(perfluorobutanesulfonate) as a reusable catalyst at 80 ºC under solvent-free condition. [66] This protocol involves the reaction between a variety of aldehydes, with aromatic/hetero aromatic aldehydes which typically follow the 1,4 addition pathway to produce a synthesis of 1,4-dihydropyridine derivatives. The method offers yields up to 95 % in 3 hours (**Scheme 17**).

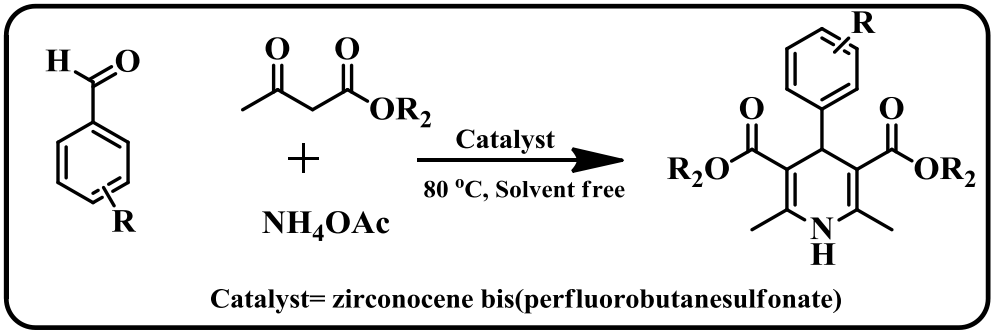

Scheme 17: Synthesis of 1,4-dihydropyridine derivatives.

Maddila *et al*., used Mn doped ZrO_2 as a catalyst for the Knoevenagel-Michael addition for the synthesis of pyrano[2,3-c]pyrazoles.[67] This procedure involves the reaction between various ring activating and ring deactivating aromatic aldehydes with malononitrile as the active methylene group, and dimethylacetylenedicarboxylate/ethyl acetoacetate it usually occurs with ultrasound irradiation (**Scheme 18**). The reaction offers yields of 88 - 98 % in aqueous ethanol as the solvent in under 10 min. The synergetic effects between Mn and zirconia provide an added advantage for the activation of the carbonyl group and the malononitrile moiety for the present condensation.

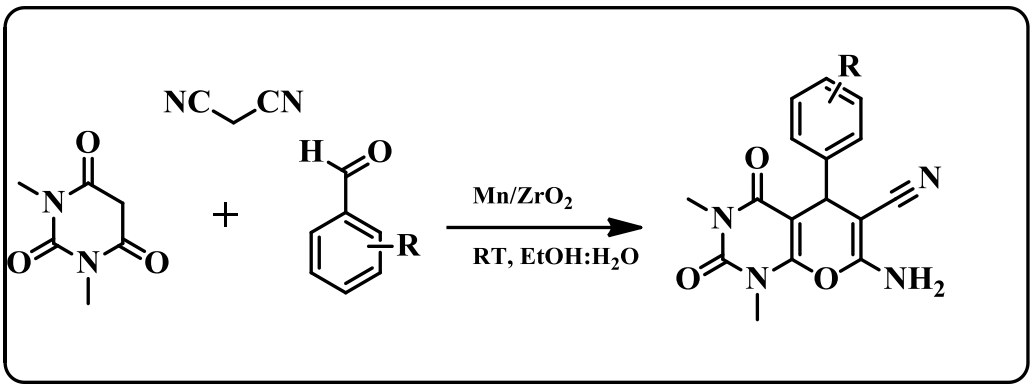

Scheme 18: Synthesis of pyranopyrazole derivatives.

Manouchehr *et al.*,[68] reported zirconia nanoparticles as a catalytic material for the synthesis of multi-substituted 1,4-dihydropyridine derivatives. This reported protocol involves reacting substituted benzaldehyde, 2,6-diaminopyrimidine-4(1*H*)-one and 5,5-dimethyl-1,3-cyclohexanedione. The mechanism of formation of new C-C bonds between 5,5-dimethyl-1,3-cyclohexanedione and substituted benzaldehyde through Knovenengal condensation, further the intermolecular Michael addition and intramolecular cyclization with 2,6-diaminopyrimidine-4(1*H*)-one to afford substituted 1,4-dihydropyridine`s. This protocol offers 96 % yields in 1 h (**Scheme 19**).

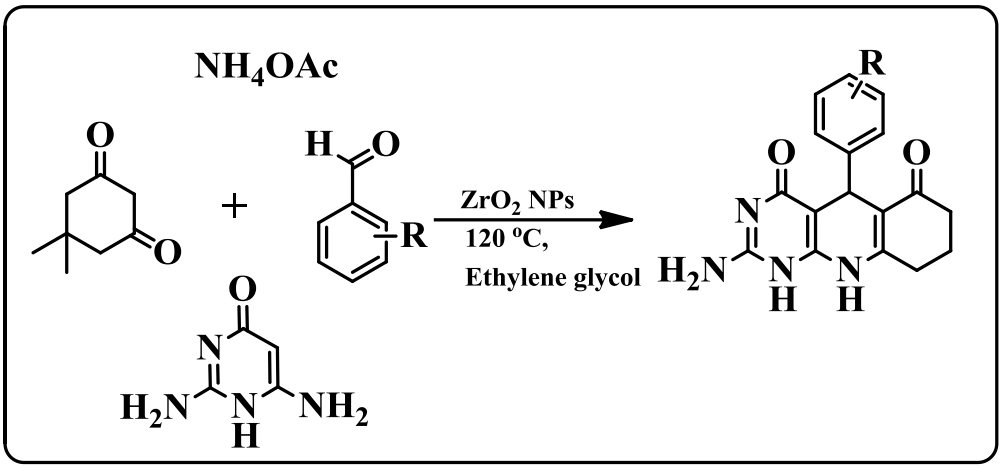

Scheme 19: Synthesis of 1,4-dihydropyridine derivatives.

Khazaei *et al.,*[69] used $ZrOCl_2.8H_2O$ as a catalyst for the synthesis of pyridine derivatives under solvent-free conditions (**Scheme 20**). This procedure involves the reaction between aromatic aldehyde, ethyl acetoacetate, ammonium acetate and 5,5-dimethyl-1,3-cyclohexanedione at 85 ºC. The reaction offers yields of 97 % in 5 min. Broad substrate scope under milder reaction conditions are the main advantage of this protocol.

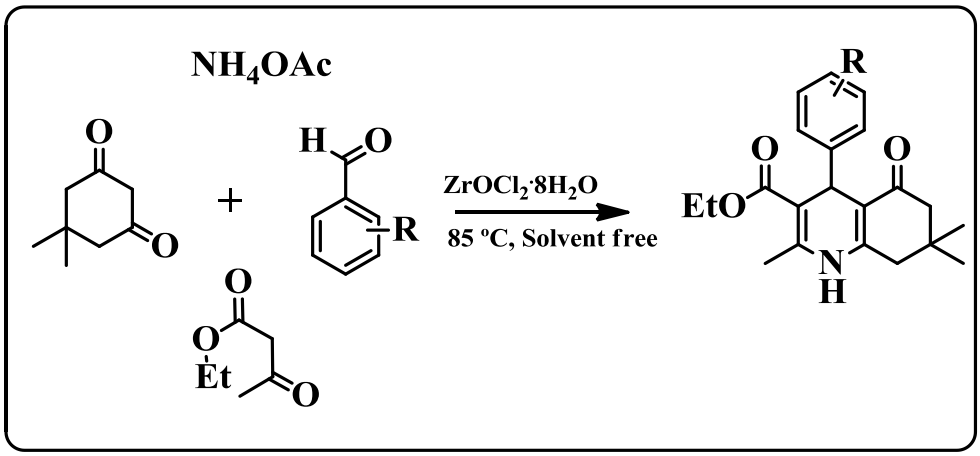

Scheme 20: Synthesis of pyridine derivatives.

1.7 Ruthenium

Ruthenium has an electronic configuration [Kr] $4d^7 5s^1$, with possible oxidation states from +I to +VIII. Ruthenia exist as an amphoteric metal oxide which possesses both Lewis acid/base sites. Instead of using strong Lewis acids, low valent ruthenia can be used for this purpose. An attractive feature of using ruthenia as a heterogeneous catalyst is its leaching stability which can be used several times.[70]

Maddila *et al*., reported Ru-loaded hydroxyapatite (Ru-HAp) and its catalytic activity was studied *via* the synthesis of pyrano[2,3-c]pyrazoles at room temperature in the presence of EtOH:H_2O as solvent.[24] The one-pot reaction involved coupling between substituted benzaldehydes, malononitrile, hydrazine hydrate and ethyl acetoacetate. The mechanism of reaction involves Knoevenagel-Michael addition (**Scheme 21**). In this present study, Ru-HAp served as an excellent catalyst with high yields of about 98 % in 15 min.

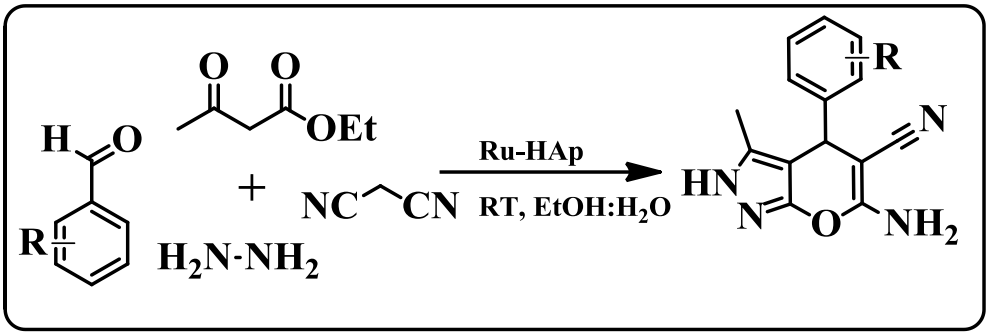

Scheme 21: Synthesis of pyrano[2,3-c]pyrazoles.

Maddila *et al*., developed a protocol for the synthesis of pyrano[2,3-c]pyrazole-3-carboxylate derivatives by using Ru loaded calcium hydroxyapatite (Ru-CaHAp) as a catalyst (**Scheme 22**).[71] The surface of the calcium hydroxyapatite was modified with ruthenia for better stability. The presence of many surface active sites facilitates the Knoevenagel-Michael addition type of reaction between aromatic aldehydes, malononitrile, dimethyl acetylenedicarboxylate, hydrazine hydrate at room temperature. Yields up to 97 % were obtained in 30 min.

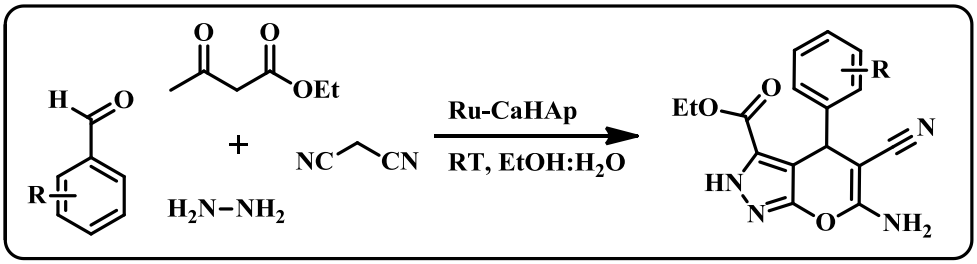

Scheme 22: Synthesis of pyrano[2,3-c]pyrazole-3-carboxylate derivatives.

1.8 Vanadium

Vanadium has an electronic configuration [Ar] $3d^3 4s^2$. Vanadium exists in different oxidation states from +II to +V and shows versatile magnetic and catalytic properties due to the vacancies in the d-orbitals. Oxides of vanadia exist in different forms like VO, V_2O_3, VO_2, and V_2O_5. The catalytic efficiency is due to empty d-orbitals of metal cation which is capable to accept a pair of electrons and act as Lewis acidic sites, whereas oxy anions act as Brønsted acidic sites.[72]

Derivatives of pyridine have been reported by Maddila *et al*., using Mg-V hydrotalcite (Mg-VCO_3 HTlc) catalyst in the presence of ethanol as the solvent. [73] The classical three-component reaction involved the reaction between aromatic aldehydes, malononitrile and acetoacetanilide at 60 ºC (**Scheme 23**). This protocol offered high yields of 85 - 93 % in 2-3 hours. The prepared catalyst had efficiency for up to four cycles of this reaction.

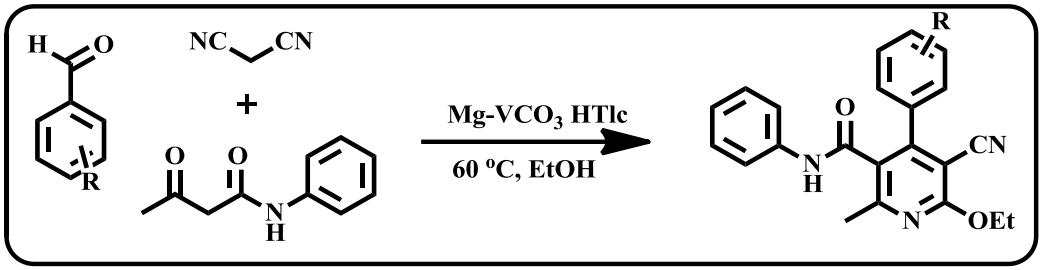

Scheme 23: Synthesis of substituted pyridines.

Pagadala *et al.*, prepared $ZnVCO_3$ hydrotalcite and utilized to synthesize 1,4-dihydropyridiene derivatives.[74] The prepared material showed excellent catalytic activity for the reaction between substituted benzaldehydes with acetoacetanilide and ammonium hydroxide to form substituted 1,4-dihydropyridines, in the presence of water. The catalyst was reusable for up to six cycles and the yields were in the range of 85-93 % in 2 - 3 h (**Scheme 24**).

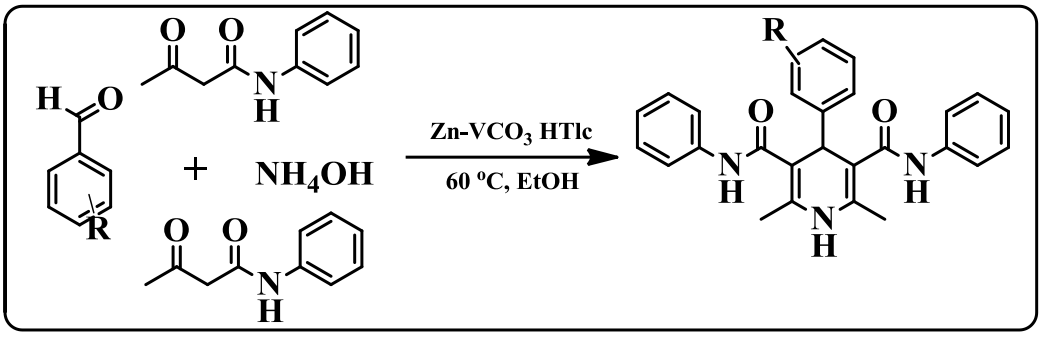

Scheme 24: Synthesis of substituted 1,4-dihydropyridines.

1.9 Bismuth

Bismuth has an electronic configuration [Xe] $4f^{14}5d^{10}6s^26p^3$. Bismuth can exist in +III to +V states. Because of the poor shielding effect of 4f-electrons bismuth can act as Lewis acidic material. The Lewis acidic nature of bismuth can be mimicked by combining bismuth with other electronegative groups such as triflates and chlorides. The low toxic nature of the bismuth is another attractive future. [75]

Brahmachari and Das used $Bi(NO_3)_3 \cdot 5H_2O$ and utilized for the synthesis of functionalized piperidine derivatives at room temperature.[76] The reaction between substituted benzaldehydes with ethyl acetoacetate, aniline give substituted piperidine derivatives, in the presence of water. The catalyst shows excellent activity and the yields were in the range of 71-80 % in 2 - 3 h (**Scheme 25**).

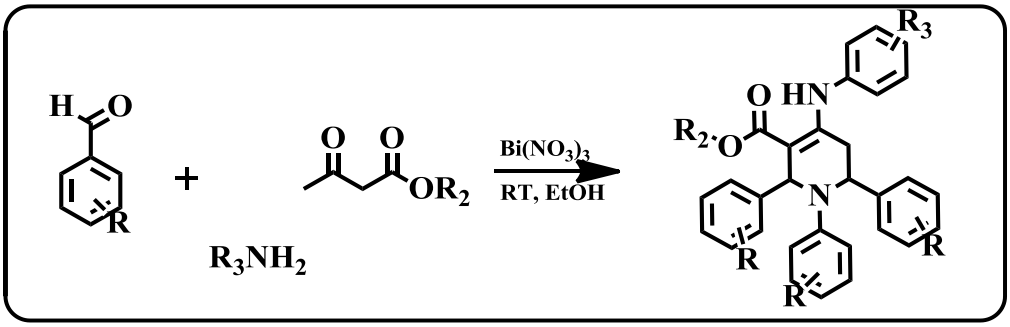

Scheme 25: Synthesis of substituted pyridine derivatives.

Derivatives of 1,8-dioxodecahydroacridine`s have been reported by Brahmachari *et al.*, using $Bi(NO_3)_3 \cdot 5H_2O$ catalyst in presence of dry ethanol at RT.[77] The tandem MCR involved the reaction between aromatic aldehydes, cyclohexane-1,3-dione and amine compound (**Scheme 26**). This protocol offered high yields of up to 96 %. The reported protocol offers a synthesis of various aromatic and hetero-aromatic derivatives.

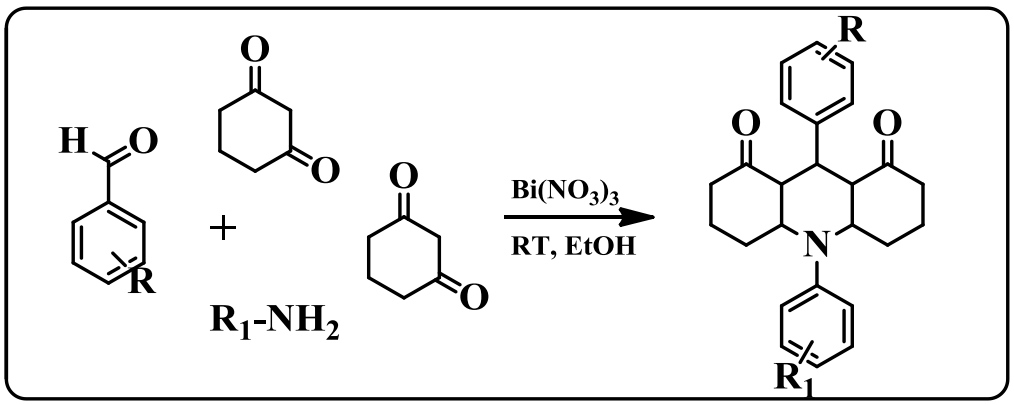

Scheme 26: Synthesis of substituted pyridine derivatives.

1.10 Silver

Silver has an electronic configuration $4d^{10}5s^1$. The mode of preparation and pre-treatment conditions affect the catalytic property of Ag catalysts. The application of Ag as a catalyst are in organic transformations like oxidations and alkylation reactions.[78]

Maddila *et al*., recently reported silver oxide on silica (Ag/SiO_2) to synthesize isoxazole derivatives in a MCR pathway, this protocol offers a wide range of substituted isoxazoles using

aqueous solvent (**Scheme 27**).[79] The starting materials for the reaction are substituted aromatic aldehyde, ethylacetoacetate and hydrazine hydrate. This protocol offers yields up to 93% in 1 hour.

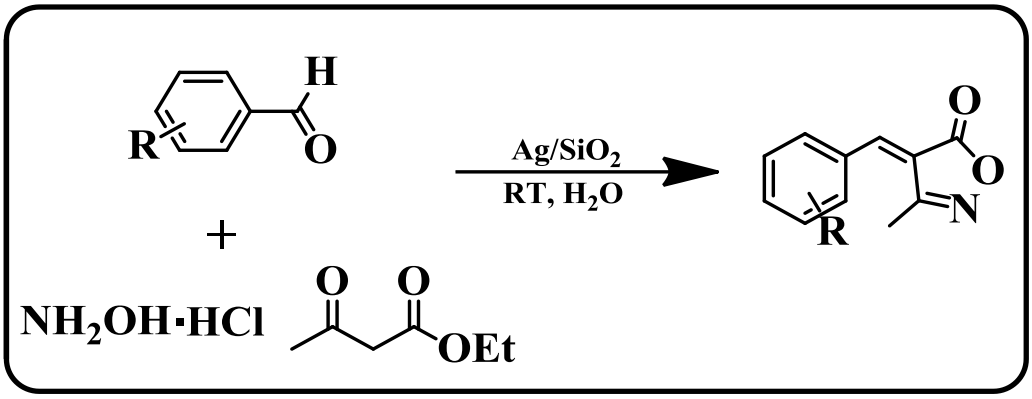

Scheme 27: Synthesis of substituted isoxazole derivatives.

Silver oxide on zirconia (AgO-ZrO_2) was prepared by Bhaskaruni *et al*.,[80] for the synthesis of indenopyrimidine derivatives in high yields of 90 to 96 % (**Scheme 28**). This protocol involved the use of ethanol as the solvent and the three-component condensation between a mixture of aromatic aldehyde, indane-1,3-dione and guanidinium hydrochloride in a short time of 30 minutes.

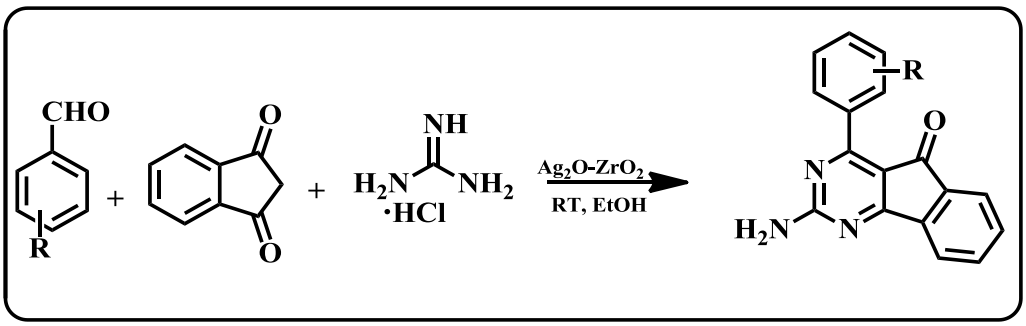

Scheme 28: Synthesis of substituted Indenopyrimidine derivatives.

1.11 Nickel

Nickel has an electronic configuration [Ar] $3d^8$ $4s^2$ or [Ar] $3d^9$ $4s^1$. Low valent Ni can act as a catalyst in many organic transformations like hydrogenation, hydrocyanation, cross-coupling reactions. [81]

Zhang *et al*.,[82] reported the synthesis of 1,2,3-triazole derivatives by using $NiFe_2O_4$ loaded glutamate-functionalized Cu. The thee-component reaction involved terminal alkynes,

sodium azide and substituted benzyl chlorides in water at room temperature. 85 - 96% yields were observed in 1.5 - 6 h (**Scheme 29**). The catalyst proved its efficiency for up to ten cycles. The higher catalytic activity of the material is due to the copper nanoparticles being strengthened on the glutamate coated $NiFe_2O_4$.

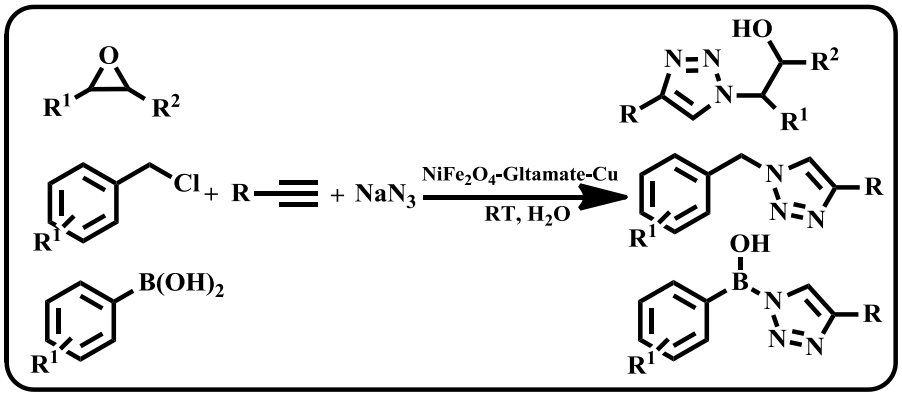

Scheme 29: Synthesis of 1,2,3-triazoles.

Demirci *et al.,* reported PdRuNi@GO nanoparticles to prepare substituted dihydropyridine derivatives at 70 °C in DCM (**Scheme 30**).[83] The four-component synthesis involved a reaction between various substituted benzaldehydes with dimedone, ammonium acetate and ethyl acetoacetate achieved yields up to 96 % in 45 min. The prepared catalyst was found to be reusable for up to five cycles.

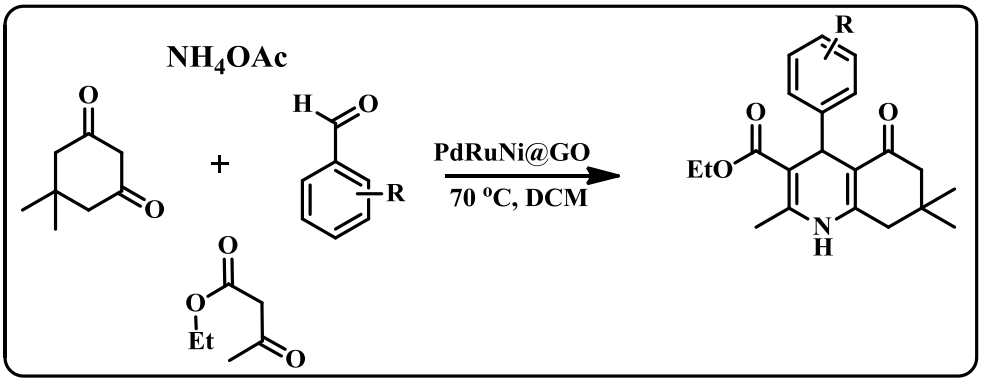

Scheme 30: Synthesis of substituted 1,4-dihydropyridine derivatives.

1.12 Iron

Iron is the second most abundant metal available on earth with an electronic configuration [Ar] $3d^6 4s^2$. Elemental iron is hard to find because it reacts with oxygen and forms oxides. The availability of four electrons in the d-orbital makes iron to accept the available electrons fast which gives the Lewis acidic nature. The Lewis acidic nature of Fe catalyzes many organic transformations.[84]

A new Fe_3O_4/SiO_2 catalyst was reported by Maleki *et al*,.[85] The catalyst contains evenly distributed iron oxide nanoparticles on silica which act as a promoter of the Lewis acidic nature of the catalytic material, which is stable for up to six catalytic cycles. (**Scheme 31**). The reaction involved the new C-C bonds forming between the aromatic aldehyde, benzyl and ammonium acetate. High yields of up to 95 % were obtained.

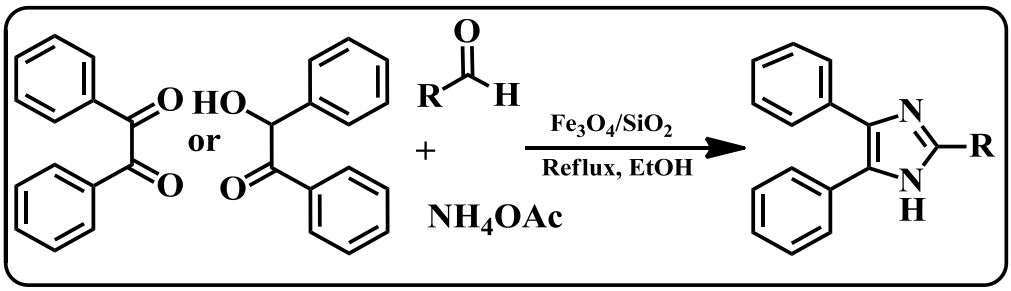

Scheme 31: Synthesis of functionalized imidazoles.

Saha *et al*.,[86] reported the synthesis of chromeno-[4,3-b]pyrrol-4(1H)-one derivatives by using copper ferrite ($CuFe_2O_4$) as a heterogeneous catalyst (**Scheme 32**). This protocol involved the reaction between an amine, 4-aminocoumarin and glyoxal monohydrate in H_2O at 70 °C. This reaction, together with its short reaction times yielded 70 to 92 % of the desired product. The presence of two cation sites namely Fe^{+3} and Cu^{+2} and their synergetic effects makes the material more Lewis acidic, which is one of the main reasons why it was chosen as the catalyst. The catalyst is reusable for up to six cycles.

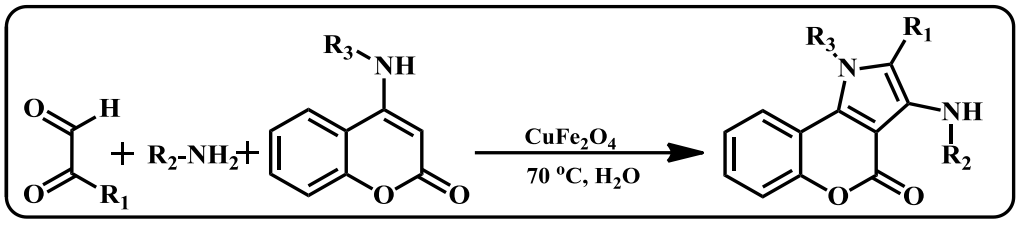

Scheme 32: Synthesis of chromeno[4,3-b]pyrrol-4(1H)-one derivatives.

In this thesis a detailed study of Ru, V, Bi, Ag, Fe, Ni loaded on ZrO_2 with different wt% were investigated as catalysts for green organic transformations.

1.13 MMO-catalysed N-heterocyclic syntheses

1.13.1 Pyrazoles

Pyrazole derivatives have found interest as pharmacologically active scaffolds with the molecular formula $C_3H_4N_2$, having two adjacent nitrogen atoms in the five-membered rings. Of

the two nitrogen atoms, one is acidic in nature and the other is neutral in nature. There are three tautomeric forms that exist in the pyrazoles **(Scheme 33)**.

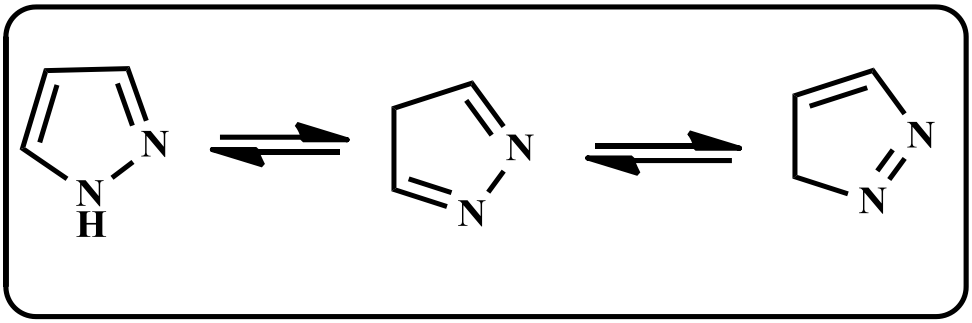

Scheme 33: Tautomeric forms of pyrazoles.

The Pyrazole ring is one of the most promising core moieties in *N*-heterocyclic chemistry, which posses a wide range of biological activities. The first pyrazole, from a natural product was 1-pyrazolyl-alanine, which was isolated from watermelon seeds in 1959.[87] These pyrazoles have been used in a number of different pharmaceutical agents like celecoxib, which is a potent anti-inflammatory drug,[88] rimonabant, the anti-obesity drug,[89] difenamizole, an analgesic drug, [90] betazole, which is an H2-receptor, [91] and phenazone which are analgesic and antipyretic agents. [92] The pyrazole moiety has found many uses in agrochemicals and as a ligand in metal catalysis.

Derivatives of 1H-3-pyrazolone have been reported by Akondi *et al*.,[93] using Ce-SiO_2 catalyst where water was used as the solvent. The classical one-pot four-component reaction involved the reaction between aromatic aldehydes, phenylhydrazine, 2-naphthol and ethyl acetoacetate as the active methylene substrate at 100 ºC (**Scheme 34**). This protocol offered high yields of 83 - 93 % in 35 - 60 min. The prepared catalyst had an efficiency for up to five cycles.

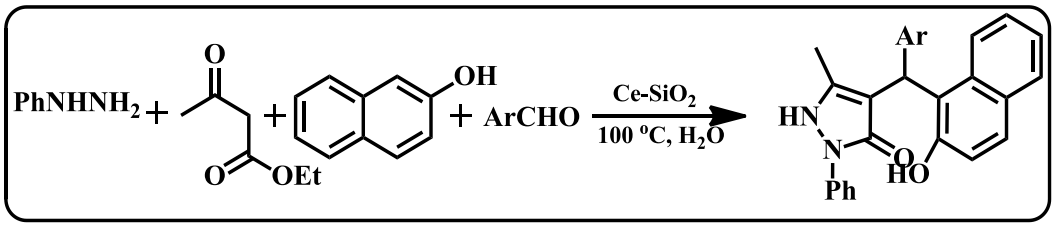

Scheme 34: General synthesis of 1H-3-pyrazolones.

CuO/ZrO_2 was used to synthesize pyrazole-4-carbonitrile derivatives [94]. This one-pot reaction involved an imine formation reaction between an aromatic aldehyde, phenyl hydrazine followed by a Michael-type reaction with malononitrile. The protocol offered yields of up to 78 - 90 % in 2 h. The catalyst showed efficiency for up to six cycles (**Scheme 35**).

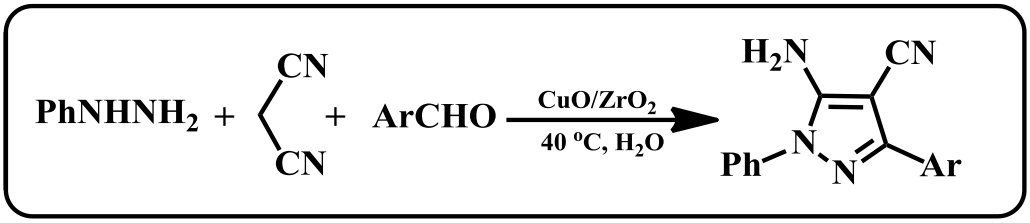

Scheme 35: Synthesis of pyrazole-4-carbonitrile derivatives.

Green synthetic procedures were used to synthesize 1,4-dihydropyrano[2,3-c]pyrazoles in a study conducted by Heravi *et al*.,[95]. This was done using MCR strategy with 84 – 95 % yields in 1 h. The protocol involved the reaction between substituted benzaldehydes and 3-methyl-1-phenyl-1*H*-pyrazole-5(4*H*)-one, and malononitrile, which was the active methylene group. The reaction took place in the presence of $H_{14}[NaP_5W_{30}O_{110}]$ and the catalyst proved its activity for up to five cycles (**Scheme 36**). The reaction was facilitated due to the strong Bronsted acidic nature of this material.

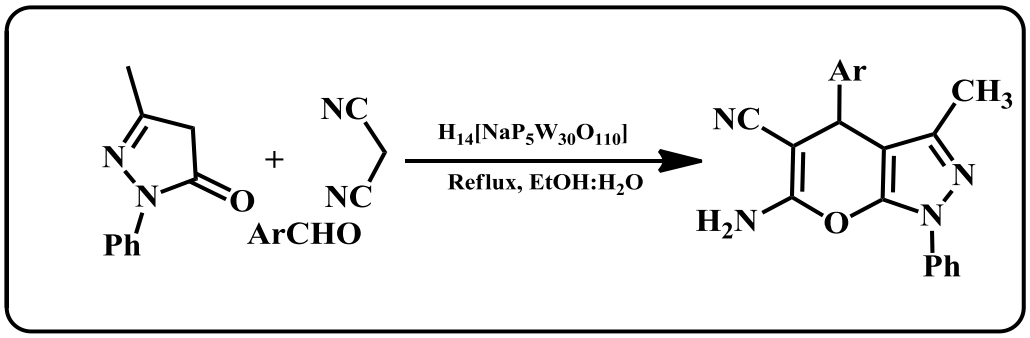

Scheme 36: One-pot three-component synthesis of 1,4-dihydropyrano[2,3-c]pyrazoles.

$La_{0.7}Sr_{0.3}MnO_3$ (LSMO) was used as a catalyst for the synthesis of 4*H*-pyrano[2,3-c] pyrazoles under ultrasound irradiation at room temperature, reported by Azarifar *et al*.[96] The LSMO catalyst was prepared by a hydrothermal process. The three-component reaction involved coupling between substituted benzaldehydes and malononitrile to give the Knoevenagel intermediate, which further reacted with 3-methyl-1-phenyl-2-pyrazolin-5-ones in a Michael addition fashion (**Scheme 37**). In this present conversion, LSMO served as an excellent catalyst with high yields of about 97 % in 9 to 150 min.

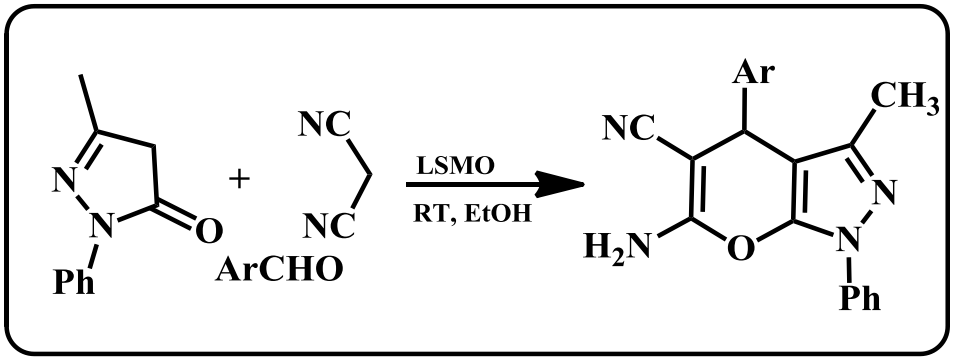

Scheme 37: Synthesis of 4H-pyrano[2,3-c]pyrazoles.

Maleki *et al*.,[97] reported the preparation of $NiFe_2O_4@SiO_2–H_3PW_{12}O_{40}$ and studied its catalytic efficiency towards the synthesis of substituted pyrazole derivatives, which have been found to be reusable for up to six catalytic cycles. Initially, the catalyst was prepared by magnetic Si-$NiFe_2O_4$ nanoparticles, and a one-pot reaction for the synthesis of substituted pyrazoles was studied by the Knoevenagel condensation between substituted aromatic aldehydes, malononitrile, and the Michael addition between 1,3-dicarbonyl compounds in 60 min with a 95 % yield (**Scheme 38**). The main advantage of this protocol was that the catalyst could be separated from the reaction mixture by a magnet.

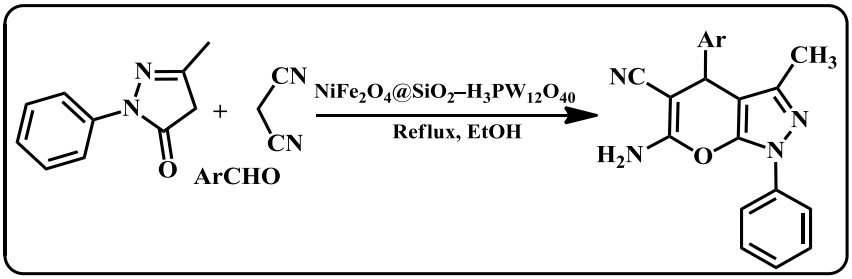

Scheme 38: One-pot synthesis of pyrano-[2,3-c]pyrazoles.

Dihydropyrano[2,3-c]pyrazole derivatives were synthesized by Pradhan *et al*.,[98] *via* a green procedure, using nanomagnetic crystalline $CuFe_2O_4$ which served as a Lewis acidic catalyst with 85 - 97 % yields in 2 - 3 h, within an aqueous system. This one-pot reaction involved the coupling of malononitrile, ethyl acetoacetate, dialkyl acetylenedicarboxylates, and different hydrazine derivatives (**Scheme 39**). The catalyst was removed by an external magnetic field and its activity was sustained for up to six cycles.

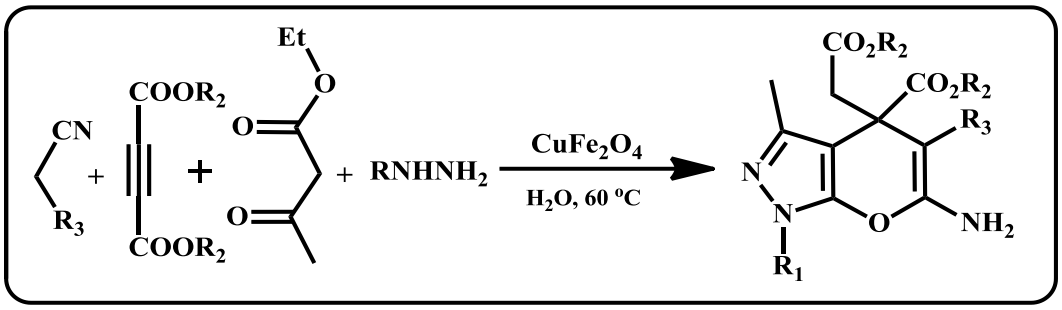

Scheme 39: Synthesis of dihydropyrano-[2,3-c]pyrazole derivatives.

Fused pyrazoles were reported by Suman *et al*.,[99] In this protocol, the authors prepared $CuFe_2O_4$@SiO_2-SO_3H (sulfonic acid functionalized silica-coated $CuFe_2O_4$ magnetic) magnetic separable material (**Scheme 40**). The catalyst proved its efficacy towards the condensation-addition method with excellent yields of 90 - 97 % in 10 min with ethanol as solvent. The catalyst was reusable for up to six cycles.

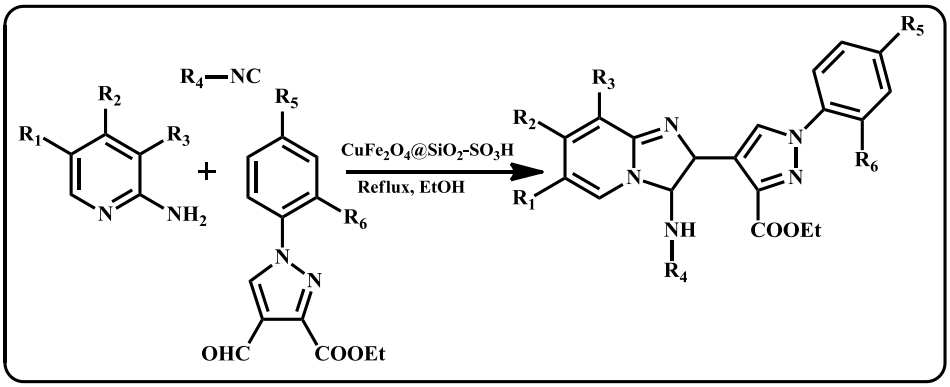

Scheme 40: Synthesis of 2-pyrazole-3-amino-imidazo-[1,2-a]pyridines.

Rakhtshah *et al*.,[100] prepared a molybdenum based material supported on iron oxide nanoparticles and these were further functionalized to afford Fe_3O_4@Si@MoO_2. The catalytic activity of the prepared material was studied by synthesizing different substituted pyrazoles in a MCR between malononitrile, substituted aromatic aldehyde, and phenylhydrazine (**Scheme 41**). Solvent-free and room temperature conditions were the main advantages of this method. This method afforded yields of 85 - 95 % in 10 – 25 min and the catalyst was reusable up to eight times.

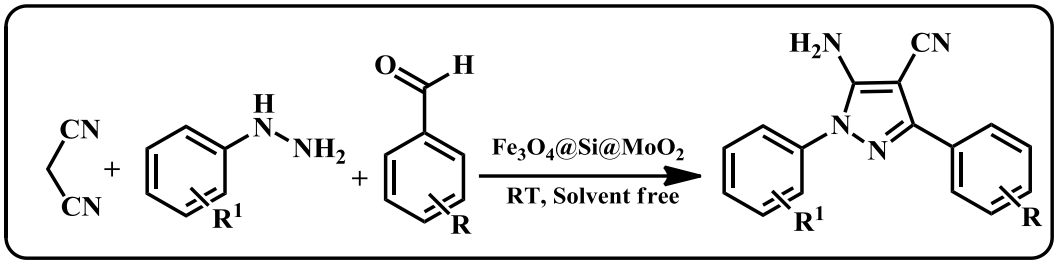

Scheme 41: The synthesis of pyrazole derivatives.

Ghomi *et al*.,[101] synthesized functionalized pyrazole derivatives using $ZnAl_2O_4$ as a base catalyst for the condensation reaction between substituted aromatic aldehydes, hydrazine hydrate and ethyl acetoacetate (**Scheme 42**). The reaction was completed in 14 - 28 min, hence, shorter reaction times are the main advantage of this protocol with yields of 80 - 92 %.

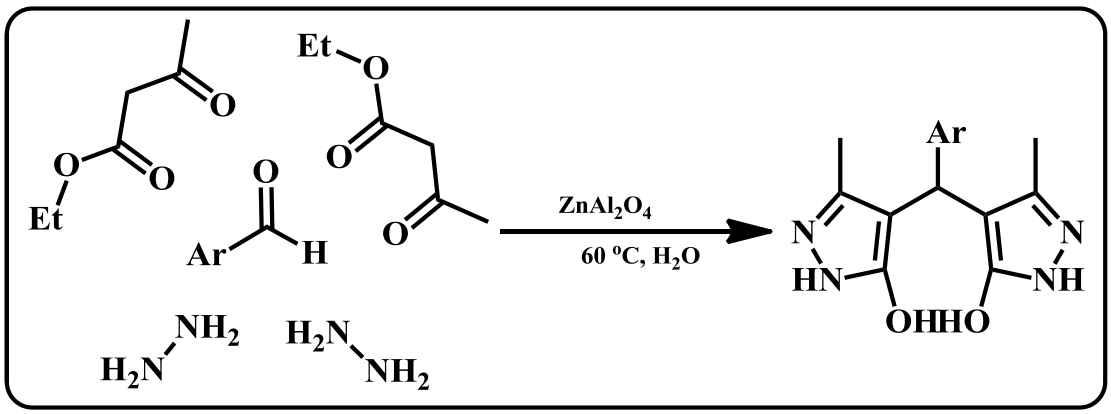

Scheme 42: Synthesis of 4,4′-(arylmethylene)-bis(3-methyl-1H-pyrazol-5-ol).

1.13.2 Pyridines

Pyridines are six-membered rings containing one nitrogen and having the molecular formula C_5H_5N. Pyridine exists in the following resonance forms.[102]

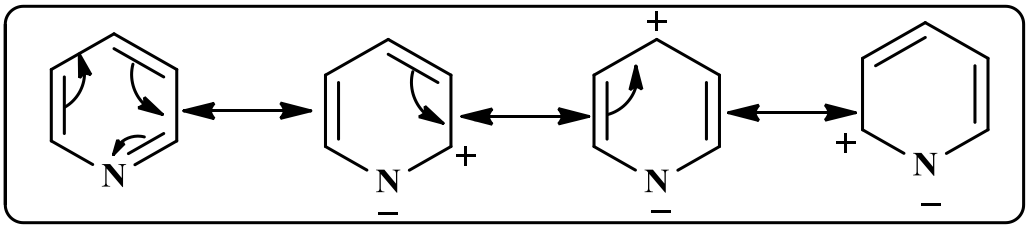

Scheme 43: Resonance forms of pyridine.

Thomas Anderson first discovered pyridine in 1849.[103] Pyridine derivatives are widely known for their broad range of biological activities like anti-inflammatory,[104] antiviral,[105] antimicrobial,[106] anticancer,[107] antidepressant,[108] antifungal,[109] and antioxidant[110] activities.

Naik and shivashankar.,[111] reported a new strategy for the synthesis of 1,4 dihydropyridine derivatives by using ethyl acetoacetate as the active methylene compound, substituted aromatic aldehydes and NH_4OAc as the nitrogen source, in the presence of nano Zn-Fe_2O_4 metal oxide catalyst in water (**Scheme 44**). This protocol offers high yields of 87 – 95% in 0.5 h.

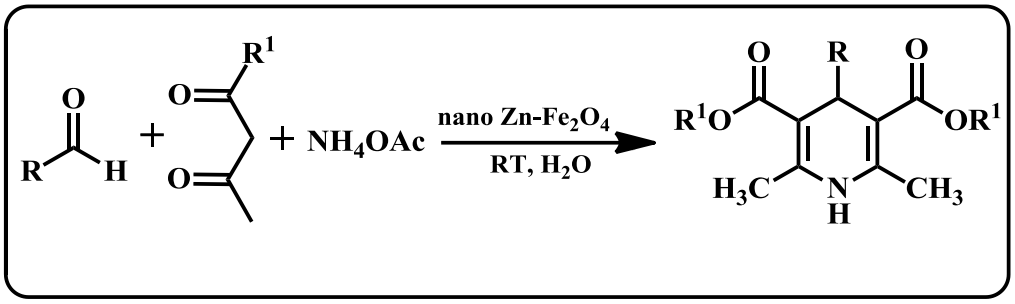

Scheme 44: Synthesis of 1,4-dihydropyridine.

Seyed *et al*.,[112] reported the use of Fe_3O_4/KCC-1/BPAT as a reusable catalyst for the synthesis of symmetrical 1,4 dihydropyridine derivatives *via* the Hantzsch reaction. This protocol involved a reaction between substituted anilines, dimethyl acetylenedicarboxylate and methyl (arylmethylide) pyruvates. Excellent yields of 79 – 88 % were obtained in 4h. Another advantage of this protocol is the use of water as a solvent (**Scheme 45**), and the catalyst was reusable for up to ten runs.

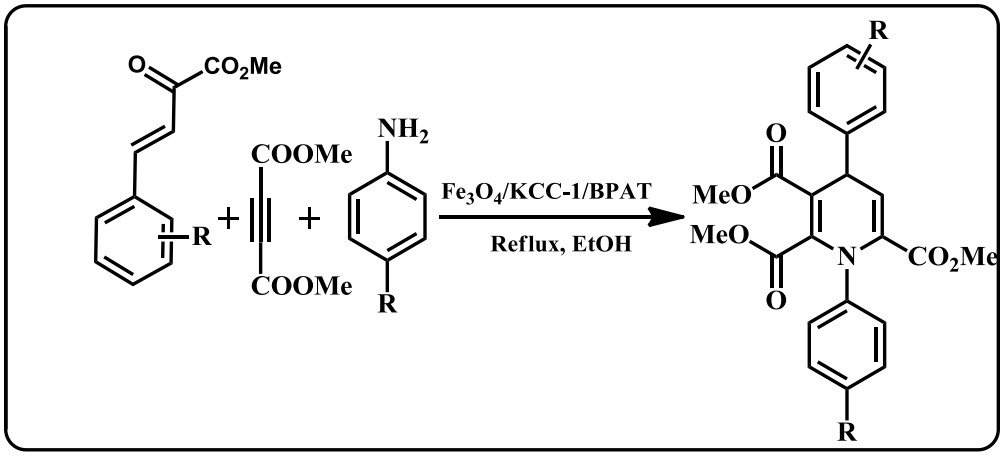

Scheme 45: 1,4 dihydropyridine derivatives synthesis.

Zhang *et al*.,[113] prepared the Fe_3O_4/GO-Mo composite to develop spirooxindole dihydropyridine derivatives. This protocol involved the reaction between malononitrile, isatins and anilinolactones under microwave irradiation. Choline chloride (ChCl) and urea was used as a cost effective deep eutectic solvent. This protocol offered high yields of 85 – 96 % in a short time of 50 - 80 min (**Scheme 46**).

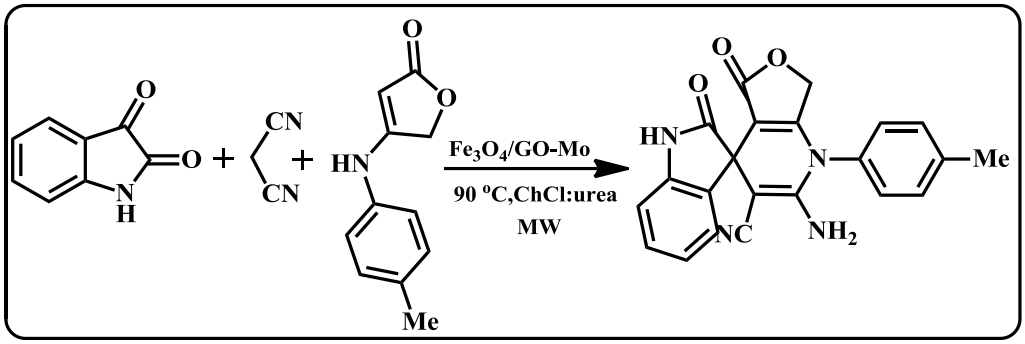

Scheme 46: Synthesis of spirooxindole dihydropyridine derivatives.

Novel indeno[1,2-*b*]pyridine derivatives were synthesized by using a Cu/ZnO catalyst in one-pot strategy at RT, in the presence of H_2O:EtOH as the solvent.[114] This protocol involved the reaction between 1,3- indandione, NH_4OAc, acetophenone and substituted aldehydes (**Scheme 47**) and it offered high yields of 85 - 95 % in 1.5 - 3 h with the catalyst being able to be reused for up to four cycles.

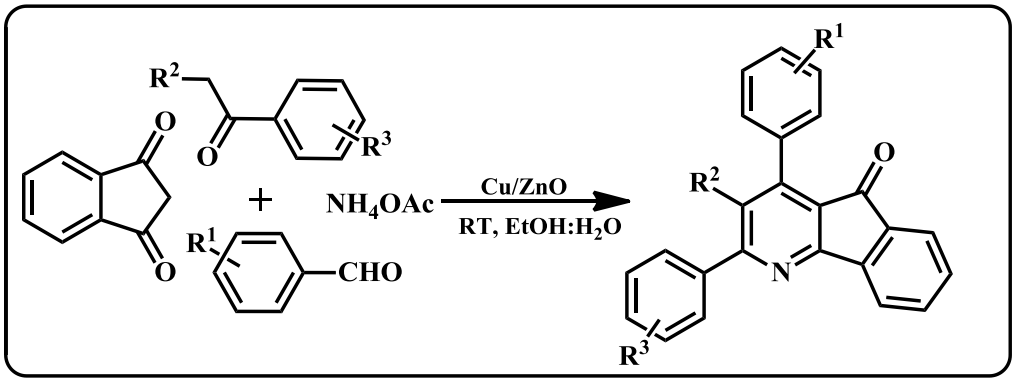

Scheme 47: Synthesis of indenopyridines.

Bamoniri and Fouladgar [115] prepared Fe_3O_4@SiO_2–$SnCl_4$ mixed metal oxide and its catalytic property was investigated *via* the synthesis of different 1,4-dihydropyridine derivatives. The one-pot reaction involved aromatic aldehydes, 1,3-dicarbonyl compound, and NH_4OAc under ultrasonic irradiation by using Fe_3O_4@SiO_2–$SnCl_4$ as a catalyst. Initially, Fe_3O_4 nanoparticles were prepared by the co-precipitation method. A solution of tetraethylorthosilicate and Fe_3O_4 was stirred to achieve Fe_3O_4@SiO_2, it was then ultra-sonicated with $SnCl_4$ to afford Fe_3O_4@SiO_2–$SnCl_4$. The highlight of this protocol is the shorter reaction times of 3 - 25 min, with excellent yields of up to 98 % (**Scheme 48**).

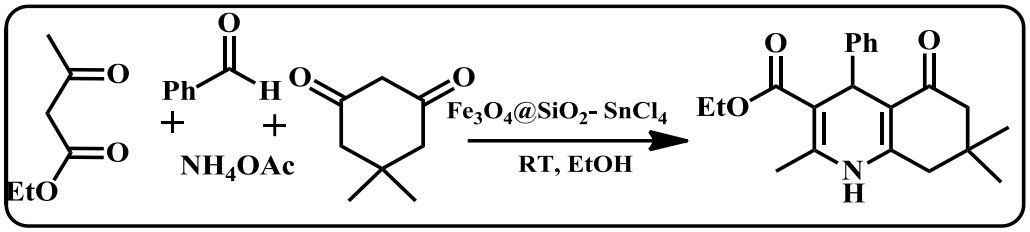

Scheme 48: Synthesis of 1,4-dihydropyridine derivatives.

Substituted 1,4-dihydropyridine derivatives were synthesized *via* a green procedure by using Sm_2O_3/ZrO_2 as a reusable catalyst[116]. This protocol involved the condensation of substituted benzaldehydes, malononitrile, dimethylacetylenedicarboxylate and 4-fluoroaniline in the presence of ethanol, at room temperature (**Scheme 49**). This method offered high yields of up to 96 % in a short time of 20 min, and the catalyst was recyclable for up to seven cycles.

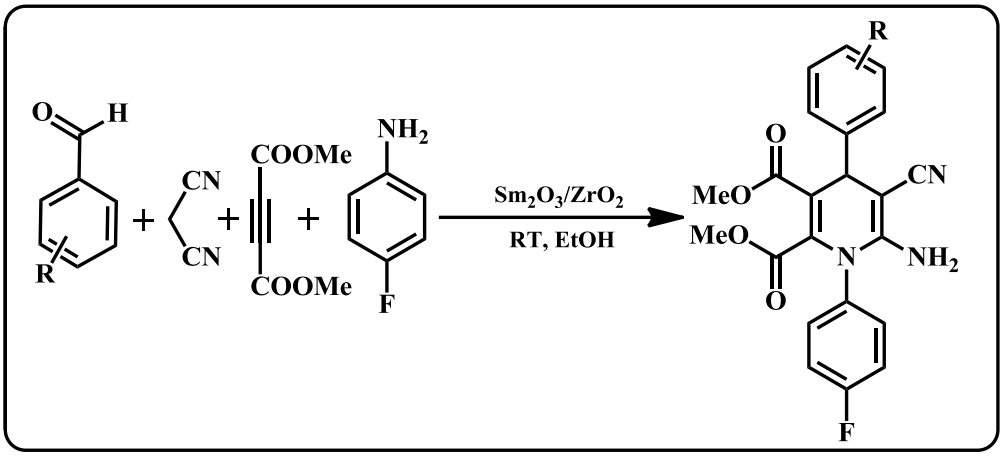

Scheme 49: Synthesis of functionalized 1,4-dihydropyridine derivatives.

Pagadala *et al*., [63] synthesized pyridine derivatives by using AAPTMS composites on m-zirconia as the reusable catalyst. The prepared catalyst consisted of diamine functionalized [N-(2 amino ethyl)-3-amino propyl trimethoxy silane (AAPTMS) on mesoporous zirconia, where the amine functionalization facilitates the condensation of reactions in an efficient way. The one-pot reaction of condensation occurred between aromatic aldehydes, malononitrile, thiazolidine-2,4-dione and NH_4OAc to obtain functionalized pyridine derivatives, utilizing water as the solvent at 70 °C (**Scheme 50**). High yields of 84 to 93 % in 1.5 - 3 h were obtained, and the prepared catalyst was reusable for up to six cycles.

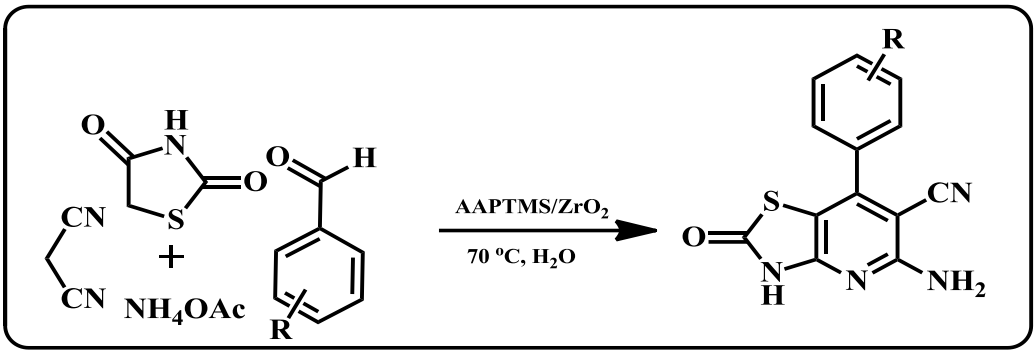

Scheme 50: Four-component synthesis of heterocycle-fused pyridines.

Cu(II)/L-His@Fe_3O_4 catalyst was prepared by Norouzi *et al.*,[117] and it was utilized in the one-pot synthesis of substituted 2-amino-6-(arylthio)pyridine-3,5-dicarbonitriles (**Scheme 51**). The condensation reaction involved aromatic aldehydes, ethyl acetoacetate, dimedone and NH_4OAc being stirred in the presence of ethanol under reflux conditions. This protocol offered high yields of up to 98 % in 15 - 100 min. The reported catalyst is reusable for up to six cycles.

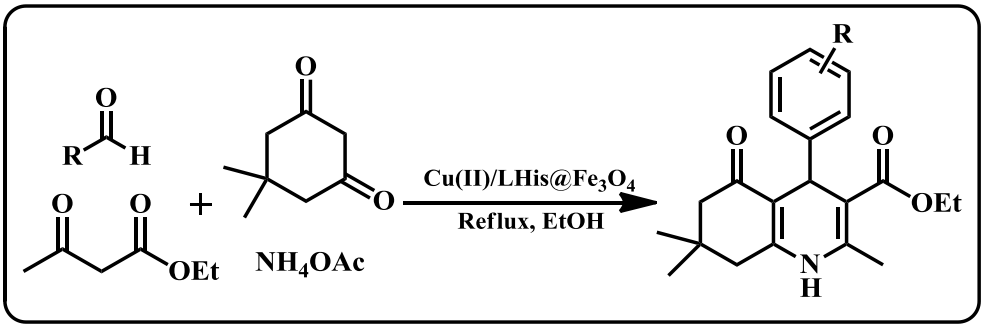

Scheme 51: Synthesis of polyhydroquinoline derivatives.

Kantevari and co-workers[118] conducted a study where they prepared new potassium dodecatangestocobaltate trihydrate ($K_5CoW_{12}O_{40}{\cdot}3H_2O$) Keggin-type heteropoly acid to synthesize substituted 2,3,6-trisubstituted pyridine derivatives. These are the type of materials which possess cobalt metal heteropolyanions synchronized by octahedral oxygen as the simple structural unit. The protocol offered an efficient strategy for MCR between aromatic aldehydes, β-dicarbonyl compounds and NH_4OAc under solvent-free conditions (**Scheme 52**). High yields of 85 – 95 % were offered within 30 - 60 min time and the catalyst was reusable for up to five cycles.

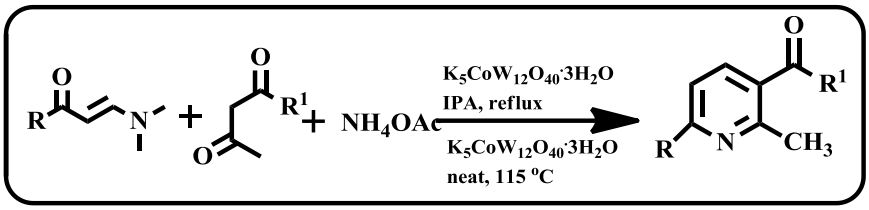

Scheme 52: Synthesis of 2,3,6-trisubstituted pyridines.

Zolfigol *et al.,* reported the preparation of $\{Fe_3O_4@SiO_2@(CH_2)_3Im\}C(CN)_3$ material and its catalytic property was examined by the one-pot synthesis of 2-amino-3-cyanopyridine derivatives[119]. This protocol involved a reaction between substituted aromatic aldehyde, malononitrile, acetophenone and NH_4OAc under solvent-free conditions at 100 ºC within short reaction times of 30 minutes, (**Scheme 53**) with yields of 80 to 91 %.

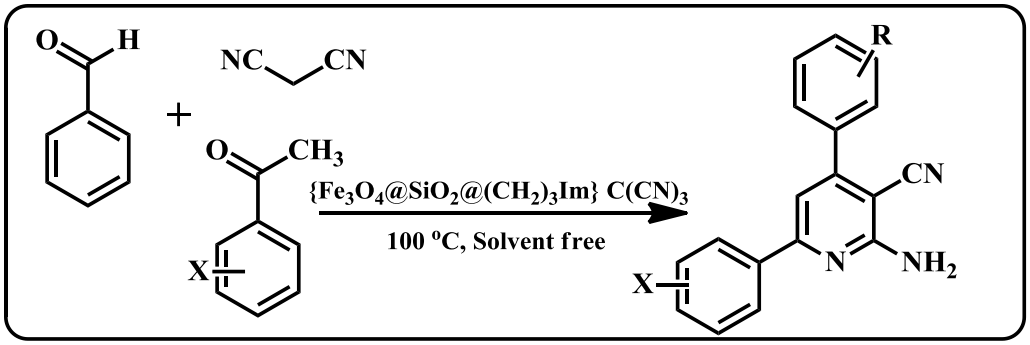

Scheme 53: One-pot synthesis of 2-amino-3-cyanopyridines.

1.13.3 Pyrimidines

Pyrimidines possess the general formula of $C_4H_4N_2$ and they contain a six-membered ring. They typically have two nitrogens at the 1 and 3 positions and can exist in the following resonance hybrids (scheme 54).[120]

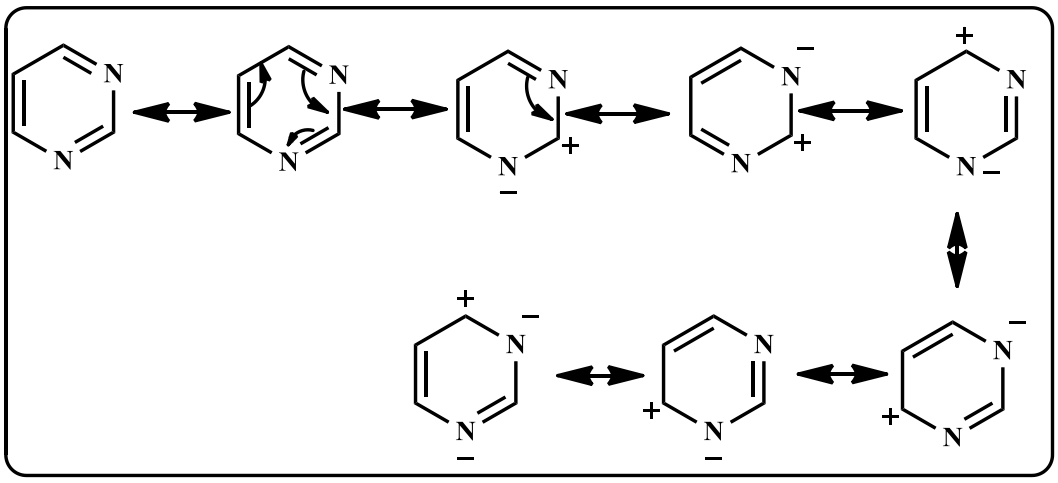

Scheme 54: Resonance structures of pyrimidine.

Pyrimidine derivatives possess a broad range of biological activity. Stavudine is a commercially available drug, which is used as an anti-HIV drug. While Fervennuline is an antibiotic, minoxidil is an anti-hypertensive,[121] and anti-cancer [122] drug. Pyrimidine and its analogues are known to possess insecticidal and pesticide activities [123]. Due to their wide applications, many protocols are reported for the synthesis of pyrimidines under MCR strategy.

Naeimi *et al*.,[124] reported the synthesis of pyrido-dipyrimidines by a one-pot green approach using microwave irradiation (**Scheme 55**). The reaction was performed using substituted benzaldehydes, 2-thiobarbituric acid, and NH_4OAc as reactants by using $CuFe_2O_4$ as a catalyst. The co-precipitation method was adopted to synthesize $CuFe_2O_4$. This protocol offers good yields of 90 - 98 % in the short time 1 - 2 min. The prepared material was reused for up to four cycles.

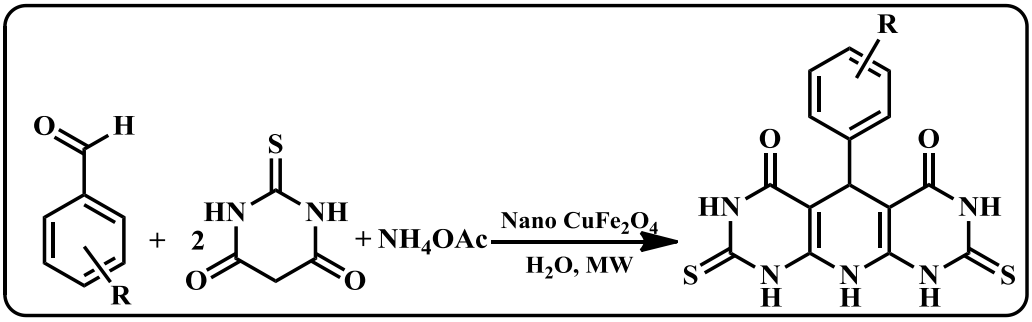

Scheme 55: Synthesis of novel pyrido[2,3-d]pyrimidine derivatives.

Shaterian and Aghakhanizadeh [125] prepared novel mixed oxide catalyst for the one-pot condensation between malononitrile, amines, and salicylaldehyde at room temperature. The reaction was performed under solvent-free conditions at room temperature. The chromeno[2,3-d]pyrimidine derivatives were obtained with 87 – 93 % yields in a short duration of 8 - 14 min and the catalyst was reusable for up to five cycles (**Scheme 56**).

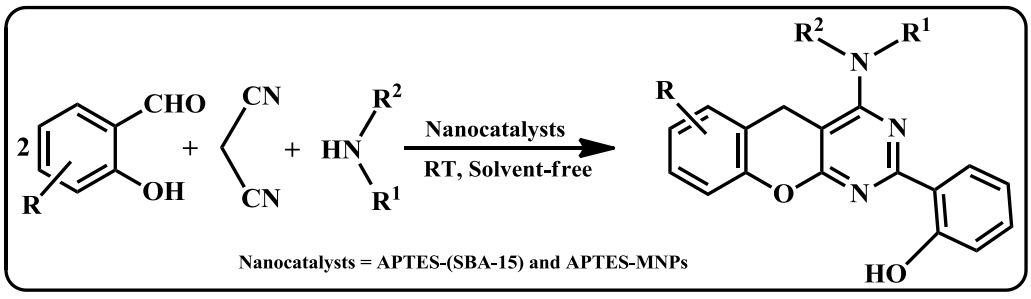

Scheme 56: Synthesis of chromeno-[2,3-d]pyrimidine derivatives.

Ghomi *et al*.,[126] reported the 3,4-dihydropyrimidine-2(1H)-one/thione synthesis by using a silica-tin(II) chloride catalyst. This protocol involved condensation between aryl

aldehydes, urea/thiourea, and ethyl acetoacetate (**Scheme 57**). The acidic sites and the synergetic effect on the surface of the catalyst makes for a fruitful reaction with shorter reaction times and high yields of 94 % in 40 min. The catalyst was proven to be efficient for up to four cycles.

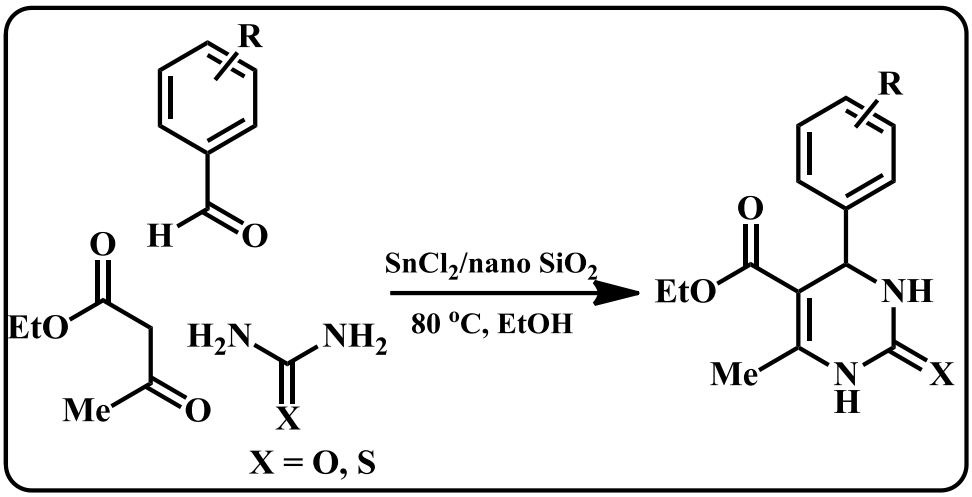

Scheme 57: Synthesis of 3,4-dihydropyrimidine-2(1H)-one/thione derivatives.

Valeria *et al*., [127] reported $H_3PMo_{12}O_{40}$ as catalyst for the synthesis of pyrimidine derivatives under solvent-free conditions. This one-pot reaction involves condensation and cyclization between substituted benzaldehydes, ethyltrifluoroacetoacetate and urea. This protocol typically offers good yields of 75 - 90 % in 15 h (**Scheme 58**).

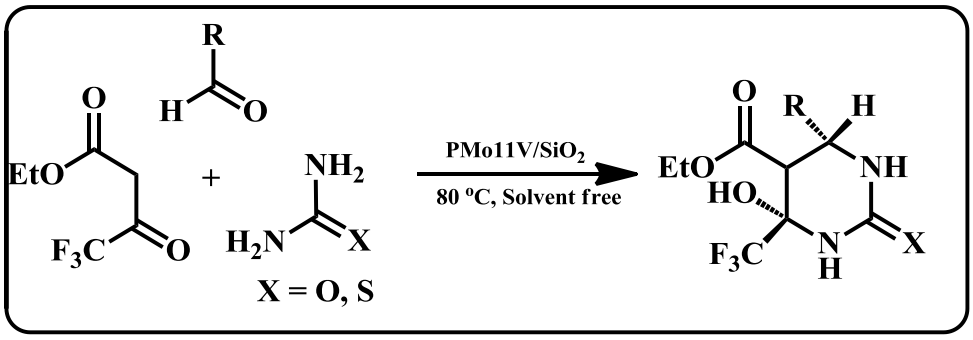

Scheme 58: Synthesis of fluorinated hexahydropyrimidine.

Sabour *et al*.,[128] prepared Al-HMS-20 as a catalyst for the synthesis of fused pyrimidine derivatives at room temperature. This reaction involved the reaction between benzaldehyde and malanonitrile to give the Knoevenagel product, which can be further cyclized with pyrimidine in a Michael addition fashion to yield pyrimidines (**Scheme 59**). The targeted molecules were synthesized with excellent yields of 87 – 95 % in 12 h and the catalyst was reusable for up to six cycles.

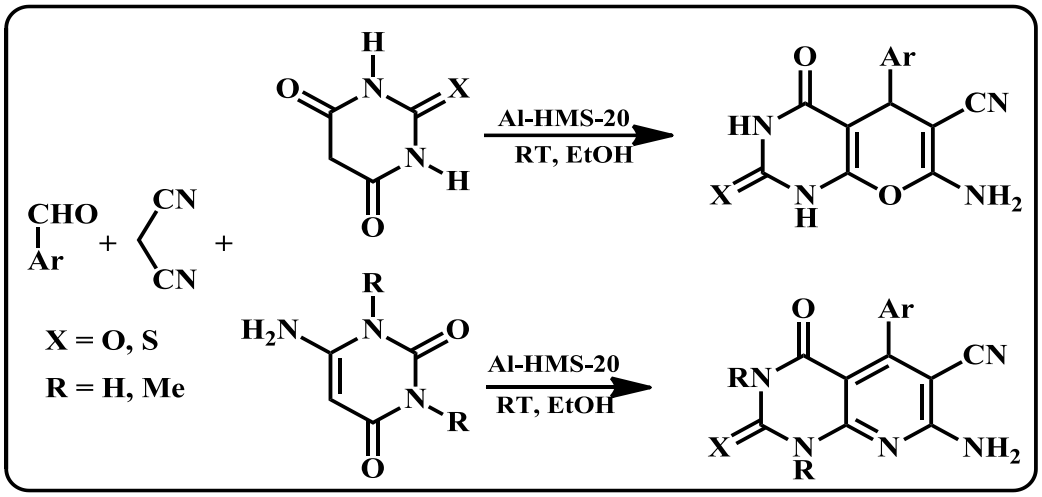

Scheme 59: Synthesis of pyrano-[2,3-d]pyrimidines.

Maleki and Agheni [129] proposed an environmentally benign Michael-type protocol, which utilizes ultrasound irradiation for the preparation of polycyclic imidazo(thiazolo)pyrimidine derivatives through the reaction between dimedone, 2-aminobenzothiazole and substituted benzaldehydes. This was done in the presence of Fe_3O_4@clay, with 93 – 98 % of yield within 15 min. The prepared Fe_3O_4@clay shows its activity for up to six cycles (**Scheme 60**).

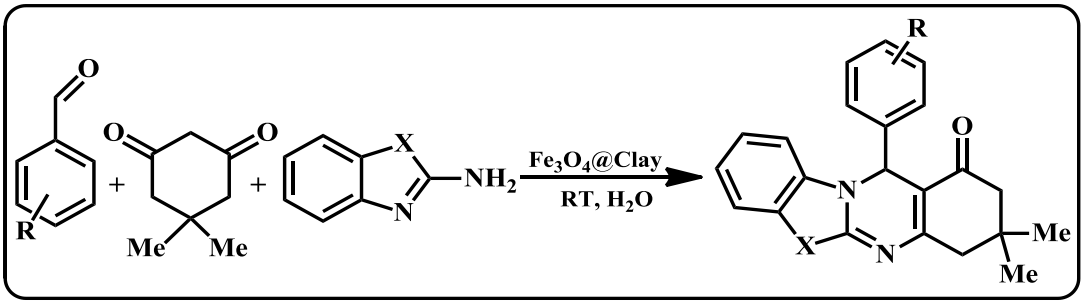

Scheme 60: Ultrasonic-assisted synthesis of imidazo-(thiazolo) pyrimidines.

Mohsenimehr *et al.*, [130] reported substituted pyrimidine derivatives by using γ-Fe_2O_3@HAp-SO_3H as a catalyst at room temperature, in the presence of DMF. This reaction involves condensation between aryl aldehydes, 5,5-dimethyl-1,3-cyclohexadione and butylthiopyrimidin-4(3H)-one (**Scheme 61**). The method offered high yields of 89 - 95 % in a short time 30 - 45 min.

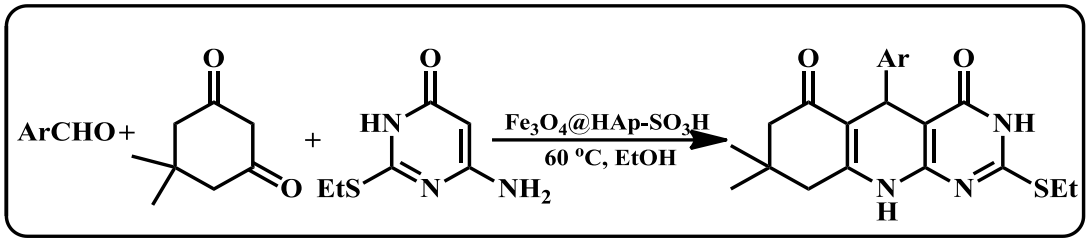

Scheme 61: Synthesis of pyrimido-[4,5−*b*]quinolines derivatives.

Dam *et al.*,[131] developed a solvent-free synthetic protocol for the synthesis of dihydropyrimidine derivatives by using Fe_3O_4@SiO_2-HSO_3 as a catalyst (**Scheme 62**). The surface of the ferrate nanoparticles is modified with SiO_2 for better stability of the material. It was then further reacted with hydrogen sulphite for the formation of Fe_3O_4@SiO_2-HSO_3. The presence of many active acidic sites on the surface is what facilitates the Knoevenagel-Michael addition type of reaction between aromatic aldehydes, β-dicarbonyl compounds and 2-aminobenzimidazole at 60 ºC. Yields of 83 - 96 % were obtained in 1.5 - 3 h.

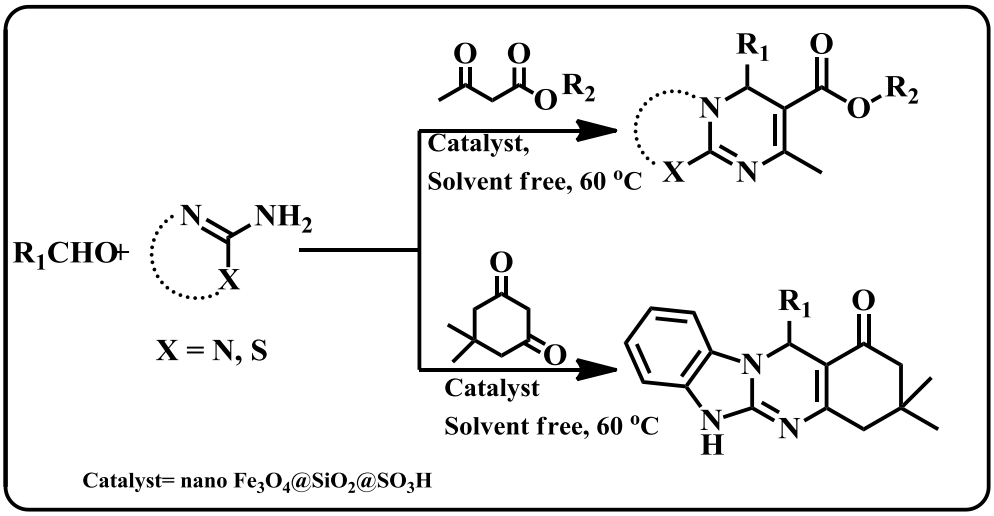

Scheme 62: Synthesis of fused pyrimidine derivatives.

Ramalingam *et al.*,[132] reported a green one-pot strategy by using ultrasound irradiation as an alternative energy source. This method offers the synthesis of 3,4-dihydropyrimidin-2-(1H)-one derivatives by using yttria-doped-zirconia in H_2O:CH_3CN solvent (**Scheme 63**). The Lewis acidic nature of yttria with the help of amphoteric zirconia accelerates the reaction for the formation of new C-C and C-N bonds in the current transformation. This step involved the reaction between aromatic aldehyde, urea/thio urea and 1,3 dicarbonyl compound to achieve the targeted molecules, in yields of 62 - 95 % in 5 - 16 hours.

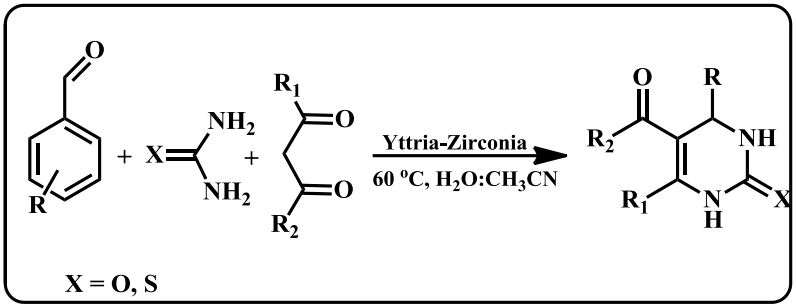

Scheme 63: Synthesis of dihydropyrimidones (DHPM).

1.14 Objectives of the study

This work described in the thesis aimed to study and designed zirconia-supported mixed metal oxide catalysts to synthesize various novel core *N*-heterocyclic moieties. During the study, an attempt was made to develop fast reaction protocols to synthesize various pyridine, pyrimidine and pyrazole derivatives with excellent yields using green solvents and mild conditions. These new protocols demonstrated efficacy and high selectivity under eco-friendly conditions. The following six series of reactions were studied which are detailed as follows:

i) Synthesis of functionalized 1,4-dihydropyridine derivatives.

ii) Synthesis of functionalized halopyridine derivatives.

iii) Synthesis of 2,4-dihydropyrano[2,3-c]pyrazole-3-carboxylate derivatives.

iv) Synthesis of indenopyrimidine derivatives.

v) Synthesis of 1,4-dihydropyridines derivatives.

vi) Synthesis of polysubstituted 1,4-dihydropyridine derivatives.

1.15. References

[1] R. A. Sheldon, *Chem. Soc. Rev.* **2012**, *41*, 1437–1451.

[2] G. Szőllősi, *Catal. Sci. Technol.* **2018**, *8*, 389–422.

[3] M. Li, F. Xu, H. Li, Y. Wang, *Catal. Sci. Tech.* **2016**, *6*, 3670–3693.

[4] S. Schauermann, H.-J. Freund, *Acc. Chem. Res.* **2015**, *48*, 2775–2782.

[5] J. Matthiesen, S. Wendt, J. Ø. Hansen, G. K. H. Madsen, E. Lira, P. Galliker, E. K. Vestergaard, R. Schaub, E. Lægsgaard, B. Hammer, et al., *ACS Nano* **2009**, *3*, 517–526.

[6] M. W. Roberts, *Catal. Lett.* **2000**, *67*, 1–4.

[7] F. Ahmad, L. Luo, X. Li, H. Huang, J. Zeng, *Chin. J. Catal.* **2018**, *39*, 1202–1209.

[8] M. A. A. Aziz, H. D. Setiabudi, L. P. Teh, N. H. R. Annuar, A. A. Jalil, *J. Taiwan Inst. Chem. Eng.* **2019**, *101*, 139–158.

[9] Y. Fang, Y. Guo, *Chinese J. Catal.* **2018**, *39*, 566–582.

[10] H. Dai, *Sci. Bull.* **2015**, *60*, 1708–1710.

[11] J. S. Dordick, *Enzyme Microb. Technol.* **1989**, *11*, 194–211.

[12] F. Zaera, A. J. Gellman, G. A. Somorjai, *Acc. Chem. Res.* **1986**, *19*, 24–31.

[13] S. T. Oyama, G. A. Somorjai, *J. Chem. Educ.* **1988**, *65*, 765.

[14] M. K. Lam, K. T. Lee, A. R. Mohamed, *Biotechnol. Adv.* **2010**, *28*, 500–518.

[15] B. Helms, J. M. J. Fréchet, *Adv. Synth. Catal.* **2006**, *348*, 1125–1148.

[16] J. Pritchard, G. A. Filonenko, R. van Putten, E. J. M. Hensen, E. A. Pidko, *Chem. Soc. Rev.* **2015**, *44*, 3808–3833.

[17] A. Jourdant, E. González-Zamora, J. Zhu, *J. Org. Chem.* **2002**, *67*, 3163–3164.

[18] Y. Matsui, M. Orchin, *J. Organomet. Chem.* **1983**, *246*, 57–60.

[19] Y. V Kissin, A. J. Brandolini, *J. Polym. Sci. Pt. A Polym. Chem.* **1999**, *37*, 4273–4280.

[20] R. De Clercq, M. Dusselier, B. F. Sels, *Green Chem.* **2017**, *19*, 5012–5040.

[21] I. Vural Gürsel, T. Noël, Q. Wang, V. Hessel, *Green Chem.* **2015**, *17*, 2012–2026.

[22] N. Mizuno, M. Misono, *Chem. Rev.* **1998**, *98*, 199–218.

[23] A. K. Datye, Q. Xu, K. C. Kharas, J. M. McCarty, *Catal. Today* **2006**, *111*, 59–67.

[24] K. Kaneda, T. Mizugaki, *Green Chem.* **2019**, *21*, 1361–1389.

[25] M. B. Gawande, R. K. Pandey, R. V Jayaram, *Catal. Sci. Technol.* **2012**, *2*, 1113–1125.

[26] J. G. de Vries, S. D. Jackson, *Catal. Sci. Technol.* **2012**, *2*, 2009.

[27] C. Perego, R. Millini, *Chem. Soc. Rev.* **2013**, *42*, 3956–3976.

[28] C. M. Marson, *Chem. Soc. Rev.* **2012**, *41*, 7712–7722.

[29] J. D. Sunderhaus, S. F. Martin, *Chem. Eur. J.* **2009**, *15*, 1300–1308.

[30] S. N. Maddila, S. Maddila, W. E. Van Zyl, S. B. Jonnalagadda, *ChemistryOpen* **2016**, *5*, 38–42.

[31] N. Pal, A. Bhaumik, *Dalton Trans.* **2012**, *41*, 9161–9169.

[32] A. Nagaraju, B. J. Ramulu, G. Shukla, A. Srivastava, G. K. Verma, K. Raghuvanshi, M. S. Singh, *Green Chem.* **2015**, *17*, 950–958.

[33] B. H. Rotstein, S. Zaretsky, V. Rai, A. K. Yudin, *Chem. Rev.* **2014**, *114*, 8323–8359.

[34] R. C. Cioc, E. Ruijter, R. V. A. Orru, *Green Chem.* **2014**, *16*, 2958–2975.

[35] B. Rajarathinam, G. Vasuki, *Org. Lett.* **2012**, *14*, 5204–5206.

[36] C. Kalinski, M. Umkehrer, L. Weber, J. Kolb, C. Burdack, G. Ross, *Mol. Divers.* **2010**, *14*, 513–522.

[37] M. Adib, E. Sheikhi, M. Azimzadeh, *Tetrahedron Lett.* **2015**, *56*, 1933–1936.

[38] H. Nagarajaiah, A. Mukhopadhyay, J. N. Moorthy, *Tetrahedron Lett.* **2016**, *57*, 5135–5149.

[39] V. V Kouznetsov, C. E. P. Galvis, *Tetrahedron* **2018**, *74*, 773–810.

[40] V. K. Sharma, S. K. Singh, *RSC Adv.* **2017**, *7*, 2682–2732.

[41] A. E. A. O. Sarhan, S. H. Abdel-Hafez, H. El-Sherief, T. Aboel-Fadl, *Synth. Commun.* **2006**, *36*, 987–996.

[42] K. Vazdar, I. Jerić, *Tetrahedron* **2018**, *74*, 7495–7506.

[43] N. A. Petasis, I. Akritopoulou, *Tetrahedron Lett.* **1993**, *34*, 583–586.

[44] K. Gewald, E. Schinke, H. Böttcher, *Chem. Ber.* **1966**, *99*, 94–100.

[45] O. H. Oldenziel, D. Van Leusen, A. M. Van Leusen, *J. Org. Chem.* **1977**, *42*, 3114–3118.

[46] S. Shaaban, B. F. Abdel-Wahab, *Mol. Divers.* **2016**, *20*, 233–254.

[47] E. Ware, *Chem. Rev.* **1950**, *46*, 403–470.

[48] S. D. Larsen, P. A. Grieco, *J. Am. Chem. Soc.* **1985**, *107*, 1768–1769.

[49] E. D. Matveeva, N. S. Zefirov, *Dokl. Chem.* **2008**, *420*, 137–140.

[50] E. Vitaku, D. T. Smith, J. T. Njardarson, *J. Med. Chem.* **2014**, *57*, 10257–10274.

[51] R. B. Bakr, A. A. Azouz, K. R. A. Abdellatif, *J. Enzyme Inhib. Med. Chem.* **2016**, *31*, 6–12.

[52] M. H. Ahmed, M. A. El-Hashash, M. I. Marzouk, A. M. El-Naggar, *J. Heterocycl. Chem.* **2019**, *56*, 114–123.

[53] A. M. Salaheldin, A. M. F. Oliveira-Campos, L. M. Rodrigues, *Synth. Commun.* **2009**, *39*, 1186–1195.

[54] M. Shokouhimehr, *Catalysts* **2015**, *5*, 534–560.

[55] S. N. Maddila, S. Maddila, K. K. Gangu, W. E. van Zyl, S. B. Jonnalagadda, *J. Fluor. Chem.* **2017**, *195*, 79–84.

[56] S. Semlitsch, S. Torron, M. Johansson, M. Martinelle, *Green Chem.* **2016**, *18*, 1923–1929.

[57] S. Maddila, V. D. B. C. Dasireddy, S. B. Jonnalagadda, *Appl. Catal. B* **2013**, *138–139*, 149–160.

[58] N. G. Shabalala, S. Maddila, S. B. Jonnalagadda, *Res. Chem. Intermed.* **2016**, *42*, 8097–8108.

[59] H. Song, X. Bao, C. M. Hadad, U. S. Ozkan, *Catal. Letters* **2011**, *141*, 43–54.

[60] M. Bowker, *Top. Catal.* **2016**, *59*, 663–670.

[61] S. Kouva, K. Honkala, L. Lefferts, J. Kanervo, *Catal. Sci. Technol.* **2015**, *5*, 3473–3490.

[62] Y. Zhao, W. Li, M. Zhang, K. Tao, *Catal. Commun.* **2002**, *3*, 239–245.

[63] R. Pagadala, D. R. Kommidi, S. Rana, S. Maddila, B. Moodley, N. A. Koorbanally, S. B. Jonnalagadda, *RSC Adv.* **2015**, *5*, 5627–5632.

[64] S. N. Maddila, S. Maddila, W. E. van Zyl, S. B. Jonnalagadda, *Res. Chem. Intermed.* **2017**, *43*, 4313–4325.

[65] A. Amoozadeh, S. Rahmani, M. Bitaraf, F. B. Abadi, E. Tabrizian, *New J. Chem.* **2016**, *40*, 770–780.

[66] J. Wang, N. Li, R. Qiu, X. Zhang, X. Xu, S.-F. Yin, *J. Organomet. Chem.* **2015**, *785*, 61–67.

[67] S. Maddila, S. Gorle, S. Shabalala, O. Oyetade, S. N. Maddila, P. Lavanya, S. B. Jonnalagadda, *Arab. J. Chem.* **2016**, DOI: 10.1016/j.arabjc.2016.04.016.

[68] M. Mamaghani, M. Jamali Moghadam, R. Hossein Nia, *J. Iran. Chem. Soc.* **2017**, *14*, 395–401.

[69] A. Khazaei, N. Sarmasti, J. Y. Seyf, M. Tavasoli, *RSC Adv.* **2015**, *5*, 101268–101275.

[70] P. Kluson, L. Cerveny, *J. Mol. Catal. A: Chem.* **1996**, *108*, 107–112.

[71] S. N. Maddila, S. Maddila, W. E. van Z. and S. B. Jonnalagadda, *Curr. Org. Synth.* **2016**, *13*, 893–900.

[72] Y. Habuta, N. Narishige, K. Okumura, N. Katada, M. Niwa, *Catal. Today* **2003**, *78*, 131–138.

[73] S. Maddila, R. Pagadala, S. Rana, S. Kankala, S. B. Jonnalagadda, *Res. Chem. Intermed.* **2015**, *41*, 8269–8278.

[74] R. Pagadala, S. Maddila, V. D. B. C. Dasireddy, S. B. Jonnalagadda, *Catal. Commun.* **2014**, *45*, 148–152.

[75] J. M. Bothwell, S. W. Krabbe, R. S. Mohan, *Chem. Soc. Rev.* **2011**, *40*, 4649–4707.

[76] G. Brahmachari, S. Das, *Tetrahedron Lett.* **2012**, *53*, 1479–1484.

[77] G. Brahmachari, S. Begam, K. Nurjamal, *ChemistrySelect* **2017**, *2*, 3311–3316.

[78] R. H. Pouwer, C. M. Williams, *Silver Org. Chem.* **2010**,

DOI: 10.1002/9780470597521.ch1.

[79] S. N. Maddila, S. Maddila, W. E. van Zyl, S. B. Jonnalagadda, *Res. Chem. Intermed.* **2016**, *42*, 2553–2566.

[80] S. Bhaskaruni, S. Maddila, W. van Zyl, S. Jonnalagadda, *Molecules* **2018**, *23*, 1648.

[81] V. P. Ananikov, *ACS Catal.* **2015**, *5*, 1964–1971.

[82] J. Lu, E.-Q. Ma, Y.-H. Liu, Y.-M. Li, L.-P. Mo, Z.-H. Zhang, *RSC Adv.* **2015**, *5*, 59167–59185.

[83] T. Demirci, B. Çelik, Y. Yıldız, S. Eriş, M. Arslan, F. Sen, B. Kilbas, *RSC Adv.* **2016**, *6*, 76948–76956.

[84] A. Fürstner, *ACS Cent. Sci.* **2016**, *2*, 778–789.

[85] A. Maleki, Z. Alrezvani, S. Maleki, *Catal. Commun.* **2015**, *69*, 29–33.

[86] M. Saha, K. Pradhan, A. R. Das, *RSC Adv.* **2016**, *6*, 55033–55038.

[87] V. Kumar, K. Kaur, G. K. Gupta, A. K. Sharma, *Eur. J. Med. Chem.* **2013**, *69*, 735–753.

[88] P. L. McCormack, *Drugs* **2011**, *71*, 2457–2489.

[89] M. Waterlow, P. Chrisp, *Core Evid.* **2008**, *2*, 173–187.

[90] A. Rauf, N. N. Farshori, Microwave-Induced Synthesis of Aromatic Heterocycles, Springer Netherlands, Dordrecht, **2012**, pp. 39–46.

[91] J. Zaiter, H. Achibat, O. Amiri, A. Hafid, M. Khouili, E. M. Rakib, C. M. B. Neves, M. G. P. M. S. Neves, A. M. S. Silva, J. A. S. Cavaleiro, et al., *New J. Chem.* **2015**, *39*, 6738–6741.

[92] K. M. Elattar, A. A. Fadda, *Synth. Commun.* **2016**, *46*, 1567–1594.

[93] A. M. Akondi, M. L. Kantam, R. Trivedi, J. Bharatam, S. P. B. Vemulapalli, S. K. Bhargava, S. K. Buddana, R. S. Prakasham, *J. Mol. Catal. A: Chem.* **2016**, *411*, 325–336.

[94] S. N. Maddila, S. Maddila, W. E. van Zyl, S. B. Jonnalagadda, *RSC Adv.* **2015**, *5*, 37360–37366.

[95] M. M. Heravi, A. Ghods, F. Derikvand, K. Bakhtiari, F. F. Bamoharram, *J. Iran. Chem.*

Soc. **2010**, *7*, 615–620.

[96] A. Azarifar, R. Nejat-Yami, M. Al Kobaisi, D. Azarifar, *J. Iran. Chem. Soc.* **2013**, *10*, 439–446.

[97] B. Maleki, H. Eshghi, M. Barghamadi, N. Nasiri, A. Khojastehnezhad, S. Sedigh Ashrafi, O. Pourshiani, *Res. Chem. Intermed.* **2016**, *42*, 3071–3093.

[98] K. Pradhan, S. Paul, A. R. Das, *Catal. Sci. Technol.* **2014**, *4*, 822–831.

[99] S. Swami, A. Agarwala, R. Shrivastava, *New J. Chem.* **2016**, *40*, 9788–9794.

[100] J. Rakhtshah, S. Salehzadeh, E. Gowdini, F. Maleki, S. Baghery, M. A. Zolfigol, *RSC Adv.* **2016**, *6*, 104875–104885.

[101] J. Safaei-Ghomi, B. Khojastehbakht-Koopaei, H. Shahbazi-Alavi, *RSC Adv.* **2014**, *4*, 46106–46113.

[102] L. Bauer, L. A. Gardella, *J. Org. Chem.* **1963**, *28*, 1320–1323.

[103] K. C. Nicolaou, R. Scarpelli, B. Bollbuck, B. Werschkun, M. M. A. Pereira, M. Wartmann, K.-H. Altmann, D. Zaharevitz, R. Gussio, P. Giannakakou, *Chem. Biol.* **2000**, *7*, 593–599.

[104] C. Gao, X.-X. Huang, M. Bai, J. Wu, J.-Y. Li, Q.-B. Liu, L.-Z. Li, S.-J. Song, *Fitoterapia* **2015**, *105*, 49–54.

[105] A. Gueiffier, S. Mavel, M. Lhassani, A. Elhakmaoui, R. Snoeck, G. Andrei, O. Chavignon, J.-C. Teulade, M. Witvrouw, J. Balzarini, et al., *J. Med. Chem.* **1998**, *41*, 5108–5112.

[106] S. R. El-Zemity, *Arch. Phytopathol. Plant Prot.* **2011**, *44*, 381–389.

[107] C.-W. Fu, Y.-J. Hsieh, T. T. Chang, C.-L. Chen, C.-Y. Yang, A. Liao, P.-W. Hsiao, W.-S. Li, *Eur. J. Med. Chem.* **2015**, *104*, 165–176.

[108] N. Siddiqui, Andalip, S. Bawa, R. Ali, O. Afzal, M. J. Akhtar, B. Azad, R. Kumar, *J. Pharm. Bioallied Sci.* **2011**, *3*, 194–212.

[109] K. Nakamoto, I. Tsukada, K. Tanaka, M. Matsukura, T. Haneda, S. Inoue, N. Murai, S. Abe, N. Ueda, M. Miyazaki, et al., *Bioorg. Med. Chem. Lett.* **2010**, *20*, 4624–4626.

[110] M. Mojarrab, R. Soltani, A. Aliabadi, *Jundishapur J. Nat. Pharm. Prod.* **2013**, *8*, 125–

130.

[111] T. R. Ravikumar Naik, S. A. Shivashankar, *Tetrahedron Lett.* **2016**, *57*, 4046–4049.

[112] S. M. Sadeghzadeh, *RSC Adv.* **2016**, *6*, 99586–99594.

[113] M. Zhang, Y.-H. Liu, Z.-R. Shang, H.-C. Hu, Z.-H. Zhang, *Catal. Commun.* **2017**, *88*, 39–44.

[114] H. Alinezhad, S. M. Tavakkoli, P. Biparva, *Chin. J. Catal.* **2014**, *35*, 560–564.

[115] A. Bamoniri, S. Fouladgar, *RSC Adv.* **2015**, *5*, 78483–78490.

[116] S. Shabalala, S. Maddila, W. E. van Zyl, S. B. Jonnalagadda, *Catal. Commun.* **2016**, *79*, 21–25.

[117] M. Norouzi, A. Ghorbani-Choghamarani, M. Nikoorazm, *RSC Adv.* **2016**, *6*, 92387–92401.

[118] S. Kantevari, M. V. Chary, S. V. N. Vuppalapati, *Tetrahedron* **2007**, *63*, 13024–13031.

[119] M. A. Zolfigol, M. Kiafar, M. Yarie, A. Taherpour, M. Saeidi-Rad, *RSC Adv.* **2016**, *6*, 50100–50111.

[120] S. Kumar, B. Narasimhan, *Chem. Cent. J.* **2018**, *12*, 38.

[121] S. Mohana Roopan, R. Sompalle, *Synth. Commun.* **2016**, *46*, 645–672.

[122] S. A. Al-Issa, *Saudi Pharm. J. SPJ Off. Publ. Saudi Pharm. Soc.* **2013**, *21*, 305–316.

[123] K. Shrivas, S. Sahu, B. Sahu, R. Kurrey, T. K. Patle, T. Kant, I. Karbhal, M. L. Satnami, M. K. Deb, K. K. Ghosh, *J. Mol. Liq.* **2019**, *275*, 297–303.

[124] H. Naeimi, A. Didar, Z. Rashid, *J. Iran. Chem. Soc.* **2017**, *14*, 377–385.

[125] H. R. Shaterian, M. Aghakhanizadeh, *Catal. Sci. Technol.* **2013**, *3*, 425–428.

[126] J. Safaei Ghomi, R. Teymuri, A. Ziarati, *monatsh.Chem.* **2013**, *144*, 1865–1870.

[127] V. Palermo, Á. Sathicq, T. Constantieux, J. Rodríguez, P. Vázquez, G. Romanelli, *Catal. Lett.* **2015**, *145*, 1022–1032.

[128] B. Sabour, M. H. Peyrovi, M. Hajimohammadi, *Res. Chem. Intermed.* **2015**, *41*, 1343–1350.

[129] A. Maleki, M. Aghaei, *Ultrason. Sonochem.* **2017**, *38*, 585–589.

[130] M. Mohsenimehr, M. Mamaghani, F. Shirini, M. Sheykhan, S. Abbaspour, L. Shafei Sabet, *J. Chem. Sci.* **2015**, *127*, 1895–1904.

[131] B. Dam, A. K. Pal, A. Gupta, *Synth. Commun.* **2016**, *46*, 275–286.

[132] S. Ramalingam, P. Kumar, *Synth. Commun.* **2009**, *39*, 1299–1309.

Chapter 2

V_2O_5/ZrO_2 as an efficient reusable catalyst for the facile, green, one-pot synthesis of novel functionalized 1,4-dihydropyridine derivatives

Sandeep V.H.S. Bhaskaruni, Suresh Maddila, Werner E. van Zyl, Sreekantha B. Jonnalagadda*

**School of Chemistry & Physics, University of KwaZulu-Natal, Westville Campus, Chiltern Hills, Durban-4000, South Africa.*

*Corresponding author: Prof. S.B. Jonnalagadda,
School of Chemistry & Physics,
University of KwaZulu-Natal,
Westville campus, Chiltern Hills,
Durban-4000, South Africa.
E-mail: **jonnalagaddas@ukzn.ac.za**
Tel.: +27 31 260 7325,
Fax: +2731 260 3091.

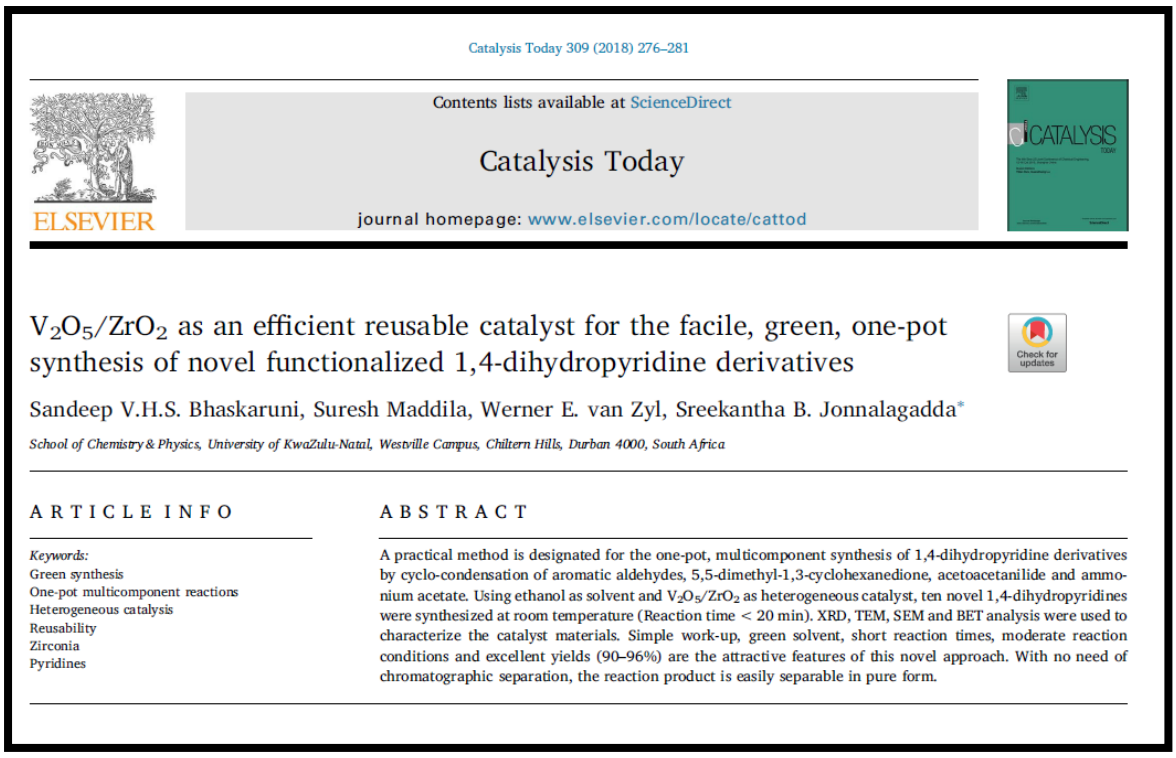

Catalysis Today 309 (2018) 276–281

Contents lists available at ScienceDirect

Catalysis Today

journal homepage: www.elsevier.com/locate/cattod

V_2O_5/ZrO_2 as an efficient reusable catalyst for the facile, green, one-pot synthesis of novel functionalized 1,4-dihydropyridine derivatives

Sandeep V.H.S. Bhaskaruni, Suresh Maddila, Werner E. van Zyl, Sreekantha B. Jonnalagadda*

School of Chemistry & Physics, University of KwaZulu-Natal, Westville Campus, Chiltern Hills, Durban 4000, South Africa

ARTICLE INFO

Keywords:
Green synthesis
One-pot multicomponent reactions
Heterogeneous catalysis
Reusability
Zirconia
Pyridines

ABSTRACT

A practical method is designated for the one-pot, multicomponent synthesis of 1,4-dihydropyridine derivatives by cyclo-condensation of aromatic aldehydes, 5,5-dimethyl-1,3-cyclohexanedione, acetoacetanilide and ammonium acetate. Using ethanol as solvent and V_2O_5/ZrO_2 as heterogeneous catalyst, ten novel 1,4-dihydropyridines were synthesized at room temperature (Reaction time < 20 min). XRD, TEM, SEM and BET analysis were used to characterize the catalyst materials. Simple work-up, green solvent, short reaction times, moderate reaction conditions and excellent yields (90–96%) are the attractive features of this novel approach. With no need of chromatographic separation, the reaction product is easily separable in pure form.

This chapter is published in the journal **Catalysis Today,** and has been structured according to the journal's format.

V_2O_5/ZrO_2 as an efficient reusable catalyst for the facile, green, one-pot synthesis of novel functionalized 1,4-dihydropyridine derivatives

Sandeep V.H.S. Bhaskaruni, Suresh Maddila, Werner E. van Zyl, Sreekantha B. Jonnalagadda*

**School of Chemistry & Physics, University of KwaZulu-Natal, Westville Campus, Chiltern Hills, Durban-4000, South Africa.*

*Corresponding author: Prof. S.B. Jonnalagadda,
School of Chemistry & Physics,
University of KwaZulu-Natal,
Westville campus, Chiltern Hills,
Durban-4000, South Africa.
E-mail: **jonnalagaddas@ukzn.ac.za**
Tel.: +27 31 260 7325,
Fax: +2731 260 3091.

Abstract

A practical method is designated for the one-pot, multi-component synthesis of 1,4-dihydropyridine derivatives by cyclo-condensation of aromatic aldehydes, 5,5-dimethyl-1,3-cyclohexanedione, acetoacetanilide and ammonium acetate. Using ethanol as solvent and V_2O_5/ZrO_2 as heterogeneous catalyst, ten novel 1,4-dihydropyridines were synthesized at room temperature (Reaction time <20 min). XRD, TEM, SEM and BET analysis were used to characterize the catalyst materials. Simple work-up, green solvent, short reaction times, moderate reaction conditions and excellent yields (90–96%) are the attractive features of this novel approach. With no need for chromatographic separation, the reaction product is easily separable in pure form.

Keywords: Green synthesis, One-pot multicomponent reactions, Heterogeneous catalysis, Reusability, Zirconia, Pyridines.

2.1 Introduction

In recent years, mixed oxides and bimetallic compounds were amongst the most extensively explored class of solid catalyst materials, either as active phases or as supports [1–3]. The presence of two or more metal cations in mixed oxides provide an opportunity to control and design the morphologies and properties of the materials [4,5]. In general, the mixed oxides are crystalline [6,7], but the nature depends on calcination temperatures as at moderate calcination, some phases may remain amorphous [8]. Due to their varied characteristics and composition, the benefits accrued from the crystalline mixed oxides are many [9]. Literature shows the use of numerous mixed oxides and bimetallic materials in various applications, as adsorbents, catalysts or photo catalysts in water treatment and as catalysts in value added conversions [10–15]. In the recent past, zirconium oxide (ZrO_2) received significant attention due to its amphoteric nature, as it can act as bi-functional material [16]. High specific surface area, better flexibility, active metal centre, thermal satiability and cost-effectiveness make it appropriate choice over wide-ranging temperatures [17]. Literature reports show its usage both as active material and support of mixed catalysts in synthetic chemistry [18]. Zirconia as catalyst has been employed in many organic shift reactions, such as epoxidation [19], isomerization [20], alkylation [21], C-C bond formation [22], to mention a few. The scope for dispersion of active material as nanoparticles on zirconia makes it an ideal support material for various applications. Vanadia is well known material as catalyst, alone or doped on different supports. It is used in variety reactions including oxidations, reductions, and many synthetic transformation reactions [23]. In the current study, the synergic properties of Zr plus V as catalyst are explored and its activity as bimetallic catalyst is optimized. Classical organic chemistry is in pursuit of opt environmentally friendly synthetic methodologies for chemical, pharmaceutical industries [24]. Main principles of green chemistry are to create environmentally benign products with high atom efficiency, prevention of waste, use of nontoxic materials and use of catalysts rather than stoichiometric reagents [25]. In order to fulfil the green chemistry principles, carrying out a reaction in heterogeneous environment makes the route more economical and eco-friendly [26], as recovery and reusability of heterogeneous catalysts is simple [27]. In contrast to multi-step reactions, multi-component reactions (MCRs) can synthesize complex molecules in one-pot with good atom-economy, selectivity and in high yields [28], providing a quick access to new organic molecules [28–30]. The combination of the MCR approach and with the use of heterogeneous catalyst is most effective option in synthetic chemistry [31,32]. Heterocyclic compounds are key moieties in many bioactive

pharmaceuticals, medicinal, computational and natural products, which inspires synthetic chemist towards the synthesis of larger and novel molecules. The 1,4-dihydropyridine nucleus is one of the most attractive heterocyclic framework that is present in many drugs and pharmaceuticals. The dihydropyridine scaffold has received greater attention due to its breadth of biological activities, ranging from cardiovascular disease [33], anti-cancer [34], anti-microbial [35], anti-oxidant [36], anti-coagulant [37], anti-leishmanial and anti-trypanosomal [38], anti-tubercular agents [39], HIV-1 protease inhibitors [40] to antioxidant activities [41]. Due their pecuniary and scientific relevance, many synthetic methods were described in literature for production of different dihydropyridines. The Hantzsch synthesis is the well-known technique for the preparation of 1,4-dihydropyridines [42]. Some of such methods employed I_2 [43], TMSI [44], Et_3N [45], polyethylene glycol (PEG-600) [46] nano-γ-Fe_2O_3-SO_3H [47], [PVPH]ClO_4 [48], L-proline [49], NaOH [50] etc., as catalysts. Many those reactions either demand high energy and expensive reagents or punitive reaction conditions and long reaction times or give low yields. Consequently, continued pursuit for improved and greener approaches for the synthesis of dihydropyridine derivatives is paramount. To the best of our knowledge, there are no reports on the use of vanadia loaded zirconia as a catalyst for the synthesis of dihydropyridines via multi-component reactions. Encouraged by the promising results in developing synthetic methods for a variety of heterocyclic molecules [51–58], we recently, we have reported different approaches for preparation of various medicinally interesting heterocyclic protocols [59–64]. In this communication, we report the synthesis and characterization of vanadia doped zirconia and its versatility as catalyst in one-pot synthesis of novel functionalized dihydropyridine derivatives using a four-component reaction and ethanol as solvent at room temperature.

2.2 Experimental Section

2.2.1 Catalyst preparation

Using simple wet-impregnation technique, materials with different loading of vanadia on zirconia (1, 2.5, & 5 wt% of V on Zr) were prepared by previously reported method [65-67]. To prepare the materials, a mixture of zirconia, ZrO_2 (3 g), (Alfa Aesar) and appropriate amount (wt%) of vanadium (V) oxide, 99.9% [V_2O_5 (Alfa Aesar)] in distilled water (100-150 mL) were used. The reaction mixture was stirred at room temperature (RT) for 6 h, followed by filtering the resultant slurry under vacuum. The material was dried for 5 h in an oven at 120–150 °C and calcined at 450 °C for 5 h in the presence of air, to obtain different weight loadings of V_2O_5/ZrO_2 catalysts.

2.2.2 General procedure for the synthesis of dihydropyridine derivatives (5a-j)

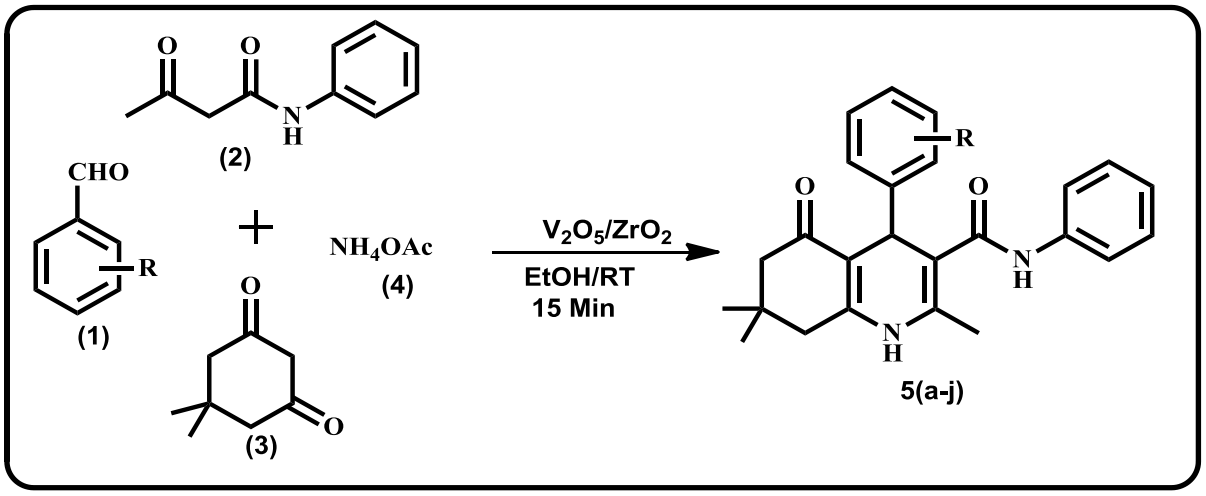

Scheme 1. Synthesis of novel 1,4-dihydropyridine derivatives.

In initial study, equimolar mixture of 2-methoxy benzaldehyde (1 mmol) (1), 5,5-dimethyl-1,3-cyclohexanedione (1 mmol) (3), acetoacetanilide (1 mmol) (2) and ammonium acetate (1 mmol) (4) were stirred at room temperature in 5 mL of ethanol as a green reaction medium followed by addition of catalyst (60 mg) at RT (15 min), reaction progress was monitered by TLC (Scheme 1). After the completion of the reaction, catalyst was filtered and the crude product was extracted by ethyl acetate, followed by evaporation of solvent under vacuum to recover the product. Ethanol was used to dissolve the crude product and to obtain pure compounds (**5a-j**). Reaction products from every reaction were characterised by ^{1}H-NMR, ^{15}N NMR, ^{13}C-NMR, HRMS and FT-IR. The related details and spectra are assimilated to the supplementary information file.

4-(2-Methoxyphenyl)-2,7,7-trimethyl-5-oxo-N-phenyl-1,4,5,6,7,8-hexahydroquinoline-3-carboxamide (5a)*:*

^{1}H NMR (400 MHz, $CDCl_3$): δ 0.87 (s, 3H, CH_3), 0.99 (s, 3H, CH_3), 2.05 (t, *J* = 17.72 Hz, 2H, CH_2), 2.25 (t, *J* = 16.52 Hz, 2H, CH_2), 2.34 (s, 3H, CH_3), 3.98 (s, 3H, -OCH_3), 5.28 (s, 1H, CH), 6.14 (s, 1H, NH), 6.82 (t, *J* = 8 Hz, 2H, Ar-H), 6.96 (t, *J* = 7.36, 1H, Ar-H), 7.03-7.07 (m, 1H, Ar-H), 7.18 (s, 1H, Ar-H), 7.20 (t, *J* = 2.88 Hz, 2H, Ar-H), 7.38 (d, *J* = 7.64Hz, 2H, Ar-H), 8.57 (s, 1H, NH); ^{13}C NMR (400 MHz, $CDCl_3$): δ 20.11, 27.07, 29.22, 29.46, 32.71, 40.96, 50.58, 56.93, 108.19, 112.02, 112.06, 120.60, 122.22, 123.63, 128.07, 128.69, 129.78, 136.12, 138.93, 142.32, 148.68, 154.10,165.94, 195.05; ^{15}N NMR (400 MHz, $CDCl_3$): δ 6.14 (s, 1H,

NH), 8.57 (s, 1H, NH). FT-IR: 3374, 3290, 3073, 2953, 1605, 1530, 1436, 1380, 1230. HRMS of $[C_{26}H_{28}N_2O_3 + Na]^+$ (m/z): 439.2010; Calcd.: 439.1998.

4-(4-Methoxyphenyl)-2,7,7-trimethyl-5-oxo-N-phenyl-1,4,5,6,7,8-hexahydroquinoline-3-carboxamide (5b):

^{1}H NMR (400 MHz, $CDCl_3$): δ 0.86 (s, 3H, CH_3), 1.04 (s, 3H, CH_3), 2.15 (t, *J* = 16.32 Hz, 2H, CH_2), 2.26 (t, *J* = 16.56 Hz, 2H, CH_2), 2.36 (s, 3H, CH_3) 3.78 (s, 3H, -OCH_3), 4.88 (s, 1H, CH), 6.32 (s, 1H, NH), 6.86 (d, *J* = 8.6 Hz, 2H, Ar-H), 7.00- 7.04 (m, 2H, Ar-H), 7.21-7.27 (m,4H, Ar-H), 7.37 (d, *J*= 5.12 Hz, 1H, NH), 7.40 (s, 1H, Ar-H); ^{13}C NMR (400 MHz, $CDCl_3$): δ 18.77, 27.05, 29.26, 32.66, 36.99, 41.04, 50.62, 55.24, 108.38, 111.21, 114.37, 123.90, 129.03, 132.03, 137.57, 138.16 ,140.96, 148.26, 158.69, 166.44, 190.93, 195.36; ^{15}N NMR (400 MHz, $CDCl_3$): 6.32 (s, 1H, NH), 7.37 (s, 1H, NH). FT-IR: 3245, 1595, 1487, 1380, 1221. HRMS of $[C_{26}H_{28}N_2O_3 + Na]^+$ (m/z): 439.1461; Calcd.: 439.1465.

4-(2-Chlorophenyl)-2,7,7-trimethyl-5-oxo-N-phenyl-1,4,5,6,7,8-hexahydroquinoline-3-carboxamide (5c):

^{1}H NMR (400 MHz, $CDCl_3$): δ 0.84 (s, 3H, CH_3), 0.97 (s, 3H, CH_3), 2.05(d, *J* = 16.36 Hz, 2H, CH_2), 2.10-2.16 (m, 2H, CH_2), 2.21 (s, 3H, CH_3), 5.30 (s, 1H, CH), 6.31 (s, 1H, NH), 6.97-7.04 (m, 2H, Ar-H), 7.10-7.14 (m, 2H, Ar-H), 7.20-7.23 (m, 1H, Ar-H), 7.34-7.37 (m, 3H, Ar-H), 7.36 (s, 1H, NH); ^{13}C NMR (400 MHz, $CDCl_3$): δ 19.27, 27.11, 29.31, 32.56, 35.43, 41.04, 50.53, 108.57, 110.68, 120.38, 124.03, 128.26, 128.80, 129.40, 129.71, 131.06, 131.65, 138.15, 140.46, 143.60, 149.11, 166.00, 195.04; ^{15}N NMR (400 MHz, $CDCl_3$): 6.31 (s, 1H, NH), 7.36 (s, 1H, NH). FT-IR: 3264, 3063, 2958, 1595, 1439, 1380, 1220. HRMS of $[C_{25}H_{25}ClN_2O_2 + Na]^+$ (m/z): 443.1510 ; Calcd.: 443.1502.

4-(2,3-Dimethoxyphenyl)-2,7,7-trimethyl-5-oxo-N-phenyl-1,4,5,6,7,8-hexahydroquinoline -3-carboxamide (5d):

^{1}H NMR (400 MHz, $CDCl_3$): δ 1.00 (s, 3H, CH_3), 1.09 (s, 3H, CH_3), 2.17 (t, *J* = 4.24 Hz, 2H, CH_2), 2.27 (d, *J* = 17.88 Hz, 2H, CH_2), 2.44 (s, 3H, CH_3), 3.84 (s, 3H, -OCH_3), 4.32 (s, 1H, CH), 5.31 (s, 1H, CH), 6.17 (s, 1H, NH), 6.73 (dd, *J* = 1.44 Hz, *J* = 1.4 Hz 1H, Ar-H), 6.87 (dd, *J* = 1.48 Hz, *J* = 1.4 Hz, 1H, Ar-H), 6.96 (t, *J* = 7.96 Hz, 1H, Ar-H), 7.04 (t, *J* = 7.36 Hz, 1H, Ar-H), 7.31 (d, *J* = 7.52 Hz, 2H, Ar-H), 7.65 (t, *J* = 7.6 Hz, 2H, Ar-H), 9.32 (s, 1H, NH); ^{13}C NMR (400 MHz, $CDCl_3$): δ 20.57, 27.13, 29.35, 29.55, 32.76, 41.10, 50.66, 55.75, 60.92, 108.23, 110.79, 111.82, 120.69, 120.98, 123.39, 124.89, 128.61, 139.36, 140.43, 142.86, 143.07, 149.10, 152.37, 165.75, 195.09; ^{15}N NMR (400 MHz, $CDCl_3$): 6.17 (s, 1H, NH), 9.32 (s, 1H, NH). FT-IR: 3262, 3063, 2956, 1995, 1488, 1380, 1220. HRMS of $[C_{27}H_{30}N_2O_4 + Na]^+$ (m/z): 469.2114 ; Calcd.: 469.2103.

4-(3,4-Dimethoxyphenyl)-2,7,7-trimethyl-5-oxo-N-phenyl-1,4,5,6,7,8-hexahydro quinoline -3-carboxamide (5e):

^{1}H NMR (400 MHz, $CDCl_3$): δ 0.81 (s, 3H, CH_3), 0.98 (s, 3H, CH_3), 2.06-2.10 (m, 2H, CH_2), 2.21 (t, *J* = 16.76 Hz, 2H, CH_2), 2.30 (s, 3H, CH_3), 3.78 (s, 6H, 2-OCH_3), 4.80 (s, 1H, CH), 6.08 (s, 1H, NH), 6.75 (d, *J* = 8.24 Hz, 1H, Ar-H), 6.89- 6.98 (m, 3H, Ar-H), 7.15 (t, *J* = 15.44 Hz, 1H, Ar-H), 7.30 (s, 1H, Ar-H); ^{13}C NMR (400 MHz, $CDCl_3$): δ 18.74, 27.00, 29.29, 32.67, 37.29, 41.13, 50.61, 55.96, 108.35, 111.40, 111.46, 119.80, 119.91, 123.92, 128.86, 137.94, 138.14, 140.83, 148.15, 148.19, 149.28, 166.39,191.00, 195.36; ^{15}N NMR (400 MHz, $CDCl_3$): 6.08 (s, 1H, NH), 7.30 (s, 1H, NH). FT-IR: 3274, 2957, 1594, 1488, 1380, 1137. HRMS of $[C_{27}H_{30}N_2O_4 + Na]^+$ (m/z): 469.0338; Calcd.: 469.0331.

2,7,7-Trimethyl-5-oxo-N-phenyl-4-(2,4,6-trimethoxyphenyl)-1,4,5,6,7,8-hexahydro quinoline -3-carboxamide (5f):

^{1}H NMR (400 MHz, $CDCl_3$): δ 0.89 (s, 3H, CH_3), 1.03 (s, 3H, CH_3), 2.08 (d, *J* = 16.24 Hz, 2H, CH_2), 2.15-2.28 (m, 2H, CH_2), 2.40 (s, 3H, CH_3), 3.75 (s, 9H, 3-OCH_3), 5.51 (s, 1H, CH), 6.13 (s, 2H, Ar-H), 6.26 (s, 1H, NH), 7.02 (t, *J* = 7.36 Hz, 1H, Ar-H), 7.26 (t, *J* = 7.52 Hz, 2H, Ar-H), 7.46 (d, *J* = 7.8 Hz, 2H, Ar-H), 8.64 (s, 1H, NH); ^{13}C NMR (400 MHz, $CDCl_3$): δ 20.23, 26.47, 27.01, 29.61, 32.40, 41.08, 50.68, 55.18, 55.79, 104.78, 109.15, 114.43, 120.50, 123.28, 128.62, 139.22, 142.91, 149.61, 159.81, 166.54, 195.23; ^{15}N NMR (400 MHz, $CDCl_3$): 6.26 (s, 1H, NH), 8.64 (s, 1H, NH). FT-IR: 3387, 2941, 2838, 1662, 1594, 1484, 1203. HRMS of $[C_{28}H_{32}N_2O_5 + Na]^+$ (m/z): 499.2213 ; Calcd.: 499.2209.

4-(4-Bromophenyl)-2,7,7-trimethyl-5-oxo-N-phenyl-1,4,5,6,7,8-hexahydroquinoline-3-carboxamide (5g):

^{1}H NMR (400 MHz, $CDCl_3$): δ 0.87 (s, 3H, CH_3), 1.06 (s, 3H, CH_3), 2.17 (t, *J* = 6.5 Hz, 2H, CH_2), 2.20-2.32 (m, 2H, CH_2), 2.36 (s, 3H, CH_3), 4.94 (s, 1H, CH), 6.25 (s, 1H, NH), 7.06 (s, 1H, NH), 7.23-7.27 (m, 5H, Ar-H), 7.33 (d, *J* =8.4 Hz, 2H,Ar-H), 7.44 (d, *J* = 8.4 Hz, 2H, Ar-H), 7.47 (s, 1H, NH) ; ^{13}C NMR (400 MHz, $CDCl_3$): δ 18.80, 27.02,29.30, 32.66, 37.45, 41.06, 50.56, 108.03, 110.52, 120.02, 121.10, 124.19, 128.91, 129.58, 132.04, 137.90, 140.82, 144.17, 148.69, 166.11, 195.22; ^{15}N NMR (400 MHz, $CDCl_3$): 6.25 (s, 1H, NH), 7.06 (s, 1H, NH). FT-IR: 3278, 295, 1595, 1438, 1379, 1220.

4-(4-Ethylphenyl)-2,7,7-trimethyl-5-oxo-N-phenyl-1,4,5,6,7,8-hexahydroquinoline-3-carboxamide (5h):

^{1}H NMR (400 MHz, $CDCl_3$): δ 0.80 (s, 3H, CH_3), 0.97 (s, 3H, CH_3), 1.13 (t, *J* = 7.64 Hz, 2H, CH_2), 2.08 (d, *J* = 3.12 Hz, 2H, CH_2), 2.11-2.18 (m, 2H, CH2), 2.27 (s, 3H, CH_3), 2.50-2.56

(m, 3H, CH_3), 4.80 (s, 1H, CH), 6.11 (s, 1H, NH), 7.08 (t, *J* = 15.28 Hz, 2H, Ar-H), 7.14-7.21(m, 5H, Ar-H), 7.26 (s, 1H, NH), 7.29 (d, *J* = 8.04 Hz, 2H); ^{13}C NMR (400 MHz, $CDCl_3$): δ= 15.43, 18.83, 27.20, 28.46, 29.19, 32.70, 37.49, 41.13, 50.62, 108.50, 111.20, 119.82, 123.83, 127.90, 128.53, 128.80, 129.99, 138.23, 140.91, 142.65, 143.24, 148.28, 166.38, 192.12, 195.27; ^{15}N NMR (400 MHz, $CDCl_3$): 6.11 (s, 1H, NH), 7.26 (s, 1H, NH). FT-IR: 3271, 2960, 1595, 1438, 1380, 1220. HRMS of $[C_{27}H_{30}N_2O_2 + Na]^+$ (m/z): 437.1474; Calcd.: 437.1465.

4-(2-Bromophenyl)-2,7,7-trimethyl-5-oxo-N-phenyl-1,4,5,6,7,8-hexahydroquinoline-3-carboxamide (5i):

^{1}H NMR (400 MHz, $CDCl_3$): δ 0.84 (s, 3H, CH_3), 0.98 (s, 3H, CH_3), 2.05 (d, *J* = 16.36 Hz, 2H, CH_2), 2.09-2.16 (m, 2H, CH_2), 2.19 (s, 3H, CH_3), 5.27 (s, 1H, CH), 6.22 (s, 1H, NH), 6.92-7.00 (m, 2H, Ar-H), 7.15-7.21 (m, 4H, Ar-H), 7.34-7.42 (m, 3H, Ar-H), 7.47 (s, 1H, NH); ^{13}C NMR (400 MHz, $CDCl_3$): δ 19.21, 27.18, 29.28, 32.56, 37.98, 41.13, 50.57, 109.19, 110.92, 120.56, 122.32, 124.08, 128.35, 128.77, 131.19, 133.06, 138.06, 139.85, 145.41, 148.99, 166.05, 195.06; ^{15}N NMR (400 MHz, $CDCl_3$): 6.22 (s, 1H, NH), 7.47 (s, 1H, NH). FT-IR: 3243, 3063, 2957, 1647, 1598, 1495, 1380, 1209.

4-(4-(Dimethylamino)phenyl)-2,7,7-trimethyl-5-oxo-N-phenyl-1,4,5,6,7,8-hexahydro quinoline-3-carboxamide (5j):

^{1}H NMR (400 MHz, $CDCl_3$): δ 0.79 (s, 3H, CH_3), 0.95 (s, 3H, CH_3), 2.02-2.15 (m, 2H, CH_2), 2.23 (d, *J* = 19.72 Hz, 2H, CH_2), 2.28 (s, 3H, CH_3), 2.83 (s, 6H, $N(CH_3)_2$), 4.72 (s, 1H, CH), 6.34 (s, 1H, NH), 6.61 (d, *J* = 8.6 Hz, 2H, Ar-H), 6.92 (t, *J* = 7.12 Hz, 1H, Ar-H), 7.14 (t, *J* = 8.16 Hz, 2H, Ar-H), 7.19 (d, *J* = 7.48 Hz, 2H, Ar-H), 7.24 (d, *J* = 8.6 Hz, 2H, Ar-H), 7.40 (s, 1H, NH); ^{13}C NMR (400 MHz, $CDCl_3$): δ 18.74, 27.26, 29.18, 32.67, 36.80, 40.07, 40.55, 41.01, 50.67, 108.50, 111.02, 111.47, 113.01, 123.69, 128.76, 132.04, 133.37, 138.37, 140.93, 148.40, 149.78, 154.41, 166.68, 190.42,195.40; ^{15}N NMR (400 MHz, $CDCl_3$): 6.34 (s, 1H, NH), 7.40 (s, 1H, NH). FT-IR: 3263, 2959, 1594, 1438, 1380, 1221. HRMS of $[C_{27}H_{31}N_3O_2 + Na]^+$ (m/z): 452.1432; Calcd.: 452.1437.

2.3 Results and discussion

2.3.1 Powder X-ray diffractogram (XRD)

The phase and crystallinity of the prepared catalyst was analysed by X-ray diffraction studies. XRD patterns of the calcinated 2.5% V_2O_5/ZrO_2 catalyst is shown in Fig. 1. The distinctive X-ray diffraction patterns at 2θ = 24.8°, 28.6°, 31.9°, 34.7°, 41.3°, 50.8° and 60.4°

of ZrO_2 (JCPDS 37-1484) recognized by an assessment with literature records and conform that the particles are polycrystalline structure [68]. As can be observed from the image, intensive peaks of V_2O_5, the diffractions at 2θ = 17.29°, 26.48°, 36.17°, and 49.79° (JCPDS41-1426) [69]. The average crystallite size of the sample was calculated by using Scherrer equation. It was about 7.6 nm, based on maximum intensity diffraction peak of V_2O_5/ZrO_2.

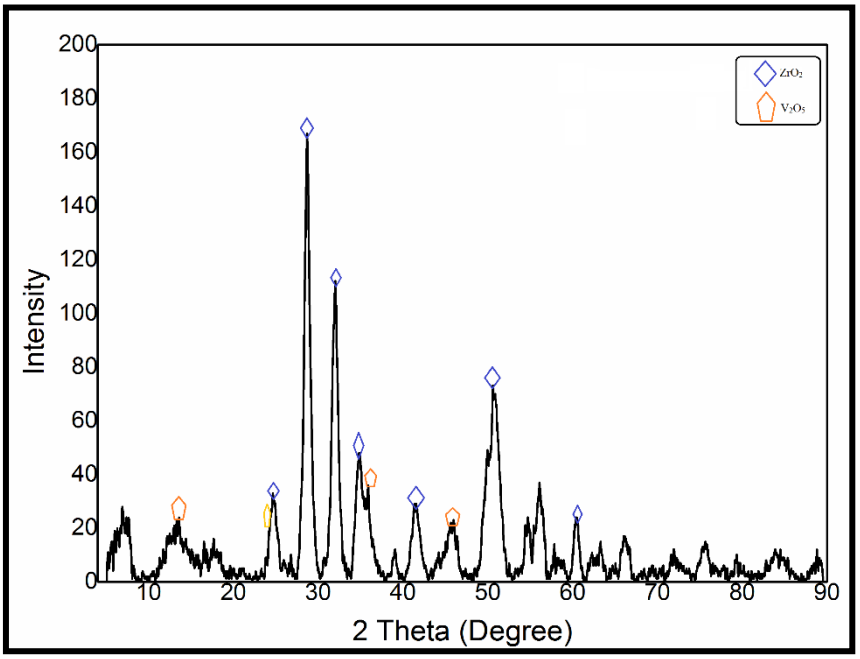

Fig. 1. Powder X-ray diffractogram of 2.5% V_2O_5/ZrO_2 catalyst.

2.3.2 SEM and TEM analysis

Fig. 2a. reveals a distinctive SEM surface morphology micrograph of the catalytic sample vanadia loaded on zirconia material. On keen examination of SEM micrograph the catalyst material displayed and settled as a large irregular shapes. It demonstrates that the agglomeration state of the zirconia units with vanadia due to its homogenous dispersion. The micrographs of SEM–EDX approved the similar dispersal of vanadia on the zirconia surface (Fig. 2b.). The SEM-EDX supports with the records from ICP elemental analysis it shows the 2.32 wt% of vanidia in the prepared catalyst. Additionally, the morphology of the catalyst as per the SEM micrographs to a crystalline and homogenous material.

The TEM images of the V_2O_5/ZrO_2 catalysts showed the arrangement of vanadium particles on the surface of zirconia support (Fig. 3.). The blacker parts of the image represent the existence of vanadium spread evenly on the surface.

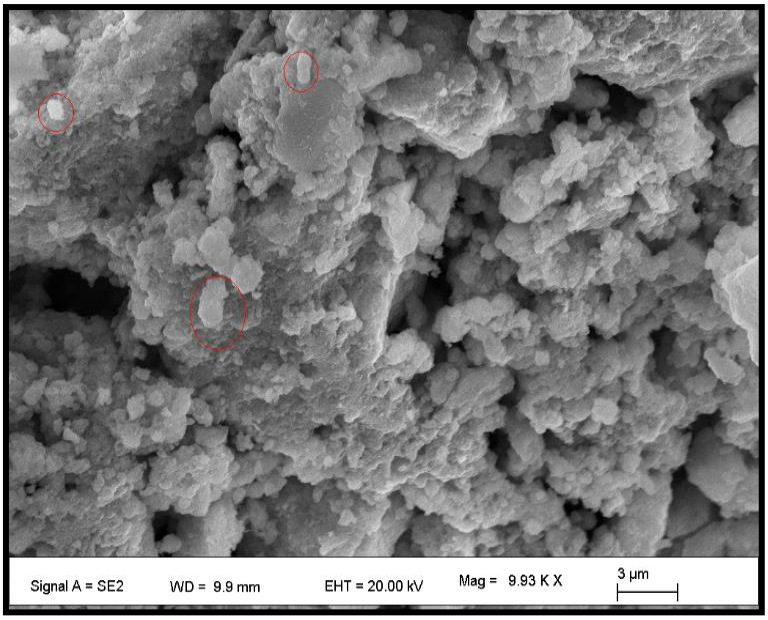

Fig. 2(a). SEM micrograph of 2.5% V_2O_5/ZrO_2 catalyst.

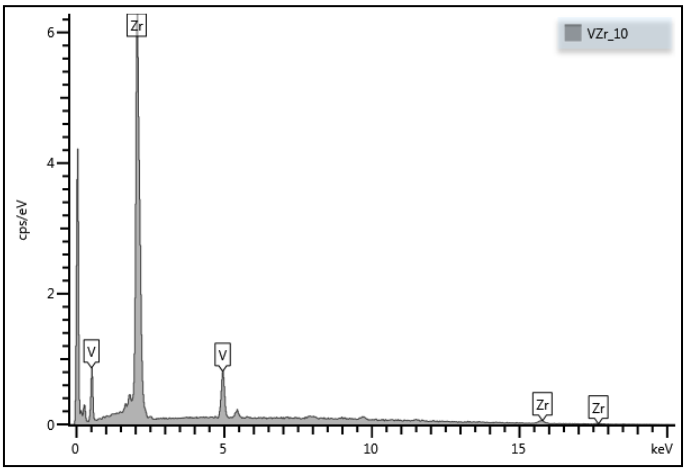

Fig. 2(b). EDS spectra of 2.5% V_2O_5/ZrO_2 catalyst.

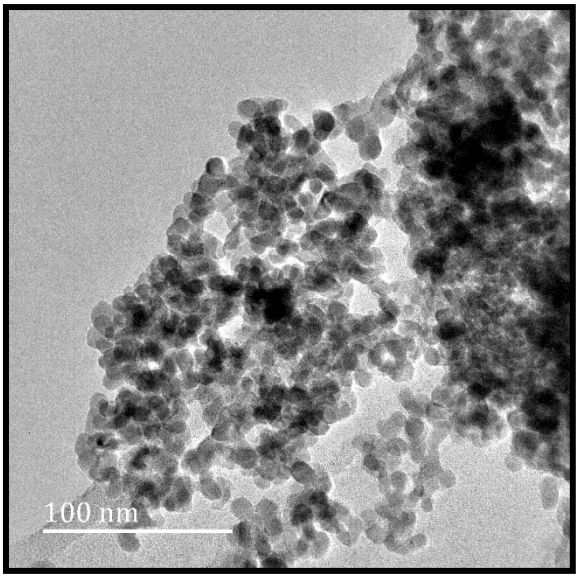

Fig. 3. TEM micrograph of 2.5%V_2O_5/ZrO_2 catalyst.

2.3.3 BET Analysis

The BET surface area and porous properties of the prepared catalyst (Fig. 4.) were obtained from N_2 adsorption studies. The V_2O_5/ZrO_2 catalyst was characterized by N_2 adsorption at 77 K using analyser. To remove the moisture in the catalytic sample, they are kept to degassing at 200^o C for a certain amount of time. The BET adsorption statistics was obtained by the creator's software by applying the BET equation. The nature of the material was meso porous which was confirmed by the type-IV adsorption isotherm, which having 0.6-0.9 P/Po range, surface are of 89.2219 m²/g, pore size of 103.249 Å and a pore volume of 0.326684 cm³/g. The pore size distribution plot is incorporated in fig. 4, illustrating the distribution of the calculated pore size from desorption data using BJH method.

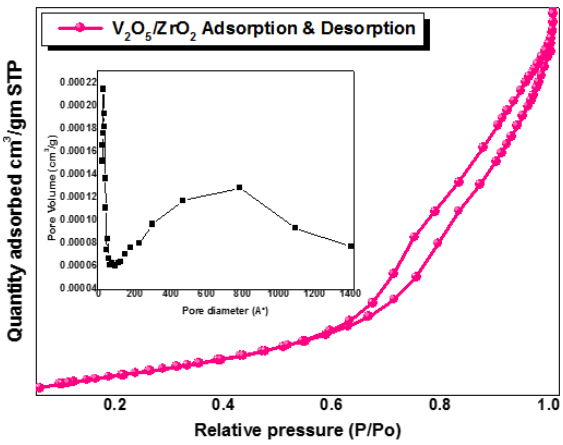

Fig. 4. N_2 adsorption-desorption isotherms and pore size distribution curve of 2.5% V_2O_5/ZrO_2 catalyst.

2.3.4 Reusability of the catalyst

Important benefit of using heterogeneous catalysts is that they are easily recyclable, which generates their use a superb alternate, particularly in view of cost-effective and environmental features. Thus to find the stability of catalyst recycling investigates was carried out. After the completion of each run, the catalyst was detached from the reaction mixture using with the vacuum, washed with ethanol solvent and dried in oven at 120 to 130 °C for 4 h. The recycled catalyst exhibited no significant loss of catalytic activity even after the five runs (Fig. 5), suggesting that there is no leaching or loss of vanadia during reaction and it is intact in the zirconia lattice. The XRD of the recycled catalyst after 5^{th} run, illustrated in Fig. 5 is much similar to the new material, confirming that no chemical or physical changes occurred on the catalyst surface.

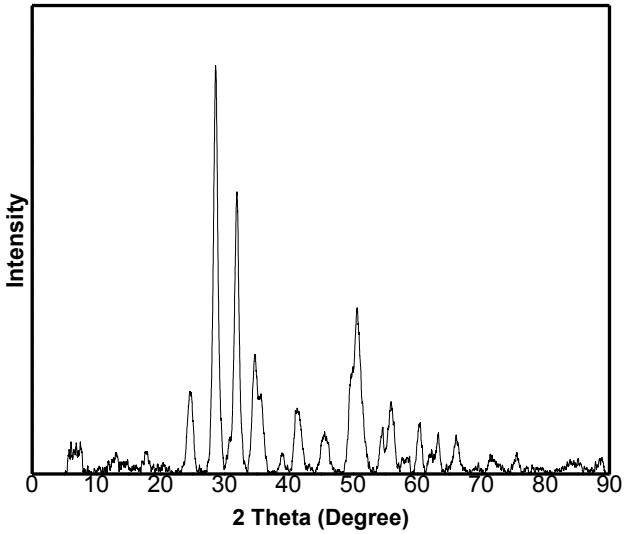

Fig. 5. XRD diffractogram of 2.5% V_2O_5/ZrO_2 catalyst recycled (after 5^{th} run).

2.3.5 Reaction optimization

In a preliminary endeavor, the reaction of 2-methoxy benzaldehyde, 5,5-Dimethyl-1,3-cyclohexanedione, acetoacetanilide and ammonium acetate was performed with various solvents, catalysts and temperature conditions. No reaction was observed under solvent-free and catalyst-free conditions, even after 12 h stirring either at RT or under reflux conditions (Table 1, entries 1 & 2). Furthermore, the primary reactants were mostly unaffected by the presence of acidic catalysts such as acetic acid, TsOH, HCl and $FeCl_3$ under ethanol solvent at RT for 8 h reaction time (Table 1, entries 3-6), but with ionic liquids like $(Bmim)BF_4$ or DABCO (Table 1, entry 7 & 8) trace yields were observed. With different basic inorganic and organic catalysts, such as NaOH, K_2CO_3, TEA and pyridine and EtOH solvent, the yield of

expected product was low at RT (Table 1, entries 9-12). The presence of heterogeneous catalysts, like silica (SiO_2), titania (TiO_2) and zirconia (ZrO_2) was effective and anticipated product yields at RT after 3 h were 50-68% (Table 1, entries 13-15). Amongst the heterogeneous catalysts examined, ZrO_2 was conceivable giving relatively higher yields (Table 1, entry 15). As doped metals with support will amend the activity of the catalytic substance, relative activity of Cu, Ce and V metals as active metals was examined. 2.5% metal loaded on Zr, i.e. 2.5% CuO/ZrO_2, CeO_2/ZrO_2, and V_2O_5/ZrO_2 were synthesised and was activity tested. Good to excellent yields (79-96%) were afforded by using three mixed oxide bimetallic catalysts in ethanol at RT (Table 1, entry 16-18). From the results of above three catalysts, vanadia doped zirconia proved efficient, which gave 96% yield of the target dihydropyridine compound in 15 min reaction time at RT. When effect of varied loading of V_2O_5 on ZrO_2 was examined, using 1% V_2O_5/ZrO_2 catalyst yielded 88% product in 45 min under same reaction conditions (Table 1, entry 19). An increase of metal loading (5%) led to a minor decreased yield (95%) with no benefit in reaction time (Table 1, entry 20). Finest activity was observed with 2.5% V_2O_5/ZrO_2, hence it was taken as optimum loading. This could be due to optimum dispersion of V_2O_5 on ZrO_2, when compared to the 5% V_2O_5/ZrO_2, where dispersion of vanadia was less uniform due to possible oligomerisation of vanadia particles. Thus, catalytic activity was lower compared to 2.5% loading. 2.5% loading recorded greater activity than the 1% V_2O_5/ZrO_2. Possibly, the former had more active sites than latter had insufficient sites for optimum activity. The perceived preeminence 2.5% metal oxide on zirconia could due to adequate and uniform presence of active metal oxides on surface of the support, while the superiority of V_2O_5/ZrO_2 catalyst could be due to relatively higher acidity of vanadia relative to copper oxide and ceria. Although, CuO on ZrO_2 was cheaper and next best, it was losing activity by 3rd run due to leaching of Cu.

Table 1: Optimal condition for the synthesis of **5a** by 2.5% V_2O_5/ZrO_2 catalyst [a].

Entry	Catalyst	Solvent	Condition	Time (h)	Yield (%)[b]
1	--	--	RT	12	--
2	--	--	Reflux	12	--
3	AcOH	EtOH	RT	8.0	--
4	TsOH	EtOH	RT	8.0	--
5	HCl	EtOH	RT	8.0	--
6	$FeCl_3$	EtOH	RT	8.0	--
7	$(Bmim)BF_4$	EtOH	RT	6.5	09
8	DABCO	EtOH	RT	6.0	12
9	NaOH	EtOH	RT	5.0	31
10	K_2CO_3	EtOH	RT	4.5	36
11	TEA	EtOH	RT	5.5	19
12	Pyridine	EtOH	RT	6.0	26
13	SiO_2	EtOH	RT	3.5	57
14	TiO_2	EtOH	RT	4.0	50
15	ZrO_2	EtOH	RT	3.0	68
16	2.5% CuO/ZrO_2	EtOH	RT	2.5	79
17	2.5% CeO_2/ZrO_2	EtOH	RT	1.0	88
18	2.5% V_2O_5/ZrO_2	EtOH	RT	0.15	96
19	1.0% V_2O_5/ZrO_2	EtOH	RT	0.45	88
20	5.0% V_2O_5/ZrO_2	EtOH	RT	0.15	95

[a] All products were characterised by ^{1}H-NMR, ^{15}N NMR, ^{13}C-NMR, HRMS and FT-IR spectral analysis.

[b] Isolated yields.

-- No reaction.

Based on the observations that 2.5% V_2O_5/ZrO_2 was ideal; we screened the efficancy of model reaction using different amounts of the catalyst under RT conditions (Table 2). An examination of the results in Table 2 indicate that an increase in mass of catalyst from 20 mg to 60 mg, resulted in increase of yield from 55% to 96% with decrease in reaction time. This product yield increase can be accredited to the proportional increase in the numeral of accessible active sites required for this reaction. No significant improvement in the yield of the product was perceived with further increase the catalyst amount from 60 mg to 120 mg. Thus, 60 mg of catalyst should be the most appropriate quantity of 2.5% V_2O_5/ZrO_2 with the conditions employed in this work.

Table 2: Optimization of various amounts of 2.5% V_2O_5/ZrO_2 for the model reaction [a].

Entry	Catalyst (mg)	Time (min)	Yield (%)
1	20	90	55
2	40	45	77
3	60	15	96
4	80	15	96
5	100	15	96
6	120	20	96

[a]Reaction conditions: arylaldehyde (1 mmol), 5,5-Dimethyl-1,3-cyclohexanedione (1 mmol), and aceto acetanilide (1 mmol), ammonium acetate (1 mmol) and solvent (5 mL) were stirred at room temperature.

Based on the promising results, to compare the efficiency of solvents, the title reaction was evaluated using 2.5% V_2O_5/ZrO_2 (60 mg) as catalyst was examined in the presence of various polar and non-polar solvents, and without solvent at RT condition (Table 3). The reaction did not occur under the solvent-free conditions (Table 3, entry 1). In various non-polar solvents, such as toluene and n-hexane, with no reaction was perceived (Table 3, entries 2 & 3), whereas with polar aprotic solvents, DMF and THF moderate yields were obtained (Table 3, entries 4 & 5). Interestingly, excellent yield of the product was afforded using with polar protic solvents MeOH and EtOH. The hydrophobicity of the catalyst and organic starting materials in ethanol might indorse their interaction with each other and even alteration to the desired product. Based on the criteria such as reaction times, greener approach, cost-effectiveness and excellent yields, EtOH proved to be the best solvent for the present procedure and it was used for all further investigations.

Table 3: Optimization of various solvent condition for the model reaction[a].

Entry	Solvent	Time (minutes)	Yield* (%)
1	No solvent	120	0
2	n-hexane	120	0
3	toluene	90	0
4	THF	60	2
5	DMF	60	5
6	MeOH	45	6
7	EtOH	25	13

[a]Reaction conditions: arylaldehyde (1 mmol), 5,5-Dimethyl-1,3-cyclohexanedione (1 mmol), and aceto acetanilide (1 mmol), ammonium acetate (1 mmol) and solvent (5 mL) were stirred at room temperature.

The wider efficacy and capability of the 2.5% V_2O_5/ZrO_2 catalyst was tested by using different substituted aromatic aldehydes under otherwise similar conditions and the results are summarised in Table 4. In almost all cases, good to excellent yields are obtained in very short reaction times (< 20 min), irrespective of aromatic aldehydes with electron-donating and withdrawing groups, at ortho, meta or para positions (5a-j). The outcomes were good to excellent in yields with all aromatic aldehydes, either bearing electron-withdrawing substituents or electron-donating substituents. All the products were well characterized by IR, ^{1}H NMR, ^{13}C NMR, ^{15}N NMR and HRMS. A comparison in table 5 in terms of catalytic activity of the V_2O_5/ZrO_2 with other various catalysts reported in the literature.

Table 4: Synthesis of novel functionalized 1,4-dihydropyridine derivatives by 2.5% V_2O_5/ZrO_2 catalyst[a].

Entry	**R**	**Product**	**Yield* (%)**	**Mp °C**
1	2-OMe	5a	96	210-212
2	4-OMe	5b	96	196-198
3	2-Cl	5c	90	218-220
4	2.3-OMe	5d	95	228-229
5	3,4-OMe	5e	91	235-237
6	2,4,6-OMe	5f	90	202-203
7	4-Br	5g	91	232-233
8	4-Et	5h	95	251–253
9	2-Br	5i	93	241–243
10	4-$N(CH_3)_2$	5j	92	186-189

[a]Reaction conditions: arylaldehyde (1) (1 mmol), (2) 5,5-Dimethyl-1,3-cyclohexanedione (1 mmol), and aceto acetanilide (3) (1 mmol) , ammonium acetate (1 mmol) and solvent (5 mL) were stirred at room temperature; R = substituted benzaldehydes; * = Isolated yields.

Table 5: A comparison table with various other catalysts to synthesis 1,4-dihydropyridines

Catalyst	Solvent	Reaction Conditions	Yield (%) [Ref]
I_2	EtOH	RT, 1 h,	82-92 [43]
TMSI	CH_3CN	RT, 2-3 h,	73-85 [44]
Et_3N	EtOH	Reflux, 24 h,	63-82 [45]
PEG-600	PEG-200	RT, 8-16 h,	50-85 [46]
nano-γ-Fe_2O_3-SO_3H	solvent free	Heat, 0.5-5.30 h,	90-94 [47]
[PVPH]ClO_4	Solvent free	100°C, 2-30 min,	90-96 [48]
L-proline	Solvent free	RT, 30 min,	83-96 [49]
NaOH	EtOH	RT, 8 h	75-85 [50]
2.5% V_2O_5/ZrO_2	**EtOH**	**RT, < 20 min**	**90-96[This work]**

A probable mechanism for the creation of the target molecule is illustrated in Scheme 2 [26]. The Knoevenagel reaction follows through a preliminary generation of benzylidene or imine intermediate, **(a)**, from the condensation of and acetoacetanilide, **(1)** and aromatic aldehydes, **(2)**. Further, the imine, **(a)** and 5,5-Dimethyl-1,3-cyclohexanedione, **(3)** lead to intermolecular Michael addition of carbonyl compounds facilitated by V_2O_5 doped ZrO_2 to produce another intermediate, **(5)**. Then, protonated carbonyl is attacked by the amine from ammonium acetate **(4)** to form the enamine, **(6)**. Intermediate, **(6)** further undergoes intra-molecular cyclization to finally afford functionalized 1,4-dihydropyridine derivative, **(7)**.

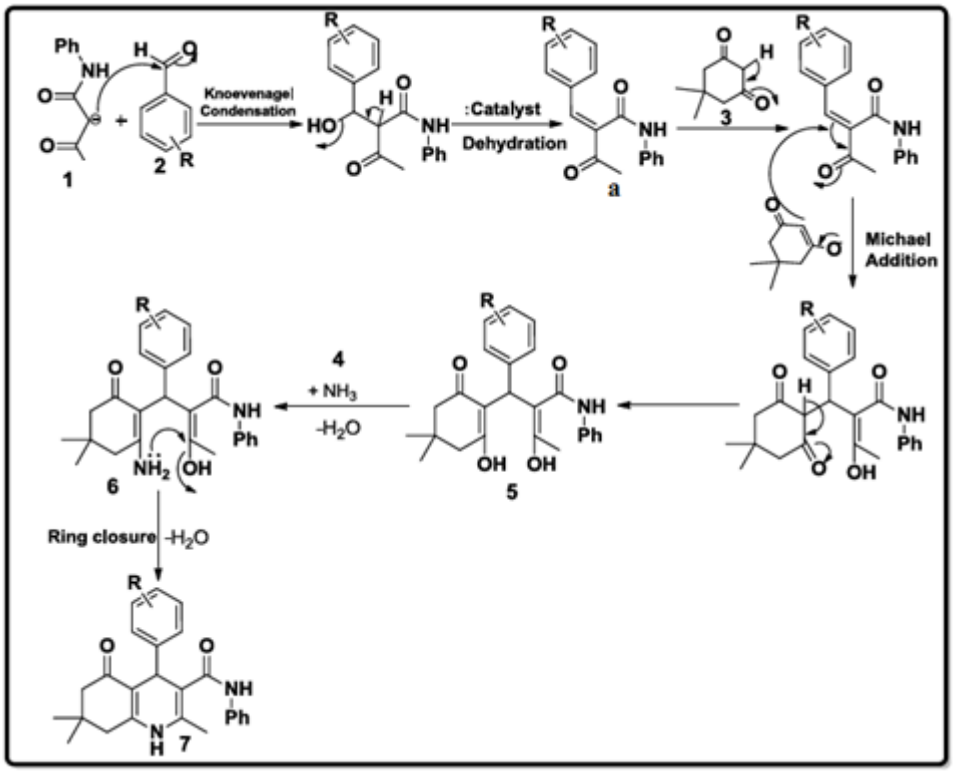

Scheme 2. Possible reaction mechanism.

2.4 Conclusions

In summary, we developed a robust and efficient recyclable catalyst, 2.5% vanadia doped zirconia to use in four-component one-pot procedure for syntheses of ten novel functionalized pyridine derivatives under green solvent conditions at RT in good to excellent yields (90-96%). The described protocol has various advantages including simple work-up, short reaction times, green solvent, impressive yields, easy purification, atom efficiency, making the procedure attractive. We believe this method will open wider catalytic applications in the fields of organic synthesis and drug discovery.

2.5 Acknowledgements

The authors are thankful to the National Research Foundation (NRF) of South Africa, and University of KwaZulu-Natal, Durban, for financial support and research facilities.

2.6 References

1. I.E. Wachs, Catal. Today. 100 (2005) 79-94.
2. Z. Guo, B. Liu, Q. Zhang, W. Deng, Y. Wang, Y. Yang, Chem. Soc. Rev. 43 (2014) 3480-3524.
3. A. Dastan, A. Kulkarnia, B. Torok, Green Chem. 14 (2012) 17-37.
4. S. Lin-Bing, L. Xiao-Qin, Z. Hong-Cai, Chem. Soc. Rev. 44 (2015) 5092-5147.
5. Q. Zhang, K.D.V. Vigier. S. Royer, F. Jerome, Chem. Soc. Rev. 41 (2012) 7108-7146.
6. M. Jabłonska, R. Palkovits, Catal. Sci. Technol. 6 (2016) 49-72.
7. J. Shi, Chem. Rev. 113 (3) (2013) 2139-2181.
8. M.J. Climent, A. Corma, S. Iborra, Chem. Rev. 111 (2011) 1072-1133.
9. I.E. Wachs, K. Routray, ACS Catal. 2 (2012) 1235-1246.
10. E.O. Oseghe, P.G. Ndungu, S.B. Jonnalagadda, Environ. Sci. & Pollution Res. 22 (2015) 211-222.
11. E.O. Oseghe, P.G. Ndungu, S.B. Jonnalagadda, J.Photochem. Photobio. A, 312 (2015) 96-106.
12. S. Maddila, E.O. Oseghe, S.B. Jonnalagadda, J. Chem. Technol. Biotec. 91 (2016) 385-393.
13. A. Ibrahim, S.B. Jonnalagadda, B.S. Martincigh, Mater. Chem. Phys. 178 (2016) 196-203.
14. V.O. Ndabankulu, S. Maddila, S.B. Jonnalagadda, Global Nest J, 18 (2016) 242-250.
15. S. Rana, S.B. Jonnalagadda, RSC Adv. 7 (2017) 2869-2879.
16. S. Maddila, S. Rana, R. Pagadala, S.B. Jonnalagadda, Res. Chem. Intermed. 41 (2015) 8269-8278.
17. S. Maddila, S. Rana, R. Pagadala, S. Kankala, S.N. Maddila, S.B. Jonnalagadda, Catal. Commun. 61 (2015) 26–30.
18. Y. Hu, S. Jin, Z. Zhang, L. Zhang, J. Deng, H. Zhang, Catal. Commun. 54 (2014) 45-49.
19. M. Sharbatdaran, F. Farzaneh, M.M. Larijani, J. Mol. Catal. A Chem. 382 (2014) 79-85.
20. R. Akkari, A. Ghorbel, N. Essayem, F. Figueras, Micropor Mesopor Mat. 111 (2008) 62-71.
21. M.K. Mishra, B. Tyagi, R. V. Jasra, J. Mol. Catal. A Chem. 223 (2004) 61-65.
22. A.H. Hoveyda, J.P. Morken, Angew. Chem. 35 (1996) 1262-1284.
23. T. Hirao, Chem. Rev. 97 (1997) 2707-2724.
24. S.N. Maddila, S. Maddila, W.E. Van Zyl, S.B. Jonnalagadda, Curr. Org. Synth. 13 (2016)

893-900.

25. R.A. Sheldon, I.W.C.E. Arends, U. Hanefeld, Green Chemistry and Catalysis, Wiley-VCH, Germany, 2007.
26. S. Maddila, S. Gorle, S. Shabalala, O. Oyetade, S.N. Maddila, P. Lavanya, S.B. Jonnalagadda, Arab. J. Chem. (2016). doi: 10.1016/j.arabjc.2016.04.016
27. R. Pagadala, S. Maddila, V. Moodley, W.E. Van Zyl, S.B. Jonnalagadda, Tetrahedron Lett. 55 (2014) 4006-4010.
28. J. Yang, C. Jiang, J. Yang, C. Qian, D. Fang, Green Chem. Lett. Rev. 6 (2013) 262-267.
29. S.N. Maddila, S. Maddila, W.E. Van Zyl, S.B. Jonnalagadda, RSC Adv. 5 (2015) 37360-37366.
30. Y. Bai, J. Zeng, J. Ma, B.K. Gorityala, X.W. Liu, J. Comb. Chem. 12 (2010) 696-699.
31. S.N. Maddila, S. Maddila, W.E. Van Zyl, S.B. Jonnalagadda, Chem. Open. 5 (2016) 38-42.
32. Z. Du, Z. Shao, Chem. Soc. Rev. 42 (2013) 1337-1378.
33. K.S. Chandra, G. Ramesh, Indian Heart J. 65 (2013) 691-695.
34. F. Shekari, H. Sadeghpour, K. Javidnia, L. Saso, F. Nazari, O. Firuzi, R. Miri, Eur.J.Pharmacol.746 (2015)233-244.
35. F. Lentz, M. Hemmer, N. Reiling, A. Hilgeroth, Bioorg. Med. Chem. Lett. 26 (2016) 5896-5898.
36. A.M. Vijesh, A.M. Isloor, S.K. Peethambar, K.N. Shivananda, T. Arulmoli, N.A. Isloor, Eur. J. Med. Chem. 46 (2011) 5591-5597.
37. R.S. Kumar, A. Idhayadhulla, A.J. Abdul Nasser, J. Selvin, Eur. J. Med. Chem. 46 (2011) 804-810.
38. J.Q. Reimão, M.T. Scotti, A.G. Tempone, Bioorganic Med. Chem. 18 (2010) 8044-8053.
39. M. Khoshneviszadeh, N. Edraki, K. Javidnia, A. Alborzi, B. Pourabbas, J. Mardaneh, R. Miri, Bioorganic Med. Chem. 17 (2009) 1579-1586.
40. A. Hilgeroth, H. Lilie, Eur. J. Med. Chem. 38 (2003) 495-499.
41. G. Díaz-Araya, L. Godoy, L. Naranjo, A. Squella, M.E. Letelier, L.J. Núñez-Vergara, Gen. Pharmacol. Vasc. Syst. 31 (1998) 385-391.
42. A. Hantzsch, A. Hantzsch, Chem. Ber. 14 (1881) 1637.
43. S. Ko, M.N.V. Sastry, C. Lin, C.F. Yao, Tetrahedron Lett. 46 (2005) 5771-5774.
44. G. Sabitha, G.S.K.K. Reddy, C.S. Reddy, J.S. Yadav, Tetrahedron Lett. 44 (2003) 4129-4131.
45. J. Sun, E.Y. Xia, Q. Wu, C.G. Yan, Org. Lett. 12 (2010) 3678-3681.

46. S. Pal, V. Singh, P. Das, L.H. Choudhury, Bioorg. Chem. 48 (2013) 8-15.
47. S. Otokesh, N. Koukabi, E. Kolvari, A. Amoozadeh, M. Malmir, S. Azhari, S. Afr. J. Chem, 68 (2015) 15–20.
48. M. Abedini, F. Shirini, M. Mousapour, Res Chem. Intermed. DOI 10.1007/s11164-015-2150-y.
49. A. Kumar, R. A. Maurya, Tetrahedron 63 (2007) 1946–1952.
50. S. Pal, L.H. Choudhury, T. Parvin. Syn. Commun. 43 (2013) 986–992.
51. S. Maddila, K.K. Gangu, S.N. Maddila, S.B. Jonnalagadda, Mol. Divers. 21 (2017) 247-255.
52. S. Shabalala, S. Maddila, W.E. Van Zyl, S.B. Jonnalagadda, Catal. Commun. 79 (2016) 21-25.
53. S.N. Maddila, S. Maddila, K.K. Gangu, W.E. van Zyl, S.B. Jonnalagadda, J. Flu. Chem.195 (2017) 79-84.
54. K.K. Gangu, S. Maddila, S.N. Maddila, S.B. Jonnalagadda, RSC Adv. 7 (2017) 423-432.
55. N. Shabalala, S. Maddila and S. B. Jonnalagadda, New. J. Chem. 40 (2016) 5107-5112.
56. S.N. Maddila, S. Maddila, W.E. Van Zyl, S.B. Jonnalagadda, Curr. Org. Chem. 20 (2016) 2125-2133.
57. K.K. Gangu, S. Maddila, S.N. Maddila, S.B. Jonnalagadda, Molecules. 21 (2016) 1281-1296.
58. N. Shabalala, S. Maddila, S.B. Jonnalagadda, Res. Chem. Intermed. 42 (2016) 8097-8108.
59. S. Gorle, S. Maddila, S.N. Maddila, K. Naicker, M. Singh, P. Singh, S.B. Jonnalagadda, Anticancer Agents Med. Chem. 17 (2017) 464-470.
60. S. Maddila, K. Naicker, S. Gorle, S. Rana, Y. Kotaiah, S.N. Maddila, M. Singh, P. Singh, S.B. Jonnalagadda, Anticancer Agents Med. Chem. 16(8) (2016) 1031-1037.
61. S. Maddila, K. Naicker, M. Momin, S. Rana, S. Gorle, S.N. Maddila, Y. Kotaiah, M. Singh, S.B. Jonnalagadda, Med. Chem. Res. 25 (2016) 283-291.
62. S. Maddila, M. Momin, S. Gorle, P. Lavanya, S.B. Jonnalagadda, J Chil Chem Soc. 60(2) (2015) 2774-2778.
63. S. Gorle, S. Maddila, S. Chokkakula, P. Lavanya, M. Singh, S.B. Jonnalagadda, J. Heterocyclic. Chem. 53 (2016) 1852-1858.
64. S. Maddila, R. Pagadala, S.B. Jonnalagadda, Lett. Org. Chem. 10 (2013) 693-714.

65. S. Maddila, V.D.B.C. Dasireddy, S.B. Jonnalagadda, Appl. Catal. B: Env. 150-151(2014) 305-314.
66. S. Maddila, V.D.B.C. Dasireddy, S.B. Jonnalagadda, Appl. Catal. B: Env. 138-139 (2013)149-160.
67. E.C. Chetty, S. Maddila, C. Southway, S.B. Jonnalagadda, ACS- Ind. Eng. Chem. Res. 51 (2012) 2864-2873.
68. S. Shabalala, S. Maddila, W. E. van Zyl, S.B. Jonnalagadda, Catal. Commun. 79 (2016) 21-25.
69. S.N. Maddila, S. Maddila, W.E. van Zyl, S.B. Jonnalagadda, ChemistryOpen 5 (2016) 38-42.

2.7 Supplementary information

2.7.1 Catalyst instrumentation details

Employing a Bruker D8 Advance instrument (Cu K radiation source with a wave length of 1.5406 Å), the X-ray diffraction data related the structural phases of the catalyst were acquired. Using a JEOL JEM-1010 electron microscope and JEOL JSM-6100 microscope, the TEM and SEM analysis data was recorded. iTEM software was used analyse the TEM data and images. Employing the X-ray analyser (energy-dispersive), EDX-analysis on the SEM images was conducted.

2.7.2 Experimental Section

All chemicals and reagents required for the reaction were of analytical grade and were used without any further purification. Bruker AMX 400 MHz NMR spectrometer was used to record the ^{1}H NMR, ^{13}C NMR and ^{15}N NMR spectral values. High-resolution mass data were obtained using a Bruker micro TOF-Q II ESI instrument operating at ambient temperature. The $CDCl_3{-}d_6$ solution was utilized for this while TMS served as the internal standard. TMS was further used as an internal standard for reporting the all chemical shifts in δ (ppm). Purity of all the reaction products was confirmed by TLC using aluminium plates coated with silica gel (Merck Kieselgel 60 F_{254}).

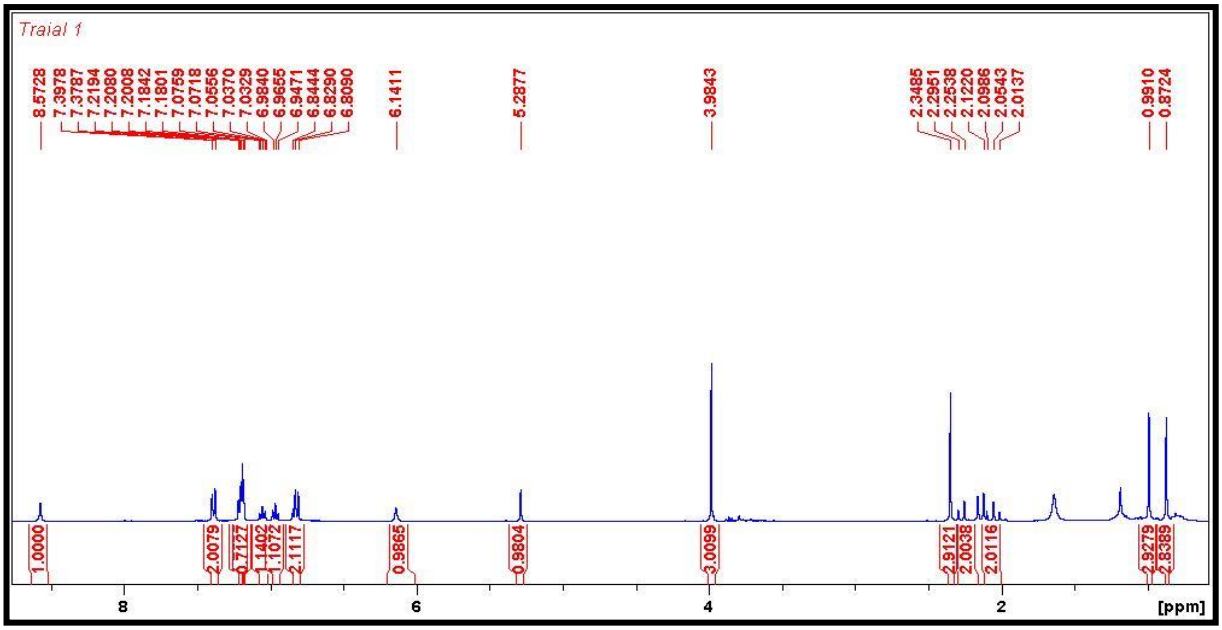

Fig.S1 ^{1}H NMR spectra of compound **5a**

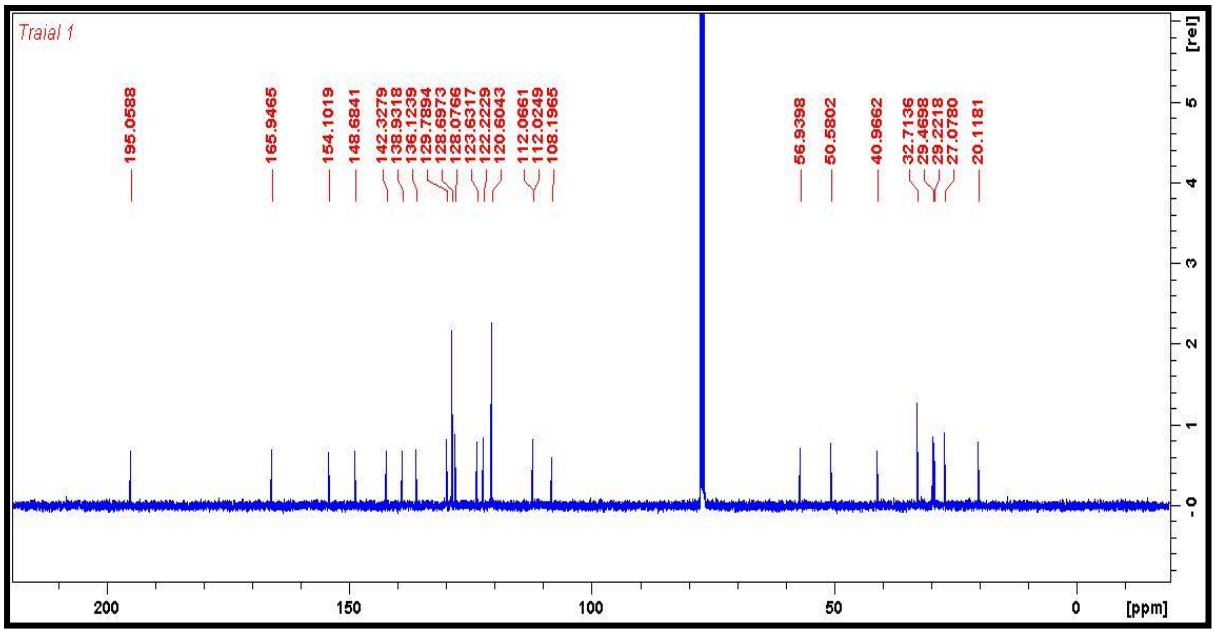

Fig.S2 ^{13}C NMR spectra of compound **5a**

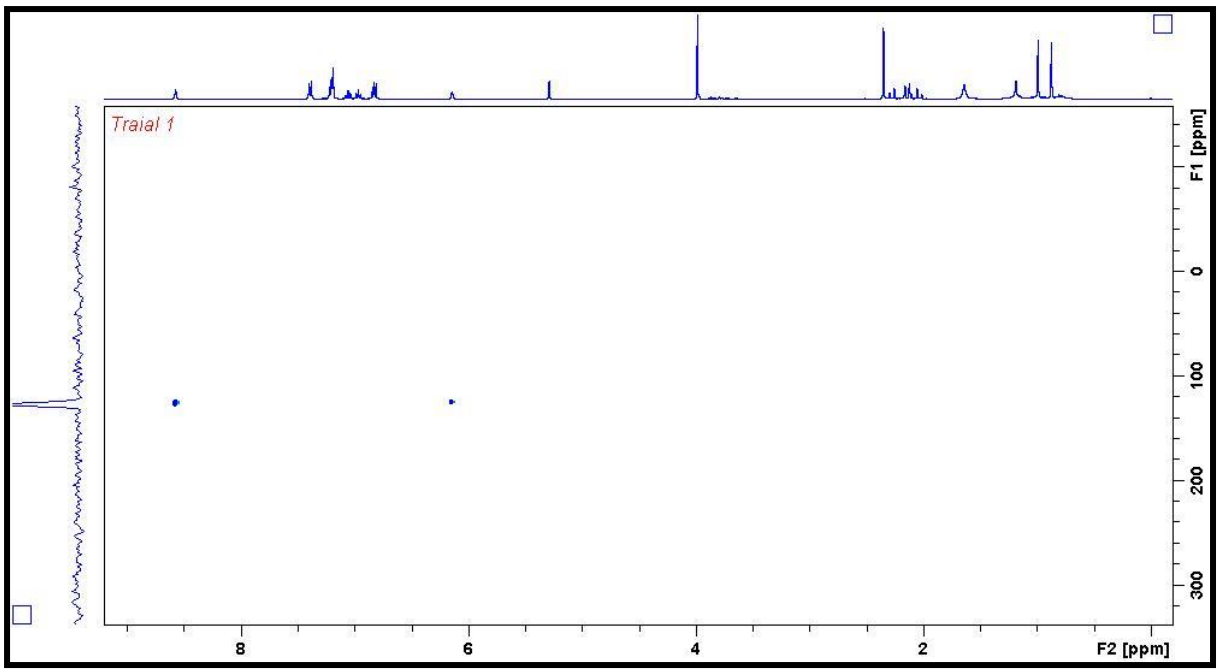

Fig.3 ^{15}N NMR spectra of compound **5a**

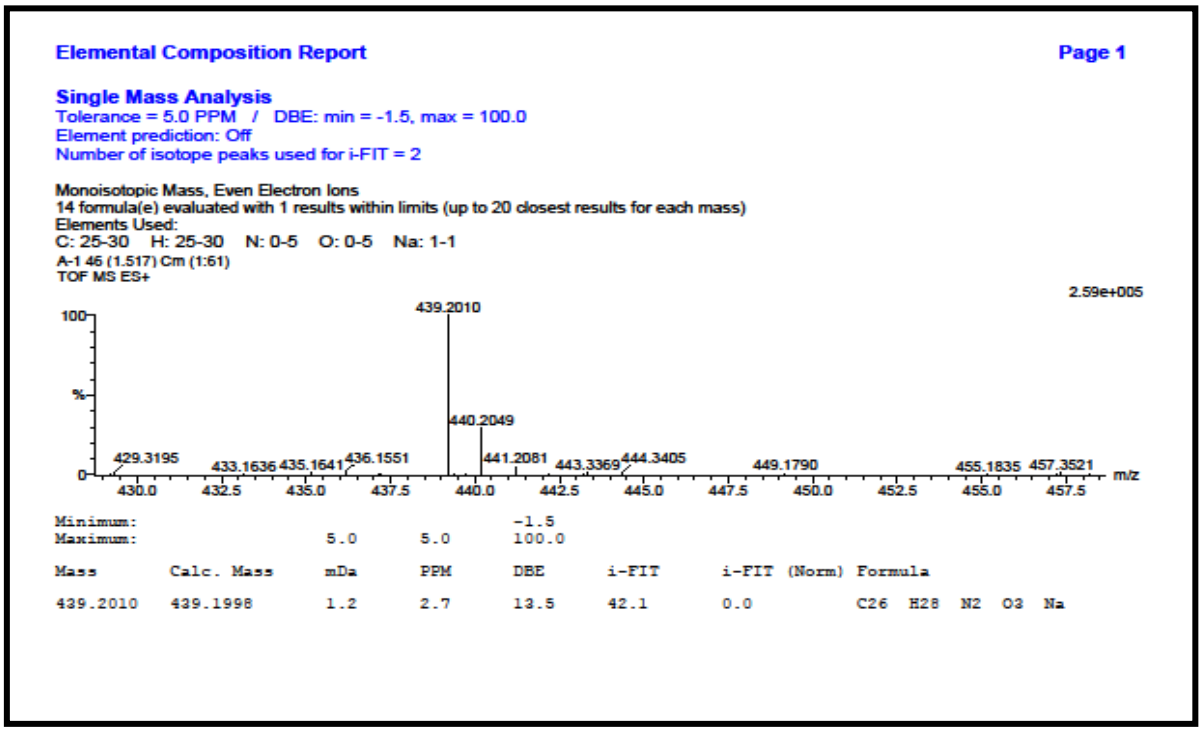

Fig.4 HRMS spectra of compound **5a**

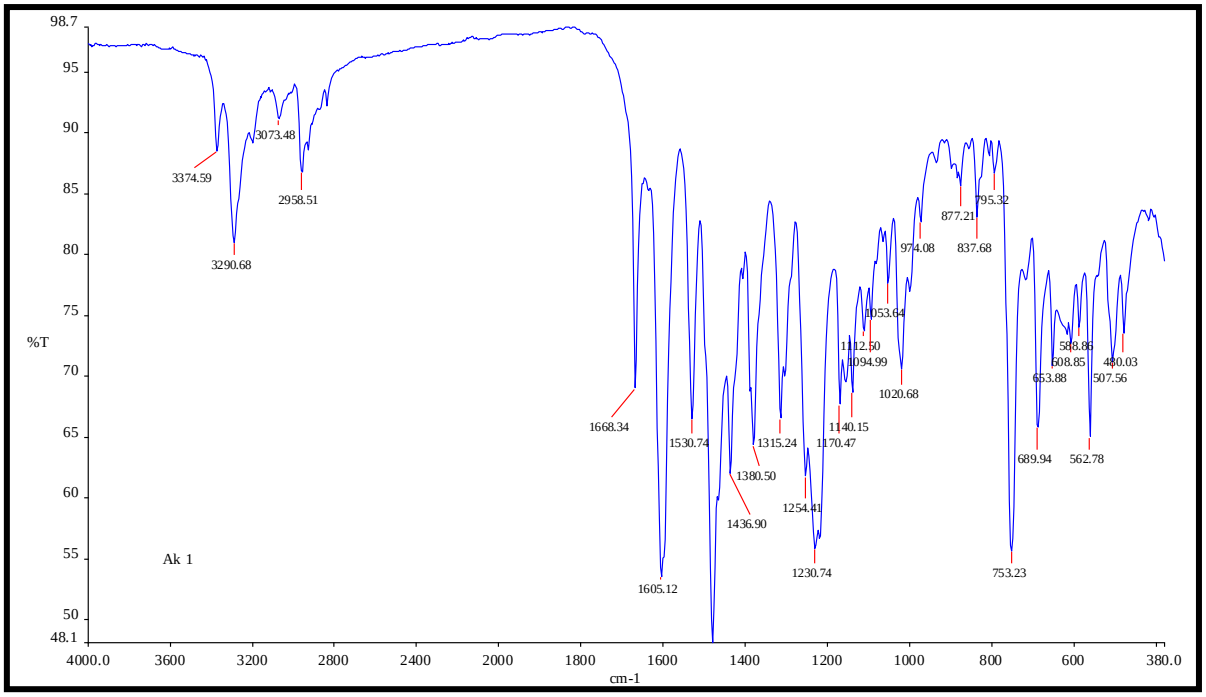

Fig.5 FT-IR spectra of compound **5a**

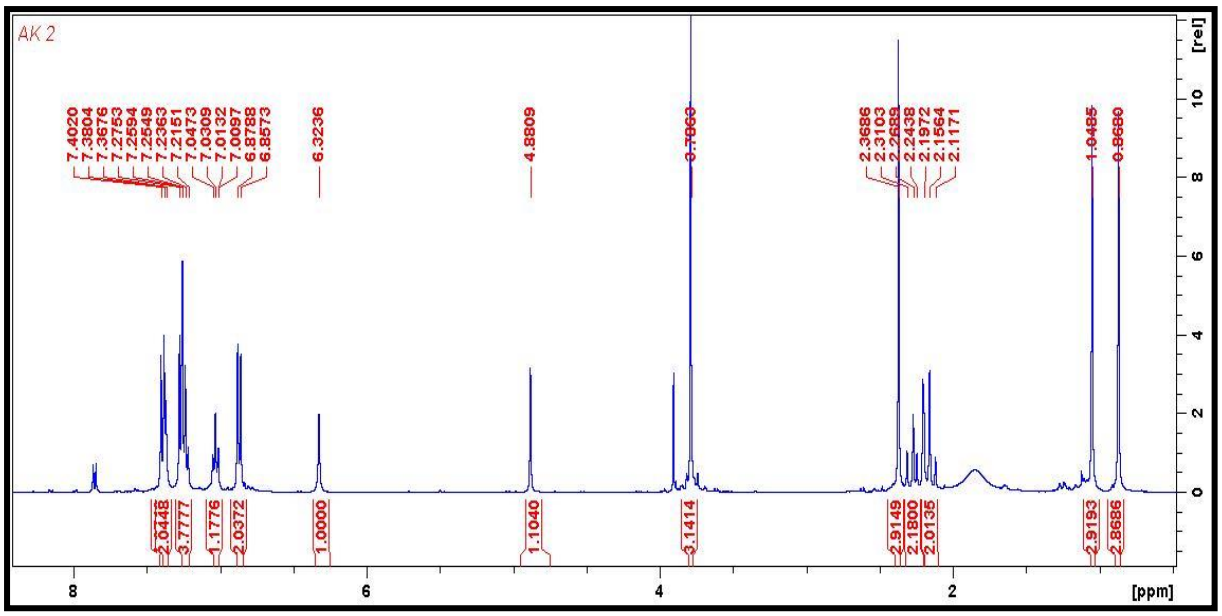

Fig.6 ^{1}H NMR spectra of compound **5b**

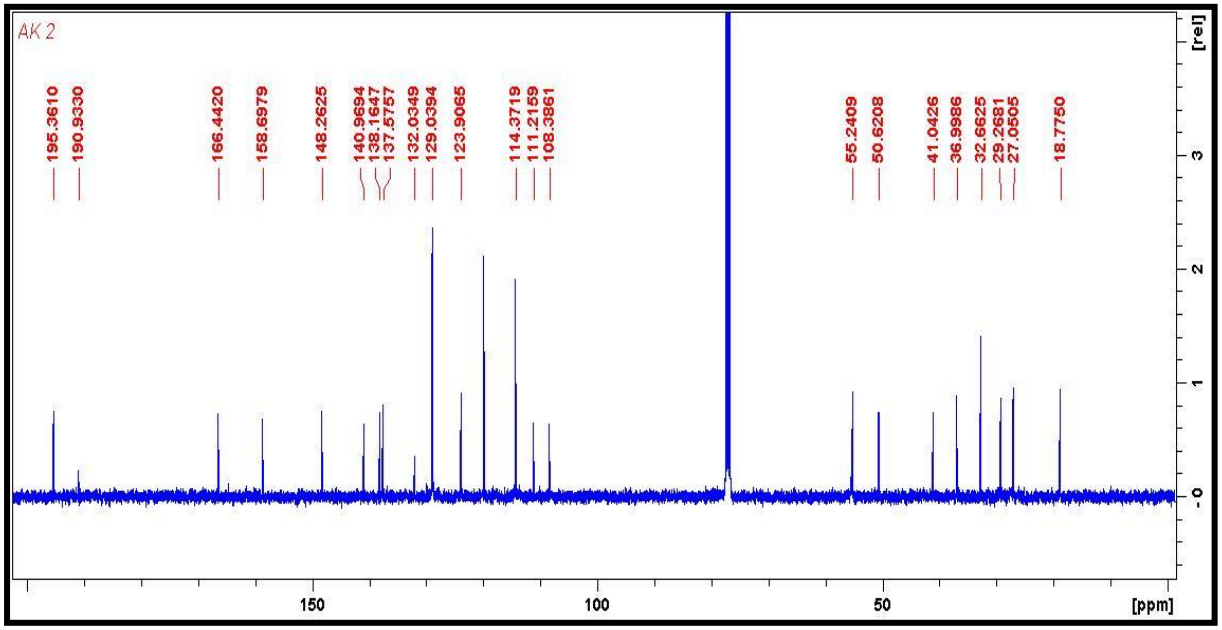

Fig.7 ^{13}C NMR spectra of compound **5b**

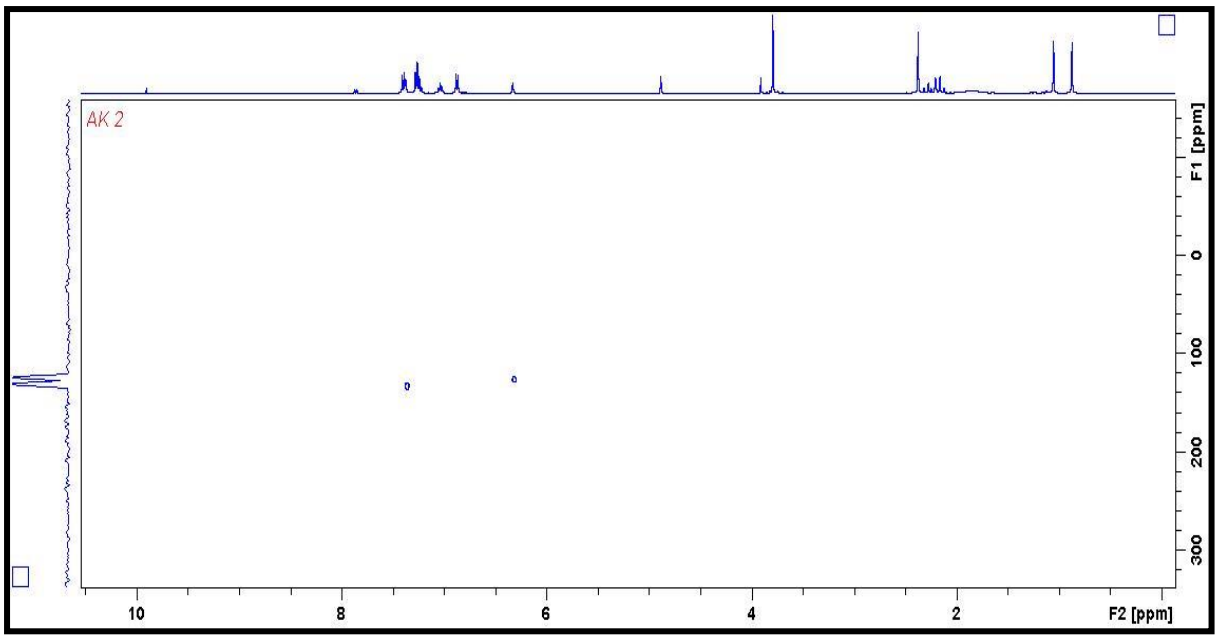

Fig.8 ^{15}N NMR spectra of compound **5b**

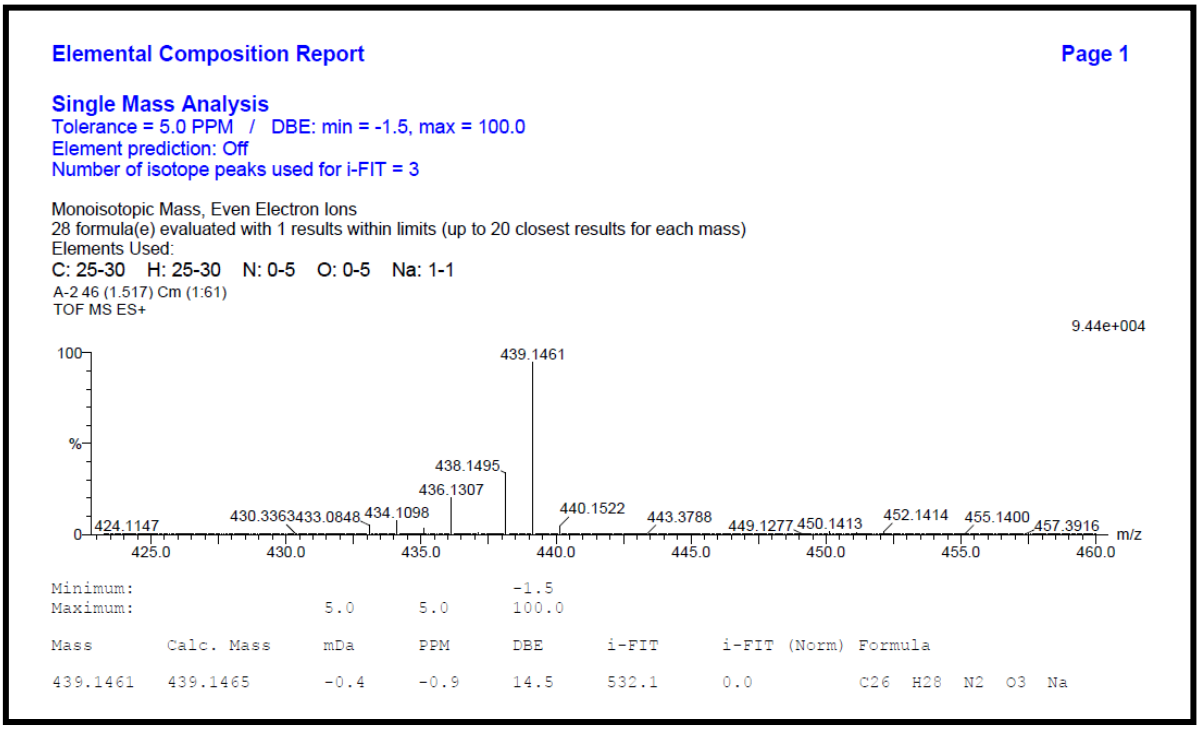

Fig.9 HRMS spectra of compound **5b**

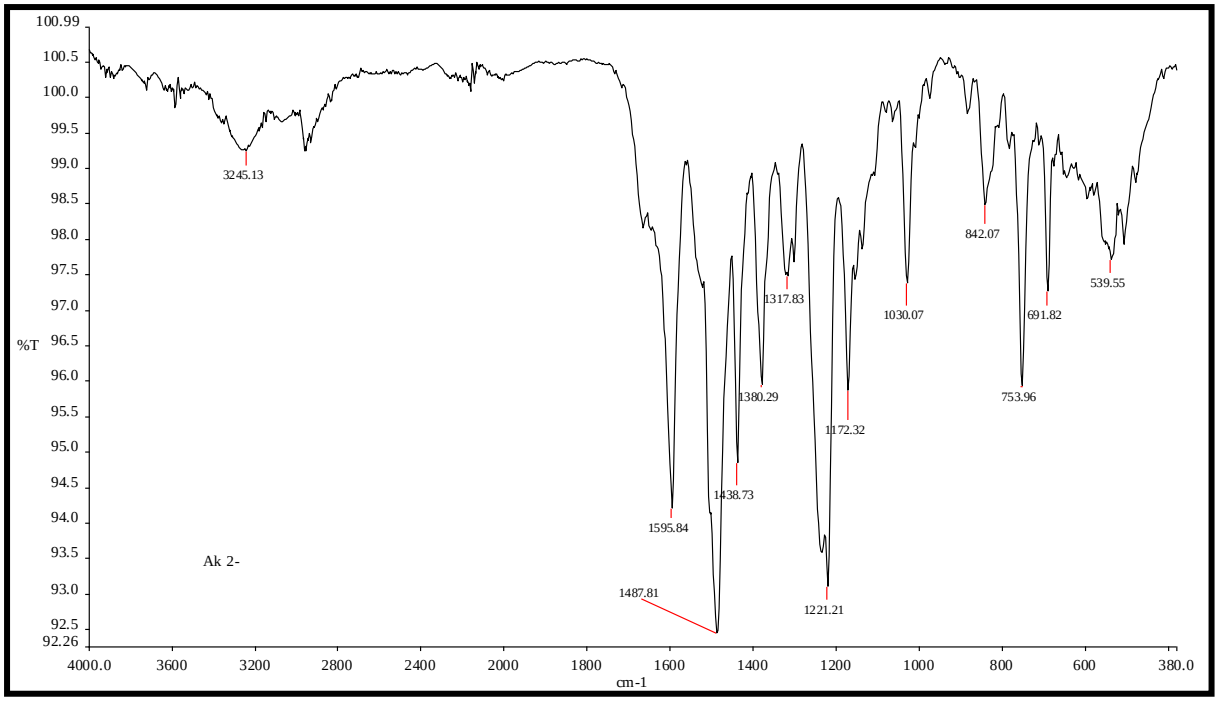

Fig.10 FT-IR spectra of compound **5b**

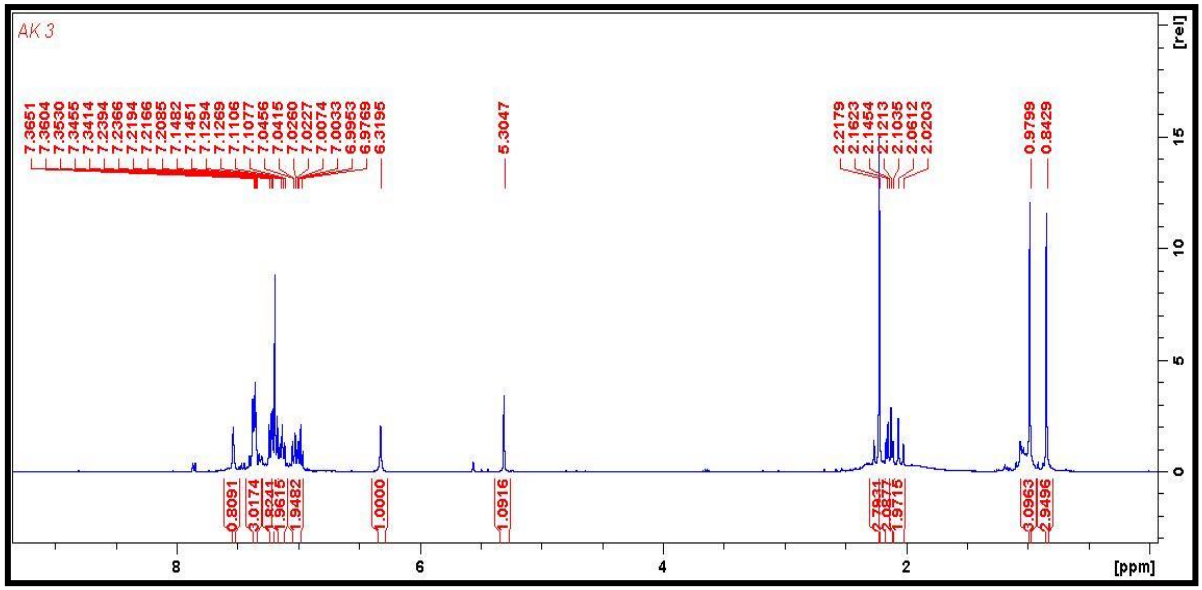

Fig.11 ^{1}H NMR spectra of compound **5c**

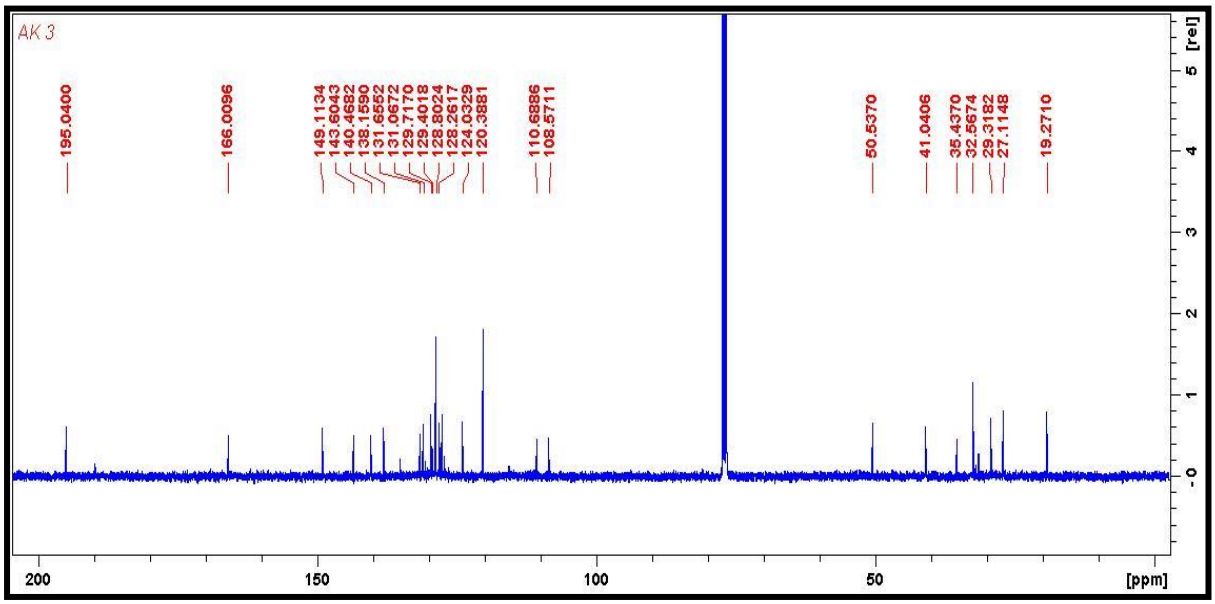

Fig.12 ^{13}C NMR spectra of compound **5c**

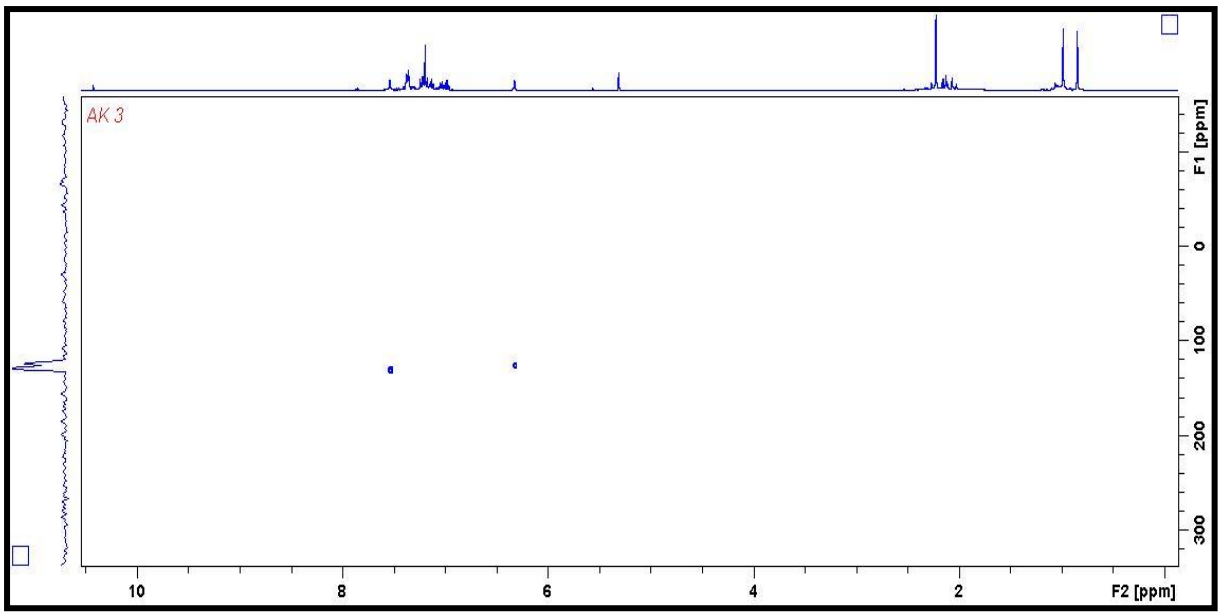

Fig.13 ^{15}N NMR spectra of compound **5c**

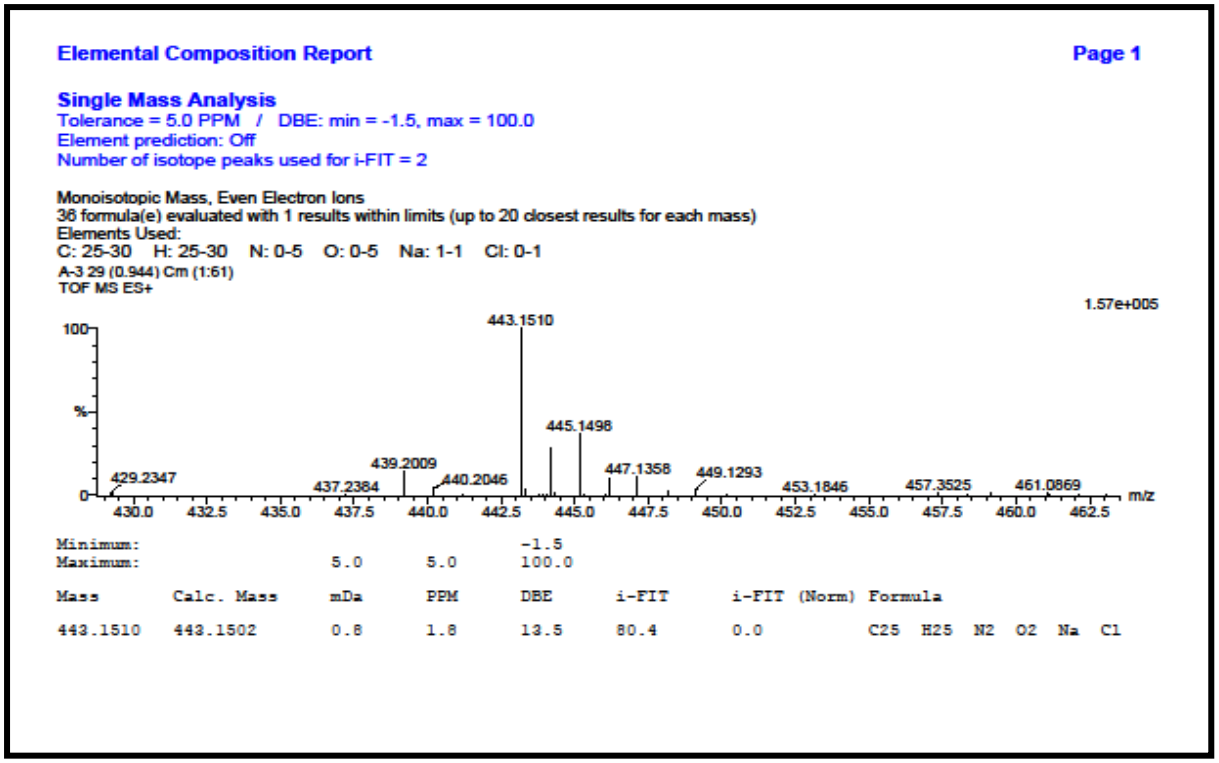

Fig.14 HRMS spectra of compound **5c**

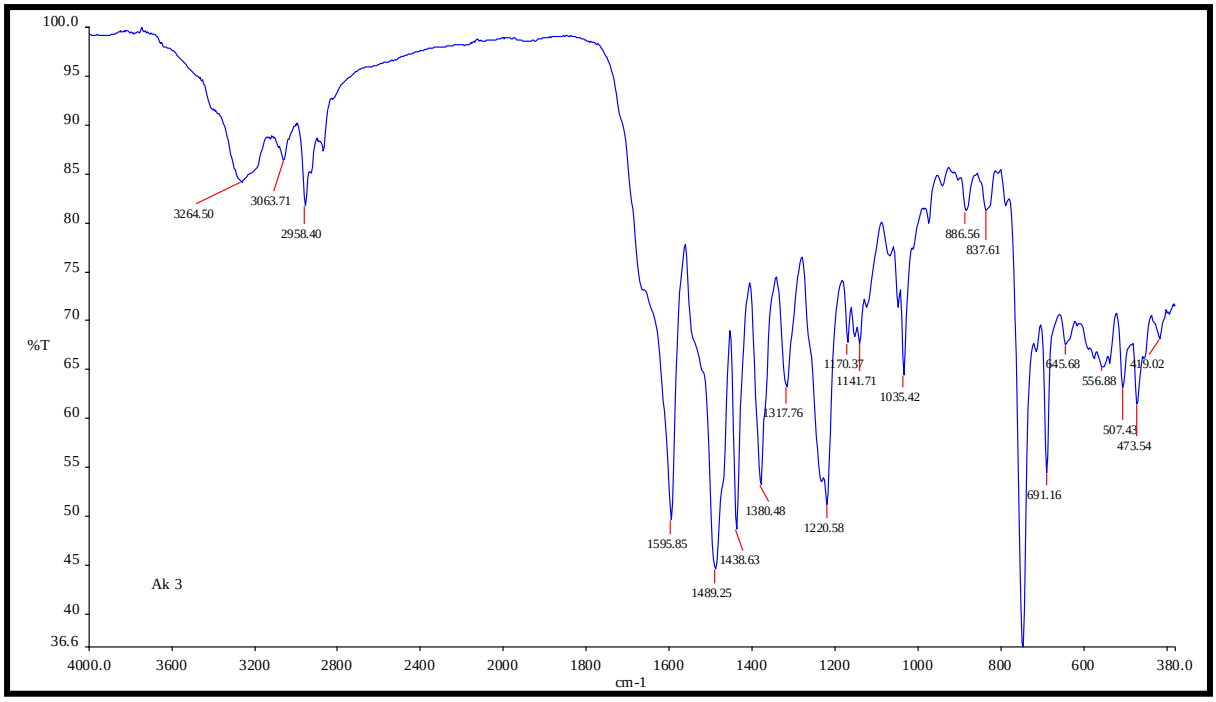

Fig.15 FT-IR spectra of compound **5c**

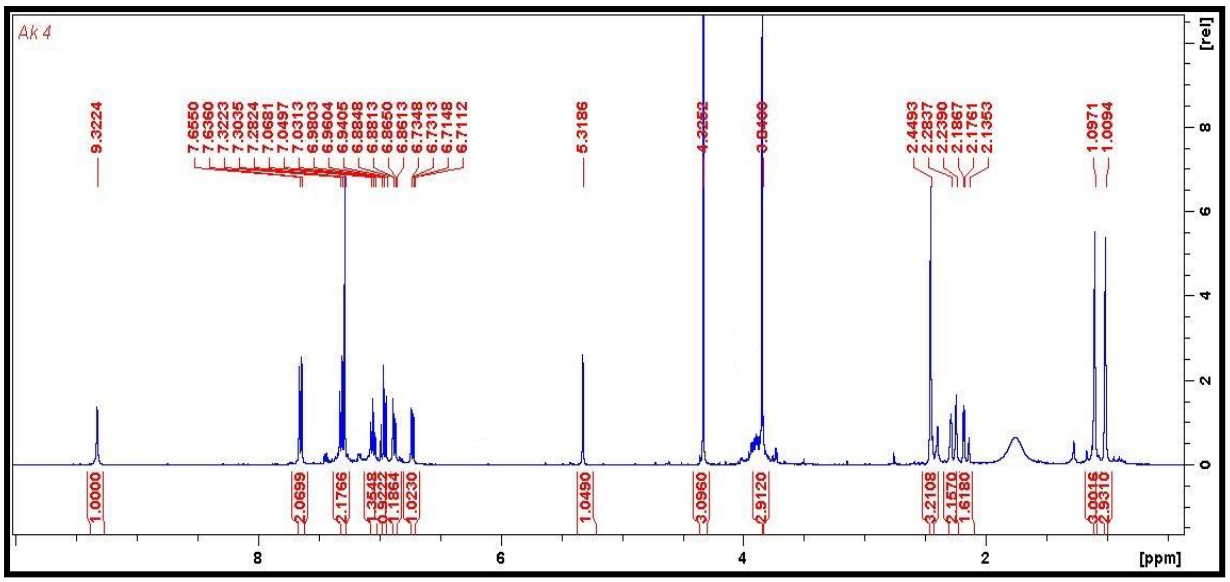

Fig.16 ^{1}H NMR spectra of compound **5d**

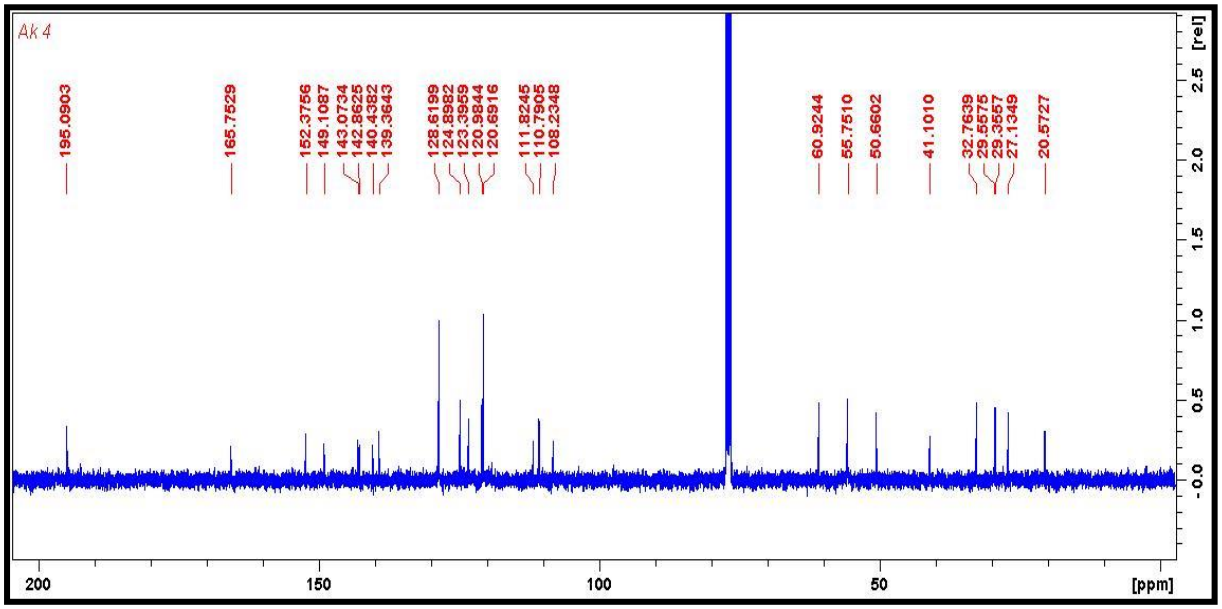

Fig.17 ^{13}C NMR spectra of compound **5d**

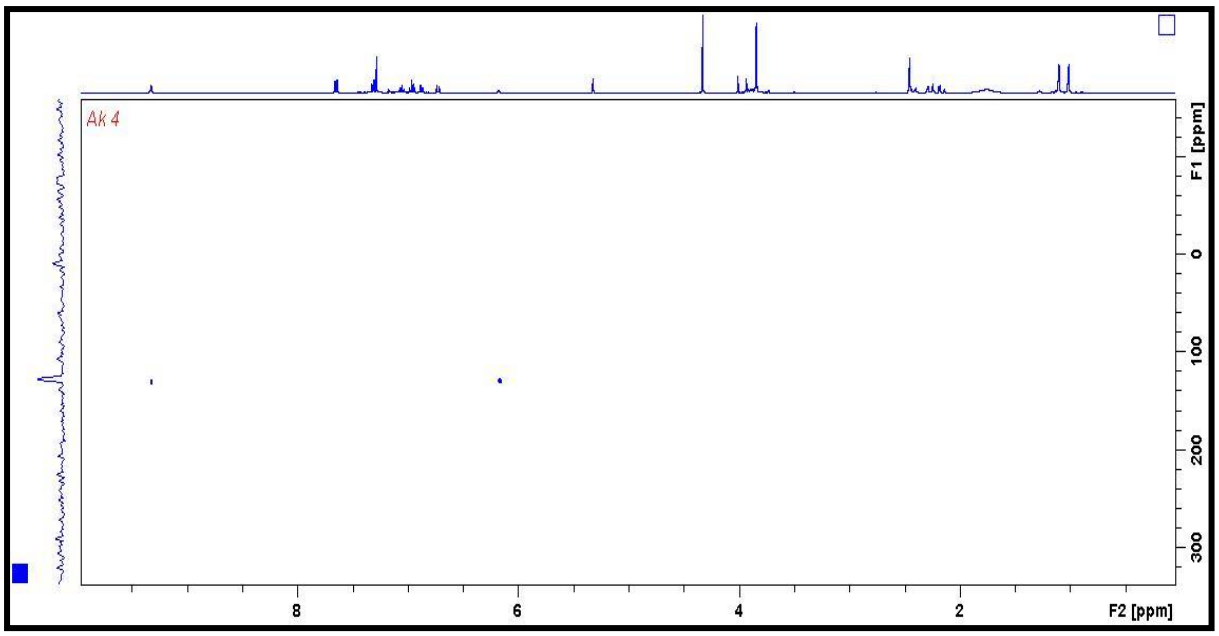

Fig.18 ^{15}N NMR spectra of compound **5d**

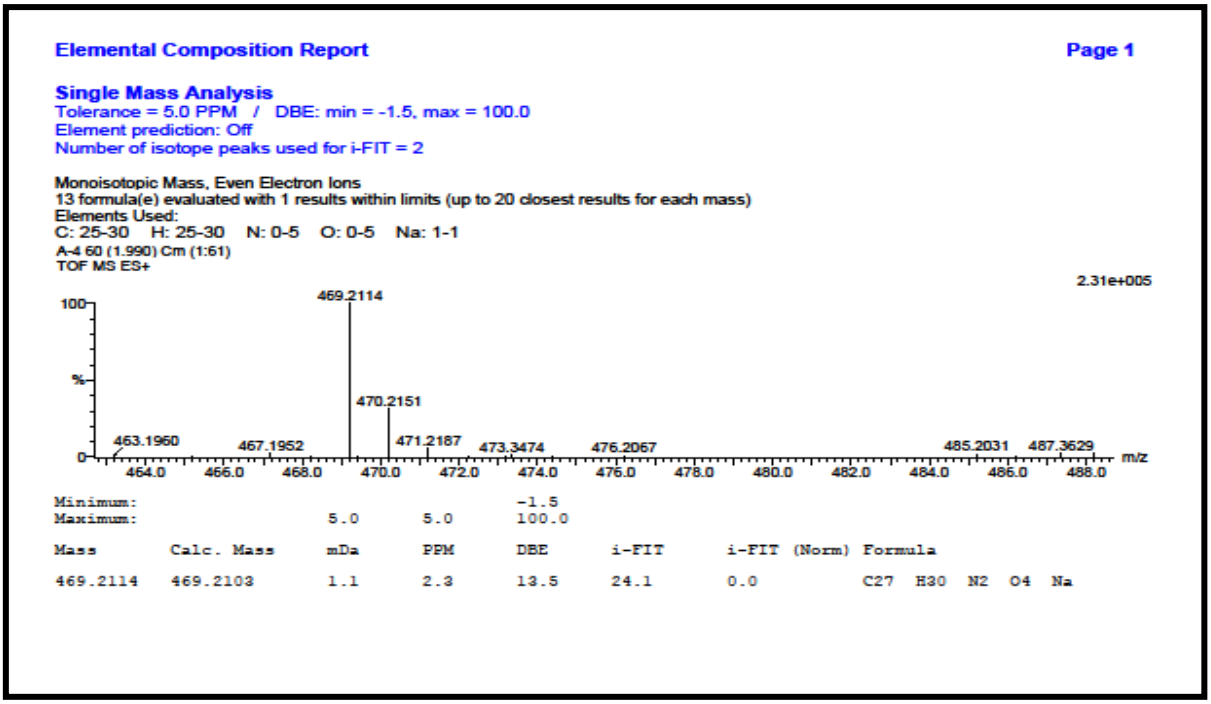

Fig.19 HRMS spectra of compound **5d**

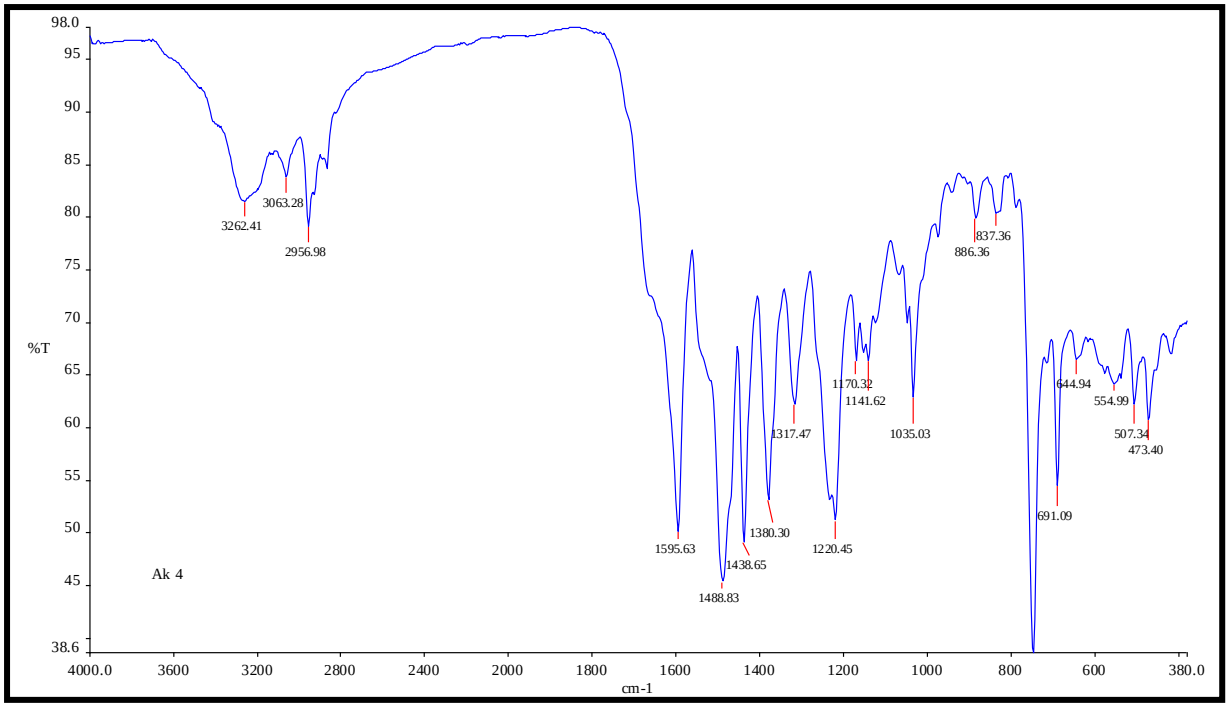

Fig.20 FT-IR spectra of compound **5d**

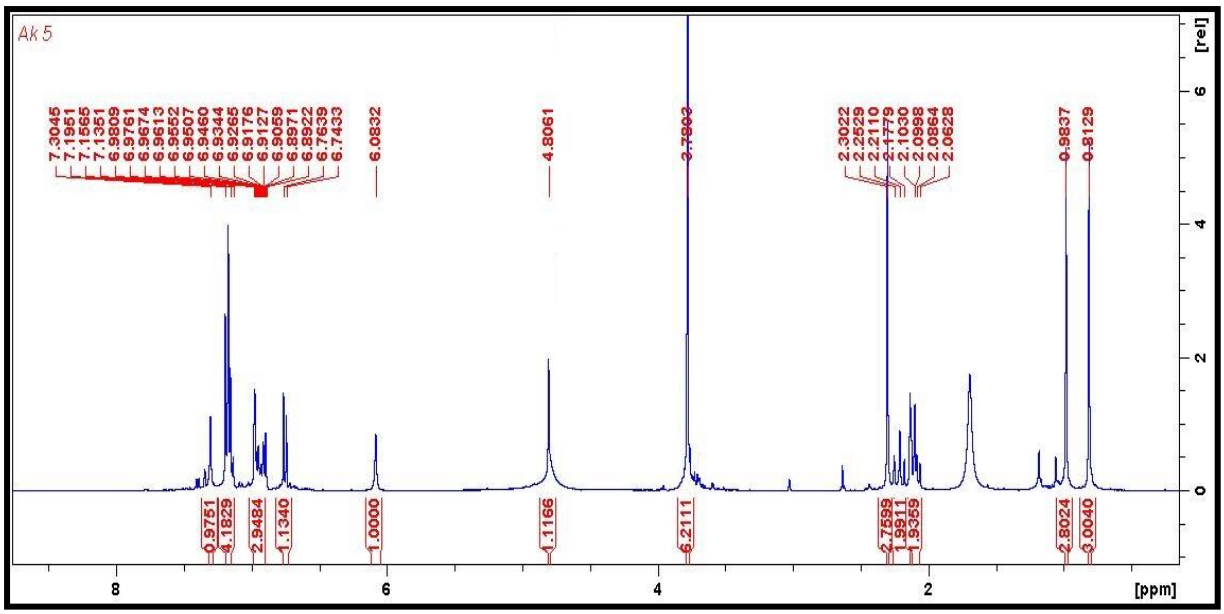

Fig.21 ^{1}H NMR spectra of compound **5e**

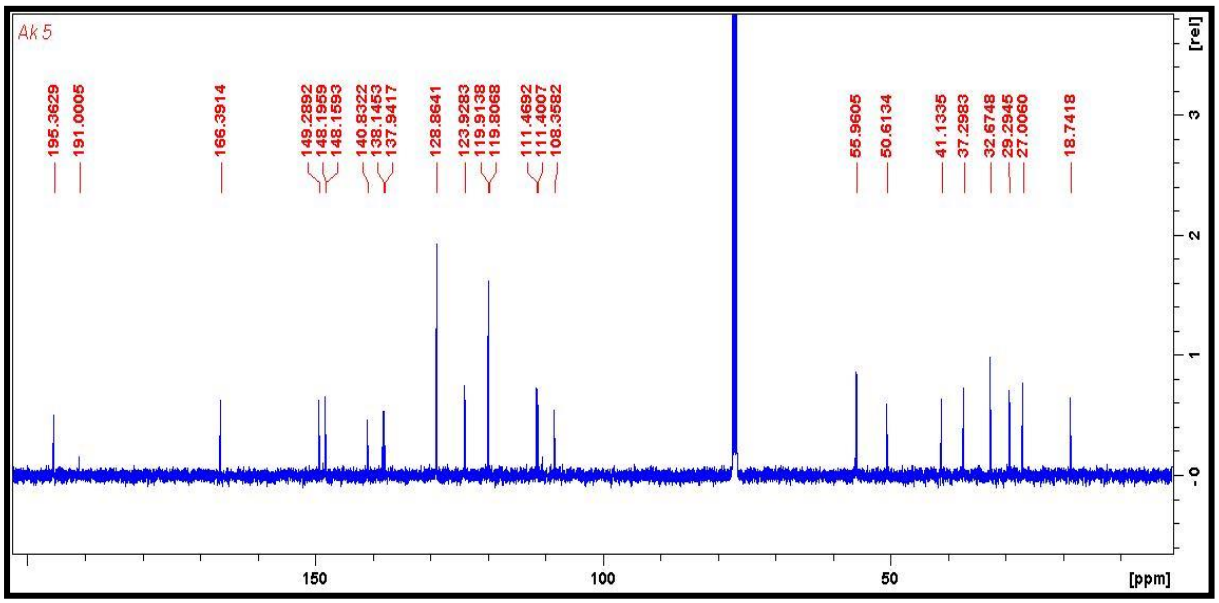

Fig.22 ^{13}C NMR spectra of compound **5e**

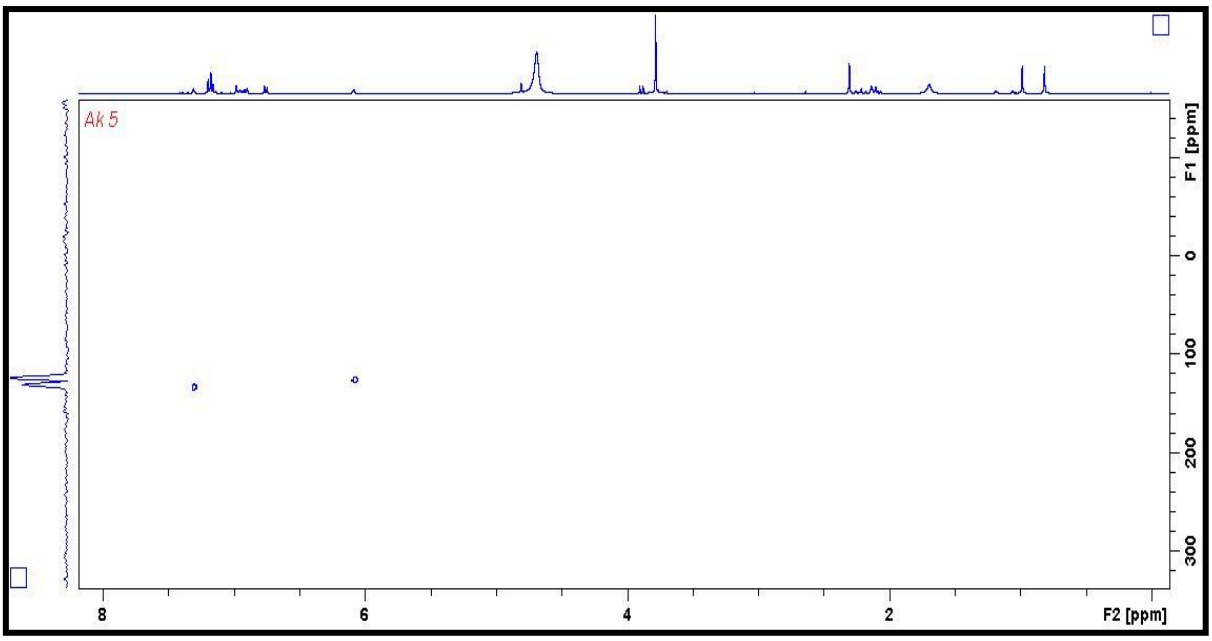

Fig.23 ^{15}N NMR spectra of compound **5e**

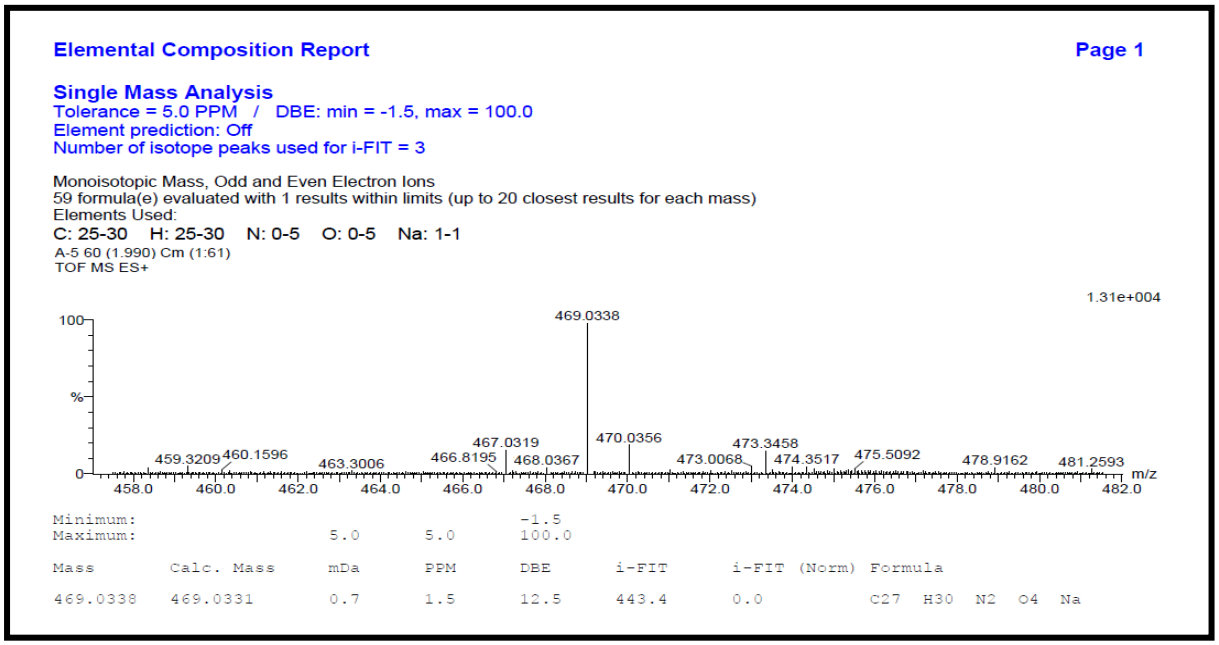

Fig.24 HRMS spectra of compound **5e**

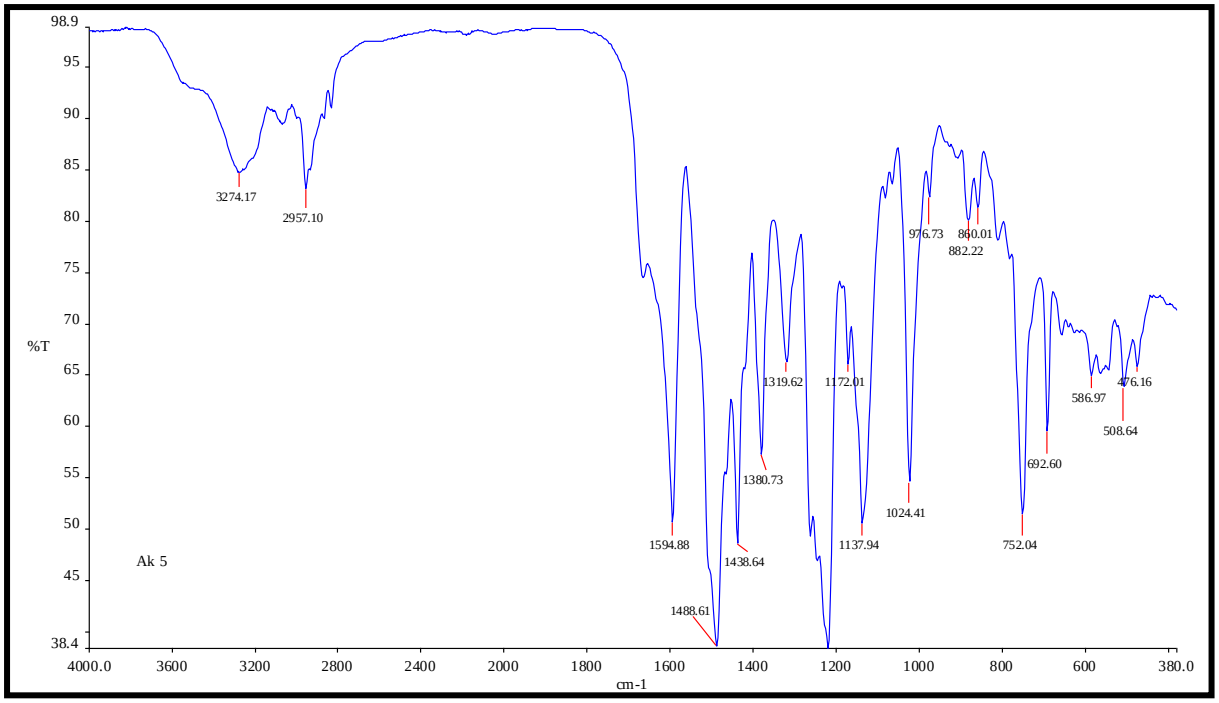

Fig.25 FT-IR spectra of compound **5e**

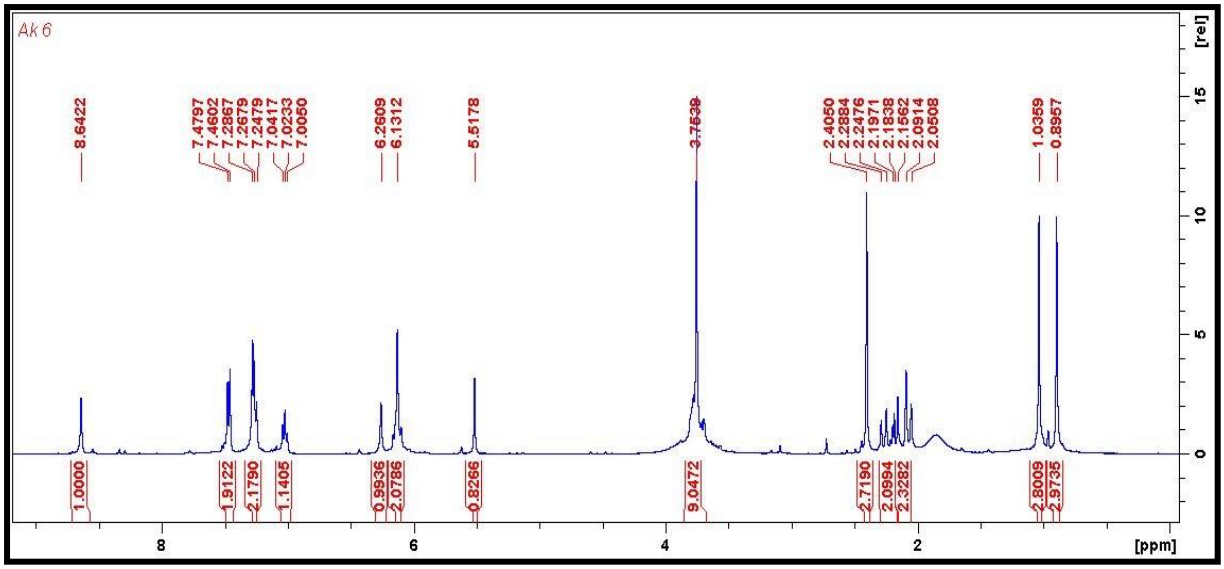

Fig.26 ^{1}H NMR spectra of compound **5f**

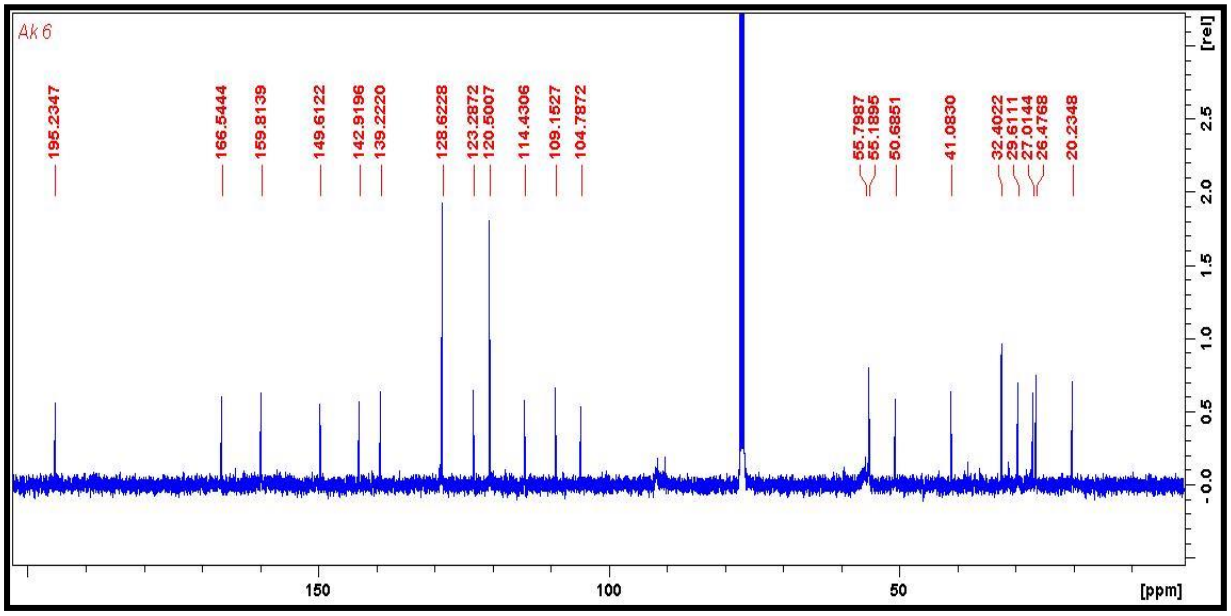

Fig.27 ^{13}C NMR spectra of compound **5f**

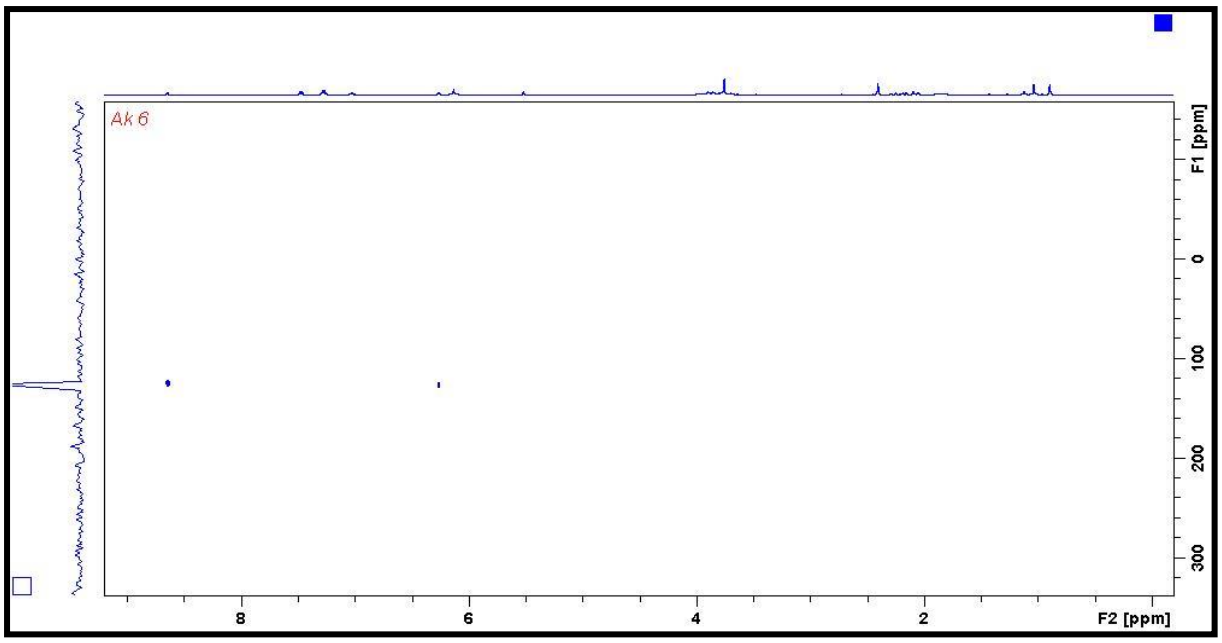

Fig.28 ^{15}N NMR spectra of compound **5f**

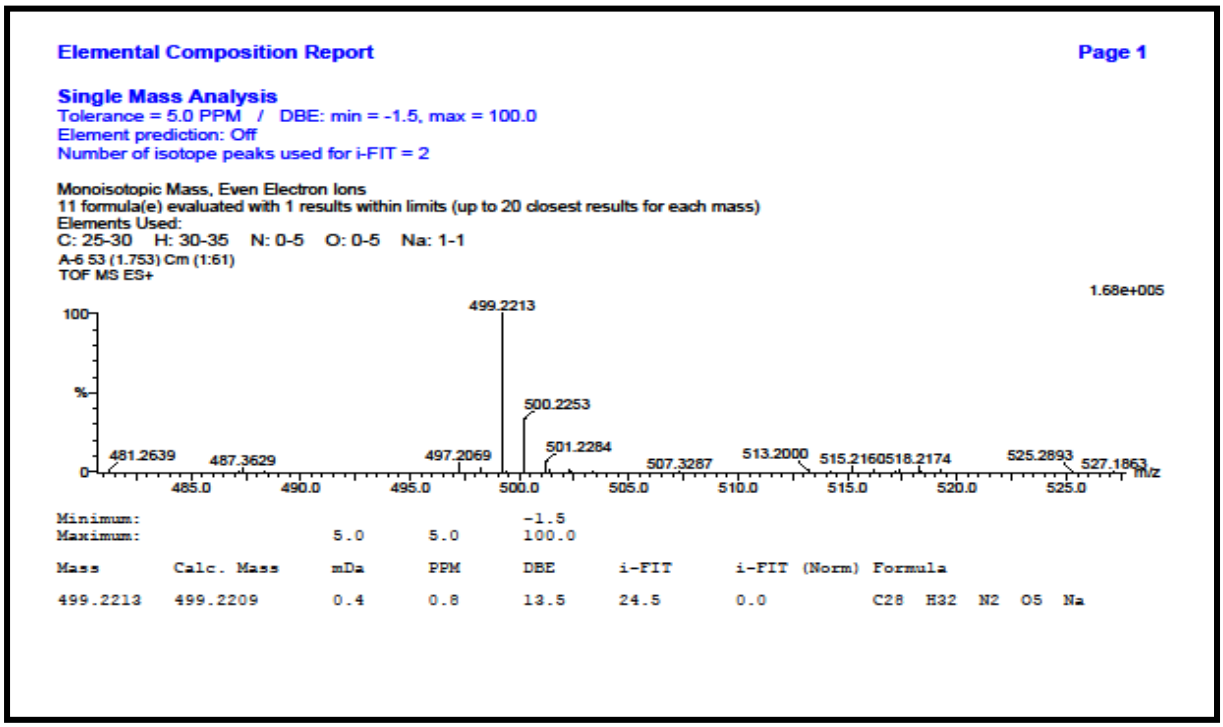

Fig.29 HRMS spectra of compound **5f**

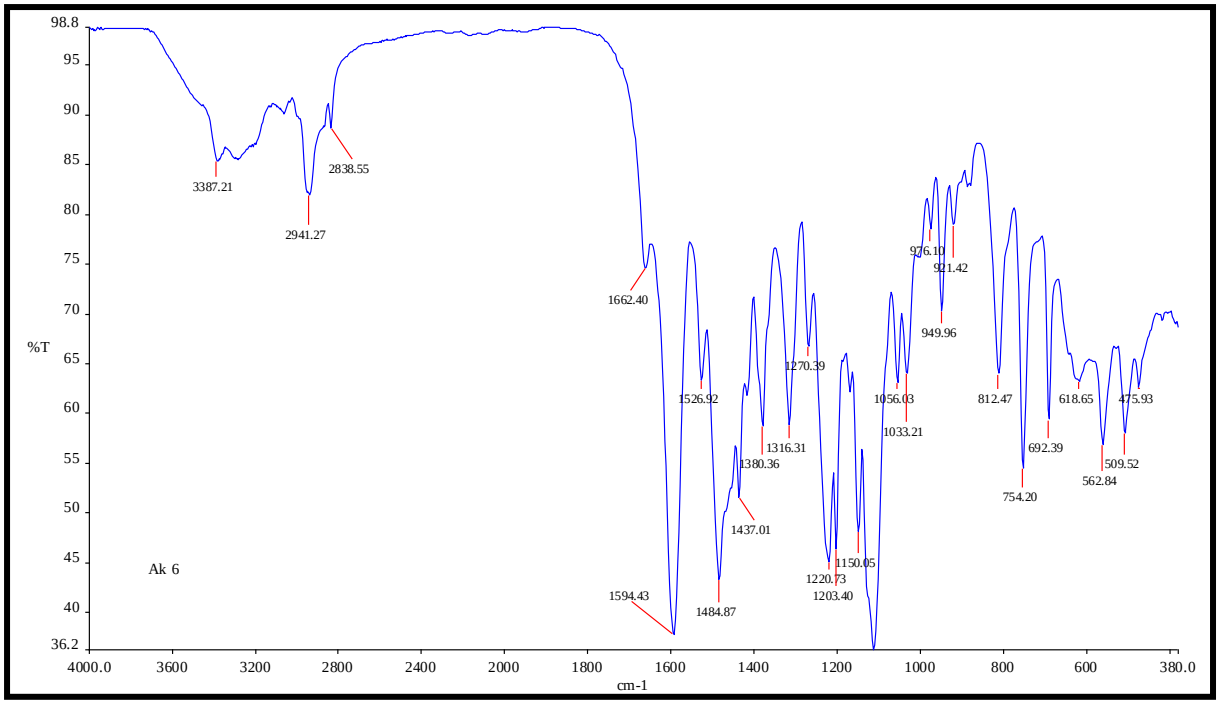

Fig.30 FT-IR spectra of compound **5f**

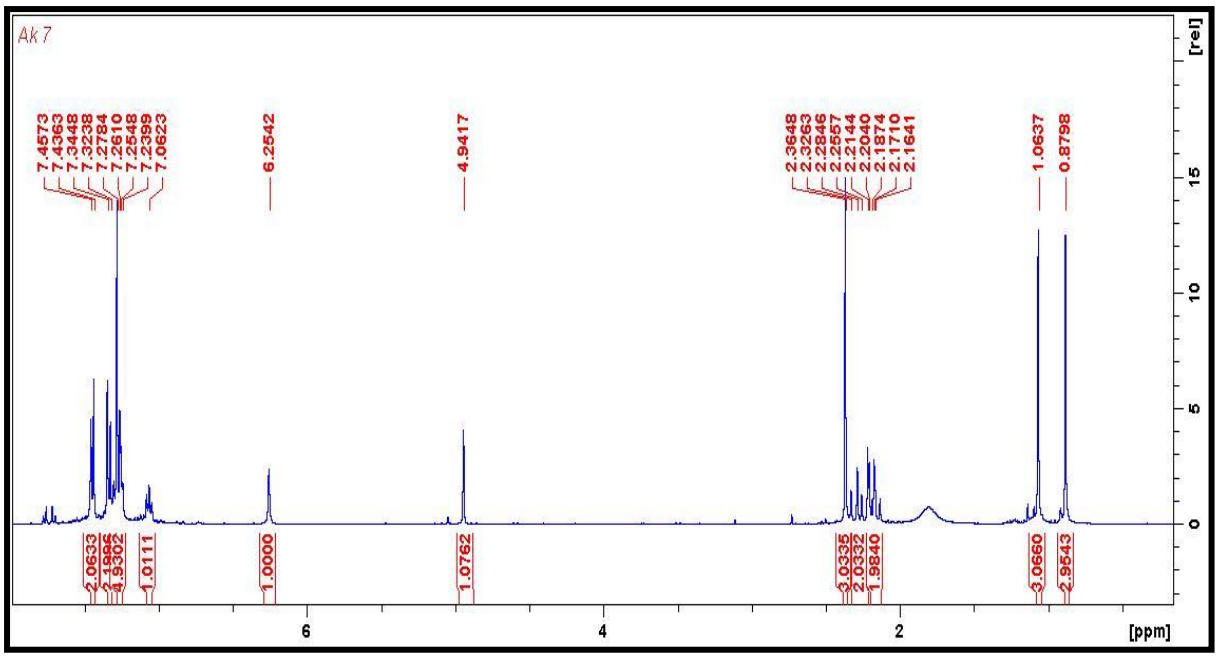

Fig.31 ^{1}H NMR spectra of compound **5g**

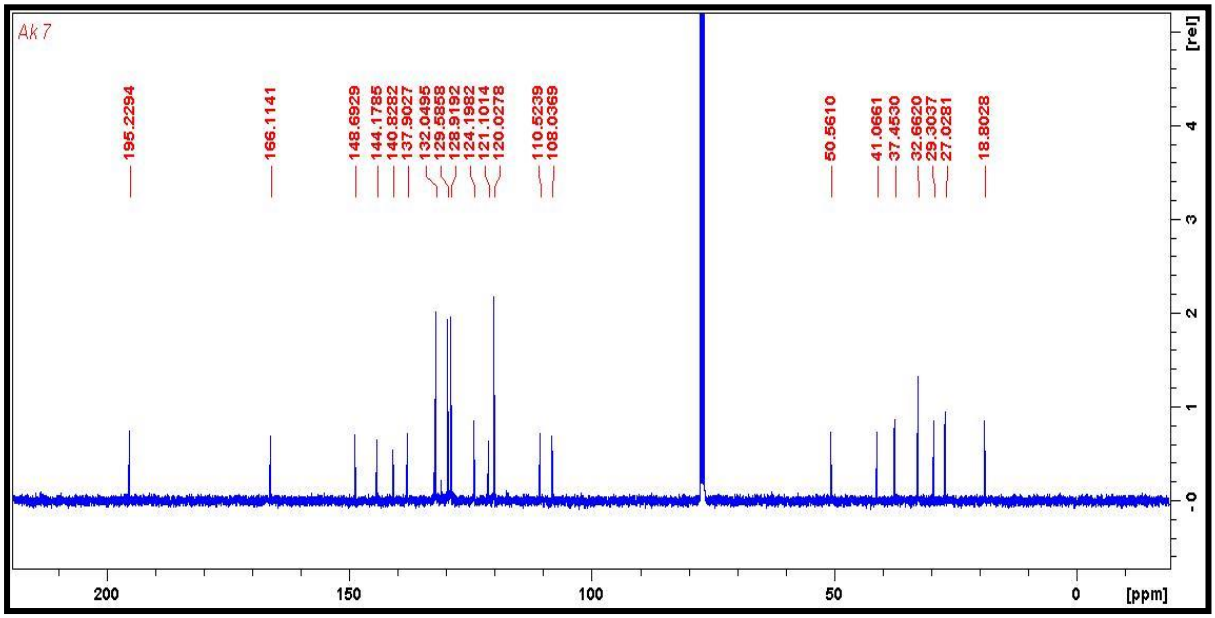

Fig.32 ^{13}C NMR spectra of compound **5g**

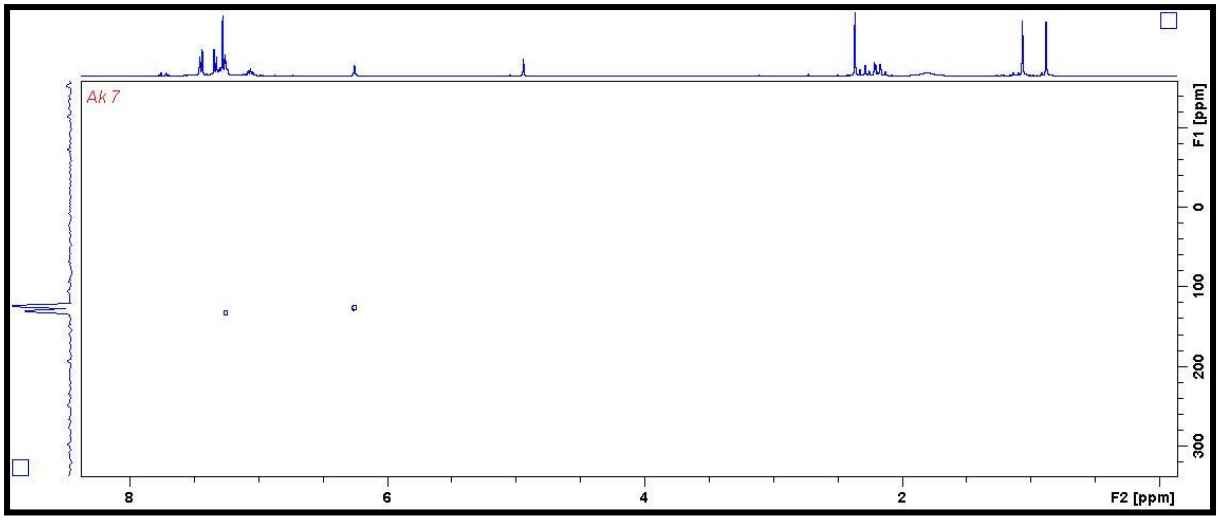

Fig.33 ^{15}N NMR spectra of compound **5g**

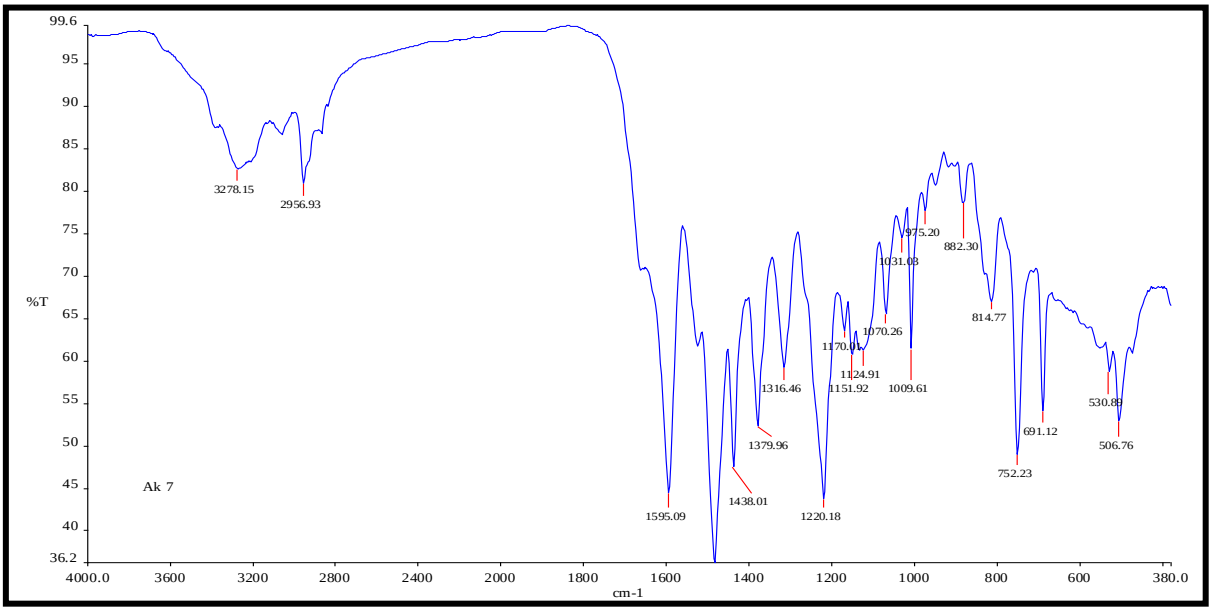

Fig.34 FT-IR spectra of compound **5g**

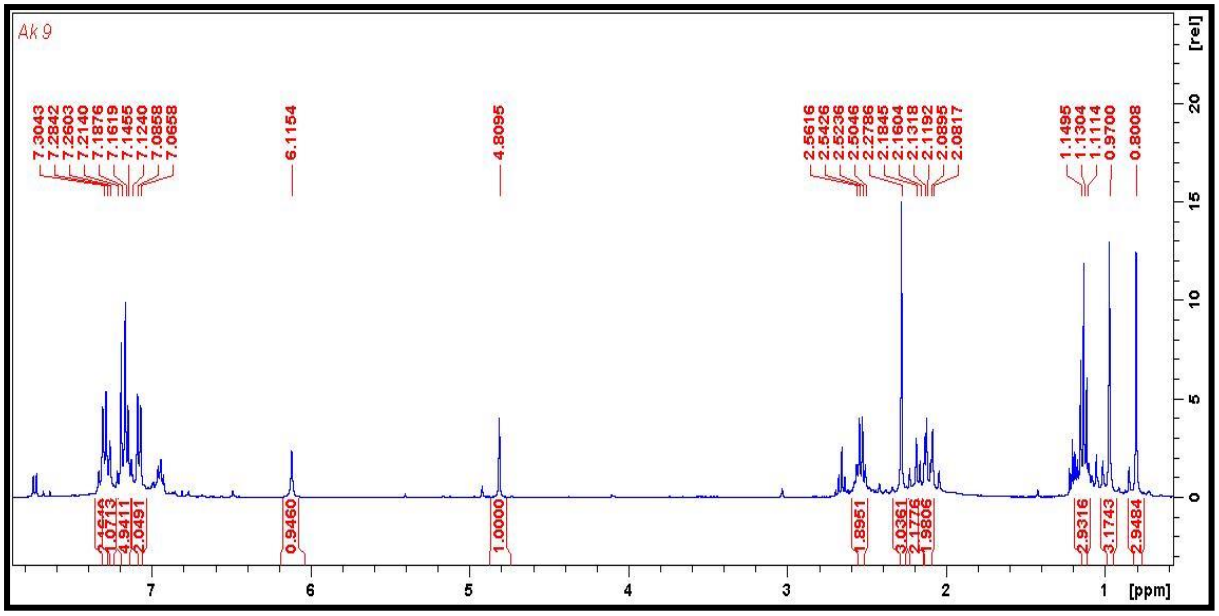

Fig.35 ^{1}H NMR spectra of compound **5h**

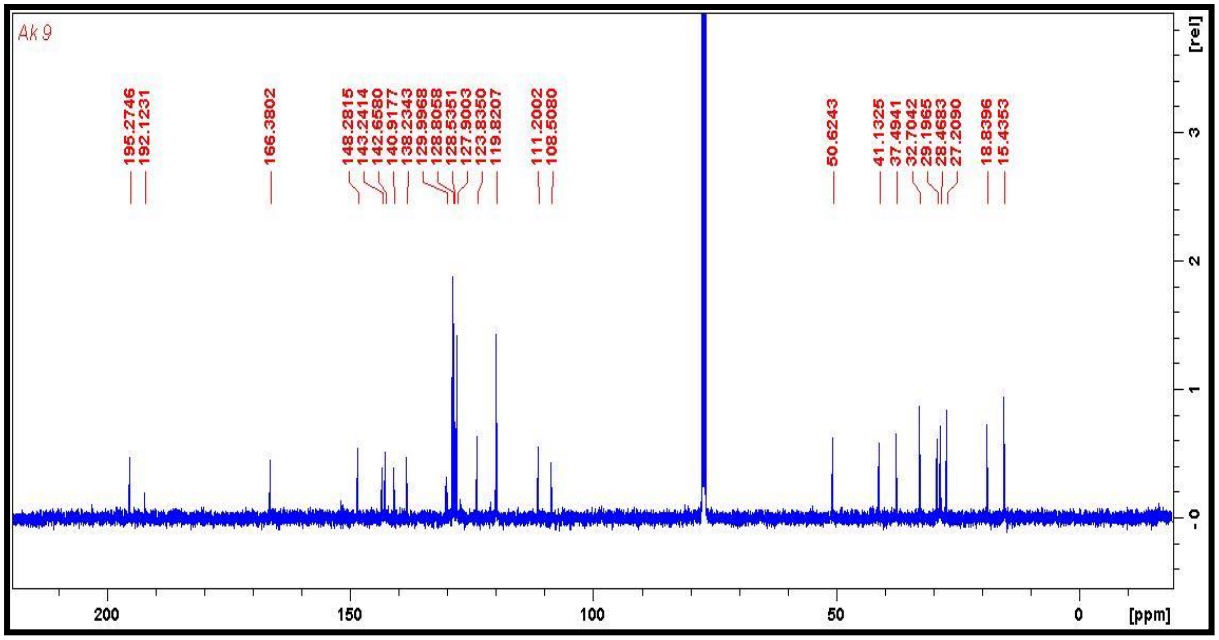

Fig.36 ^{13}C NMR spectra of compound **5h**

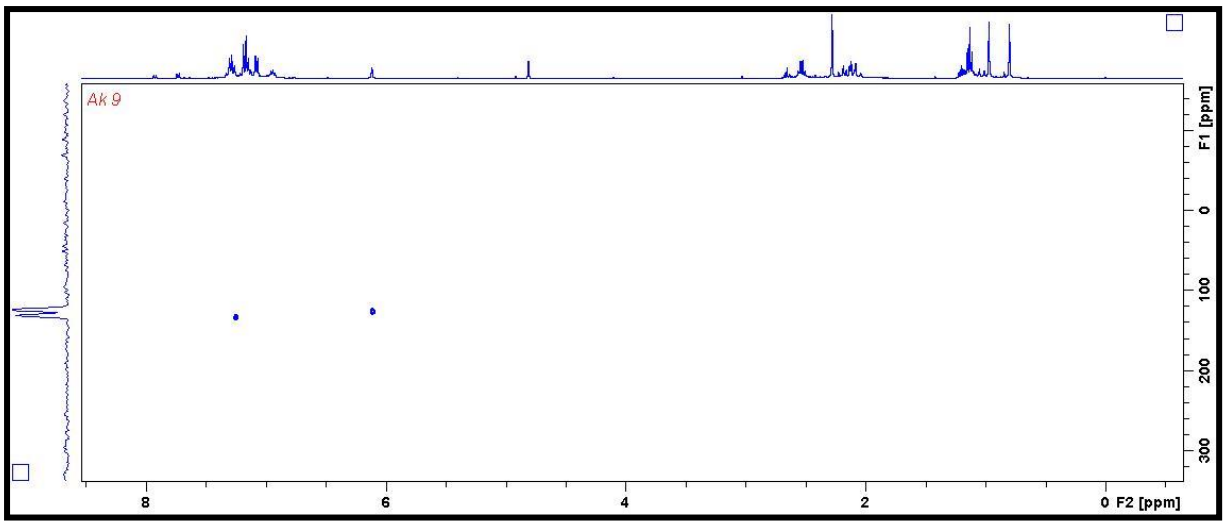

Fig.37 ^{15}N NMR spectra of compound **5h**

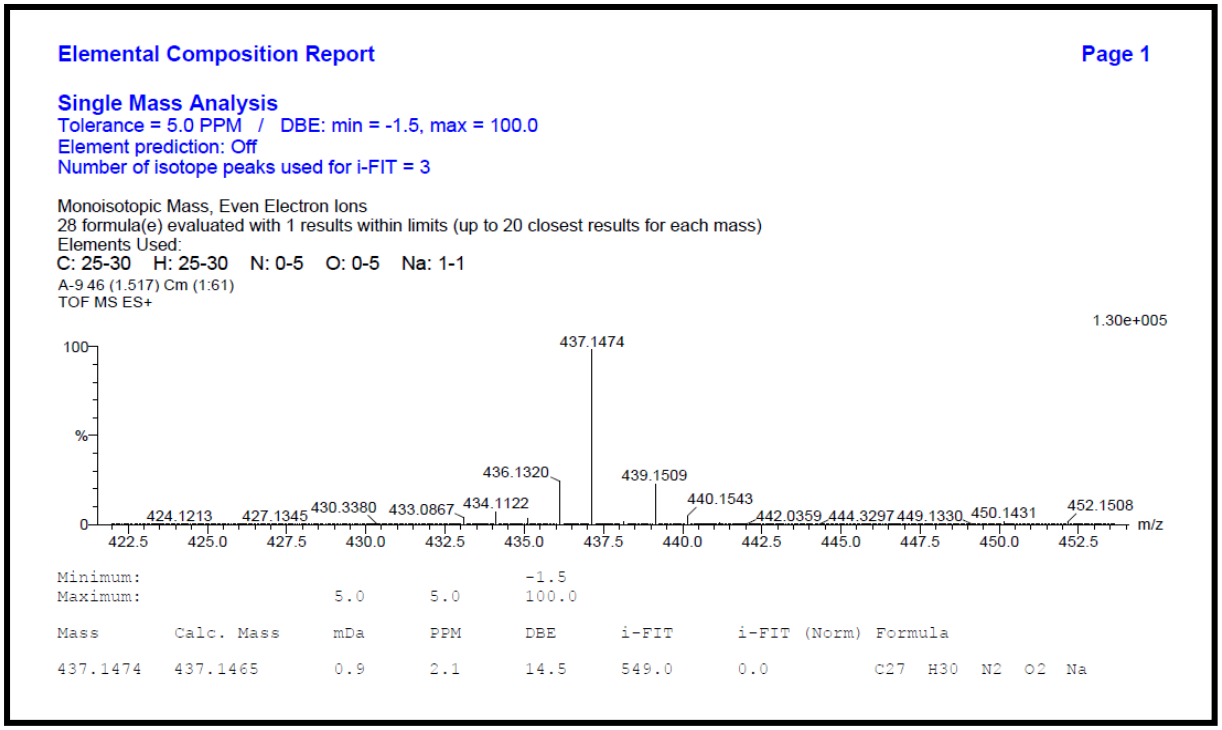

Fig.38 HRMS spectra of compound **5h**

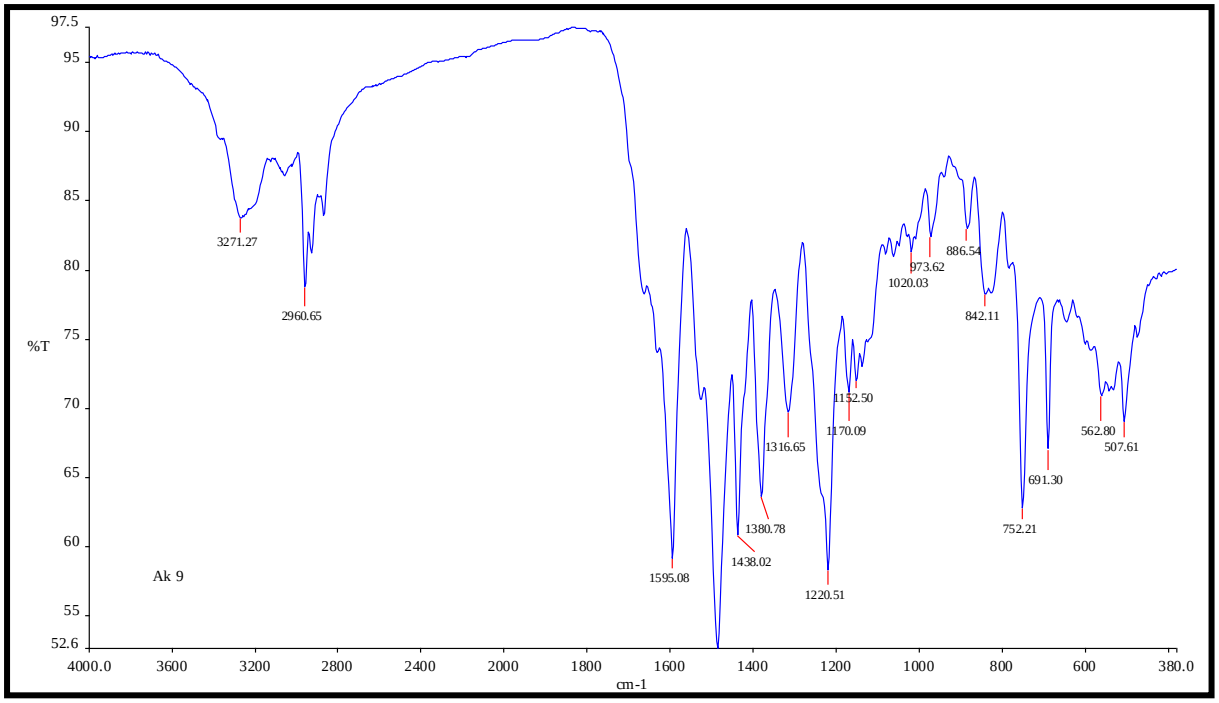

Fig.39 FT-IR spectra of compound **5h**

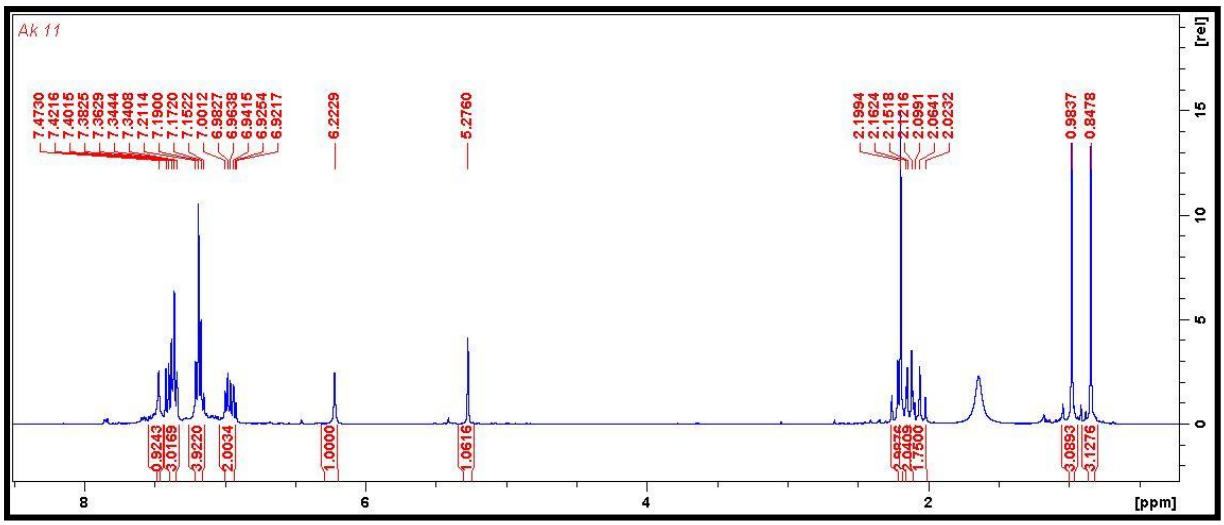

Fig.40 ^{1}H NMR spectra of compound **5i**

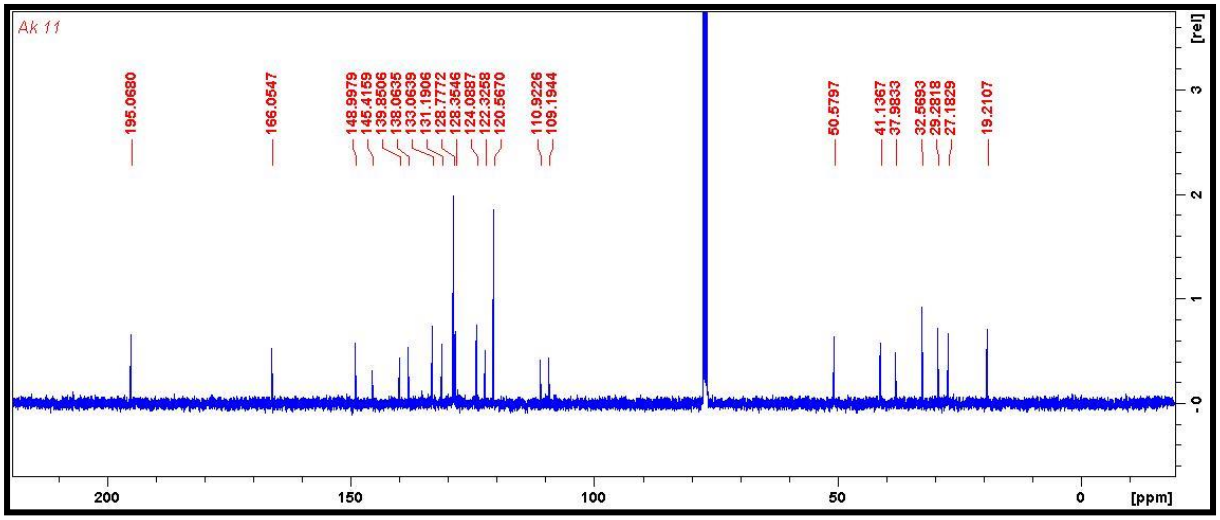

Fig.41 ^{13}C NMR spectra of compound **5i**

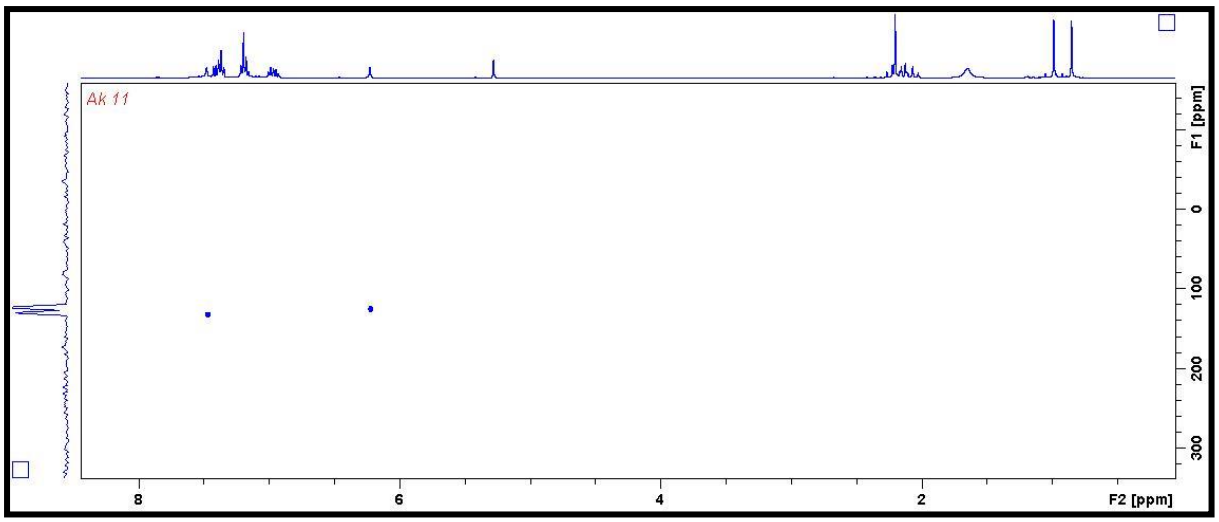

Fig.42 ^{15}N NMR spectra of compound **5i**

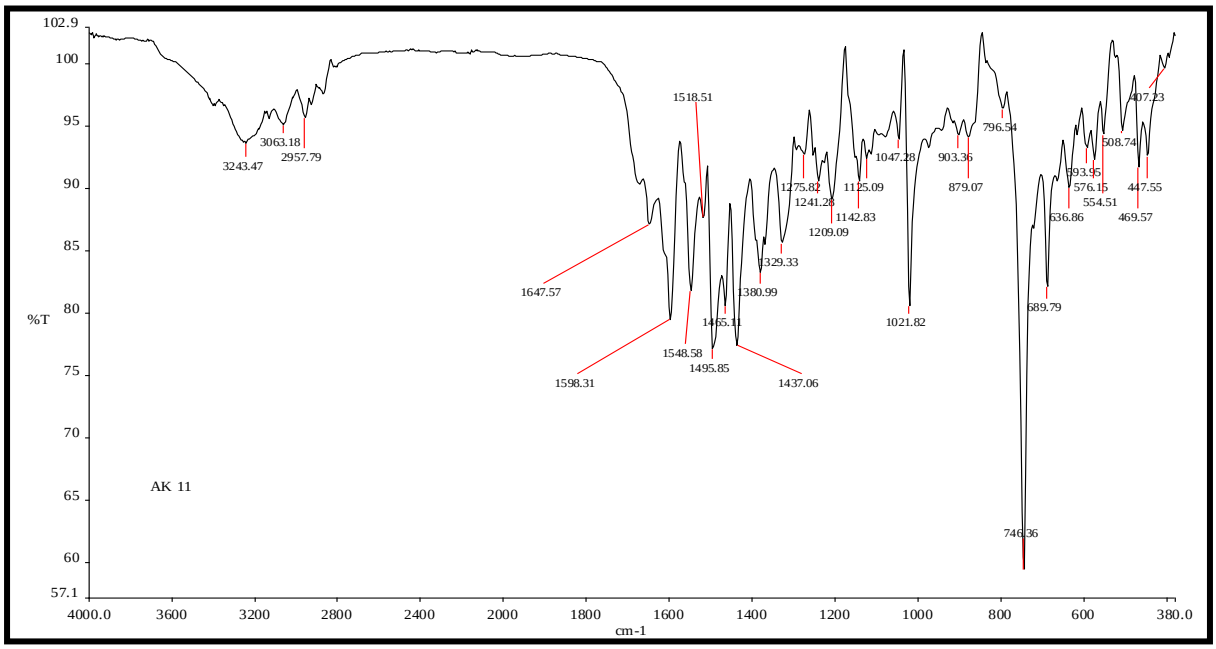

Fig.43 FT-IR spectra of compound **5i**

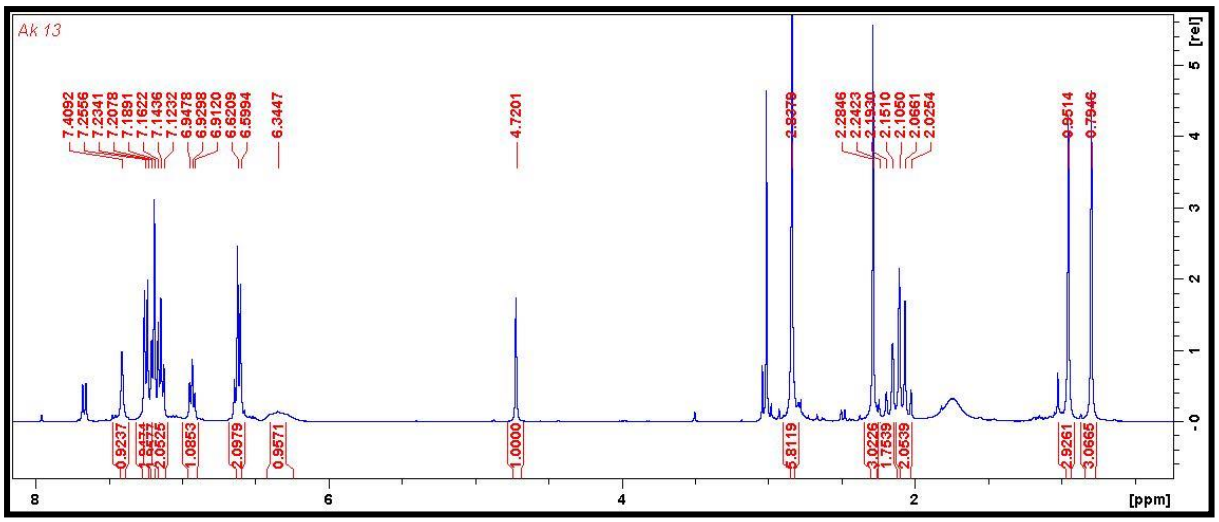

Fig.44 ^{1}H NMR spectra of compound **5j**

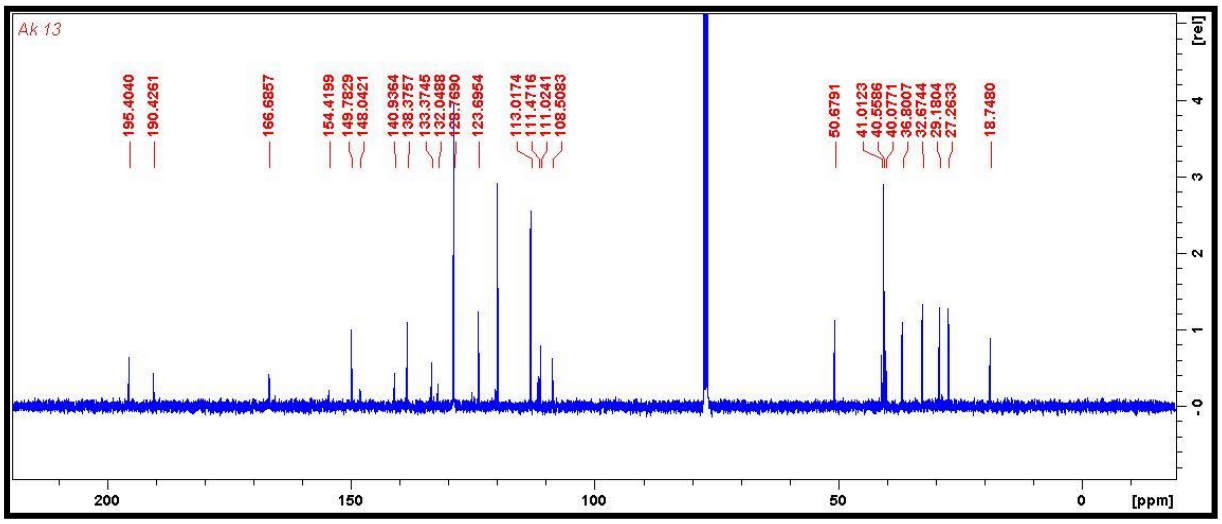

Fig.45 ^{13}C NMR spectra of compound **5j**

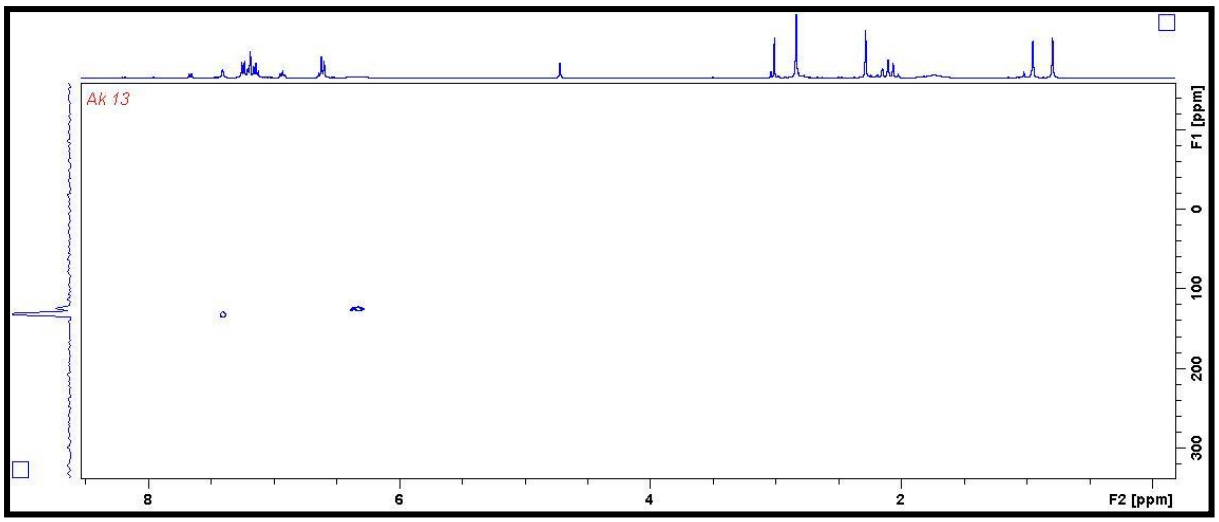

Fig.46 ^{15}N NMR spectra of compound **5j**

Elemental Composition Report **Page 1**

Single Mass Analysis
Tolerance = 5.0 PPM / DBE: min = -1.5, max = 100.0
Element prediction: Off
Number of isotope peaks used for i-FIT = 3

Monoisotopic Mass, Even Electron Ions
15 formula(e) evaluated with 1 results within limits (up to 20 closest results for each mass)
Elements Used:
C: 25-30 H: 30-35 N: 0-5 O: 0-5 Na: 1-1
A-13 53 (1.753) Cm (1:61)
TOF MS ES+

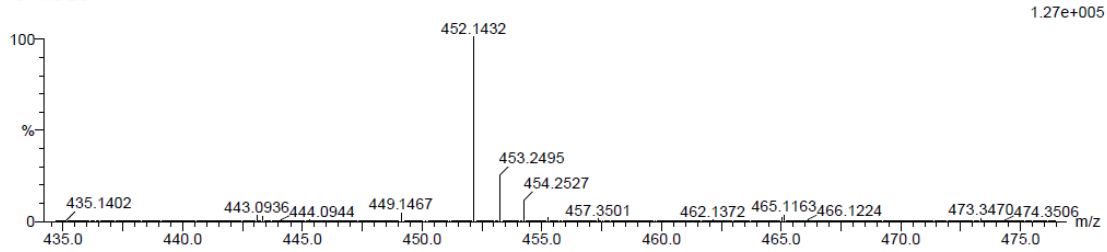

Minimum:				-1.5			
Maximum:		5.0	5.0	100.0			
Mass	Calc. Mass	mDa	PPM	DBE	i-FIT	i-FIT (Norm)	Formula
452.1432	452.1437	-0.5	-1.1	12.5	516.0	0.0	C27 H31 N3 O2 Na

Fig.47 HRMS spectra of compound **5j**

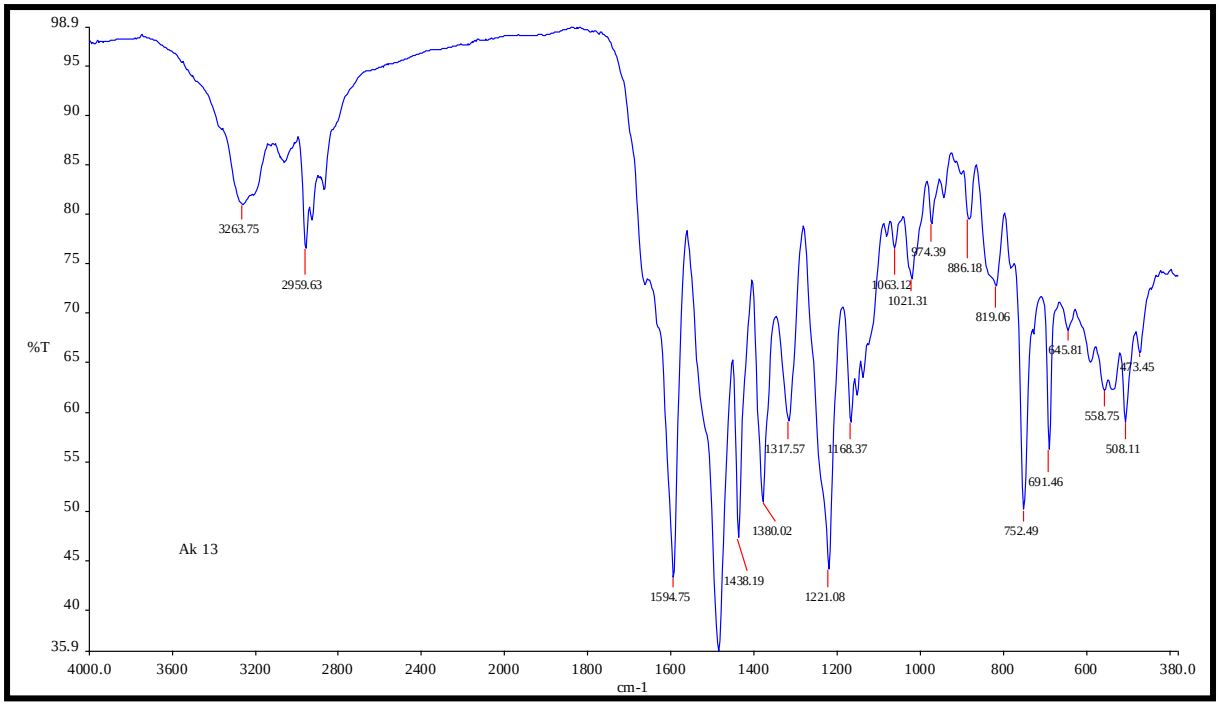

Fig.48 FT-IR spectra of compound **5j**

Chapter 3

RuO_2/ZrO_2 as an efficient reusable catalyst for the facile, green, one-pot synthesis of novel functionalized halopyridine derivatives

Sandeep V.H.S. Bhaskaruni, Suresh Maddila, Werner E. van Zyl, Sreekantha B. Jonnalagadda*

*School of Chemistry & Physics, University of KwaZulu-Natal, Westville Campus, Chiltern Hills, Durban-4000, South Africa.

*Corresponding author: Prof. S.B. Jonnalagadda,
School of Chemistry & Physics,
University of KwaZulu-Natal,
Durban-4000, South Africa.
E-mail: **jonnalagaddas@ukzn.ac.za**
Tel.: +27 31 260 7325,
Fax: +2731 260 3091.

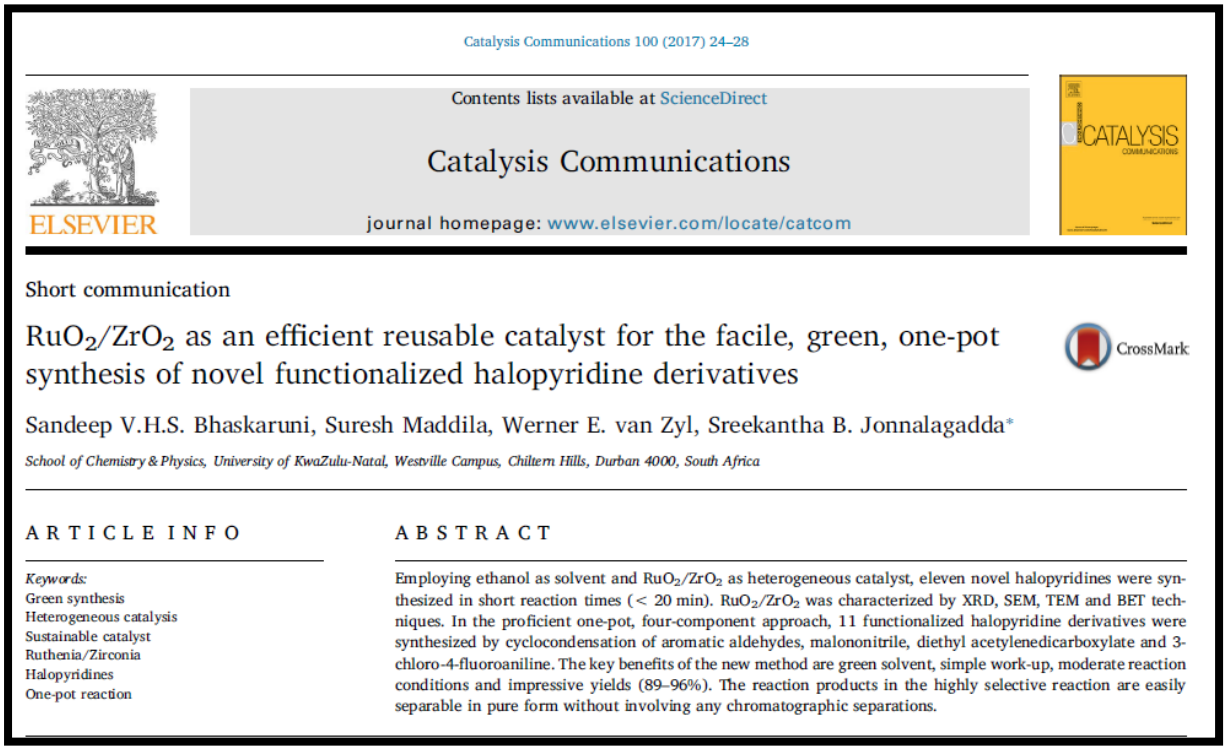

Catalysis Communications 100 (2017) 24–28

Contents lists available at ScienceDirect

Catalysis Communications

journal homepage: www.elsevier.com/locate/catcom

Short communication

RuO_2/ZrO_2 as an efficient reusable catalyst for the facile, green, one-pot synthesis of novel functionalized halopyridine derivatives

Sandeep V.H.S. Bhaskaruni, Suresh Maddila, Werner E. van Zyl, Sreekantha B. Jonnalagadda*

School of Chemistry & Physics, University of KwaZulu-Natal, Westville Campus, Chiltern Hills, Durban 4000, South Africa

ARTICLE INFO

Keywords:
Green synthesis
Heterogeneous catalysis
Sustainable catalyst
Ruthenia/Zirconia
Halopyridines
One-pot reaction

ABSTRACT

Employing ethanol as solvent and RuO_2/ZrO_2 as heterogeneous catalyst, eleven novel halopyridines were synthesized in short reaction times (< 20 min). RuO_2/ZrO_2 was characterized by XRD, SEM, TEM and BET techniques. In the proficient one-pot, four-component approach, 11 functionalized halopyridine derivatives were synthesized by cyclocondensation of aromatic aldehydes, malononitrile, diethyl acetylenedicarboxylate and 3-chloro-4-fluoroaniline. The key benefits of the new method are green solvent, simple work-up, moderate reaction conditions and impressive yields (89–96%). The reaction products in the highly selective reaction are easily separable in pure form without involving any chromatographic separations.

This chapter is published in the journal **Catalysis Communications,** and has been structured according to the journal's format.

RuO_2/ZrO_2 as an efficient reusable catalyst for the facile, green, one-pot synthesis of novel functionalized halopyridine derivatives

Sandeep V.H.S. Bhaskaruni, Suresh Maddila, Werner E. van Zyl, Sreekantha B. Jonnalagadda*

**School of Chemistry & Physics, University of KwaZulu-Natal, Westville Campus, Chiltern Hills, Durban-4000, South Africa.*

*Corresponding author: Prof. S.B. Jonnalagadda,
School of Chemistry & Physics,
University of KwaZulu-Natal,
Durban-4000, South Africa.
E-mail: **jonnalagaddas@ukzn.ac.za**
Tel.: +27 31 260 7325,
Fax: +2731 260 3091.

Abstract

Employing ethanol as solvent and RuO_2/ZrO_2 as heterogeneous catalyst, eleven novel halopyridines were synthesized in short reaction times (< 20 min). RuO_2/ZrO_2 was characterized by XRD, SEM, TEM and BET techniques. In the proficient one-pot, four-component approach, 11 functionalized halopyridine derivatives were synthesized by cyclocondensation of aromatic aldehydes, malononitrile, diethyl acetylenedicarboxylate and 3-chloro-4-fluoroaniline. The key benefits of the new method are green solvent, simple work-up, moderate reaction conditions and impressive yields (89–96%). The reaction products in the highly selective reaction are easily separable in pure form without involving any chromatographic separations.

Keywords: Green synthesis; Heterogeneous catalysis; Sustainable catalyst; Ruthenia/Zirconia; halopyridines; One-pot reaction.

3.1 Introduction

Multicomponent reaction (MCR) is one of the most effective synthetic approach for organic compounds and plays significant role in the discovery and development of new molecules in medicinal and pharmaceutical fields [1,2]. Relative to the multi-step counterparts, MCRs are widely used to produce various chemical libraries of drug-like compounds for biological screening, due to greater yields affordable avoiding the separation and purification of intermediates [3]. Other benefits include greener approaches, energy efficiency, short reaction time, good selectivity, simpler workups and high yields [4]. Moreover, MCRs recognize the principles of green chemistry in terms of atom economy, as well as numerous other criteria of the best heterocyclic syntheses [5,6].

Heterogeneous catalysis plays an important role in organic synthesis, as about 90% of the large scale chemical processes use these catalysts, in at least one step of the process [7,8]. Heterogeneous catalysts possess diverse chemical and physical characteristics that render them ideal in MCRs [8]. These properties include controlled miscibility, thermal stability, easy recovery, recyclability and minimal loss of material [9]. Heterogeneous catalysis receives greater attention due to simple approach, improved selectivity, high conversion and long catalyst life, contributing to green synthesis principles [9-11].

Many ruthenium compounds were used as homogeneous catalysts or reagents as their efficiency can be recommended by their activity, ease of handling, normal cost, low toxicity and appropriateness in condensation systems [4]. These catalysts have been employed in many industry processes including Fischer-Tropsch synthesis [12], hydrogenation [13] and steam reforming and fine chemicals manufacture [14]. The need to use these compounds in stoichiometric quantities and in non-recoverable format will impose significant financial and environmental constraints. Consequently, the use of ruthenium salts in a heterogeneous system become a desirable choice in green synthesis. Zirconia (ZrO_2) is widely used as a support material, owing to its cost-effectiveness, flexibility, high specific surface area and thermal durability, making it appropriate over wide-ranging temperatures [15-17]. Amid other metal oxides, it stands out tall as ideal support material for catalysts, facilitating good dispersion of active material on its enormous surface [18,19]. Easily separable heterogeneous materials as catalysts tend to reduce the operation costs [17-19].

Among the bulk of heterocyclic compounds used the fields of medicinal and pharmaceutical chemistry, pyridine ring is most commonly found unit in both natural products and synthesised materials [20,21]. Pyridines exhibit a wide and diverse window of biological activities, such as

antimicrobial, anti-tumor, anti-viral, anti-inflammatory and anti-oxidant activities [22- 26]. A number of pyridine derivatives are used in agrochemical industry as herbicidal and insecticidal agents [27,28]. Many synthetic procedures have been reported in the literature for production of different dihydropyridine derivatives, due to their financial and scientific relevance. Some of these methods employed TEA, PEG-600, Meglumine and NaOH as catalysts [29-32]. Some of those reactions demand costly reagents, high temperatures, long reaction times, tedious handling processes and harsh reaction conditions, while others suffer low yields, necessitating newer and efficient protocols. Consequently, pursuit for better and greener approaches for the synthesis of pyridine derivatives is paramount.

Encouraged by the promising results in developing synthetic routes for varied heterocyclic protocols, we recently reported various protocols for synthesis of different therapeutically interesting heterocycles [33,34]. In this communication, we report a new method for synthesis of functionalized halopyridine derivatives using one-pot four-component reaction at room temperature, with 2% RuO_2/ZrO_2 (i.e. 2% RuO_2 loaded onto ZrO_2 support) as recyclable catalyst and ethanol as solvent.

3.2 Experimental Section

3.2.1 Catalyst preparation

A range of supported catalysts with different weight percentages of ruthenium on zirconium, as RuO_2 loaded on ZrO_2 (1, 2, & 4 wt%), were prepared using the simple wet-impregnation technique. The heterogeneous catalyst was synthesized from a mixture of zirconia (ZrO_2 (2 g), catalyst support, Alfa Aesar) and an appropriate amount (wt%) of ruthenium chloride [$RuCl_3 \cdot XH_2O$ (Alfa Aesar)] in distilled water (100 mL). The reaction mixture was stirred at room temperature (RT) for 8 h, followed by filtering the resultant slurry under vacuum. The material was dried for 5 h in an oven at 110–120°C and calcined at 450°C for 5 h in the presence of air, to obtain different wt% of RuO_2/ZrO_2 catalysts.

3.2.2 General procedure for the synthesis of 1,4-dihydropyridine derivatives (5a-k)

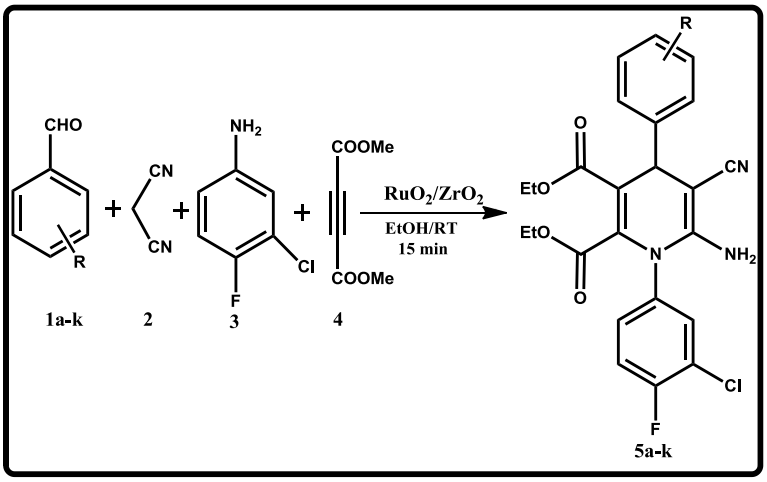

Scheme 1 Synthesis of novel 1,4-dihydropyridine derivatives.

In a typical reaction, to equimolar ratios of aldehydes (1 mmol) (1), malononitrile (1 mmol) (2), 3-chloro-4-fluoroaniline (1mmol) (3) and diethyl acetylenedicarboxylate (1 mmol) (4) were dissolved in ethanol (10 ml) at RT followed by addition of RuO_2/ZrO_2 (30 mg) as a catalyst. The reaction mixture was stirred for 15 min at RT (Scheme 1). The progress of the reaction was monitored by thin layer chromatography. The catalyst was initially removed from the reaction mixture by filtration and crude product was extracted using ethyl acetate followed by evaporation of solvent under vacuum. Ethanol was used to dissolve the crude product and to obtain pure compounds (**5a-k**). All the reaction products were characterised by analysis using ^{1}H NMR, ^{13}C NMR, ^{15}N NMR, ^{19}F NMR, HR-MS and FT-IR. The details and spectra are assimilated to the supplementary information file.

Diethyl 6-amino-1-(3-chloro-4-fluorophenyl)-4-(2-chlorophenyl)-5-cyano-1,4-dihydro-pyridine-2,3-dicarboxylate (5a):

^{1}H NMR (400 MHz, DMSO-d_6) δ = 0.89–0.97 (m, 6H, 2×CH_3), 3.83–3.92 (m, 4H, 2×CH_2), 5.10 (s, 1H, CH), 5.84 (s, 2H, NH_2), 7.24–7.29 (m, 1H, ArH), 7.40–7.47 (m, 4H, ArH), 7.55 (t, 1H, ArH), 7.73 (dd, *J* = 6.56 Hz, 2.52 Hz, 1H, ArH); ^{13}C NMR (100 MHz, DMSO-d_6): 13.10, 13.52, 18.49, 30.63, 35.49, 55.99, 58.48, 60.36, 61.60, 103.60, 117.40, 117.63, 120.33, 128.07, 128.41, 129.16, 130.04, 131.36, 131.96, 132.03, 133.49, 142.22, 143.04, 150.58, 156.87, 159.36, 162.17, 164.23; ^{15}N NMR (40.55 MHz, DMSO-d_6) δ 5.84 (s, 2H, NH_2); ^{19}F NMR (376.58 MHz, DMSO-d_6): ─123.09; FT-IR: 3334, 3066, 2984, 2187, 1734, 1616, 1492, 1363, 1216. HRMS of $[C_{24}H_{20}Cl_2FN_3O_4 + H]^+$ (m/z): 504.2189; Calcd.:504.2178.

Diethyl 6-amino-1-(3-chloro-4-fluorophenyl)-5-cyano-4-(2-fluorophenyl)-1,4-dihydro pyridine-2,3-dicarboxylate (5b):

^{1}H NMR (400 MHz, DMSO-d_6) δ = 0.89-0.97 (m, 6H, 2×CH_3), 3.83–3.92 (m, 4H, 2×CH_2), 5.10 (s, 1H, CH), 5.84 (s, 2H, NH_2), 7.24–7.29 (m, 1H, ArH), 7.40–7.47 (m, 4H, ArH), 7.55 (t, 1H, ArH), 7.72-7.74 (dd, *J* = 2.52 HZ, 2.52 HZ 1H, ArH); ^{13}C NMR (100 MHz, DMSO-d_6): 8.60, 13.10, 13.51, 33.17, 33.27, 45.75, 58.05, 60.41, 61.58, 62.50, 102.90, 113.27, 113.33, 114.03, 117.15, 122.66, 127.91, 132.08, 133.33, 133.93, 134.01, 136.87, 142.03, 146.25, 148.33, 148.36, 150.86, 156.83, 156.93, 158.55, 159.31, 160.92, 160.99, 162.20, 163.43, 164.13, 164.22, 187.81; ^{15}N NMR (40.55 MHz, DMSO-d_6) δ 5.88 (s, 2H, NH_2); ^{19}F NMR (376.58 MHz, DMSO-d_6): ─120.95, ─134.41; FT-IR: 3473, 3363, 2984, 2186, 1730, 1615, 1489, 1366, 1216. HRMS of $[C_{24}H_{20}ClF_2N_3O_4 + H]^+$ (m/z): 488.1405; Calcd.: 488.1390.

Diethyl 6-amino-1-(3-chloro-4-fluorophenyl)-5-cyano-4-(4-ethylphenyl)-1,4-dihydro-pyridine-2,3-dicarboxylate (5c):

^{1}H NMR (400 MHz, DMSO-d_6) δ = 0.90 (t, 3H, CH_3), 1.04 (t, 3H, CH_3), 1.18 (t, 3H, CH_3), 2.56–2.62 (q, 2H, CH_2), 3.82-3.87 (q, 2H, CH_2), 3.93-3.98 (q, 2H, CH_2), 4.43 (s, 1H, CH), 5.83 (s, 2H, NH_2), 7.21 (s, 4H, ArH), 7.34–7.37 (m, 1H, ArH), 7.54 (t, 1H, ArH), 7.62–7.64 (dd, *J* = 2.52 Hz, 2.56 Hz,1H, ArH); ^{13}C NMR (100 MHz, DMSO-d_6): 13.11, 13.66, 15.49, 27.76, 30.64, 59.55, 60.46, 61.56, 105.01, 117.45, 117.68, 120.08, 120.27, 120.95, 126.96, 128.01, 131.69, 131.77, 132.24, 133.25, 140.89, 142.34, 142.76, 150.57, 156.77, 162.34, 164.46; ^{15}N NMR (40.55 MHz, DMSO-d_6) δ 5.83 (s, 2H, NH_2); ^{19}F NMR (376.58 MHz, DMSO-d_6): ─123.66; FT-IR: 3466, 3345, 3098, 2970, 2188, 1730, 1694, 1651, 1583, 1488, 1367.

Diethyl 6-amino-1-(3-chloro-4-fluorophenyl)-4-(4-chlorophenyl)-5-cyano-1,4-dihydro pyridine-2,3-dicarboxylate (5d):

^{1}H NMR (400 MHz, DMSO-d_6) δ = 0.89 (t, 3H, CH_3), 1.03 (t, 3H, CH_3), 3.81-3.85 (m, 2H, CH_2), 3.92–3.96 (m, 2H, CH_2), 4.50 (s, 1H, CH), 5.91 (s, 2H, NH_2), 7.33 (d, *J* = 8.44 Hz, 2H, ArH), 7.37–7.41 (m, 1H, ArH), 7.44 (d, *J* = 8.44 Hz, 1H, ArH), 7.54 (t, *J* = 8.92 Hz,1H, ArH), 7.68–7.70 (dd, *J* = 2.6 Hz, *J* = 2.6 Hz); ^{13}C NMR (100 MHz, DMSO-d_6): 13.10, 13.65, 30.64, 58.90, 60.52, 61.62, 104.26, 117.42, 117.65, 120.73, 128.59, 129.04, 131.46, 131.98, 133.39, 141.30, 144.50, 150.63, 156.84, 162.18, 164.29; ^{15}N NMR (40.55 MHz, DMSO-d_6) δ 5.91 (s, 2H, NH_2); ^{19}F NMR (376.58 MHz, DMSO-d_6): ─120.19; FT-IR: 3483, 3315, 2985, 2195, 1746, 1693, 1578, 1491, 1369, 1209.

Diethyl 6-amino-1-(3-chloro-4-fluorophenyl)-5-cyano-4-(3,4-dimethoxy phenyl)-1,4-dihydropyridine-2,3-dicarboxylate (5e):

^{1}H NMR (400 MHz, DMSO-d_6) δ = 0.90 (t, 3H, CH_3), 1.07 (t, 3H, CH_3), 3.75 (s, 6H, 2×OCH_3), 3.82–3.86 (q, 2H, CH_2), 3.95–4.01 (q, 2H, CH_2), 4.42 (s, 1H, CH), 5.84 (s, 2H, NH_2), 6.84 (t, 2H, ArH), 6.98 (d, *J* = 8.8 Hz, 1H, ArH), 7.30–7.33 (m, 1H, ArH), 7.57–7.60 (dd, *J* =2.56, 2.72 Hz, 2H, ArH), ^{13}C NMR (100 MHz, DMSO-d_6): 13.10, 13.72, 30.62, 38.14, 55.34, 55.50, 59.73, 60.47, 61.55, 105.22, 110.75, 112.30, 117.48, 117.71, 118.95, 120.27, 120.93, 131.64, 132.33, 133.11, 138.01, 140.75, 147.78, 148.48, 150.57, 162.35, 164.53; ^{15}N NMR (40.55 MHz, DMSO-d_6) δ 5.84 (s, 2H, NH_2); ^{19}F NMR (376.58 MHz, DMSO-d_6): ─123.11; FT-IR: 3438, 3321, 3232, 2960, 2190, 1741, 1690, 1775, 1496, 1227.

Diethyl 6-amino-1-(3-chloro-4-fluorophenyl)-5-cyano-4-(2,3-dimethoxy phenyl)-1,4-dihydropyridine-2,3-dicarboxylate (5f):

^{1}H NMR (400 MHz, DMSO-d_6) δ = 0.91 (t, 3H, CH_3), 0.98 (t, 3H, CH_3), 3.80 (s, 3H, OCH_3), 3.81 (s, 3H, OCH_3), 3.83–3.87 (q, 2H, CH_2), 3.89–3.94 (q, 2H, CH_2), 4.82 (s, 1H, CH), 5.73 (m, 2H, NH_2), 6.83–6.86 (dd, 1H, *J* = 1.32,1.32 Hz,1H,ArH), 6.93–6.95 (dd, *J* = 1.32 Hz, *J* = 1.36 Hz, 1H, ArH), 7.07 (t, 1H, ArH), 7.36–7.39 (m, 1H, ArH), 7.56 (t, 1H, ArH), 7.0–7.62 (dd, *J* = 2.6 Hz, *J* = 2.56 Hz, 1H, ArH); ^{13}C NMR (100 MHz, DMSO-d_6): 13.12, 13.64, 18.50, 20.71, 30.63, 33.43, 55.56,55.98, 59.36, 59.71, 61.50, 104.50, 111.46, 117.47, 120.03, 120.22, 123.94, 131.70, 131.78, 132.44, 133.20, 138.17, 141.58, 146.05, 150.73, 152.26, 156.72, 159.20, 162.44, 164.52, 170.30; ^{15}N NMR (40.55 MHz, DMSO-d_6) δ 5.73 (s, 2H, NH_2); ^{19}F NMR (376.58 MHz, DMSO-d_6): ─126.81; FT-IR: 3449, 3358, 2982, 2180, 1730, 1691, 1585, 1482, 1370, 1217. HRMS of $[C_{26}H_{25}N_3O_6ClF + H]^+$ (m/z): 530.2393; Calcd.: 530.2409.

Diethyl 6-amino-1-(3-chloro-4-fluorophenyl)-5-cyano-4-(4-fluorophenyl)-1,4-dihydro pyridine-2,3-dicarboxylate (5g):

^{1}H NMR (400 MHz, DMSO-d_6) δ = 0.90 (t, 3H, CH_3), 1.03 (t, 3H, CH_3), 3.82–3.96 (m, 4H, 2×CH_2), 4.50 (s, 1H, CH), 5.88 (s, 2H, NH_2), 7.20 (t, 2H, ArH),7.33–7.36 (m, 2H, ArH), 7.38–7.40 (m,1H, ArH), 7.54 (t, 1H, ArH), 7.68–7.70 (dd, *J* = 2.6 Hz, *J* = 2.6 Hz, 1H, ArH) ;^{13}C NMR (100 MHz, DMSO-d_6): 13.10, 13.63, 14.03, 18.49, 20.70, 30.62, 38.26, 55.98, 59.27, 59.70, 60.46, 61.58, 104.60, 115.20, 117.41, 117.63, 120.09, 120.28, 120.78, 129.00, 129.08, 131.79, 131.87, 133.37, 141.12, 141.80, 150.54, 156.82, 159.30, 162.22, 162.33, 164.35, 170.29 ^{15}N NMR (40.55 MHz, DMSO-d_6) δ 5.88 (s, 2H, NH_2); ^{19}F NMR (376.58 MHz, DMSO-d_6): ─114.10, ─115.86 ; FT-IR: 3459,3322,2181,1733,1654, 1576,1495, 1367.

Diethyl 6-amino-1-(3-chloro-4-fluorophenyl)-5-cyano-4-(3-fluorophenyl)-1,4-dihydro pyridine-2,3-dicarboxylate (5h):

^{1}H NMR (400 MHz, DMSO-d_6) δ = 0.90 (t, 3H, CH_3), 1.02 (t, *J* = 7.08 Hz 3H, CH_3), 3.83–3.88 (q, 2H, CH_2), 3.95–3.97 (q, 2H, CH_2), 4.54 (s, 1H, CH), 5.92 (s, 2H, NH_2), 7.06–7.10 (m, 2H, ArH), 7.18 (d, *J* = 7.76 Hz, 1H, ArH), 7.36– 7.39 (m, 1H, ArH), 7.42–7.47 (m, 1H, ArH), 7.55 (t, 1H , ArH), 7.69–7.71 (dd, *J* = 2.56 Hz, *J* = 2.56 Hz, 1H, ArH); ^{13}C NMR (100 MHz, DMSO-d_6): 13.10, 13.62, 58.79, 60.51, 61.64, 104.06, 113.63, 113.85, 117.45, 117.67, 120.10, 120.29, 123.24, 130.65, 130.73, 131.77, 131.86, 131.98, 133.40, 141.44, 148.34, 148.40, 150.66, 156.83, 160.99, 162.17, 163.42, 164.30 ; ^{15}N NMR (40.55 MHz, DMSO-d_6) δ 5.92 (s, 2H, NH_2); ^{19}F NMR (376.58 MHz, DMSO-d_6): ─113.11, ─114.04; FT-IR: 3463, 3323, 3234, 2986, 2184, 1701, 1655, 1579, 1485, 1369.

Diethyl 6-amino-1-(3-chloro-4-fluorophenyl)-4-(3-chlorophenyl)-5-cyano-1,4-dihydro pyridine-2,3-dicarboxylate (5i):

^{1}H NMR (400 MHz, DMSO-d_6) δ = 0.90 (t, 3H, CH_3), 1.03 (t, 3H, CH_3), 3.82–3.88 (m, 2H, CH_2), 3.94–3.99 (m, 2H, CH_2), 4.53 (s, 1H, CH), 5.95 (s, 2H, NH_2), 7.30–7.37 (m, 4H, ArH), 7.45 (t, 1H, ArH), 7.56 (t, 1H, ArH), 7.67–7.70 (dd, *J* = 2.6 Hz,*J* = 2.64 Hz, 1H, ArH); ^{13}C NMR (100 MHz, DMSO-d_6): 13.10, 13.61, 58.72, 60.53, 61.65, 104.08, 117.47, 117.70, 120.68, 125.99, 126.91, 126.94, 130.76, 131.73, 131.81, 131.98, 132.01, 132.95, 133.37, 141.47, 147.93, 150.73, 156.85, 158.33, 162.14, 164.24; ^{15}N NMR (40.55 MHz, DMSO-d_6) δ 5.95 (s, 2H, NH2); ^{19}F NMR (376.58 MHz, DMSO-d_6): ─119.94; FT-IR: 3475, 3335, 2187, 1737, 1655, 1578, 1492.1257.

Diethyl 6-amino-1-(3-chloro-4-fluorophenyl)-5-cyano-4-(2-methoxy phenyl)-1,4-dihydro pyridine-2,3-dicarboxylate (5j):

^{1}H NMR (400 MHz, DMSO-d_6) δ = 0.92 (t, 3H, CH_3), 0.97 (t, 3H, CH_3), 3.82 (s, 3H, OCH_3), 3.85–3.88(q, 2H,CH_2), 3.89–3.93 (q, 2H, CH_2), 4.92 (s, 1H, CH), 5.68 (s, 2H, NH_2), 6.97–7.02 (m, 2H, ArH), 7.18–7.22 (m, 2H, ArH), 7.31–7.35 (m, 1H, ArH),7.55 (t, 1H, ArH), 7.58–7.61 (dd, *J* = 2.6 Hz, 2.6 Hz, 1H, ArH); ^{13}C NMR (100 MHz, DMSO-d_6): 13.14, 13.58, 30.64, 32.01, 55.69, 59.48, 60.23, 61.51, 104.31, 111.46, 117.44, 117.66, 120.01, 120.20, 120.79, 127.96, 128.02, 131.66, 131.75, 132.42, 132.46, 133.19, 133.40, 141.84, 150.80, 156.20, 156.69, 159.17, 162.48, 164.52; ^{15}N NMR (40.55 MHz, DMSO-d_6) δ 5.68 (s, 2H, NH_2); ^{19}F NMR (376.58 MHz, DMSO-d_6): ─120.88; FT-IR: 3460, 3313, 2986, 2186, 1704, 1652, 1579, 1490, 1243. HRMS of $[C_{25}H_{23}ClFN_3O_5 + H]^+$ (m/z): 500.2573; Calcd.: 500.2559.

Diethyl 6-amino-4-(2-bromophenyl)-1-(3-chloro-4-fluorophenyl)-5-cyano-1,4-dihydro pyridine-2,3-dicarboxylate (5k):

^{1}H NMR (400 MHz, DMSO-d_6) δ = 0.90 (t, 3H, CH_3), 0.96 (t, 3H, CH_3), 3.80–3.86 (m, 2H, CH_2), 3.88 (q, 2H, CH_2), 5.10 (s, 1H, CH), 5.84 (s, 2H, NH_2), 7.16–7.20 (m, 1H, ArH), 7.47 (t, 3H, ArH), 7.56 (t, 2H, ArH), 7.74–7.77 (m, 1H, ArH); ^{13}C NMR (100 MHz, DMSO-d_6): 13.11, 13.62, 37.83, 58.66, 60.34, 61.59, 103.87, 117.38, 117.52, 120.09, 120.21, 122.02, 122.74, 125.49, 128.16, 130.13, 131.92, 131.96, 132.06, 132.39, 133.34, 133.48, 144.85, 148.24, 156.88, 159.36, 160.29, 162.16, 164.28; ^{15}N NMR (40.55 MHz, DMSO-d_6) δ = 5.84 (s, 2H, NH2); ^{19}F NMR (376.58 MHz, DMSO-d_6): −119.77; FT-IR: 3467, 3321, 2981, 2194, 1740, 1653, 1583, 1494, 1242. HRMS of $[C_{24}H_{20}BrClFN_3O_4 + 2H]^+$ (m/z): 549.1563; Calcd.: 549.1558.

3.3 Results and Discussion

3.3.1 XRD analysis

Fig. 1 illustrates the powder XRD pattern, which is used to recognize the structure of zirconia with 2 wt% ruthenia as second phase. The diffraction peaks for 2 theta (degree) diffraction angles were observed from 5° to 90°. The major peak values perceived at 2θ of 24.2°, 28.2°, 31.3°, 35.4°, 40.5°, 45.0°, 50.3°, 55.4° and 60.1° correspond to different diffraction planes of zirconia (JCPDS card no. 37-1484). The 2% RuO_2/ZrO_2 catalyst displayed major Bragg angle diffraction peaks at 2 theta of 35.1°, 38.3°, 44.1°, 58.5°, 66.1°, 69.5° and 78.1° corresponding to the RuO_2 (JCPDS # 40-1290). Diffractogram shows that the material was of polycrystalline nature and the average crystallite size was 6.3 nm.

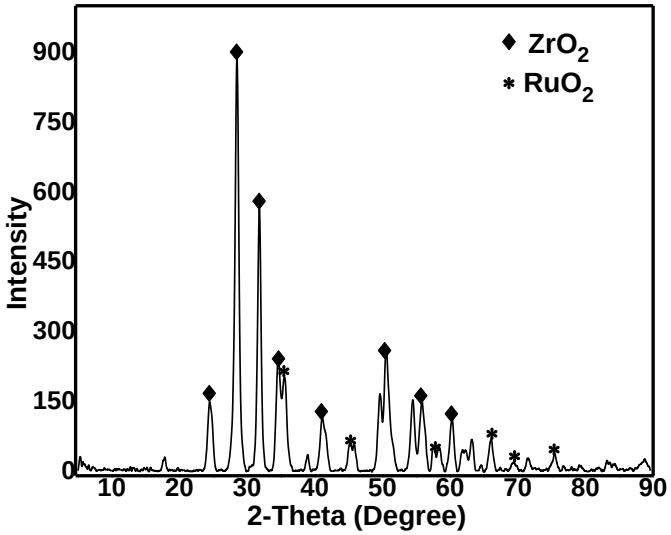

Fig. 1. Powder X-ray diffractogram of 2% RuO_2/ZrO_2 catalyst.

3.3.2 TEM analysis

Transmission Electron Microscopy (TEM) micrograph of ruthenia supported on zirconia catalyst is shown in Fig. 2. The TEM micrograph showed puffy spherical shaped zirconia particles had different shape variations. The RuO_2 particles displayed a black spotted cubic shape with an average particle size of 11 nm and are homogeneously distributed on the zirconia support.

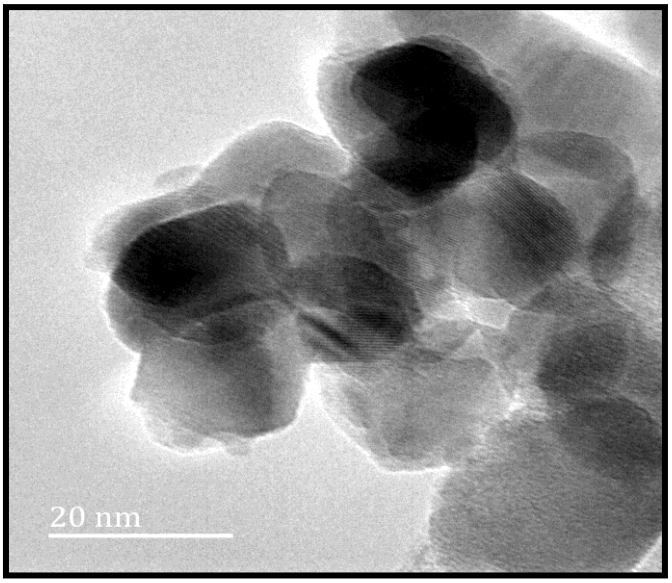

Fig. 2. TEM micrograph of 2% RuO_2/ZrO_2 catalyst.

3.3.3 SEM analysis

Fig. 3 displays a SEM micrograph of the sample of RuO_2/ZrO_2, which illustrates the catalyst's surface morphology. As observed from the high magnification SEM micrograph, zirconia particles are large with irregular shapes. This micrograph illustrates that small needle shapes particles of ruthenia on the surface of zirconia in an aggregative state. Homogeneous distribution of RuO_2 and ZrO_2 on the surface of the catalyst was quantified by the EDS analysis (Fig. 4). Moreover, the morphology of the catalyst as per the SEM micrographs points to a crystalline and homogenous sample.

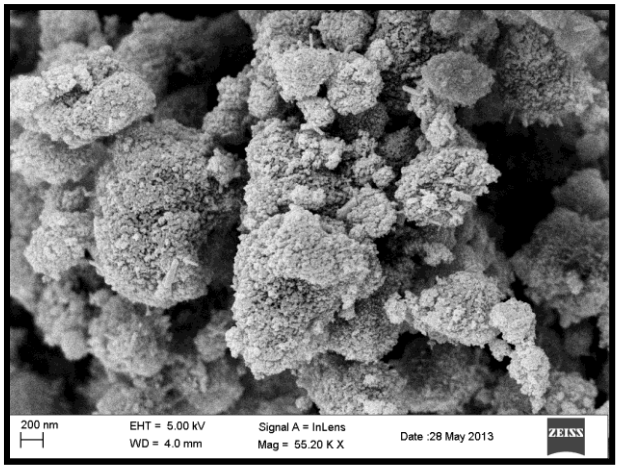

Fig. 3. SEM micrograph of 2% RuO_2/ZrO_2 catalyst.

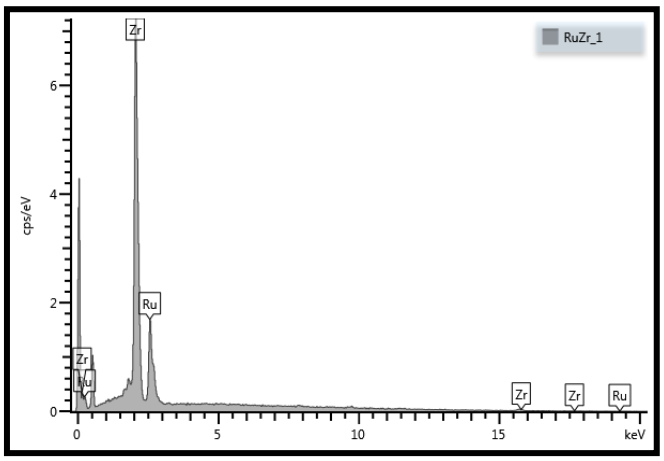

Fig. 4. EDS spectra of 2% RuO_2/ZrO_2 catalyst.

3.3.4 BET surface area analysis

The BET surface area properties of the synthesised catalyst were obtained from N_2 adsorption studies (Fig. 5.). The RuO_2/ZrO_2 composite was characterized by N_2 adsorption at 77 K using analyser. The N_2 sorption results confirms a typical type IV isotherm with a narrow H_2 hysteresis loop lying in the p/p_o range of 0.62-0.98, which is typical for mesoporous materials. The BET surface area of 2% RuO_2/ZrO_2 catalyst was 41.99 m^2/g, pore volume 0.134 cm^3/g and pore size 12.7 nm. These results suggest that the 2% RuO_2/ZrO_2 catalyst could act as good promoter for the growth of additional crystalline faces, which cooperate to enhance the catalytic activity of RuO_2/ZrO_2.

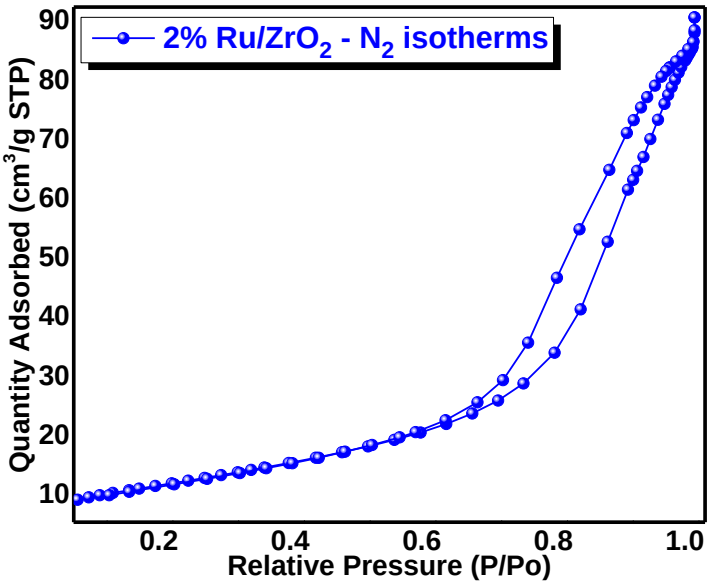

Fig. 5. N_2 adsorption-desorption isotherms of 2% RuO_2/ZrO_2 catalyst.

3.3.5 Pyridine adsorbed FT-IR spectroscopy

The nature of acidity of 2% RuO_2/ZrO_2 was examined from *ex situ* pyridine FT-IR spectroscopy (Fig. 6) [35]. The presence of Brønsted acidic sites are confirmed by the IR band at 1525 cm^{-1} and both Brønsted and Lewis acidic sites are attributed to the peak observed at 1485 cm^{-1}. The absorption band at 1460 cm^{-1} is due to the Lewis acidic sites of the catalyst. The figure reveals the presence of more Lewis acidic sites in the catalyst than the Brønsted acidic sites. Generally, more Lewis acidic sites are predicted in the RuO_2/ZrO_2 catalyst due to availability of vacant metal orbitals on the surface of catalyst, which is capable to accept a electron pair from the electron rich species. The few less intensive peaks observed in the spectrum are mainly due to the higher signal to noise ratio.

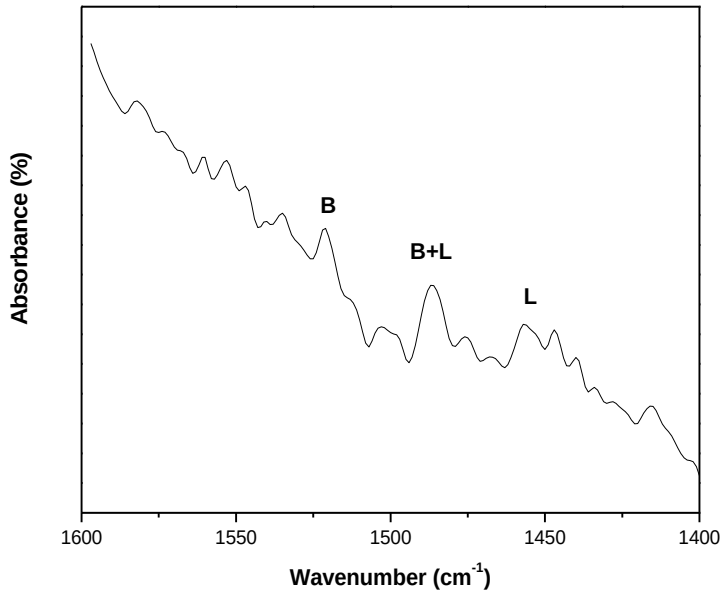

Fig. 6. Pyridine adsorbed FT-IR spectra of 2% RuO_2/ZrO_2 catalyst.

3.3.6 Reaction chemistry

The model reaction of equivalent quantities of diethylacetylenedicarboxylate, 3-chloro-4-fluoroaniline, malononitrile and 2-methoxybenzaldehyde was performed with different catalysts (Table 1). Initially, under catalyst-free and solvent-free conditions no reaction was observed, neither at RT nor reflux conditions (at 100^o C), even after 10 h of reaction time under magnetic stirring (Table 1, entries 1 & 2). For the optimization of the catalyst, in the preliminary studies, the reaction was investigated using various acidic catalysts. In the presence of AcOH, $FeCl_3$, *p*-toluenesulphonic acid (PTSA) and trifluoro acetic acid (TFA), no reaction was observed even after 8 h, at RT under ethanol solvent condition (Table 1, entries 3-6). When the reaction was conducted using ionic liquids (Bmim)BF_4 or L-proline as catalysts, only a trace amount of product yield was observed (Table 1, entries 7 & 8). Using various organic and inorganic basic catalysts like TEA, pyridine, DABCO, NaOH and K_2CO_3 at RT in EtOH solvent the yield of anticipated product was not satisfactory (Table 1, entries 9-13). With pure oxide materials such as silica, zirconia and alumina, moderate yields were obtained after 2.5 h reaction time (Table 1, entries 14-16). Results with zirconia were promising with one of the highest yield among the oxide catalysts (Table 1, entries 15). To enhance the observed activity of zirconia it was loaded with selected metals to form their bimetallic mixed oxides and activities of 2% CuO/ZrO_2, MnO_2/ZrO_2, and RuO_2/ZrO_2 in ethanol solvent at RT waere screened. These mixed oxide catalysts afforded good to excellent yields 81-96% (Table 1, entry 17-19) and 2% RuO_2/ZrO_2 proved superior with 96% yield of the target compound in 15 min under RT. While

using 1% RuO_2/ZrO_2 catalyst yielded 90% product in 30 min under similar conditions (Table 1, entry 20), 4% RuO_2/ZrO_2 led to a slight decreased yield (95%) in 15 min (Table 1, entry 21). Based on its performance, 2% RuO_2/ZrO_2 was chosen as ideal loading for the further studies. The observed superiority of RuO_2/ZrO_2 catalyst could be due to even dispersal of active ruthenia on the wide surface area of zirconia.

Table 1: Optimal condition for the synthesis of **5a** by 2% RuO_2/ZrO_2 catalyst[a]

Entry	Catalyst	Solvent	Condition	Time (h)	Yield (%)[b]
1	--	--	RT	10	--
2	--	--	Reflux	10	--
3	AcOH	EtOH	RT	8.0	--
4	$FeCl_3$	EtOH	RT	10	--
5	PTSA	--	RT	8.0	--
6	TFA	--	RT	8.0	--
7	$(Bmim)BF_4$	EtOH	RT	8.0	09
8	L-proline	EtOH	RT	7.0	14
9	TEA	EtOH	RT	6.0	37
10	Pyridine	EtOH	RT	4.5	22
11	DABCO	EtOH	RT	5.0	29
12	NaOH	EtOH	RT	3.5	28
13	K_2CO_3	EtOH	RT	3.0	40
14	SiO_2	EtOH	RT	2.5	49
15	ZrO_2	EtOH	RT	2.0	76
16	Al_2O_3	EtOH	RT	2.5	58
17	CuO/ZrO_2	EtOH	RT	1.0	81
18	MnO_2/ZrO_2	EtOH	RT	0.75	88
19	2% RuO_2/ZrO_2	EtOH	RT	0.15	96
20	1% RuO_2/ZrO_2	EtOH	RT	0.30	90
21	4% RuO_2/ZrO_2	EtOH	RT	0.20	95

[a] All products were characterised by ^{1}H-NMR, ^{15}N NMR, ^{19}F NMR, ^{13}C-NMR, HRMS and FT-IR spectral analysis; [b] Isolated yields; -- No reaction.

Next, the effect of the amount of catalyst on the reaction was screened. As shown in Table 2, the results (Table 2, entries 1-3) show that an increase in mass of catalyst from 10 mg to 30 mg, resulted in an increased yield from 55% to 96% and a decrease in reaction time. No further significant improvement in the yield of the product was observed on increasing the catalyst amount from 30 mg to 60 mg. Therefore, 30 mg of 2% RuO_2/ZrO_2 catalyst was observed ideal quantity for the reaction conditions employed.

Table 2: Optimization of various weight % for the model reaction by 2% RuO_2/ZrO_2 catalyst[a]

Entry	Catalyst (mg)	Time (min)	Yield (%)
1	10	90	55
2	20	45	77
3	30	15	96
4	40	15	96
5	50	15	96
6	60	20	96

[a]Reaction conditions: 2-methoxybenzaldehyde (1 mmol), malononitrile (1 mmol), diethyl acetylenedicarboxylate (1 mmol), 3-chloro-4-fluoroanilene (1 mmol) and catalyst and solvent (10 mL) were stirred at room temperature.

To compare of efficiency of other solvents, the model reaction was evaluated in presence of various polar and non-polar solvents as well as solvent-free conditions (Table 3). No reaction was observed under the solvent-free condition (Table 3, entry 1). In the presence of non-polar solvents like n-hexane and toluene, with no reaction was observed (Table 3, entries 2 & 3), whereas polar aprotic solvents, such as THF and DMF showed a moderate yields (Table 3, entries 4 & 5). Interestingly, better results were noticed with polar protic solvents, MeOH, EtOH and isopropyl-alcohol (Table 3, entries 6-8), but none were better than EtOH as solvent. Hence, EtOH solvent system was used for further reactions of substituted pyridines.

Table 3: Optimization of various solvent condition for the model reaction by 2% RuO_2/ZrO_2 catalyst[a]

Entry	Solvent	Time (minutes)	Yield* (%)
1	No solvent	120	0
2	n-hexane	120	0
3	toluene	90	0
4	THF	60	36
5	DMF	60	45
6	MeOH	45	84
7	EtOH	25	96
8	isoproponal	60	69

[a]Reaction conditions: 2-methoxybenzaldehyde (1 mmol), malononitrile (1 mmol), diethyl acetylenedicarboxylate (1 mmol), 3-chloro-4-fluoroanilene (1 mmol), catalyst (30 mg) and solvent (10 mL) were stirred at room temperature.

To evaluate the inclusive applicability of this process, the efficacy of the reaction with a series of substituted aromatic aldehydes was studied under the optimised conditions and the results are summarized in supporting information Table 4. In all cases, the reactions afforded the products in good to excellent yields in short reaction times (< 20 min). Interestingly, the aldehydes both with electron-donating and electron-withdrawing (ortho, meta and para)

substituents performed efficiently under reaction conditions giving the corresponding target products with high selectivity (5a-k).

Table 4: Synthesis of novel functionalized pyridine derivatives by 2% RuO_2/ZrO_2 catalyst[a]

Entry	R	Product	Yield* (%)	Mp °C
1	2-OMe	5a	96	178-180
2	2-F	5b	89	201-202
3	4-Et	5c	90	231-232
4	4-Cl	5d	91	216-218
5	3,4-OMe	5e	94	198-199
6	2,3-OMe	5f	96	240-241
7	4-F	5g	92	224-225
8	3-F	5h	90	191-192
9	3-Cl	5i	91	206–208
10	2-Cl	5j	94	221-222
11	2-Br	5k	89	208-209

[a]Reaction conditions: substituted benzaldehyde (1 mmol), malononitrile (1 mmol), diethyl acetylenedicarboxylate (1 mmol), 3-chloro-4-fluoroanilene (1mmol), catalyst (30 mg) and ethanol solvent (10 mL) were stirred at room temperature.
R = substituted benzaldehydes
* = Isolated yields.

Based on the results, a probable reaction mechanism for the RuO_2/ZrO_2 catalysed synthesis of functionalized halo pyridines is proposed in **Scheme 2** [6]. In the first step, 2-arylidenemalononitrile (**a**) is formed by a fast Knoevenagel condensation of malononitrile **(2)** with arylaldehyde **(1)** catalyzed by the Lewis acidic sites of RuO_2/ZrO_2. The next step involves formation of a 1,3-dipole intermediate compound (**b**) by reaction of amine (**3**) with diethylacetylenedicarboxylate (**4**). In the third step, a Michael addition of (**a)** to (**b)** on catalyst surface produces an intermediate. Finally, an intramolecular cyclization affords the desired functionalized halo 1,4-dihydropyridine derivative.

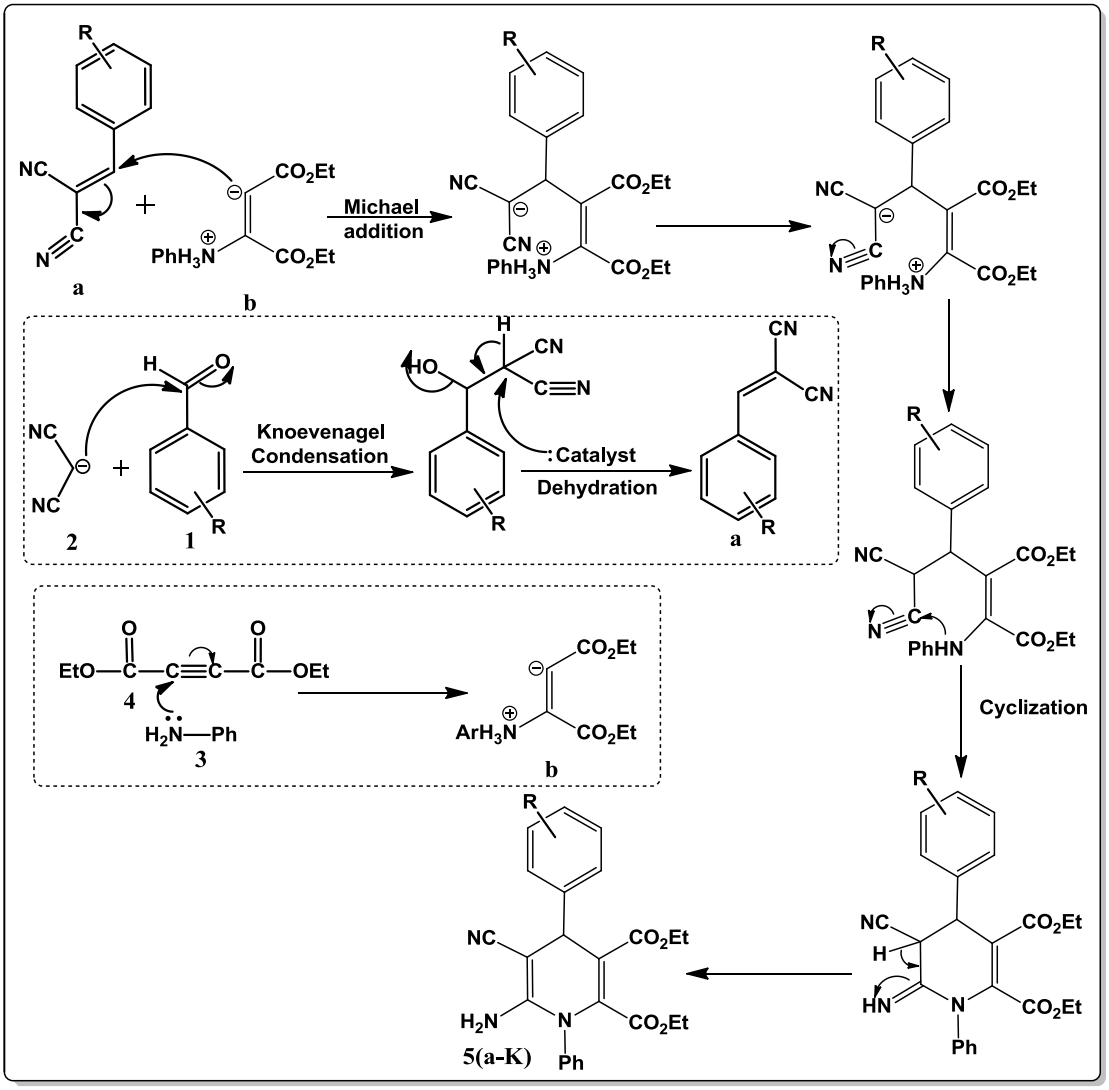

Scheme 2: Possible reaction mechanism.

3.4 Reusability of catalyst

The reusability of the heterogeneous catalysts is an important requirement from the environmental and economic point of view. In heterogeneous catalysis, poisoning of the catalyst and leaching of metal are the common constraints, which diminish the catalyst activity for further reuse. To examine the stability of the catalyst, recycling experiments were performed. After each run, the catalyst was separated by filtration, and recovered catalyst was washed in replicate with ethanol and dried at 120°C for 4 h. When the recovered catalyst was reemployed repeatedly, no significant loss was observed either in the material recovered or in its activity in the first six runs. The catalytic activity of the RuO_2/ZrO_2 decreased by about 4%, when the recovered catalyst material was reused in the 7^{th} run.

3.5 Conclusion

In summary, we have described a simple and feasible four-component procedure using 2% RuO_2/ZrO_2 as catalyst, for the preparation of eleven novel functionalized pyridine derivatives under green solvent conditions in excellent yields (89-96%). The procedure comprises numerous benefits including simple workup, short reaction times, green solvent, high yields and easy purification, waste minimization and catalyst reusability, which makes it advantageous. We believe this method will open wider applications in the fields of medicinal chemistry, molecular diversity synthesis and drug design.

3.6 Acknowledgements

The authors are thankful to the National Research Foundation (NRF) of South Africa, and University of KwaZulu-Natal, Durban, for financial support and research facilities. Authors are also thank full to Dr. Viswanadham Balaga, UKZN for the discussion about the catalyst characterisation.

3.7 References

[1] A. Domling, W. Wang, K. Wang, Chem. Rev. 122 (2012) 3083–3135.

[2] R.C. Cioc, E. Ruijter, R.V.A. Orru, Green Chem. 16 (2014) 2958-2975.

[3] P. Slobbe, E. Ruijter, R.V.A. Orru, Med. Chem. Commun. 3 (2012) 1189-1218.

[4] S.N. Maddila, S. Maddila, W.E. van Zyl, S.B. Jonnalagadda, Curr. Org. Chem. 20 (2016) 2125-2133.

[5] R.A. Sheldon, Chem. Soc. Rev. 41 (2012) 1437-1451.

[6] S. Maddila, K.K. Gangu, S.N. Maddila, S.B. Jonnalagadda, Mol. Diver. 21 (2017). 247–255.

[7] M.J. Climent, A. Corma, S. Iborra, Chem. Rev. 111 (2011) 1072–1133.

[8] S.N. Maddila, S. Maddila, W.E. van Zyl, S.B. Jonnalagadda. Curr. Org. Syn. 13 (2016) 893-900.

[9] S.N. Maddila, S. Maddila, W.E. van Zyl, S.B. Jonnalagadda, ChemistryOpen. 5 (2016) 38–42.

[10] S.N. Maddila, S. Maddila, W.E. van Zyl, S.B. Jonnalagadda, Res. Chem. Intermed. 42 (2016) 2553-2566.

[11] S. Rana, S. Maddila, S.B. Jonnalagadda, Catal. Sci. & Tech. 5 (2015) 3235-3241.

[12] M. Claeys, E.V. Steen, Catal. Today. 71 (2002) 419–427.

[13] R. Noyori, S. Hashiguchi, Acc. Chem. Res. 30 (1997) 97–102.

[14] K. Kusada, H. Kobayashi, T. Yamamoto, S. Matsumura, Naoya, Sumi, K. Sato, K. Nagaoka, Y. Kubota, H. Kitagawa, J. Am. Chem. Soc. 135 (2013) 5493–5496.

[15] M. Mamak, N. Coombs, G. Ozin, J. Am. Chem. Soc. 122 (2000) 8932–8939.

[16] M.N. Aboushelib, C.J. Kleverlaan, A.J. Feilzer, J. Prosth. Dentistry. 98 (2007) 379–388.

[17] S.P.S. Badwal, Solid State Ionics, 52 (1992) 23-32.

[18] S.N. Maddila, S. Maddila, K.K. Gangu, W.E. van Zyl, S.B. Jonnalagadda, J. Fluor. Chem. 195 (2017) 79-84.

[19] S.N. Maddila, S. Maddila, W.E. van Zyl, S.B. Jonnalagadda, RSC Adv. 5 (2015) 37360-37366.

[20] B. Heller, M. Hapke, Chem. Soc. Rev. 36 (2007) 1085-1094.

[21] D. M. Stout, A.I. Meyers, Chem. Rev. 82 (1982) 223–243.

[22] E. Abele, R. Abele, E. Lukevics, Chem. Heterocyc. Comp. 39 (2003) 825–865.

[23] S. Kumar, N. Sharma, I.K. Maurya, A.K. Bhasin, N. Wangoo, P. Brandao, V. Felix, K.K. Bhasin, R.K. Sharma, Eur. J. Med. Chem. 123 (2016) 916-924.

[24] M.V. Rodic, V.M. Leovac, L.S. Jovanovic, V. Spasojevic, M.D. Joksovic, T. Stanojkovic, I. Z. Matic, L.S. Vojinovic-Jesic, V. Markovic, Eur. J. Med. Chem. 115 (2016) 75-81.

[25] J. Li, S. Kovackova, S. Pu, J. Rozenski, S D. Jonghe, S. Einav, P. Herdewijn, Med. Chem. Comm. 69 (2015) 1666-1672.

[26] T. Murata, M.S.S. Sakakibara, T. Yoshino, T. Masuda, T. Shintani, H. Sato, Y. Koriyama, K. Fukushima, N. Nunami, M. Yamauchi, K. Fuchikami, H. Komura, A. Watanabe, K.B. Ziegelbauer, K.B. Bacon, T.B. Lowinger, Bioorg. & Med. Chem. Lett. 14 (2004) 4019–4022.

[27] G. Li , X. Qian, J. Cui, Q. Huang, R. Zhang, H. Guan, J. Agric. Food Chem. 54 (2006) 125–129.

[28] X.H. Liu, X.Y. Xu, C.X. Tan, J.Q. Weng, J.H. Xin, J. Chen, Pest Manage. Sci. 71 (2015) 292–301.

[29] P. Suman, H.C. Lokman, P. Tasneem, Syn. Commun. 43 (2013) 986–992.

[30] P. Suman, S. Vandana, D. Prolay, H.C Lokman, Bioorg. Chem. 48 (2013) 8–15.

[31] C. Hong-Shuo, D. Rui-Yun, Monatsh Chem. 146 (2015) 1355–1362.

[32] S. Jing, X. Er-Yan, W. Qun, Y. Chao-Guo, Org. Lett. 12 (2010) 3678–3681.

[33] S. Maddila, K. Naicker, S. Gorle, S. Rana, Y. Kotaiah, S.N. Maddila, M. Singh, P. Singh, S.B Jonnalagadda, Anti-Cancer Agents in Med. Chem. 16 (2016) 1031-1037.

[34] S. Maddila, K. Naicker, M. Momin, S. Rana, S. Gorle, S.N. Maddila, Y. Kotaiah, M. Singh, S.B. Jonnalagadda, Med. Chem. Res. 25 (2016) 283–291.

[35] B. Viswanadham, J. Pedada, H.B. Friedrich, S. Singh, K.V.R. Chary, Catal. Lett. 146 (2016) 364-372.

3.8 Supplementary information

3.8.1 Catalyst instrumentation details

Employing a Bruker D8 Advance instrument (Cu K radiation source with a wave length of 1.5406 Å), the X-ray diffraction data related the structural phases of the catalyst were acquired. Using a JEOL JEM-1010 electron microscope and JEOL JSM-6100 microscope, the TEM and SEM analysis data was recorded. iTEM software was used analyse the TEM data and images. Employing the X-ray analyser (energy-dispersive), EDX-analysis on the SEM images was conducted.

3.8.2 Experimental Section

All chemicals and reagents required for the reaction were of analytical grade and were used without any further purification. Bruker AMX 400 MHz NMR spectrometer was used to record the ^{1}H NMR, ^{13}C NMR and ^{15}N NMR spectral values. High-resolution mass data were obtained using a Bruker micro TOF-Q II ESI instrument operating at ambient temperature. The $CDCl_3{-}d_6$ solution was utilized for this while TMS served as the internal standard. TMS was further used as an internal standard for reporting the all chemical shifts in δ (ppm). Purity of all the reaction products was confirmed by TLC using aluminium plates coated with silica gel (Merck Kieselgel 60 F_{254}). Infrared (IR) spectra were recorded on a Perkin Elmer Precisely equipped with a Universal ATR sampling accessory using a diamond crystal. The powdered material was placed on the crystal and a force of 120 psi was applied to ensure proper contact between the material and the crystal.The spectra were analyzed using Spectrum 100 software. Before recording the IR spectra, pyridine was adsorbed by placing a drop of pyridine on 10 mg of the sample followed by evacuation in air for 1 h at room temperature to remove reversibly adsorbed pyridine on the surface of the catalyst.

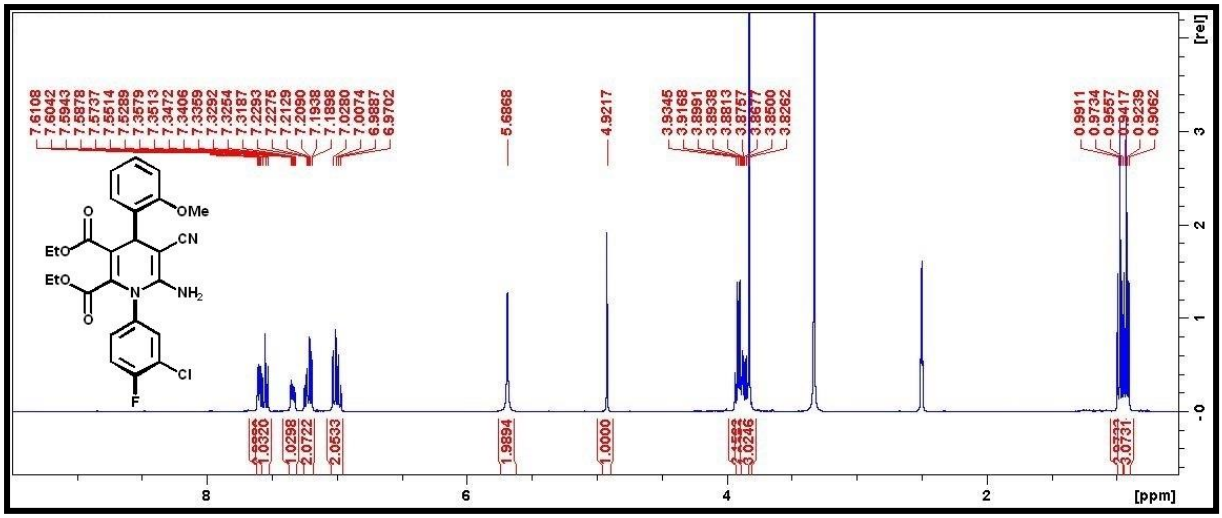

^{1}H NMR spectra of compound **5a**

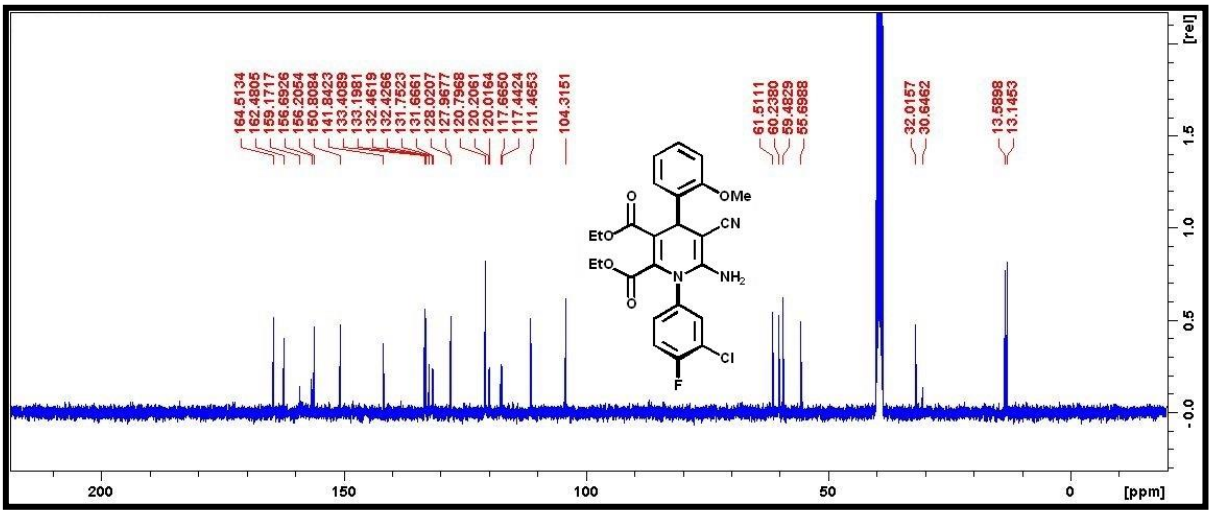

^{13}C NMR spectra of compound **5a**

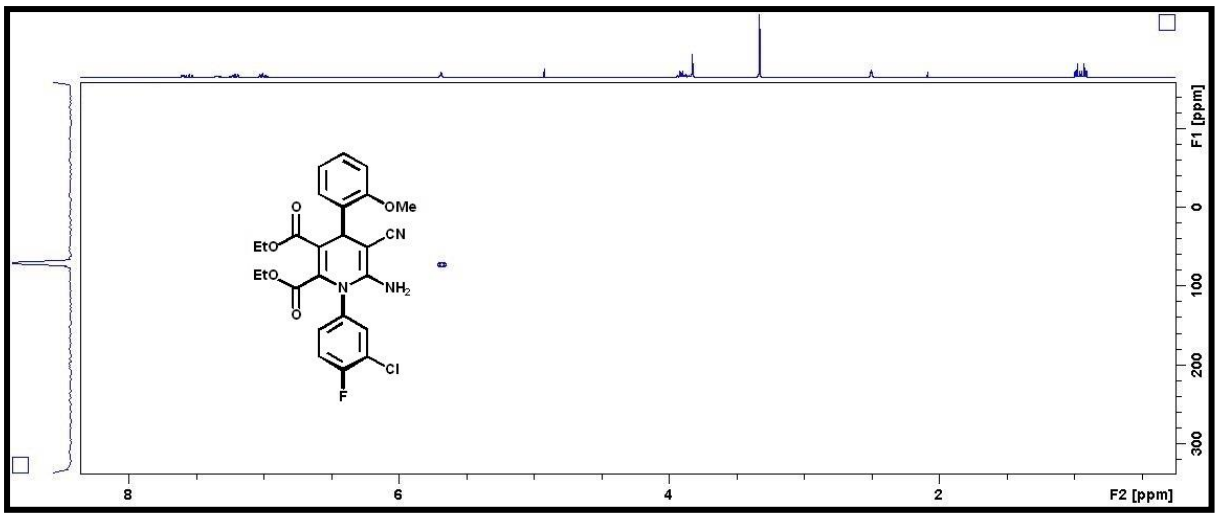

^{15}N NMR spectra of compound **5a**

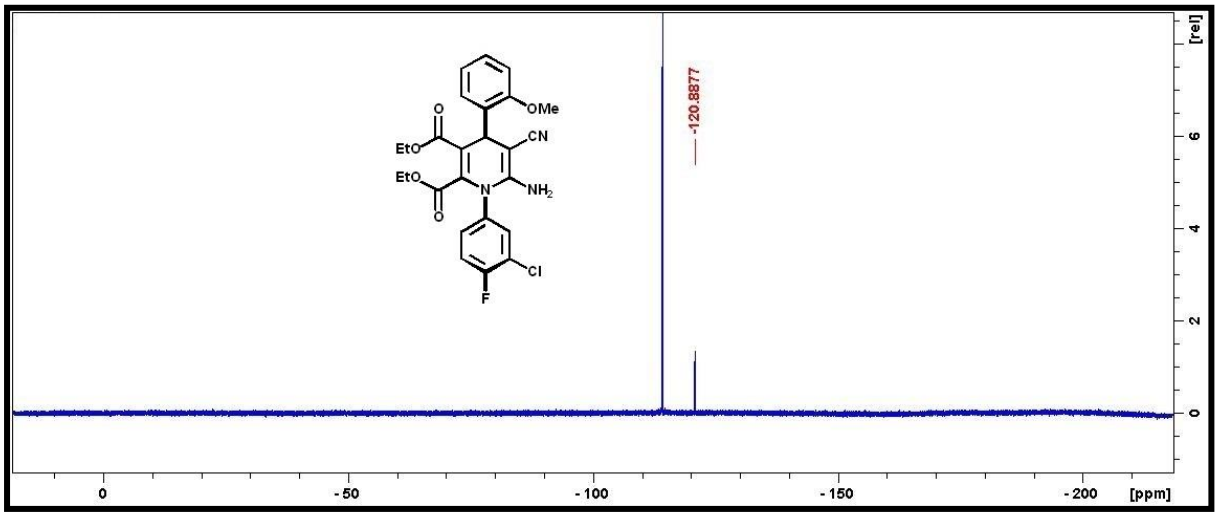

^{19}F NMR spectra of compound **5a**

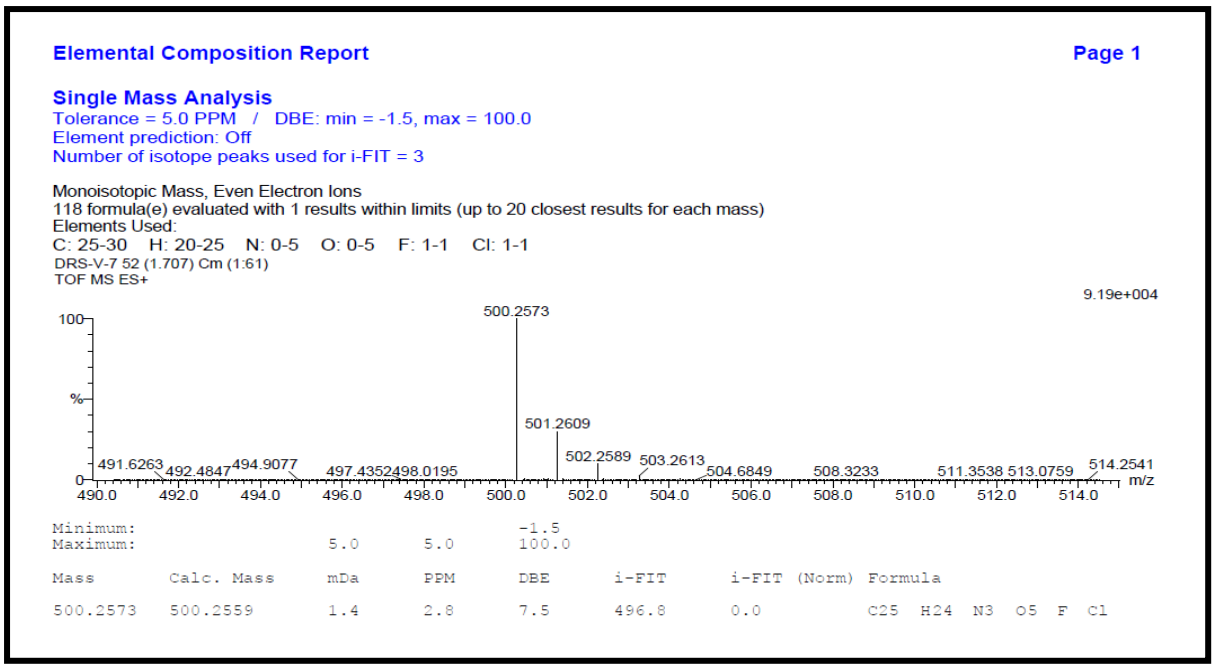

Elemental Composition Report Page 1

Single Mass Analysis
Tolerance = 5.0 PPM / DBE: min = -1.5, max = 100.0
Element prediction: Off
Number of isotope peaks used for i-FIT = 3

Monoisotopic Mass, Even Electron Ions
118 formula(e) evaluated with 1 results within limits (up to 20 closest results for each mass)
Elements Used:
C: 25-30 H: 20-25 N: 0-5 O: 0-5 F: 1-1 Cl: 1-1
DRS-V-7 52 (1.707) Cm (1:61)
TOF MS ES+
9.19e+004

Minimum:		5.0	5.0	-1.5			
Maximum:				100.0			
Mass	Calc. Mass	mDa	PPM	DBE	i-FIT	i-FIT (Norm)	Formula
500.2573	500.2559	1.4	2.8	7.5	496.8	0.0	C25 H24 N3 O5 F Cl

HRMS spectra of compound **5a**

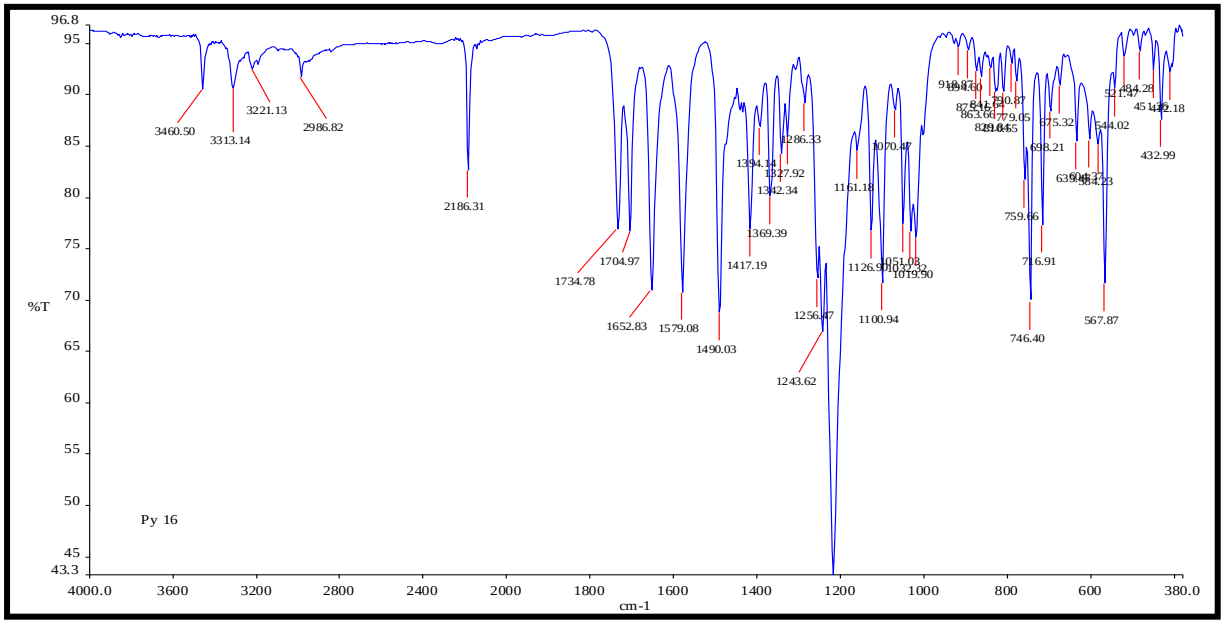

FT-IR spectra of compound **5a**

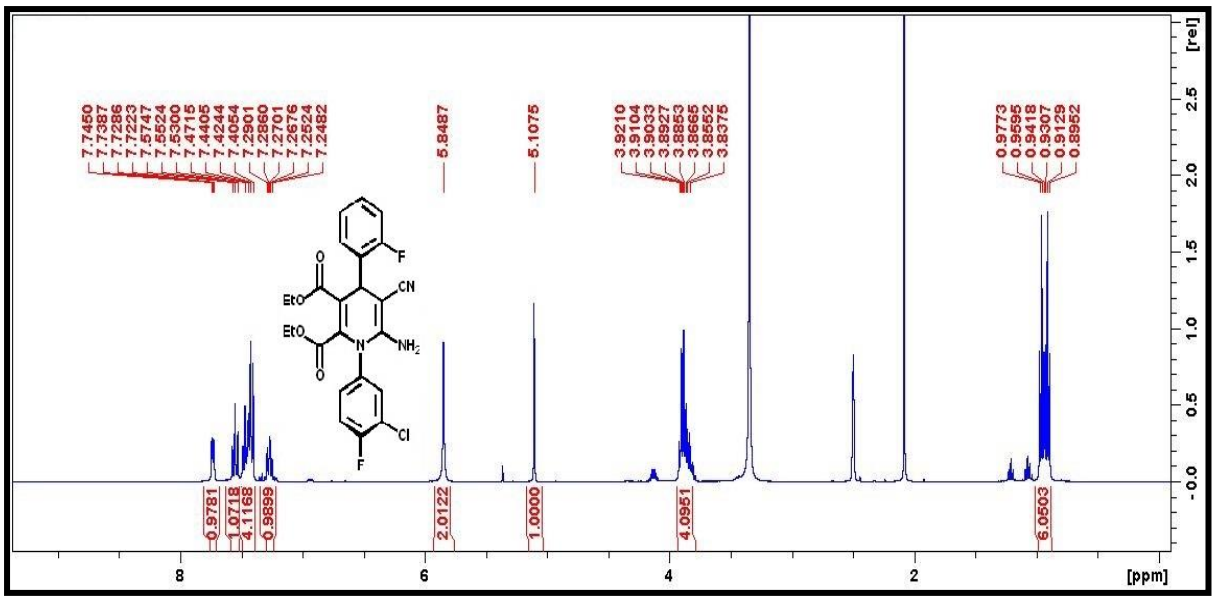

^{1}H NMR spectra of compound **5b**

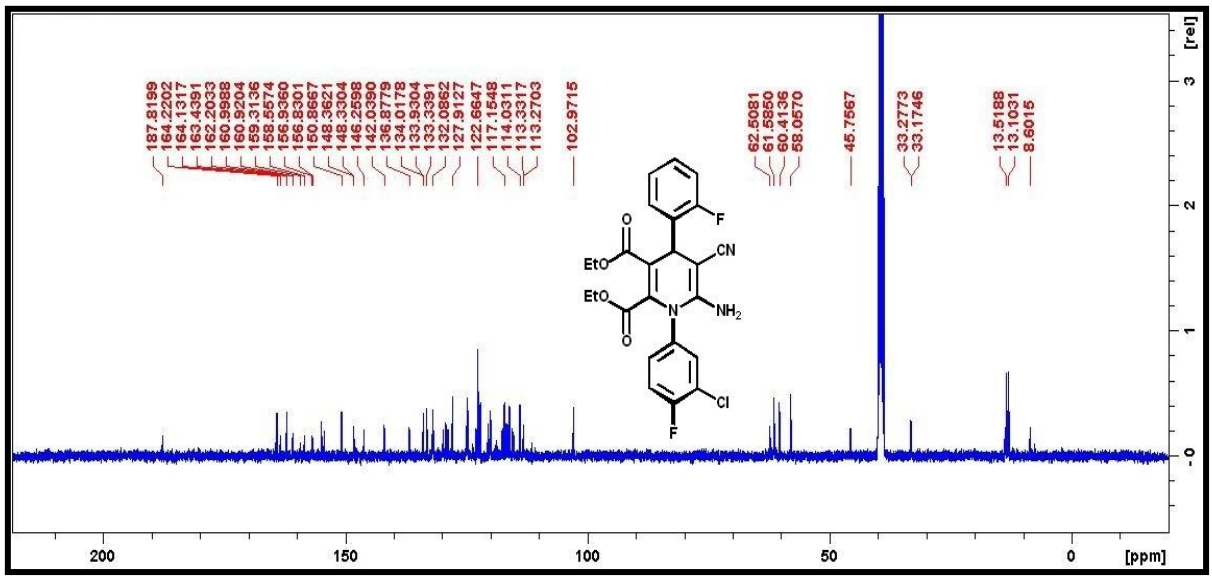

^{13}C NMR spectra of compound **5b**

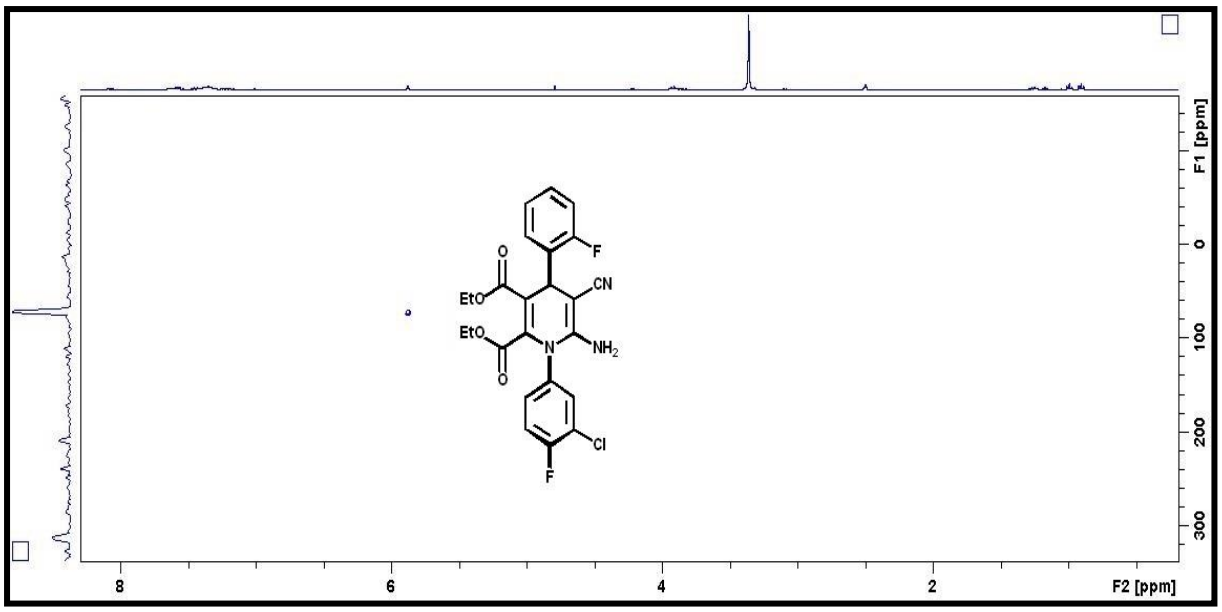

^{15}N NMR spectra of compound **5b**

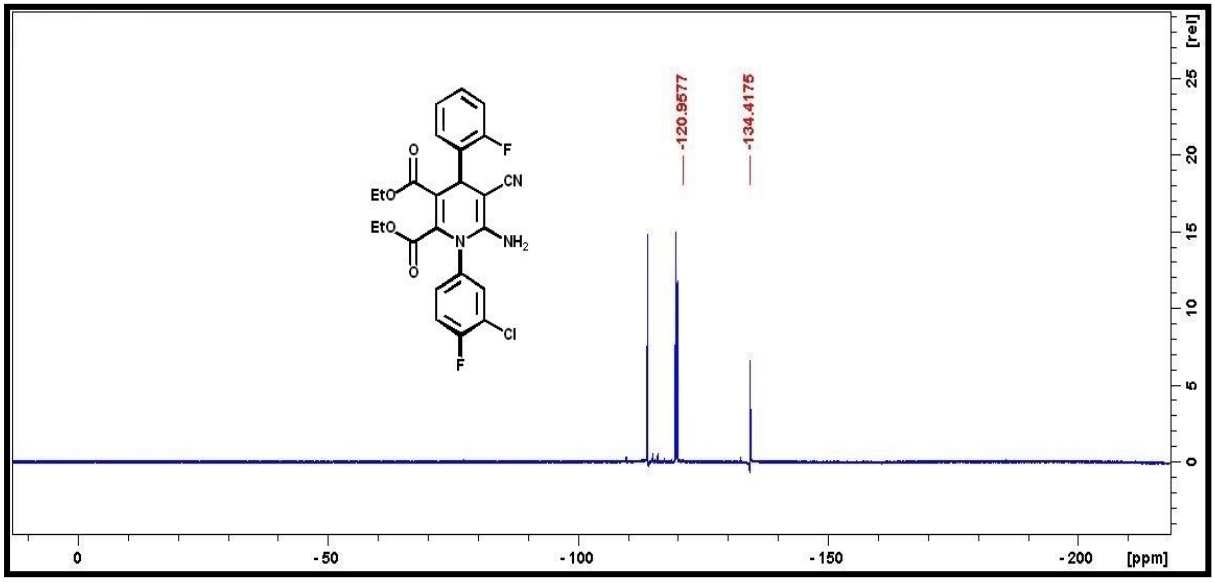

^{19}F NMR spectra of compound **5b**

Elemental Composition Report **Page 1**

Single Mass Analysis
Tolerance = 5.0 PPM / DBE: min = -1.5, max = 100.0
Element prediction: Off
Number of isotope peaks used for i-FIT = 3

Monoisotopic Mass, Even Electron Ions
27 formula(e) evaluated with 1 results within limits (up to 20 closest results for each mass)
Elements Used:
C: 20-25 H: 20-25 N: 0-5 O: 0-5 F: 0-5 Cl: 1-1

DRS-V-7 53 (1.707) Cm (1:61)
TOF MS ES+

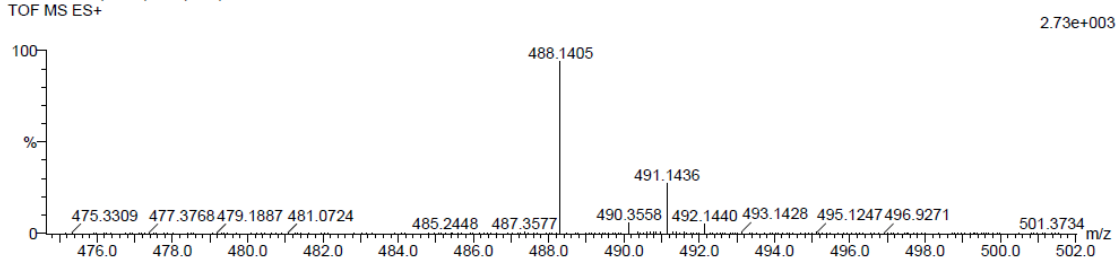

Minimum:				-1.5			
Maximum:		5.0	5.0	100.0			
Mass	Calc. Mass	mDa	PPM	DBE	i-FIT	i-FIT (Norm)	Formula
488.1405	488.1390	1.5	3.1	14.5	97.7	0.0	C24 H21 N3 O4 F2 Cl

HRMS spectra of compound **5b**

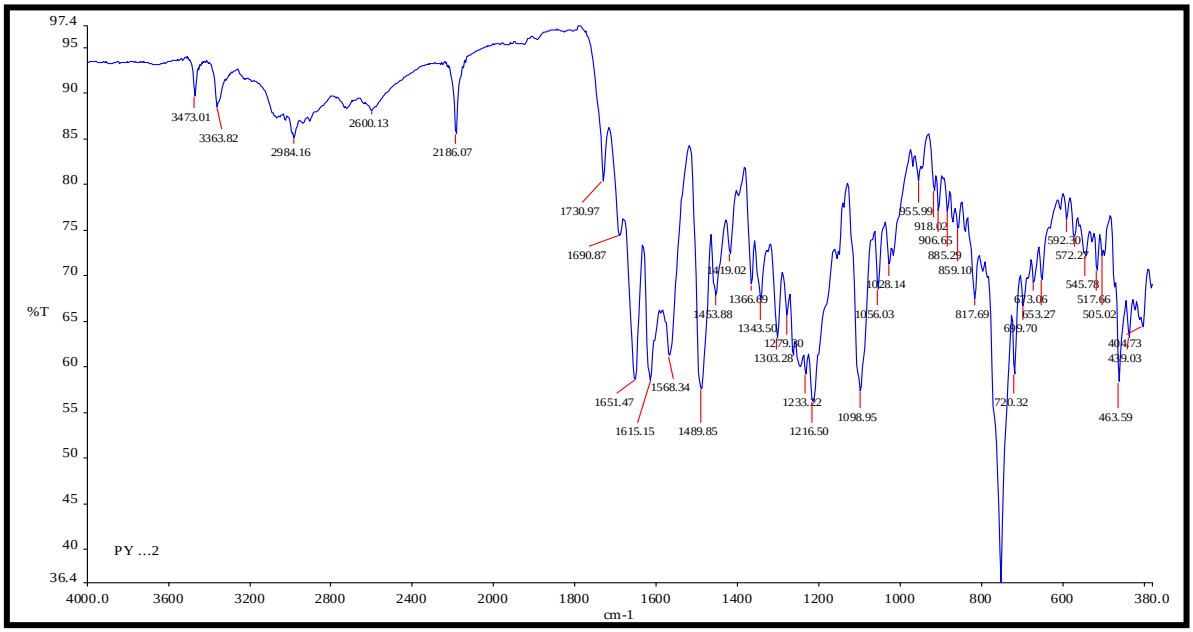

FT-IR spectra of compound **5b**

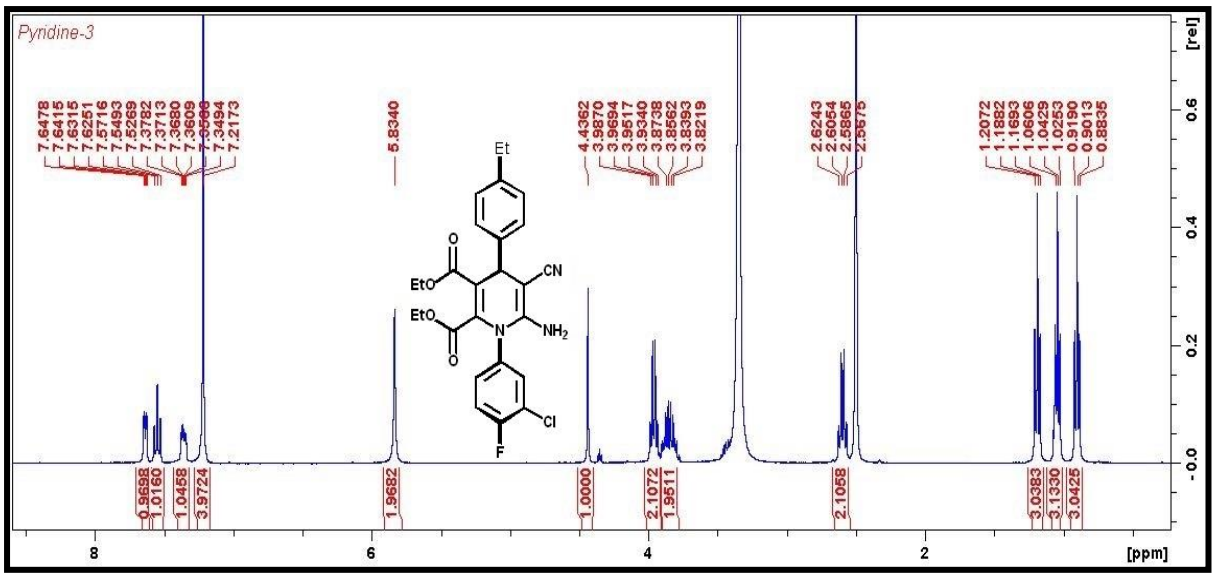

^{1}H NMR spectra of compound **5c**

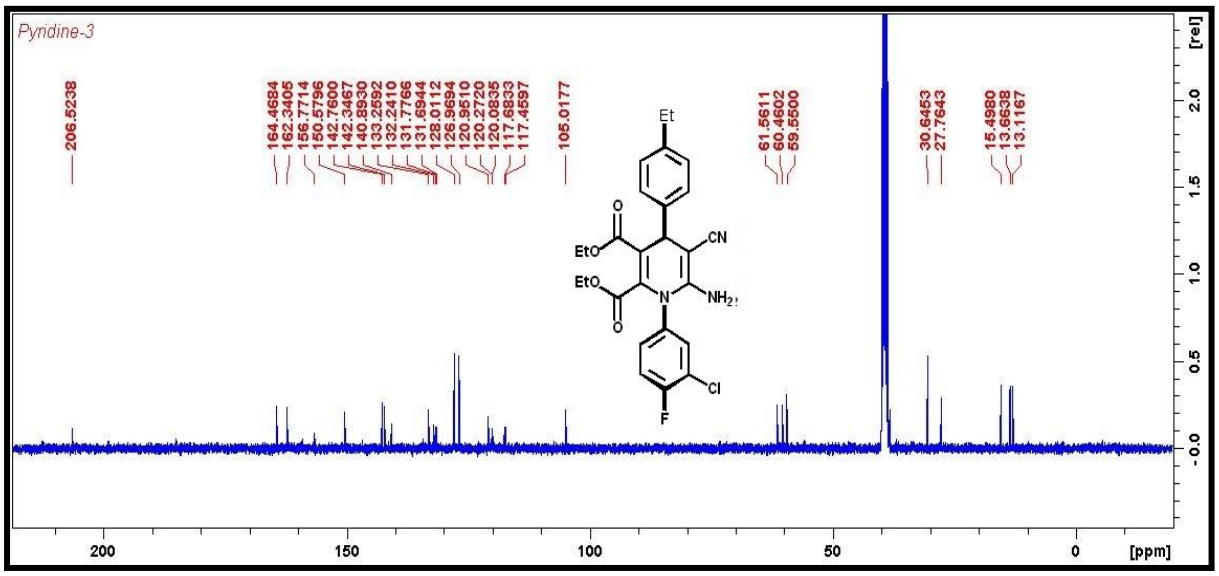

^{13}C NMR spectra of compound **5c**

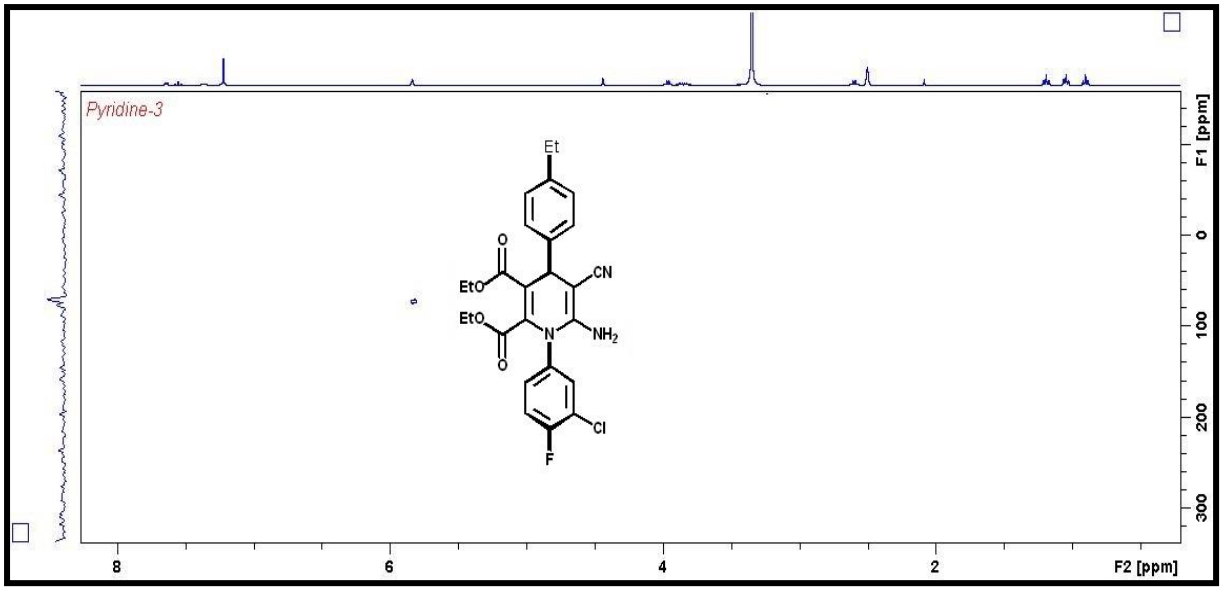

^{15}N NMR spectra of compound **5c**

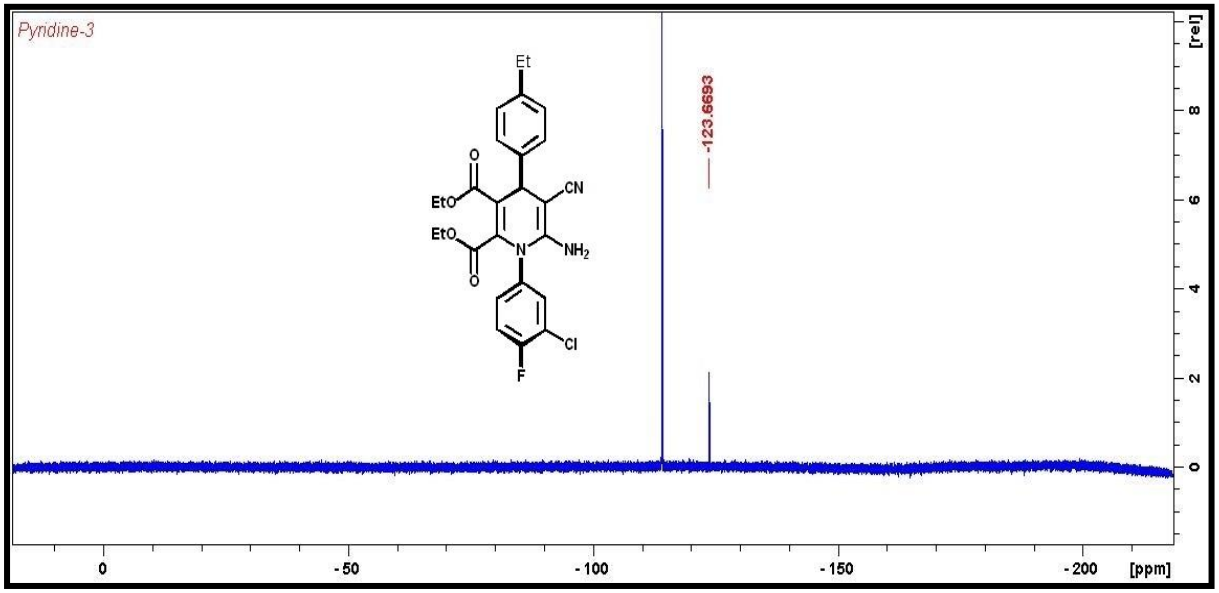

^{19}F NMR spectra of compound **5c**

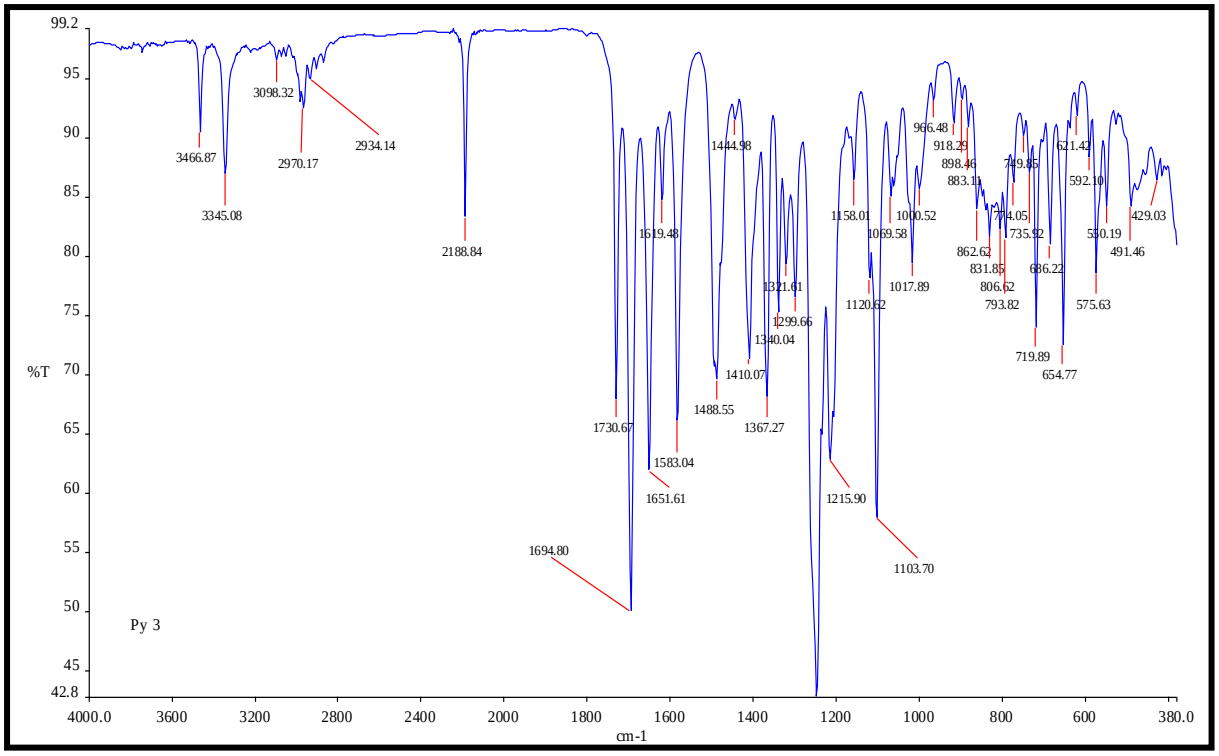

FT-IR spectra of compound **5c**

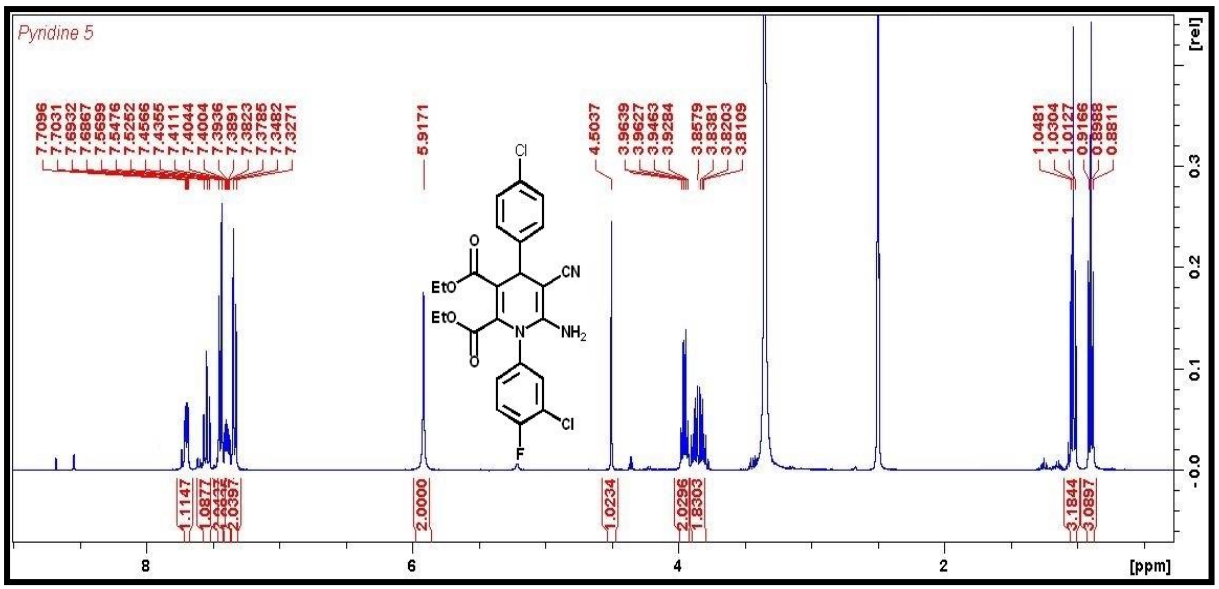

^{1}H NMR spectra of compound **5d**

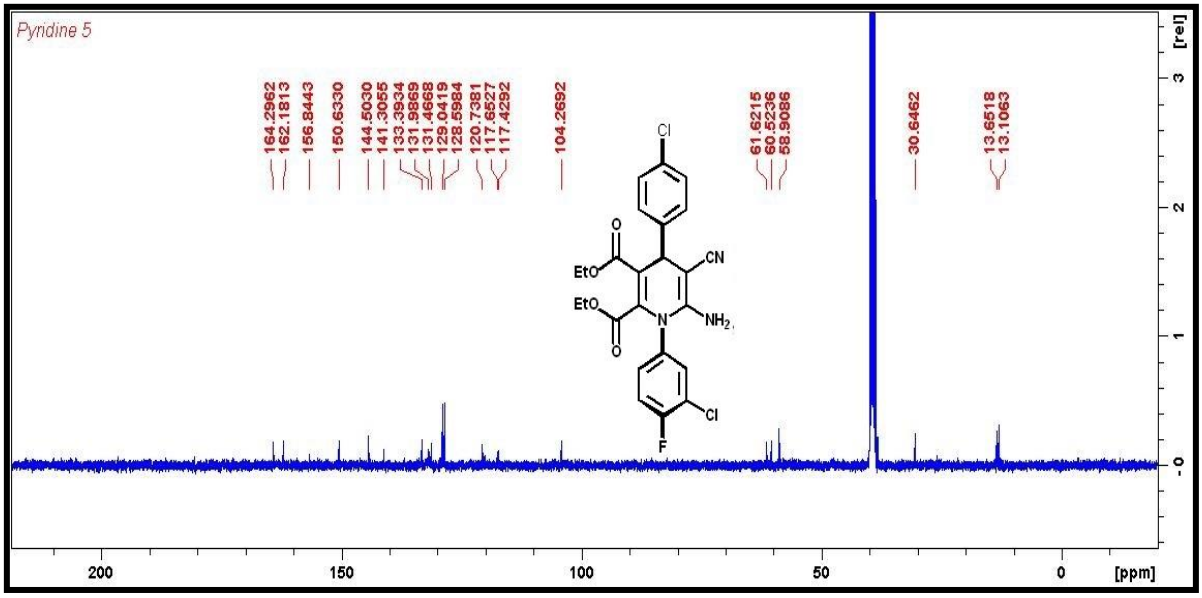

^{13}C NMR spectra of compound **5d**

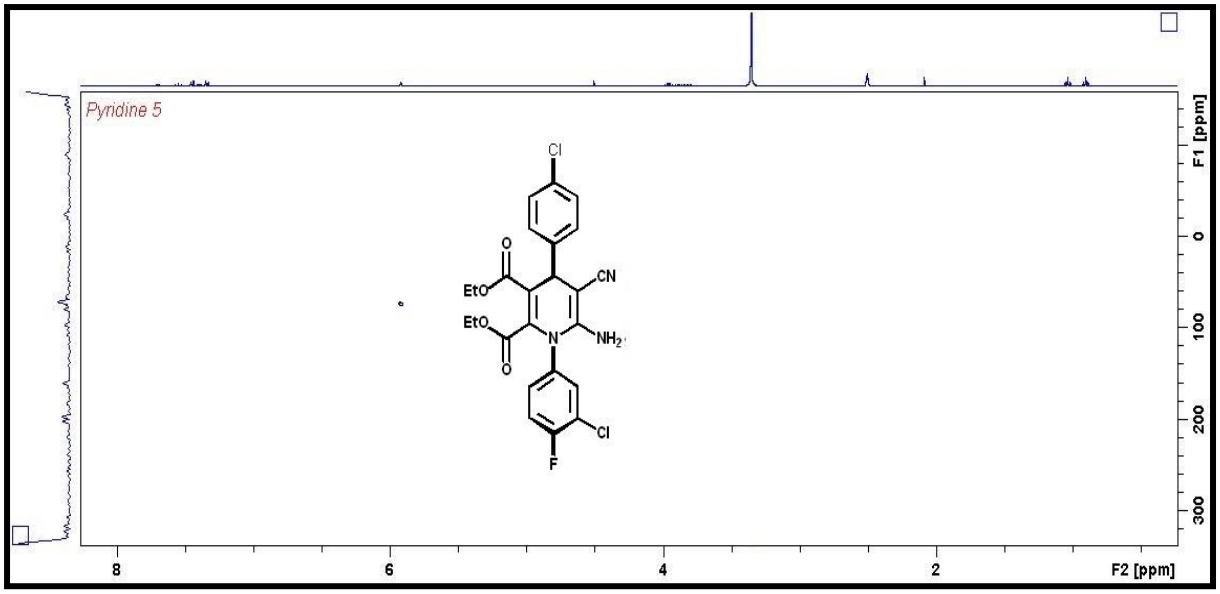

^{15}N NMR spectra of compound **5d**

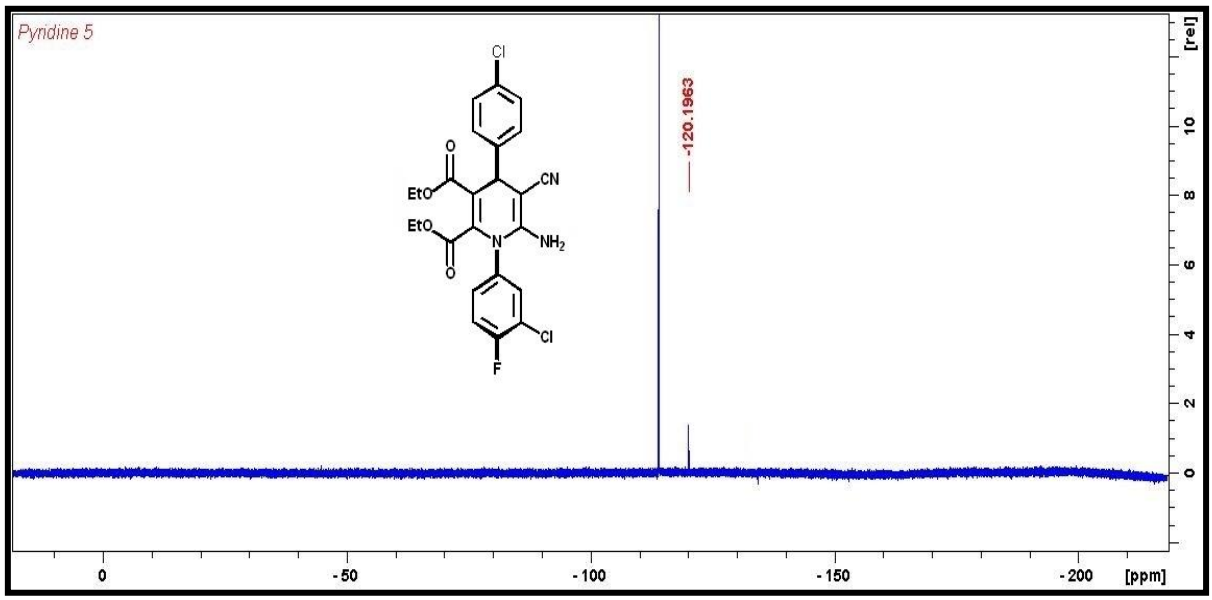

^{19}F NMR spectra of compound **5d**

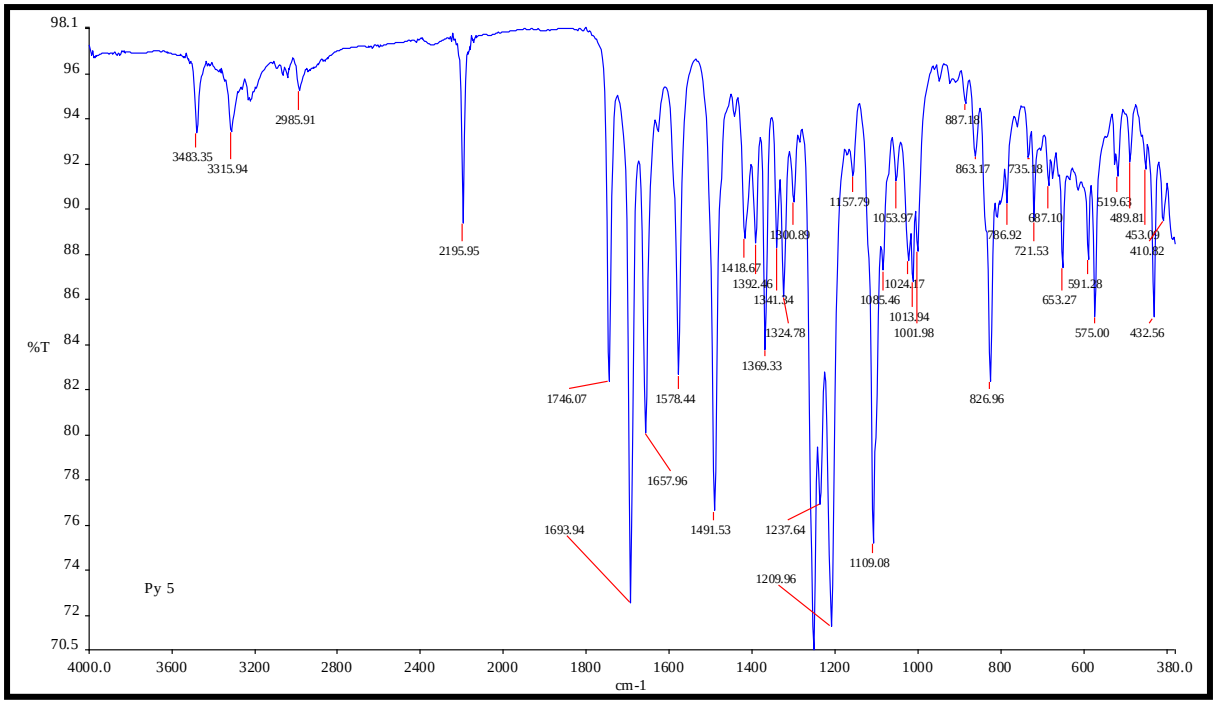

FT-IR spectra of compound **5d**

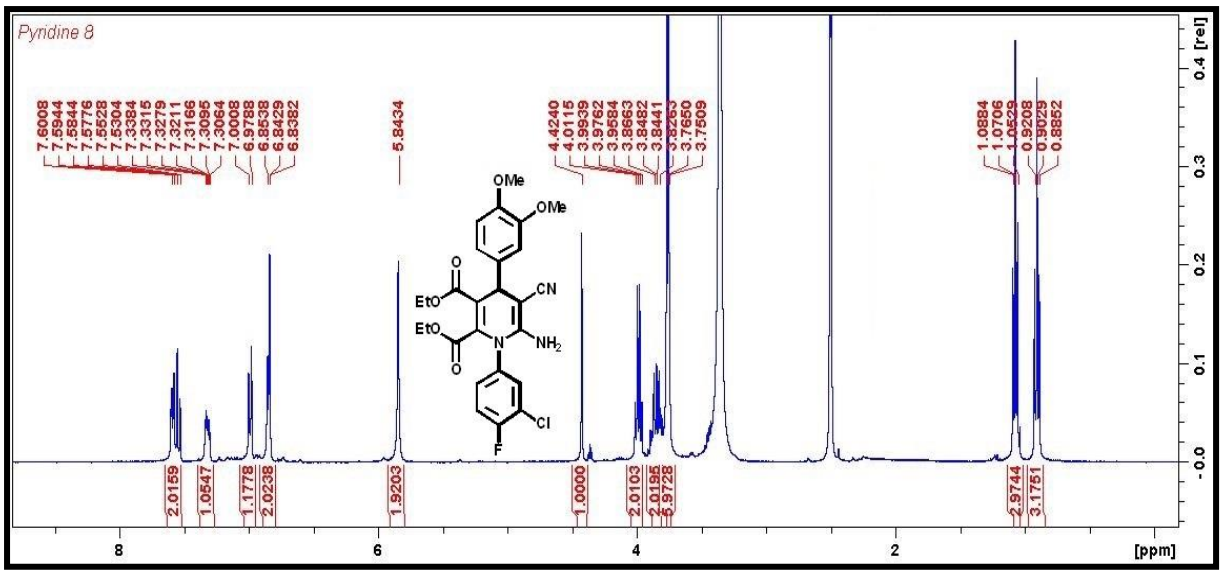

^{1}H NMR spectra of compound **5e**

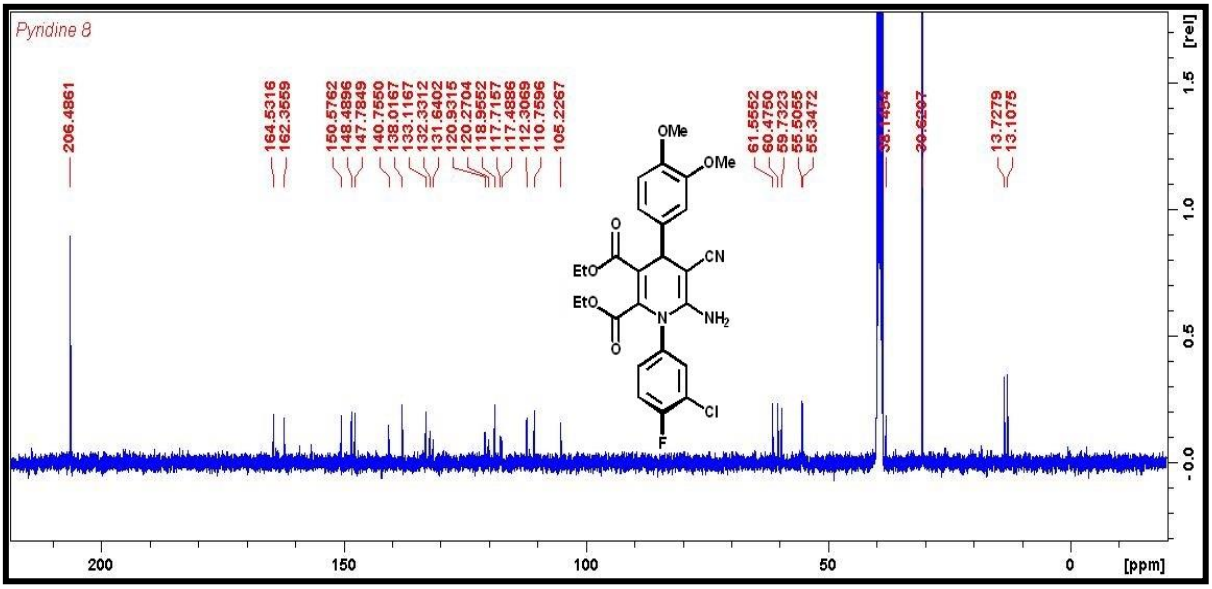

^{13}C NMR spectra of compound **5e**

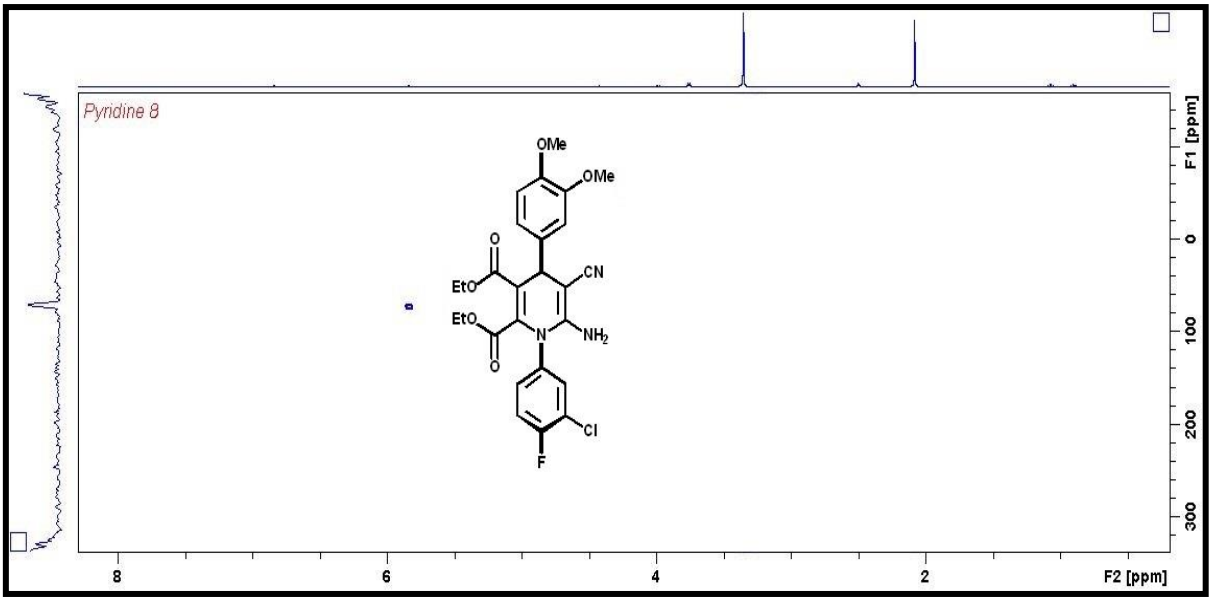

^{15}N NMR spectra of compound **5e**

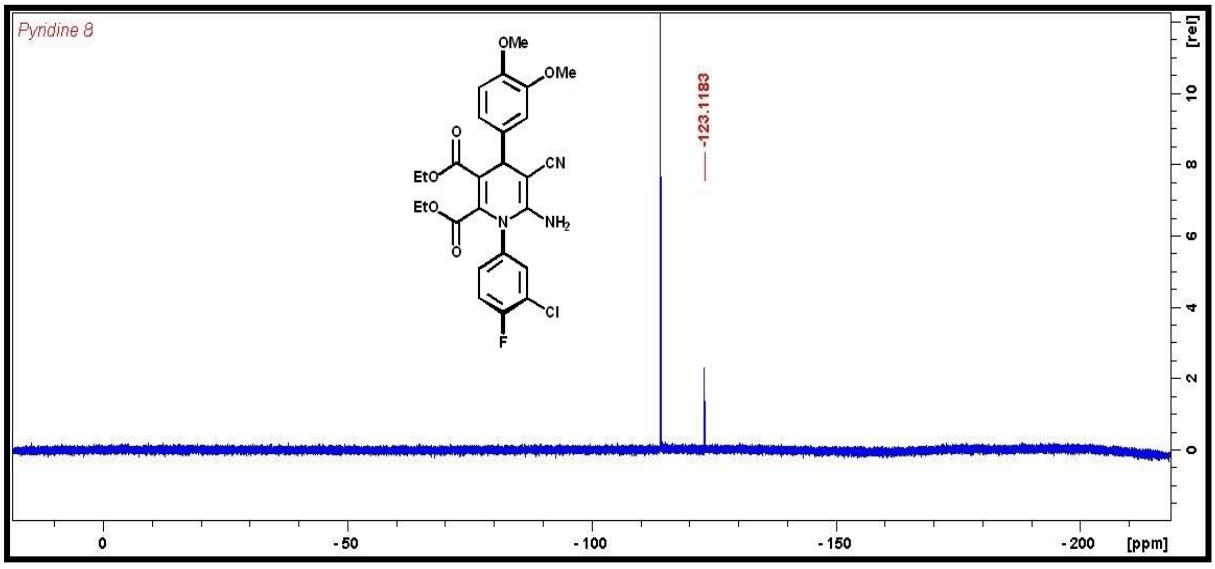

^{19}F NMR spectra of compound **5e**

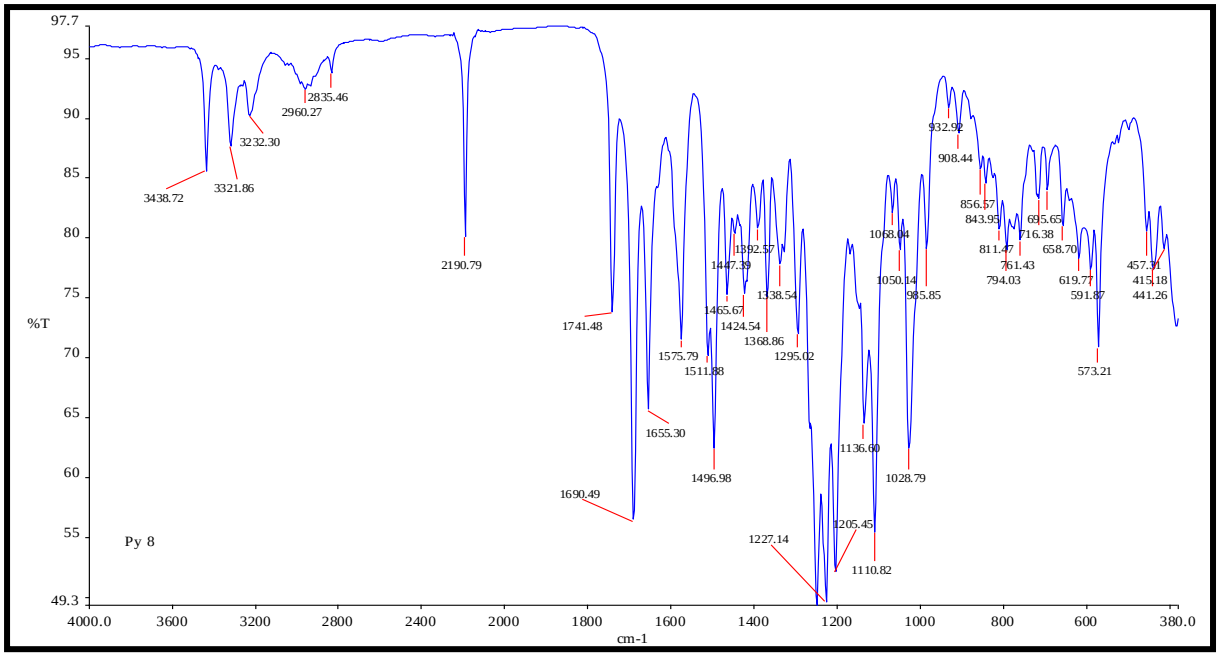

FT-IR spectra of compound **5e**

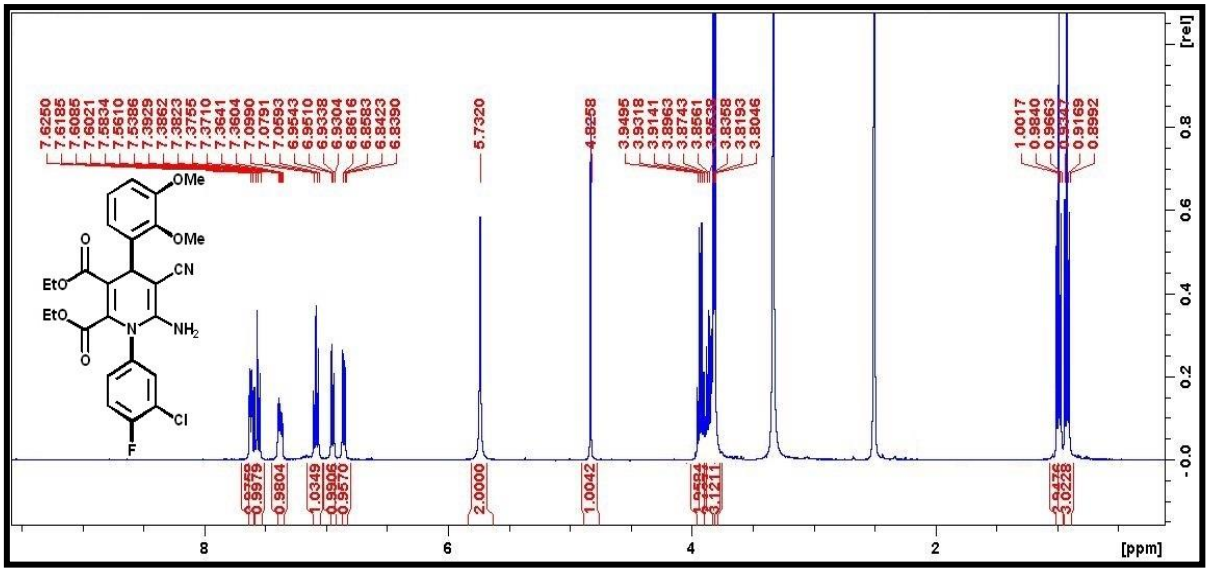

^{1}H NMR spectra of compound **5f**

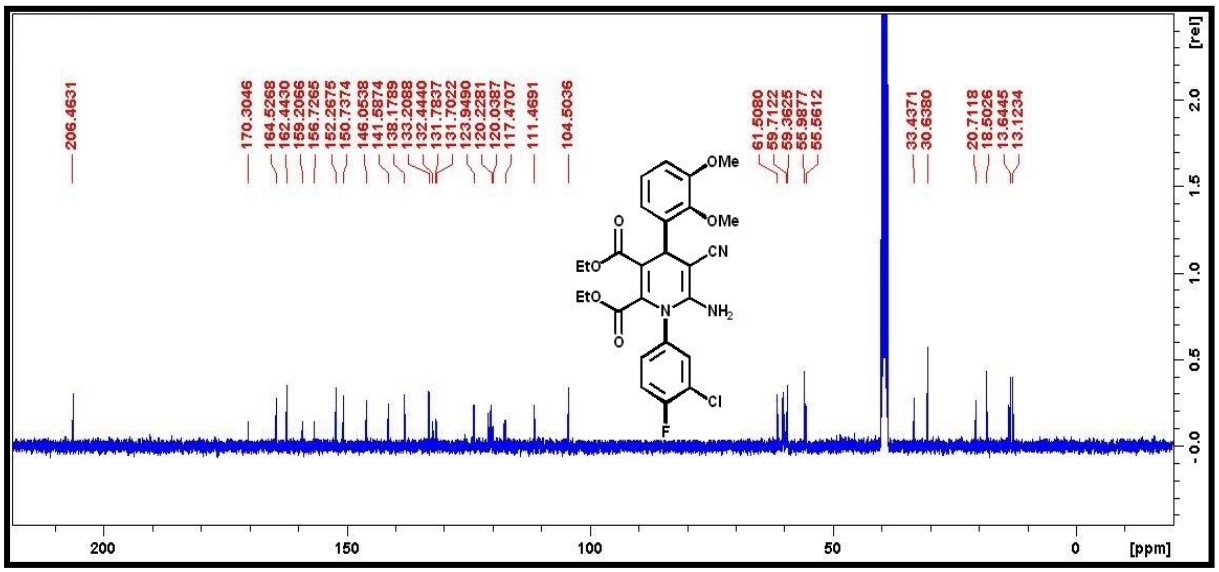

^{13}C NMR spectra of compound **5f**

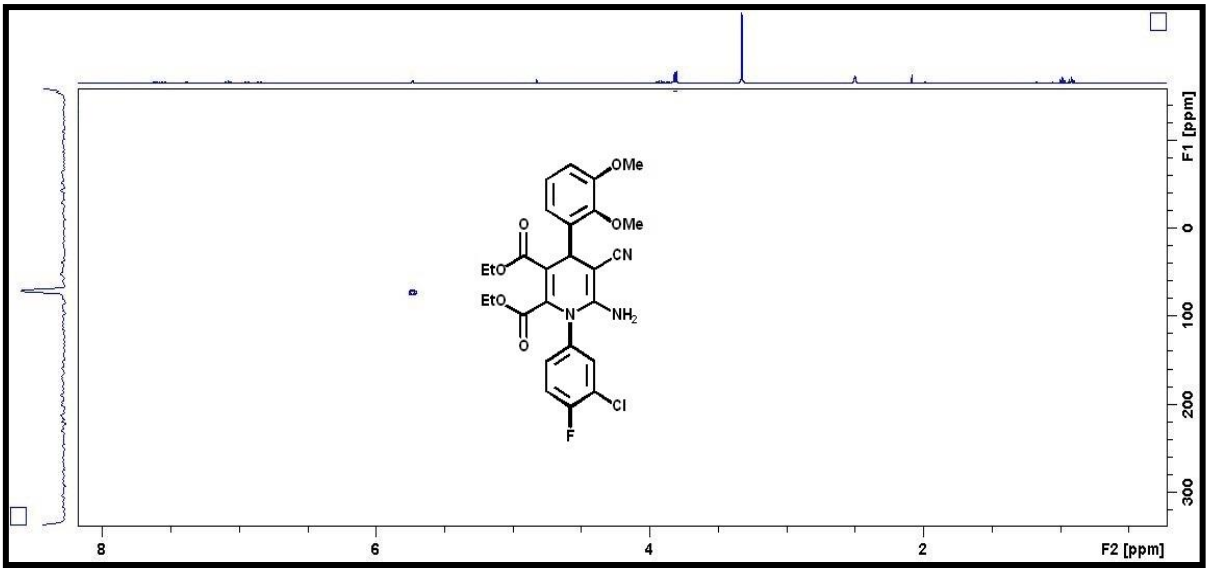

^{15}N NMR spectra of compound **5f**

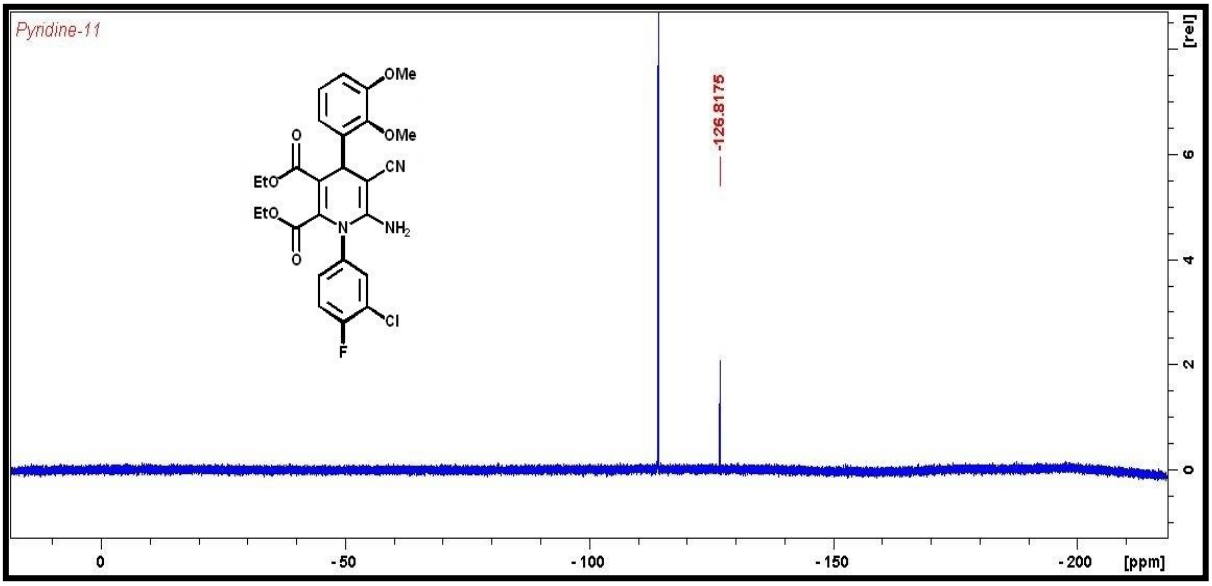

^{19}F NMR spectra of compound **5f**

Elemental Composition Report **Page 1**

Single Mass Analysis
Tolerance = 5.0 PPM / DBE: min = -1.5, max = 100.0
Element prediction: Off
Number of isotope peaks used for i-FIT = 3

Monoisotopic Mass, Even Electron Ions
120 formula(e) evaluated with 1 results within limits (up to 20 closest results for each mass)
Elements Used:
C: 25-30 H: 25-30 N: 0-5 O: 0-10 F: 1-1 Cl: 1-1
DRS-V-14 (0.101) Cm (1:61)
TOF MS ES+

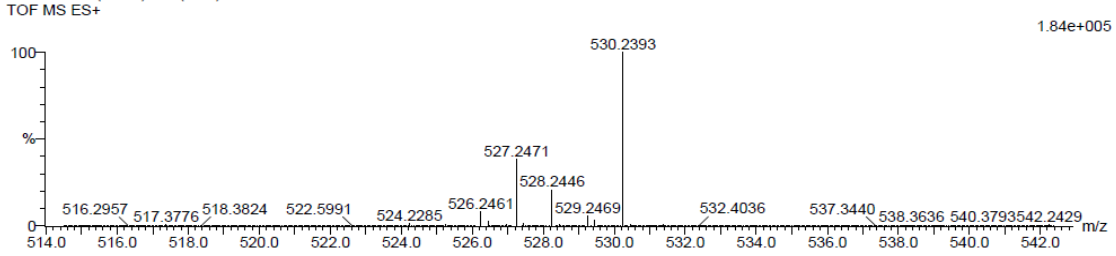

Minimum:				-1.5			
Maximum:		5.0	5.0	100.0			
Mass	Calc. Mass	mDa	PPM	DBE	i-FIT	i-FIT (Norm)	Formula
530.2393	530.2409	-1.6	-3.0	7.5	508.0	0.0	C26 H26 N3 O6 F Cl

HRMS spectra of compound **5f**

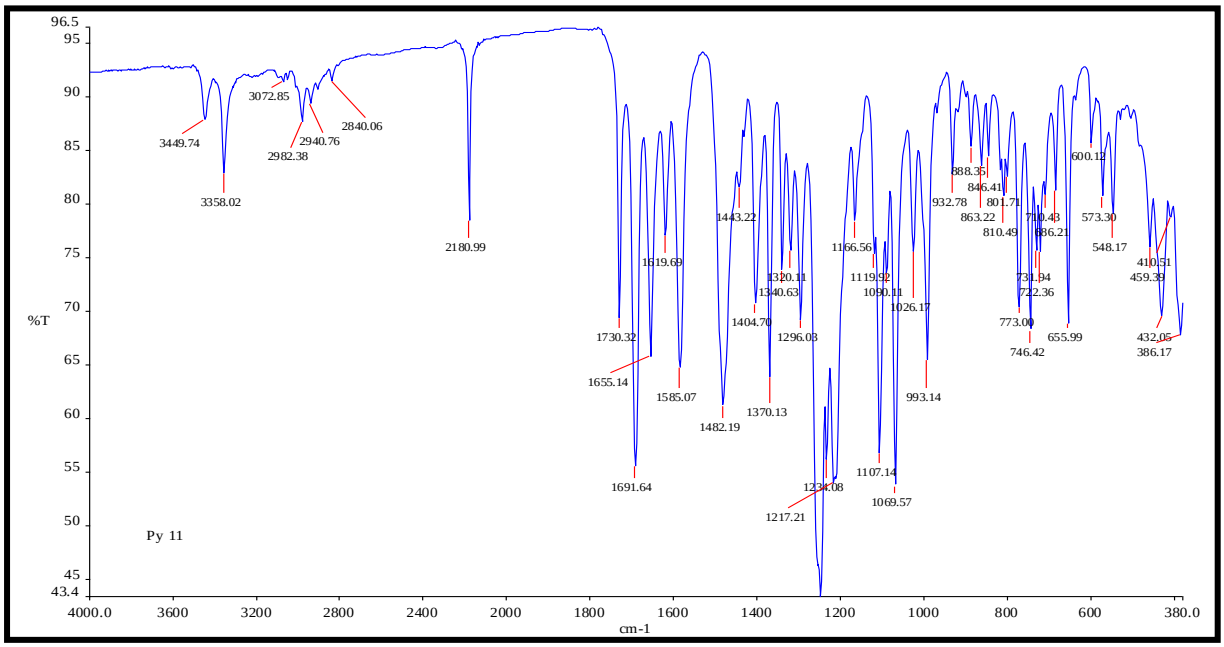

FT-IR spectra of compound **5f**

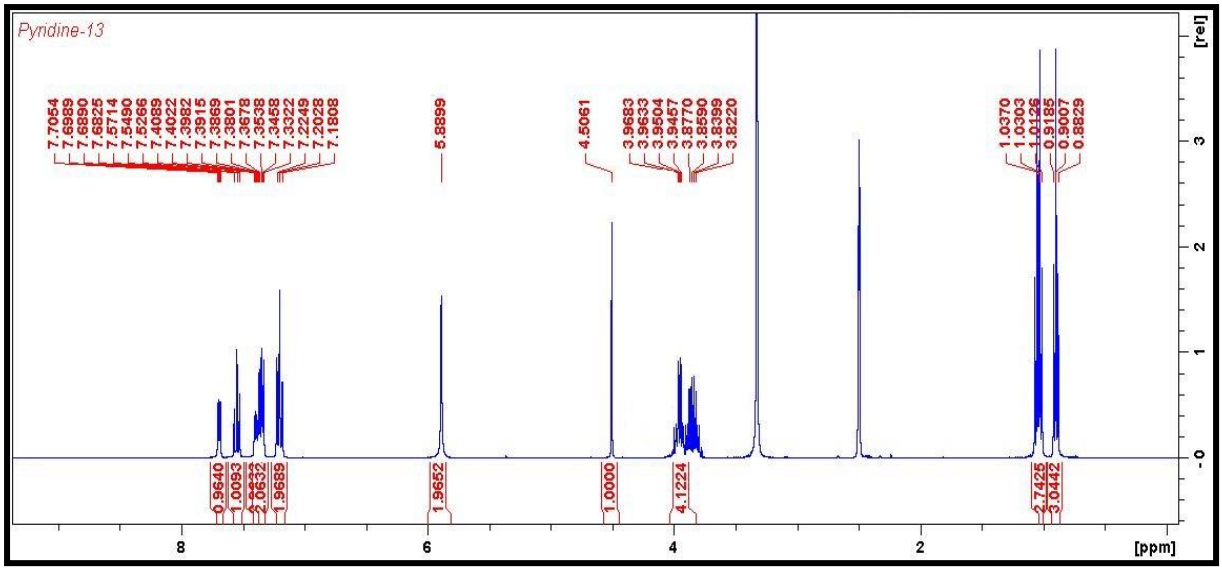

^{1}H NMR spectra of compound **5g**

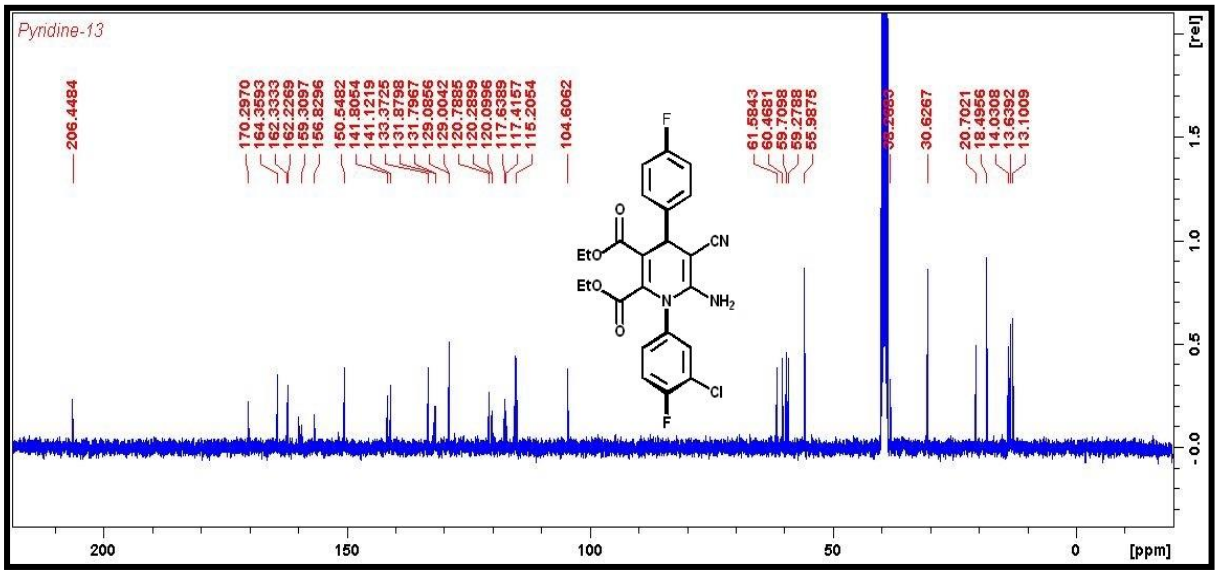

^{13}C NMR spectra of compound **5g**

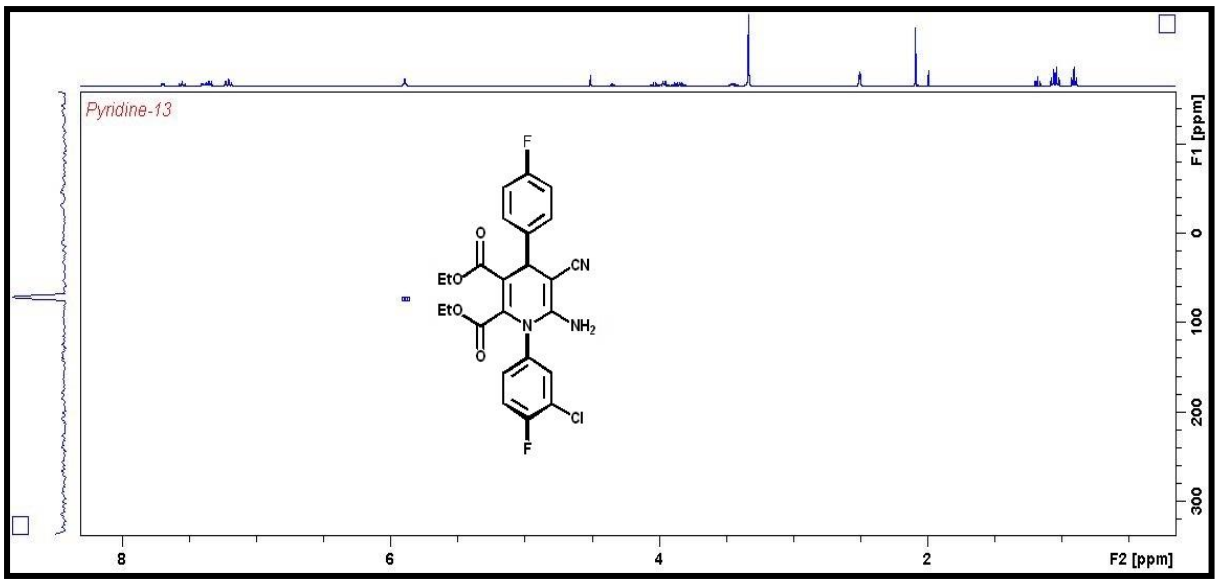

^{15}N NMR spectra of compound **5g**

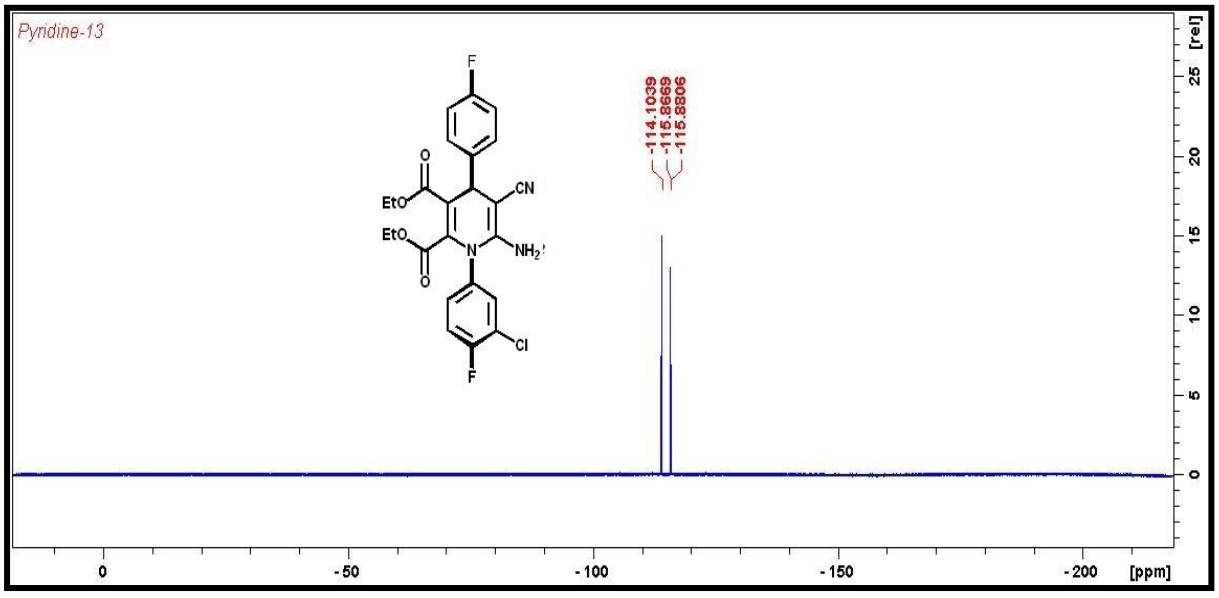

^{19}F NMR spectra of compound **5g**

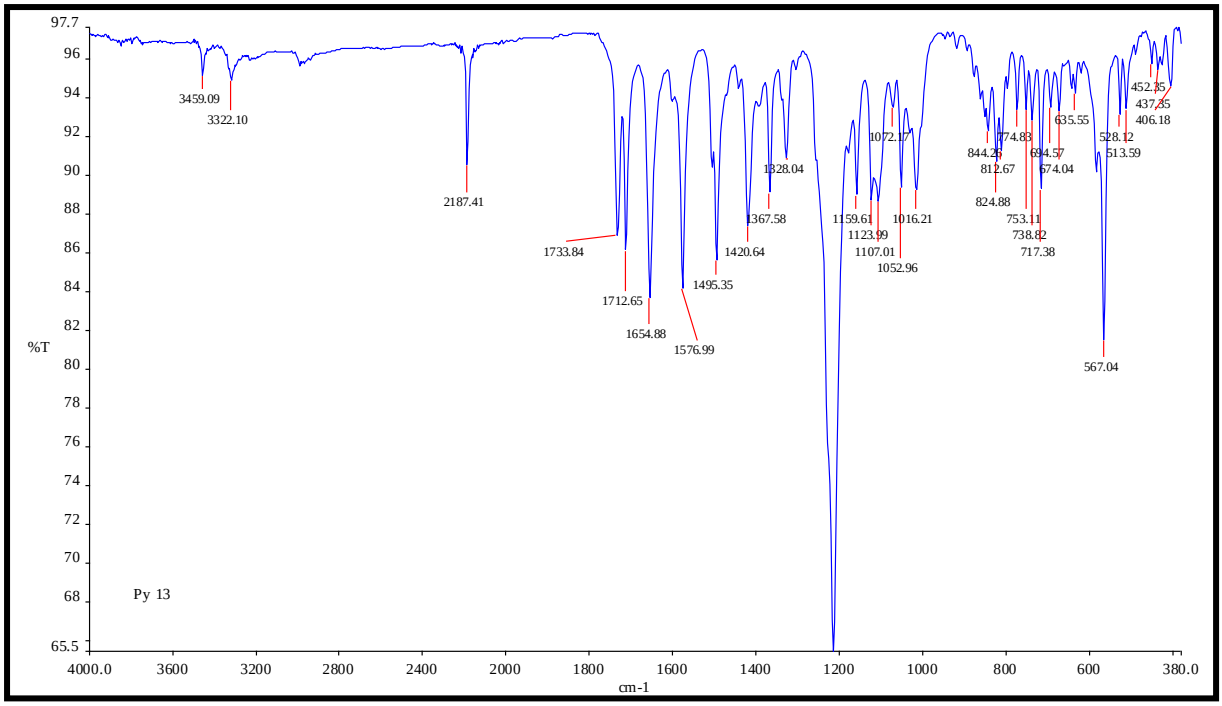

FT-IR spectra of compound **5g**

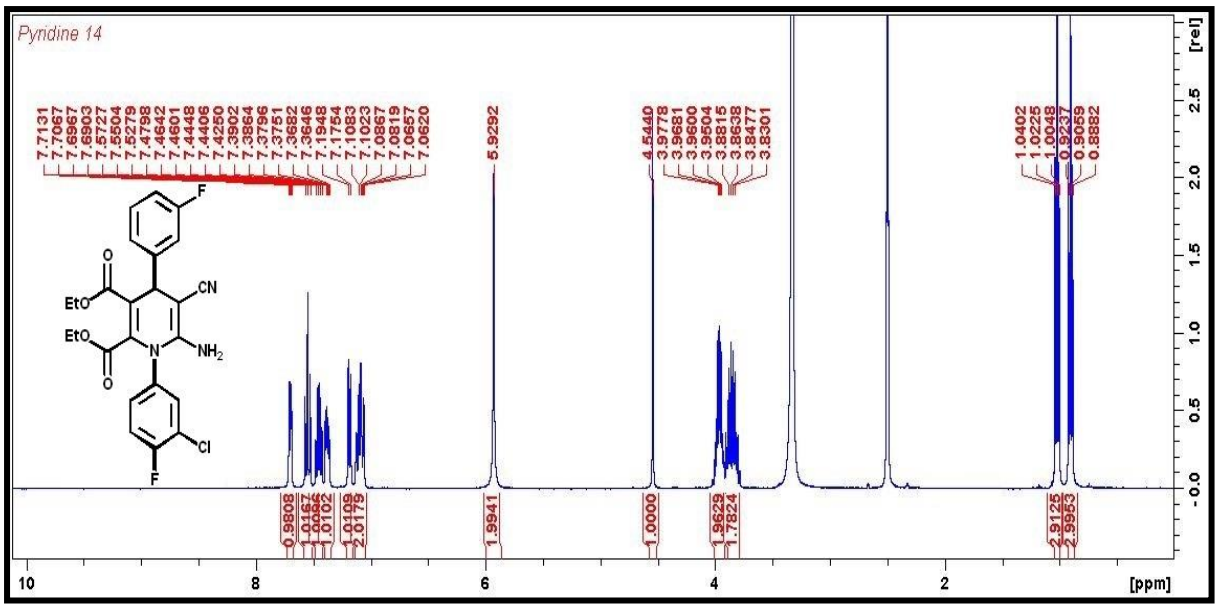

^{1}H NMR spectra of compound **5h**

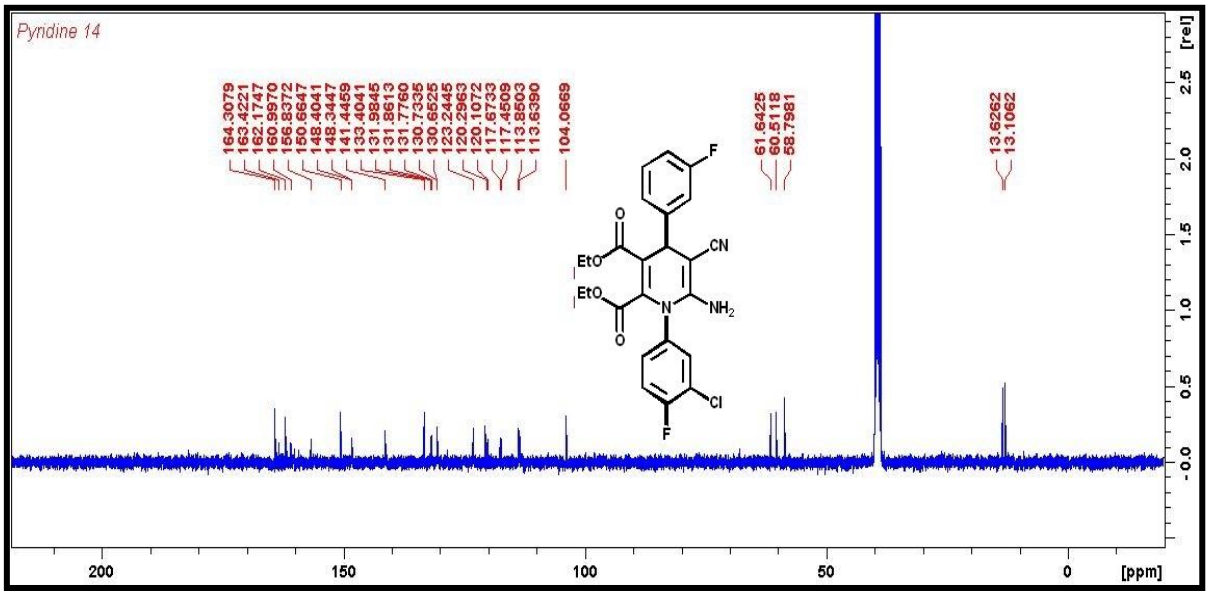

^{13}C NMR spectra of compound **5h**

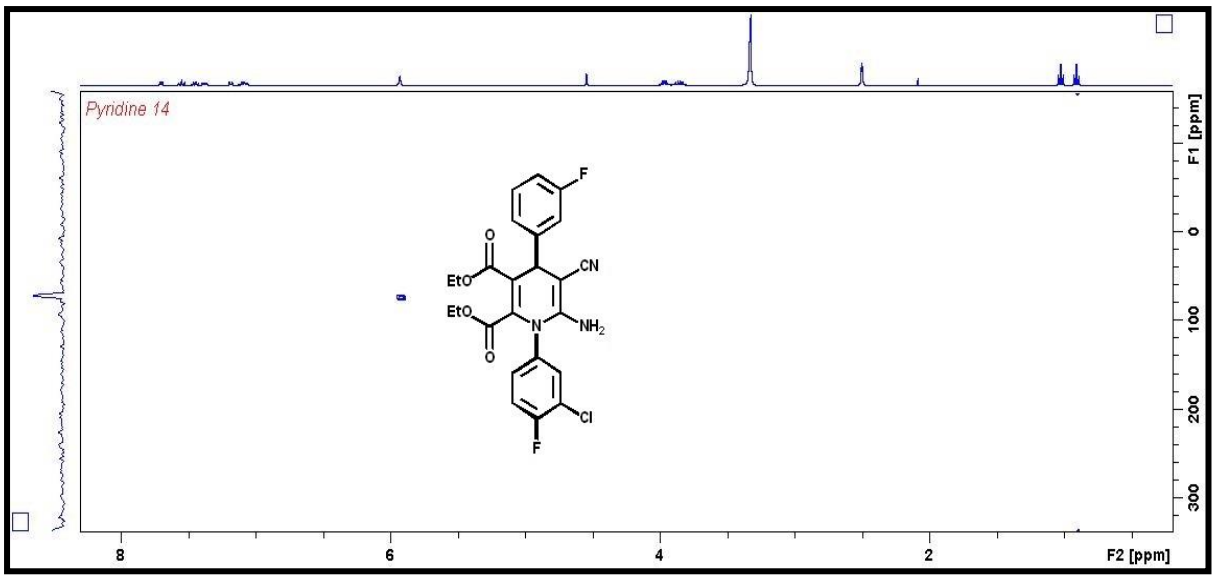

^{15}N NMR spectra of compound **5h**

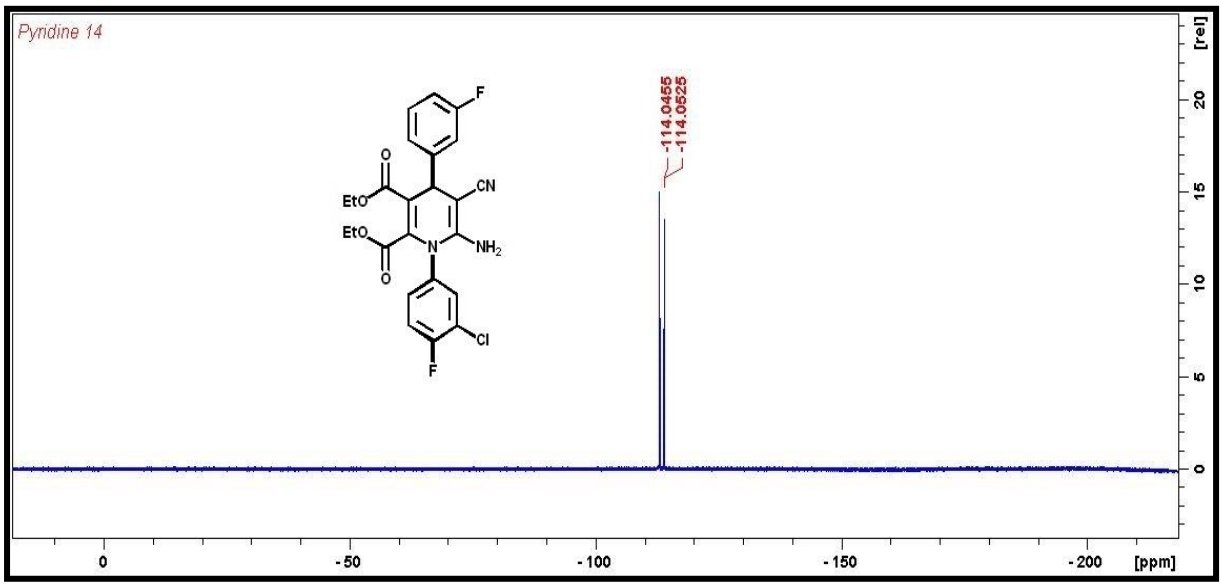

^{19}F NMR spectra of compound **5h**

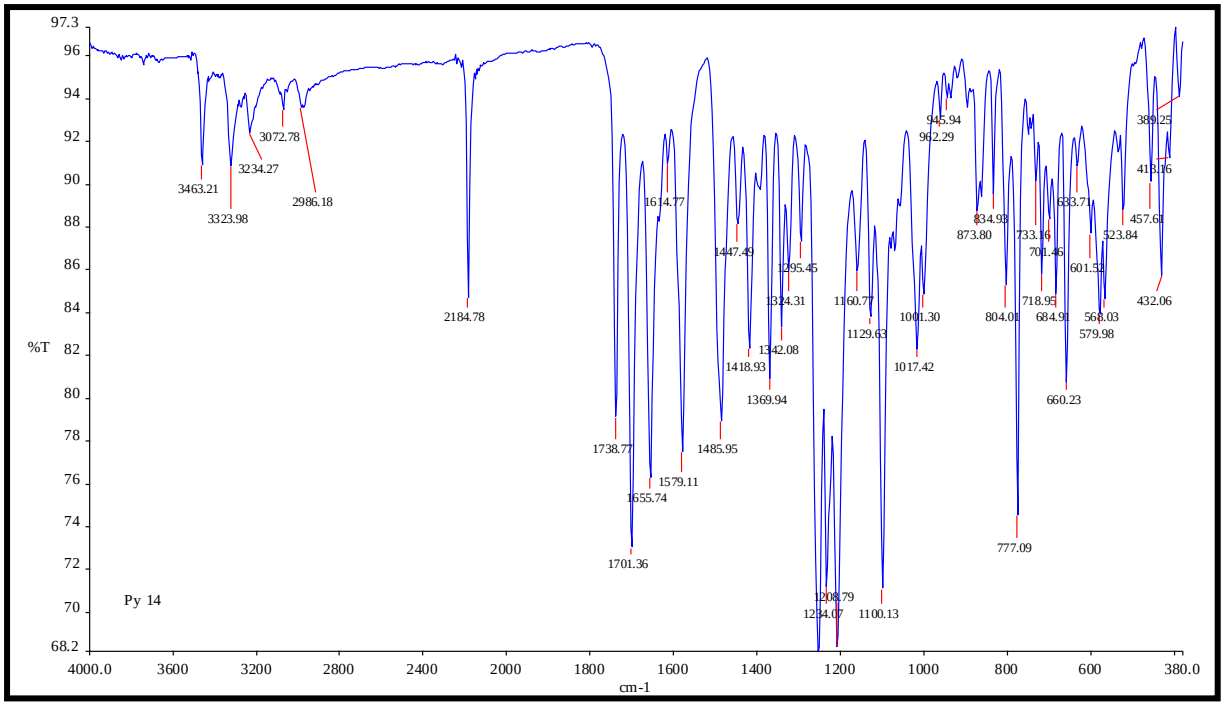

FT-IR spectra of compound **5h**

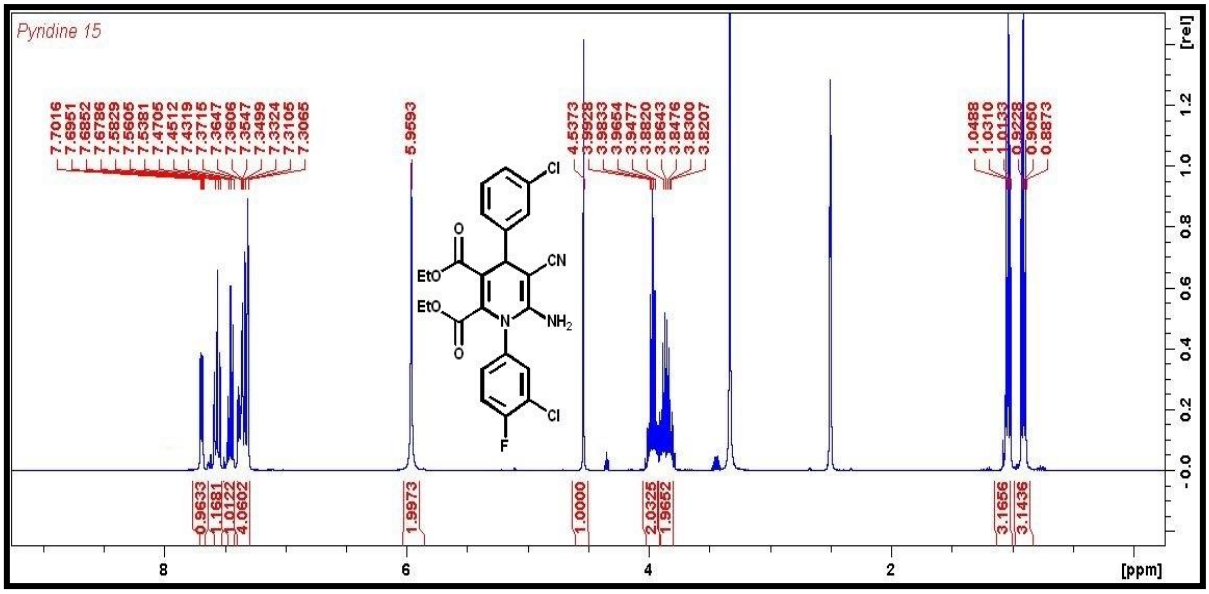

^{1}H NMR spectra of compound **5i**

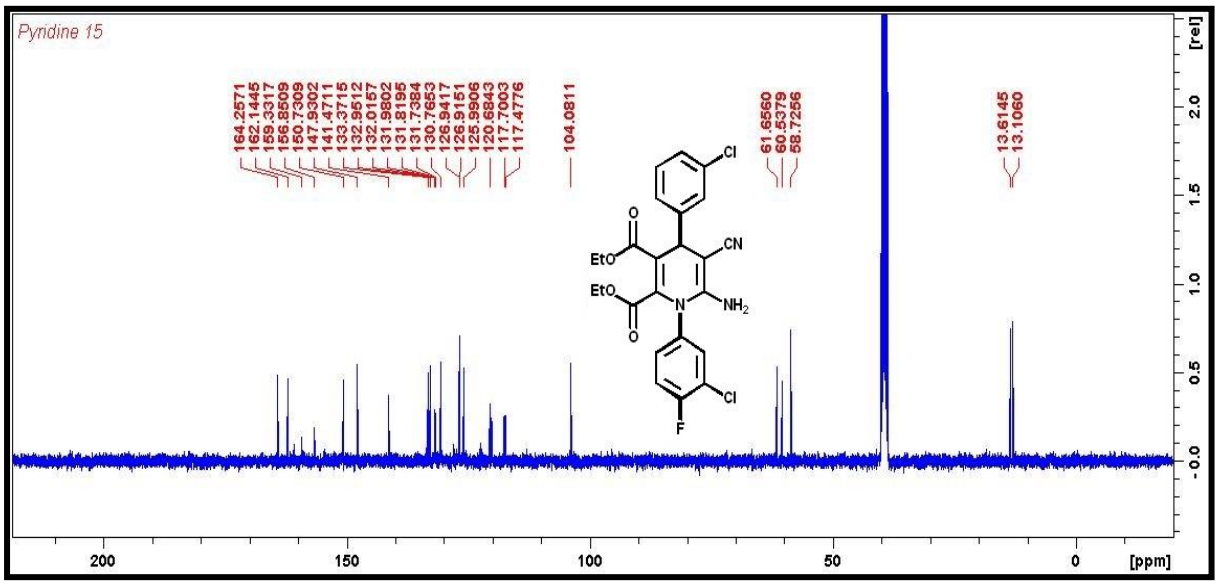

^{13}C NMR spectra of compound **5i**

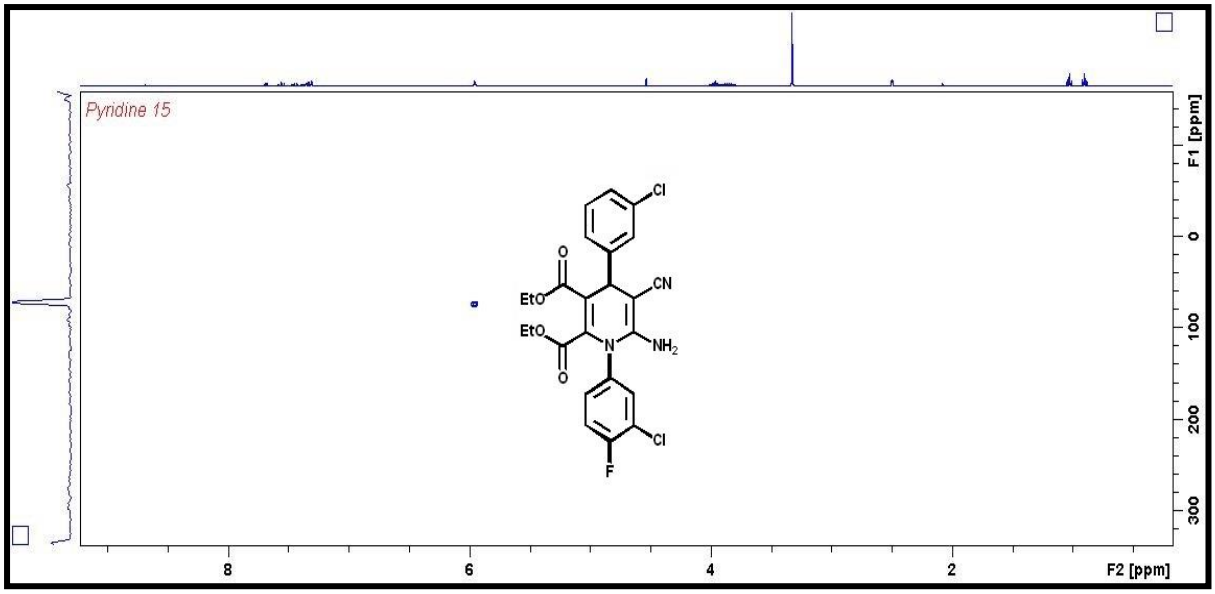

^{15}N NMR spectra of compound **5i**

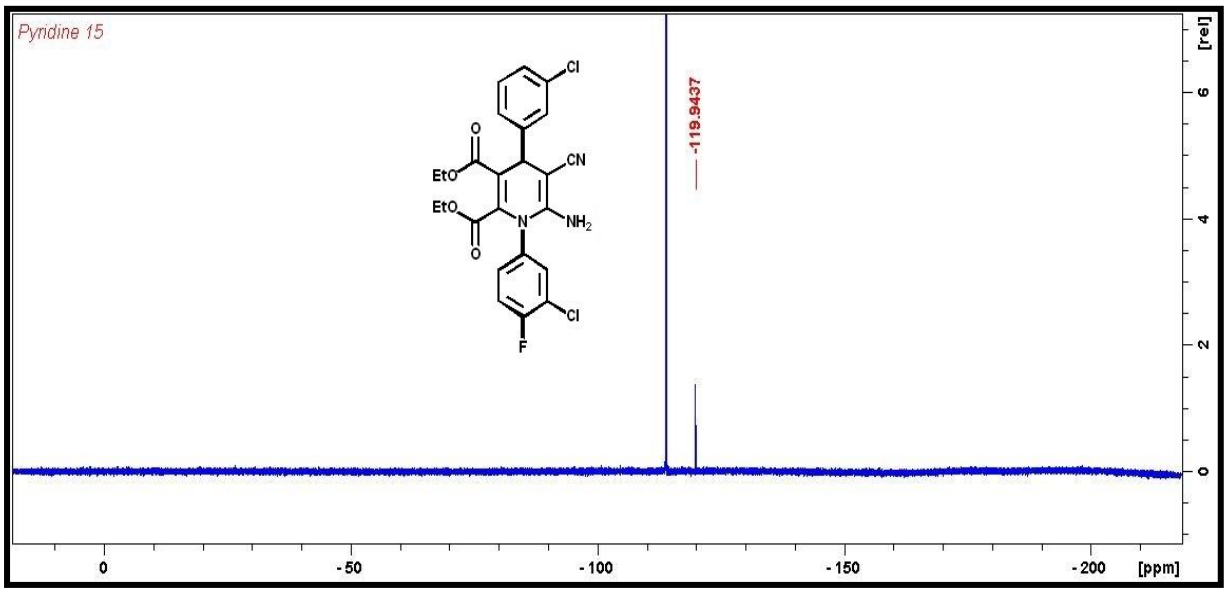

^{19}F NMR spectra of compound **5i**

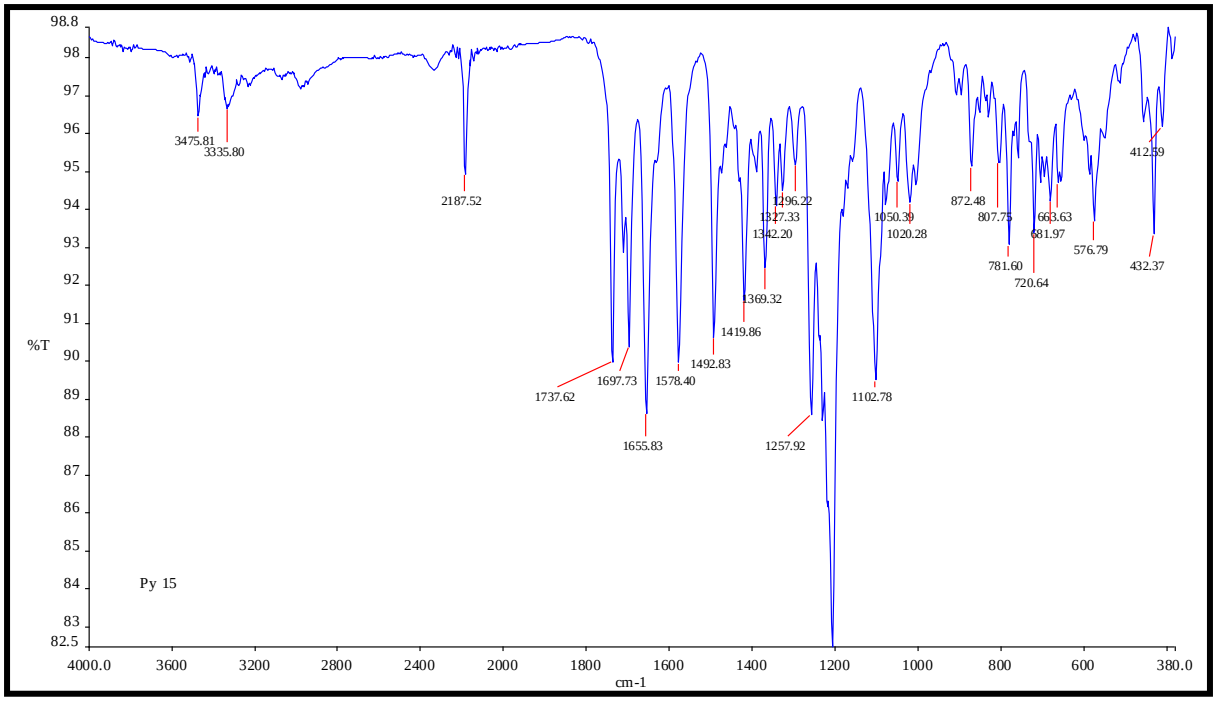

FT-IR spectra of compound **5i**

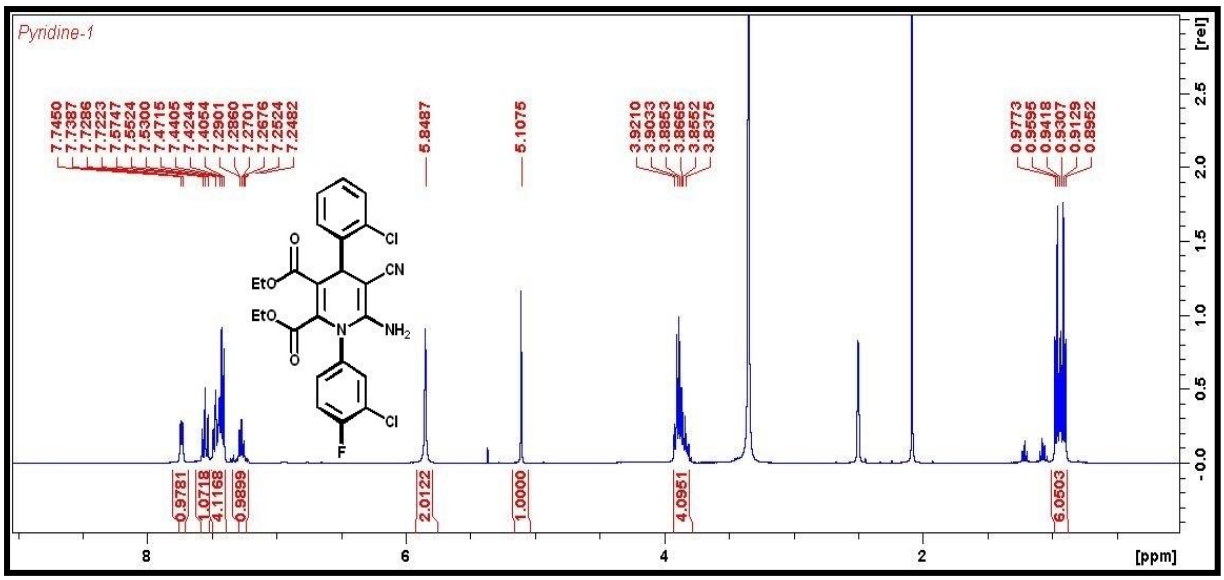

^{1}H NMR spectra of compound **5j**

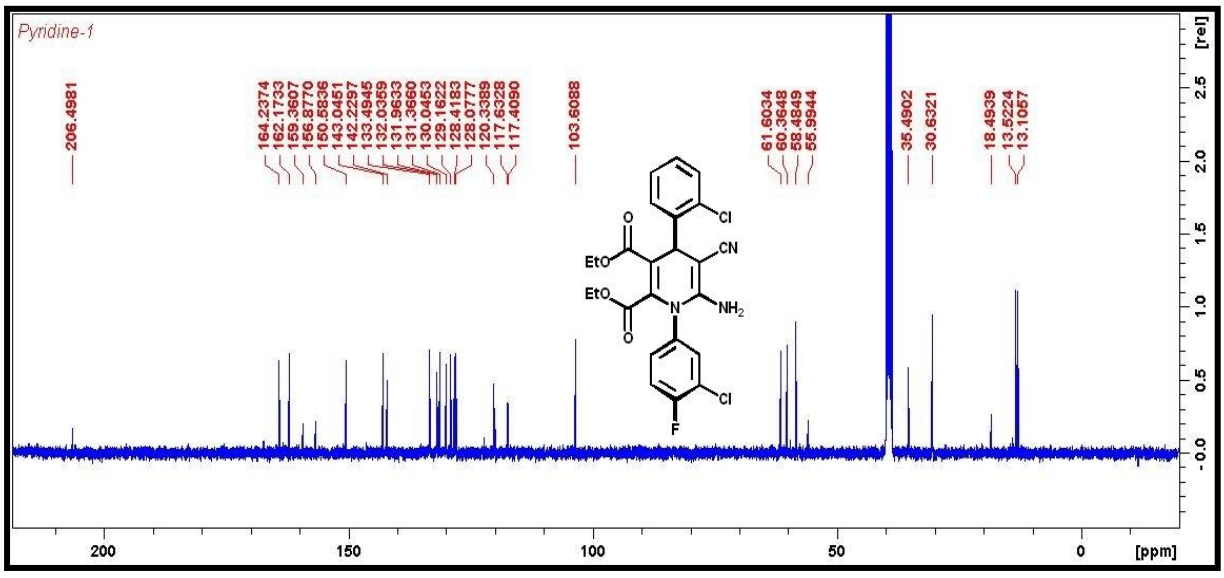

^{13}C NMR spectra of compound **5j**

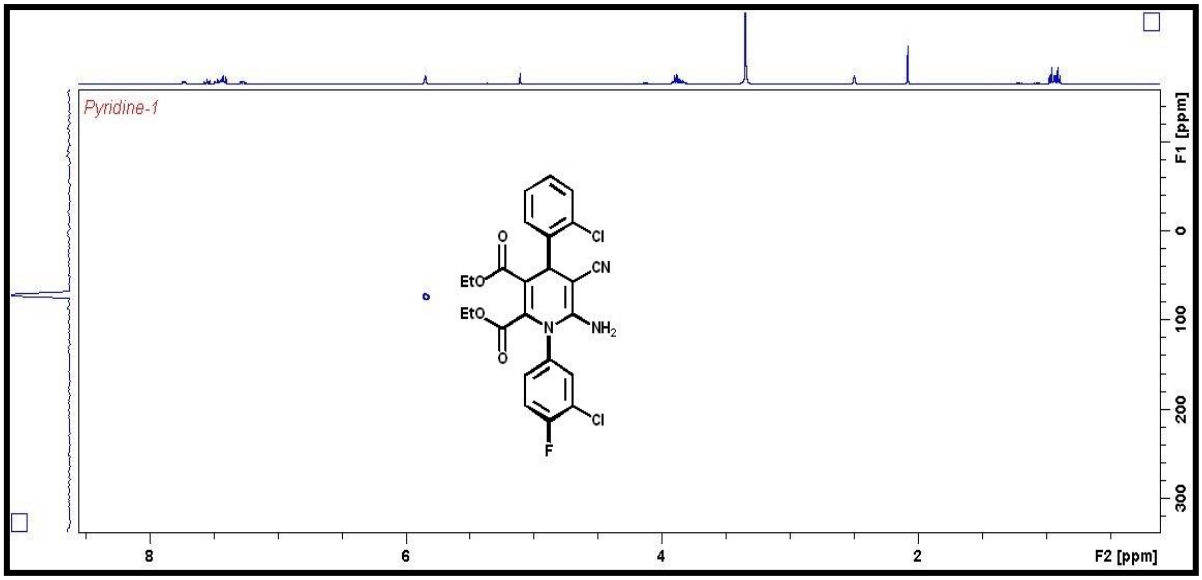

^{15}N NMR spectra of compound **5j**

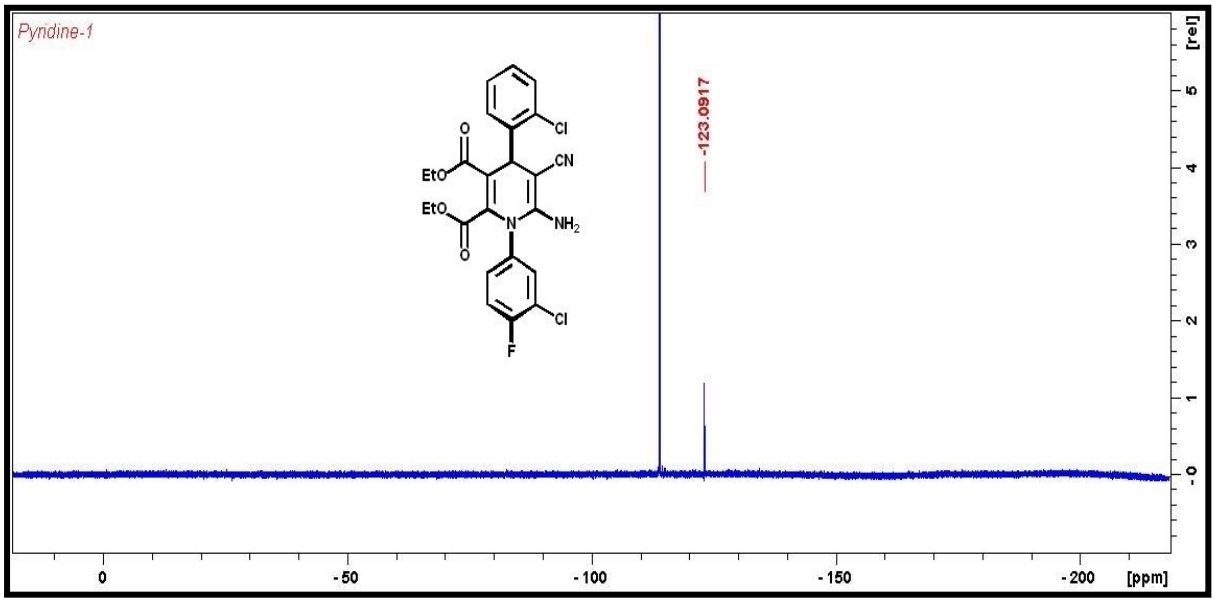

^{19}F NMR spectra of compound **5j**

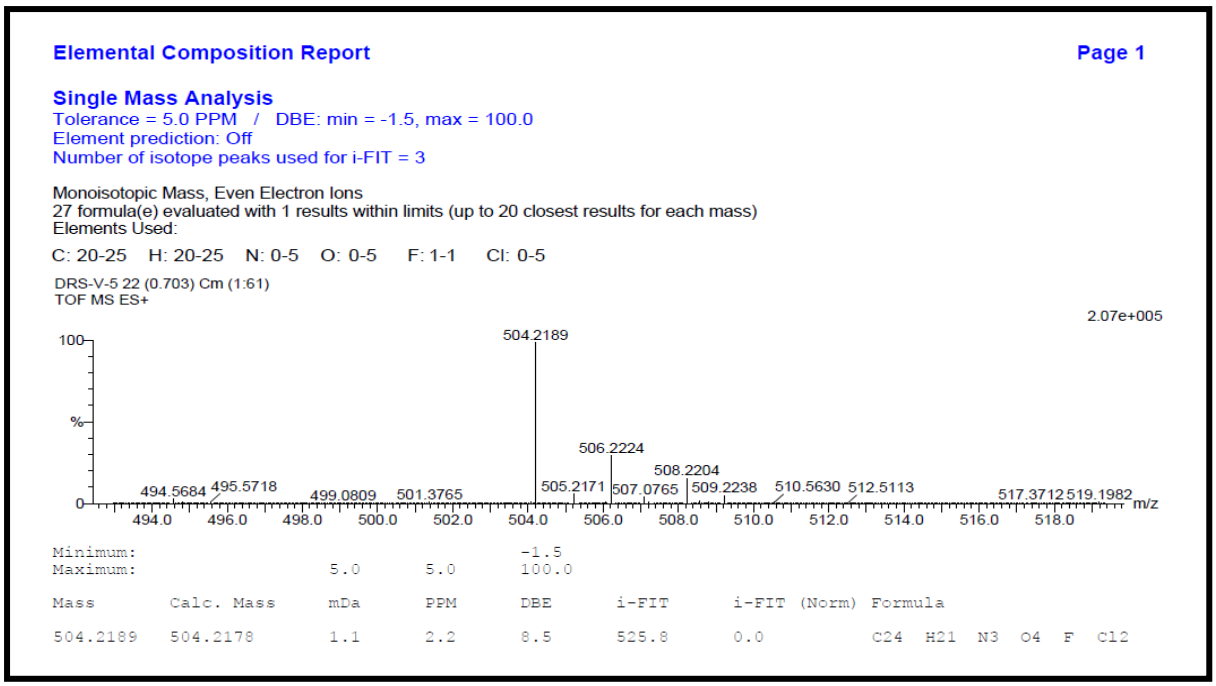

HRMS spectra of compound **5j**

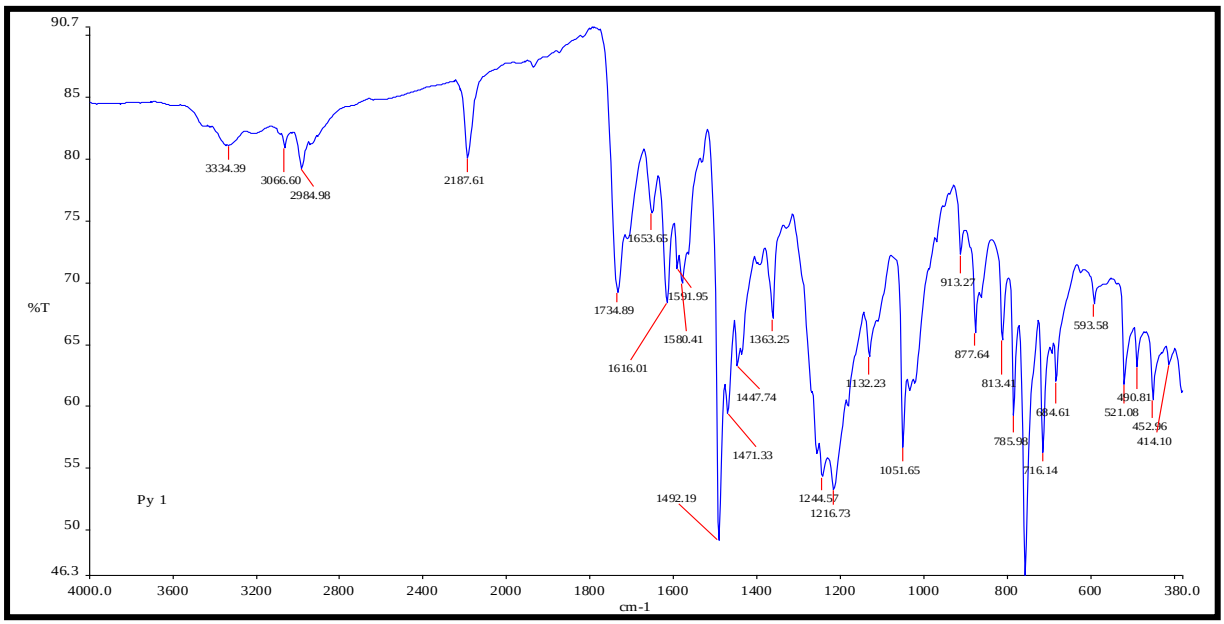

FT-IR spectra of compound **5j**

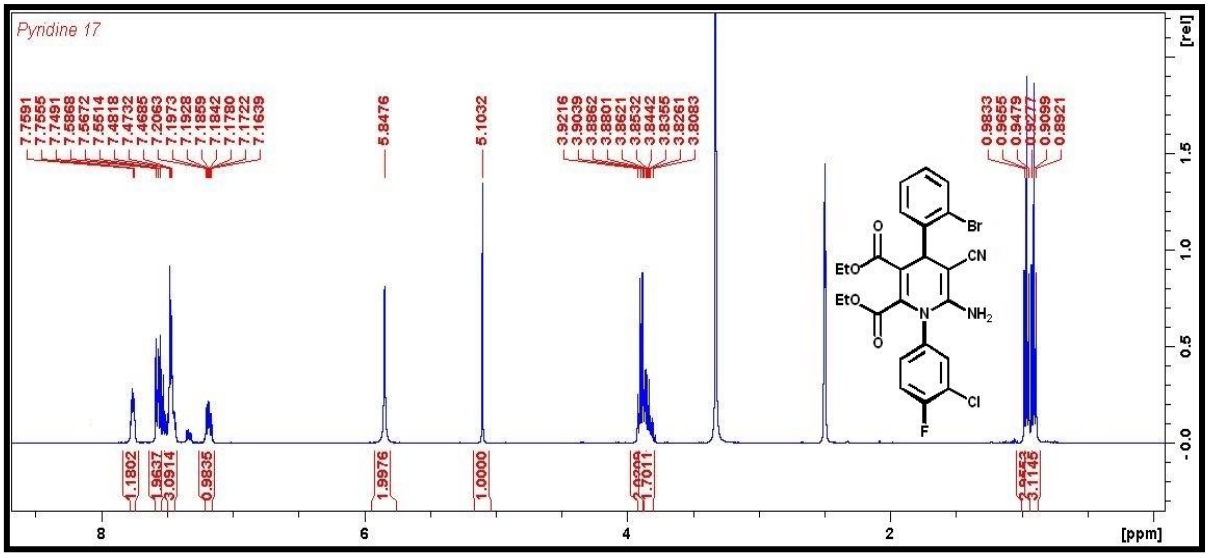

^{1}H NMR spectra of compound **5k**

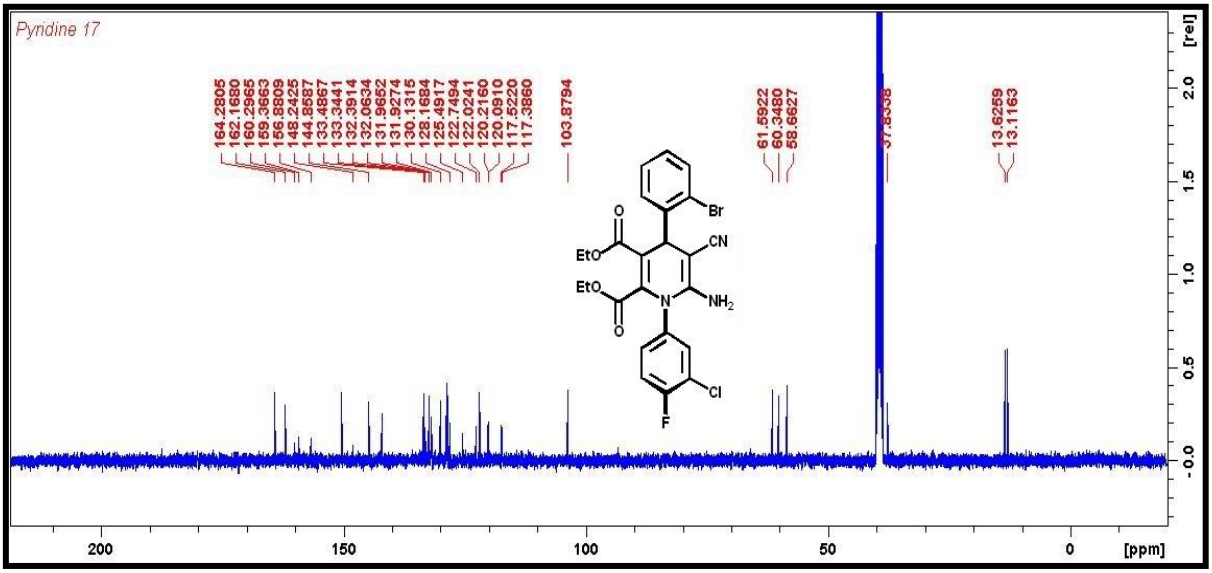

^{13}C NMR spectra of compound **5k**

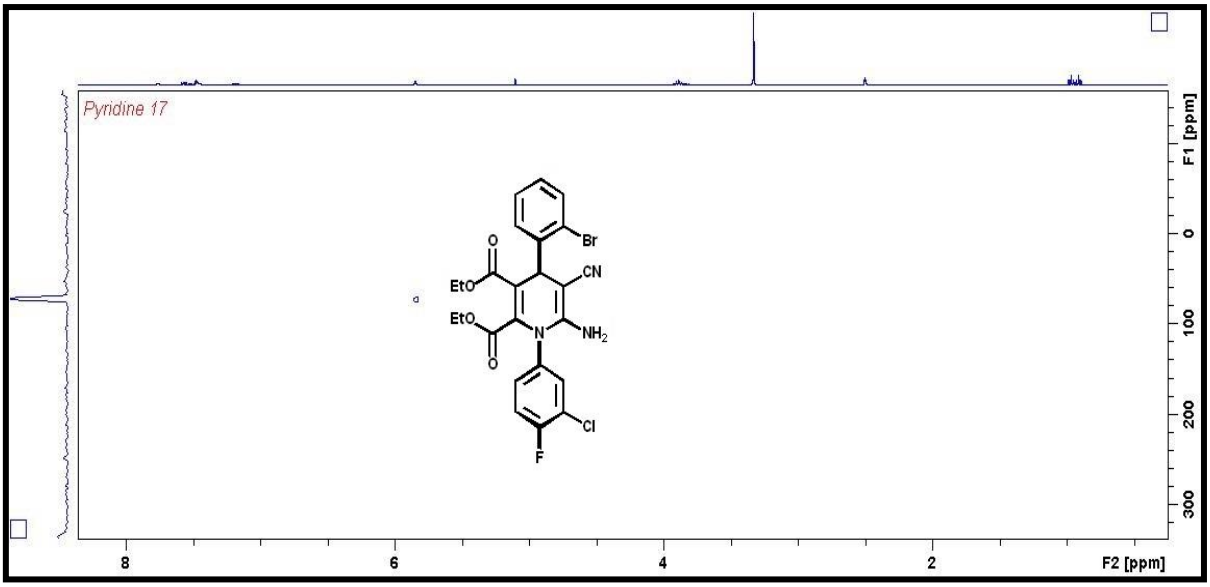

^{15}N NMR spectra of compound **5k**

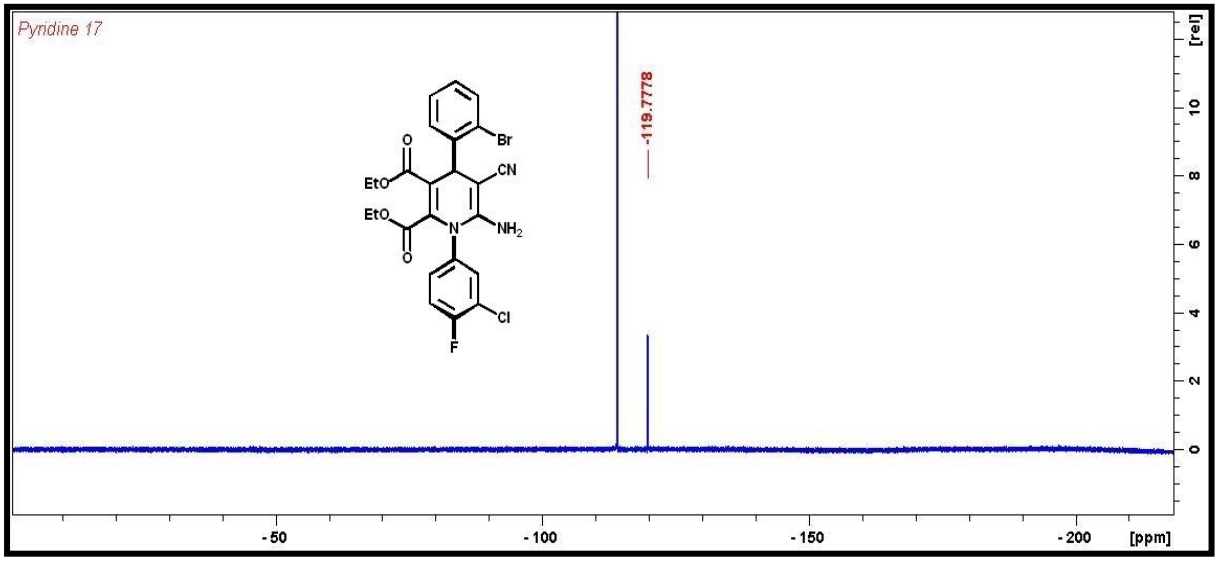

^{19}F NMR spectra of compound **5k**

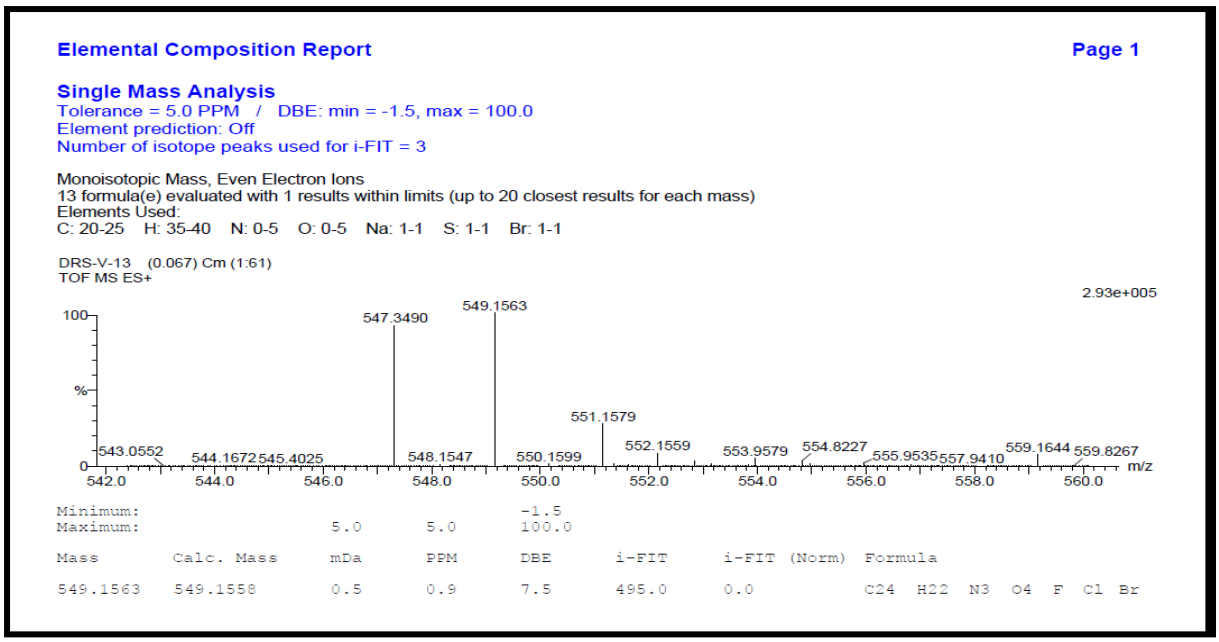

HRMS spectra of compound **5k**

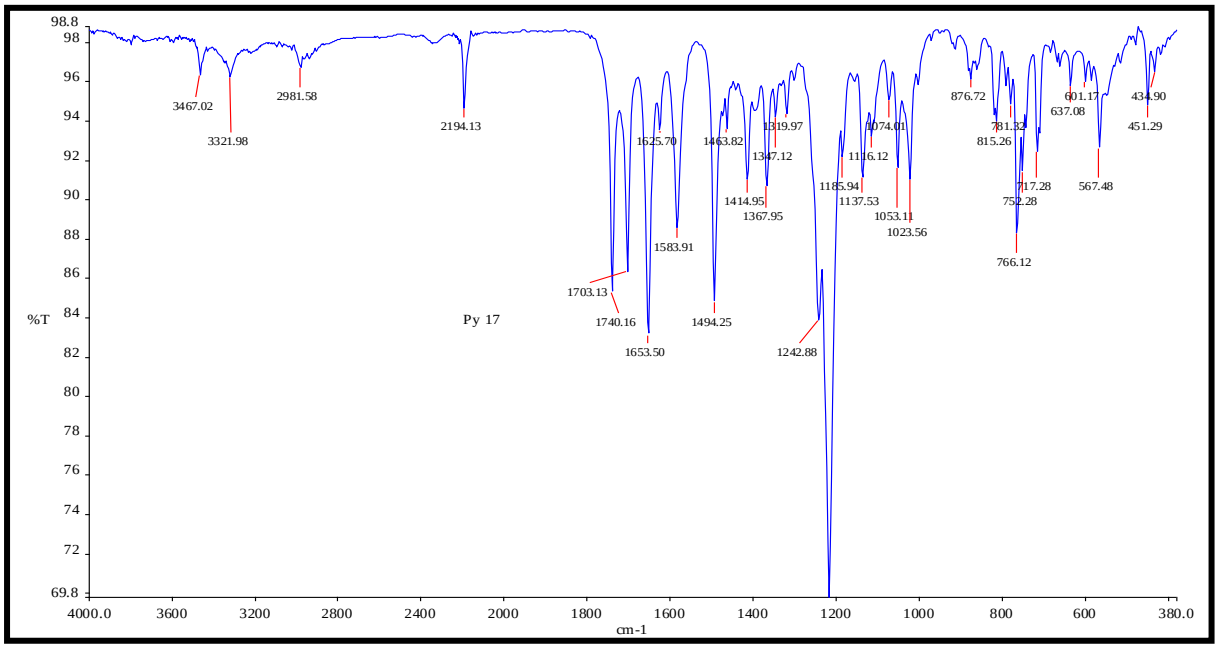

FT-IR spectra of compound **5k**

Chapter 4

An efficient and green approach for the synthesis of 2,4-dihydropyrano[2,3-c]pyrazole-3-carboxylates using Bi_2O_3/ZrO_2 as a reusable catalyst

Sandeep V.H.S. Bhaskaruni, Suresh Maddila, Werner E. van Zyl and Sreekantha B. Jonnalagadda*

*School of Chemistry & Physics, University of KwaZulu-Natal, Westville Campus, Chiltern Hills, Durban-4000, South Africa

*Corresponding Author: Prof. Sreekantha B. Jonnalagadda
School of Chemistry & Physics,
University of KwaZulu-Natal,
Durban 4000, South Africa.
Tel.: +27 31 2607325,
Fax: +27 31 2603091
E-mail address: jonnalagaddas@ukzn.ac.za

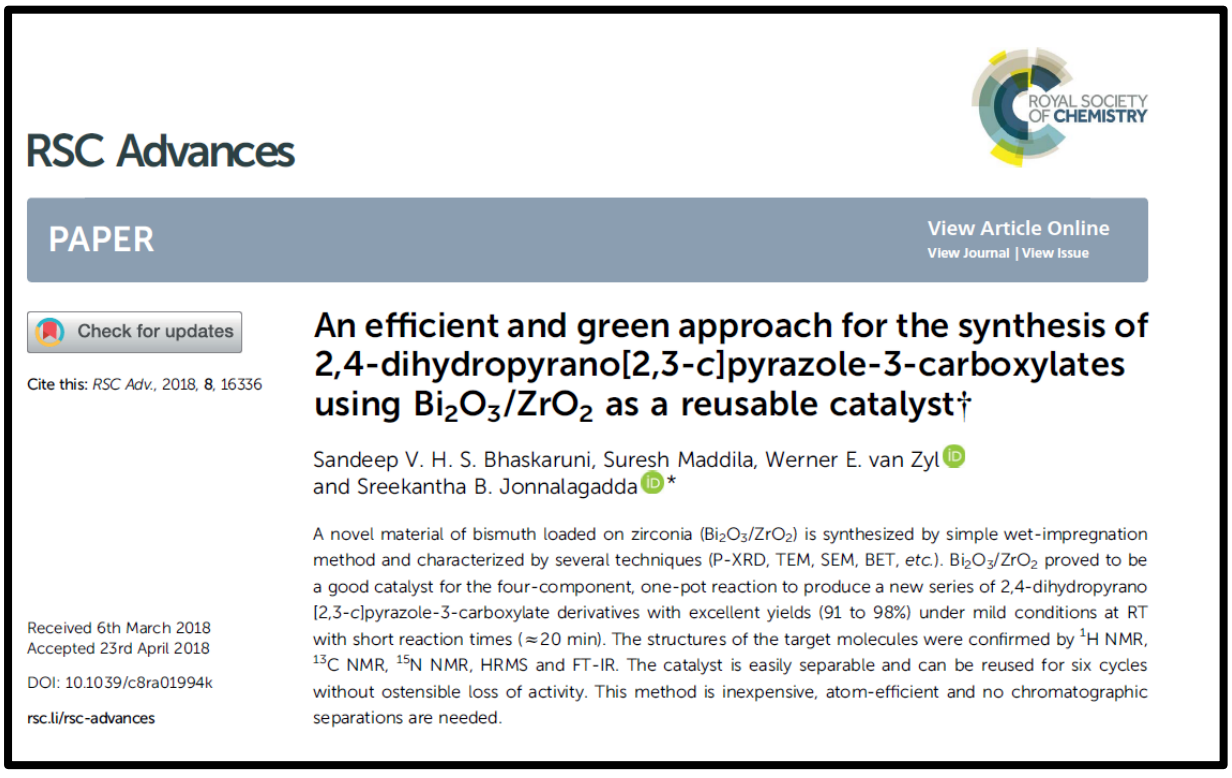

RSC Advances

ROYAL SOCIETY OF CHEMISTRY

PAPER

View Article Online
View Journal | View Issue

Check for updates

Cite this: *RSC Adv.*, 2018, **8**, 16336

An efficient and green approach for the synthesis of 2,4-dihydropyrano[2,3-*c*]pyrazole-3-carboxylates using Bi_2O_3/ZrO_2 as a reusable catalyst†

Sandeep V. H. S. Bhaskaruni, Suresh Maddila, Werner E. van Zyl and Sreekantha B. Jonnalagadda*

A novel material of bismuth loaded on zirconia (Bi_2O_3/ZrO_2) is synthesized by simple wet-impregnation method and characterized by several techniques (P-XRD, TEM, SEM, BET, *etc.*). Bi_2O_3/ZrO_2 proved to be a good catalyst for the four-component, one-pot reaction to produce a new series of 2,4-dihydropyrano [2,3-*c*]pyrazole-3-carboxylate derivatives with excellent yields (91 to 98%) under mild conditions at RT with short reaction times (≈20 min). The structures of the target molecules were confirmed by ^{1}H NMR, ^{13}C NMR, ^{15}N NMR, HRMS and FT-IR. The catalyst is easily separable and can be reused for six cycles without ostensible loss of activity. This method is inexpensive, atom-efficient and no chromatographic separations are needed.

Received 6th March 2018
Accepted 23rd April 2018

DOI: 10.1039/c8ra01994k

rsc.li/rsc-advances

This chapter is published in the journal **RSC Advances,** and has been structured according to the journal's format.

An efficient and green approach for the synthesis of 2,4-dihydropyrano[2,3-c]pyrazole-3-carboxylates using Bi_2O_3/ZrO_2 as a reusable catalyst

Sandeep V.H.S. Bhaskaruni, Suresh Maddila, Werner E. van Zyl and Sreekantha B. Jonnalagadda*

*School of Chemistry & Physics, University of KwaZulu-Natal, Westville Campus, Chiltern Hills, Durban-4000, South Africa

*Corresponding Author: Prof. Sreekantha B. Jonnalagadda
School of Chemistry & Physics,
University of KwaZulu-Natal,
Durban 4000, South Africa.
Tel.: +27 31 2607325,
Fax: +27 31 2603091
E-mail address: jonnalagaddas@ukzn.ac.za

Abstract

A novel material of bismuth loaded on zirconia (Bi_2O_3/ZrO_2) is synthesized by simple wet-impregnation method and characterized by several techniques (P-XRD, TEM, SEM, BET, etc.). Bi_2O_3/ZrO_2 proved to be a good catalyst for the four-component, one-pot reaction to produce a new series of 2,4-dihydropyrano[2,3-c]pyrazole-3-carboxylate derivatives with excellent yields (91 to 98%) under mild conditions at RT with short reaction times (≈20 min). The structures of the target molecules were confirmed by ^{1}H NMR, ^{13}C NMR, ^{15}N NMR, HRMS and FT-IR. The catalyst is easily separable and can be reused for six cycles without ostensible loss of activity. This method is inexpensive, atom-efficient and no chromatographic separations are needed.

4.1 Introduction

In pharmaceutical research, methods for the synthesis of medicinally important scaffolds in high yields under moderate conditions fascinate all.[1] Multicomponent reactions (MCRs) are one-step reactions, in which three or more starting materials are integrated together to obtain the target molecule with no need for separation of intermediates.[2] In MCRs, the product formation takes place through reaction of multiple reactive components present in the reaction media in sequence. The main characteristics are high atom economy, eco-compatibility, and efficient forming of multiple-bonds, which are the near ideal targets in the modern organic synthesis.[3,4]

Heterogeneous catalysts play a key role in the development of cost-effective and eco-friendly protocols in organic synthesis.[5] The main benefits are the recyclability and reusability of the catalytic material, which are not observed in other organic or inorganic homogenous catalysts.[6] The principal assets of heterogeneous catalysts are their high surface area, simple handling, low toxicity, short reaction times, easy separation, and thermal and mechanical stability, relative to many homogenous catalysts.[7]

To vary the surface characteristics of heterogeneous catalysts, the use of mixed oxides is an attractive option.[8,9] The recent literature reveals that zirconium oxide has been used either as an active material or a support in catalysts in the design of various organic transformations, with good product selectivity.[10–12] ZrO_2 even shows potential catalyst activity in water. Its redox properties, high surface area, and acidic and basic sites make it superior to other catalytic systems.[12] Furthermore, ZrO_2 is less-expensive, stable, non-hazardous, reusable and viably available.[3,13] Bismuth is a green grade element and its related compounds play a prominent role in many organic transformations, such as oxidation, reduction, and C–C bond formation reactions,[14] owing to the presence of Lewis acidic character. Moreover, it is non-toxic and highly stable.[15] Hence, the use of bismuth oxide-loaded zirconia catalysts is an elective choice for the present synthetic scheme.

Heterocyclic molecules have become important in the fields of pharmaceutical, agro, industrial and combinatorial chemistry.[16]Accomplishing facile and easy methods for the design of new composite heterocyclic moieties is a key aspect and ongoing challenge in the field of heterocyclic chemistry. Pyrano [2,3-c]pyrazoles and their derivatives are significant nitrogen containing heterocyclic molecules with interesting biological and pharmaceutical properties, such as anti-inflammatory,[17] anticancer,[18]antioxidant,[19]anti-bacterial[20]and anti-tubercular agents.[21] Subsequently, the preparation of several substituted pyrano[2,3-c]pyrazole derivatives

has been explored by different methods, using silica-supported tetramethylguanidine,[22] BS-2GTi,[23] $Ba(OH)_2$,[24] g-alumina,[25] Amberlyst A21,[26] acetic acid,[27] visible light-assisted synthesis[28] etc. as catalysts. All these reactions reported have low yields, with many demanding expensive chemicals, harsh reaction conditions and long reaction times. Therefore, an improvement over existing procedures with a greener approach with enhanced yields under milder conditions is necessary and vital.

With consistent interest in development of improved methods for the synthesis of different biologically active scaffolds, we have previously reported varied enriched protocols for the synthesis of novel heterocycles.[29–32] In this communication, we report a new catalyst material Bi_2O_3/ZrO_2 for MCRs for synthesis of new functionalized pyrano[2,3-c]pyrazole derivatives by using in a one-pot four component reaction.

4.2 Experimental Section

4.2.1 Catalyst preparation

A series of bismuth oxide-loaded zirconia (Bi_2O_3/ZrO_2) catalyst materials with different weight percentages were prepared (1, 2.5, & 5 wt%) by employing wet impregnation method.[31–35] A mixture of zirconium oxide (ZrO_2, 2 g, Alfa Aesar) and appropriate amount (wt%) of bismuth chloride ($BiCl_3$, Alfa Aesar) in deionised water (60 mL) were agitated with vigorous stirring at room temperature (RT) for 7 h. The resultant slurry was heated to and preserved at 75°C for 1.5 h and then allowed to cool to RT. Then, the slurry was filtered under vacuum and was dried in an oven at 120-140 °C for 8 h, and further calcined at 450 °C for 6 h in the presence of air, to afford different wt% of Bi_2O_3/ZrO_2. Instrumentation details are included in the supporting information.

4.2.2 General procedure for the synthesis of pyranopyrazole derivatives (5a-k)

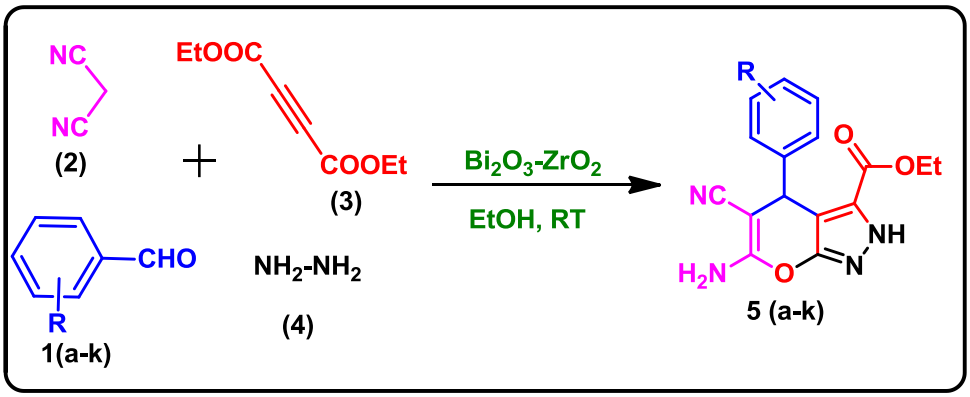

Scheme 1 Synthesis of 2,4-dihydropyrano[2,3-c] pyrazole-3-carboxylates.

In order to examine the efficiency of the prepared Bi_2O_3/ZrO_2 catalyst, in a 25 mL reaction flask at RT, the equi-molar mixture of chosen aromatic aldehyde (1 mmol) (1), malononitrile (1 mmol) (2), Diethyl acetylenedicarboxylate (1 mmol) (3), hydrazine hydrate (1 mmol) (4) and Bi_2O_3/ZrO_2 (30 mg) catalyst were added under stirring using ethanol as solvent (5 mL) for 15 minutes (Scheme 1). The progression of reaction was observed by TLC. After completion of the reaction, the catalyst material was recovered by simple filtration and the organic compound was separated by using addition of appropriate ethanol. Then, the pure target products was obtained after evaporation of ethanol under vacuum. All the reaction products were characterised by using various spectral techniques (^{1}H-NMR, ^{15}N NMR, ^{13}C-NMR, HRMS and FT-IR). The details and spectra are assimilated to the supplementary information file.

Ethyl-6-amino-5-cyano-4-(2-methoxyphenyl)-2,4-dihydropyrano[2,3-c]pyrazole-3-carboxylate (5a):

^{1}H NMR (400 MHz, DMSO-d_6) δ = 1.01 (t, *J* = 7.12 Hz, 3H, CH_3), 3.69 (s, 3H, OCH_3), 4.01-4.06 (m, 2H, CH_2), 5.05 (s, 1H, CH), 6.82 (d, *J* = 8.56 Hz, 2H, ArH), 6.85 (s,2H, NH_2), 6.89 (dd, *J* = 1.56 Hz, *J* = 1.56 Hz, 1H, ArH), 6.94 (d, *J* = 8.04, 1H, ArH), 7.15-7.22 (m, 1H, ArH), 13.57 (s, 1H, NH); ^{13}C NMR (100 MHz, DMSO-d_6): 13.57, 31.62, 55.43, 56.00, 60.62, 103.58, 111.33, 120.21, 127.87, 128.59, 132.41, 136.46, 156.25, 156.60, 158.25, 160.56; ^{15}N NMR (40.55 MHz, DMSO-d_6) δ = 6.85 (s, 2H, NH_2), 13.57 (s, 1H, NH). HRMS of [$C_{17}H_{16}N_4O_4$─H^+] (m/z): 339.1082; Calcd.: 339.0992.

Ethyl-6-amino-5-cyano-4-(4-methoxyphenyl)-2,4-dihydropyrano[2,3-c]pyrazole-3-carboxylate (5b):

^{1}H NMR (400 MHz, DMSO-d_6) δ = 1.08 (t, *J* = 7.08Hz, 3H, CH_3), 3.70 (s, 3H, OCH_3), 4.07-4.12 (m, 2H, CH_2), 4.69 (s, 1H, CH), 6.83 (d, *J* = 8.56 Hz, 2H, ArH), 6.97 (s,2H, NH_2), 7.00 (d, *J* = 8.6 Hz, 2H, ArH), 13.69 (s, 1H, NH); ^{13}C NMR (100 MHz, DMSO-d_6): 13.77, 36.16, 54.95, 58.16, 60.79, 113.53, 115.16, 120.31, 124.08, 128.31, 133.32, 137.07, 157.87, 158.12, 159.87. ^{15}N NMR (40.55 MHz, DMSO-d_6) δ = 6.97 (s, 2H, NH_2), 13.69 (s, 1H, NH). HRMS of [$C_{17}H_{16}N_4O_4$─H^+] (m/z): 339.1082; Calcd.: 339.1093.

Ethyl-6-amino-5-cyano-4-(2,3-dimethoxyphenyl)-2,4-dihydropyrano[2,3-c]pyrazole-3-carboxylate (5c):

^{1}H NMR (400 MHz, DMSO-d_6) δ = 1.06 (t, *J* = 7.04 Hz, 3H, CH_3),3.54 (s, 3H, OCH_3), 3.76 (s, 3H, OCH_3), 4.07-4.09 (m, 2H, CH_2), 4.91 (s, 1H, CH), 6.60 (d, *J* = 7.13 Hz, 2H, ArH), 6.89

(d, *J* = 8.28 Hz, 1H, ArH), 6.91 (s, 2H, NH_2), 6.95 (d, *J* = 7.92 Hz, 1H, ArH), 13.55 (s, 1H, NH); ^{13}C NMR (100 MHz, DMSO-d_6): 13.72, 32.79, 55.48, 56.90, 59.69, 60.67, 103.87, 111.46, 120.56, 121.37, 123.18, 128.68, 137.21, 146.42, 152.26, 155.91, 158.19, 160.48; ^{15}N NMR (40.55 MHz, DMSO-d_6) δ = 6.91 (s, 2H, NH_2), 13.55 (s, 1H, NH). HRMS of [$C_{18}H_{18}N_4O_5$+Na^+] (m/z): 393.1188; Calcd.: 393.1175.

Ethyl-6-amino-5-cyano-4-(3,4-dimethoxyphenyl)-2,4-dihydropyrano[2,3-c]pyrazole-3-carboxylate (5d):

^1H NMR (400 MHz, DMSO-d_6) δ = 1.08 (t, *J* = 7.12 Hz, 3H, CH_3), 3.68 (d, *J* = 5.72 6H, OCH_3), 4.08-4.13 (m, 2H, CH_2), 4.70 (s, 1H, CH), 6.56 (dd, *J* = 1.84 Hz, *J* = 1.84, 1H, ArH), 6.71 (d, *J* = 1.84 Hz, 1H, ArH), 6.55 (d, *J* = 8.32 Hz, 1H, ArH), 6.96 (s, 2H, NH_2), 13.55 (s, 1H, NH); ^{13}C NMR (100 MHz, DMSO-d_6): 13.76, 36.46, 55.44, 58.04, 60.79, 103.84, 111.73, 119.22, 127.24, 128.93, 137.55, 148.25, 154.42, 155.48, 158.15, 159.93, 160.59; ^{15}N NMR (40.55 MHz, DMSO-d_6) δ = 6.96 (s, 2H, NH_2), 13.55 (s, 1H, NH). HRMS of [$C_{18}H_{19}N_4O_5$+H^+] (m/z): 371.0389; Calcd.: 371.0395.

Ethyl-6-amino-5-cyano-4-(2,5-dimethoxyphenyl)-2,4-dihydropyrano[2,3-c]pyrazole-3-carboxylate (5e):

^1H NMR (400 MHz, DMSO-d_6) δ = 1.04 (t, *J* = 7.12 Hz, 3H, CH_3), 3.61 (d, *J* = 6.61 Hz, 6H, OCH3), 4.03-4.09 (m, 2H, CH_2), 4.97 (s, 1H, CH), 6.46 (d, *J* = 2.66 Hz, 1H, ArH), 6.74 (dd, *J* = 3 Hz, *J* = 3.04Hz, 1H, ArH), 6.85 (s, 1H, ArH), 6.87 (s, 2H, NH_2), 13.58 (s, 1H, NH); ^{13}C NMR (100 MHz, DMSO-d_6): 13.58, 32.12, 55.18, 56.05, 56.57, 60.69, 103.39, 111.52, 112.60, 115.48, 120.33, 128.61, 133.54, 150.99, 152.82, 156.18, 158.25, 160.62; ^{15}N NMR (40.55 MHz, DMSO-d_6) δ = 6.87 (s, 2H, NH_2), 13.58 (s, 1H, NH).

Ethyl-6-amino-5-cyano-4-(2,4,6-trimethoxyphenyl)-2,4-dihydropyrano[2,3-c]pyrazole-3-carboxylate (5f):

^1H NMR (400 MHz, DMSO-d_6) δ = 1.06 (t, *J* = 7.09 Hz, 3H, CH_3), 3.73 (s, 3H, OCH_3), 3.89 (d, *J* = 7.96 Hz, 6H, OCH_3), 4.02-4.11 (m, 2H, CH_2), 5.27 (s, 1H, CH), 6.33 (s, 2H, ArH), 6.88 (s,2H, NH_2), 13.25 (s, 1H, NH); ^{13}C NMR (100 MHz, DMSO-d_6): 13.78, 25.41, 55.04, 55.79, 56.11, 60.38, 103.69, 104.51, 112.39, 113.84, 116.38, 120.70, 156.67, 158.59, 159.55, 167.37. ;^{15}N NMR (40.55 MHz, DMSO-d_6) δ = 6.88 (s, 2H, NH_2), 13.25 (s, 1H, NH). HRMS of [$C_{19}H_{20}N_4O_6$+Na^+] (m/z): 423.1297; Calcd.: 423.1281.

Ethyl-6-amino-5-cyano-4-(3-hydroxyphenyl)-2,4-dihydropyrano[2,3-c]pyrazole-3-carboxylate (5g):

^{1}H NMR (400 MHz, DMSO-d_6) δ = 1.07 (t, *J* = 7.08 Hz, 3H, CH_3), 4.08-4.13 (m, 2H, CH_2), 4.63 (s, 1H, CH), 6.40 (s, 1H, ArH), 6.51-6.58 (m, 2H, ArH), 6.99 (s, 2H, NH_2), 7.05 (t, *J* = 7.79 Hz,1H, ArH), 9.27 (s, 1H, OH), 13.71 (s, 1H, NH); ^{13}C NMR (100 MHz, DMSO-d_6): 13.74, 36.85, 55.98, 60.80, 103.74, 113.59, 114.06, 117.99, 120.26, 128.95, 129.07, 146.30, 155.56, 157.16, 158.16, 160.02;^{15}N NMR (40.55 MHz, DMSO-d_6) δ = 6.99 (s, 2H, NH_2), 13.71 (s, 1H, NH)

Ethyl-6-amino-5-cyano-4-(3,4-dihydroxyphenyl)-2,4-dihydropyrano[2,3-c]pyrazole-3-carboxylate (5h):

^{1}H NMR (400 MHz, DMSO-d_6) δ = 1.12 (t, *J* = 7.12 Hz, 3H, CH_3), 4.10-4.15 (m, 2H, CH_2), 4.54 (s, 1H, CH), 6.37-6.42 (m, 2H, ArH), 6.60 (d, *J* = 8.04 Hz, 1H, ArH), 6.93 (s, 2H, NH_2), 8.67 (s, 1H, OH), 8.79 (s, 1H, OH), 13.65 (s, 1H, NH); ^{13}C NMR (100 MHz, DMSO-d_6): 13.82, 36.34, 58.42, 60.80, 104.41, 114.50, 115.04, 118.12, 120.41, 128.81, 136.05, 143.91, 144.55, 155.47, 158.23, 159.83; ^{15}N NMR (40.55 MHz, DMSO-d_6) δ = 6.93 (s, 2H, NH_2), 13.65 (s, 1H, NH). HRMS of [$C_{16}H_{14}N_4O_5$─H^+] (m/z): 341.0886; Calcd.: 341.0886.

Ethyl-6-amino-5-cyano-4-(2-nitrophenyl)-2,4-dihydropyrano[2,3-c]pyrazole-3-carboxylate (5i):

^{1}H NMR (400 MHz, DMSO-d_6) δ = 0.92 (t, *J* = 7.08 Hz, 3H, CH_3), 3.96-4.05 (m, 2H, CH_2), 5.57 (s, 1H, CH), 7.14 (s, 2H, NH_2), 7.22 (dd, *J* = 1.08, *J* = 1.08 Hz, 1H, ArH), 7.44-7.48 (m, 1H, ArH), 7.61-7.65 (m, 1H, ArH), 7.92 (dd, *J* = 1.12 Hz, *J* = 1.12 Hz, ArH), 13.79 (s, 1H, NH); ^{13}C NMR (100 MHz, DMSO-d_6): 13.63, 31.49, 56.12, 60.85, 102.33, 119.60, 128.02, 128.99, 131.07, 133.64, 138.89, 148.20, 155.58, 157.73, 160.55; ^{15}N NMR (40.55 MHz, DMSO-d_6) δ = 7.14 (s, 2H, NH_2), 13.79 (s, 1H, NH). HRMS of [$C_{16}H_{13}N_5O_5$─H^+] (m/z): 354.0850; Calcd.: 354.0838.

Ethyl-6-amino-4-(4-bromophenyl)-5-cyano-2,4-dihydropyrano[2,3-c]pyrazole-3-carboxylate (5j):

^{1}H NMR (400 MHz, DMSO-d_6) δ = 1.05 (t, *J* = 3.56 Hz, 3H, CH_3), 4.06-4.12 (m, 2H, CH_2), 4.76 (s, 1H, CH), 7.05 (s, 2H, ArH), 7.07 (s, 2H, NH_2), 7.47 (d, *J* = 8.32, 2H, ArH), 13.77 (s, 1H, NH); ^{13}C NMR (100 MHz, DMSO-d_6): 13.76, 36.37, 57.27, 60.85, 102.99, 119.59, 120.09, 129.06, 129.62, 131.11, 144.26, 155.45, 157.97, 160.00; ^{15}N NMR (40.55 MHz, DMSO-d_6) δ

= 7.07 (s, 2H, NH_2), 13.77 (s, 1H, NH). HRMS of [$C_{16}H_{13}BrN_4O_3$─H^+] (m/z): 387.0106; Calcd.: 387.0093.

Ethyl-6-amino-5-cyano-4-(4-ethylphenyl)-2,4-dihydropyrano[2,3-c]pyrazole-3-carboxylate (5k):

^{1}H NMR (400 MHz, DMSO-d_6) δ = 1.06 (d, *J* = 6.44 Hz, 3H, CH_3), 1.15 (d, *J* = 6.44 Hz, 3H, CH_3), 2.54 (d, *J* = 7.04 Hz, 2H, CH_2), 4.09 (d, *J* = 5.56 Hz, 2H, CH_2), 4.70 (s, 1H, CH), 6.99 (s, 2H, NH_2), 7.11 (d, *J* = 6.60 Hz,4H, ArH), 13.70 (s, 1H, NH); ^{13}C NMR (100 MHz, DMSO-d_6): 13.71, 15.49, 27.70, 36.55, 57.95, 60.76, 103.83, 120.31, 127.17, 127.55, 128.91, 141.93, 142.23, 155.54, 158.12, 159.97; ^{15}N NMR (40.55 MHz, DMSO-d_6) δ = 6.99 (s, 2H, NH_2), 13.70 (s, 1H, NH). HRMS of [$C_{18}H_{18}N_4O_3$─H^+] (m/z): 337.1310; Calcd.: 337.1301.

4.3 Results and Discussion

4.3.1 XRD analysis

X-ray diffraction studies were performed to analyze the phases and crystallinity size of the catalyst materials. The powdered XRD patterns of the different wt% of prepared Bi_2O_3–ZrO_2 are shown in Fig. 1 and the diffraction peaks (2 theta) were measured from 0° to 90°. The major diffraction peaks placed at 2θ of 24.5°, 27.8°, 31.3°, 35.4° and 50.3° are indexed to the (110), (-111), (111), (200) and (022) diffraction planes of ZrO_2 and also the peaks were correlated with international standard file (JCPDS 37-1484). The Bi_2O_3 peaks were displayed in the XRD diffractogram at 2θ = 27.16°, 30.3°, 35.4°,40.3°, 46.9°, 53.4°, 56.1°, 59.4°, 62.9°, 64.5° and 65.9° further these were matched with (120), (012), (031), (013), (302), (124), (222), (134), (052), (412) and (251) diffraction planes of corresponding to the standard file (JCPDS 41-1449). The diffraction pattern reveals the polycrystalline nature of the prepared catalytic material.

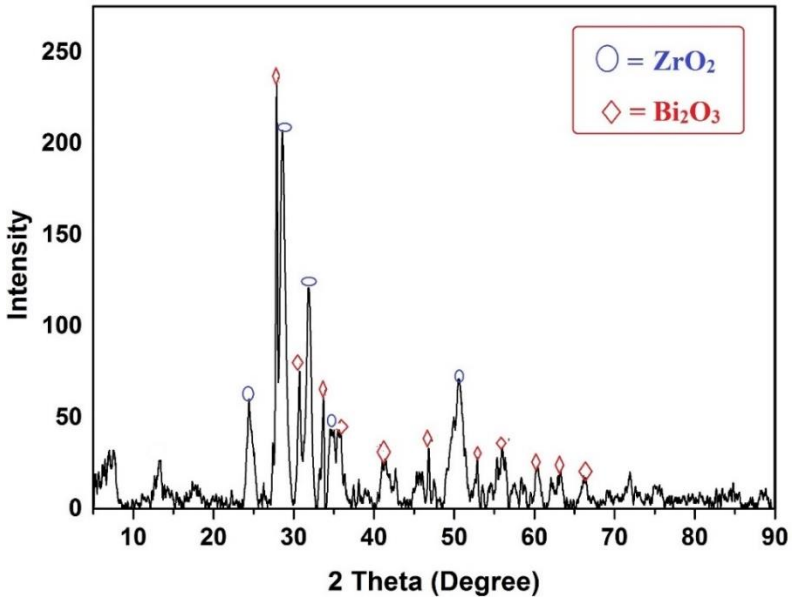

Fig. 1 Powder X-ray diffractogram of 2.5% Bi_2O_3-ZrO_2 catalyst.

4.3.2 TEM analysis

The TEM image of 2.5 wt% bismuth loaded on zirconia is shown in Fig. 2a. It shows that bismuth particles settled as irregular black particles on the spherical shaped zirconia particles. The highly dispersed bismuth particles occur due to fine interaction between bismuth and the zirconia oxides. In order to analyse the particle size distribution (Fig. 2b) quantitatively, the histogram was fitted with the Gaussian function and the mean particle size was calculated to be 8.54 nm.

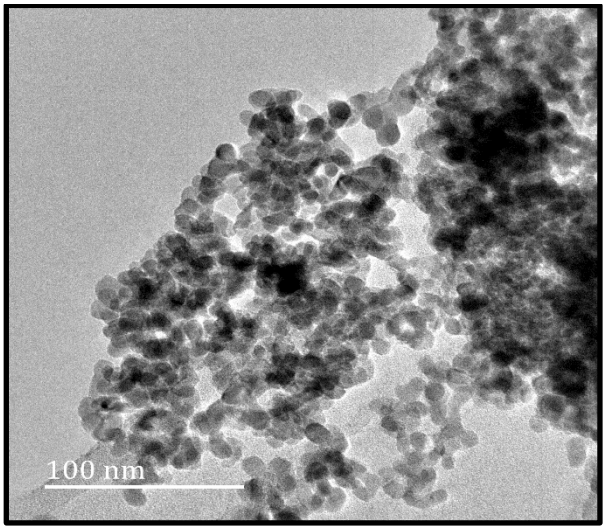

Fig. 2(a) TEM micrograph of 2.5% Bi_2O_3/ZrO_2 catalyst.

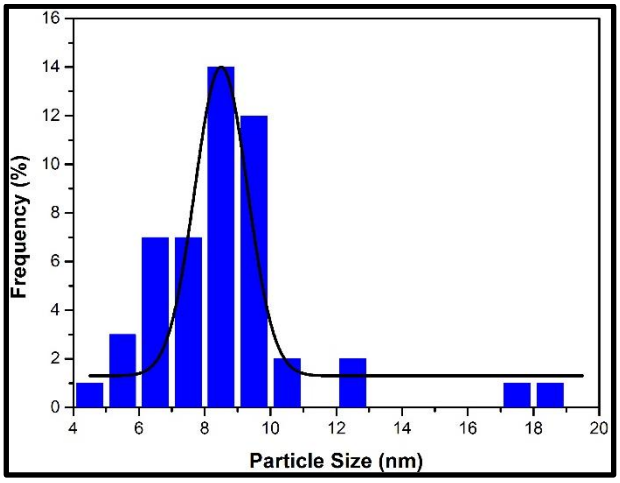

Fig. 2(b) Particle size distribution of Bi_2O_3/ZrO_2.

4.3.3 SEM analysis

Fig. 3a displays a scanning electron microscopy (SEM) image of Bi_2O_3/ZrO_2 combined, which demonstrates the catalyst surface morphology. The units are huge with oval-like irregular shapes. This micrograph displays that the Bi_2O_3 particles are aggregated and accumulated on the zirconia. A homogeneous distribution of Bi_2O_3 on the surface of the ZrO_2 catalyst was calculated by EDS analysis (Fig. 3b), with minor but prominent quantities of surface improvement of bismuth.

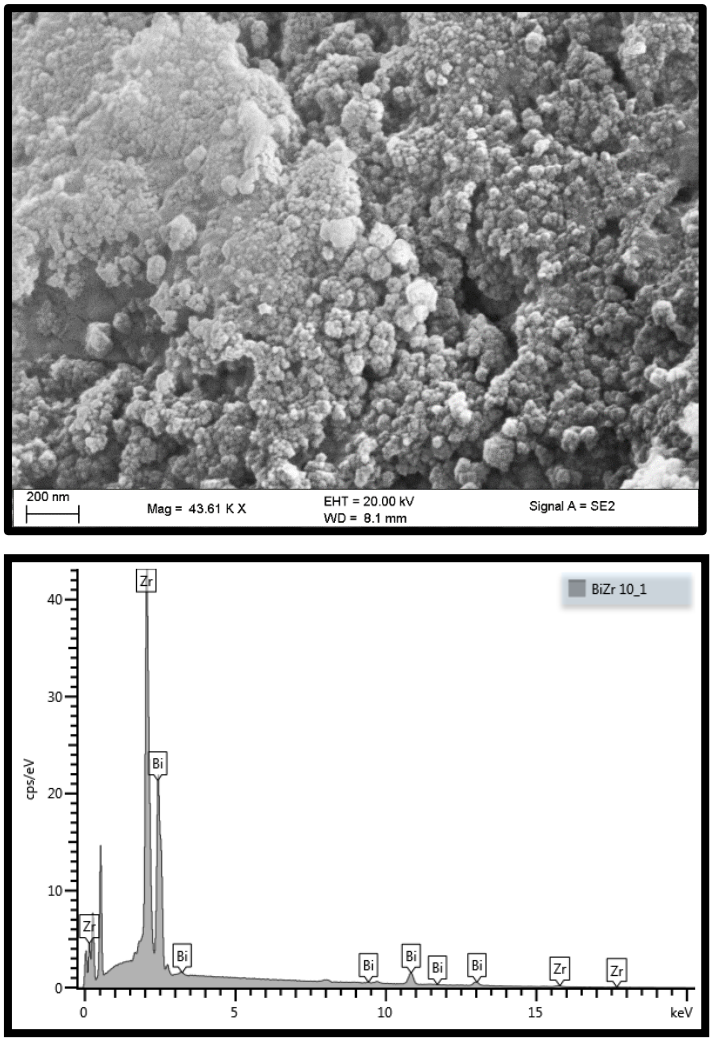

Fig. 3(a) SEM micrograph and (b) EDS spectra of 2.5% Bi_2O_3/ZrO_2 catalyst.

4.3.4 BET surface area analysis

Fig. 4 illustrates a nitrogen adsorption–desorption isotherms of Bi_2O_3/ZrO_2 catalyst material. The N_2 isotherm associated to type IV a typical H2-hysteresis loop, which describes characteristic mesoporous material lying within the p/p_o range of 0.59-0.97. The BET surface area of 2.5% Bi_2O_3/ZrO_2 catalyst material was showed to be 80.40 m^2/g, pore volume 0.320 cm^3/g and pore size 106.4 Å. For the 1% Bi_2O_3/ZrO_2 catalyst loading, the particles are small and have a high surface area (89.02 m^2/g), but had less number of active sites relative to the 2.5% Bi_2O_3/ZrO_2. With the 5% Bi_2O_3/ZrO_2 loading, the bismuth particles are visibly larger, hence had smaller surface area (70.38 m^2/g) when compared to the 2.5% loading and thus slightly lower yield. Hence, Bi_2O_3 on ZrO_2, acts as good promoter for the present transformation. These results suggest that bismuth on zirconia could act as good promoter for the growth of additional crystalline faces, which cooperate to enhance the catalytic activity.

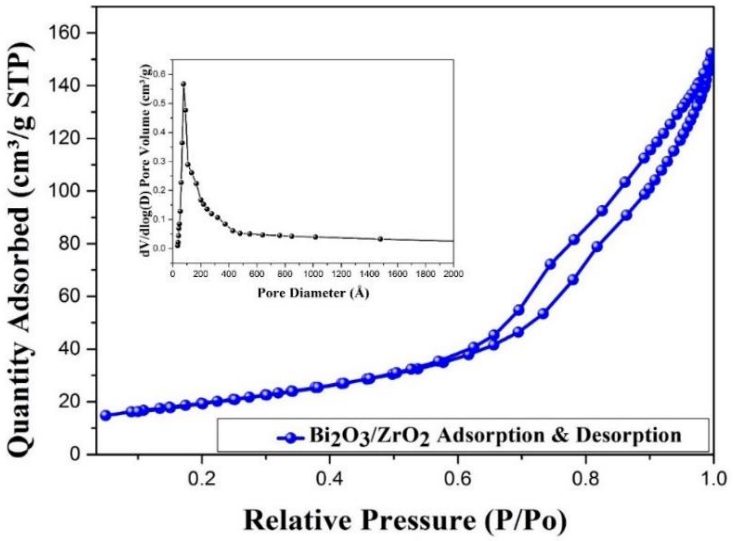

Fig. 4. N_2 adsorption-desorption isotherms of 2.5% Bi_2O_3/ZrO_2 catalyst.

4.3.5 Pyridine IR analysis

The ex situ pyridine[36] adsorbed FT-IR spectra range of 1600–1400 cm^{-1} of prepared Bi_2O_3/ZrO_2 were analysed in the Fig. 5 Corresponding bands at 1449 cm^{-1}, 1487 cm^{-1} and 1530 cm^{-1} were attributed to Lewis, Brønsted and Lewis and Brønsted acidic sites respectively. Upon the careful examination, the prepared catalyst material reveals strong Lewis acidic and weak Brønsted acidic sites.

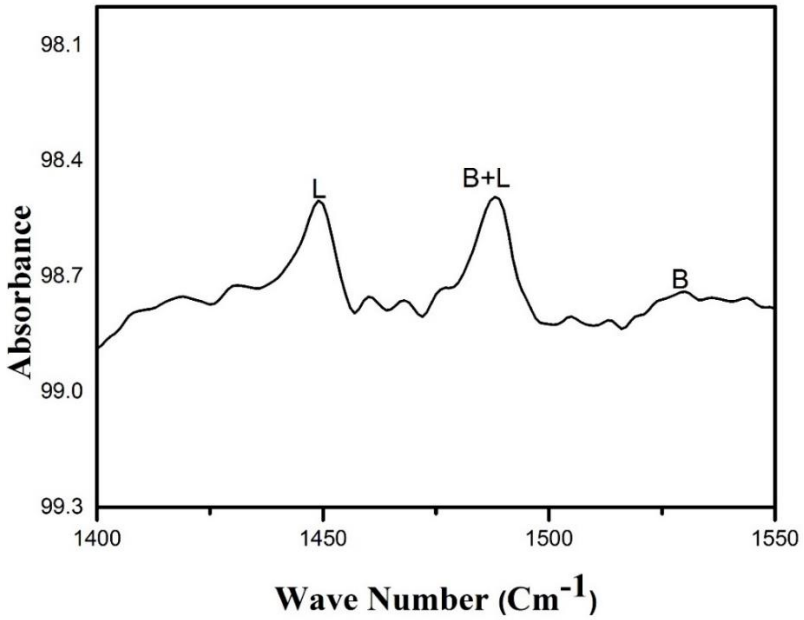

Fig. 5 Pyridine IR spectra of 2.5% Bi_2O_3/ZrO_2 catalyst.

4.3.6 Reaction optimization

The four-component reaction protocol of substituted aromatic aldehydes, malononitrile, hydrazine hydrate and diethyl acetylenedicarboxylate using a Bi_2O_3/ZrO_2 catalyst is shown in

Scheme 1. To optimise the reaction, decrease the reaction time and increase the product yield, the effects of variation of catalysts, solvents etc., were examined on this model reaction. Initially, the reaction of 2-methoxy benzaldehyde, malanonitrile, hydrazine hydrate and diethyl acetylenedicarboxylate was performed under catalyst-free conditions. Only a trace of product was observed under RT reflux conditions or after 10 h of stirring (Table 1, entries 1 and 2). Different catalysts were employed in the presence of EtOH as the solvent at RT. The reaction was studied with commercially available acidic catalysts like acetic acid, $FeCl_3$, and p-toluenesulfonic acid (PTSA). Low product yields were observed even after 9.5 h of stirring at RT (Table 1, entries 3–5). Next, trace amounts of yields were observed when the reaction was carried out with ionic liquids such as (Bmim)BF_4 or L-proline (Table 1, entries 6 and 7) as catalysts. When the same reaction was performed in the presence of various basic organic and inorganic catalysts, such as TEA, pyridine, DABCO, NaOH and K_2CO_3 at RT, very low yields were observed (Table 1, entries 8–12). The reaction was conducted by using several pure metal oxide catalysts, such as SiO_2, ZrO_2 and Al_2O_3. Moderate yields were afforded at RT after 2.0–3.0 h reaction time (Table 1, entries 13–15). Among the selected heterogeneous catalysts, ZrO_2 exhibited promising results with the highest yield (Table 1, entry 14). It is well known that mixed oxides are better catalysts compared to single oxides. Based on the results with ZrO_2, to improve the yield and reaction times the reaction was attempted with various mixed metal oxides (2.5% CuO/ZrO_2, MnO_2/ZrO_2, and Bi_2O_3/ZrO_2), which all gave good to excellent yields (81–98%) at RT with EtOH as the solvent (Table 1, entries 16–18), and Bi proved to be superior. Hence, the effect of varied loading of Bi_2O_3 on ZrO_2 was examined by using different wt% (1%, 2.5% and 5%) of Bi_2O_3 on ZrO_2 supports; the results were impressive with excellent yields within short times (Table 1, entries 18–20). Using 1% Bi_2O_3 loaded on ZrO_2 (Table 1, entry 19), the product yield was 90% in 45 min of stirring under the optimized conditions. A further increase of Bi loading (5%) led to a slightly decreased yield (96%) without any improvement in reaction time. While with 1% loading there were less active sites, the good activity with 2.5% loading may be because the dispersion of Bi_2O_3 on the surface of ZrO_2 is uniform; with 5% loading, oligomerisation of Bi_2O_3 on the surface of ZrO_2 may have happened, which decreases the activity of the sites. Thus, the catalytic activity was lower when compared with 2.5% loading. Based on this evaluation of the results, it is noticeable that 2.5% Bi_2O_3 loaded on zirconia catalyst has a higher surface area and subsequently the most reactive acidic sites owing to its nature and exhibited better catalytic activity compared to the other mixed catalysts. Furthermore, these catalysts have higher surface area, smaller particle sizes and more catalytic

active sites than the related oxide homologues. Therefore, 2.5% Bi_2O_3/ZrO_2 catalyst was preferred for all further reactions to attain excellent product yields.

Table 1: Optimal condition for the synthesis of **5a** by 2.5% Bi_2O_3/ZrO_2 catalyst[a]

Entry	Catalyst	Condition	Time (h)	Yield (%)[b]
1	--	RT	10	11
2	--	Reflux	10	12
3	AcOH	RT	9.5	36
4	$FeCl_3$	RT	9.5	41
5	PTSA	RT	9.5	30
6	$(Bmim)BF_4$	RT	8.0	6
7	L-proline	RT	7.0	8
8	TEA	RT	6.0	17
9	Pyridine	RT	4.5	21
10	DABCO	RT	5.0	23
11	NaOH	RT	4.5	20
12	K_2CO_3	RT	4.0	25
13	SiO_2	RT	3.0	49
14	ZrO_2	RT	2.0	76
15	Al_2O_3	RT	2.5	58
16	2.5% CuO/ZrO_2	RT	1.0	81
17	2.5% MnO_2/ZrO_2	RT	0.90	88
18	2.5% Bi_2O_3/ZrO_2	RT	0.25	98
19	1% Bi_2O_3/ZrO_2	RT	0.75	90
20	5% Bi_2O_3/ZrO_2	RT	0.25	96

[a] All products were characterised by ^{1}H-NMR, ^{15}N NMR, ^{13}C-NMR, HRMS and FT-IR spectral analysis.
[b] Isolated yields.
-- No reaction.

The model reaction with 2.5% Bi_2O_3/ZrO_2 was conducted using varied non-polar and polar (protic and aprotic) solvents, such as n-hexane, toluene, THF, DMF, H_2O, MeOH and EtOH, at RT (Table 2). No reaction was observed with non-polar solvents (n-hexane and toluene; Table 2, entries 1 and 2). However, polar aprotic solvents (THF and DMF) revealed a very low yield (Table 2, entries 3 and 4). Further, the reaction occurred efficiently with polar solvents (H_2O, MeOH and EtOH) and with excellent yields in short reaction times except with H_2O (Table 2, entries 5–7). When using H_2O, as a polar green solvent, the reaction time increased and the yield was decreased. Based on these results, ethanol was chosen as the ideal solvent, which is also environmentally friendly and cost-effective.

Table 2: Optimization of various solvent condition for the model reaction.

Entry	Solvent	Time (minutes)	Yield* (%)
1	n-hexane	120	--
2	toluene	90	--
3	THF	60	8
4	DMF	60	12
5	H_2O	60	45
6	MeOH	45	86
7	EtOH	15	98

[a]Reaction conditions: aromatic aldehydes (1 mmol), malononitrile (1 mmol), hydrazine hydrate (1 mmol), Diethyl acetylenedicarboxylate (1 mmol) and solvent (5 mL) were stirred at room temperature.

Next, the model reaction was evaluated by employing different amounts of 2.5% Bi_2O_3/ZrO_2 catalyst. The summarized outcomes (Table 3, entries 1–3) show that the increase in amount of catalyst from 10 mg to 30 mg leads to an increase in the product yield from 58% to 98% plus decreased reaction time. No significant change was observed in the yield of product with further increase in the amount of catalyst from 30 mg to 60 mg. Therefore, 30 mg of Bi_2O_3/ZrO_2 catalyst was used for the further reactions.

Table 3: Optimization of various weight % for the model reaction by 2.5% Bi_2O_3/ZrO_2 catalyst[a]

Entry	Catalyst (mg)	Time (min)	Yield (%)
1	10	90	58
2	20	45	80
3	30	15	98
4	40	15	98
5	50	15	98
6	60	20	98

[a]Reaction conditions: aromatic aldehydes (1 mmol), malononitrile (1 mmol), hydrazine hydrate (1 mmol), Diethyl acetylenedicarboxylate (1 mmol), and solvent (5 mL) were stirred at room temperature.

For the optimised reaction conditions, to establish the wider scope of the protocol, the method was applied for the synthesis of different pyranopyrazoles using various substituted aromatic aldehydes (Table 4) and the results are summarized in Table 4. The 2.5% Bi_2O_3/ZrO_2 catalyst material catalysed the facile one-pot synthesis of pyranopyrazole derivatives with excellent yields in short reaction times (<20 min). Remarkably, the aldehydes with both electron donating

and electron withdrawing (ortho, meta and para) substituents worked efficiently under the reaction conditions, producing the corresponding target products (5a–k).

Table 4: Synthesis of novel functionalized pyridine derivatives by 2.5% Bi_2O_3/ZrO_2 catalyst[a].

Entry	R	Product	Yield* (%)	Mp °C
1	2-OMe	5a	97	205-207
2	4-OMe	5b	98	208-210
3	2,3-OMe	5c	94	230-232
4	3,4-OMe	5d	91	243-245
5	2,5-OMe	5e	93	257-259
6	2,4,6-OMe	5f	96	240-242
7	3-OH	5g	92	221-223
8	3,4-OH	5h	98	204-206
9	2-NO_2	5i	95	235–237
10	4-Br	5j	94	225-227
11	4-Et	5k	96	210-212

[a]Reaction conditions: aromatic aldehydes (1 mmol), malononitrile (1 mmol), hydrazine hydrate (1 mmol), Diethyl acetylenedicarboxylate (1 mmol), and solvent (5 mL) were stirred at room temperature.

4.4 Reusability of catalyst

The reusability and recyclability of a solid catalyst material is an important parameter as per green chemistry principles. Several recycling experiments were conducted to examine the stability and sustainability of the catalyst material. After completion of every run, filtration was employed to separate the catalyst from the crude product. Then the catalyst was washed with ethanol and dried at 120˚C for 3 h for up to seven runs. Marginal loss of less than 5% of the catalyst was observed in the recovery procedure. Then it was washed with ethanol and dried at 120˚C for 3 h. The loss was supplemented to 30 mg by adding the minute amount required. Activity was retained with no loss in the first six runs, then the material's catalytic activity weakened by 4% in the 7^{th} cycle. No loss of catalytic activity could be observed up to the 6^{th} run owing to the minor losses in the recovery process and nonleaching of the active material.

4.5 Mechanism

From the experimental results, a plausible mechanism is suggested in Scheme 2. The presence of Lewis acidity on the catalyst surface would facilitate the reaction. It may be assumed that in the first step Knoevenagel condensation[37] is achieved by the coordination of Lewis acidic sites with the oxygen of the carbonyl group, forming a carbocation intermediate **(a)**. In the next step, the active methylene group reacts with the carbocation intermediate giving (b); next it will dissociate from the catalyst surface taking a proton from the protic solvent (EtOH) and gives (c). It will further undergo dehydration giving (d). In the next step, ethyl 5-

oxo-2,5-dihydro-1H-pyrazole-3-carboxylate (e) is possibly formed by the reaction between hydrazine hydrate (4) with diethyl acetylenedicarboxylate (3). Finally, a Michael addition between (d) and (e) occurs, yielding the desired product selectively through 6-exo-dig cyclization. The catalytic efficiency of the Bi_2O_3/ZrO_2 on the title reaction in comparison with other reported catalysts is summarized in the Table 5.

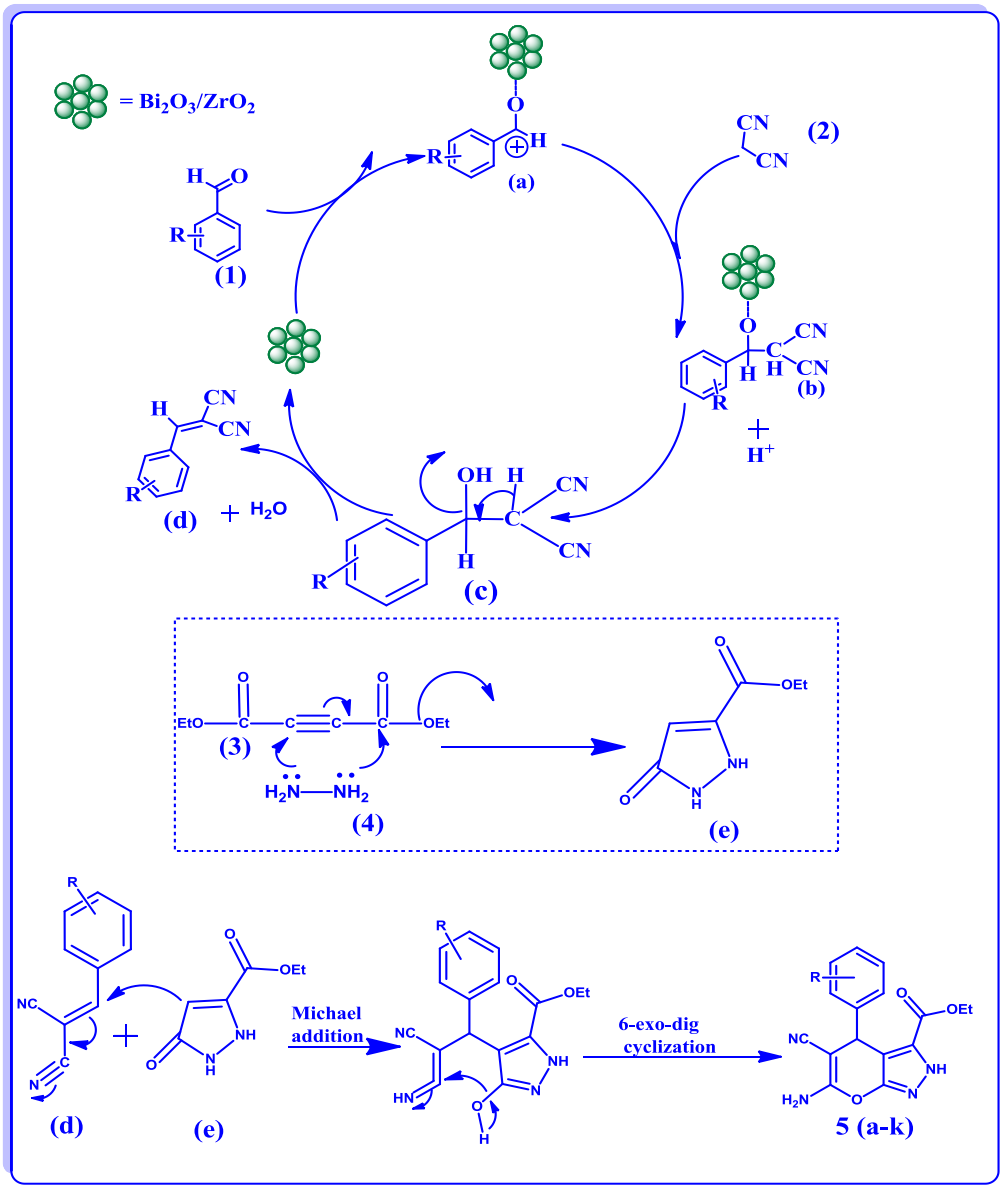

Scheme 2 Plausible reaction mechanism for the formation of 2,4-dihydropyrano[2,3-c] pyrazole-3-carboxylate derivatives.

Table 5 Comparison of various catalysts for the synthesis of pyrano[2,3-c]pyrazole derivatives.

Catalyst	**Solvent**	**Reaction Condition**	**Time**	**Yield (%)[Ref]**
Silica-supported tetramethylguanidine	Neat	RT	15-60 min	79-98[22]
BS-2G-Ti	H_2O	Heating	60-100 min	45-96[23]
$Ba(OH)_2$	H_2O	Reflux	60-120 min	81-93[24]
γ-Alumina	H_2O	Reflux	35-90 min	61-90[25]
Amberlyst A21	EtOH	RT	10-65 min	73-98[26]
AcOH	AcOH	Reflux	72-90 min	71-92[27]
Visible light assisted	Neat condition	RT	15-25 min	56-90[28]
2.5% Bi_2O_3-ZrO_2	EtOH	RT	≈ 20 min	91-98 [Present]

4.6 Conclusion

In summary, we designed a highly efficient and cost-effective method for the synthesis of pyranopyrazole derivatives via a one-pot, four-component reaction in ethanol as a green solvent, using environmentally benign Bi_2O_3/ZrO_2 as selective catalyst. Of the 11 derivatives synthesised, eight are new molecules. The operational simplicity of this approach, short reaction times, high yields, eco-friendly solvent, mild reaction conditions make this method attractive. Additionally, the catalyst can be easily recovered and recycled for at least six runs without loss of efficiency. Moreover, expansion of the reaction scope and synthetic and medicinal applications of this methodology are in progress in our laboratory.

4.7 Acknowledgements

The authors are thankful to the National Research Foundation (NRF) of South Africa, and University of KwaZulu-Natal, Durban, for financial support and research facilities.

4.8 References

1 B. H. Rotstein, S. Zaretsky, V. Rai and A. K. Yudin, Chem. Rev., 2014, 114, 8323–8359.

2 A. Domling, W. Wang and K. Wang, Chem. Rev., 2012, 112, 3083–3135.

3 S. N. Maddila, S. Maddila, W. E. van Zyl and S. B. Jonnalagadda, RSC Adv., 2015, 5, 37360–37366.

4 S. Maddila, K. K. Gangu, S. N. Maddila and S. B. Jonnalagadda, Mol. Diversity, 2017, 21, 247–255.

5 S. N. Maddila, S. Maddila, K. K. Gangu, W. E. van Zyl and S. B. Jonnalagadda, J. Fluorine Chem., 2017, 195, 79–84.

6 S. V. H. S. Bhaskaruni, S. Maddila, K. K. Gangu and S. B. Jonnalagadda, Arabian J. Chem., DOI: 10.1016/j.arabjc.2017.09.016.

7 S. Shabalala, S. Maddila, W. E. van Zyl and S. B. Jonnalagadda, Catal. Commun., 2016, 79, 21–25.

8 S. Shabalala, S. Maddila, W. E. van Zyl and S. B. Jonnalagadda, Ind. Eng. Chem. Res., 2017, 56, 11372–11379.

9 M. B. Gawande, R. K. Pandey and R. V Jayaram, Catal. Sci.Technol., 2012, 2, 1113–1125.

10 S. V. H. S. Bhaskaruni, S. Maddila, W. E. van Zyl and S. B. Jonnalagadda, Catal. Commun., 2017, 100, 24–28.

11 S. V. H. S. Bhaskaruni, S. Maddila, W. E. van Zyl and S. B. Jonnalagadda, Catal. Today, 2018, 309, 276–281.

12 S. Maddila, S. Rana, R. Pagadala, S. Kankala, S. N. Maddila and S. B. Jonnalagadda, Catal. Commun., 2015, 61, 26–30.

13 S. Shabalala, S. Maddila, W. E. van Zyl and S. B. Jonnalagadda, Catal. Commun., 2016, 79, 21–25.

14 M. Wada, H. Ohki and K. Akiba, Tetrahedron Lett., 1986, 27,4771–4774.

15 J. M. Bothwell, S. W. Krabbe and R. S. Mohan, Chem. Soc.Rev., 2011, 40, 4649.

16 R. Pagadala, S. Maddila, V. D. B. C. Dasireddy and S. B. Jonnalagadda, Catal. Commun., 2014, 45, 148–152.

17 H. M. Faidallah and S. A. F. Rostom, Arch. Pharm., 2017, 350, 1–17.

18 A. Sharma, R. Chowdhury, S. Dash, B. Pallavi and P. Shukla, Curr. Microwave Chem., 2016, 3, 78–84.

19 R. S. Aliabadi and N. O. Mahmoodi, RSC Adv., 2016, 6, 85877–85884.

20 S. R. Mandha, S. Siliveri, M. Alla, V. R. Bommena, M. R. Bommineni and S. Balasubramanian, Bioorg. Med. Chem. Lett., 2012, 22, 5272–5278.
21 Z. Xu, C. Gao, Q.-C. Ren, X.-F. Song, L.-S. Feng and Z.-S. Lv, Eur. J. Med. Chem., 2017, 139, 429–440.
22 A. B. Atar, J. T. Kim, K. T. Lim and Y. T. Jeong, Synth. Commun., 2014, 44, 2679–2691.
23 P. S. Sinija and K. Sreekumar, RSC Adv., 2015, 5, 101776–101788.
24 S. H. S. Azzam and M. A. Pasha, Tetrahedron Lett., 2012, 53, 6834–6837.
25 H. Mecadon, M. R. Rohman, M. Rajbangshi and B. Myrboh, Tetrahedron Lett., 2011, 52, 2523–2525.
26 M. Bihani, P. P. Bora, G. Bez and H. Askari, ACS Sustainable Chem. Eng., 2013, 1, 440–447.
27 V. L. Gein, T. M. Zamaraeva and P. A. Slepukhin, Tetrahedron Lett., 2014, 55, 4525–4528.
28 B. Pati Tripathi, A. Mishra, P. Rai, Y. Kumar Pandey, M. Srivastava, S. Yadav, J. Singh and J. Singh, New J. Chem., 2017, 41, 11148–11154.
29 S. Gorle, S. Maddila, S. N. Maddila, K. Naicker, M. Singh, P. Singh and S. B. Jonnalagadda, Anti-Cancer Agents Med. Chem., 2017, 17, 464–470.
30 S. Maddila, K. Naicker, M. I. K. Momin, S. Rana, S. Gorle, S. Maddila, K. Yalagala, M. Singh, N. A. Koorbanally and S. B. Jonnalagadda, Med. Chem. Res., 2016, 25, 283–291.
31 S. Maddila, K. Naicker, S. Gorle, S. Rana, K. Yalagala, S. N. Maddila, M. Singh, P. Singh and S. B. Jonnalagadda, Anti-Cancer Agents Med. Chem., 2016, 16, 1031–1037.
32 S. Maddila, S. Gorle, N. Seshadri, P. Lavanya and S. B. Jonnalagadda, Arabian J. Chem., 2016, 9, 681–687.
33 S. Maddila, V. D. B. C. Dasireddy and S. B. Jonnalagadda, Appl. Catal., B, 2014, 150–151, 305–314.
34 V. Moodley, S. Maddila, S. B. Jonnalagadda and W. E. van Zyl, New J. Chem., 2017, 41, 6455–6463.
35 S. Maddila, V. D. B. C. Dasireddy and S. B. Jonnalagadda, Appl. Catal., B, 2013, 138–139, 149–160.
36 V. Balaga, J. Pedada, H. B. Friedrich and S. Singh, J. Mol. Catal. A: Chem., 2016, 425, 116–123.
37 Q. Li, X. Wang, Y. Yu, Y. Chen and L. Dai, Tetrahedron, 2016, 72, 8358–8363.

4.9 Supplementary information

4.9.1 Catalyst instrumentation details

Employing a Bruker D8 Advance instrument (Cu K radiation source with a wave length of 1.5406 Å), the X-ray diffraction data related the structural phases of the catalyst were acquired. Using a JEOL JEM-1010 electron microscope and JEOL JSM-6100 microscope, the TEM and SEM analysis data was recorded. iTEM software was used analyse the TEM data and images. Employing the X-ray analyser (energy-dispersive), EDX-analysis on the SEM images was conducted.

4.9.2 Experimental Section

All chemicals and reagents required for the reaction were of analytical grade and were used without any further purification. Bruker AMX 400 MHz NMR spectrometer was used to record the ^{1}H NMR, ^{13}C NMR and ^{15}N NMR spectral values. High-resolution mass data were obtained using a Bruker micro TOF-Q II ESI instrument operating at ambient temperature. The DMSO−d_6 solution was utilized for this while TMS served as the internal standard. TMS was further used as an internal standard for reporting the all chemical shifts in δ (ppm). Purity of all the reaction products was confirmed by TLC using aluminium plates coated with silica gel (Merck Kieselgel 60 F_{254}). Infrared (IR) spectra were recorded on a Perkin Elmer Precisely equipped with a Universal ATR sampling accessory using a diamond crystal. The powdered material was placed on the crystal and a force of 120 psi was applied to ensure proper contact between the material and the crystal.The spectra were analyzed using Spectrum 100 software. Before recording the IR spectra, pyridine was adsorbed by placing a drop of pyridine on 10 mg of the sample followed by evacuation in air for 1 h at room temperature to remove reversibly adsorbed pyridine on the surface of the catalyst.

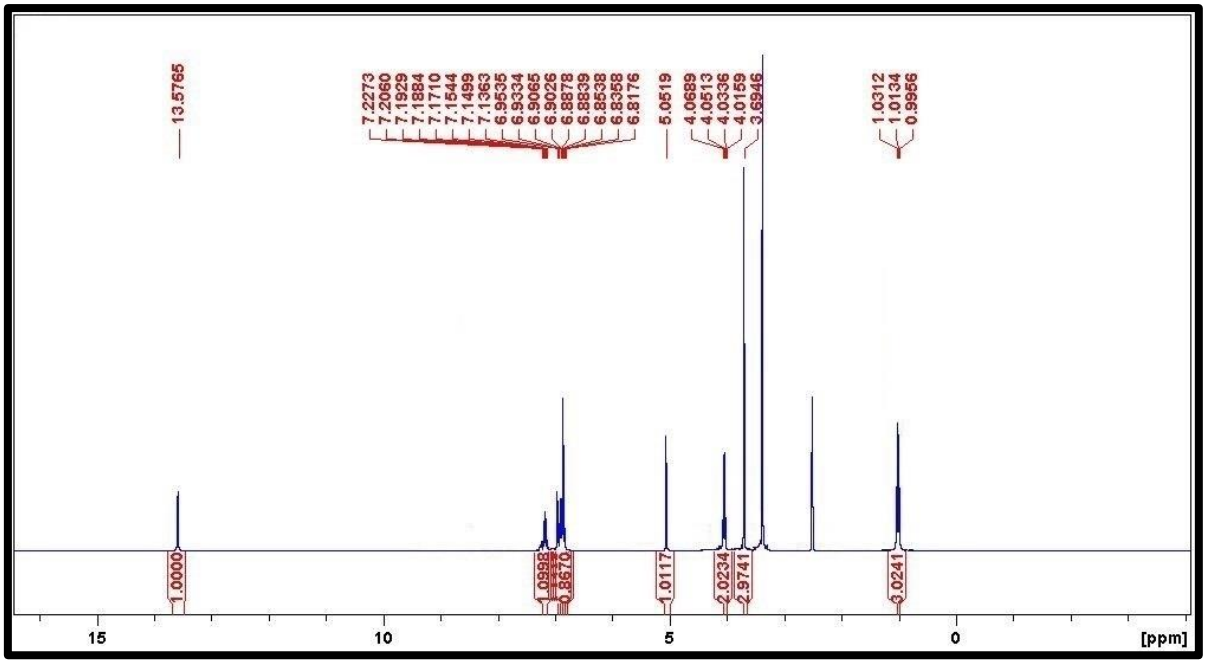

^{1}H NMR spectra of compound **5a**

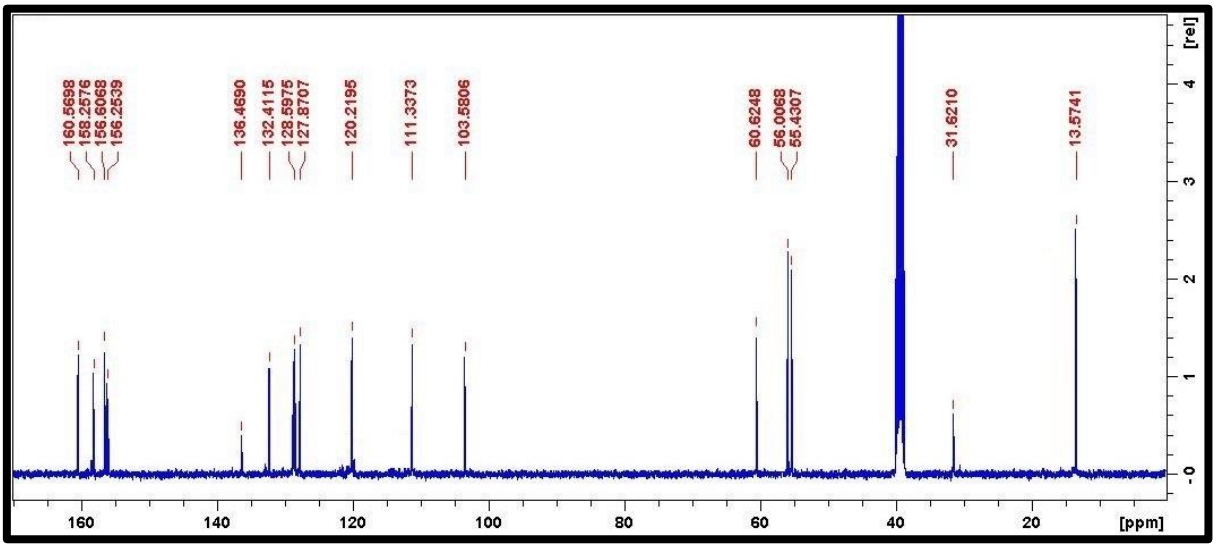

^{13}C NMR spectra of compound **5a**

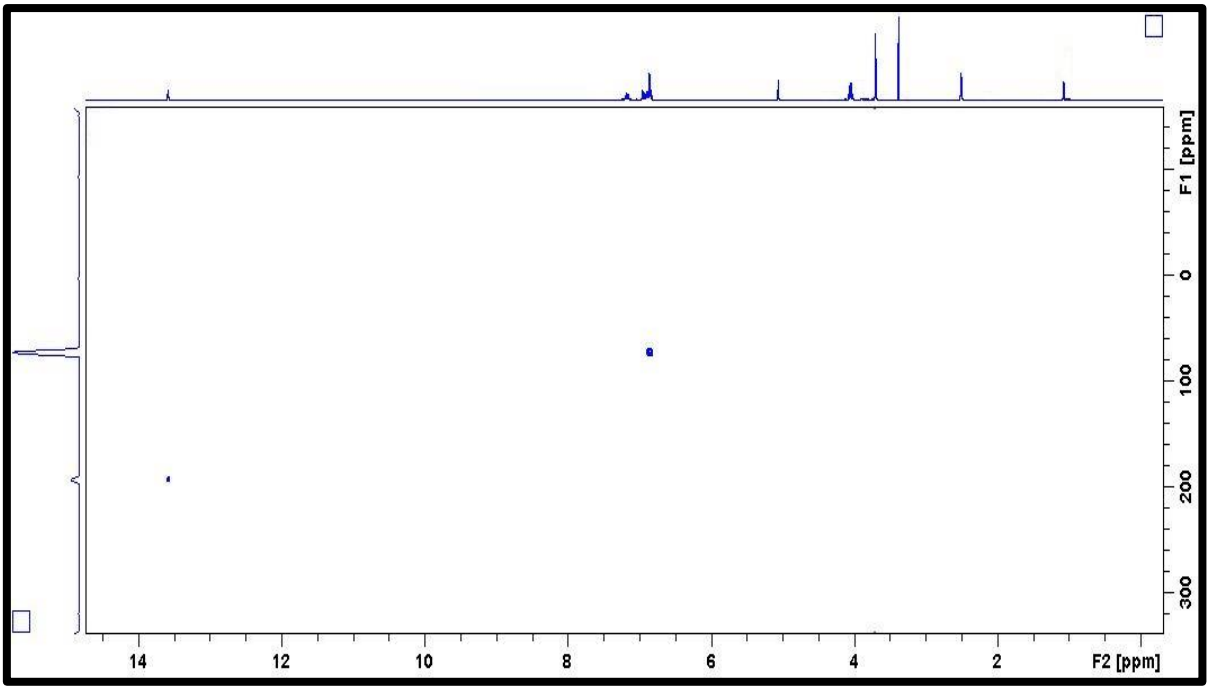

^{15}N NMR spectra of compound **5a**

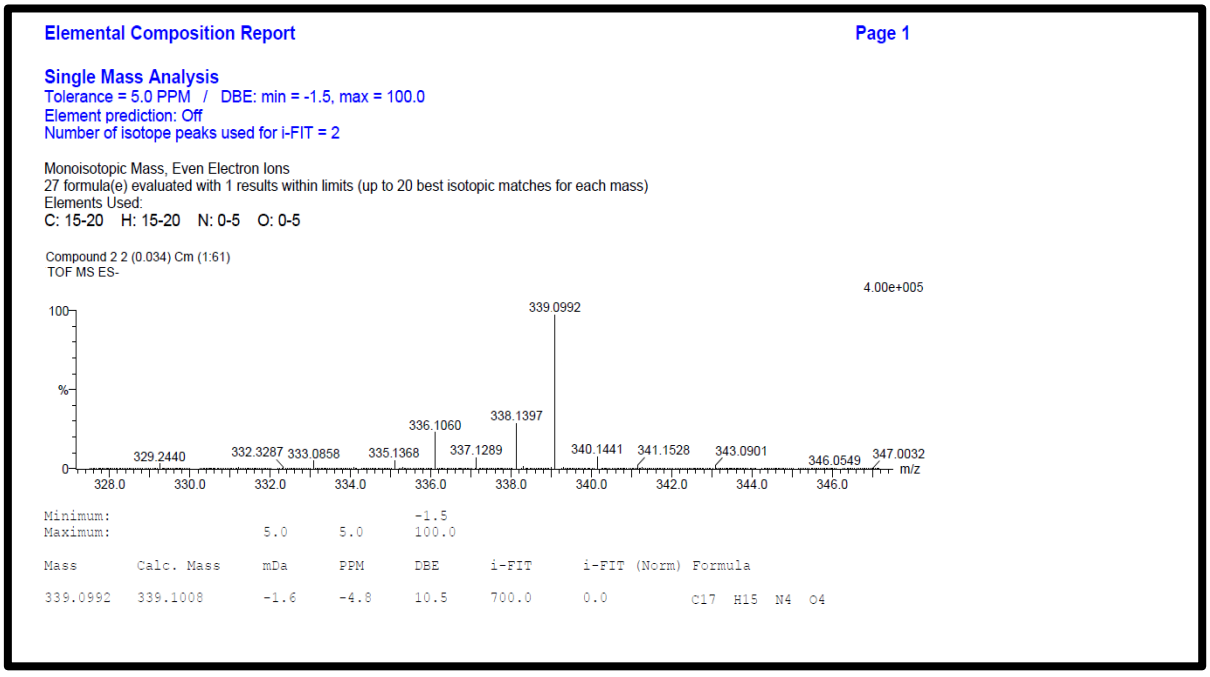

HRMS spectra of compound **5a**

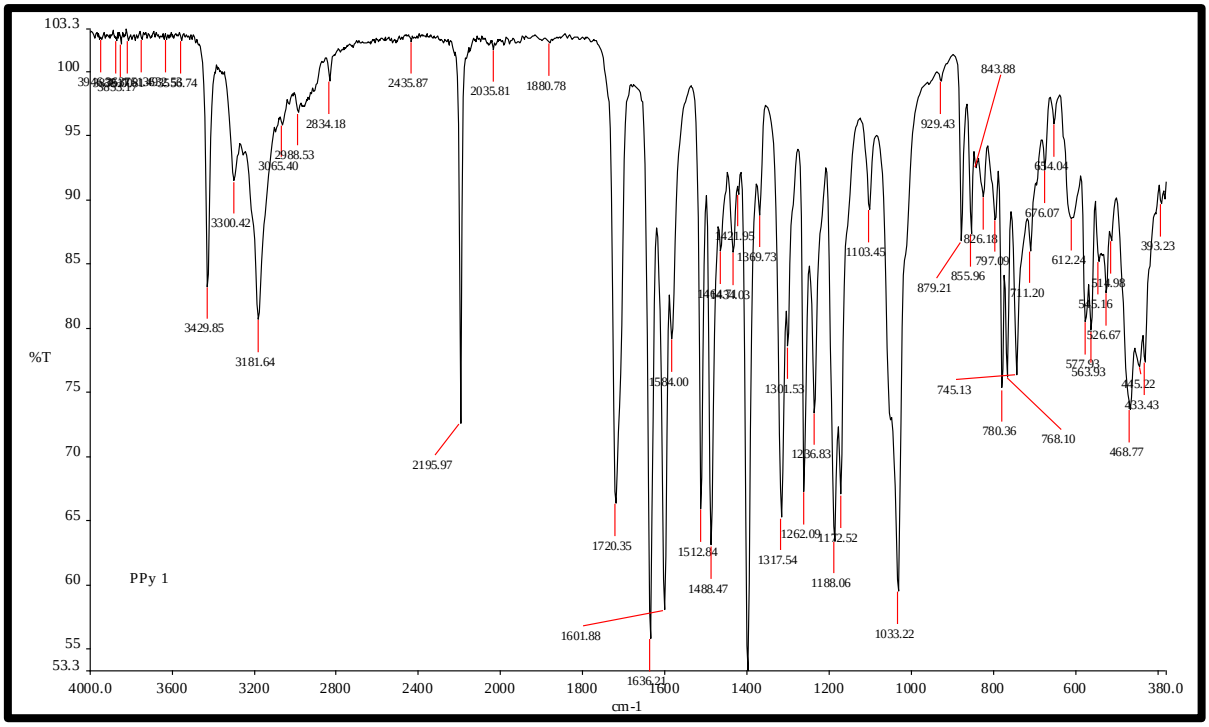

FT-IR spectra of compound **5a**

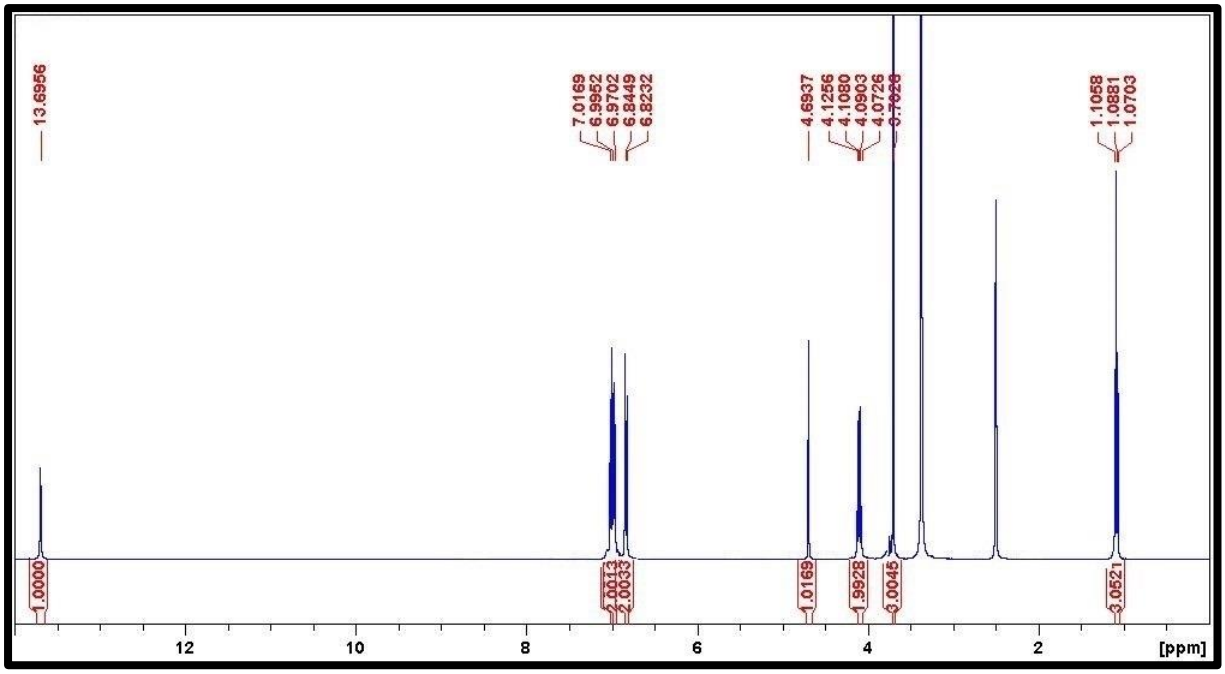

^{1}H NMR spectra of compound **5b**

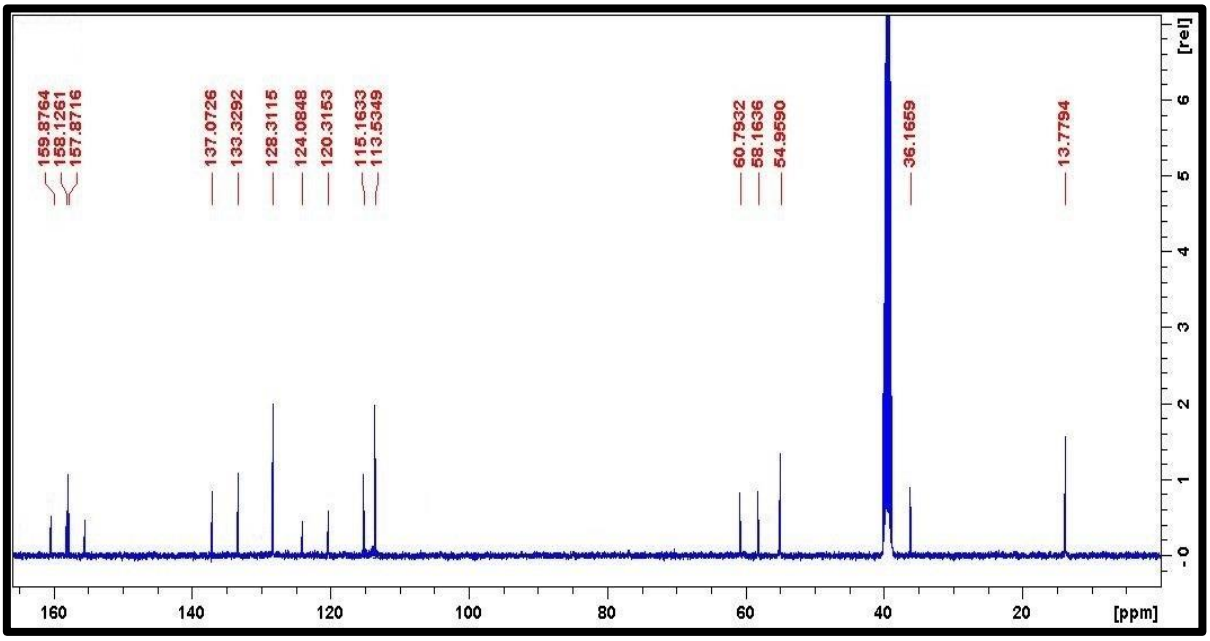

^{13}C NMR spectra of compound **5b**

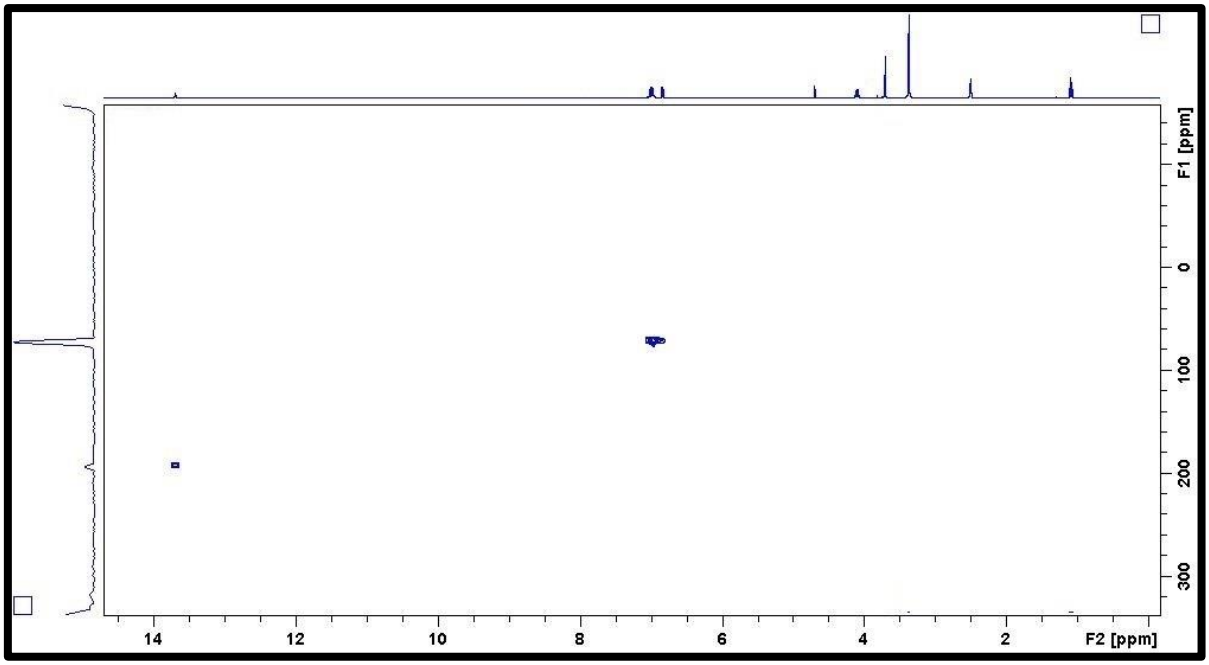

^{15}N NMR spectra of compound **5b**

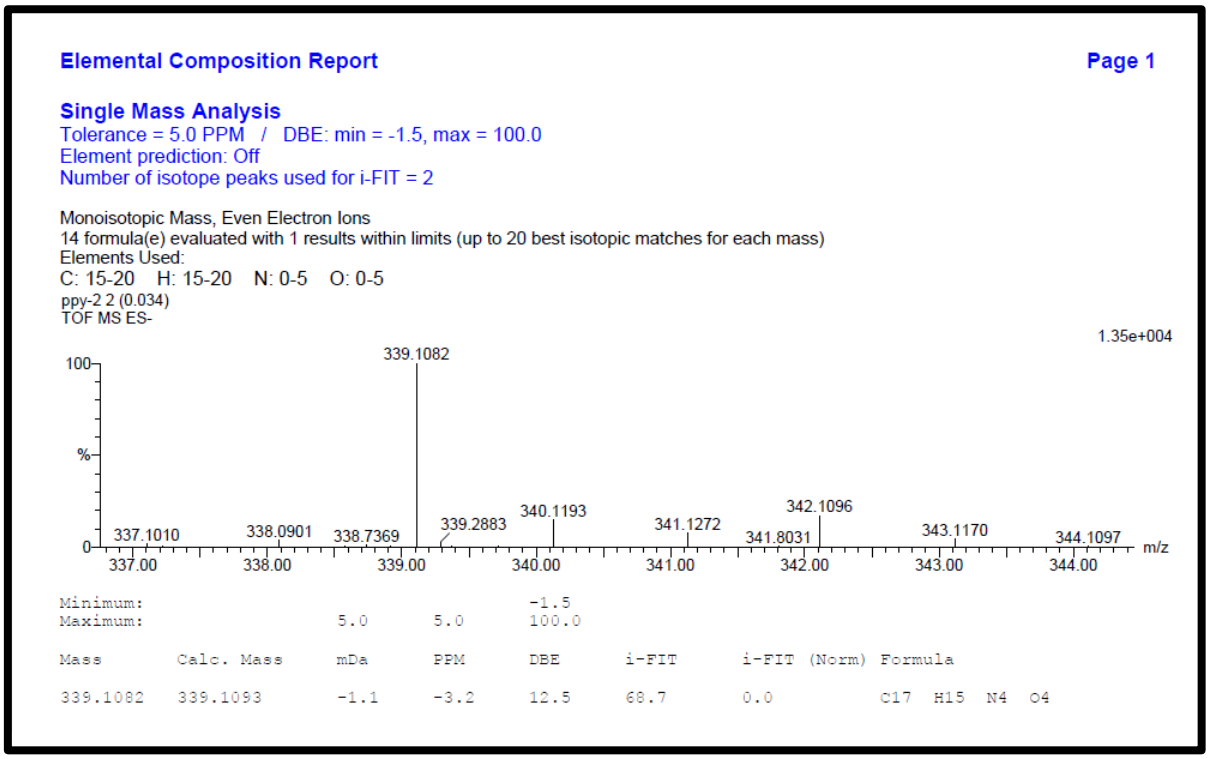

HRMS spectra of compound **5b**

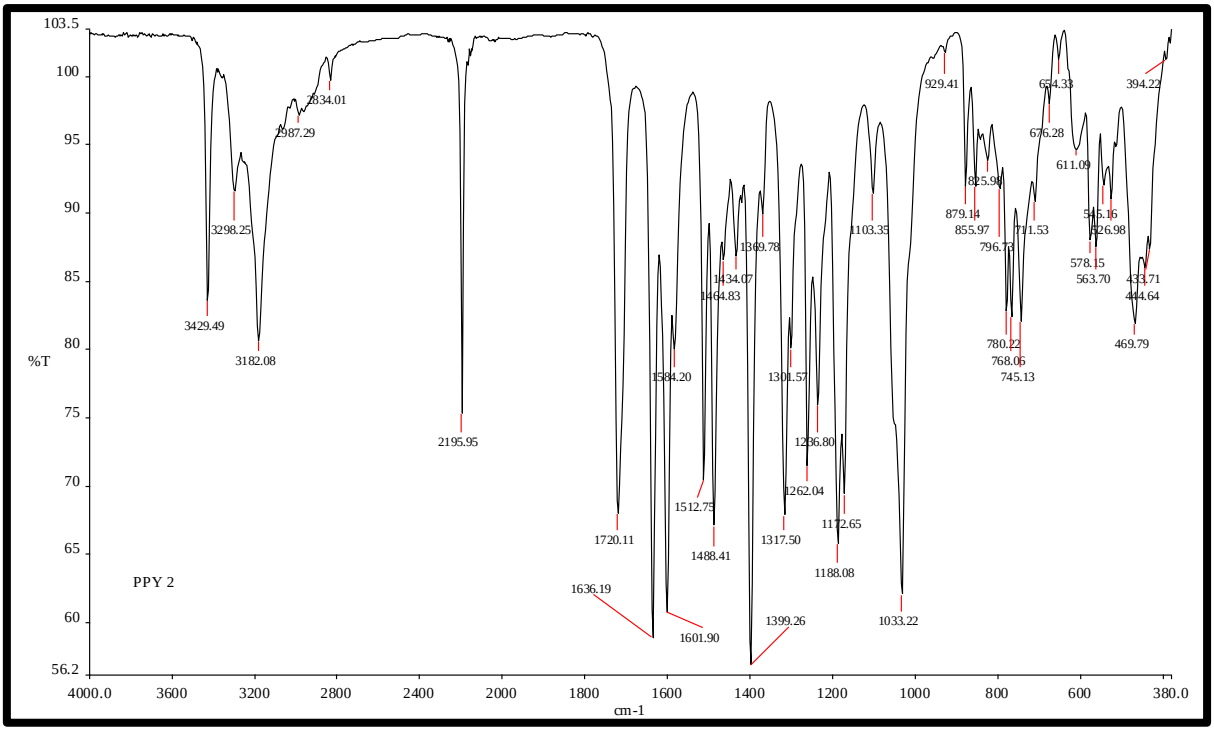

FT-IR spectra of compound **5b**

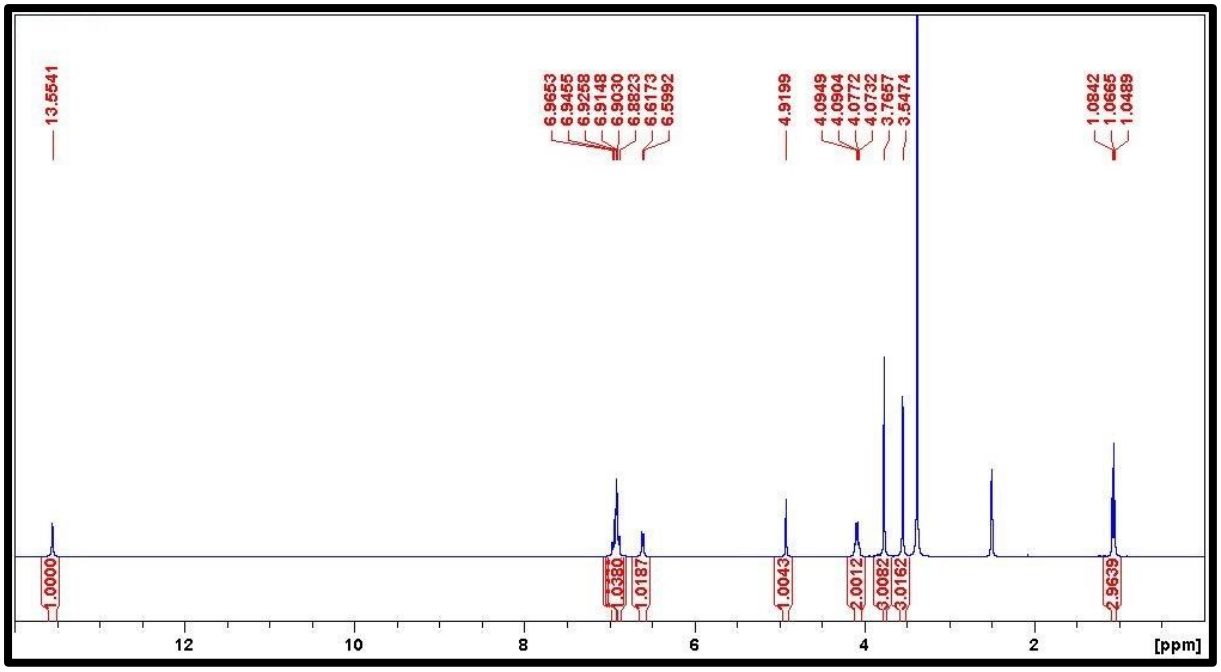

^{1}H NMR spectra of compound **5c**

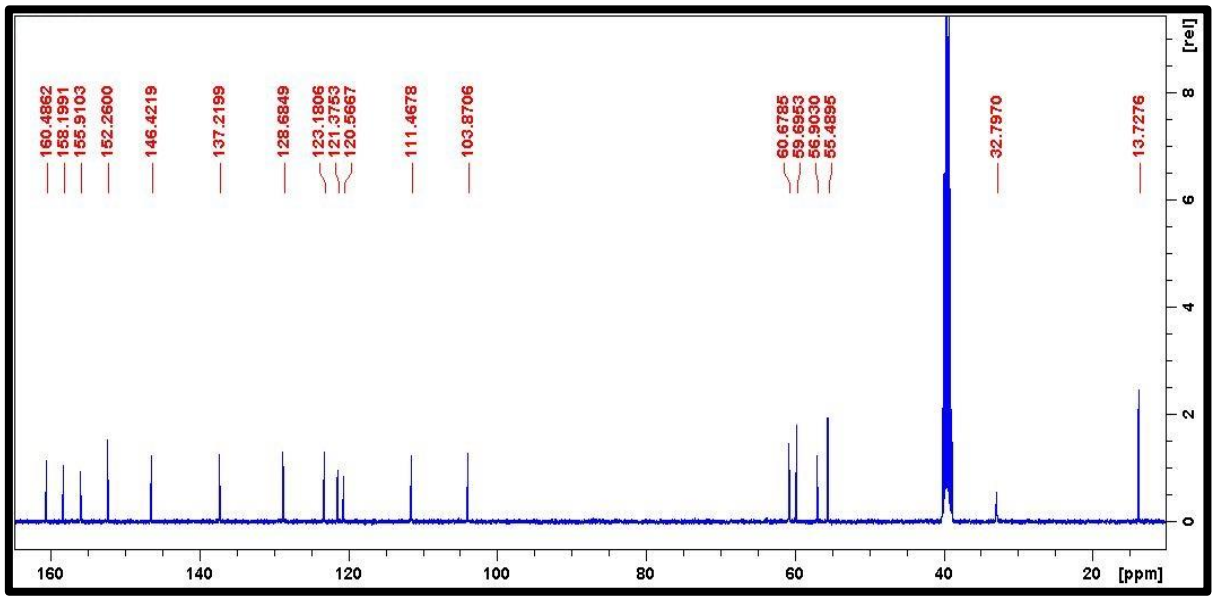

^{13}C NMR spectra of compound **5c**

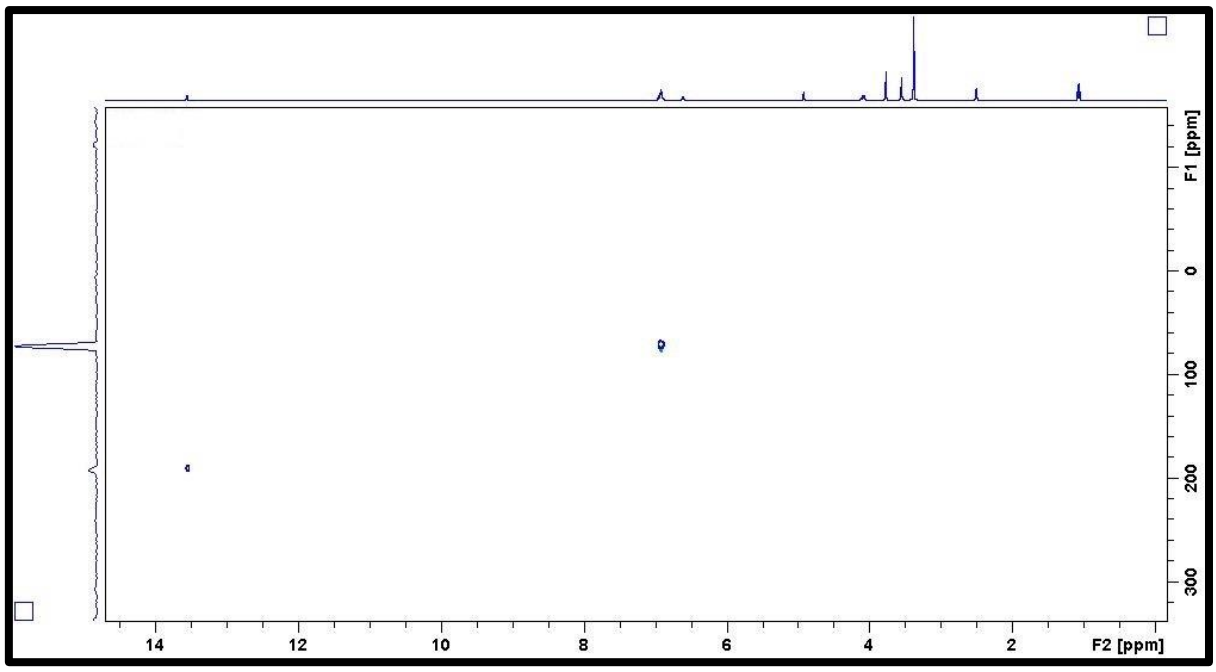

^{15}N NMR spectra of compound **5c**

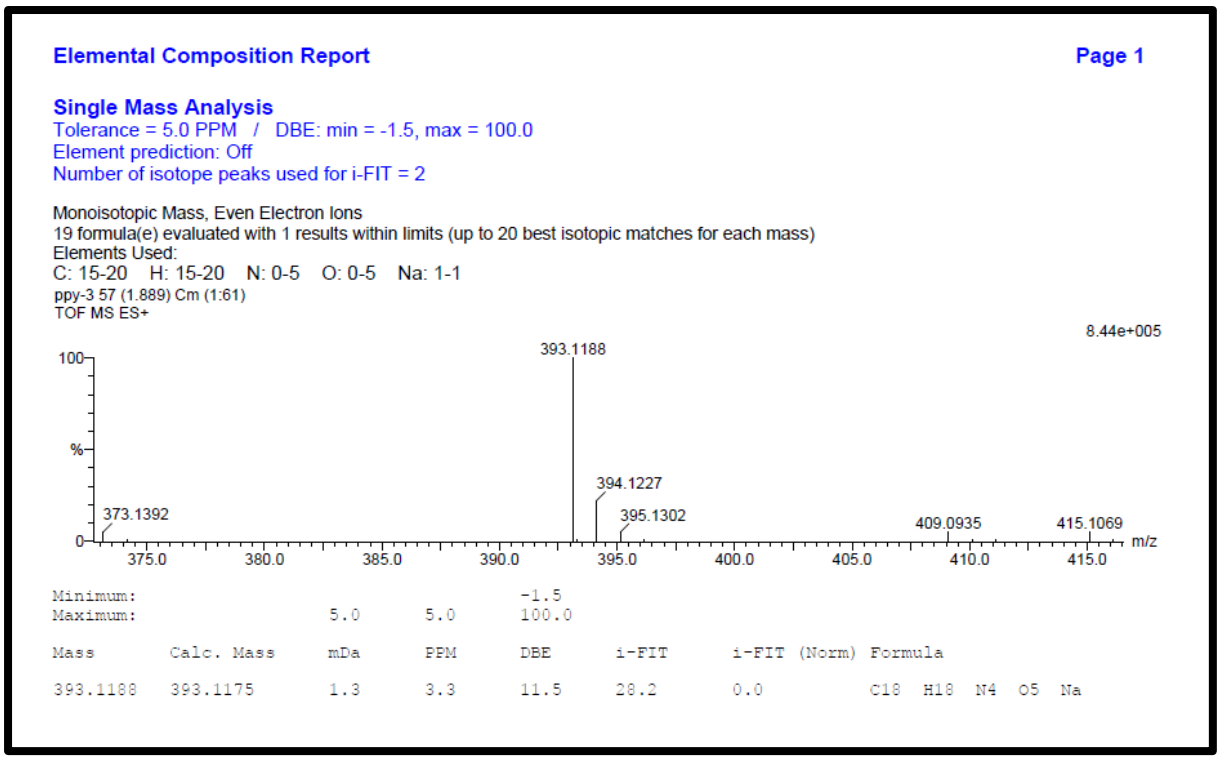

HRMS spectra of compound **5c**

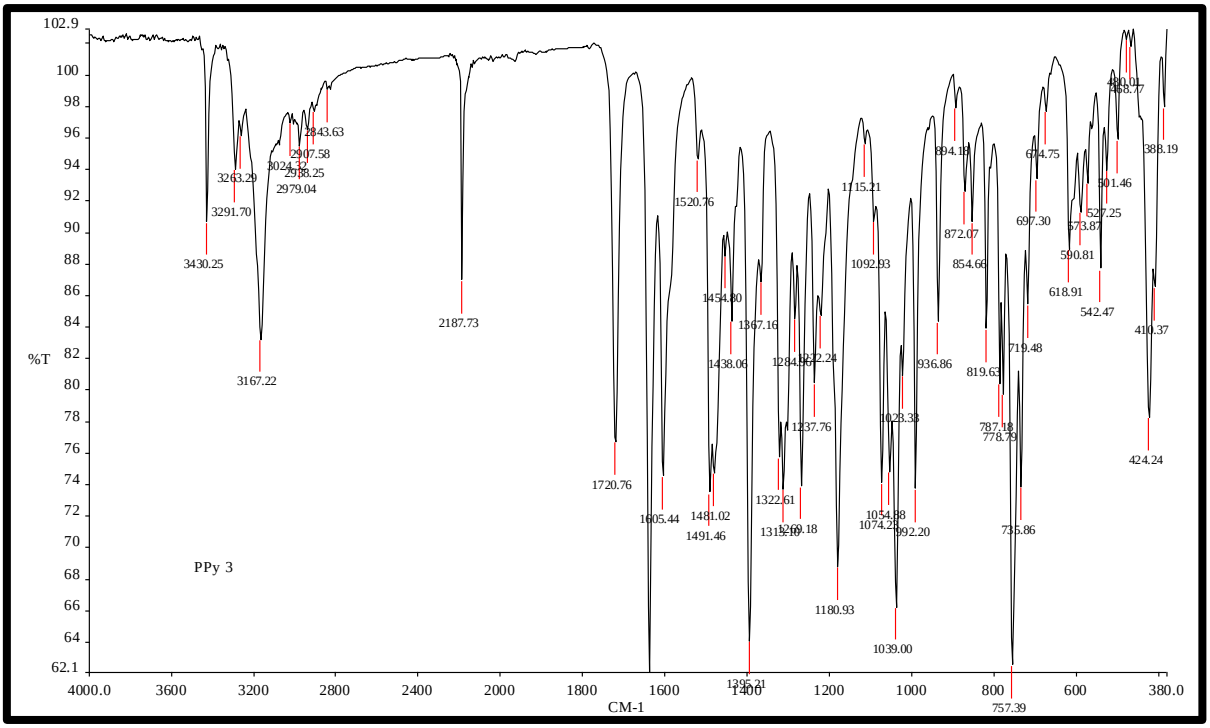

FT-IR spectra of compound **5c**

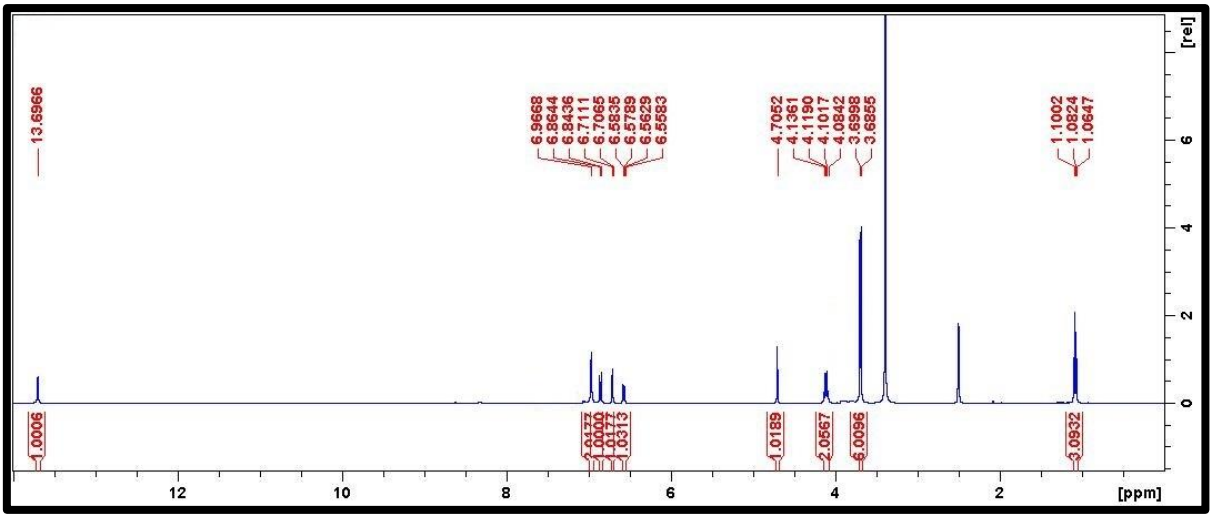

^{1}H NMR spectra of compound **5d**

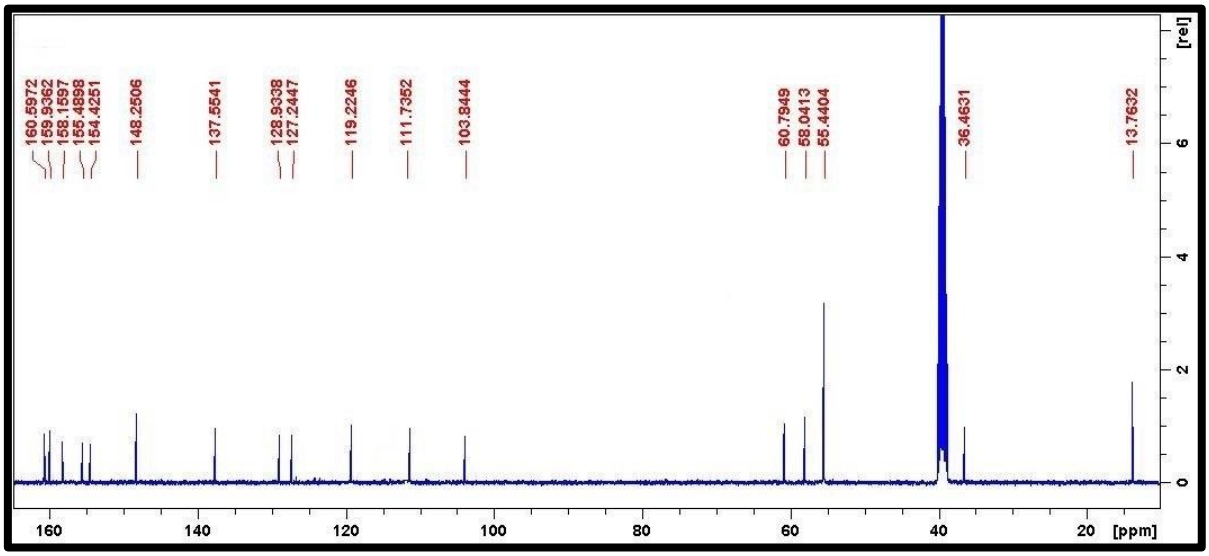

^{13}C NMR spectra of compound **5d**

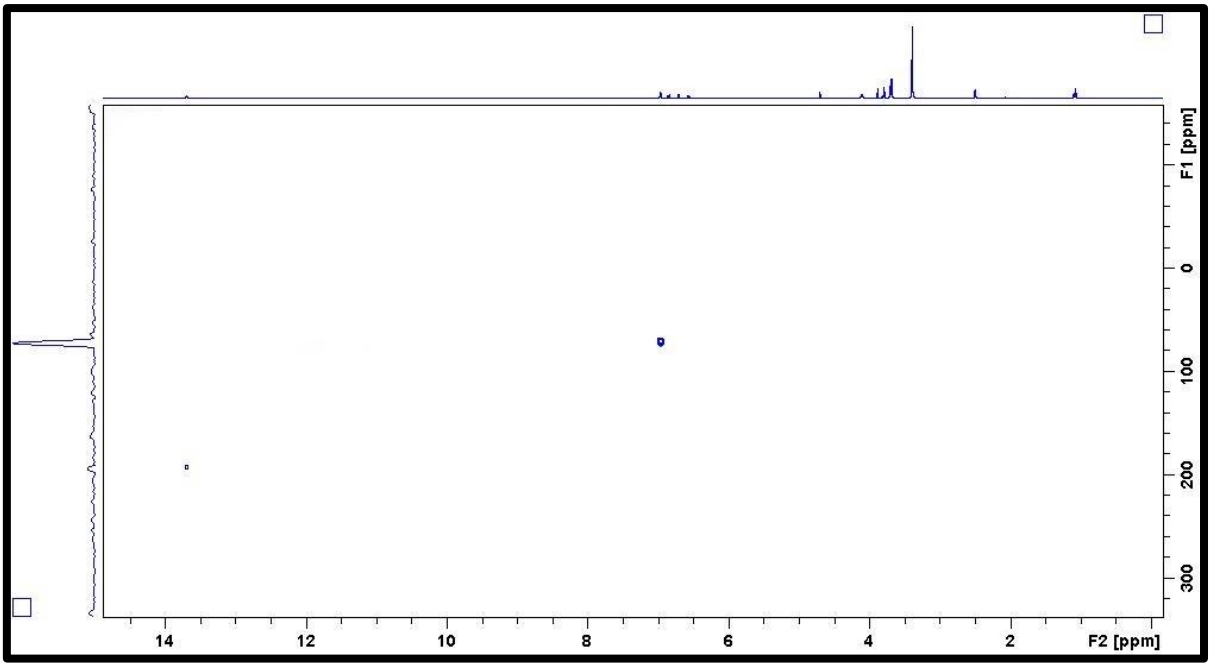

^{15}N NMR spectra of compound **5d**

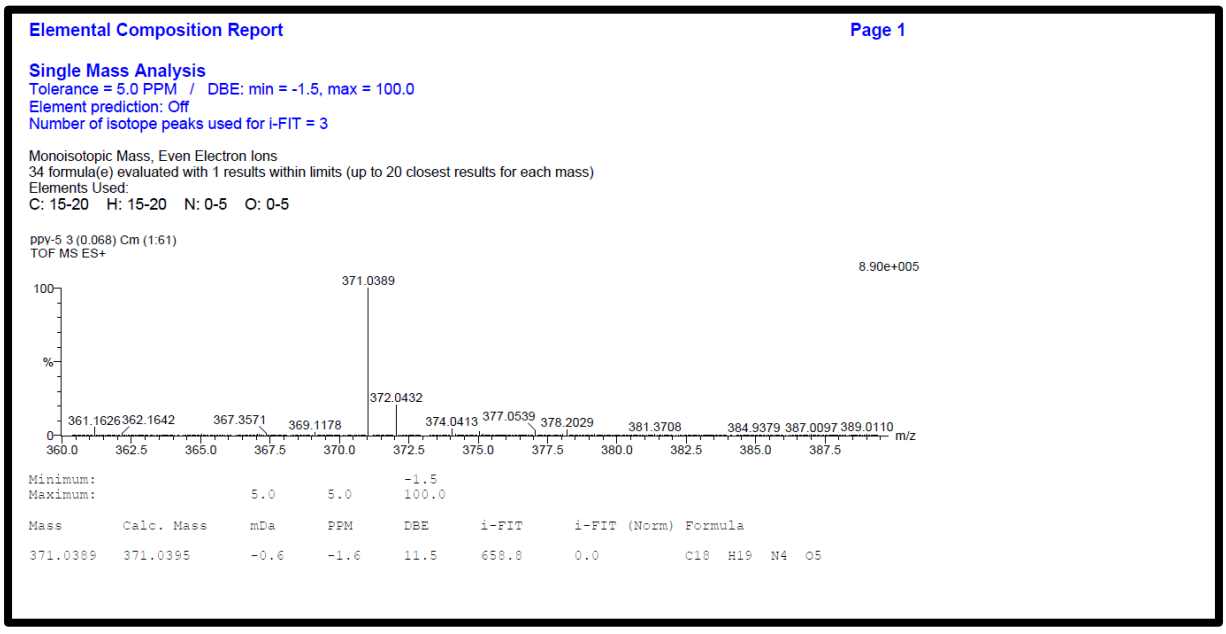

HRMS spectra of compound **5d**

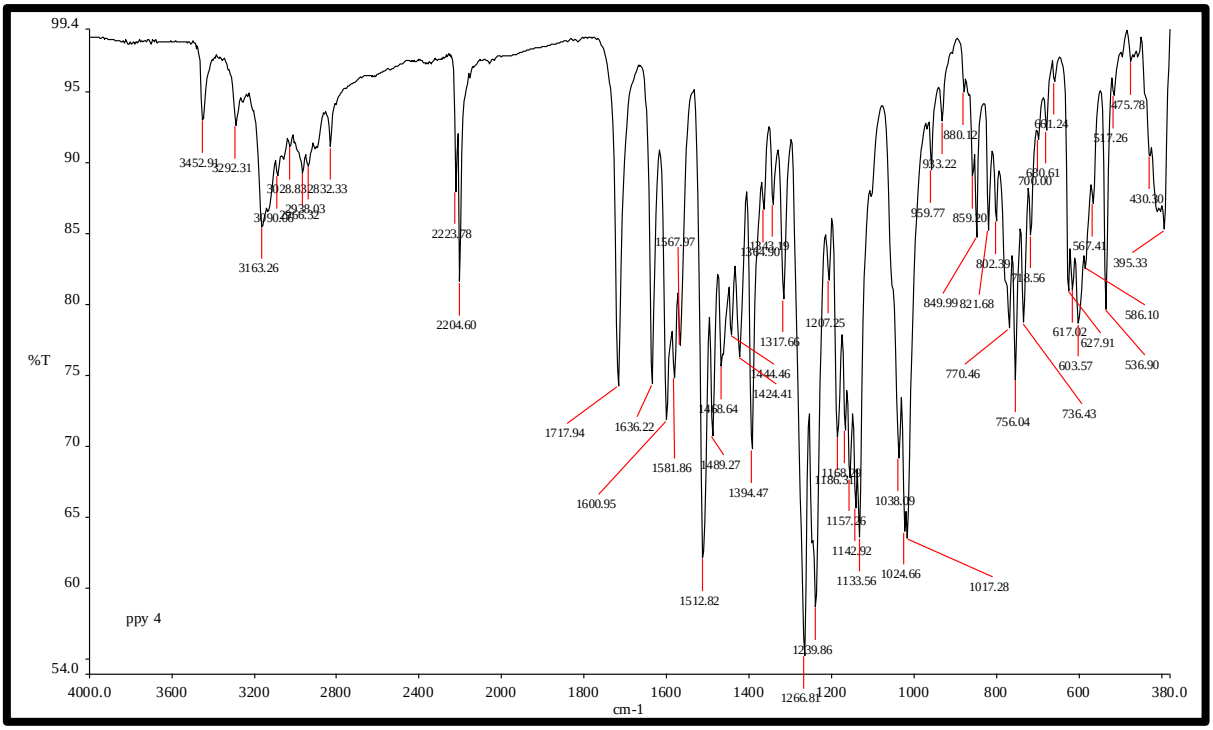

FT-IR spectra of compound **5d**

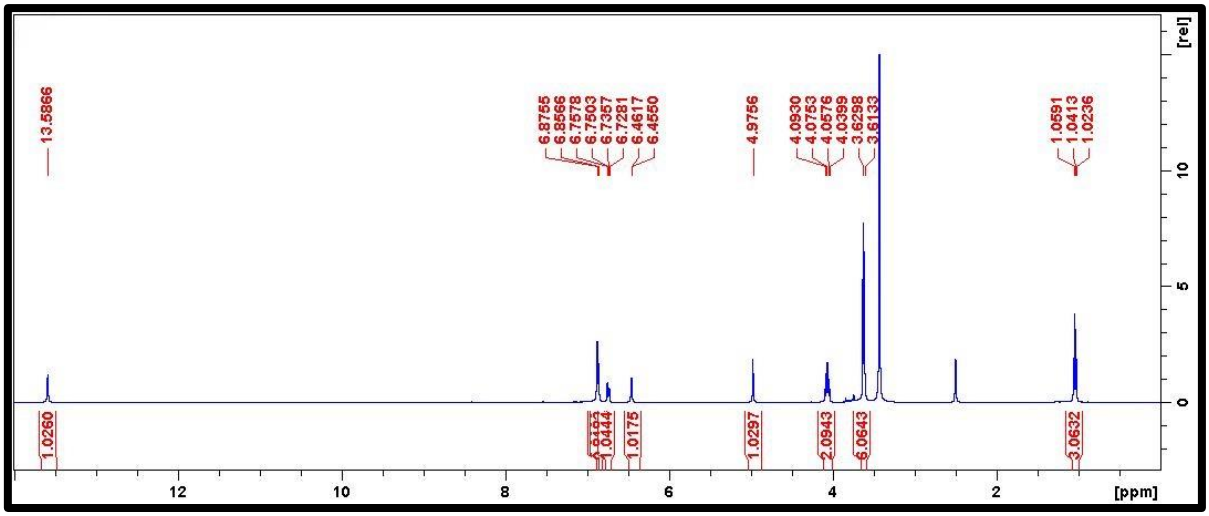

^{1}H NMR spectra of compound **5e**

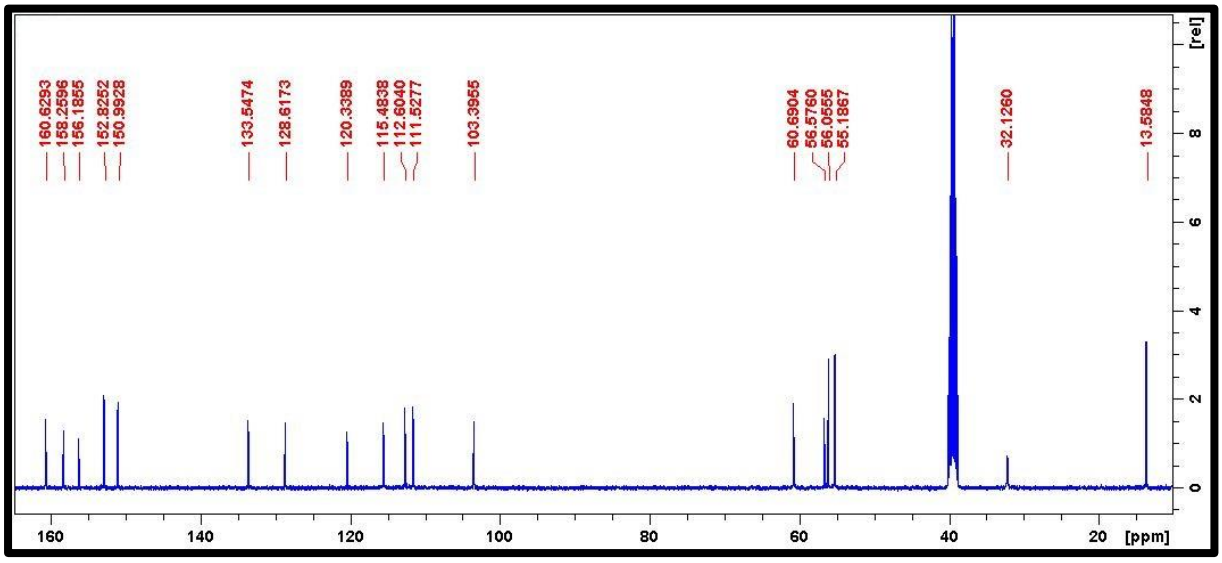

^{13}C NMR spectra of compound **5e**

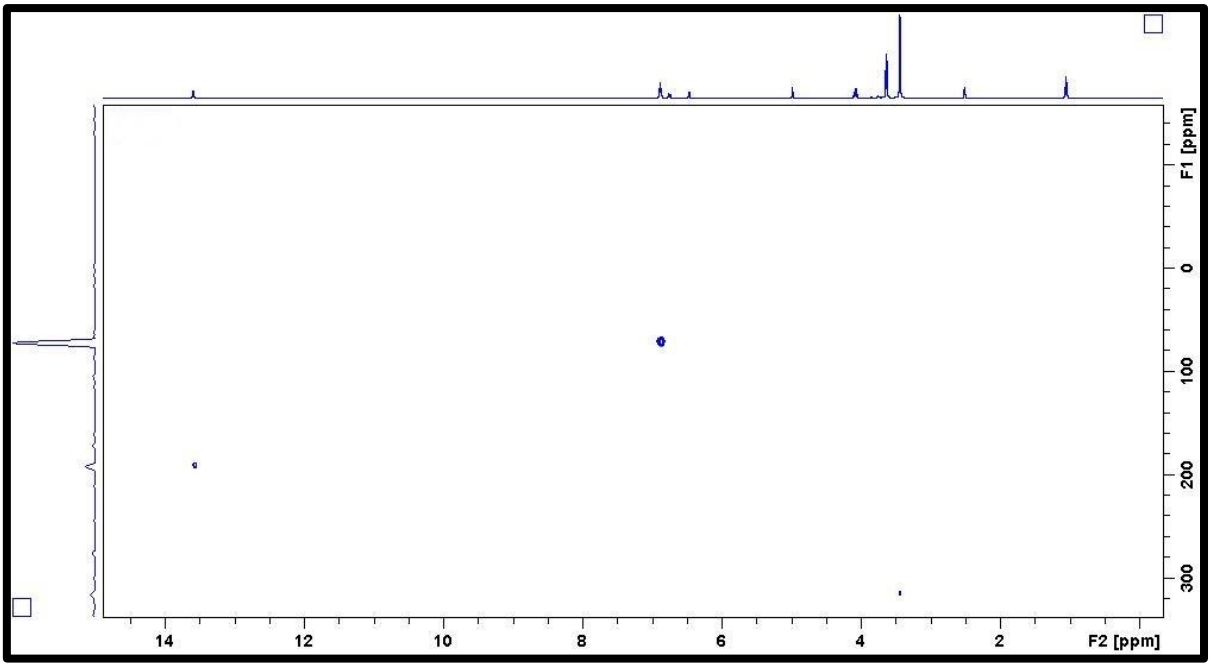

^{15}N NMR spectra of compound **5e**

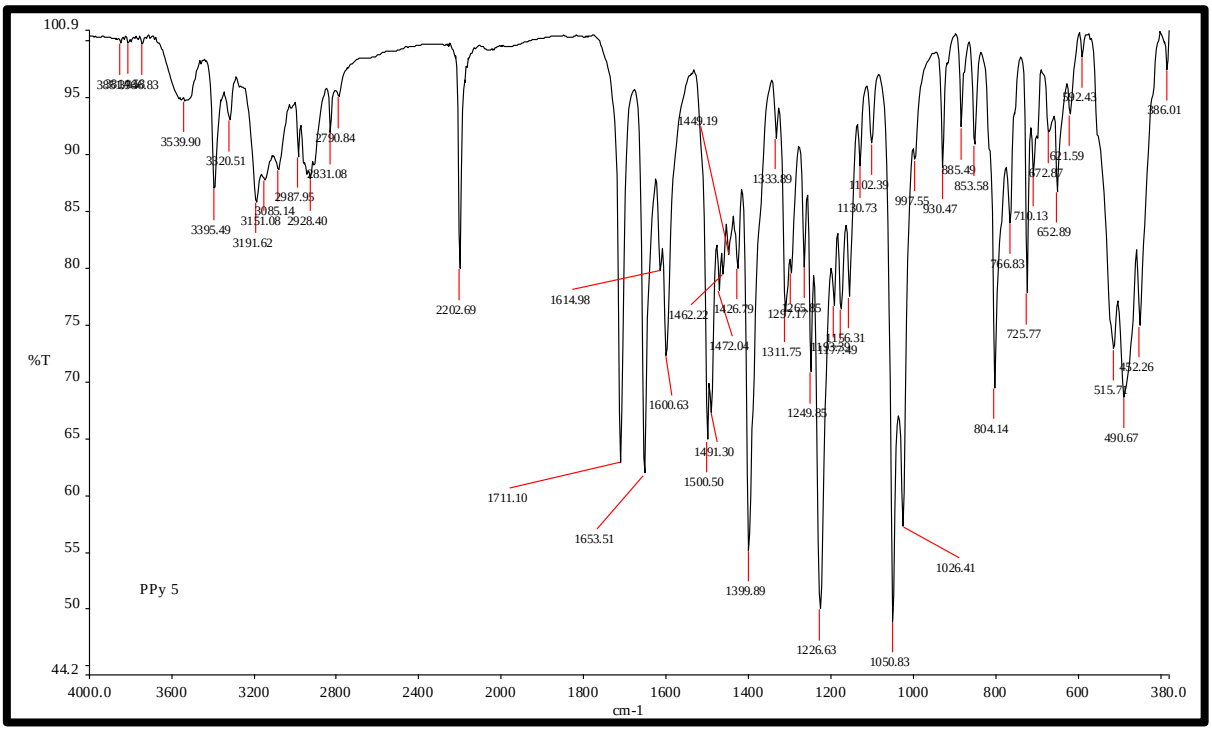

FT-IR spectra of compound **5e**

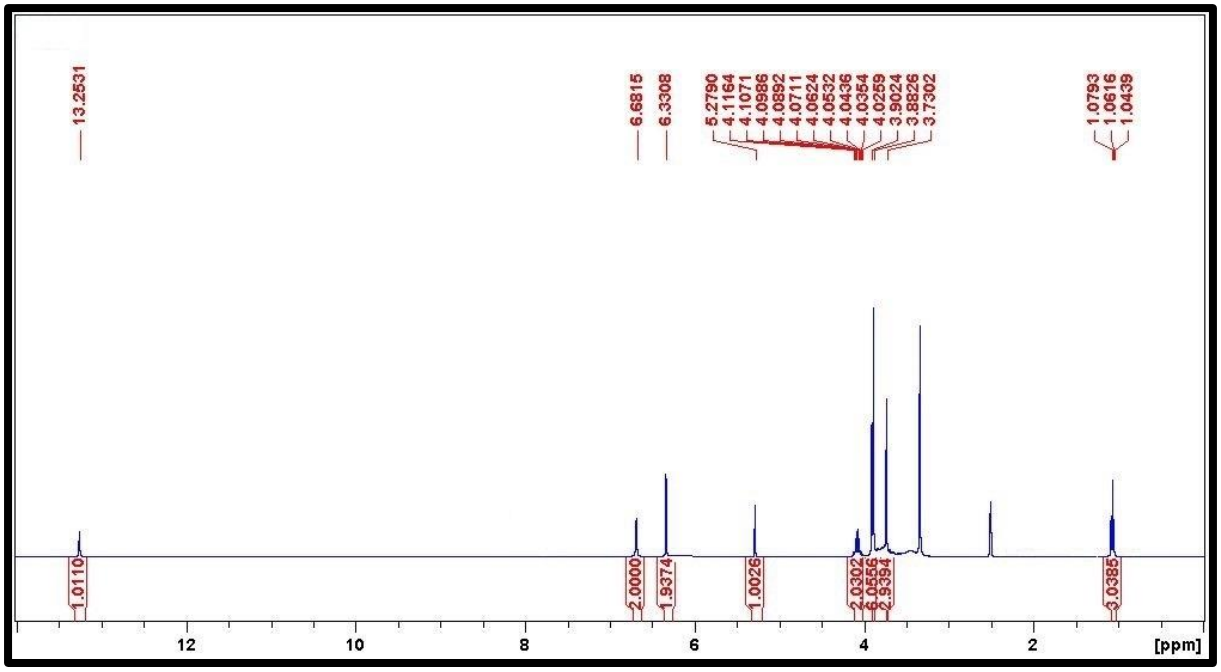

^{1}H NMR spectra of compound **5f**

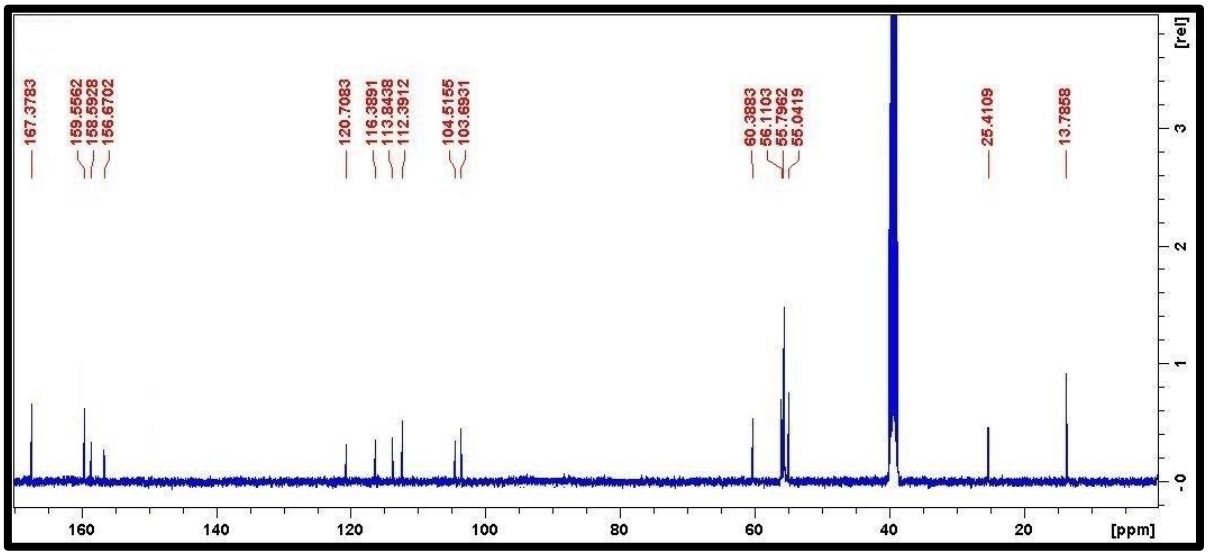

^{13}C NMR spectra of compound **5f**

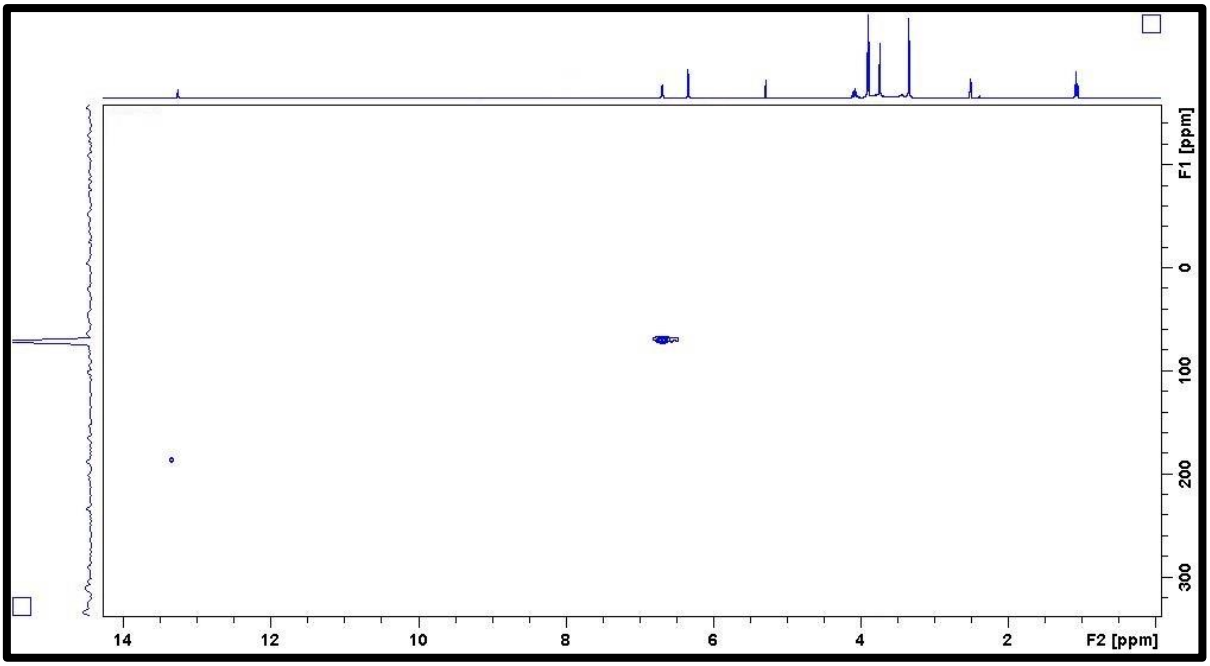

^{15}N NMR spectra of compound **5f**

Elemental Composition Report **Page 1**

Single Mass Analysis
Tolerance = 5.0 PPM / DBE: min = -1.5, max = 100.0
Element prediction: Off
Number of isotope peaks used for i-FIT = 2

Monoisotopic Mass, Even Electron Ions
15 formula(e) evaluated with 1 results within limits (up to 20 best isotopic matches for each mass)
Elements Used:
C: 15-20 H: 15-20 N: 0-5 O: 5-10 Na: 1-1
ppy-6 3 (0.068) Cm (1:61)
TOF MS ES+

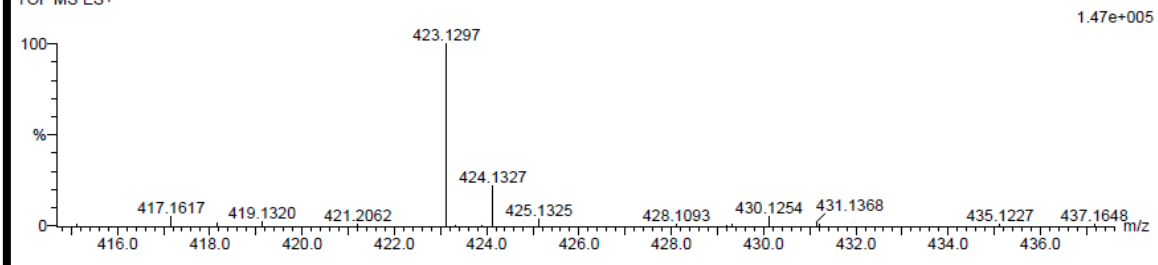

Minimum:				-1.5			
Maximum:		5.0	5.0	100.0			
Mass	Calc. Mass	mDa	PPM	DBE	i-FIT	i-FIT (Norm)	Formula
423.1297	423.1281	1.6	3.8	11.5	39.8	0.0	C19 H20 N4 O6 Na

HRMS spectra of compound **5f**

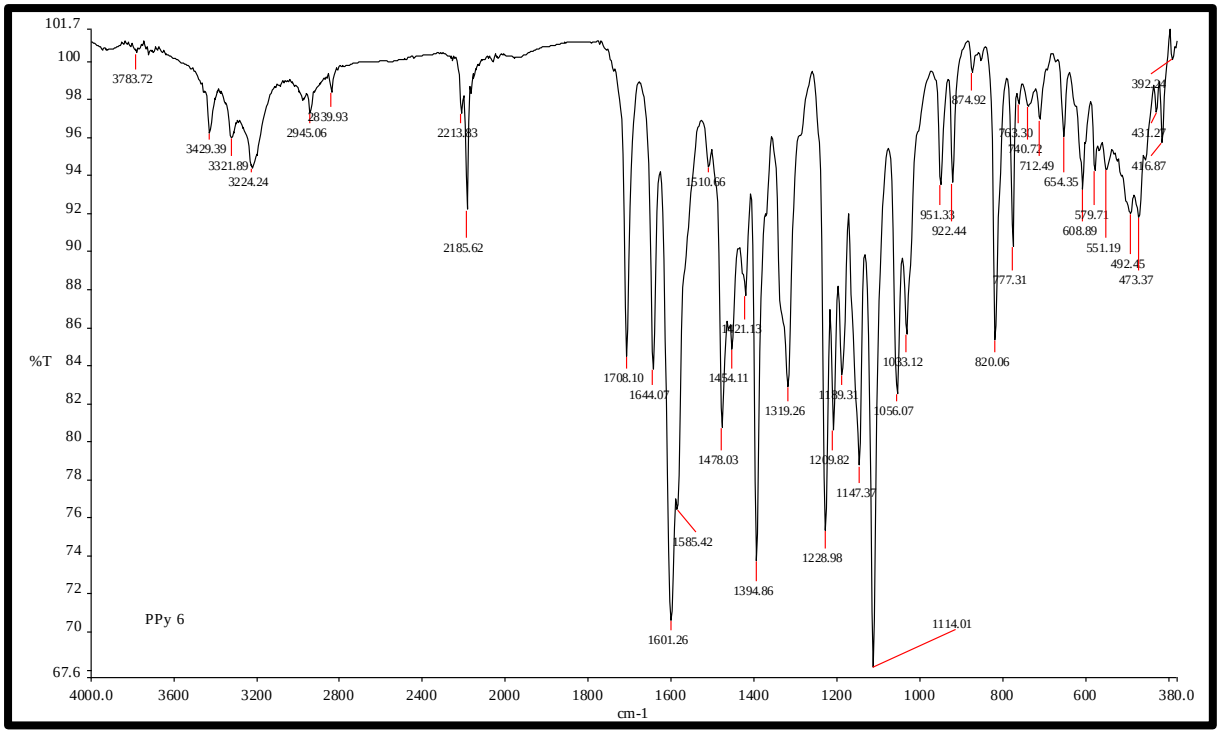

FT-IR spectra of compound **5f**

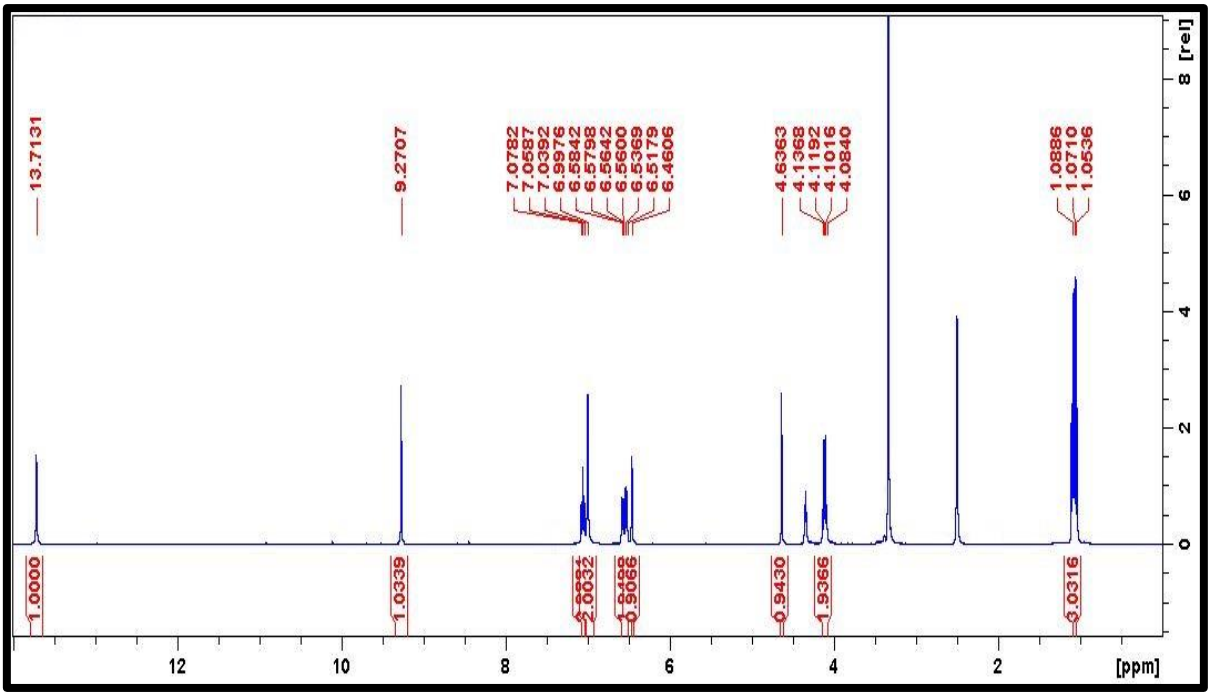

^{1}H NMR spectra of compound **5g**

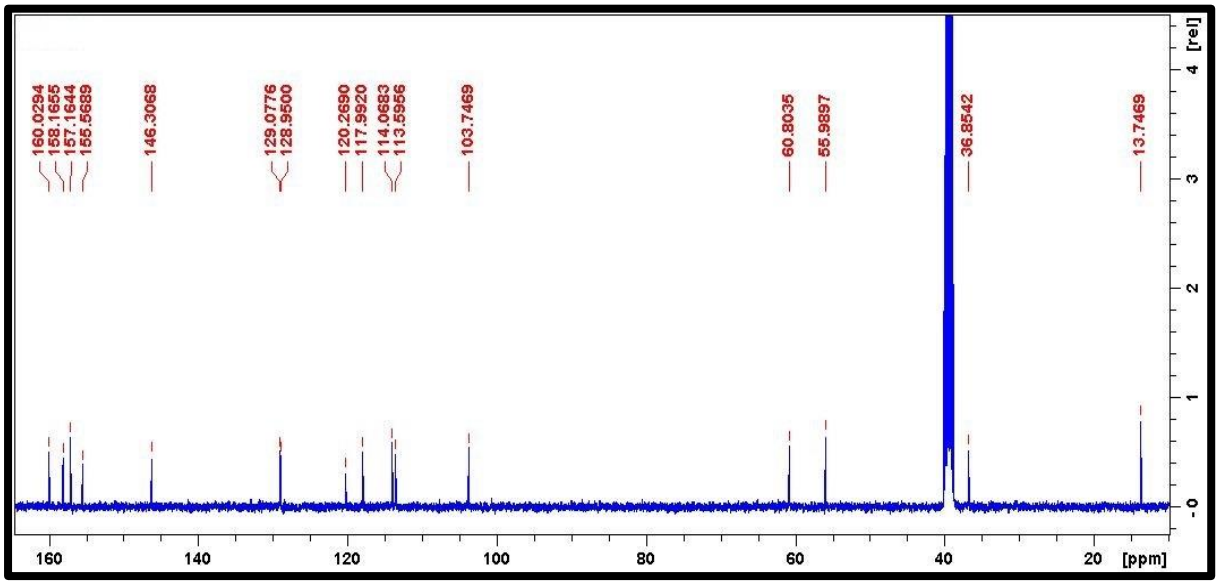

^{13}C NMR spectra of compound **5g**

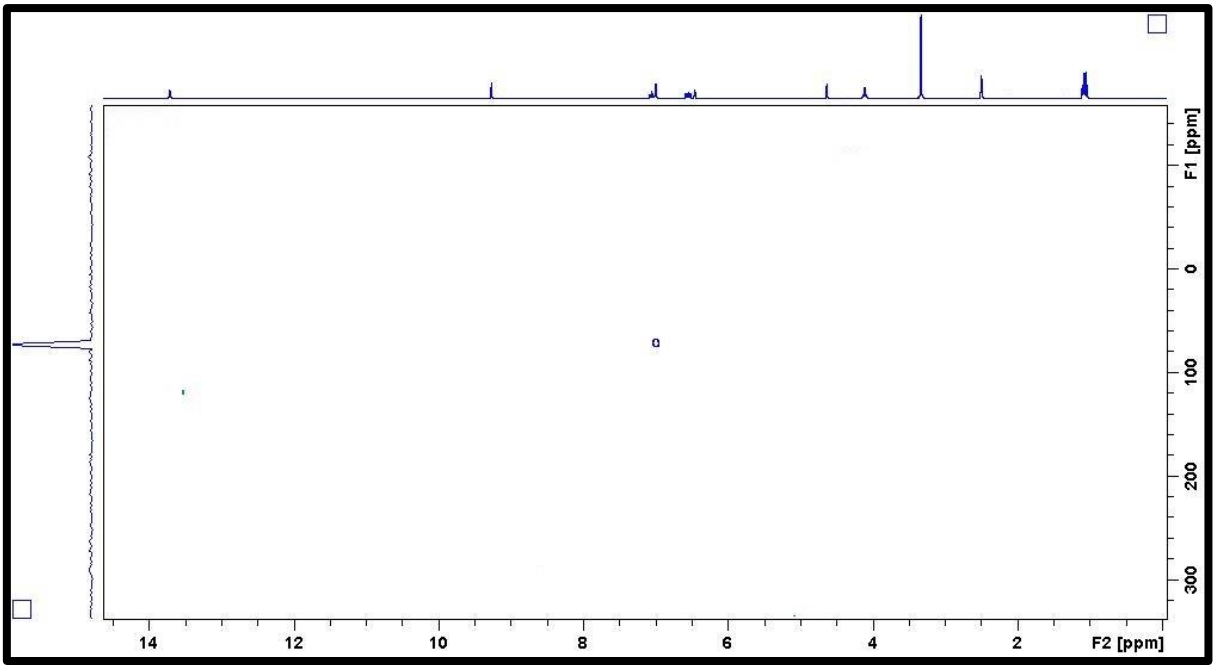

^{15}N NMR spectra of compound **5g**

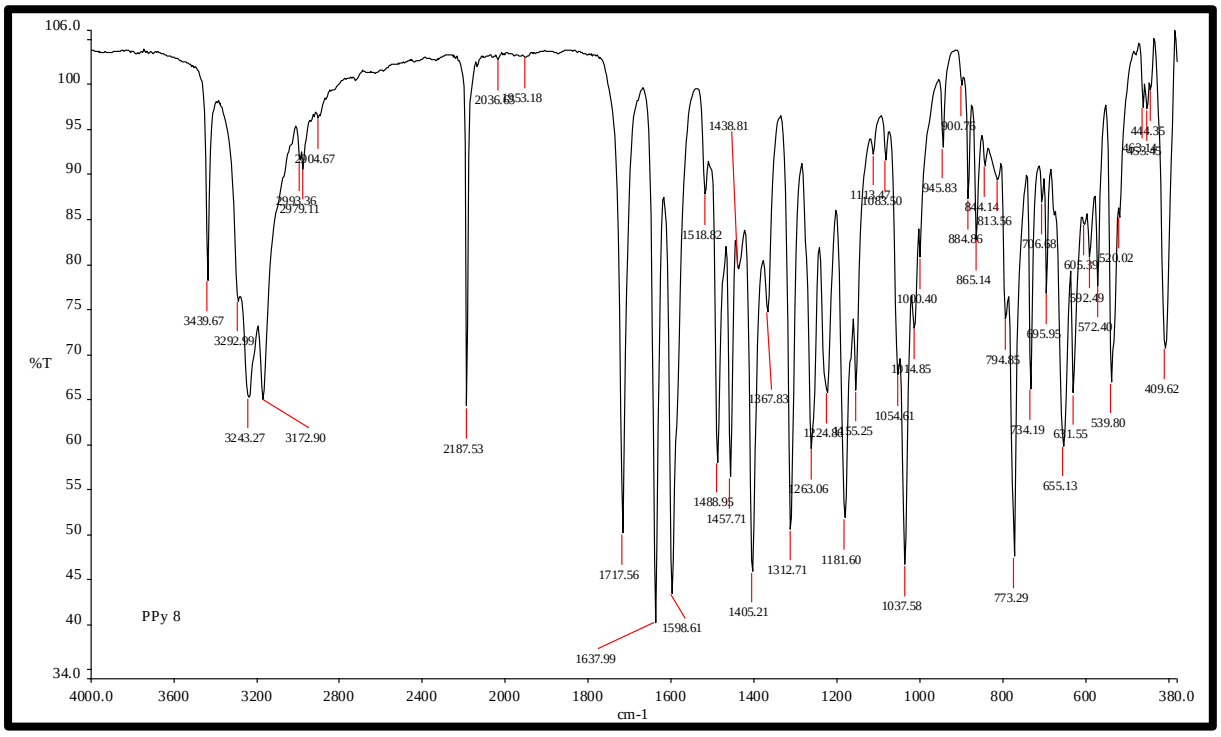

FT-IR spectra of compound **5g**

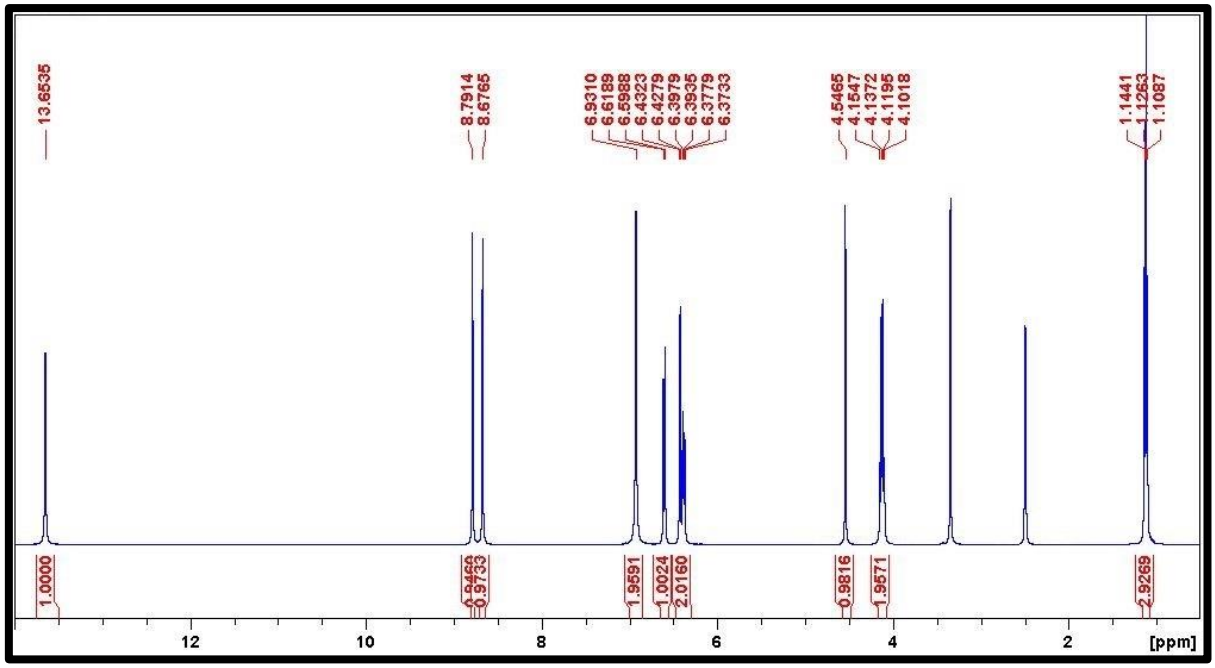

^{1}H NMR spectra of compound **5h**

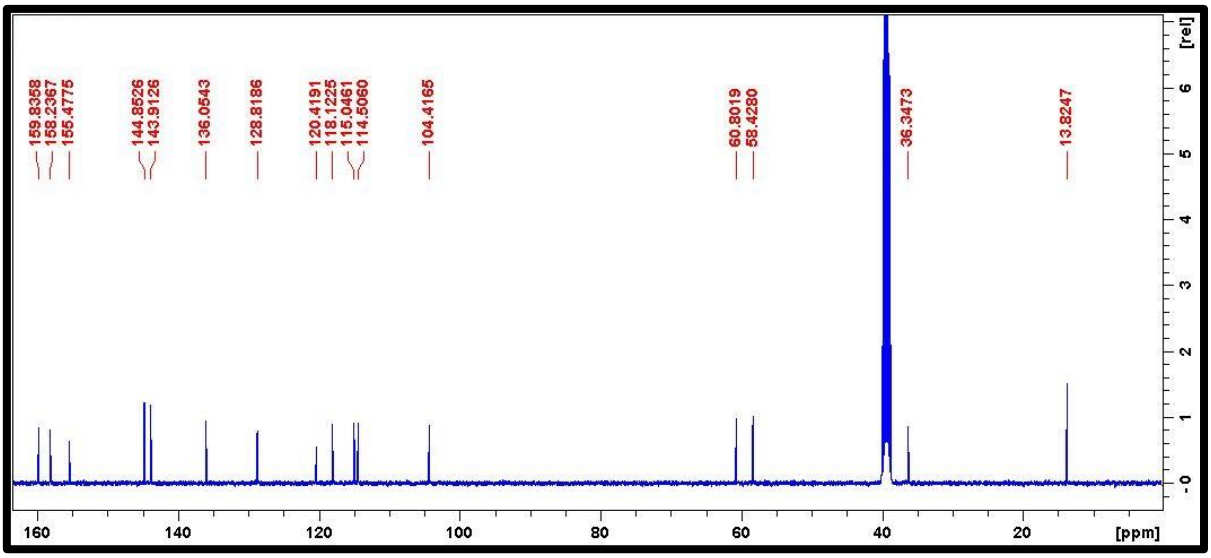

^{13}C NMR spectra of compound **5h**

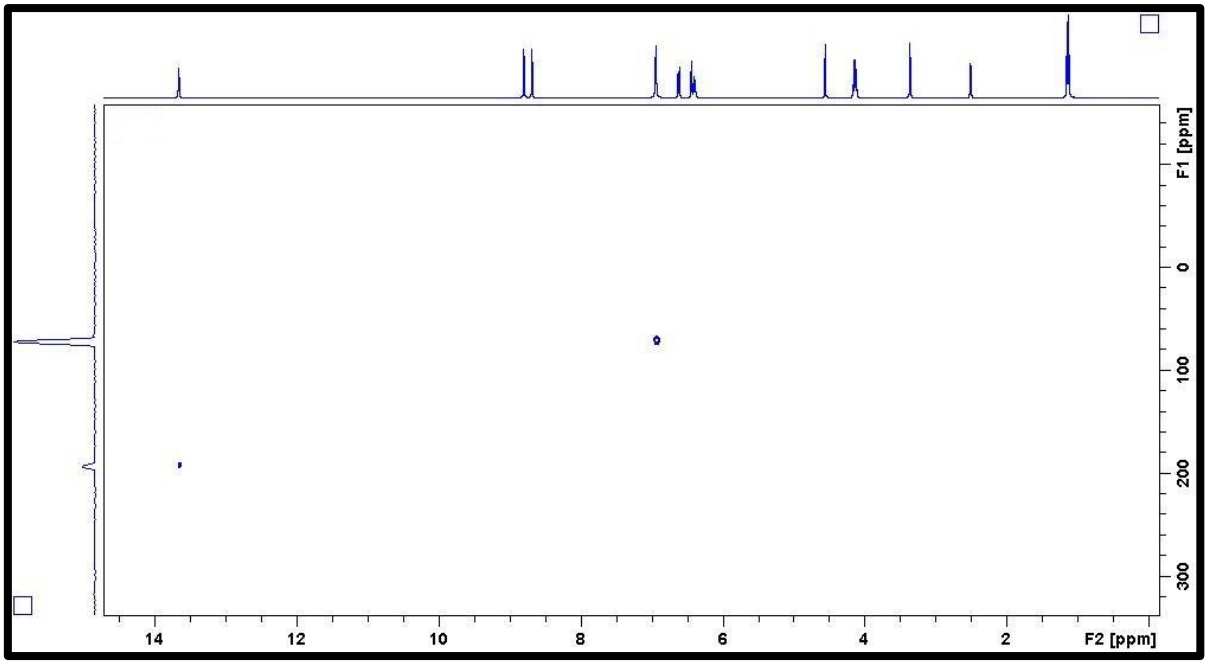

^{15}N NMR spectra of compound **5h**

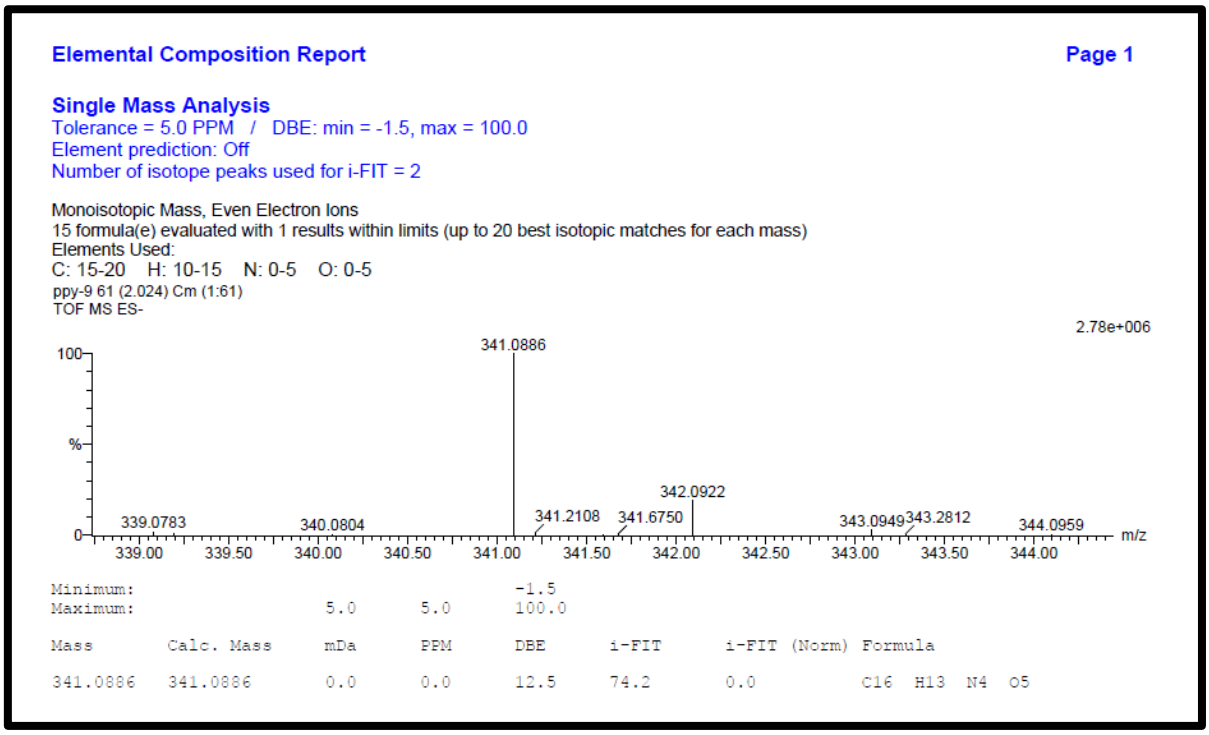

HRMS spectra of compound **5h**

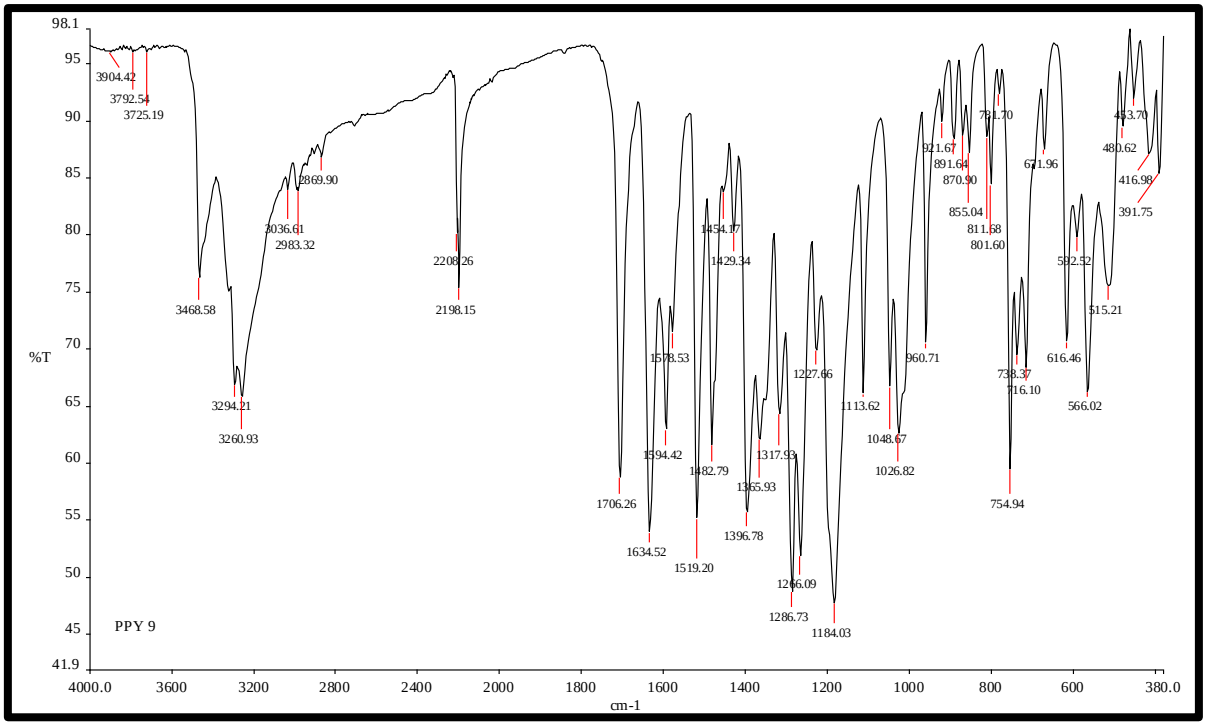

FT-IR spectra of compound **5h**

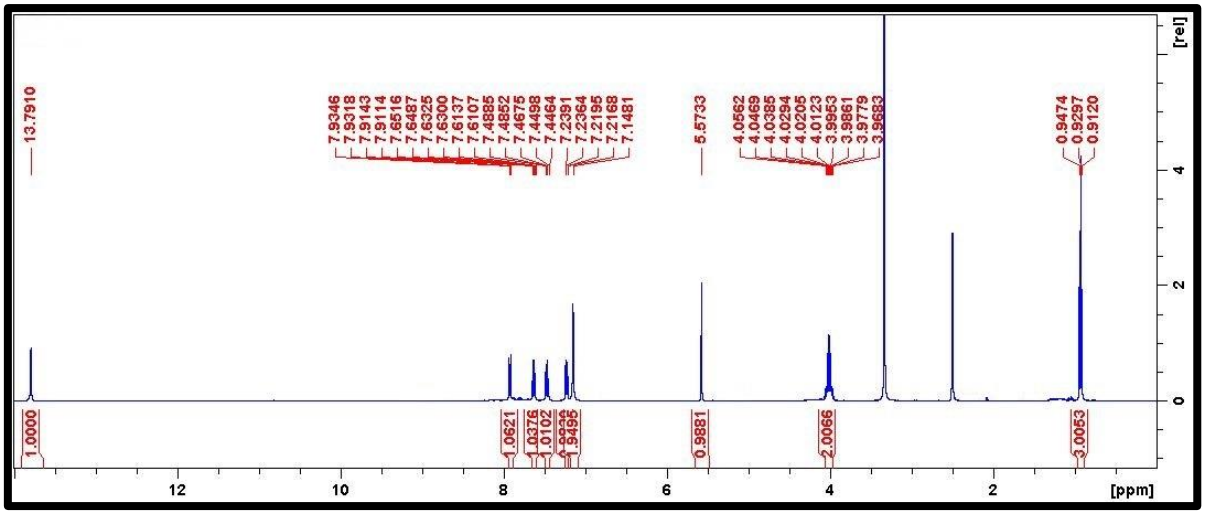

^{1}H NMR spectra of compound **5i**

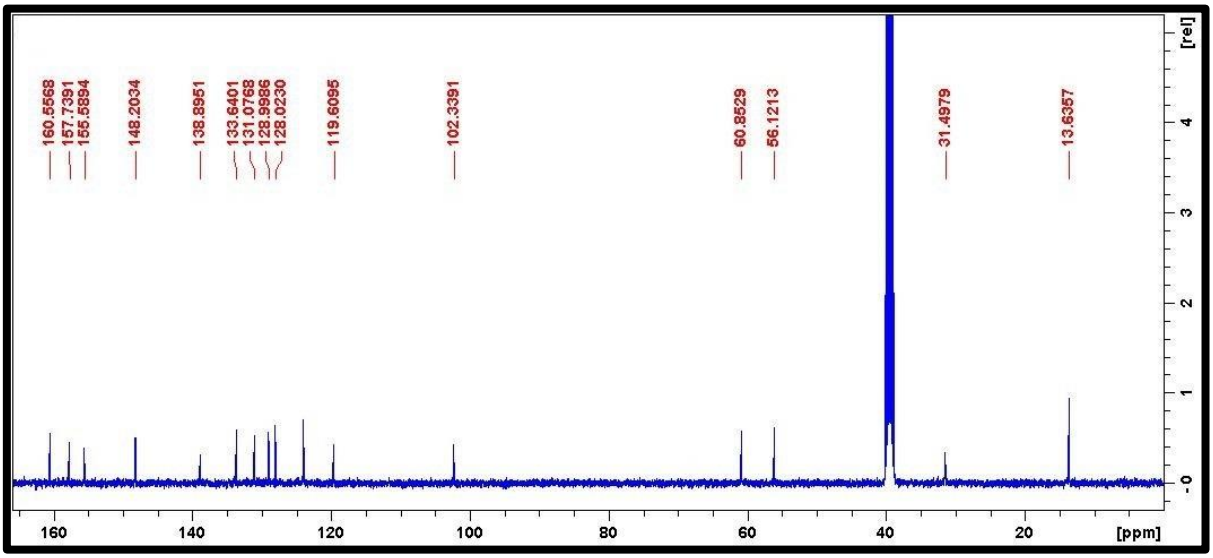

^{13}C NMR spectra of compound **5i**

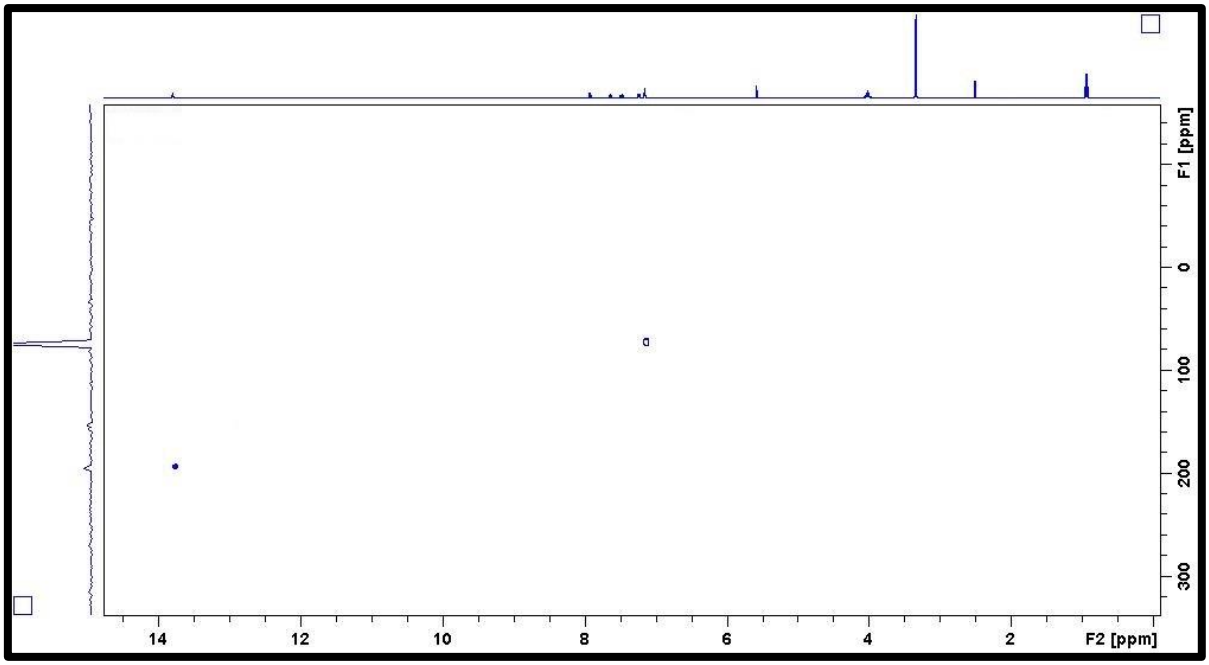

^{15}N NMR spectra of compound **5i**

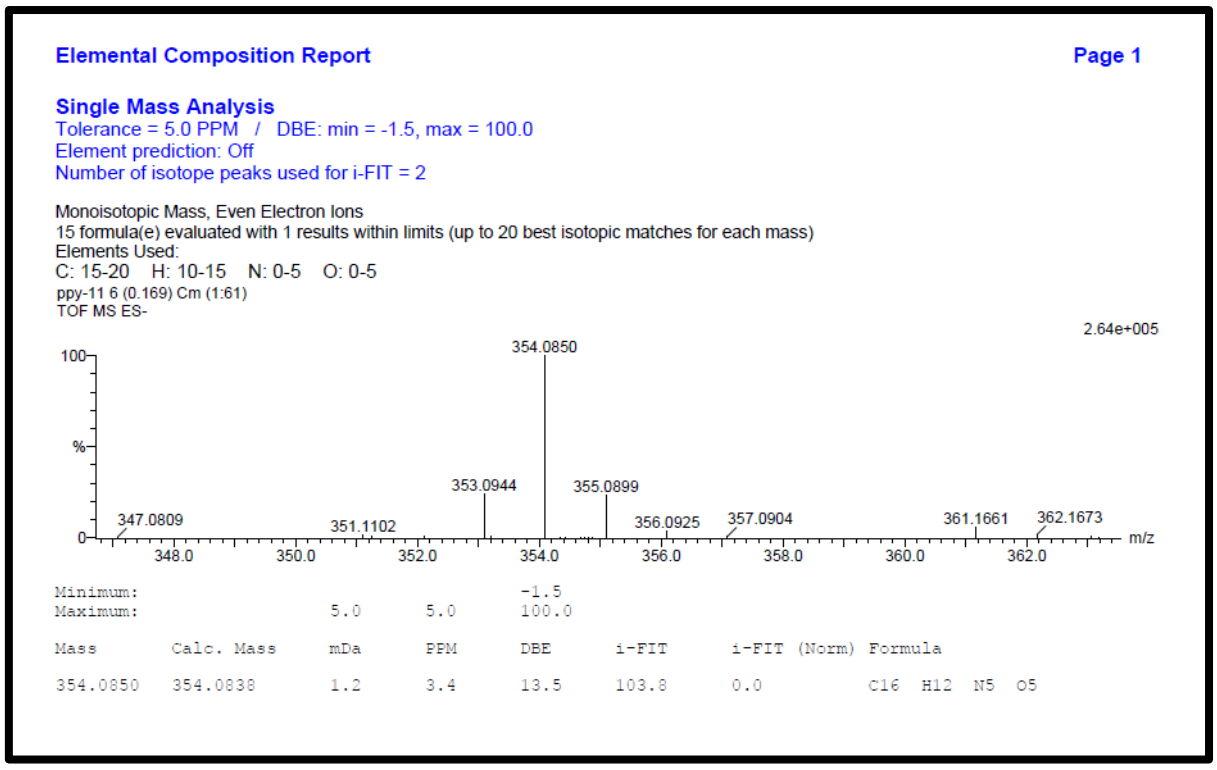

HRMS spectra of compound **5i**

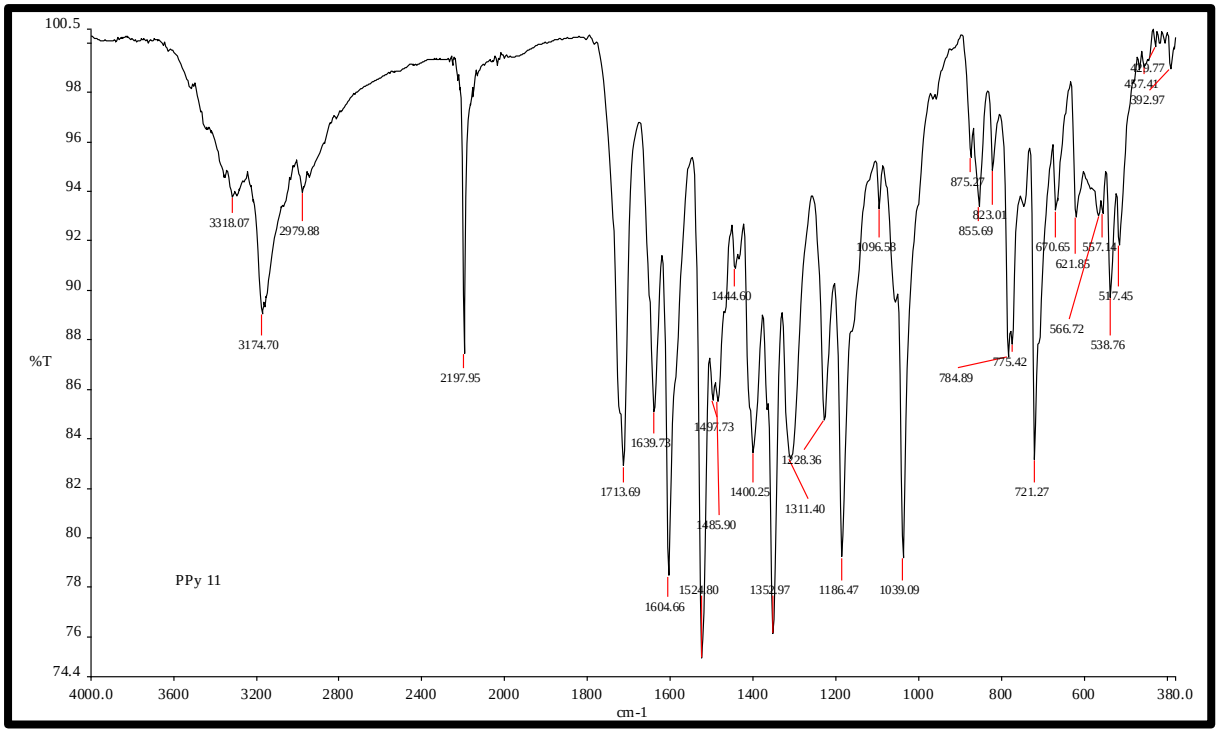

FT-IR spectra of compound **5i**

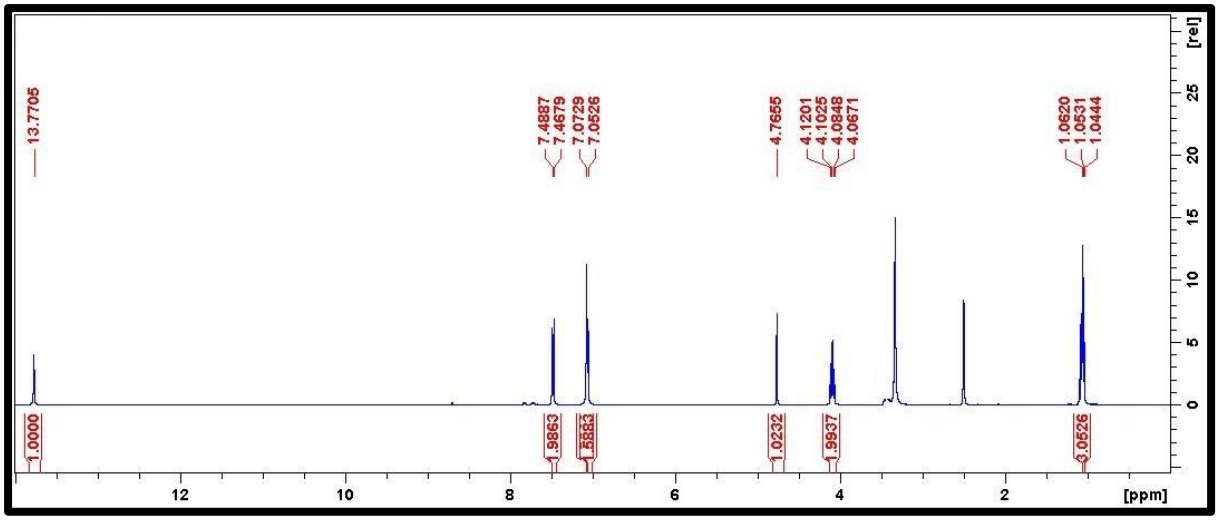

^{1}H NMR spectra of compound **5j**

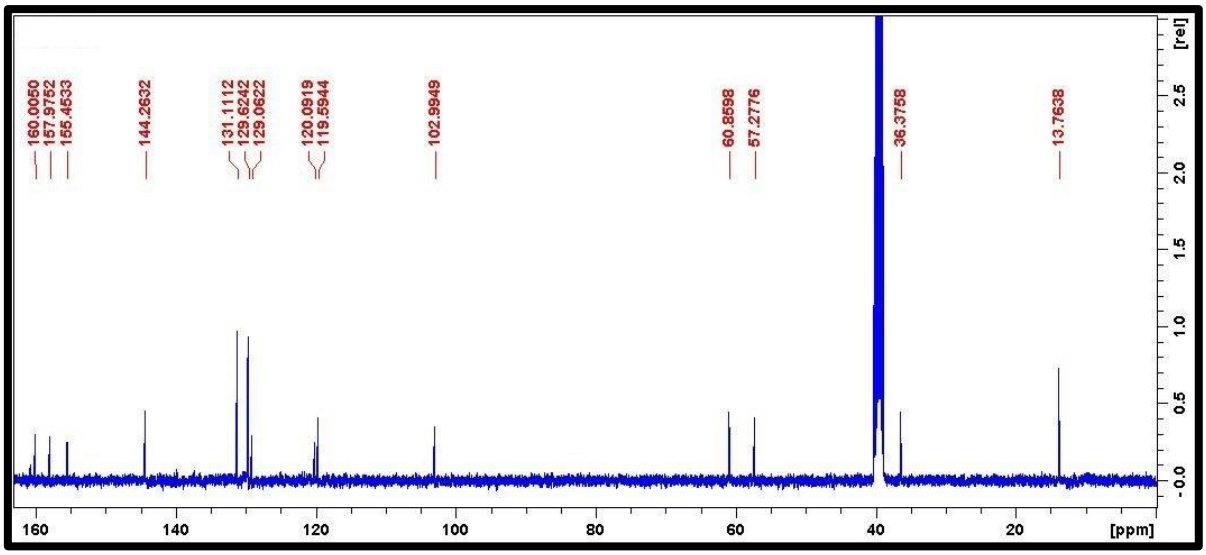

^{13}C NMR spectra of compound **5j**

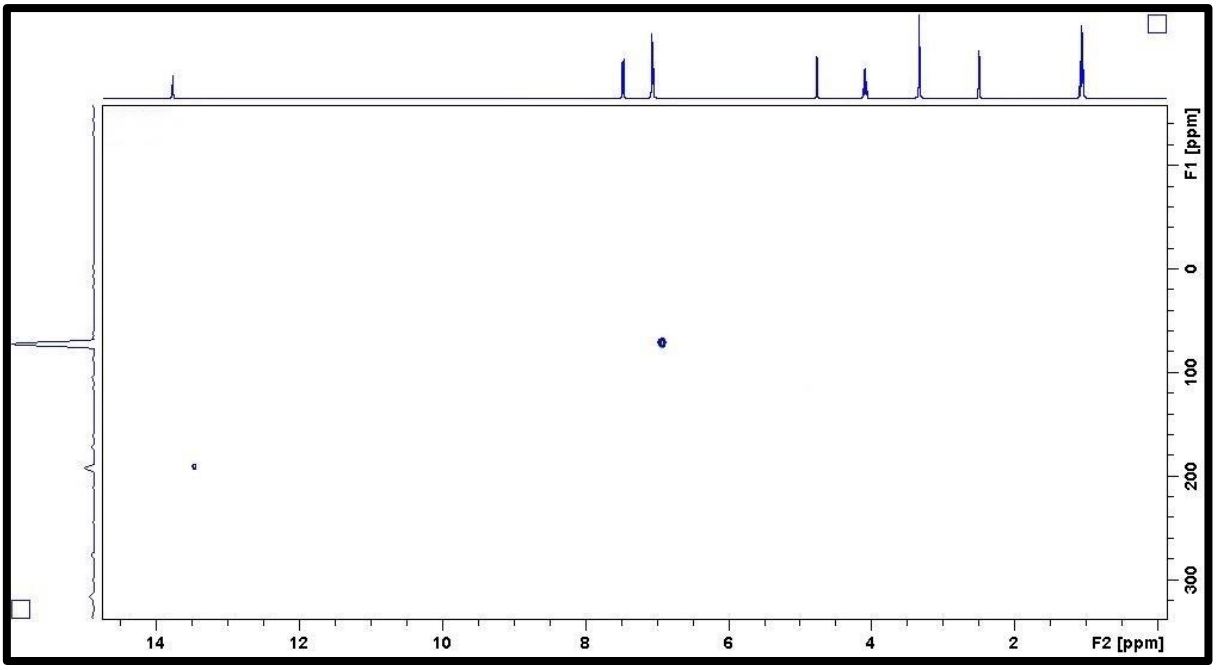

^{15}N NMR spectra of compound **5j**

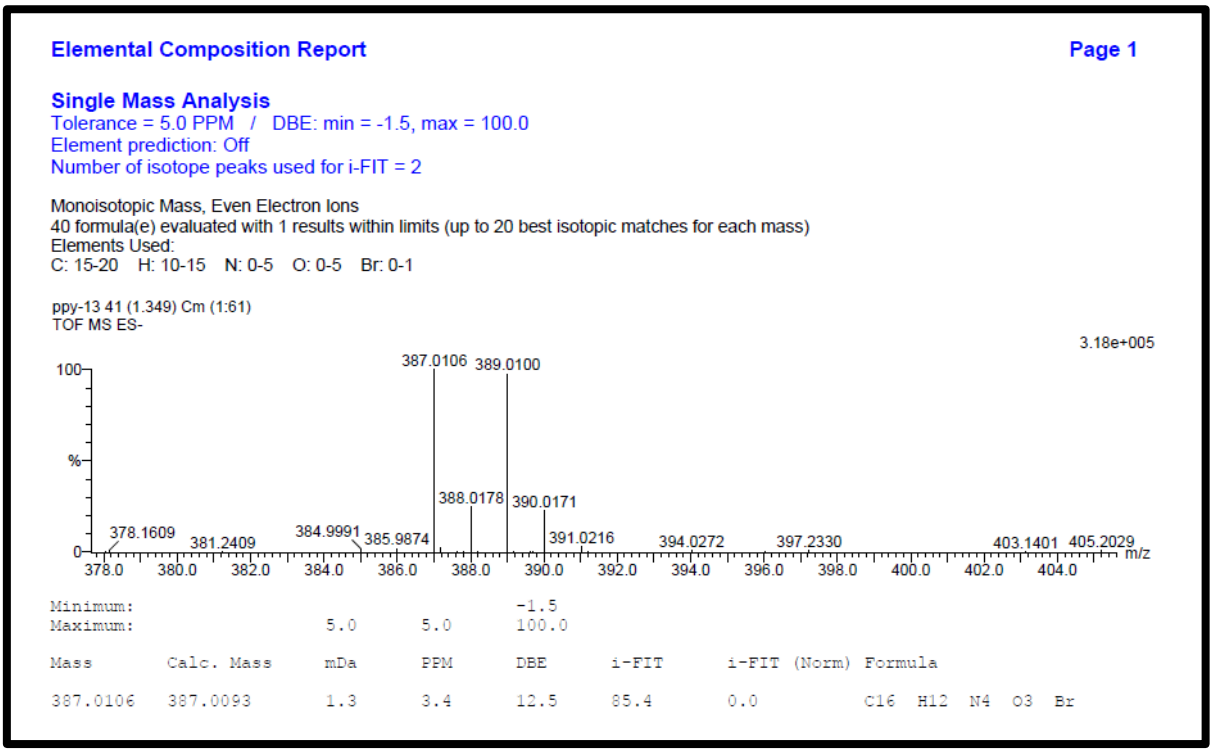

HRMS spectra of compound **5j**

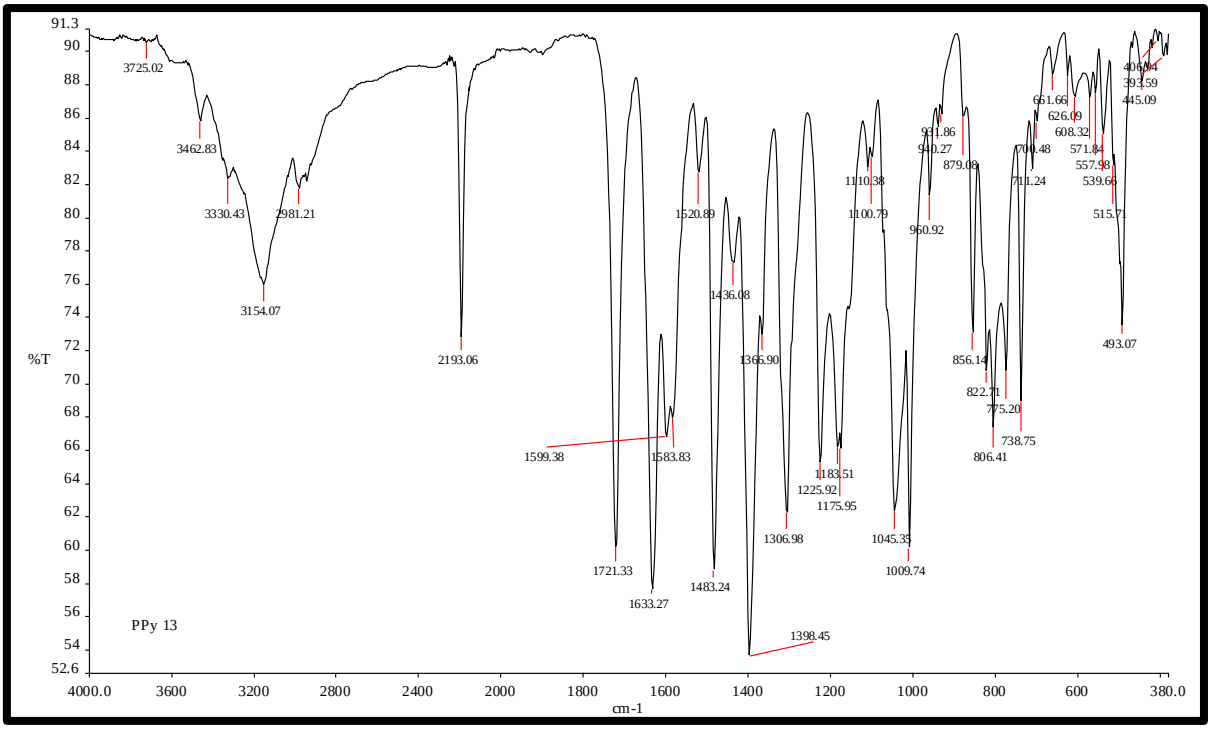

^{1}H NMR spectra of compound **5j**

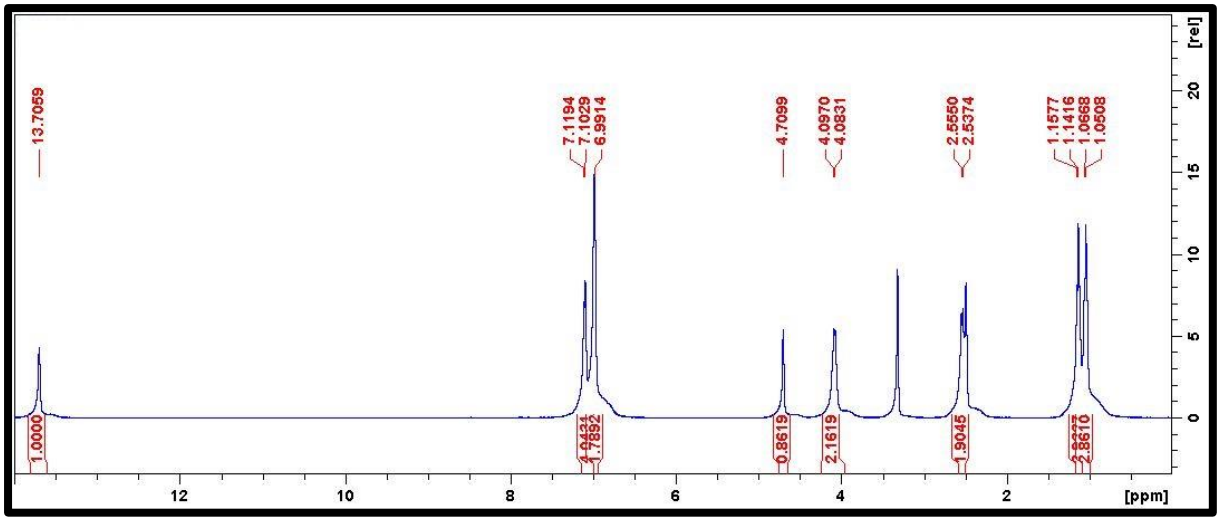

^{1}H NMR spectra of compound **5k**

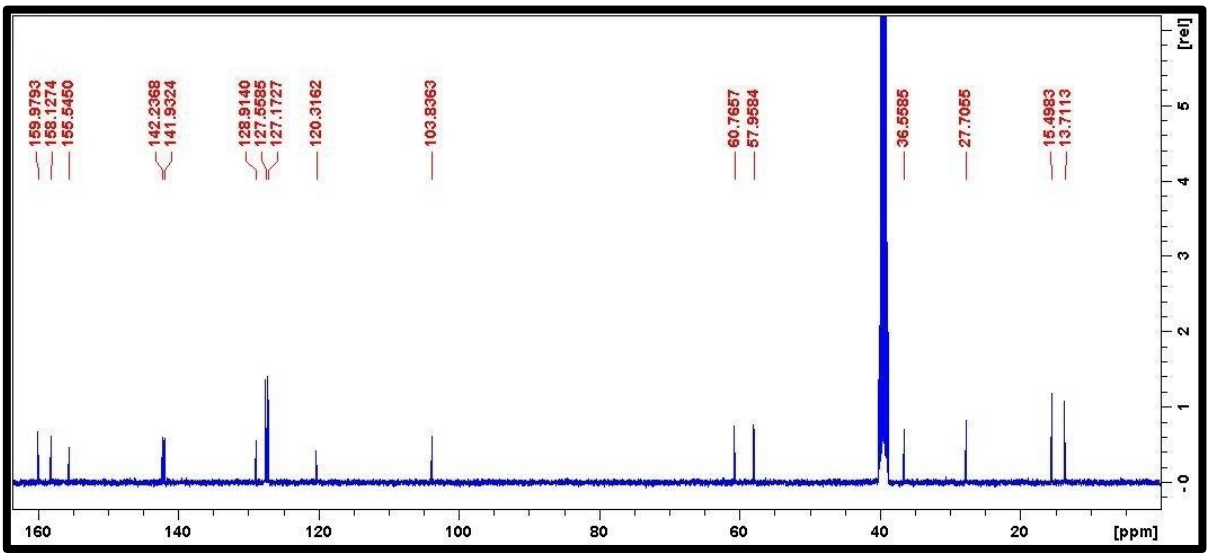

^{13}C NMR spectra of compound **5k**

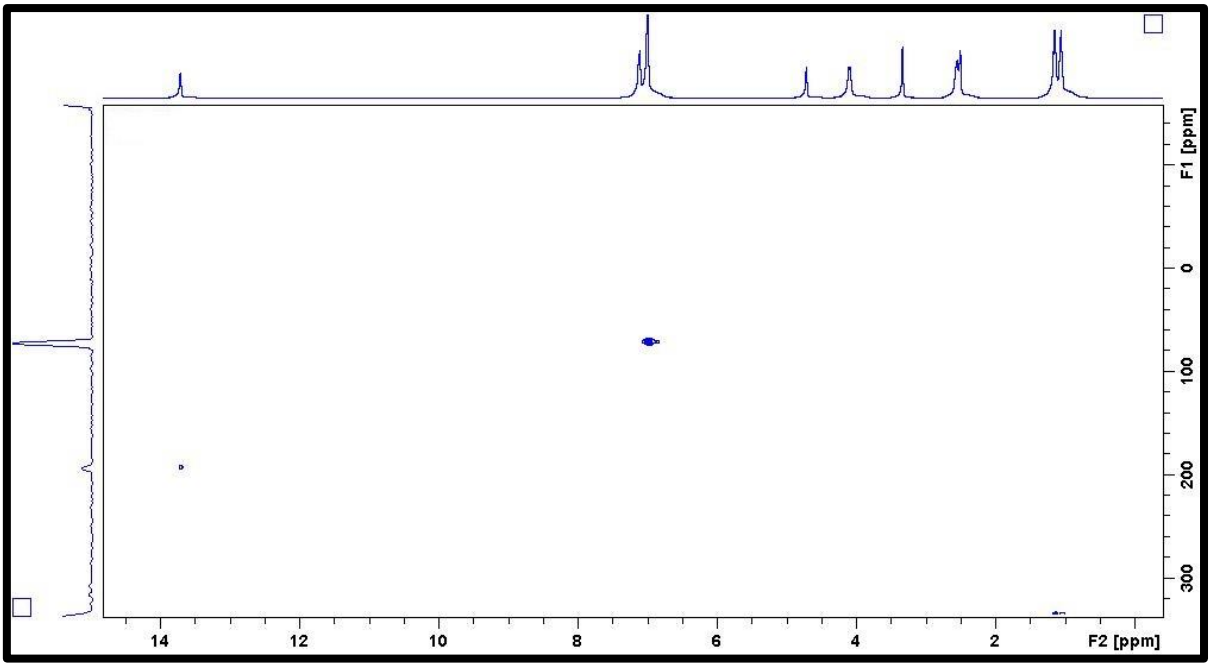

^{15}N NMR spectra of compound **5k**

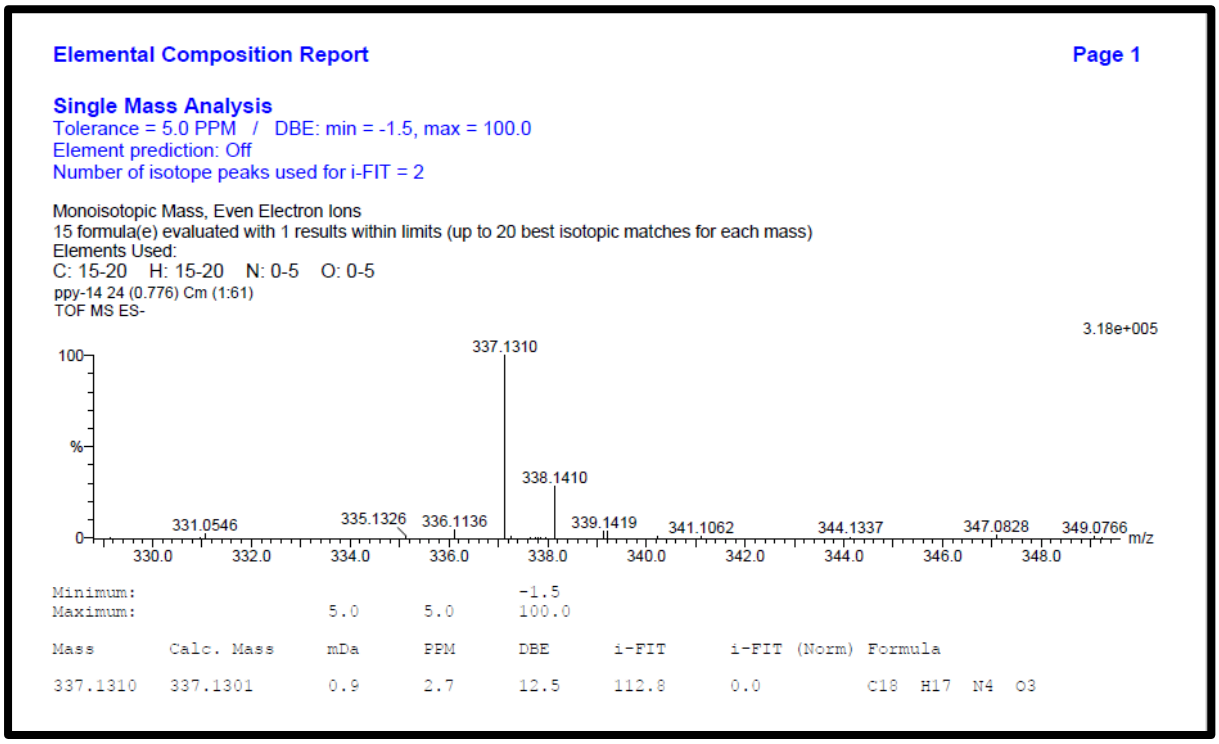

HRMS spectra of compound **5k**

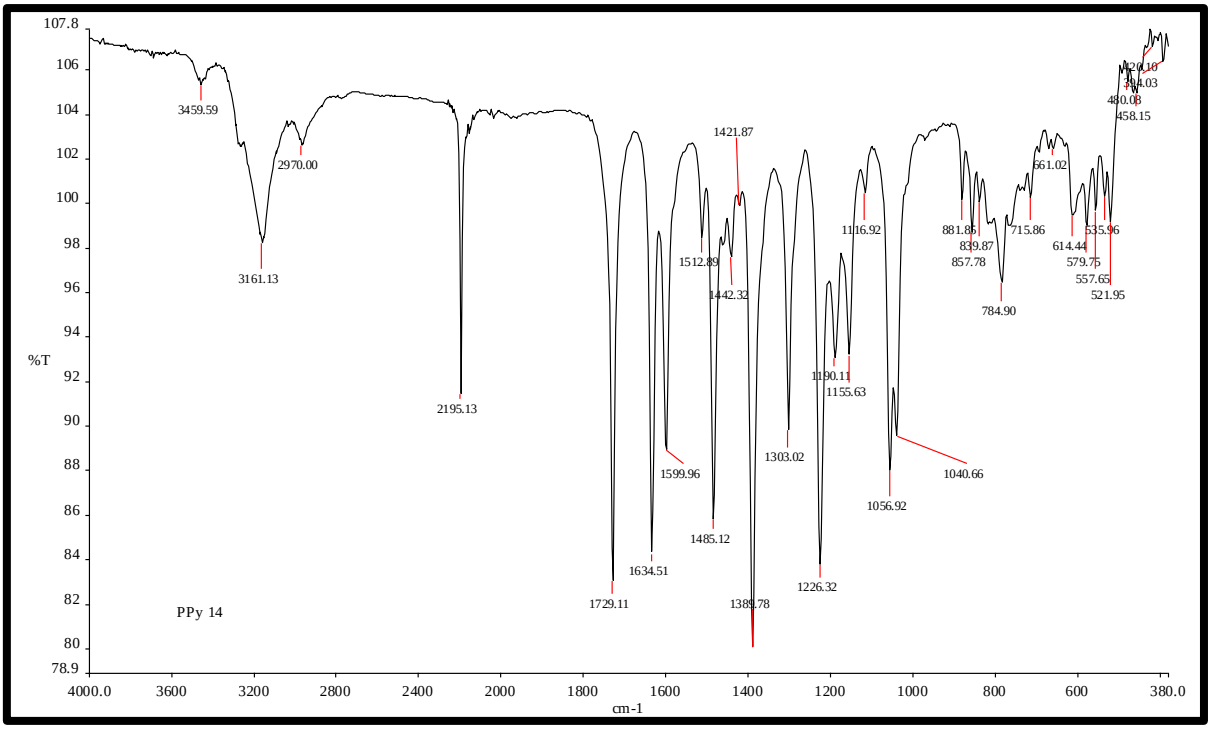

FT-IR spectra of compound **5k**

Chapter 5

Ag_2O on ZrO_2 as Recyclable Catalyst for Multicomponent Synthesis of Indenopyrimidine Derivatives

Sandeep V.H.S. Bhaskaruni, Suresh Maddila, Werner E. van Zyl and Sreekantha B. Jonnalagadda*

*School of Chemistry & Physics, University of KwaZulu-Natal, Westville Campus, Chiltern Hills, Durban-4000, South Africa

*Corresponding Author: Prof. Sreekantha B. Jonnalagadda
School of Chemistry & Physics,
University of KwaZulu-Natal,
Durban 4000, South Africa.
Tel.: +27 31 2607325,
Fax: +27 31 2603091
E-mail address: jonnalagaddas@ukzn.ac.za

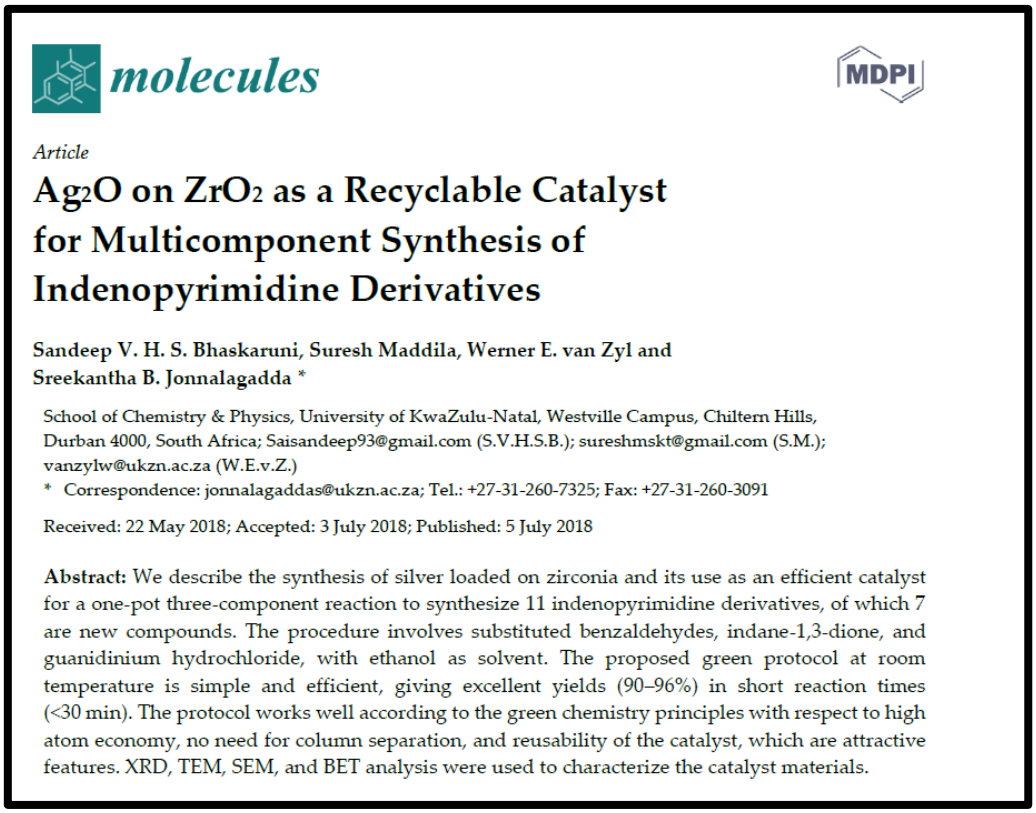

molecules

MDPI

Article

Ag_2O on ZrO_2 as a Recyclable Catalyst for Multicomponent Synthesis of Indenopyrimidine Derivatives

Sandeep V. H. S. Bhaskaruni, Suresh Maddila, Werner E. van Zyl and Sreekantha B. Jonnalagadda *

School of Chemistry & Physics, University of KwaZulu-Natal, Westville Campus, Chiltern Hills, Durban 4000, South Africa; Saisandeep93@gmail.com (S.V.H.S.B.); sureshmskt@gmail.com (S.M.); vanzylw@ukzn.ac.za (W.E.v.Z.)

* Correspondence: jonnalagaddas@ukzn.ac.za; Tel.: +27-31-260-7325; Fax: +27-31-260-3091

Received: 22 May 2018; Accepted: 3 July 2018; Published: 5 July 2018

Abstract: We describe the synthesis of silver loaded on zirconia and its use as an efficient catalyst for a one-pot three-component reaction to synthesize 11 indenopyrimidine derivatives, of which 7 are new compounds. The procedure involves substituted benzaldehydes, indane-1,3-dione, and guanidinium hydrochloride, with ethanol as solvent. The proposed green protocol at room temperature is simple and efficient, giving excellent yields (90–96%) in short reaction times (<30 min). The protocol works well according to the green chemistry principles with respect to high atom economy, no need for column separation, and reusability of the catalyst, which are attractive features. XRD, TEM, SEM, and BET analysis were used to characterize the catalyst materials.

This chapter is published in the journal **Molecules,** and has been structured according to the journal's format.

Ag_2O on ZrO_2 as Recyclable Catalyst for Multicomponent Synthesis of Indenopyrimidine Derivatives

Sandeep V.H.S. Bhaskaruni, Suresh Maddila, Werner E. van Zyl and Sreekantha B. Jonnalagadda*

*School of Chemistry & Physics, University of KwaZulu-Natal, Westville Campus, Chiltern Hills, Durban-4000, South Africa

*Corresponding Author: Prof. Sreekantha B. Jonnalagadda
School of Chemistry & Physics,
University of KwaZulu-Natal,
Durban 4000, South Africa.
Tel.: +27 31 2607325,
Fax: +27 31 2603091
E-mail address: jonnalagaddas@ukzn.ac.za

Abstract:

We describe the synthesis of silver loaded on zirconia and its use as an efficient catalyst for a one-pot three-component reaction to synthesize 11 indenopyrimidine derivatives, of which 7 are new compounds. The procedure involves substituted benzaldehydes, indane-1,3-dione, and guanidinium hydrochloride, with ethanol as solvent. The proposed green protocol at room temperature is simple and efficient, giving excellent yields (90–96%) in short reaction times (<30 min). The protocol works well according to the green chemistry principles with respect to high atom economy, no need for column separation, and reusability of the catalyst, which are attractive features. XRD, TEM, SEM, and BET analysis were used to characterize the catalyst materials.

5.1 Introduction

Multicomponent reactions (MCRs) are cherished protocols in organic synthesis due to their vast potential in the fields of medicinal, pharmaceutical, and agro-chemistry [1]. MCRs are different from the other classical synthesis approaches due to their facile synthesis protocols, high atom efficiency, high yields, and minimal by-product formation [2]. Further, the efficacy of MCRs when compared with multistep synthetic protocols lies in the selective formation of several bonds in a single reaction flask with highly desirable yield over a short interval of time [3].

Currently, heterogeneous catalysts play a key role in organic synthesis because they meet most of the goals of green and sustainable chemistry [4]. Researchers have made remarkable improvements in the design of well-defined catalyst materials. Innovative methods have allowed the coherent design and preparation of very active and selective catalyst materials by governing the structure and composition of the active particles [5]. Furthermore, heterogeneous catalysts offer many benefits in synthetic transformations such as outstanding chemical and thermal stability, noncorrosiveness, nonflammability, eco-friendliness, nontoxicity, ease of separation, reusability, and commercial availability [6].

In recent years, zirconium oxide (ZrO_2) have been effusively revealed as a catalyst or a supported catalyst in various potential chemical applications due to its extensive properties such as acidic and basic sites [7], high stability in the presence of redox conditions, active phase support, and chemical consistency related to other supports like alumina and silica. Further, ZrO_2 is low cost, stable, nonhazardous, reusable, and readily available [8]. Silver salts are widely used as catalysts and their efficacy has been demonstrated in terms of being cost-effective, non-toxic, simple to handle, and appropriate for usage as a one-electron redox system [9]. However, their use in large amounts is unwarranted, but if used in a green-manner as a recyclable catalyst, it has many advantages. Hence, the use of silver-loaded zirconia catalysts is a desirable choice for eco-friendly synthesis.

Among the known heterocyclic compounds, N-heterocyclic scaffolds are very important in medicinal chemistry [10]. In the N-heterocyclic class of scaffolds, pyrimidine and its derivatives play a prominent role [11]. Being the main constituents of several natural products, these pyrimidines represent a significant class of molecules which have been of increased interest in recent years owing to their valuable pharmacological and biological applications in antimicrobial [12], antifungal [13], anti-tumor [14], anti-HIV [15], anti-tubercular [16], anti-inflammatory [17], and antimalarial [18] activities. Moreover, aryl-indenopyrimidines have

been used as adenosine A2A receptor antagonists [19], which are useful, and many reports have dealt with the preparation of different types of pyrimidine derivatives via multicomponent reactions. Owing to their economic viability and scientific importance, methodologies have been described for the synthesis of various types of substituted pyrimidines. Diverse catalytic systems such as NaOH, [20–22] sodium methoxide [23], 1-sulfonic acid-3-methyl imidazolium ferric chloride/NaY [24], α-Fe_2O_3-MCM-41-P [25], and uranyl acetate/succinimide sulfonic acid [26] have been used in the synthesis of pyrimidine derivatives. However, these protocols invariably demand expensive reagents, high energy input, and lengthy reaction times. Other limitations are lower yields and the need for solvents and column separations. There is, thus, a demand for a greener preparation method for indenopyrimidines. We found no literature reports to date using metal complexes or metal oxides as catalysts in their synthesis. Although silver-loaded ZrO_2 have been reported as a catalyst for varied reactions [27,28], no protocols have been described for the synthesis of indenopyrimidines via MCRs.

We recently reported several green synthetic approaches of various medicinally interesting heterocyclic scaffolds [29–37]. Encouraged by those favorable results with different substituted heterocyclic scaffolds, here we describe the synthesis and characterization of silver loaded on zirconia and its efficiency in the one-pot synthesis of functionalized indenopyrimidines via a three-component reaction at room temperature (RT).

5.2 Experimental Section

5.2.1 Catalyst preparation

Supported catalysts with different wt % (weight percentage) of silver-loaded zirconia (1, 2.5, and 5.0 wt %) were synthesized following a wet impregnation process [38,39]. The solid heterogeneous catalyst was prepared by combining zirconia (ZrO_2, 3 g, Alfa Aesar, Ward Hill, MA, USA) and a suitable quantity of silver chloride ($AgCl_2$, Alfa Aesar) dissolved in distillated water (60 mL). The mixture was stirred at room temperature (RT) for 5–7 h. After this time, the ensuing slurry was filtered under vacuum. It was dried in an oven at 120–130 °C for 6 h and calcined in the presence of air at 450 °C for 5 h to afford the (1.0, 2.5, and 5.0 wt %) silver on zirconia.

5.2.2 General procedure for the synthesis of indeno-pyrimidine derivatives (4a-k)

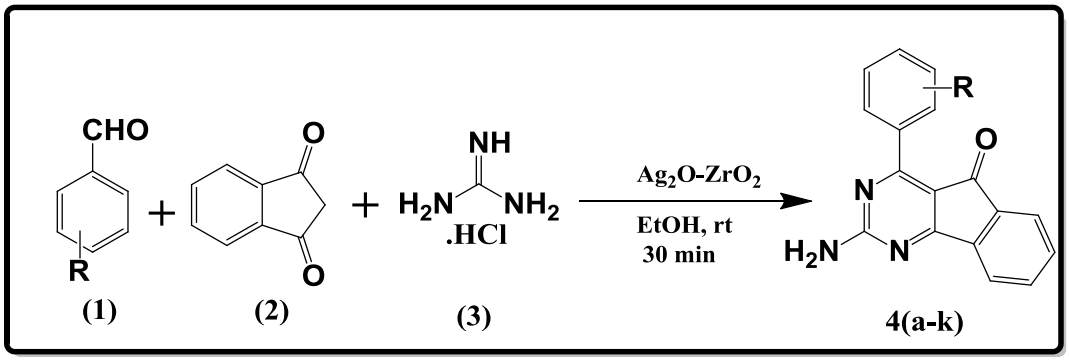

Scheme 1 Synthesis of novel indenopyrimidine derivatives.

In a typical reaction, an equi-molar mixture of aldehydes (1 mmol) (1), indane-1,3-dione (1 mmol) (2), and guanidinium hydrochloride (1 mmol) (3) were dissolved in ethanol (5 ml) at R.T., followed by addition of Ag_2O-ZrO_2 (60 mg) as a catalyst. The reaction mixture was held at R.T. for 30 min under stirring (Scheme 1), while the reaction progress was monitored by TLC at regular time intervals. When the reaction was complete, the mixture was filtered and ethyl acetate was used to extract the filtrate, evaporated under reduced pressure to obtain the crude product and washed with ethanol. The reaction product was recrystallized in ethanol to obtain the pure target compound, which was further characterized by ^{1}H-NMR, ^{13}C-NMR, HRMS and FT-IR analysis. The related details and spectra are given in the supplementary information file.

2-Amino-4-(2-methoxyphenyl)-5H-indeno[1,2-d]- pyrimidine-5-one (4a)

^{1}H NMR (DMSO-d6, 400 MHz) δ = 3.83 (s, 3H, -OCH_3), 7.09 (d, J= 7.6Hz, 1H, Ar-H), 7.16 (d, J = 8.16Hz,1H, Ar-H), 7.61 (t, J = 1.2, 1H, Ar-H), 7.92-7.95 (m, 4H, Ar-H), 8.22 (s, 2H, -NH_2), 8.77-8.79 (m, 1H, Ar-H).^{13}C NMR δ = 56.03, 111.56, 120.10, 121.00, 122.94, 122.98, 128.16, 133.09, 135.69, 135.78, 135.86, 138.96, 139.32, 141.79, 160.05, 188.50, 189.61; FT-IR: 3269.10 (-NH), 2957.02 (-CH), 1710 (-C=O), 1593.28 (-C=C), 1483.73(-C=N), 733.81 (-CH).

2-Amino-4-(4-methoxyphenyl)-5H-indeno[1,2-d]- pyrimidine-5-one (4b)

^{1}H NMR (DMSO-d6, 400 MHz) δ = 3.89 (s, 3H, -OCH_3), 7.13 (d, J= 8.92 Hz,2H, Ar-H,), 7.80 (s, 2H, -NH_2), 7.71 (s, 2H, NH_2), 7.93-7.95 (m, 4H, Ar-H), 8.60 (d, J= 8.92 Hz, 2H, Ar-H.^{13}C NMR δ = 55.72,114.49, 122.86, 125.86, 126.28, 135.54, 135.69, 136.98, 139.27, 141.69, 145.72, 163.77, 188.96, 189.80; FT-IR: 3010.13 (-NH), 2941.01 (-CH), 1712.14 (-C=O), 1673.42 (-C=C), 1468.81 (-C=N), 771.95 (-CH);HRMS of $[C_{18}H_{13}N_3O_2 + H]^+$ (m/z) :304.0766; Calcd.: 304.0763.

2-Amino-4-(2,3-dimethoxyphenyl)-5H-indeno[1,2-d]- pyrimidine-5-one (4c)

^{1}H NMR (DMSO-d6, 400 MHz) δ = 3.91 (s, 6H, -OCH_3), 7.21 (t, J = 8.08 Hz, 1H, Ar-H,), 7.32-7.34 (m, 1H, Ar-H), 7.94-8.14 (m, 4H, Ar-H), 8.36 (s, 2H, -NH_2), 8.38 (t, J = 1.04 Hz, 1H, Ar-H).^{13}C NMR δ = 55.95, 61.49,118.22,123.05, 123.10, 123.61, 124.23, 126.21, 129.53, 136.02, 139.00, 139.42, 141.89, 150.23, 152.19; FT-IR: 3087.99 (-NH), 2939.24 (-CH), 1711.98 (-C=O), 1673.55 (-C=C), 1469.79 (-C=N), 771.94 (-CH); HRMS of $[C_{19}H_{15}N_3O_3 + H]^+$ (m/z) :334.0992; Calcd.: 334.1008.

2-Amino-4-(2,5-dimethoxyphenyl)-5H-indeno[1,2-d]- pyrimidine-5-one (4d)

^{1}H NMR (DMSO-d6, 400 MHz) δ = 3.82 (s, 3H, -OCH3), 3.89 (s, 3H, -OCH3),7.11 (d, J = 9.12 Hz, 1H, Ar-H,), 7.21 (d, J= 3.12 Hz, 1H, Ar-H), 7.93-7.97 (m, 4H, Ar-H), 8.23 (s, 2H, -NH_2), 8.64 (d, J = 3.2 Hz, 1H, ArH).^{13}C NMR δ = 55.51, 56.38, 112.72, 116.49, 121.32, 123.07, 128.11, 135.75, 135.89, 138.84, 139.29, 141.87, 152.29, 154.92, 188.82, 189.64, 206.58; FT-IR: 3087.87 (-NH), 2950.12(-CH), 1746.67(-C=O), 1683.90 (-C=C), 1588.60 (-C=N) ,780.18 (-CH); HRMS of $[C_{19}H_{15}N_3O_3 + H]^+$ (m/z) :334.0434; Calcd.: 334.0441.

2-Amino-4-(2-bromophenyl)-5H-indeno[1,2-d]- pyrimidine-5-one (4e)

^{1}H NMR (DMSO-d6, 400 MHz) δ = 7.52-7.59 (m, 2H, NH_2), 7.89-7.98 (m,7H, Ar-H),8.00 (s, 1H, Ar-H).^{13}C NMR δ = 122.83, 122.91, 124.36, 130.67, 132.12, 132.32, 135.70, 135.92, 140.42, 141.20, 141.35, 141.67, 142.03, 142.98, 197.19, 198.68; FT-IR: 3089.08(-NH), 2941.43 (-CH), 1745.65(-C=O), 1673.02(-C=C), 1564.46 (-C=N), 771.47 (-CH), 619.03 (-C-Br); HRMS of $[C_{17}H_{10}BrN_3O + H]^+$ (m/z) :353.1042; Calcd.: 353.1042.

2-Amino-4-(2-fluorophenyl)-5H-indeno[1,2-d]- pyrimidine-5-one (4f)

^{1}H NMR (DMSO-d6, 400 MHz) δ =7.39 (s, 1H, NH_2), 7.68 (t J= 1.08 Hz, 2H, Ar-H), 7.92-7.99 (m, 6H, Ar-H).^{13}C NMR δ =115.65, 115.86, 123.24 , 124.49, 124.52, 133.07, 136.07, 136.21, 139.60, 141.99, 160.66, 188.07, 188.85, 197.56, 198.69;FT-IR: 3275.94 (-NH), 2956.87 (-CH), 1740.56 (-C=O), 1620.19 (-C=C),1485.01(-C=N), 1008.10 (-C-F), 757.33(-CH); HRMS of $[C_{17}H_{10}BrN_3O + H]^+$ (m/z) :292.0732; Calcd.: 292.0732.

2-Amino-4-(3,4-dimethoxyphenyl)-5H-indeno[1,2-d]- pyrimidine-5-one (4g)

^{1}H NMR (DMSO-d6, 400 MHz) δ = 3.90 (d, J= 3.84 Hz, 6H, -OCH_3), 7.16 (d, J = 8.52 Hz, 1H, Ar-H,), 7.80 (s, 1H, NH_2), 7.92-7.97 (m, 4H, Ar-H), 8.02-8.04 (m, 1H, Ar-H), 8.68 (d, J = 1.92 Hz, 1H, ArH).^{13}C NMR δ =55.18, 111.53, 115.74, 122.78, 122.91, 126.09, 131.08, 135.56, 135.69, 139.22, 146.43, 148.31, 153.91, 189.85 ; FT-IR: 3088.10 (-NH), 2942.06 (-CH), 1712.66(-C=O), 1673.31(-C=C),1468.88 (-C=N), 772.61 (-CH), 801.96 (-CH).

2-Amino-4-(3-hydroxyphenyl)-5H-indeno[1,2-d]- pyrimidine-5-one (4h)

^{1}H NMR (DMSO-d6, 400 MHz) δ = 7.01-7.04 (m,1H, Ar-H,), 7.35 (t, J= 7.88 Hz, 1H, Ar-H), 7.71 (s, 2H, NH_2), 7.82 (d, J= 7.72 Hz, 1H, Ar-H), 7.92-7.96 (m, 5H, Ar-H), 9.86 (s, 1H,-OH).^{13}C NMR δ =119.61, 120.67, 123.00, 123.04, 125.46, 128.94, 129.69, 133.84, 135.77, 135.93, 139.33, 141.89, 145.82, 157.33, 188.45, 189.43.; FT-IR: 3241.25 (-OH), 3088.13 (-NH), 1745.77(-C=O), 1665.42 (-C=C), 1484.83(-C=N), 780.62 (-CH); HRMS of $[C_{17}H_{11}N_3O_2 + H]^+$ (m/z) :290.0732; Calcd.: 290.0732.

2-Amino-4-(4-bromophenyl)-5H-indeno[1,2-d]- pyrimidine-5-one (4i)

^{1}H NMR (DMSO-d6, 400 MHz) δ = 7.77 (d, J= 8.52 Hz, 2H, Ar-H), 7.81 (s, J= 8.56 Hz, 2H, -NH_2), 7.95-7.99 (m, 4H, Ar-H), 8.41 (d, J= 8.52 Hz, 2H, Ar-H).^{13}C NMR δ = 103.27, 109.58, 110.67, 112.60, 116.48, 136.51, 143.42, 151.63, 151.95, 152.67, 167.34, 194.19; FT-IR: 3087.96 (-NH), 1724.92 (-C=O), 1685.17 (-C=C), 1485.31 (-C=N), 828.42 (-CH), 606.46 (-C-Br).

2-Amino-4-(4-chlorophenyl)-5H-indeno[1,2-d]- pyrimidine-5-one (4j)

^{1}H NMR (DMSO-d6, 400 MHz) δ = 7.36 (d, J= 8.52 Hz, 2H, -NH_2), 7.64 (d, J= 8.56 Hz, 1H, Ar-H), 7.85-7.97 (m, 6H, Ar-H), 7.82 (d, J= 7.72 Hz, 1H, Ar-H), 8.51 (d, J= 8.6 Hz,1H, Ar-H).^{13}C NMR δ =122.57, 122.79, 123.13, 127.74, 127.82, 128.85, 130.79, 135.36, 135.59, 137.85, 141.51, 143.73, 197.94, 198.14, 199.07. 4; FT-IR: 3089.02 (-NH), 1712.07(-C=O), 1673.33 (-C=C), 1469.06 (-C=N), 802.02 (-CH), 702.10 (-C-Cl); HRMS of $[C_{17}H_{10}ClN_3O + H]^+$ (m/z) :308.1139; Calcd.: 308.114.

2-Amino-4-(4-ethylphenyl)-5H-indeno[1,2-d]- pyrimidine-5-one (4k)

^{1}H NMR (DMSO-d6, 400 MHz) δ = 1.22 (t, J= 7.56 Hz, 3H, -CH_3), 2.68-2.79 (m, 2H, -CH_2), 7.42 (d, J= 8.2 Hz, 2H, Ar-H), 7.83 (s, 2H, -NH_2), 7.93-7.96 (m, 4H, Ar-H), 8.46 (d, J= 8.24 Hz, 2H, Ar-H).^{13}C NMR δ = 15.03, 28.42, 30.63, 122.56,122.98, 123.04, 128.30, 130.48, 134.22, 135.57, 135.75, 135.90, 139.39, 141.86, 142.99, 145.64, 150.32, 188.69, 189.56, 206.47 ; FT-IR: 3088.40 (-NH), 2941.60 (-CH) , 1712.33(-C=O), 1673.31(-C=C), 1469.87 (-C=N), 802.02 (-CH).

5.3 Results and Discussion

5.3.1 Crystallinity by powder XRD (PXRD) studies

Figure 1. Illustrate the crystalline phases of calcined silver oxide-zirconia catalyst material. The PXRD patterns of catalytic sample displays the major 2θ peak values at 24.2°,

28.2°, 31.3°, 35.4°, 40.5°, 45.0°, 50.3°, 55.4° and 60.1° correspond to zirconia and the peak values were correlated with international standard file (JCPDS file no. 37-1484). In addition, the catalyst material revealed diffraction patterns at 2θ angles of 38.1°, 44.3°, 64.4°, and 77.4° corresponding to the Ag_2O (JCPDS file no 72-2108). The peaks recognized in the diffractogram indicate the polycrystalline nature of the catalyst materials. Further, the average crystallite size of the catalyst was measured by the Debye-Scherrer formula using the strongest maximum intensity diffraction peak, about 9.2 nm for 2.5 % Ag_2O/ZrO_2.

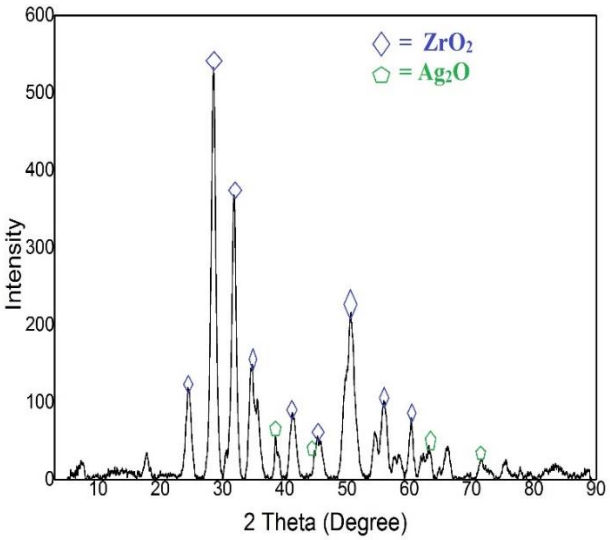

Figure 1. Powder X-ray diffractogram of 2.5 % Ag_2O-ZrO_2 catalyst.

5.3.2 TEM analysis

The transition electron microscopy image (Figure 2) provides the morphology of prepared Ag_2O/ZrO_2 of different wt % . In this image, the silver oxide particle dimensions are mostly in the range between 10-16 nm, with black sphere-shape and seemingly well distributed. Further, zirconia revealed as white globular shape particles. It is clearly observed that 1% has less dispersion of Ag, whereas for 5 % has more Ag agglomerated on the surface of Zr, which fails to provide the active sites to facilitate the reaction. Changes in the morphology of the recovered catalyst after reaction were marginal.

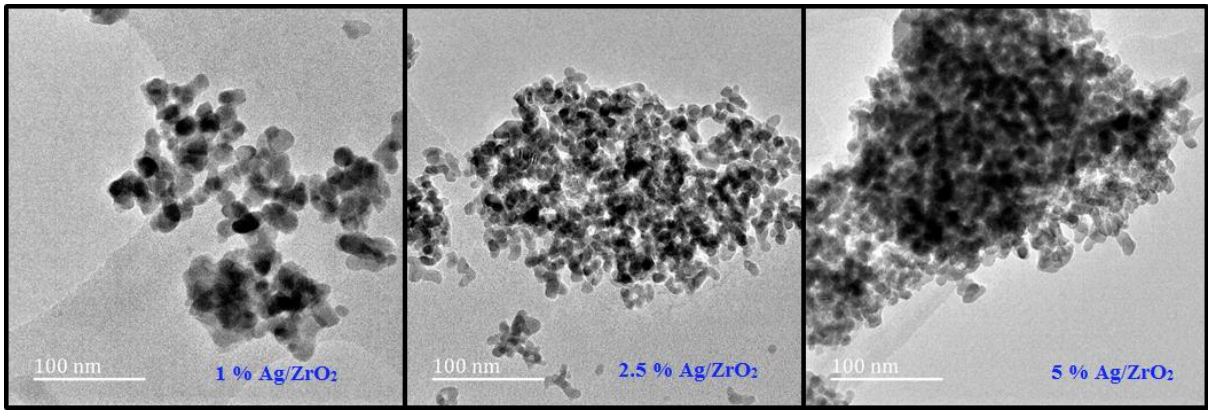

Figure 2. TEM micrograph of 1, 2.5 & 5 % Ag_2O-ZrO_2 catalyst.

5.3.3 SEM analysis

The morphology and size dispersion of the catalyst material were determined with SEM analysis. In Figure 3, a large number of, white and irregular shapes are observed for 2.5 % Ag_2O loaded on ZrO_2. Small silver oxide particles were revealed as white irregular aggregates on the zirconia surface. The micrographs of SEM–EDX validate the even distribution of silver oxide on zirconia surface. Results also confirms with the data from ICP elemental analysis (2.18 wt% Ag). The mapping also shows the presence of Ag on ZrO_2. Furthermore, the morphology of the catalyst from the SEM images also show the crystallinity and homogeneity of the sample.

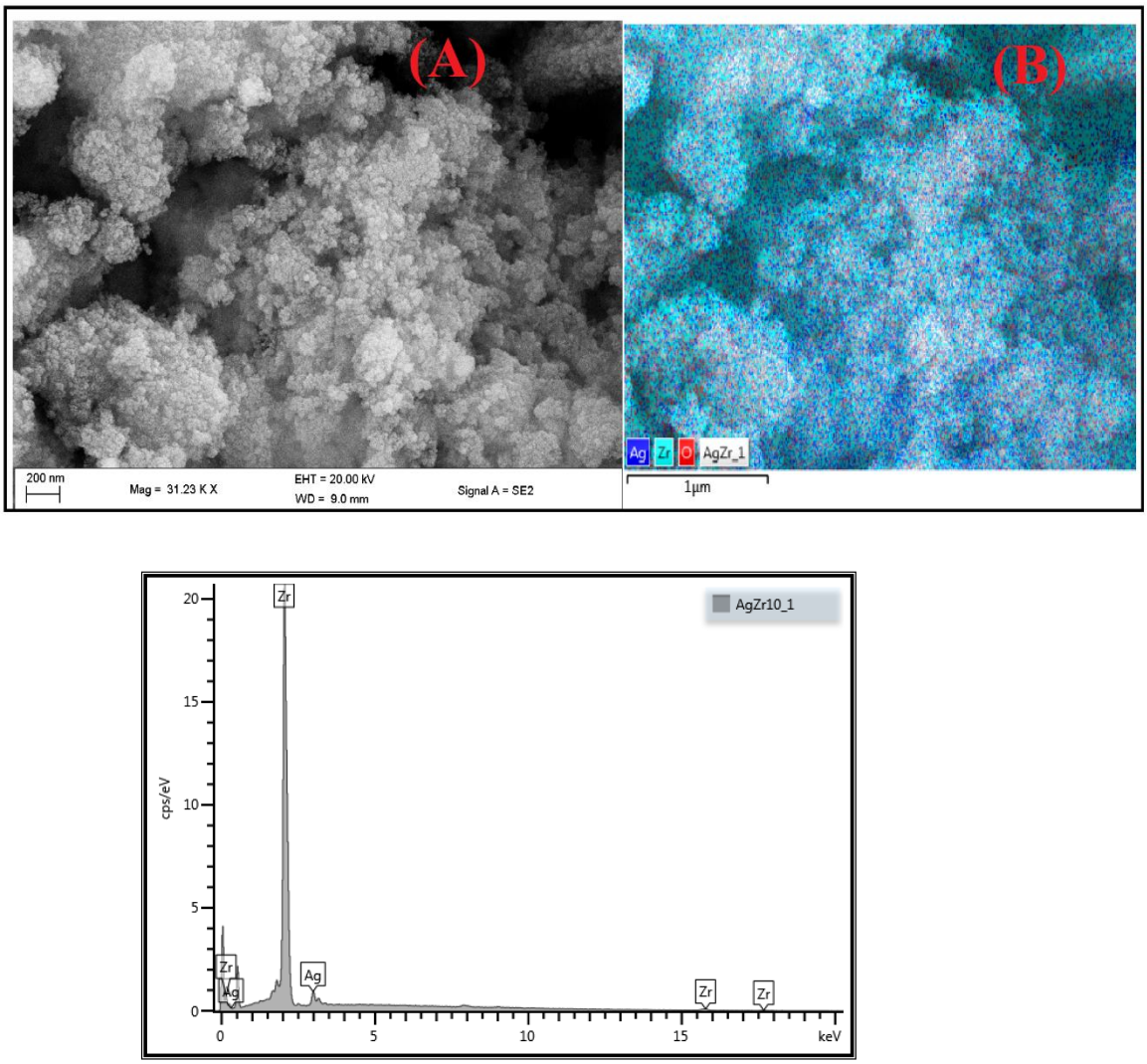

Figure 3. (A) SEM micrograph; (B) SEM Mapping (c) EDS spectra of of 2.5 % Ag_2O-ZrO_2 catalyst.

5.3.4 BET surface area analysis

The nitrogen adsorption/desorption isotherm and resulting pore size dispersion of the 2.5 % Ag_2O/ZrO_2 catalyst material is shown in Figure 4. The catalyst material exhibits type-IV isotherm with the presence of a typical H2-hysteresis loop, which designates the mesoporous nature of the material as per the IUPAC classification. The BJH pore size distribution describes a mesoporous texture for the material, and the isotherms P/Po range was 0.61-0.98. The BET surface area was measured at 89.52 m^2/g with a pore volume of 0.330 cm^3/g and pore size of 10.3 nm. The ICP study indicates the presence of >1.98 wt % of silver in the catalyst material.

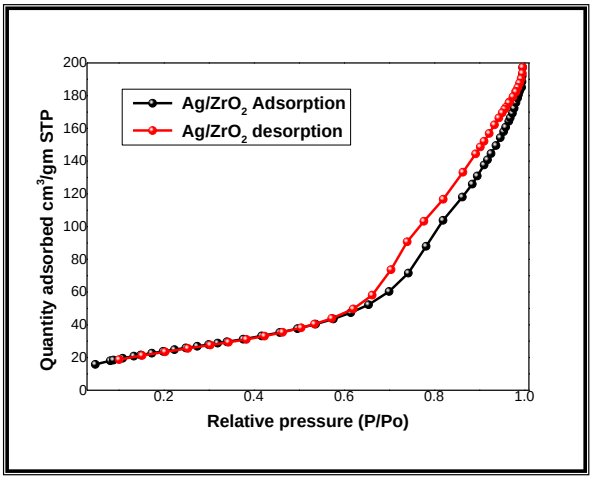

Figure 4. N_2 adsorption-desorption isotherms of 2.5 % Ag_2O-ZrO_2 catalyst.

5.3.5 Pyridine IR analysis

The nature of acidic sites on the 2.5% Ag_2O-loaded ZrO_2 surface was examined by employing ex situ pyridine FT-IR spectroscopy (Figure 5) [40]. The IR band at 1540 cm^{-1} confirmed the presence of Brønsted acidic sites (B). The peak observed at 1485 cm^{-1} is attributed to both Brønsted and Lewis acidic sites (B + L). The prominent absorption band at 1450 cm^{-1} is due to the pyridine adsorbed on Lewis acidic sites (L) of the catalyst. The presence of more Lewis acidic sites on the catalyst surface than Brønsted acidic sites is shown in Figure 5. Generally, more Lewis acidic sites are anticipated in the Ag_2O–ZrO_2 catalyst due to the availability of vacant metal orbitals on the surface of the catalyst, which are capable of accepting electron pairs from the electron-rich species [41]. Except for the assigned peaks, the other IR bands are mostly less intensive, mainly due to the signal-to-noise ratio, which was unavoidable.

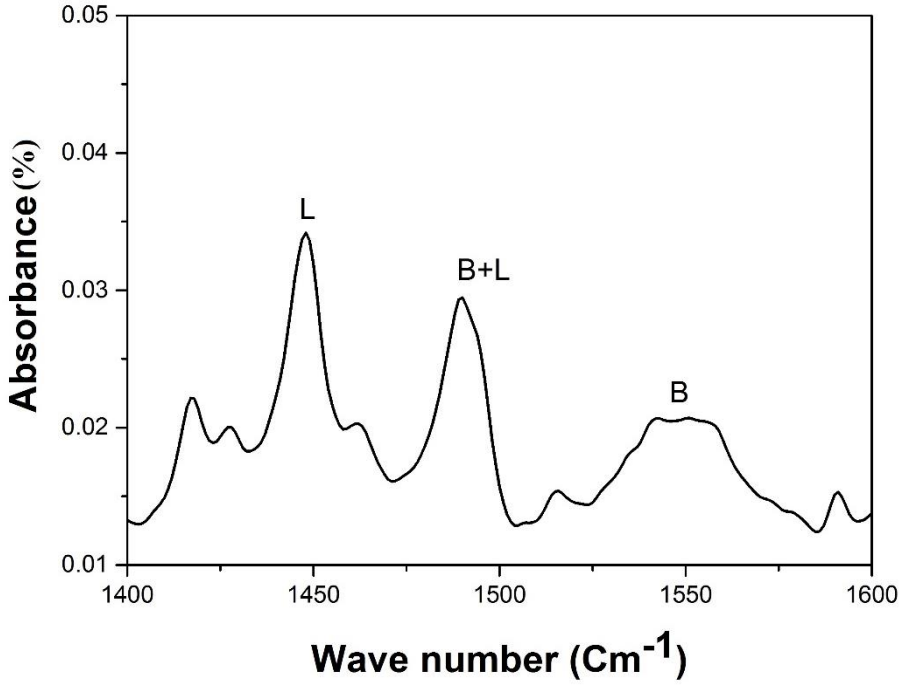

Figure 5. Pyridine FT-IR spectra of 2.5 % Ag_2O/ZrO_2 catalyst.

5.3.6 Reaction optimization

For optimization of the reaction conditions for a one-pot, three-component reaction involving 2-methoxy benzaldehyde (1 mmol), indane-1,3-dione (1 mmol), and guanidinium hydrochloride (1 mmol), various reaction conditions such as effect of temperature, solvents and catalysts were investigated. In the absence of solvent and catalyst, no product occurred at R.T. or reflux conditions, even after 10 h of reaction (Table 1, entry 1 & 2). The reaction was carried out in ethanol, in presence of various basic catalysts, like TEA, pyridine, NaOH and K_2CO_3 at R.T., only trace amounts of material was obtained (Table 1, entries 3–6). Reactions with ionic liquids such as $(Bmim)BF_4$ or L-proline (Table 1, entries 7 & 8) as a catalysts gave low yields.. When the reaction was conducted using acidic catalysts, such as AcOH, $FeCl_3$ and PTSA, moderate yields of product were attained after 4 h (Table 1, entries 9–11). Consequently, reaction was attempted in presence of pure metal oxide catalysts, such as SiO_2, ZrO_2 and Al_2O_3, and the reaction showed good yields after 2.0-3.0 h reaction time (Table 1, entries 12-14). Based on the promising outcome with zirconia oxide, to enhance the reaction performance, efficiency of different metal oxides loaded on zircania, such as 2.5% CuO/ZrO_2, MnO_2/ZrO_2, and Ag_2O/ZrO_2 were examined. These mixed oxide heterogeneous catalysts gave very good to excellent yields (82-96%) (Table 1, entry 15-17), while the best result was obtained with Ag_2O/ZrO_2 (96% yield, 30 min)**.** Bimetallic metal oxides showed higher activity than their parent metal oxides presumably due to better distribution of the active metal on the support and

the synergistic activity between the loaded and support materials, providing optimum distribution and increased number of active sites compared to their oxide homologues.

Table 1. Effect of catalysts on the synthesis of **4a**[a.]

Entry	Catalyst	Solvent	Condition	Time (h)	Yield (%)[b]
1	--	--	RT	10	--
2	--	--	Reflux	10	--
3	TEA	EtOH	RT	8.0	09
4	Pyridine	EtOH	RT	8.5	13
5	NaOH	EtOH	RT	7.5	25
6	K_2CO_3	EtOH	RT	7.0	19
7	$(Bmim)BF_4$	EtOH	RT	10	23
8	L-proline	EtOH	RT	10	27
9	AcOH	EtOH	RT	5.0	43
10	$FeCl_3$	EtOH	RT	4.5	50
11	PTSA	EtOH	RT	5.0	45
12	SiO_2	EtOH	RT	2.5	62
13	ZrO_2	EtOH	RT	2.0	79
14	Al_2O_3	EtOH	RT	3.0	59
15	$2.5\%CuO/ZrO_2$	EtOH	RT	1.5	82
16	$2.5\%MnO_2/ZrO_2$	EtOH	RT	1.0	87
17	$2.5\%Ag_2O/ZrO_2$	EtOH	RT	0.20	96

[a] All products were characterised by ^{1}H-NMR, ^{13}C-NMR, HRMS and FT-IR spectral analysis. [b] Isolated yields after recrystallization. -- No reaction.

The effect of solvents on the title reaction was investigated in presence of varied nonpolar solvents. No reaction occurred in n-hexane or toluene. When the reaction was performed in polar aprotic solvents such as THF, DMF, MeCN, the yield of product was low. In polar protic solvent, MeOH, yield was good, but lower than with EtOH. Hence, EtOH was chosen as solvent for the remainder of the studies. The optimized results are shown in Table 2. (entries 1-8).

Table 2 Optimization of various solvent condition for the model reaction.

Entry	**Solvent**	**Time (minutes)**	**Yield* (%)**
1	No solvent	120	--
2	n-hexane	120	--
3	toluene	90	--
4	THF	75	10
5	DMF	65	18
6	MeCN	60	25
7	MeOH	45	81
8	EtOH	30	96

[a]Reaction conditions: arylaldehyde **(1)** (1 mmol),1,3-Indandione (1 mmol) **(2)**, and gunadium hydrochloride **(3)** (1mmol) and solvent (5 mL) were stirred at room temperature.

-- No isolated yields.

Assuming silver oxide loaded on zirconia as the ideal model catalyst, the contribution of % silver loading on zirconia was 1.0, 2.5 and 5.0% Ag_2O/ZrO_2. While 1% Ag loading gave 90% yield in 45 min, relative to the 2.5 % Ag, the 5% Ag neither improved the yield nor decreased the reaction time. The best activity was observed with 2.5% Ag_2O/ZrO_2, hence this was taken as the optimum loading. This could be due to optimum dispersion of Ag_2O on ZrO_2, when compared to 5% $Ag_2O//ZrO_2$, where dispersion was less uniform due to possible aggregation of silver particles. Hence, catalytic activity was lower compared to the 2.5% loading. 2.5% loading recorded greater activity than 1% $Ag_2O//ZrO_2$. Possibly the former had more active sites than the latter. A discussion on the role of the Lewis acidic sites in the reaction is part of the mechanism section. The efficacy of the reaction, including yield and reaction times for 2.5 wt% Ag_2O/ZrO_2 are summarized in Table 3. An increase in catalyst amount from 20 mg to 60 mg, improved the yield from 52% to 96% and reduced the reaction time. The increase in the product may be attributed to the comparative increase in the number of available active sites possibly accelerating the reaction. An increase in the amount of catalyst from 60 mg to 120 mg registered no significant change in the yield of product or reaction time. Hence, 60 mg of the catalyst was considered the ideal amount for the chosen synthesis.

Table 3 Optimization of various weight % for the model reaction by 2.5 % Ag_2O/ZrO_2 catalyst[a.]

Entry	Catalyst (mg)	Time (min)	Yield (%)
1	20	100	56
2	40	50	79
3	60	30	96
4	80	30	96
5	100	30	96
6	120	40	96

[a]Reaction conditions: arylaldehyde **(1)** (1 mmol), 1,3-indanedione **(2)** (1 mmol), and guanidine hydrochloride **(3)** (1 mmol) and catalyst and solvent (5 mL) were stirred at room temperature.

Encouraged by the results, we further explored the applicability of the protocol for other substituted aldehydes under the optimized reaction conditions, by using 10 other substituted aldehydes. The corresponding indeno-pyrimidines afforded excellent yields in similar reaction times (30 min). (Table 4, entries 1–11). All the reactions, irrespective of electron withdrawing or electron-donating groups at ortho, meta or para positions, generally gave excellent yields. All the product molecules were fully characterized employing ^{1}H NMR,^{13}C NMR, FT-IR and HR-MS spectral analysis.

Table 4 Synthesis of novel functionalized pyridine derivatives by 2.5 % Ag_2O/ZrO_2 catalyst[a.]

Entry	R	Product	Yield* (%)	Mp °C	Lit Mp (◦C)
1	2-OMe	4a	94	119-121	-
2	4-OMe	4b	93	136-137	100[20]
3	2,3-$(OMe)_2$	4c	94	183-184	-
4	2,5-$(OMe)_2$	4d	92	200-201	-
5	2-Br	4e	94	197-198	-
6	2-F	4f	92	239-241	-
7	3,4-$(OMe)_2$	4g	96	176–178	178[20]
8	3-OH	4h	95	246–248	-
9	4-Br	4i	94	221-223	210[20]
10	4-Cl	4j	90	239-241	244[20]
11	4-Et	4k	94	204-206	-

[a]Reaction conditions: arylaldehyde **(1)** (1 mmol), 1,3-indanedione **(2)** (1 mmol), and guanidine hydrochloride **(3)** (1mmol), catalyst (60 mg) and ethanol solvent (5 mL) were stirred at room temperature. R = substituted benzaldehydes. - New compounds/no literature data. * = Isolated yields after recrystallization.

A proposed mechanism for the one-pot three-component reaction is outlined in Scheme 2. The presence of Lewis acidic sites on the catalyst surface facilitates the reactants to undergo reaction in a shorter time. It is assumed that in the first step, the Lewis acidic sites with the carbonyl oxygen generate the carbocation (**a**) [42]. In a fast reaction with the carbocation, the active methylene group affords intermediate (**b**), which desorbs from the catalyst surface by abstracting a proton from the protic solvent, EtOH (**b**), to form (**c**). On further dehydration (**c**), it produces the condensation product (**A**). Next, a Michael addition occurs between the intermediate (**A**) and the guanidinium, followed by cyclization and aromatization, and the transient intermediate yields the target compound—the substituted pyrimidine-5-one derivative [20]. The catalytic efficiency of the Ag_2O/ZrO_2 on the title reaction in comparison with other reported catalysts is summarized in the Table 5.

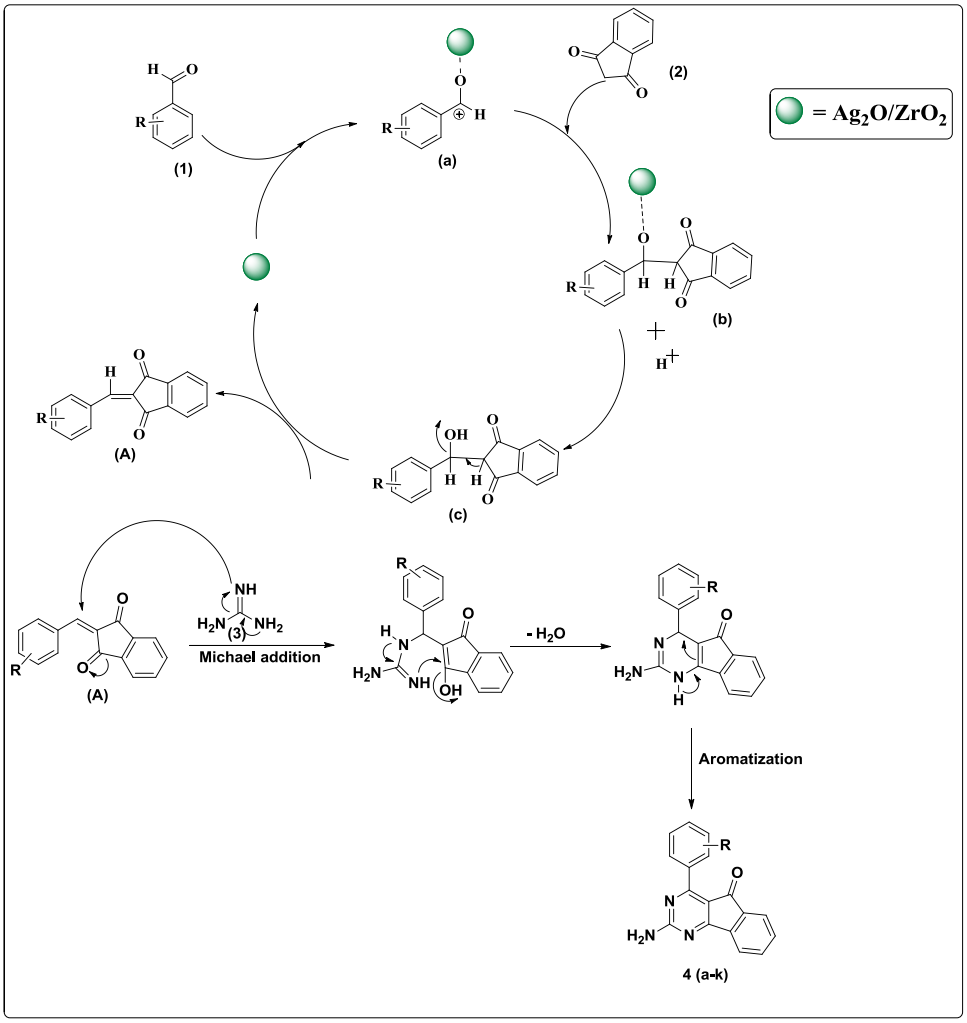

Scheme 2. Probable mechanism for the synthesis of novel indeno-pyrimidine derivatives.

Table 5 A comparison table with various other catalysts to synthesis pyrimidine derivatives.

Catalyst	Solvent	Reaction Condition	Yield (%) [Ref]
NaOH	EtOH	Reflux, 6-10h	81-94 [20]
NaOH	EtOH	Reflux, 7-8.4h	75-86 [21]
NaOH	EtOH	Reflux, 0.5-1h	85-94 [22]
NaOMe	EtOH	Reflux, 10-14h	60-70[23]
α-Fe_2O_3-MCM-41-P	Solvent free	80°C, 1 h	82-95 [25]
Uranyl acetate/ succinimide sulfonic acid	Solvent free	90°C, 4 h	75-96[26]
2.5% Ag_2O-ZrO_2	EtOH	Rt, 30 min	90-96 [Present Work]

5.4 Reusability of catalyst

The main objective and attraction of heterogeneous catalysts are its reusability. We thus examined the recovery and reusability of the Ag_2O/ZrO_2 catalyst. The solid catalyst from the reaction mixture was separated by simple filtration under vacuum, followed by washing with acetone solvent and drying at 100 °C for 3 h. The recovered catalyst was re-used in subsequent reactions. Six runs in successive reactions gave yields without significant loss in product yield.

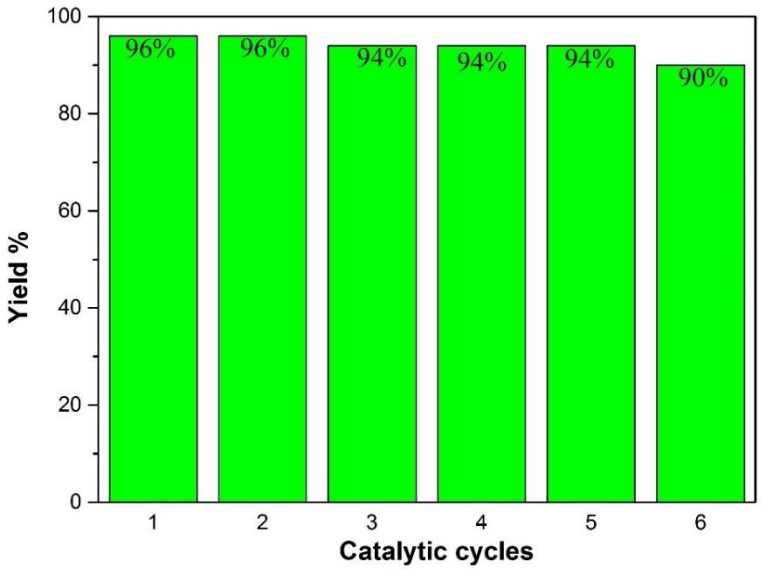

Figure 6. Recyclability of Ag_2O/ZrO_2 catalyst.

5.5 Conclusion

In conclusion, we report a simple and green protocol for the synthesis of indeno-pyrimidines by three-component reaction. All the reactions with eleven different aromatic aldehydes with 1,3-indandione, and gunadium hydrochloride using (2.5 %) silver loaded on zirconia catalyst gave excellent yields (90-96%). The proposed catalyst proved efficient, stable and reusable. This method offers easy workup, excellent selectivity and high yields in short reaction times at room temperature using ethanol, a green solvent. All the products were purified by re-crystallization from ethanol and no need for chromatographic separation by this method. Consequently, the use of volatile and hazardous solvents has been evaded. This synthesis method is useful to synthesize privileged pyrimidine scaffolds in a short time in a one pot strategy under green conditions.

5.6 Acknowledgements

The authors are thankful to the National Research Foundation (NRF) of South Africa, and University of KwaZulu-Natal, Durban, for financial support and research facilities.

5.7 References

1. Rotstein, B.H.; Zaretsky, S.; Rai, V.; Yudin, A.K. Small heterocycles in multicomponent reactions. Chem. Rev. 2014, 114, 8323–8359, doi:10.1021/cr400615v.

2. Domling, A.; Wang, W.; Wang, K. Chemistry and biology of multicomponent reactions. Chem. Rev. 2012, 112, 3083–3135, doi:10.1021/cr100233r.Chemistry.

3. Gangu, K.K.; Maddila, S.; Maddila, S.N.; Jonnalagadda, S.B. Novel iron doped calcium oxalates as promising heterogeneous catalysts for one-pot multi-component synthesis of pyranopyrazoles. RSC Adv. 2017, 7, 423–432, doi:10.1039/C6RA25372E.

4. Bhaskaruni, S.V.H.S.; Maddila, S.; Gangu, K.K.; Jonnalagadda, S.B. A review on multi-component green synthesis of N-containing heterocycles using mixed oxides as heterogeneous catalysts. *Arab. J. Chem.* **2017**, doi:10.1016/j.arabjc.2017.09.016.

5. Bhaskaruni, S.V.H.S.; Maddila, S.; van Zyl, W.E.; Jonnalagadda, S.B. RuO_2/ZrO_2 as an efficient reusable catalyst for the facile, green, one-pot synthesis of novel functionalized halopyridine derivatives. *Catal. Commun.* **2017**, *100*, 24–28, doi:10.1016/j.catcom.2017.06.023.

6. Pagadala, R.; Maddila, S.; Moodley, V.; van Zyl, W.E.; Jonnalagadda, S.B. An efficient method for the multicomponent synthesis of multisubstituted pyridines, a rapid procedure using Au/MgO as the catalyst. *Tetrahedron Lett.* **2014**, *55*, 4006–4010, doi:10.1016/j.tetlet.2014.05.089.

7. Bhaskaruni, S.V.H.S.; Maddila, S.; van Zyl, W.E.; Jonnalagadda, S.B. V_2O_5/ZrO_2 as an efficient reusable catalyst for the facile, green, one-pot synthesis of novel functionalized 1,4-dihydropyridine derivatives. *Catal. Today* **2017**, doi:10.1016/j.cattod.2017.05.038.

8. Maddila, S.N.; Maddila, S.; van Zyl, W.E.; Jonnalagadda, S.B. Mn doped ZrO_2 as a green, efficient and reusable heterogeneous catalyst for the multicomponent synthesis of pyrano[2,3-D]-pyrimidine derivatives. *RSC Adv.* **2015**, *5*, 37360–37366, doi:10.1039/C5RA06373F.

9. Wen, C.; Yin, A.; Dai, W.-L. Recent advances in silver-based heterogeneous catalysts for green chemistry processes. *Appl. Catal. B Environ.* **2014**, *160–161*, 730–741, doi:10.1016/j.apcatb.2014.06.016.

10. Maddila, S.; Jonnalagadda, S.B.; Gangu, K.K.; Maddila, S.N. Recent Advances in the

Synthesis of Pyrazole Derivatives Using Multicomponent Reactions. *Curr. Org. Synth.* **2017**, *14*, 634–653.

11. Gore, R.P.; Rajput, A.P. A review on recent progress in multicomponent reactions of pyrimidine synthesis. *Drug Invent. Today* **2013**, *5*, 148–152, doi:10.1016/j.dit.2013.05.010.

12. Yalagala, K.; Maddila, S.; Rana, S.; Maddila, S.N.; Kalva, S.; Skelton, A.A.; Jonnalagadda, S.B. Synthesis, antimicrobial activity and molecular docking studies of pyrano[2,3-D]pyrimidine formimidate derivatives. *Res. Chem. Intermed.* **2016**, *42*, 3763–3774, doi:10.1007/s11164-015-2243-7.

13. Maddila, S.; Gorle, S.; Seshadri, N.; Lavanya, P.; Jonnalagadda, S.B. Synthesis, antibacterial and antifungal activity of novel benzothiazole pyrimidine derivatives. *Arab. J. Chem.* **2016**, *9*, 681–687, doi:10.1016/j.arabjc.2013.04.003.

14. Raić-Malić, S.; Svedružić, D.; Gazivoda, T.; Marunović, A.; Hergold-Brundić, A.; Nagl, A.; Balzarini, J.; De Clercq, E.; Mintas, M. Synthesis and Antitumor Activities of Novel Pyrimidine Derivatives of 2,3-*O*,*O*Dibenzyl- 6-deoxy-L-ascorbic Acid and 4,5-Didehydro-5,6-dideoxy-L-ascorbic Acid. *J. Med. Chem.* **2000**, *43*, 4806–4811, doi:10.1021/jm0009540.

15. Miazga, A.; Ziemkowski, P.; Siwecka, M.A.; Lipniacki, A.; Piasek, A.; Kulikowski, T. Synthesis, biological properties and anti-HIV-1 activity of new pyrimidine P1,P2-dinucleotides. *Nucleosides Nucleotides Nucleic Acids* **2010**, *29*, 438–444, doi:10.1080/15257771003738642.

16. Yadlapalli, R.K.; Chourasia, O.P.; Vemuri, K.; Sritharan, M.; Perali, R.S. Synthesis and in vitro anticancer and antitubercular activity of diarylpyrazole ligated dihydropyrimidines possessing lipophilic carbamoyl group. *Bioorg. Med. Chem. Lett.* **2012**, *22*, 2708–2711, doi:10.1016/j.bmcl.2012.02.101.

17. De Assis, S.P.O.; da Silva, M.T.; de Oliveira, R.N.; de Lima, V.L.M. Synthesis and Anti-Inflammatory Activity of New Alkyl-Substituted Phthalimide 1*H*-1,2,3-Triazole Derivatives. *Sci. World J.* **2012**, *2012*, 925925, doi:10.1100/2012/925925.

18. Singh, K.; Kaur, T. Pyrimidine-based antimalarials: Design strategies and antiplasmodial effects. *Medchemcomm* **2016**, *7*, 749–768, doi:10.1039/C6MD00084C.

19. Lim, H.-K.; Chen, J.; Sensenhauser, C.; Cook, K.; Preston, R.; Thomas, T.; Shook, B.; Jackson, P.F.; Rassnick, S.; Rhodes, K.; et al. Overcoming the Genotoxicity of a Pyrrolidine Substituted Arylindenopyrimidine As a Potent Dual Adenosine A2A/A1 Antagonist by Minimizing Bioactivation to an Iminium Ion Reactive Intermediate. *Chem. Res. Toxicol.* **2011**, *24*, 1012–1030, doi:10.1021/tx1004437.

20. Patravale, A.A.; Gore, A.H.; Patil, D.R.; Kolekar, G.B.; Deshmukh, M.B.; Anbhule, P.V. Trouble-Free Multicomponent Method for Combinatorial Synthesis of 2-Amino-4-phenyl-5-*H*-indeno[1,2-*d*]pyrimidine- 5-one and Their Screening against Cancer Cell Lines. *Ind. Eng. Chem. Res.* **2014**, *53*, 16568–16578, doi:10.1021/ie5013618.

21. Undare, S.S.; Valekar, N.J.; Patravale, A.A.; Jamale, D.K.; Vibhute, S.S.; Walekar, L.S.; Kolekar, G.B.; Deshmukh, M.B.; Anbhule, P.V. Synthesis, anti-inflammatory, ulcerogenic and cyclooxygenase activities of indenopyrimidine derivatives. *Bioorg. Med. Chem. Lett.* **2016**, *26*, 814–818, doi:10.1016/j.bmcl.2015.12.088.

22. Xia, S.; Yin, S.; Tao, S.; Shi, Y.; Rong, L.; Wei, X.; Zong, Z. An efficient and facile synthesis of novel substituted pyrimidine derivatives: 4-amino-5-carbonitrile-2-nitroaminopyrimidine. Res. Chem. Intermed. 2012, 38, 2435–2442, doi:10.1007/s11164-012-0559-0.

23. Jagadale, S.D.; Sawant, A.D.; Deshmukh, M.B. Synthesis and Antimicrobial Evaluation of Novel Dibenzo- 18-Crown-6-Ether Functionalized Pyrimidines. J. Heterocycl. Chem. 2017, 54, 2307–2312, doi:10.1002/jhet.2818.

24. Gogoi, P.; Dutta, A.K.; Saikia, S.; Borah, R. Heterogenized hybrid catalyst of 1-sulfonic acid-3-methyl imidazolium ferric chloride over NaY zeolite for one-pot synthesis of 2-amino-4-arylpyrimidine derivatives: A viable approach. Appl. Catal. A Gen. 2016, 523, 321–331, doi:10.1016/j.apcata.2016.06.015.

25. Aryan, R.; Beyzaei, H.; Nojavan, M.; Dianatipour, T. Secondary amines immobilized inside magnetic mesoporous materials as a recyclable basic and oxidative heterogeneous nanocatalyst for the synthesis of trisubstituted pyrimidine derivatives. Res. Chem. Intermed. 2016, 42, 4417–4431, doi:10.1007/s11164-015- 2284-y.

26. Kamali, M.; Shockravi, A.; Doost, M.S.; Hooshmand, S.E. One-pot, solvent-free synthesis via Biginelli reaction : Catalyst-free and new recyclable catalysts. Cogent Chem. 2015, 24, 1–6, doi:10.1080/23312009.2015.1081667.

27. Zhang, J.; Li, L.; Wang, S.; Huang, T.; Hao, Y.; Qi, Y. Multi-mode photocatalytic degradation and photocatalytic hydrogen evolution of honeycomb-like three-dimensionally ordered macroporous composite Ag/ZrO_2. RSC Adv. 2016, 6, 13991–14001, doi:10.1039/C5RA18964K.

28. Lee, C.; Shul, Y.-G.; Einaga, H. Silver and manganese oxide catalysts supported on mesoporous ZrO_2 nanofiber mats for catalytic removal of benzene and diesel soot. Catal. Today 2017, 281, 460–466, doi:10.1016/j.cattod.2016.05.050.

29. Shabalala, N.G.; Maddila, S.; Jonnalagadda, S.B. Facile one-pot green synthesis of tetrahydrobiphenylene- 1,3-dicarbonitriles in aqueous media under ultrasound irradiation. Res. Chem. Intermed. 2016, 42, 8097–8108, doi:10.1007/s11164-016-2581-0.

30. Shabalala, N.; Maddila, S.; Jonnalagadda, S.B. Catalyst-free, one-pot, four-component green synthesis of functionalized 1-(2-fluorophenyl)-1,4-dihydropyridines under ultrasound irradiation. New J. Chem. 2016, 40, 5107–5112, doi:10.1039/C5NJ03574K.

31. Shabalala, S.; Maddila, S.; van Zyl, W.E.; Jonnalagadda, S.B. Sustainable CeO_2/ZrO_2 Mixed Oxide Catalyst For the Green Synthesis of Highly Functionalized 1,4-Dihydropyridine-2,3-dicarboxylate Derivatives. Curr. Org. Synth. 2017, 14, 1–8.

32. Shabalala, S.; Maddila, S.; van Zyl, W.E.; Jonnalagadda, S.B. Innovative Efficient Method for the Synthesis of 1,4-Dihydropyridines Using Y_2O_3 Loaded on ZrO_2 as Catalyst. Ind. Eng. Chem. Res. 2017, 56, 11372–11379, doi:10.1021/acs.iecr.7b02579.

33. Gangu, K.K.; Maddila, S.; Maddila, S.N.; Jonnalagadda, S.B. Nanostructured samarium doped fluorapatites and their catalytic activity towards synthesis of 1,2,4-triazoles. Molecules 2016, 21, 1281, doi:10.3390/molecules21101281.

34. Maddila, S.; Lavanya, P.; Jonnalagadda, S.B. Cesium loaded on silica as an efficient and recyclable catalyst for the novel synthesis of selenophenes. Arab. J. Chem. 2016, 9, 891–897, doi:10.1016/j.arabjc.2013.09.030.

35. Maddila, S.; Valand, J.; Bandaru, H.; Yalagala, K.; Lavanya, P. Ag Loaded on SiO_2 as an Efficient and Recyclable Heterogeneous Catalyst for the Synthesis of Chloro-8-substituted-9H-purines. J. Heterocycl. Chem. 2016, 53, 319–324, doi:10.1002/jhet.2407.

36. Maddila, S.; Maddila, S.N.; Jonnalagadda, S.B.; Lavanya, P. Reusable Ce-V Loaded

Alumina Catalyst for Multicomponent Synthesis of Substituted Pyridines in Green Media. J. Heterocycl. Chem. 2016, 53, 658–664, doi:10.1002/jhet.2430.

37. Maddila, S.; Gorle, S.; Shabalala, S.; Oyetade, O.; Maddila, S.N.; Lavanya, P.; Jonnalagadda, S.B. Ultrasound mediated green synthesis of pyrano[2,3-c]pyrazoles by using Mn doped ZrO_2. Arab. J. Chem. 2016, doi:10.1016/j.arabjc.2016.04.016.

38. Maddila, S.; Dasireddy, V.D.B.C.; Jonnalagadda, S.B. Ce-V loaded metal oxides as catalysts for dechlorination of chloronitrophenol by ozone. Appl. Catal. B Environ. 2014, 150–151, 305–314, doi:10.1016/j.apcatb.2013.12.036.

39. Maddila, S.; Dasireddy, V.D.B.C.; Jonnalagadda, S.B. Dechlorination of tetrachloro-o-benzoquinone by ozonation catalyzed by cesium loaded metal oxides. Appl. Catal. B Environ. 2013, 138–139, 149–160, doi:10.1016/j.apcatb.2013.02.017.

40. Balaga, V.; Pedada, J.; Friedrich, H.B.; Singh, S. Tuning surface composition of Cs exchanged phosphomolybdic acid catalysts in CH bond activation of toluene to benzaldehyde at room temperature. *J. Mol. Catal. A Chem.* **2016**, *425*, 116–123, doi:10.1016/j.molcata.2016.10.007.

41. Védrine, J.C. Acid-base characterization of heterogeneous catalysts: An up-to-date overview. *Res. Chem. Intermed.* **2015**, *41*, 9387–9423, doi:10.1007/s11164-015-19829.

42. Li, Q.; Wang, X.; Yu, Y.; Chen, Y.; Dai, L. Tailoring a magnetically separable $NiFe_2O_4$ nanoparticle catalyst for Knoevenagel condensation. *Tetrahedron* **2016**, *72*, 8358–8363, doi:10.1016/j.tet.2016.11.011.

5.8 Supplementary information

5.8.1 Catalyst instrumentation details

Employing a Bruker D8 Advance instrument (Cu K radiation source with a wave length of 1.5406 Å), the X-ray diffraction data related the structural phases of the catalyst were acquired. Using a JEOL JEM-1010 electron microscope and JEOL JSM-6100 microscope, the TEM and SEM analysis data was recorded. iTEM software was used analyse the TEM data and images. Employing the X-ray analyser (energy-dispersive), EDX-analysis on the SEM images was conducted.

5.8.2 Experimental Section

All chemicals and reagents required for the reaction were of analytical grade and were used without any further purification. Bruker AMX 400 MHz NMR spectrometer was used to record the ^{1}H NMR, and ^{13}C NMR spectral values. High-resolution mass data were obtained using a Bruker micro TOF-Q II ESI instrument operating at ambient temperature. The $CDCl_3{-}d_6$ solution was utilized for this while TMS served as the internal standard. TMS was further used as an internal standard for reporting the all chemical shifts in δ (ppm). Purity of all the reaction products was confirmed by TLC using aluminium plates coated with silica gel (Merck Kieselgel 60 F_{254}). Infrared (IR) spectra were recorded on a Perkin Elmer Precisely equipped with a Universal ATR sampling accessory using a diamond crystal. The powdered material was placed on the crystal and a force of 120 psi was applied to ensure proper contact between the material and the crystal.The spectra were analyzed using Spectrum 100 software. Before recording the IR spectra, pyridine was adsorbed by placing a drop of pyridine on 10 mg of the sample followed by evacuation in air for 1 h at room temperature to remove reversibly adsorbed pyridine on the surface of the catalyst.

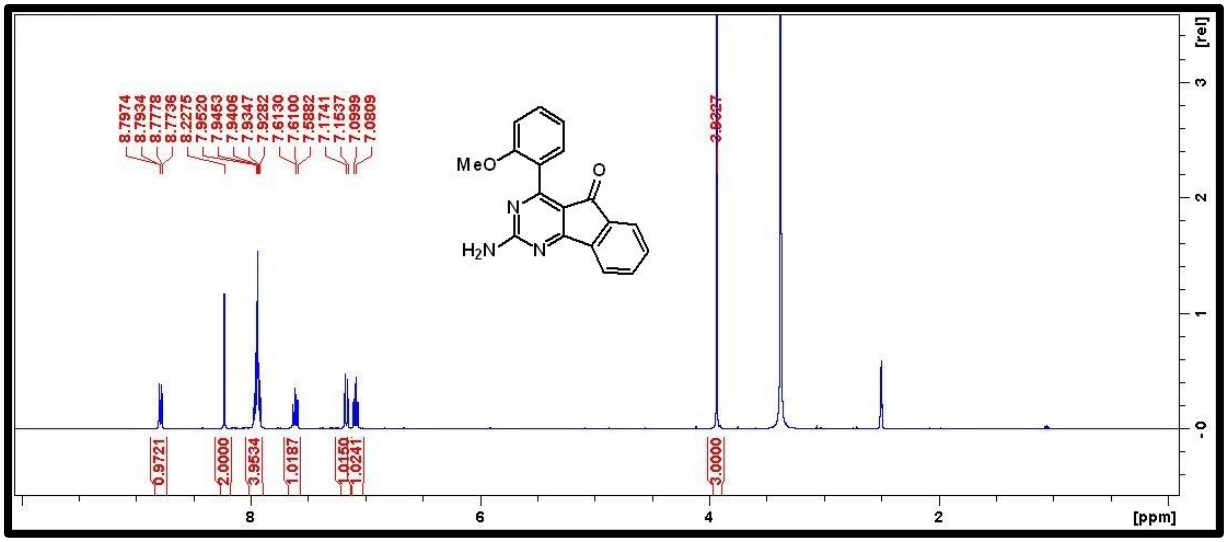

^{1}H NMR spectra of compound **4a**

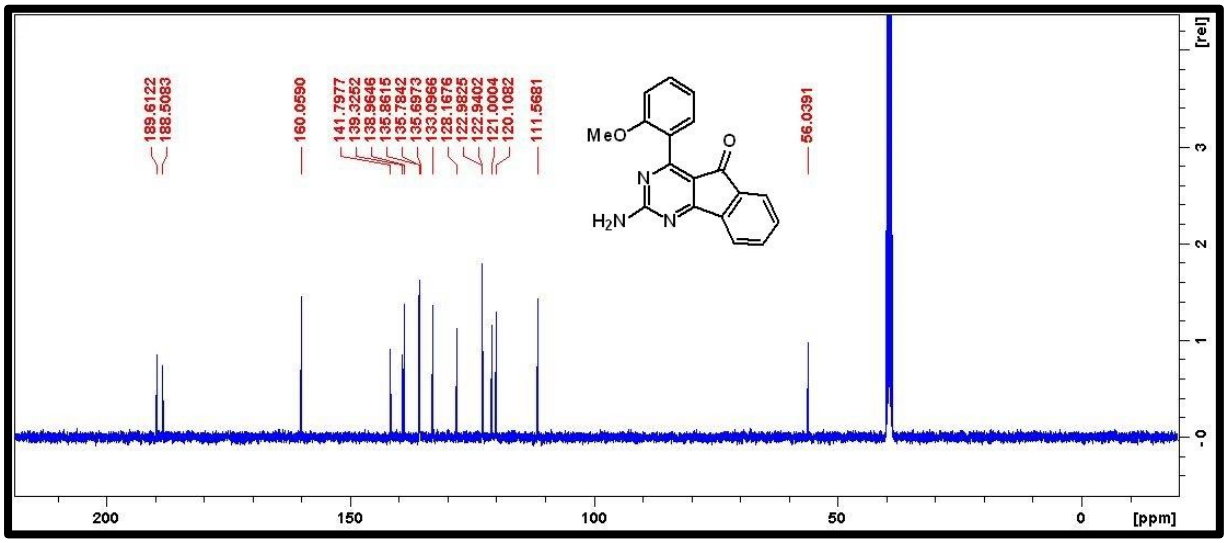

^{13}C NMR spectra of compound **4a**

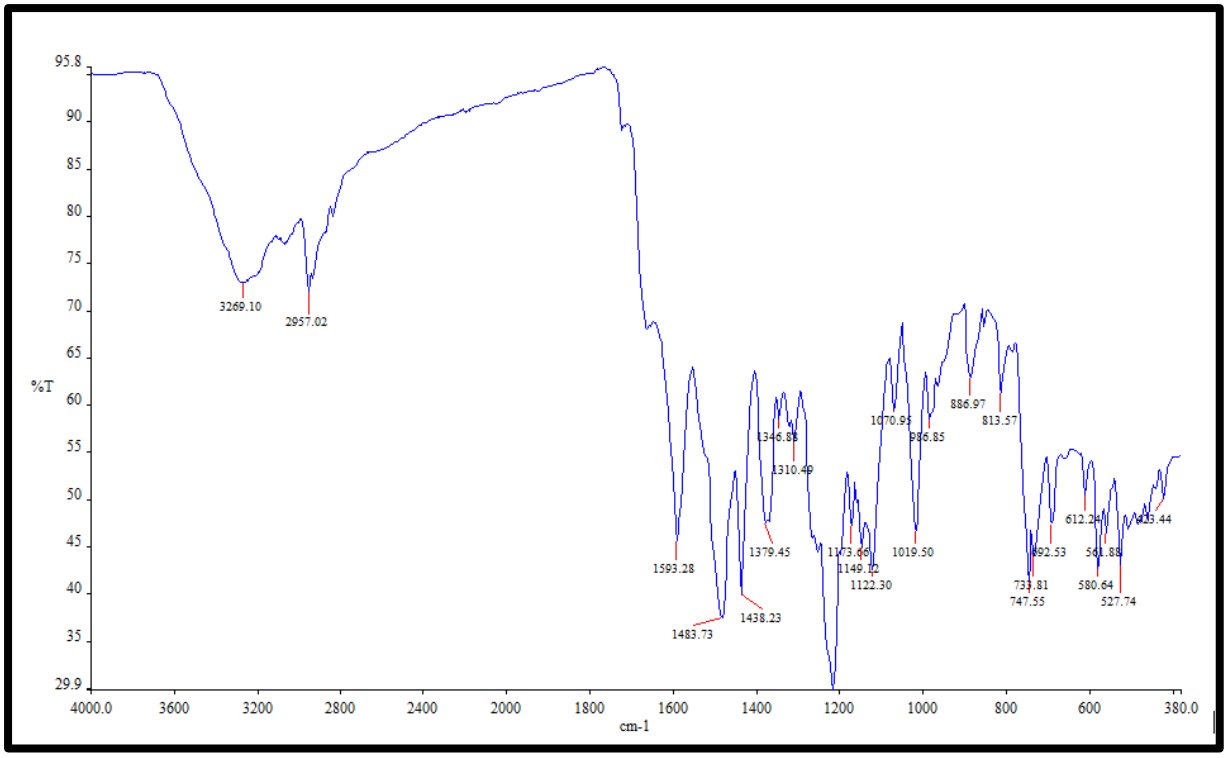

FT-IR spectra of compound **4a**

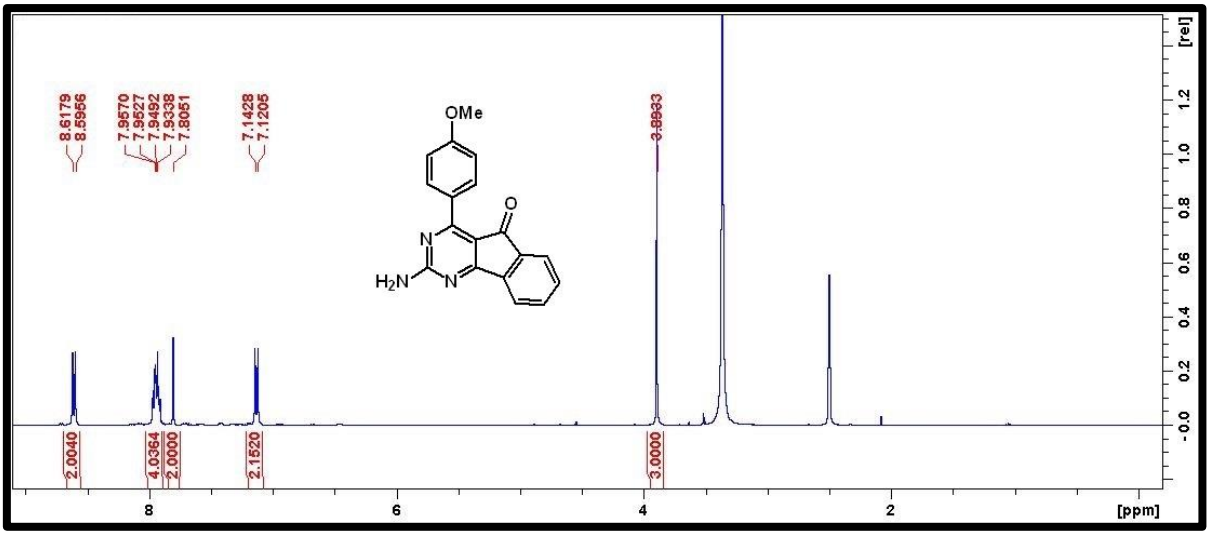

^{1}H NMR spectra of compound **4b**

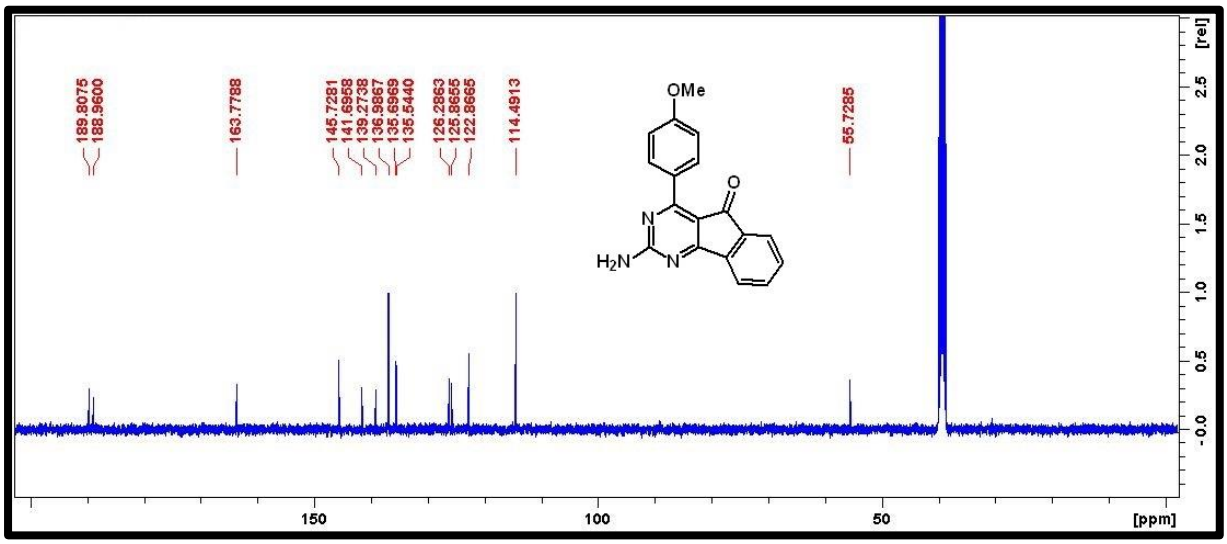

^{13}C NMR spectra of compound **4b**

Elemental Composition Report **Page 1**

Single Mass Analysis
Tolerance = 4.0 PPM / DBE: min = -1.5, max = 100.0
Element prediction: Off
Number of isotope peaks used for i-FIT = 3

Monoisotopic Mass, Even Electron Ions
30 formula(e) evaluated with 1 results within limits (up to 20 best isotopic matches for each mass)
Elements Used:
C: 15-20 H: 10-15 N: 0-5 O: 0-5
Compound 10 31 (1.012) Cm (1:61)
TOF MS ES-

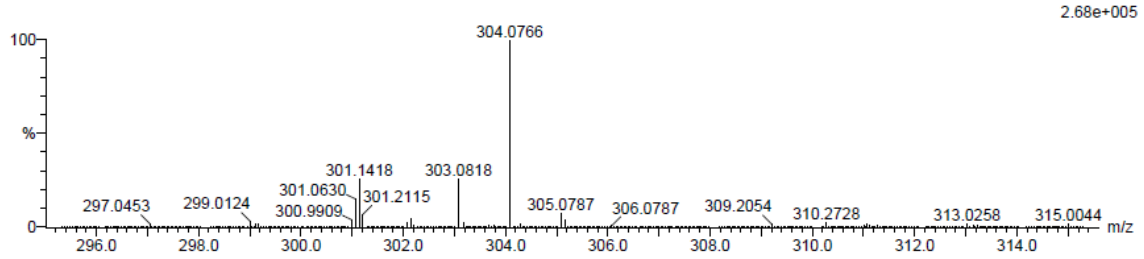

Minimum:				-1.5			
Maximum:		5.0	4.0	100.0			
Mass	Calc. Mass	mDa	PPM	DBE	i-FIT	i-FIT (Norm)	Formula
304.0766	304.0763	0.3	1.0	5.5	668.7	0.0	C18 H14 N3 O2

HRMS spectra of compound **4b**

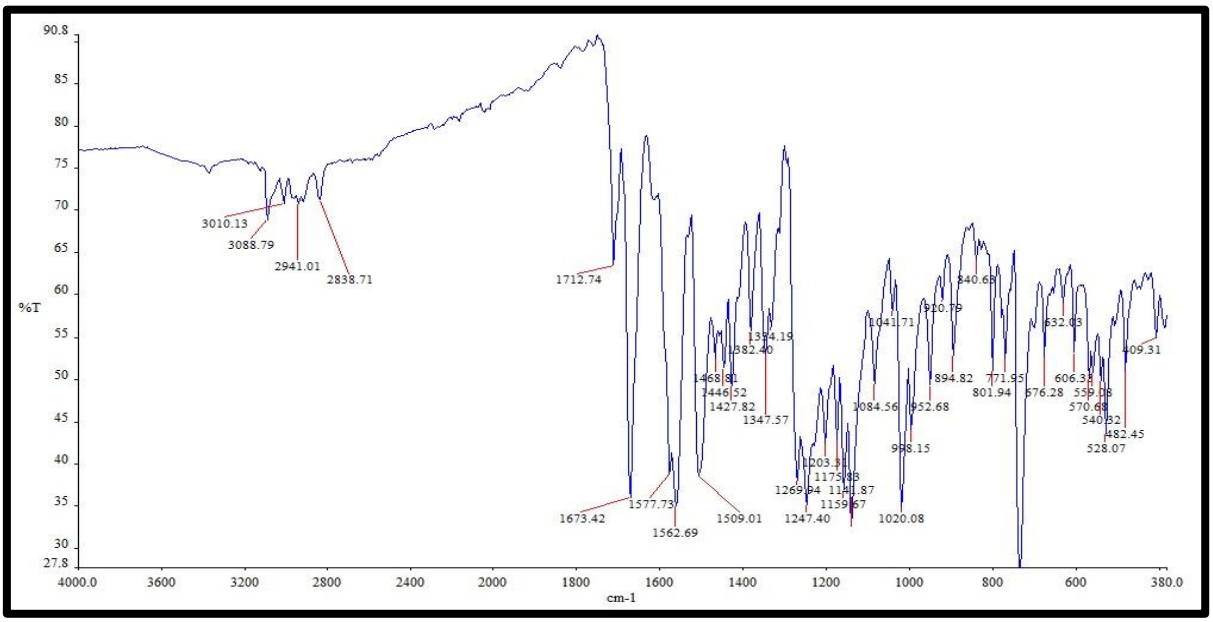

FT-IR spectra of compound **4b**

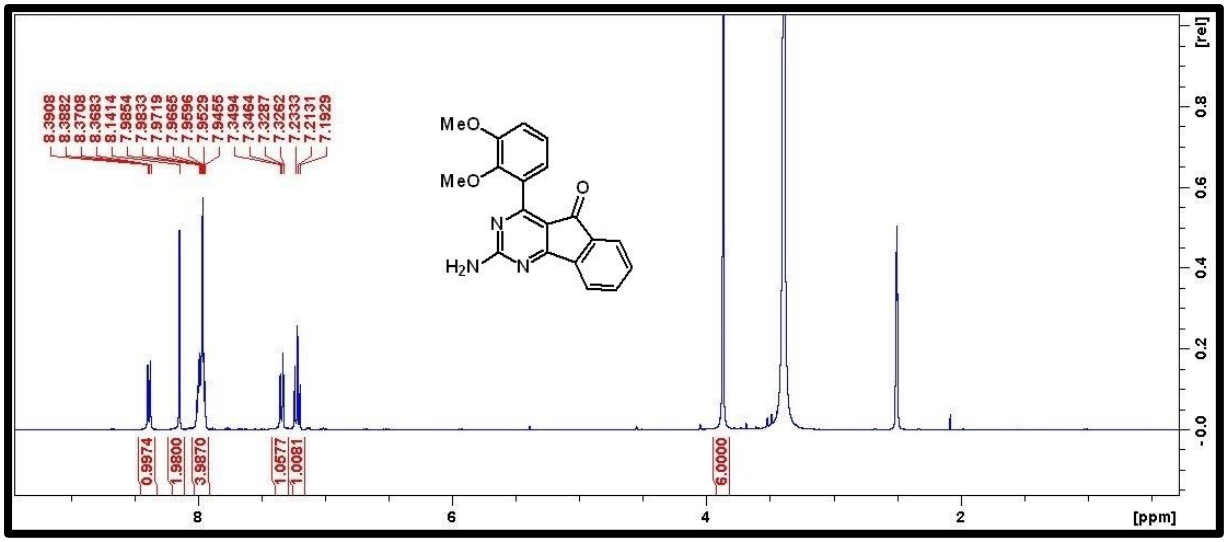

^{1}H NMR spectra of compound **4c**

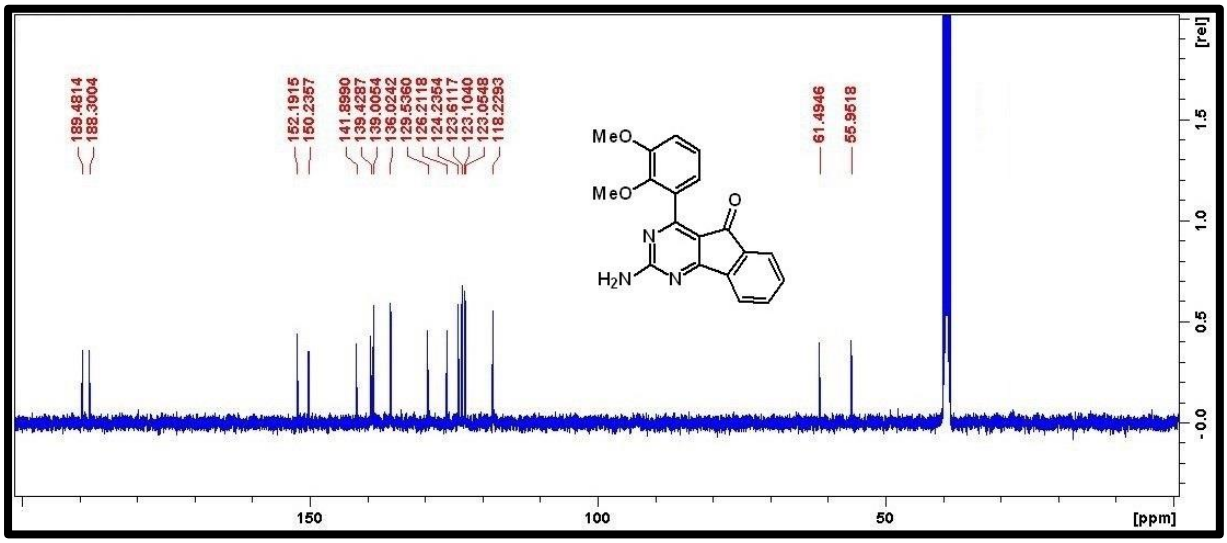

^{13}C NMR spectra of compound **4c**

Elemental Composition Report **Page 1**

Single Mass Analysis
Tolerance = 5.0 PPM / DBE: min = -1.5, max = 100.0
Element prediction: Off
Number of isotope peaks used for i-FIT = 3

Monoisotopic Mass, Even Electron Ions
16 formula(e) evaluated with 1 results within limits (up to 20 closest results for each mass) mass)
Elements Used:
C: 15-20 H: 15-20 N: 0-5 O: 0-5
S6 51 (1.788) Cm (1:61)
TOF MS ES-

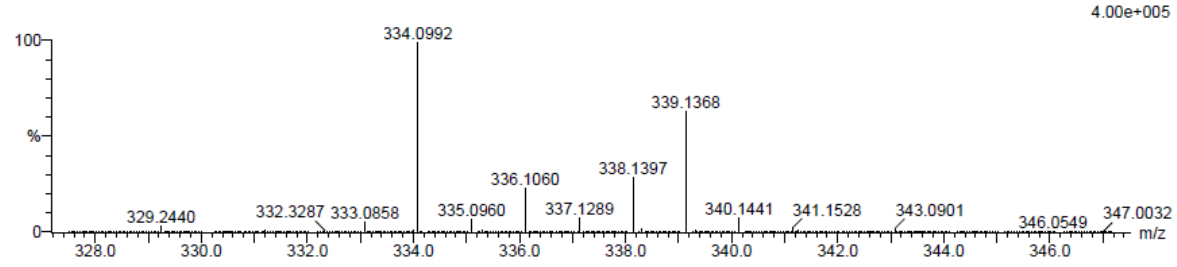

Minimum:				-1.5			
Maximum:		5.0	5.0	100.0			
Mass	Calc. Mass	mDa	PPM	DBE	i-FIT	i-FIT (Norm)	Formula
334.0992	334.1008	-1.6	-4.8	10.5	700.0	0.0	C19 H16 N3 O3

HRMS spectra of compound **4c**

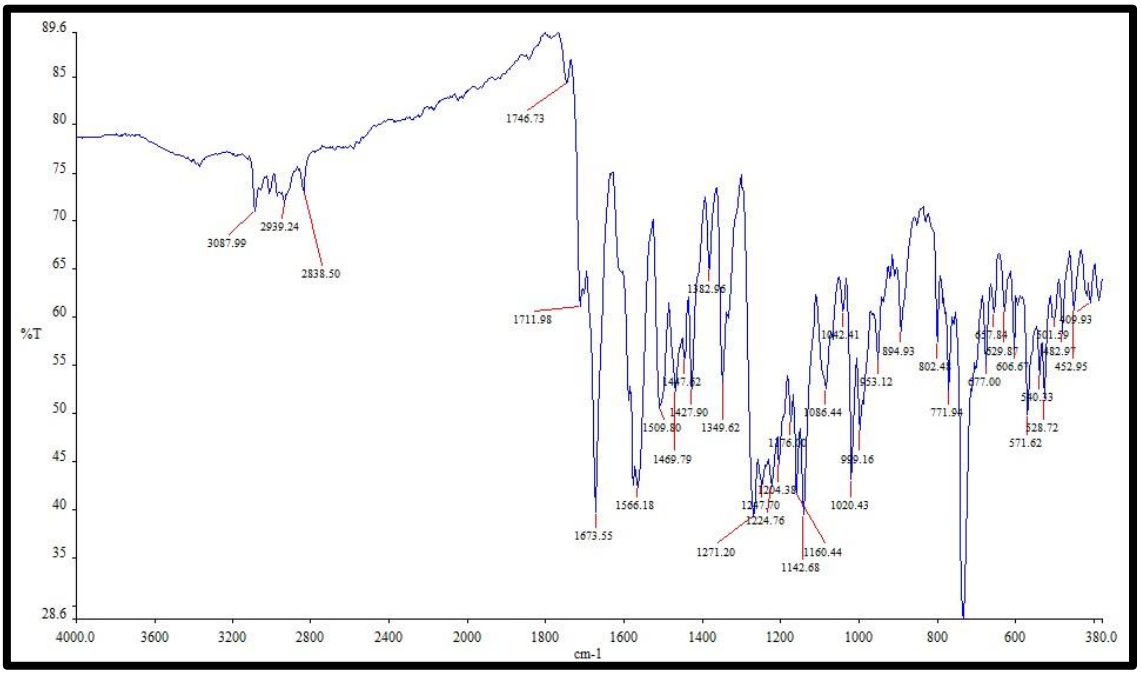

FT-IR spectra of compound **4c**

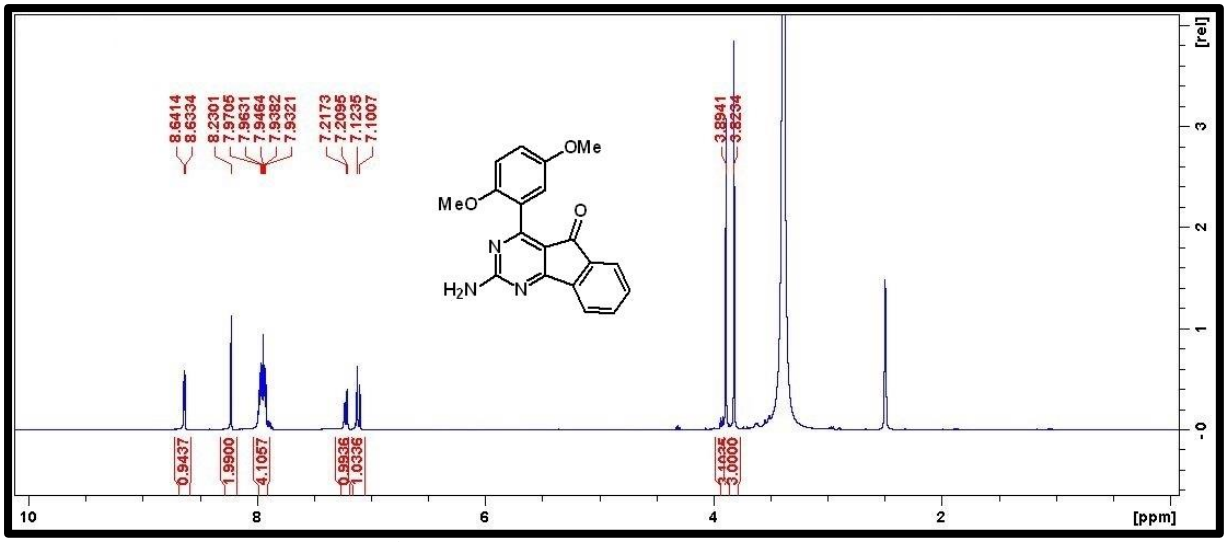

^{1}H NMR spectra of compound **4d**

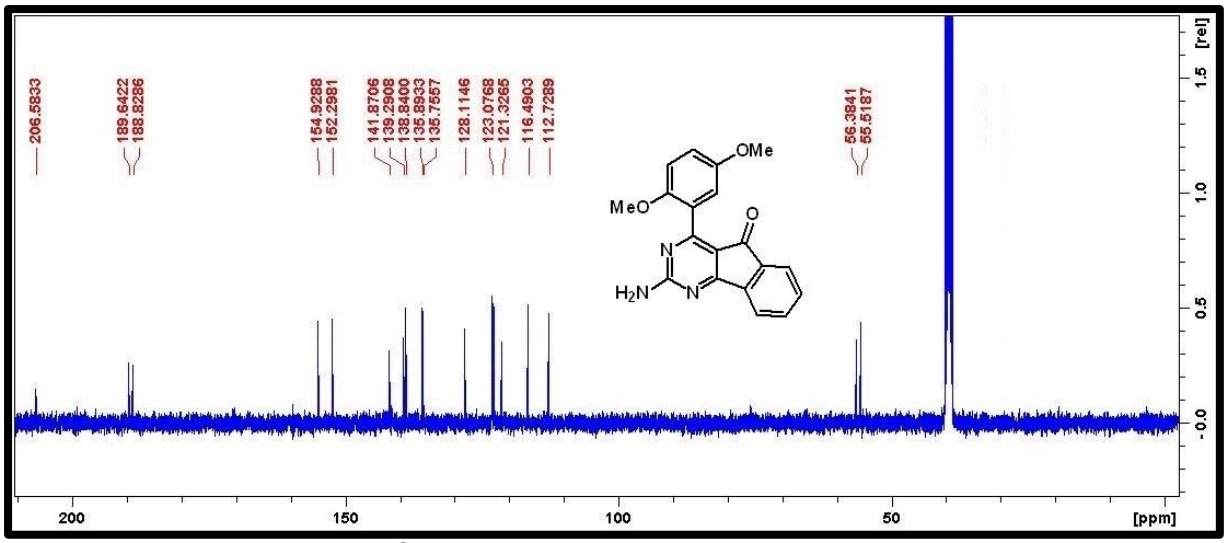

^{13}C NMR spectra of compound **4d**

Elemental Composition Report **Page 1**

Single Mass Analysis
Tolerance = 5.0 PPM / DBE: min = -1.5, max = 100.0
Element prediction: Off
Number of isotope peaks used for i-FIT = 3

Monoisotopic Mass, Even Electron Ions
16 formula(e) evaluated with 1 results within limits (up to 20 closest results for each mass)
Elements Used:
C: 15-20 H: 15-20 N: 0-5 O: 0-5
S3 54 (1.788) Cm (1:61)
TOF MS ES-

2.20e+005

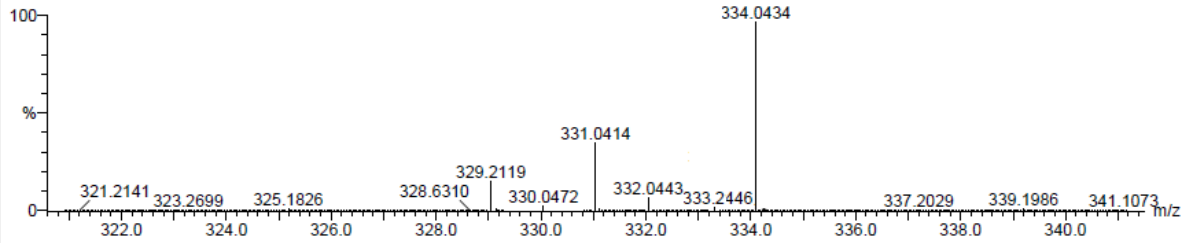

Minimum:				-1.5			
Maximum:		5.0	5.0	100.0			
Mass	Calc. Mass	mDa	PPM	DBE	i-FIT	i-FIT (Norm)	Formula
334.0434	334.0441	-0.7	-2.1	12.5	652.1	0.0	C19 H16 N3 O3

HRMS spectra of compound **4d**

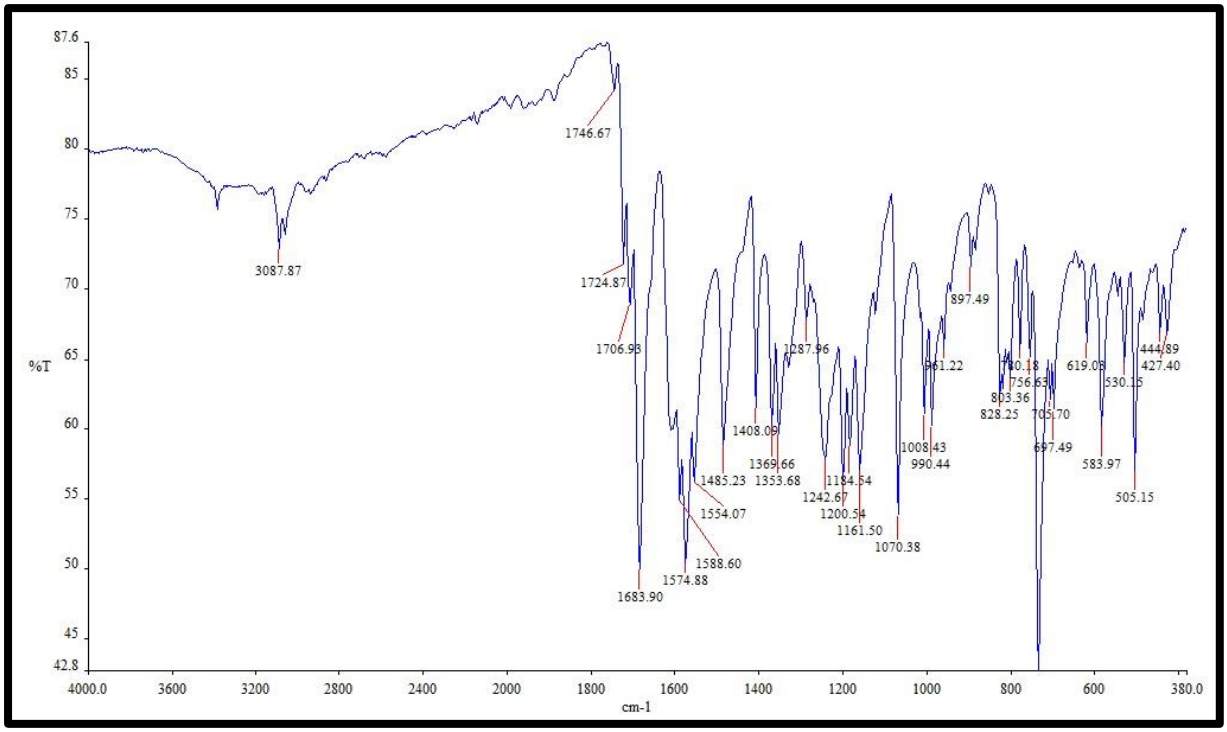

FT-IR spectra of compound **4d**

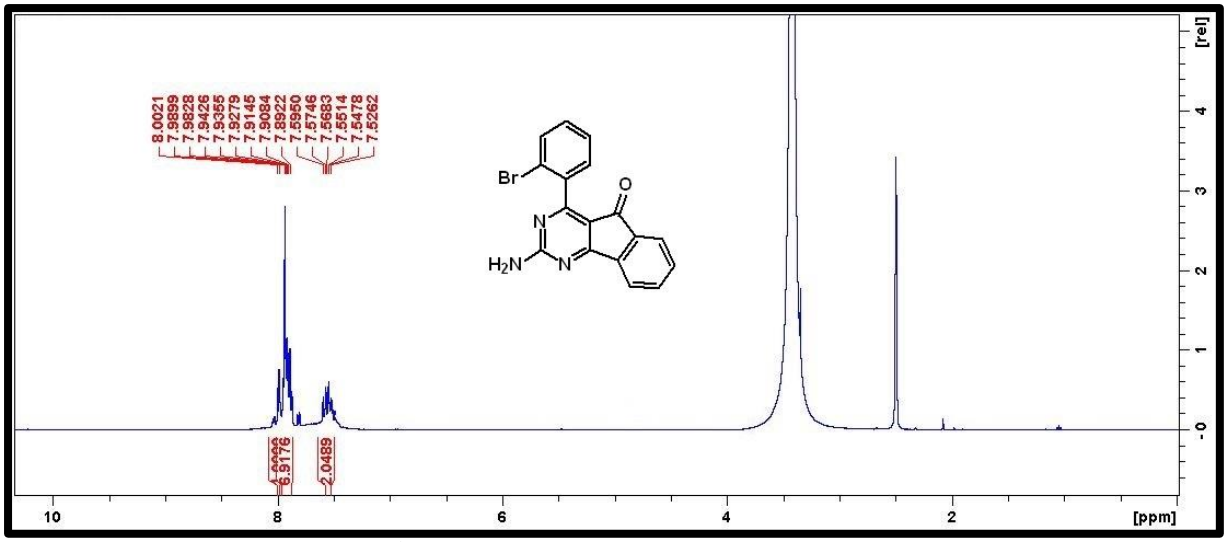

^{1}H NMR spectra of compound **4e**

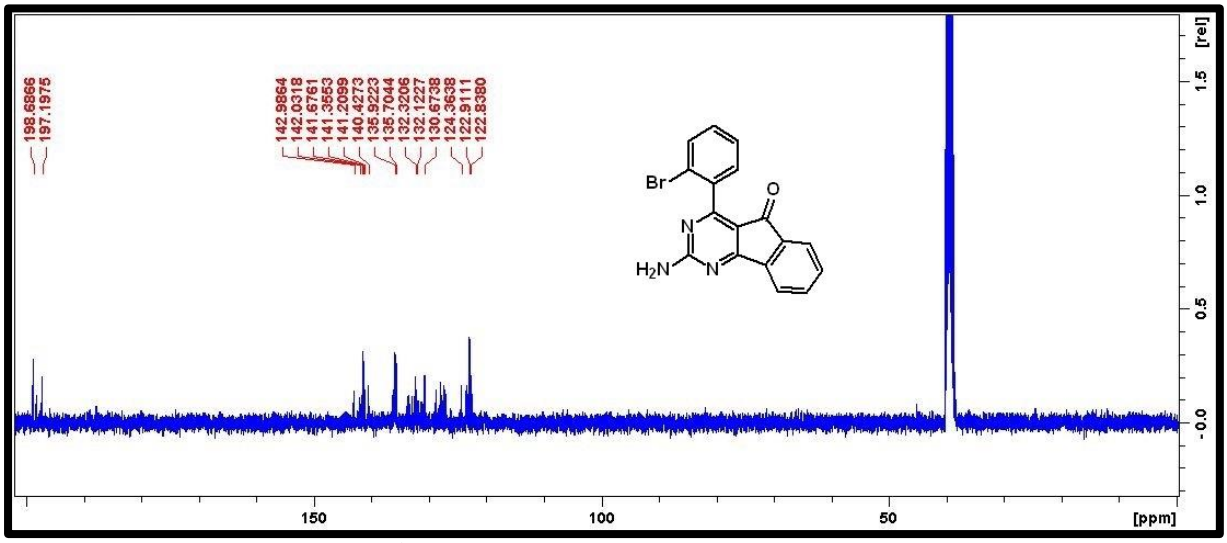

^{1}C NMR spectra of compound **4e**

Elemental Composition Report **Page 1**

Single Mass Analysis
Tolerance = 5.0 PPM / DBE: min = -1.5, max = 100.0
Element prediction: Off
Number of isotope peaks used for i-FIT = 3

Monoisotopic Mass, Even Electron Ions
15 formula(e) evaluated with 1 results within limits (up to 20 closest results for each mass)
Elements Used:
C: 15-20 H: 10-15 N: 0-5 O: 0-5 Br: 1-1
S4 sm 35 (1.148) Cm (1:61)
TOF MS ES-

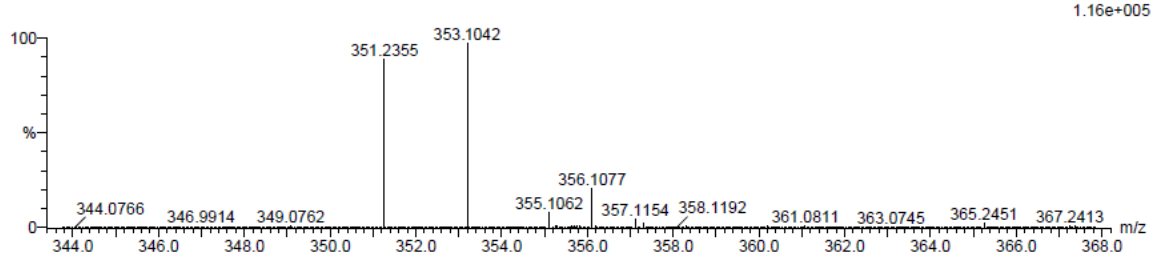

Minimum:				-1.5			
Maximum:		5.0	5.0	100.0			
Mass	Calc. Mass	mDa	PPM	DBE	i-FIT	i-FIT (Norm)	Formula
353.1042	353.1042	0.0	0.0	12.5	617.1	0.0	C17 H11 N3 O Br

HRMS spectra of compound **4e**

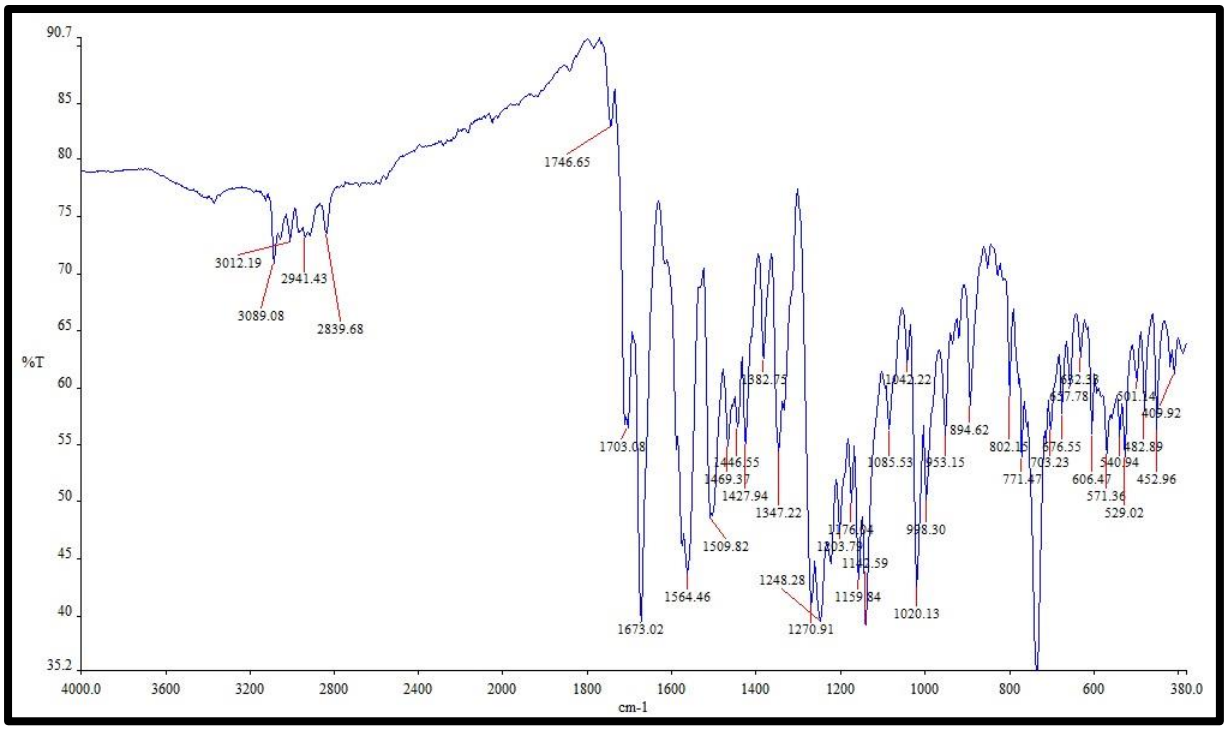

FT-IR spectra of compound **4e**

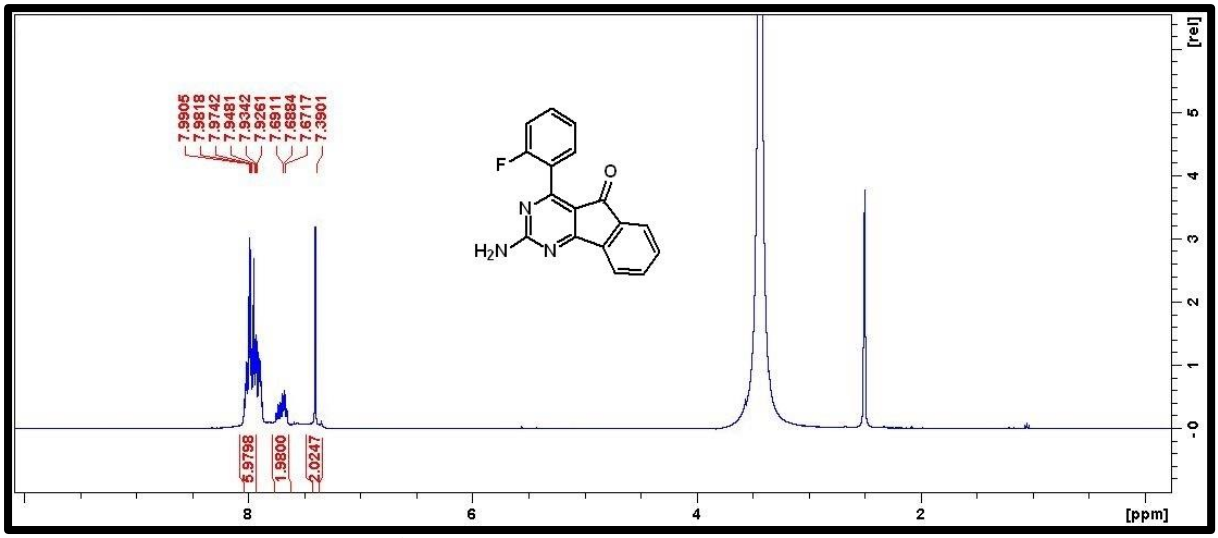

^{1}H NMR spectra of compound **4f**

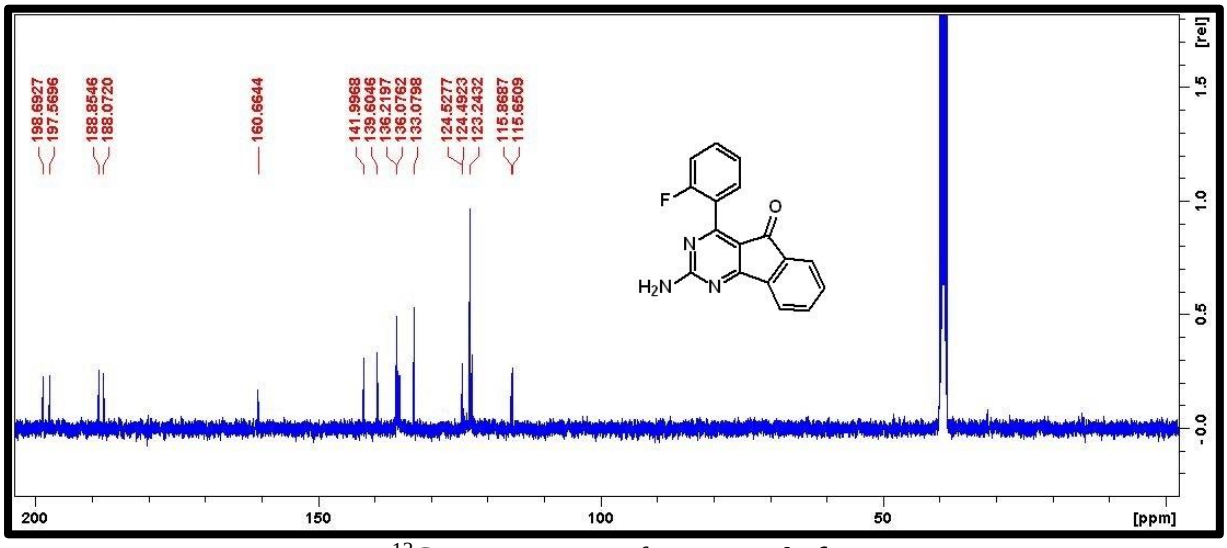

^{13}C NMR spectra of compound **4f**

Elemental Composition Report **Page 1**

Single Mass Analysis
Tolerance = 5.0 PPM / DBE: min = -1.5, max = 100.0
Element prediction: Off
Number of isotope peaks used for i-FIT = 3

Monoisotopic Mass, Even Electron Ions
71 formula(e) evaluated with 1 results within limits (up to 20 closest results for each mass)
Elements Used:
C: 15-20 H: 10-15 N: 0-5 O: 0-5 F: 0-1
S13 3 (0.068) Cm (1:61)
TOF MS ES-

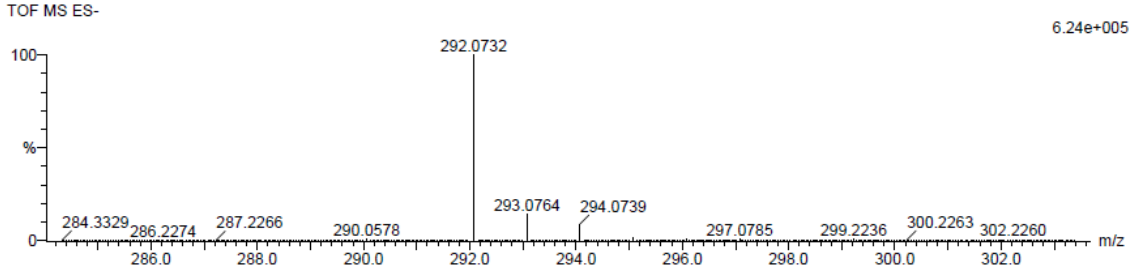

Minimum:				-1.5			
Maximum:		5.0	5.0	100.0			
Mass	Calc. Mass	mDa	PPM	DBE	i-FIT	i-FIT (Norm)	Formula
292.0732	292.0732	0.0	0.0	5.5	721.3	0.0	C17 H11 N3 O F

HRMS spectra of compound **4f**

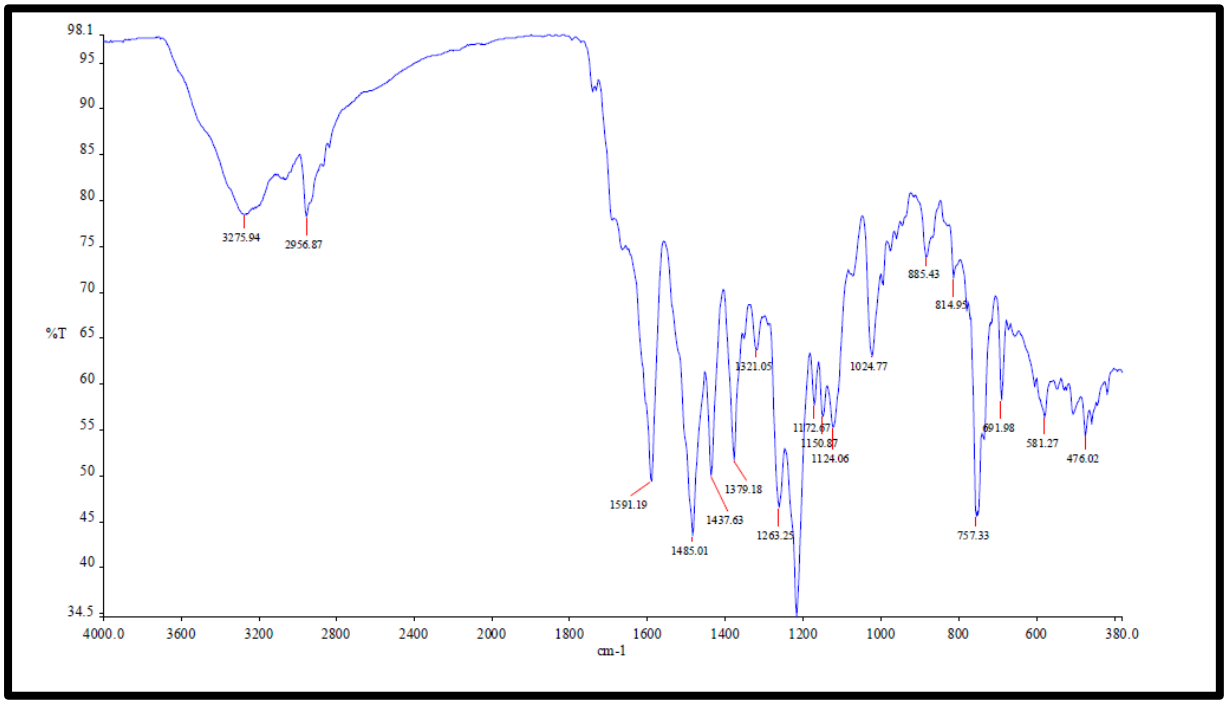

FT-IR spectra of compound **4f**

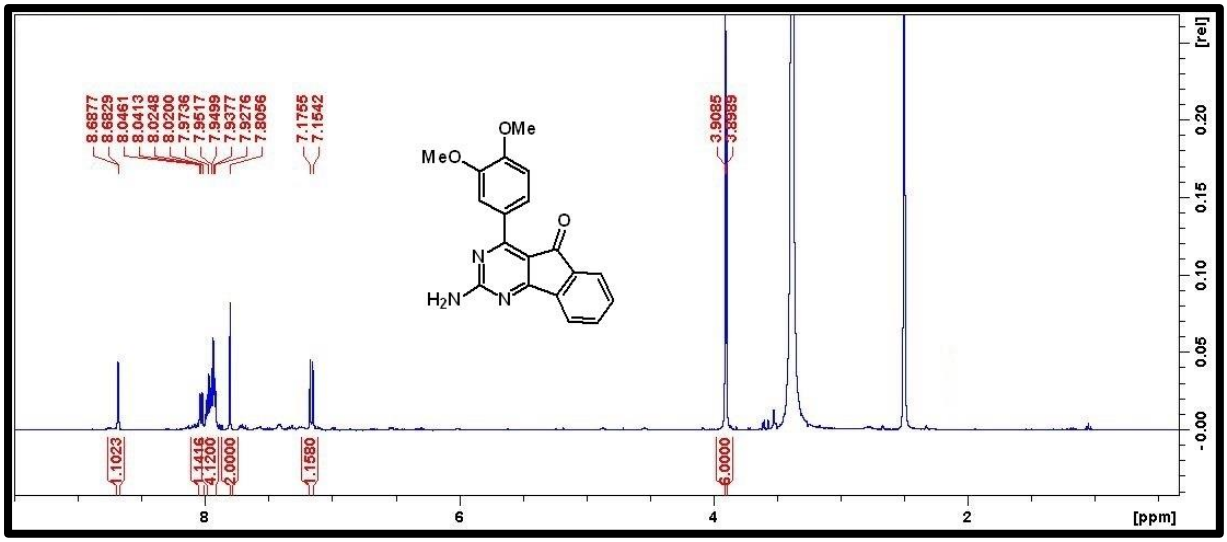

FT-IR spectra of compound **4g**

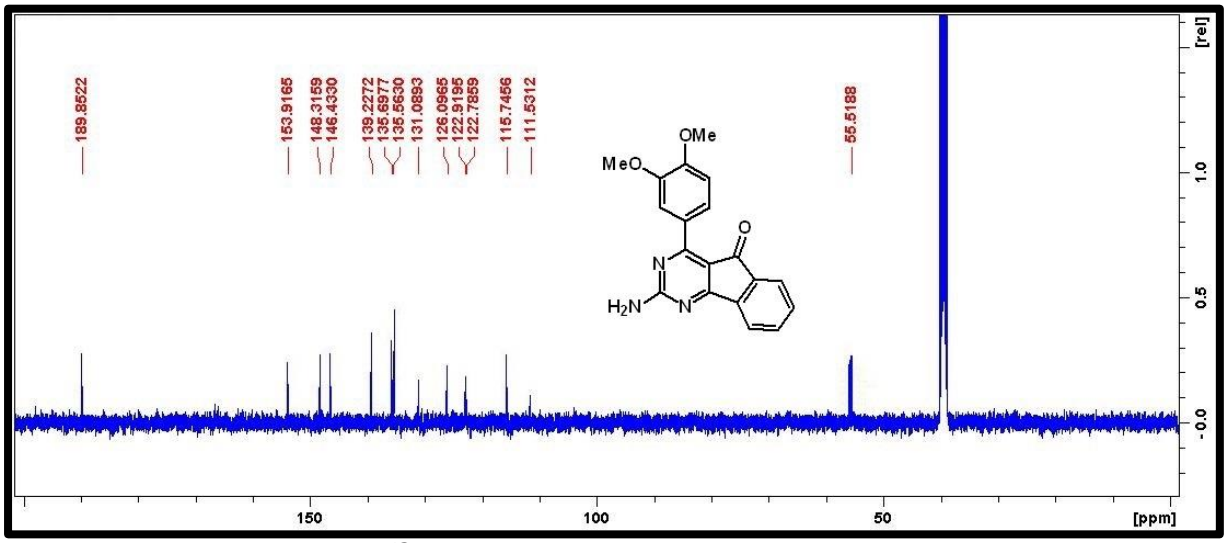

^{13}C NMR spectra of compound **4g**

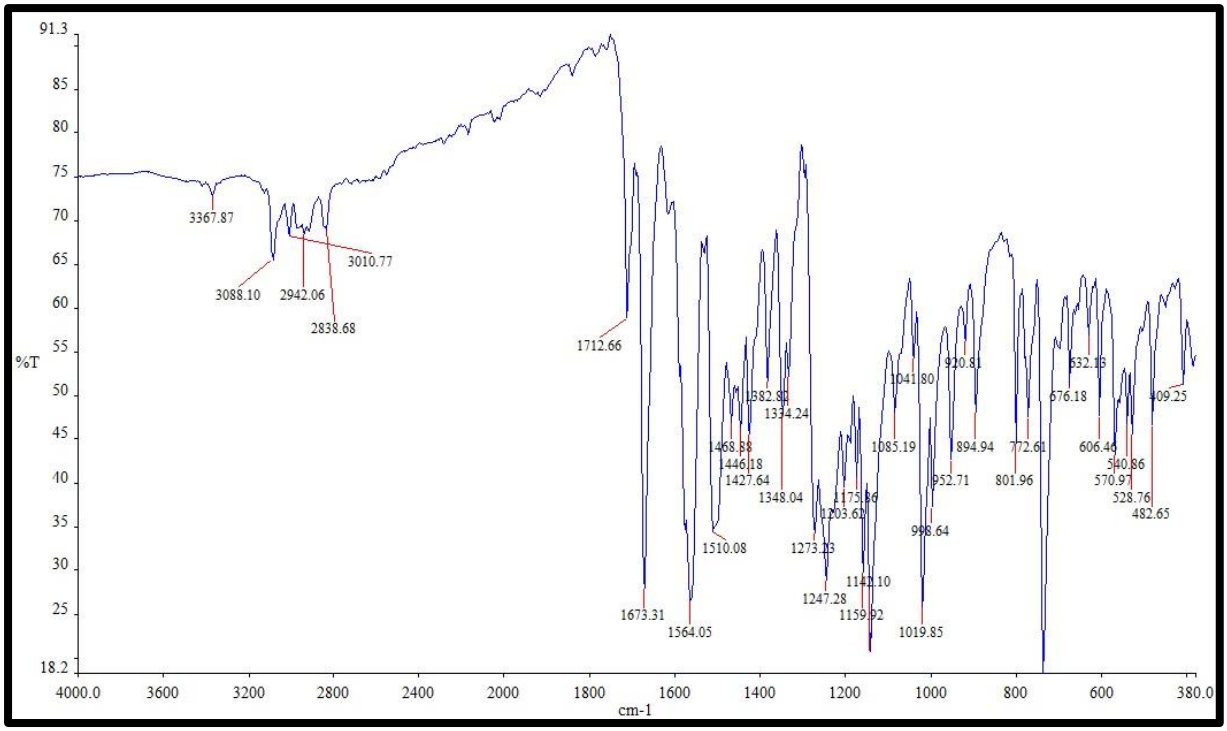

FT-IR spectra of compound **4g**

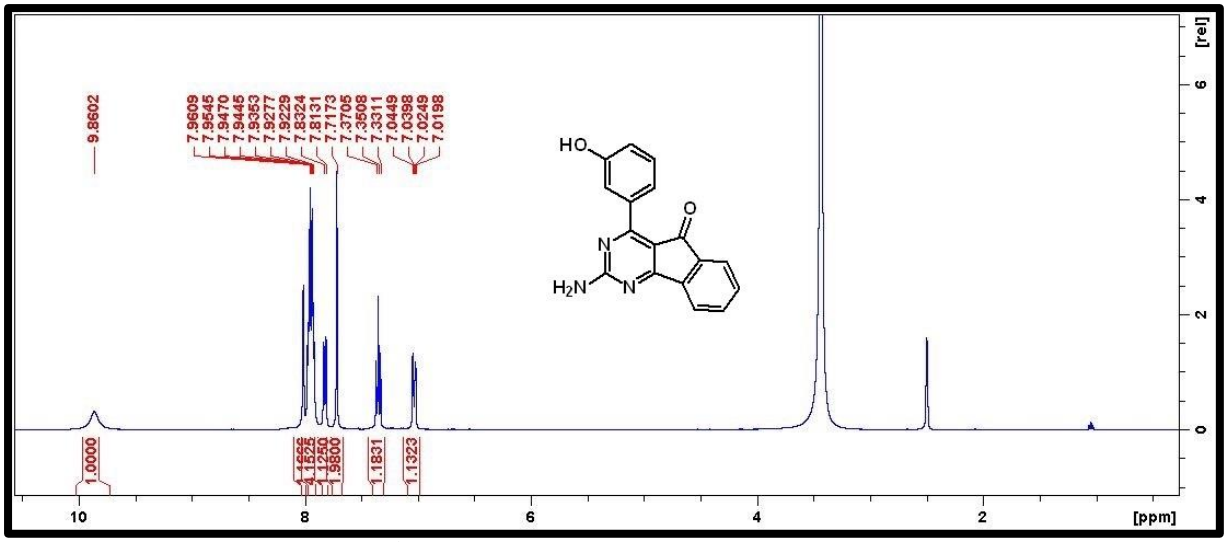

^{1}H NMR spectra of compound **4h**

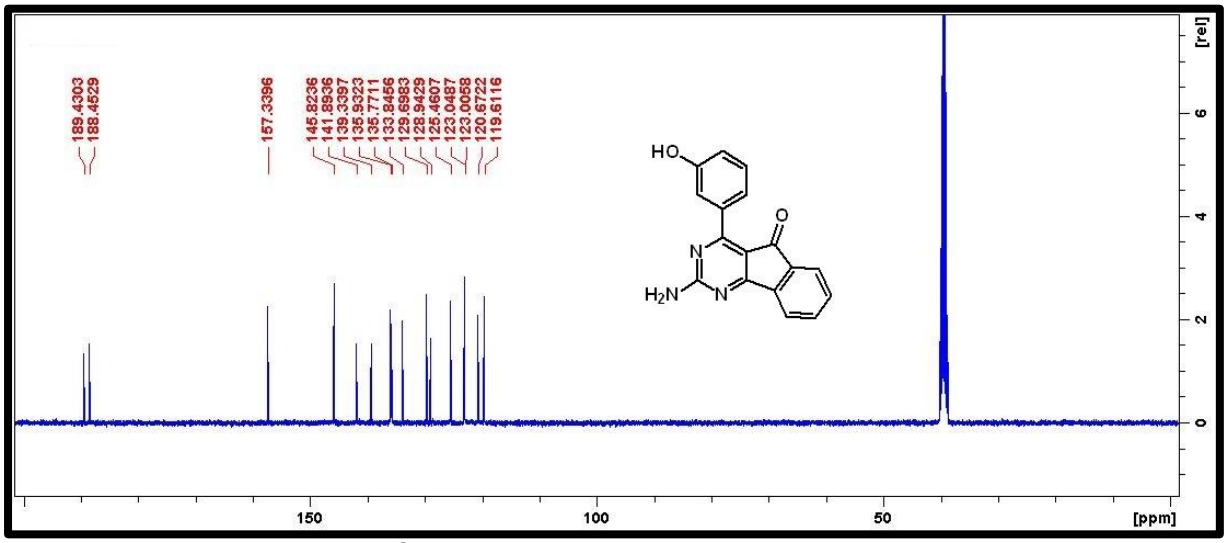

^{13}C NMR spectra of compound **4h**

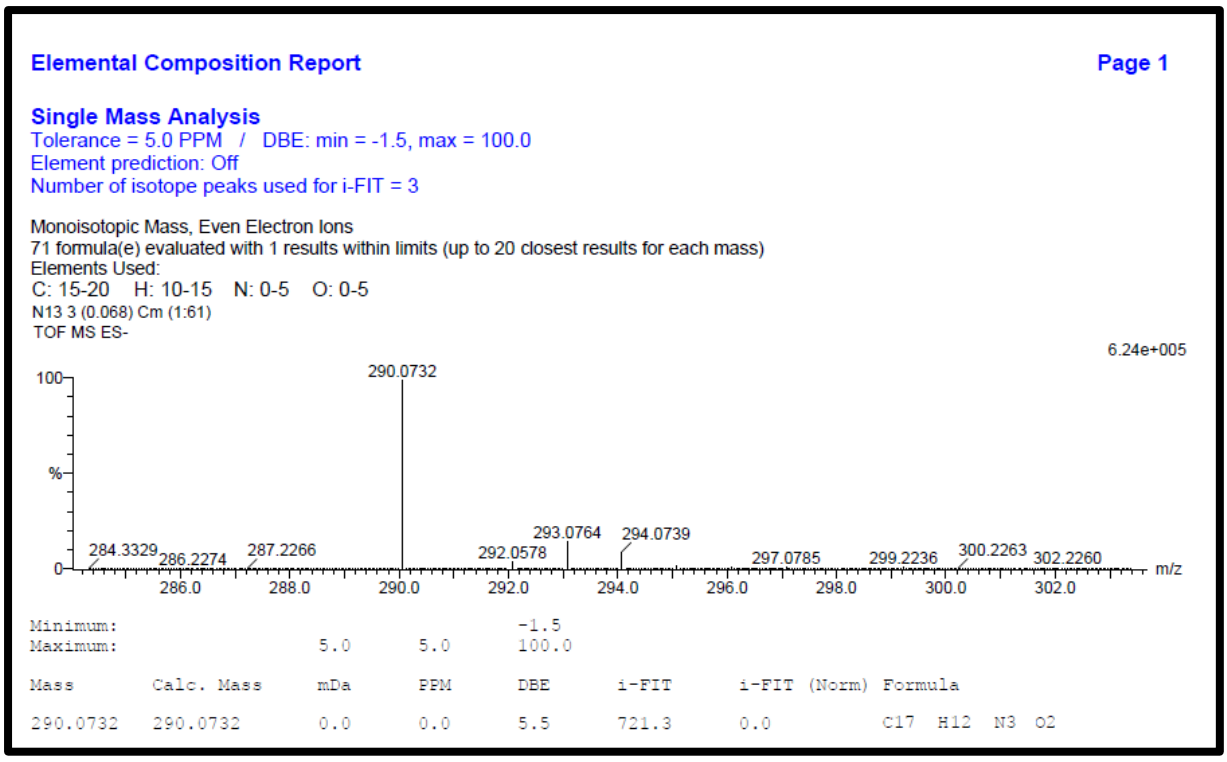

HRMS spectra of compound **4h**

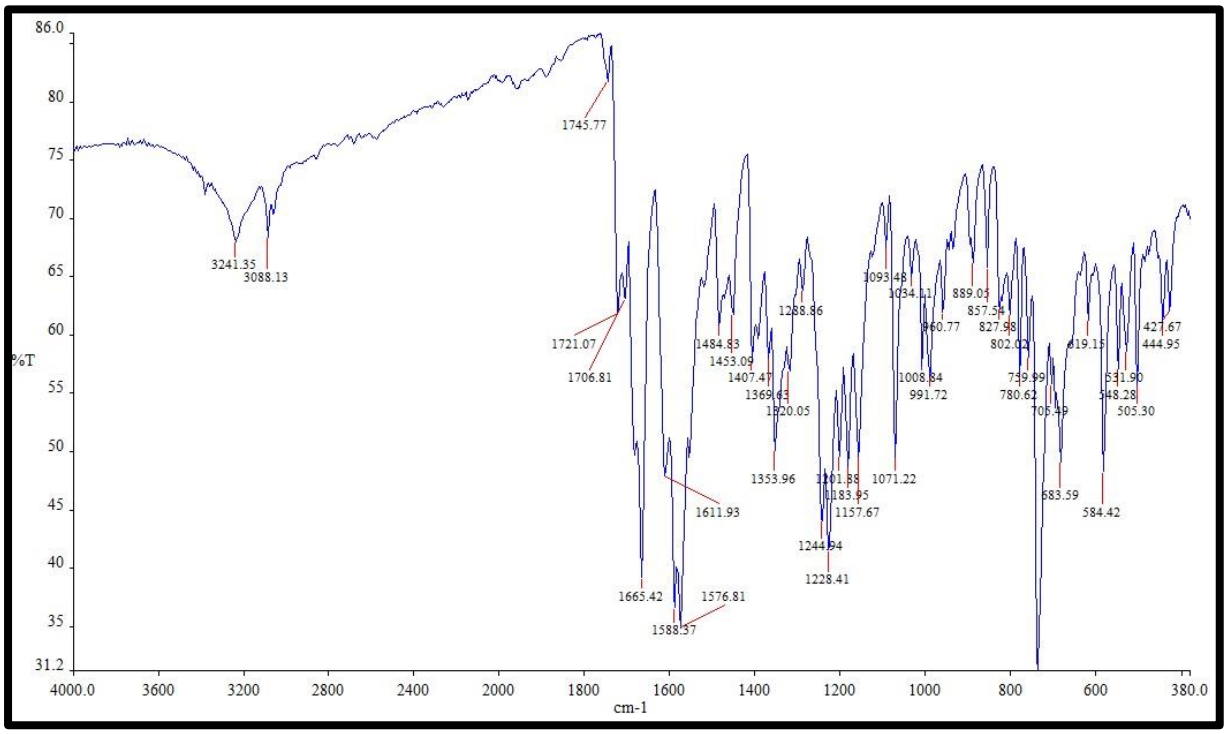

FT-IR spectra of compound **4h**

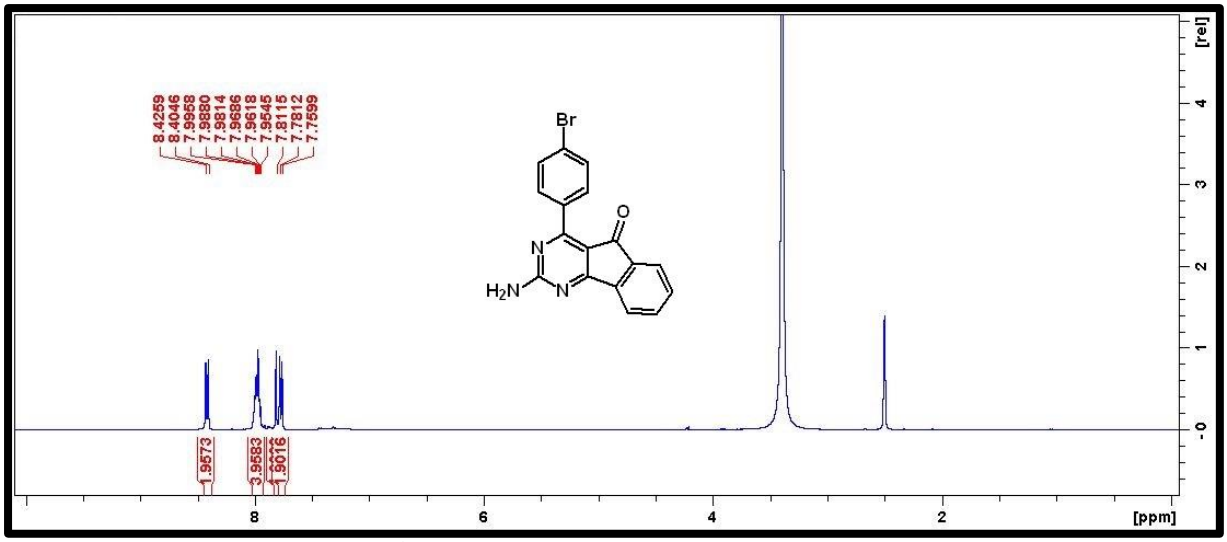

^{1}H NMR spectra of compound **4i**

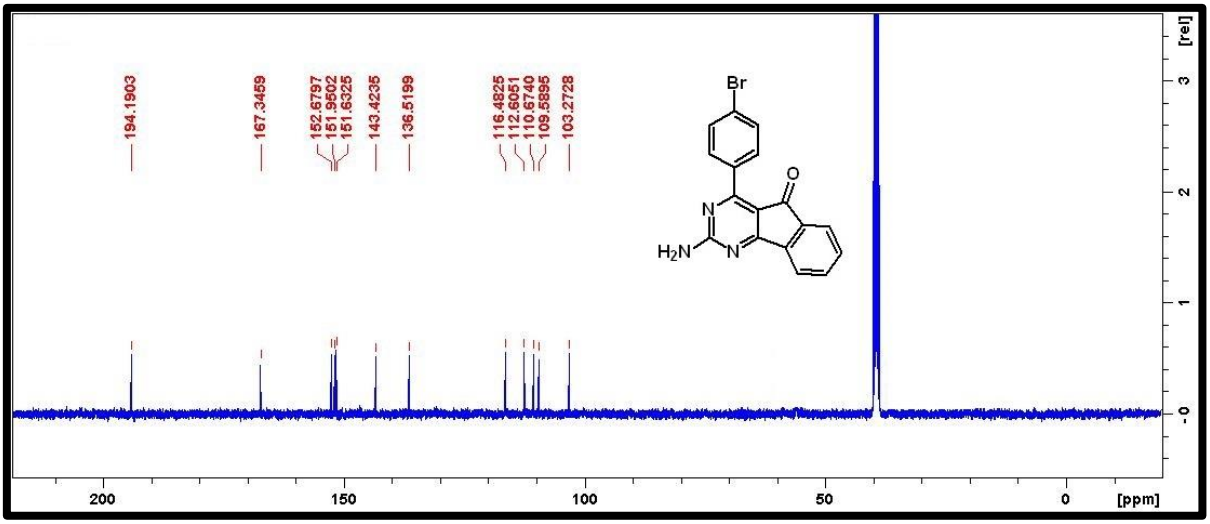

^{13}C NMR spectra of compound **4i**

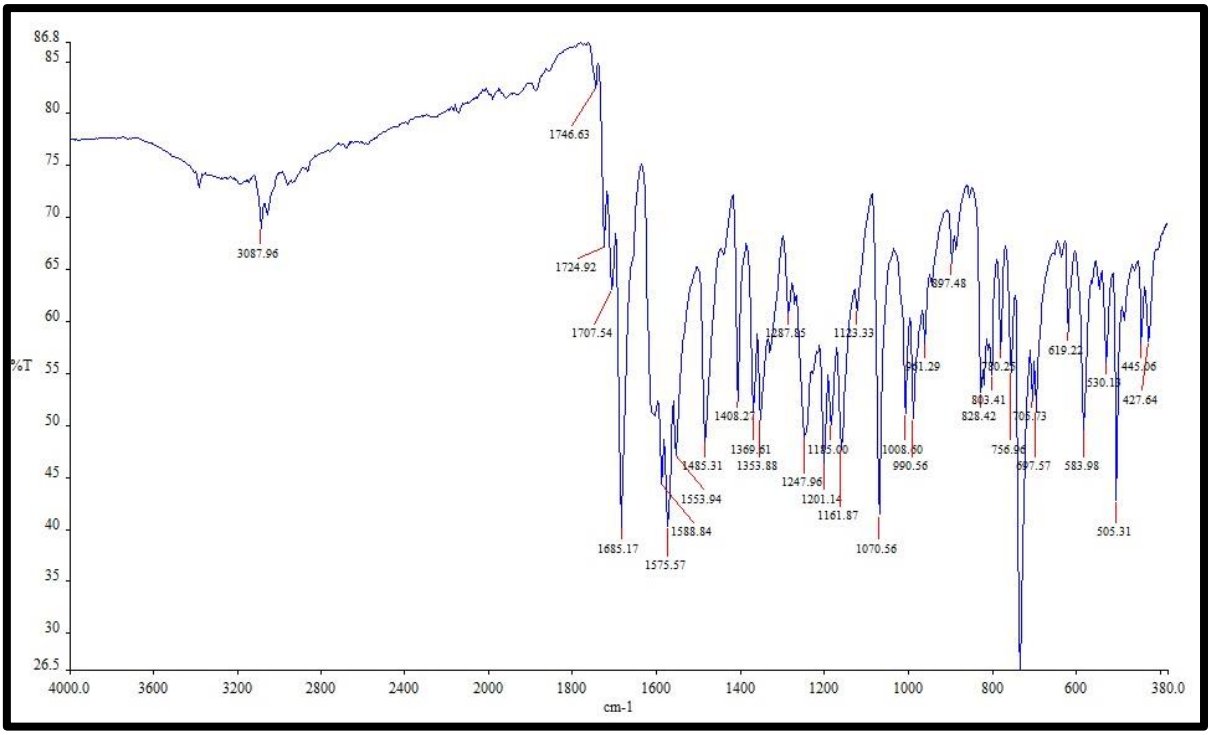

FT-IR spectra of compound **4i**

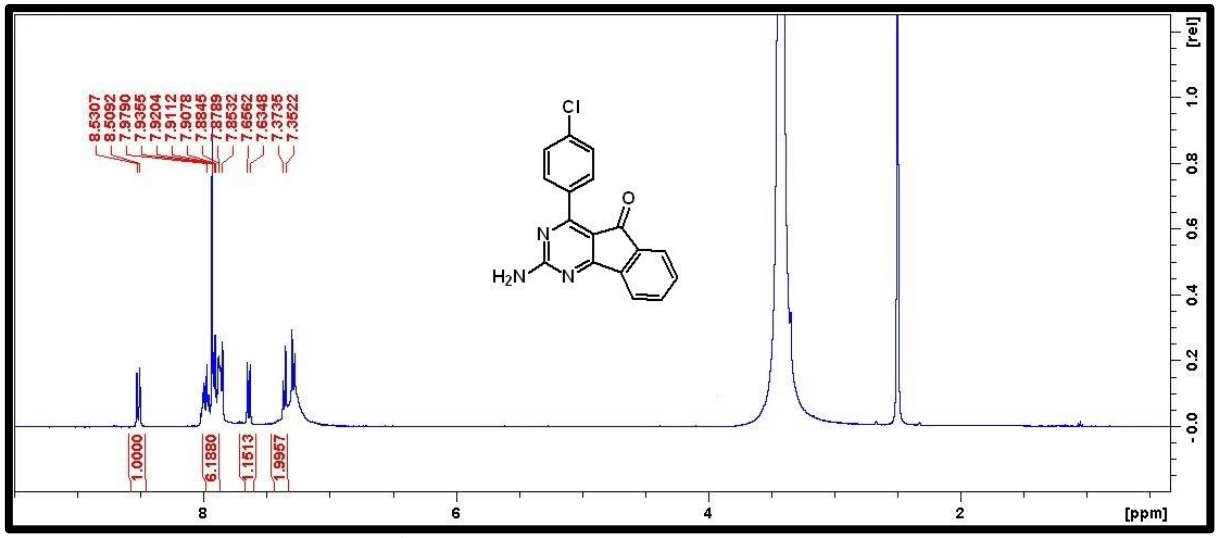

^{1}H NMR spectra of compound **4j**

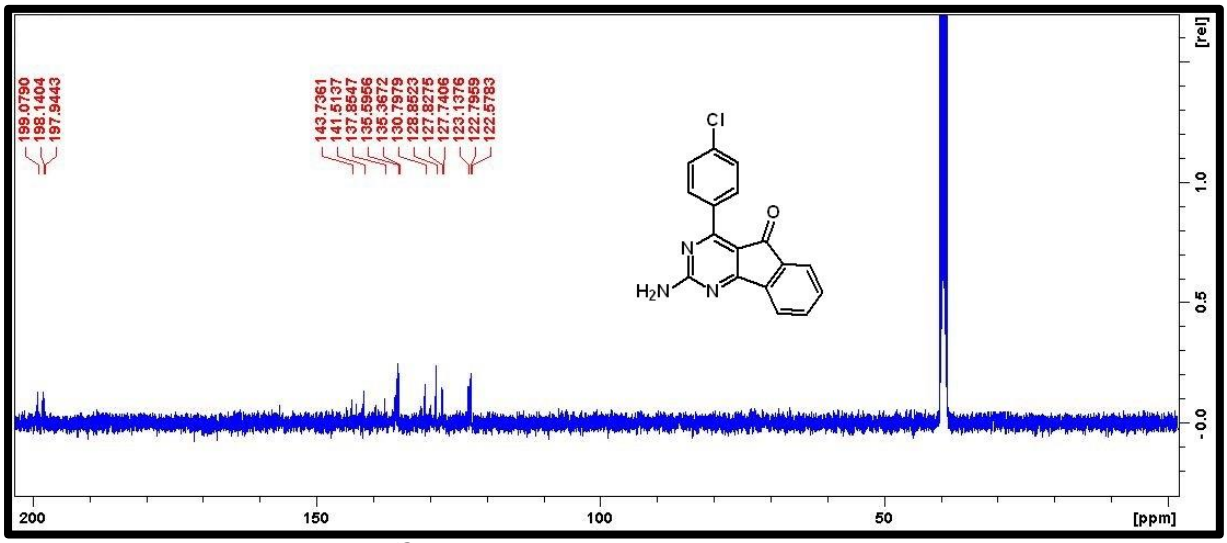

^{13}C NMR spectra of compound **4j**

Elemental Composition Report **Page 1**

Single Mass Analysis
Tolerance = 5.0 PPM / DBE: min = -1.5, max = 100.0
Element prediction: Off
Number of isotope peaks used for i-FIT = 3

Monoisotopic Mass, Even Electron Ions
9 formula(e) evaluated with 1 results within limits (up to 20 closest results for each mass)
Elements Used:
C: 15-20 H: 10-15 N: 0-5 O: 0-5 Cl: 1-1
S9 22 (0.709) Cm (1:61)
TOF MS ES-

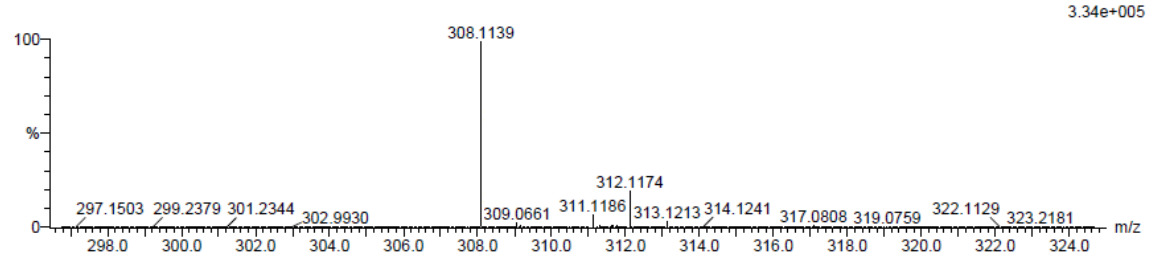

Minimum:				-1.5			
Maximum:		5.0	5.0	100.0			
Mass	Calc. Mass	mDa	PPM	DBE	i-FIT	i-FIT (Norm)	Formula
308.1139	308.1144	-0.5	-1.6	11.5	691.8	0.0	C17 H11 N3 O Cl

HRMS spectra of compound **4j**

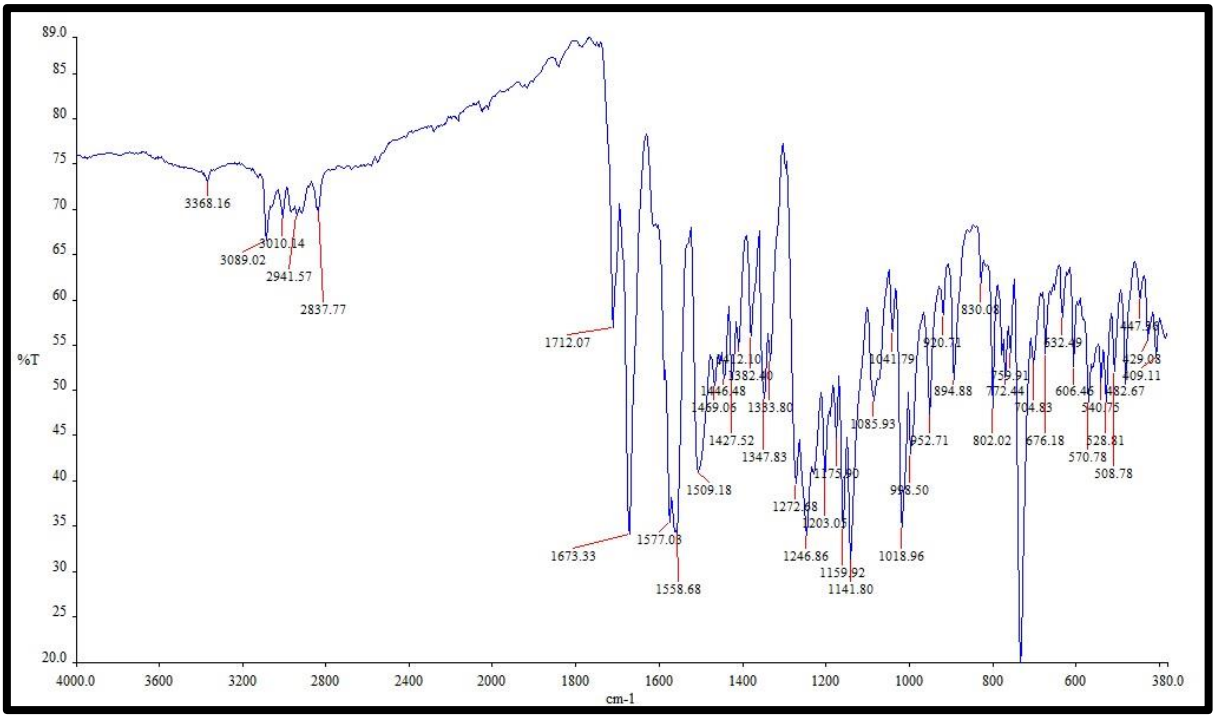

FT-IR spectra of compound **4j**

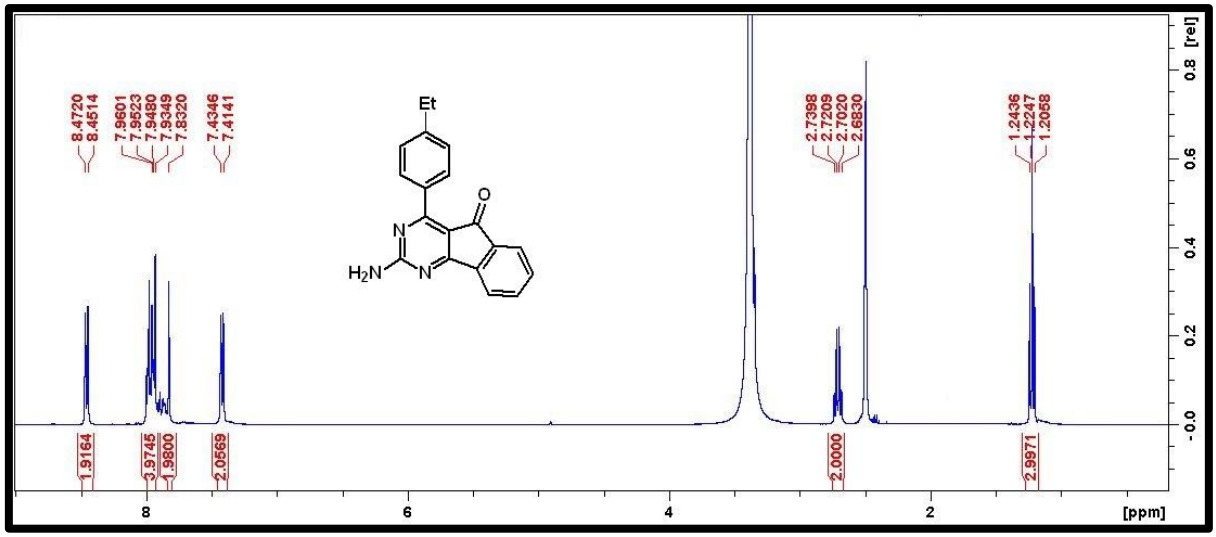

^{1}H NMR spectra of compound **4k**

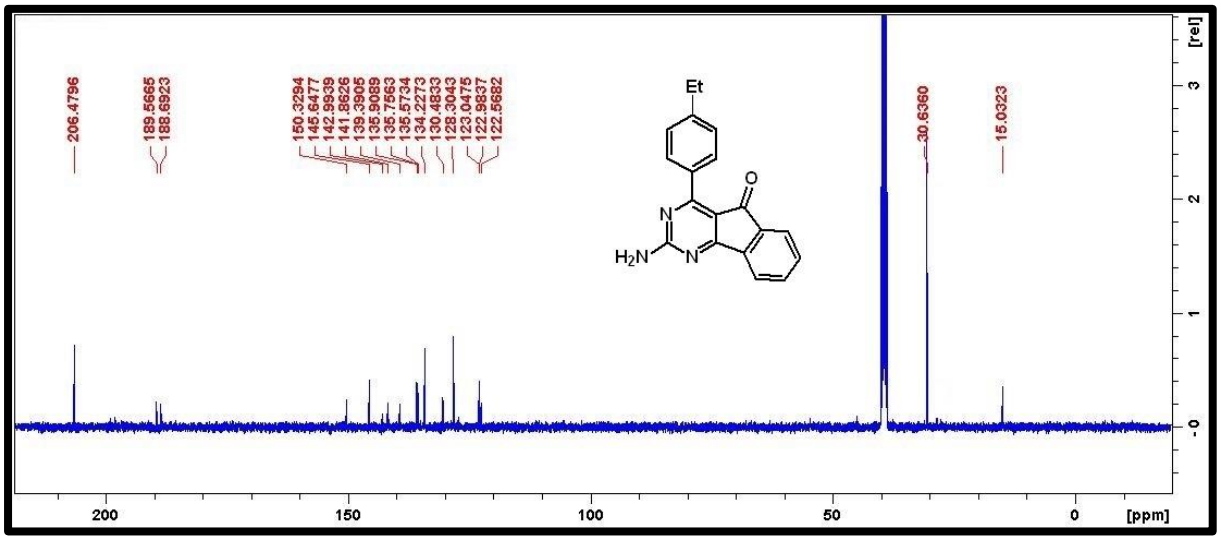

^{13}C NMR spectra of compound **4k**

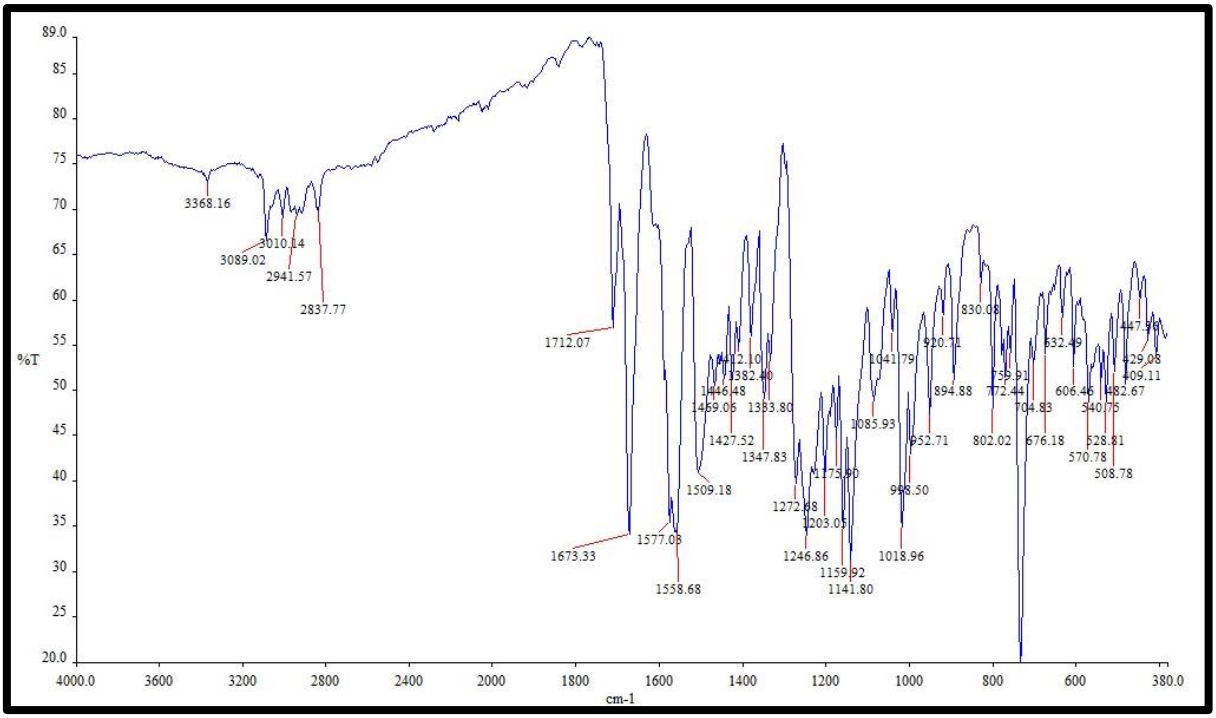

FT-IR spectra of compound **4k**

Chapter 6

A green protocol for the synthesis of new 1,4-dihydropyridine derivatives using Fe_2O_3/ZrO_2 as a reusable catalyst

Sandeep V.H.S. Bhaskaruni, Suresh Maddila, Werner E. van Zyl and Sreekantha B. Jonnalagadda*

*School of Chemistry & Physics, University of KwaZulu-Natal, Westville Campus, Chiltern Hills, Durban-4000, South Africa

*Corresponding Author: Prof. Sreekantha B. Jonnalagadda
School of Chemistry & Physics,
University of KwaZulu-Natal,
Durban 4000, South Africa.
Tel.: +27 31 2607325,
Fax: +27 31 2603091
E-mail address: jonnalagaddas@ukzn.ac.za

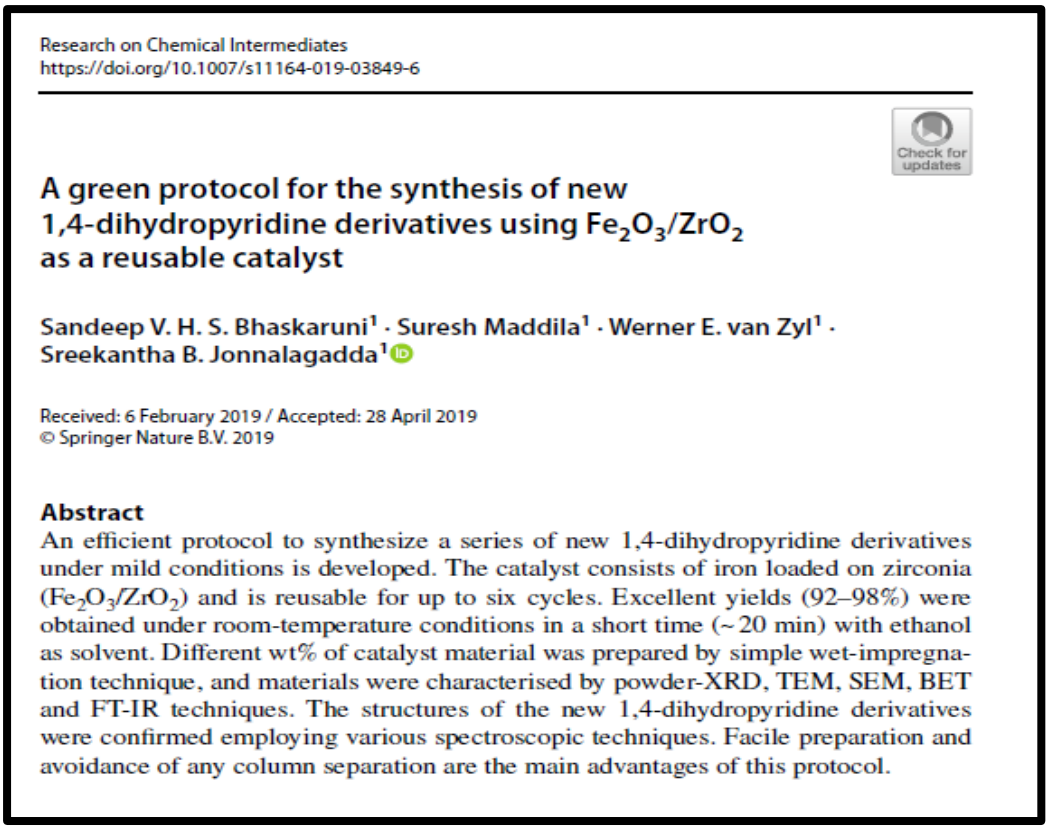

Research on Chemical Intermediates
https://doi.org/10.1007/s11164-019-03849-6

Check for updates

A green protocol for the synthesis of new 1,4-dihydropyridine derivatives using Fe_2O_3/ZrO_2 as a reusable catalyst

Sandeep V. H. S. Bhaskaruni[1] · Suresh Maddila[1] · Werner E. van Zyl[1] · Sreekantha B. Jonnalagadda[1]

Received: 6 February 2019 / Accepted: 28 April 2019

Abstract
An efficient protocol to synthesize a series of new 1,4-dihydropyridine derivatives under mild conditions is developed. The catalyst consists of iron loaded on zirconia (Fe_2O_3/ZrO_2) and is reusable for up to six cycles. Excellent yields (92–98%) were obtained under room-temperature conditions in a short time (~20 min) with ethanol as solvent. Different wt% of catalyst material was prepared by simple wet-impregnation technique, and materials were characterised by powder-XRD, TEM, SEM, BET and FT-IR techniques. The structures of the new 1,4-dihydropyridine derivatives were confirmed employing various spectroscopic techniques. Facile preparation and avoidance of any column separation are the main advantages of this protocol.

This chapter is published in the journal, **Research on Chemical Intermediates**, and has been structured according to the journal's format.

A green protocol for the synthesis of new 1,4-dihydropyridine derivatives using Fe_2O_3/ZrO_2 as a reusable catalyst

Sandeep V.H.S. Bhaskaruni, Suresh Maddila, Werner E. van Zyl and Sreekantha B. Jonnalagadda*

*School of Chemistry & Physics, University of KwaZulu-Natal, Westville Campus, Chiltern Hills, Durban-4000, South Africa

*Corresponding Author: Prof. Sreekantha B. Jonnalagadda
School of Chemistry & Physics,
University of KwaZulu-Natal,
Durban 4000, South Africa.
Tel.: +27 31 2607325,
Fax: +27 31 2603091
E-mail address: jonnalagaddas@ukzn.ac.za

Abstract:

An efficient protocol to synthesize a series of new 1,4-dihydropyridine derivatives under mild conditions is developed. The catalyst consists of iron loaded on zirconia (Fe_2O_3/ZrO_2) and is reusable for up to six cycles. Excellent yields (92–98%) were obtained under room-temperature conditions in a short time (~ 20 min) with ethanol as solvent. Different wt% of catalyst material was prepared by simple wet-impregnation technique, and materials were characterised by powder-XRD, TEM, SEM, BET and FT-IR techniques. The structures of the new 1,4-dihydropyridine derivatives were confirmed employing various spectroscopic techniques. Facile preparation and avoidance of any column separation are the main advantages of this protocol.

6.1 Introduction

The design and development of efficient protocols for synthesis of bio-active scaffolds with excellent yields under green conditions using recyclable materials is a challenge [1]. Multicomponent reactions (MCRs) are good strategies involving single- pot reactions to afford the targeted molecules with high functional group tolerance [2]. When compared to linear and convergent synthetic methods, MCRs are advantageous due to high atom economy and short reaction times, as both are the sought-after green parameters in synthesis. Thus, MCRs offer a powerful tool for preparation of complex heterocyclic molecules [3].

Green chemistry, in the context of synthetic procedures, focuses on the use of materials and reaction conditions that do not have a negative impact on human health and the environment [4]. Eco-friendly processes and reusable materials, the two main goals of green synthesis, have motivated the use of heterogeneous catalysts in various MCRs [5, 6]. Heterogeneous catalysts are crucial for efficiency in various MCRs, due to the active phase and support interactions. The surface and interfacial free energies are responsible for such interactions. [7, 8]. In the MCRs, zirconia-based materials as catalysts have gained importance in MCR reactions due to their unique properties, such as thermal stability, high porosity, less corrosion, low cost, ease of recovery and recyclability [9–11]. Zirconia has been solely used as catalyst in many reactions, including C–C bond formation [12], epoxidation [13, 14] and isomerization [9]. The even distribution of the active material on the surface of zirconia makes it an ideal support for various applications. The active catalyst material needs to provide not only the active sites, but also large surface area and increased mechanical strength [15, 16].

Iron is a non-toxic, earth-abundant metal which plays a crucial role in human health and also in many organic transformations [17, 18]. It acts as a nucleophile in the lower oxidation states, and catalyses a variety of transformations like nucleophilic substitutions [19], hydrogenation/hydro-silylation [20, 21], cyclo-isomerization reactions [22] and C–C and C–heteroatom bond-forming reactions [23]. Although iron-loaded ZrO_2 has been reported as a catalyst for some reactions [24,25], Fe_2O_3/ZrO_2 as a catalyst in an MCR synthesis protocol is demonstrated for the first time in this communication.

Substituted dihydropyridines are a class of calcium channel blockers and are known for an wide range of biological activities, including anti-cancer [29] and anti-tubercular properties [30]. In the recent past, a few reviews have been dedicated towards the synthetic methods of producing various dihydropyridine derivatives [26–28]. The literature also reveals various methods for the synthesis of substituted 1,4-dihydropyridine derivatives using different

catalysts. Such materials include $MIIZr_4(PO_4)_6$ [31], zirconocene bis(perfluorobutanesulphonate) [32], sulphated polyborate [33], silica-functionalized sulphonic acid coated with ionic liquid [34], chitosan-supported oxo-vanadium [35], sulphated boric acid nanoparticles [36], DBU [37], nicotinic acid [38] γ-Fe_2O_3/Cu@cellulose [39], SBA-15@AMPDCo[40], Fe_3O_4@ D-NH-$(CH_2)_4$-SO_3H [41] and Cu-adenine@boehmite [42]. However, many of the reported methodologies suffer from either low yields, demand for expensive chemicals, prolonged reaction times or extreme conditions. In this study, we report the synthesis and characterization of Fe_2O_3/ZrO_2 and its catalytic activityin synthesis of 1,4-dihydropyridine derivatives.

6.2 Experimental Section

6.2.1 Catalyst preparation

A simple wet impregnation technique was adopted to synthesize a series of different wt% (1, 2.5, 5.0) iron-loaded zirconia materials. The method involved mixing of zirconium oxide (ZrO_2, 2 g, Alfa Aesar) and appropriate amounts (wt%) of iron nitrate [$Fe(NO_3)_3 \cdot 9H_2O$, Alfa Aesar] in deionised water (50 mL), while stirring at room temperature (RT) for 7 h. The resultant slurry was filtered by vacuum and kept in an oven at 120 °C for 5 h, and further calcined at 450 °C for 4 h in the presence of air to afford materials of different wt% of Fe_2O_3/ZrO_2.

6.2.2 Synthesis of novel 1,4‑dihydropyridine derivatives (5a-j)

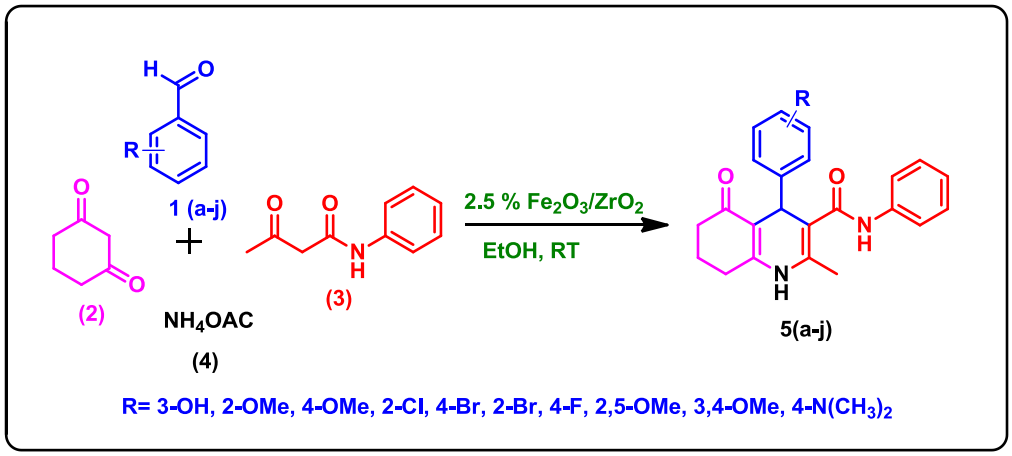

Scheme 1: Synthesis of new 1,4-dihydropyridine derivatives.

To evaluate the activity of the prepared Fe_2O_3/ ZrO_2 as catalyst, a one-pot reaction was performed using the chosen aromatic aldehyde (1 mmol) (1), 1,3-cyclohexadione (1 mmol) (2),

acetoaccetanilide (1 mmol) (3) and ammonium acetate (1 mmol) (4). The reaction mixture and 45 mg of Fe_2O_3/ ZrO_2 catalyst were added to 5 mL of ethanol in a 25-mL reaction flask, and stirred at RT for 20 min (Scheme 1). Thin-layer chromatography (TLC) was used to monitor the reaction progress. Catalyst was separated from the reaction mixture by simple filtration. The product was extracted with ethylacetate, and the solvent was evaporated under reduced pressure to obtain the crude product. The crude product was recrystallized from ethanol to obtain the pure target compound, which was characterised by various spectral techniques.

4-(3-hydroxyphenyl)-2-methyl-5-oxo-N-phenyl-1,4,5,6,7,8-hexahydroquinoline-3-carboxamide(5a): ^{1}H NMR (400 MHz, DMSO-d_6): δ= 1.75-1.94 (m, 2H, CH_2), 2.03 (s, 3H, CH_3), 2.19-2.22 (m, 2H, CH_2), 2.42-2.49 (m, 2H, CH_2), 4.90 (s, 1H, CH), 6.45-6.48 (m, 1H, Ar-H), 6.60 (t, *J*= 6.88 Hz, 2H, Ar-H), 6.93-7.01 (m, 2H, Ar-H), 7.24 (d, *J*= 7.68 Hz, 2H, Ar-H), 7.56 (d, *J* = 7.8 Hz, 2H, Ar-H), 8.74 (s, 1H, NH), 9.11 (s, 1H, NH), 9.50 (s, 1H, NH); ^{13}C NMR (100 MHz, DMSO-d_6): 16.97, 20.86, 26.44, 36.86, 37.63, 108.92, 111.02, 112.67, 114.37, 118.05, 119.59, 122.88, 128.42, 128.71, 134.52, 139.37, 148.47, 152.36, 157.00, 167.50, 194.10; ^{15}N NMR (40.55 MHz, DMSO-d_6) δ= 123.8, 134.3 ;HRMS of [$C_{23}H_{22}N_2O_3$+Na^+] (m/z): 397.1546; Calcd.: 397.1528.

4-(2-methoxyphenyl)-2-methyl-5-oxo-N-phenyl-1,4,5,6,7,8-hexahydroquinoline-3-carboxamide(5b):^{1}H NMR (400 MHz, DMSO-d_6): δ= 1.70-1.90 (m, 2H, CH_2), 1.95 (s, 3H, CH_3), 2.17-2.21 (m, 2H, CH_2), 2.54-2.60 (m, 2H, CH_2), 3.71 (s, 3H, -OCH_3), 5.22 (s, 1H, CH), 6.82 (d, *J*= 7.12 Hz, 2H, Ar-H), 6.99 (dd, *J* = 6.56 Hz, *J* = 5.96 Hz, 2H, Ar-H), 7.03-7.07 (m, 1H, Ar-H), 7.25 (t, *J* = 7.72 Hz, 2H, Ar-H), 7.61 (d, *J* = 7.88 Hz, 2H, Ar-H), 8.70 (s, 1H, NH), 9.44 (s, 1H, NH); ^{13}C NMR (100 MHz, DMSO-d_6): δ= 16.83, 21.06, 26.51,31.21, 36.95, 55.59, 108.36, 110.89, 111.11, 119.21, 120.63, 122.55, 126.89, 128.23, 128.38, 134.17, 135.42, 139.80, 153.13, 155.62, 167.27, 193.72; ^{15}N NMR (40.55 MHz, DMSO-d_6) δ= 124.6, 132.5; HRMS of [$C_{24}H_{24}N_2O_3$+Na^+] (m/z): 411.0985; Calcd.: 411.0983.

4-(4-methoxyphenyl)-2-methyl-5-oxo-N-phenyl-1,4,5,6,7,8-hexahydroquinoline-3-carboxamide(5c): ^{1}H NMR (400 MHz, DMSO-d_6): δ= 1.87-1.93 (m, 2H, CH_2), 2.03 (s, 3H, CH_3), 2.13-2.25 (m, 2H, CH_2), 2.40-2.47 (m, 2H, CH_2), 3.65 (s, 3H, -OCH_3), 4.92 (s, 1H, CH), 6.73 (d, *J*= 8.52 Hz, 2H, Ar-H), 6.98 (t, *J*= 7.28 Hz, 1H, Ar-H), 7.07 (d, *J*= 8.48 Hz, 2H, Ar-H), 7.23 (t, *J*= 7.68 Hz, 2H, Ar-H), 7.55 (d, *J*= 8Hz, 2H, Ar-H), 8.71 (s, 1H, NH), 9.48 (s, 1H, NH); ^{13}C NMR (100 MHz, DMSO-d_6): δ=17.00, 20.90, 26.40, 36.90, 54.84, 109.34, 111.09, 113.27, 114.49, 119.52, 122.82, 128.30, 128.40, 134.54, 138.30, 139.39, 152.03, 157.29,

167.48, 194.00; ^{15}N NMR (40.55 MHz, DMSO-d_6) δ= 123.7, 134.3; [$C_{24}H_{24}N_2O_3$+Na^+] (m/z): 411.1684; Calcd.: 411.1685.

4-(2-chlorophenyl)-2-methyl-5-oxo-N-phenyl-1,4,5,6,7,8-hexahydroquinoline-3-carboxamide(5d): ^{1}H NMR (400 MHz, DMSO-d_6): δ= 1.76-1.87 (m, 2H, CH_2), 1.91 (s, 3H, CH_3), 2.12-2.19 (m, 2H, CH_2), 2.51-2.57 (m, 2H, CH_2), 5.33 (s, 1H, CH), 6.95-6.99 (m, 1H, Ar-H), 7.06-7.08 (m, 1H, Ar-H), 7.16-7.24 (m, 5H, Ar-H), 7.52 (s, 1H, Ar-H), 7.54 (d, *J* = 1.04 Hz, 1H, Ar-H), 8.76 (s, 1H, NH), 9.67 (s, 1H, NH); ^{13}C NMR (100 MHz, DMSO-d_6):δ=18.51, 21.02, 26.27, 33.37, 56.00, 109.62, 114.21, 119.45, 123.01, 126.90, 128.41, 128.57, 131.30, 133.07, 135.88, 141.22, 147.84, 152.33, 166.31, 171.98, 193.74.^{15}N NMR (40.55 MHz, DMSO-d_6) δ=122.1, 133.7; HRMS of [$C_{23}H_{21}N_2O_2Cl$+Na^+] (m/z): 415.1188; Calcd.:415.1189.

***4-(4-bromophenyl)-2-methyl-5-oxo-N-phenyl-1,4,5,6,7,8-hexahydroquinoline-3-carboxamide(5e)*:** ^{1}H NMR (400 MHz, DMSO-d_6): δ= 1.79-1.92 (m, 2H, CH_2), 2.03 (s, 3H, CH_3), 2.19 (t, *J*= 10 Hz, 2H, CH_2), 2.78-3.03 (m, 2H, CH_2), 4.96 (s, 1H, CH), 6.99 (t, *J*= 7.32 Hz, 1H, Ar-H), 7.11 (d, *J*= 8.36Hz, 2H, Ar-H), 7.23 (t, *J*= 7.68 Hz, 2H, Ar-H), 7.37 (d, *J*= 8.36 Hz, 2H, Ar-H), 7.54 (d, *J*= 7.8 Hz, 2H, Ar-H), 8.81 (s, 1H, NH), 9.58 (s, 1H, NH); ^{13}C NMR (100 MHz, DMSO-d_6): δ=16.99, 20.84, 26.39, 37.54, 55.99, 108.62, 110.43, 118.70, 119.60, 122.96, 128.42, 129.62, 130.72, 134.88, 139.28, 146.40, 152.54, 167.20, 194.00; ^{15}N NMR (40.55 MHz, DMSO-d_6) δ= 125.4, 133.8; HRMS of [$C_{23}H_{21}N_2O_2Br$+Na^+] (m/z): 459.0689; Calcd.: 459.0684.

4-(2-bromophenyl)-2-methyl-5-oxo-N-phenyl-1,4,5,6,7,8-hexahydroquinoline-3-carboxamide(5f): ^{1}H NMR (400 MHz, DMSO-d_6): δ= 1.84-1.88 (m, 2H, CH_2), 1.90 (s, 3H, CH_3), 2.13 (t, *J*=6.16Hz, 2H, CH_2), 2.43 (t, *J*= 5.28 Hz, 2H, CH_2), 5.28 (s, 1H, CH), 7.00-7.04 (m, 2H, Ar-H), 7.20-7.25 (m, 4H, Ar-H), 7.34 (d, *J*= 7.88 Hz, 1H, Ar-H), 7.53 (d, *J*= 7.8Hz, 2H, Ar-H), 8.75 (s, 1H, NH), 9.68 (s, 1H, NH); ^{13}C NMR (100 MHz, DMSO-d_6): δ=16.43, 20.52, 28.42, 36.69, 56.19, 101.10, 109.23, 110.70, 111.63, 119.52, 121.93, 126.22, 127.21, 128.33, 131.71, 132.58, 139.40, 142.20, 152.90, 166.87, 193.54; ^{15}N NMR (40.55 MHz, DMSO-d_6) δ= 120.1, 130.1.

4-(4-fluorophenyl)-2-methyl-5-oxo-N-phenyl-1,4,5,6,7,8-hexahydroquinoline-3-carboxamide(5g): ^{1}H NMR (400 MHz, DMSO-d_6): δ= 1.87-1.94 (m, 2H, CH_2), 2.04 (s, 3H, CH_3), 2.17-2.21 (m, 2H, CH_2), 2.34-2.42 (t, 2H, CH_2), 4.98 (s, 1H, CH), 6.91-7.01 (M, 3h, Ar-H), 7.16-7.25 (m, 4H, Ar-H), 7.54 (d, *J*= 7.8 Hz, 2H, Ar-H), 8.78 (s, 1H, NH), 9.55 (s, 1H, NH); ^{13}C NMR (100 MHz, DMSO-d_6): δ=17.00, 20.85, 26.39, 36.79, 37.18, 108.95, 110.78, 114.37, 114.58, 119.58, 122.91, 128.41, 129.07, 134.75, 139.312, 143.25, 152.40, 167.31; ^{15}N

NMR (40.55 MHz, DMSO-d_6) δ= 122.3, 133.7; HRMS of [$C_{23}H_{21}N_2O_2F$+Na^+] (m/z): 399.1470; Calcd.: 399.1485.

4-(2,5-dimethoxyphenyl)-2-methyl-5-oxo-N-phenyl-1,4,5,6,7,8-hexahydroquinoline-3-carboxamide(5h): ^{1}H NMR (400 MHz, DMSO-d_6): δ= 1.84-1.94 (m, 2H, CH_2), 1.96 (s, 3H, CH_3), 2.20 (t, *J*= 6.32 Hz, 2H, CH_2), 2.54-2.63 (m, 2H, CH_2), 3.52 (s, 3H, -OCH_3), 3.61 (s, 3H, -OCH_3), 5.17 (s, 1H, CH), 6.52 (d, *J*= 3.04 Hz, 1H, Ar-H), 6.61-6.14 (m, 1H, Ar-H), 6.75 (d, *J*= 8.84 Hz, 1H, Ar-H), 6.98 (t, *J*= 7.36 Hz, 1H, Ar-H), 7.24 (t, *J*= 7.6 Hz, 2H, Ar-H), 7.59 (d, *J*= 7.72 Hz, 2H, Ar-H), 8.71 (s, 1H, NH), 9.42 (s, 1H, NH); ^{13}C NMR (100 MHz, DMSO-d_6): δ=16.90, 21.12, 26.47, 31.33, 36.92, 54.93, 56.39, 108.44, 110.38, 110.89, 112.11, 115.10, 119.24, 122.58, 128.37, 134.48, 136.93, 139.77, 149.88, 153.05, 153.49, 167.10, 193.70; ^{15}N NMR (40.55 MHz, DMSO-d_6) δ= 125.3, 131.5; HRMS of [$C_{25}H_{26}N_2O_4$+Na^+] (m/z): 441.1800; Calcd.: 441.1790.

4-(3,4-dimethoxyphenyl)-2-methyl-5-oxo-N-phenyl-1,4,5,6,7,8-hexahydroquinoline-3-carboxamide(5i): ^{1}H NMR (400 MHz, DMSO-d_6): δ= 1.80-1.91 (m, 2H, CH_2), 2.03 (s, 3H, CH_3), 2.20 (t, *J*= 4 Hz, 2H, CH_2), 2.63-2.67 (m, 2H, CH_2), 3.57 (s, 3H, -OCH_3), 3.65 (s, 3H, -OCH_3), 4.94 (s, 1H, CH), 6.63-6.66 (m, 1H, Ar-H), 6.75 (t, *J*= 8.48 Hz, 2H, Ar-H), 6.97-7.03 (m, 1H, Ar-H), 7.22-7.26 (m, 2H, Ar-H), 7.40 (d, *J* = 7.64 Hz, 1H, Ar-H), 7.57 (d, *J* = 7.68, 1H, Ar-H), 8.71 (s, 1H, NH), 9.51 (s, 1H, NH); ^{13}C NMR (100 MHz, DMSO-d_6): δ=16.99, 21.10, 26.43, 32.90, 37.12, 55.15, 55.45, 108.88, 111.10, 111.41, 111.74, 119.54, 122.87, 128.40, 134.41, 139.40, 139.78, 146.90, 148.13, 152.27, 165.02, 167.57, 194.10; ^{15}N NMR (40.55 MHz, DMSO-d_6) δ= 124.6, 134.9; HRMS of [$C_{25}H_{26}N_2O_4$─H^+] (m/z): 441.1798; Calcd.: 441.1790.

4-(4-(dimethylamino)phenyl)-2-methyl-5-oxo-N-phenyl-1,4,5,6,7,8-hexahydroquinoline-3-carboxamide(5j): ^{1}H NMR (400 MHz, DMSO-d_6): δ= 1.88-1.92 (m, 2H, CH_2), 2.03 (s, 3H, -OCH_3), 2.11-2.24 (m, 2H, CH_2), 2.45 (t, *J*= 5.24 Hz, 2H, CH_2), 2.79 (s, 6H, $N(CH_3)_2$), 4.86 (s, 1H, CH), 6.55 (d, *J*= 8.68 Hz, 2H, Ar-H), 6.97 (t, *J*= 8.44 Hz, 3H, Ar-H), 7.23 (t, *J*= 7.68Hz, 2H, Ar-H), 7.55 (d, *J*= 7.8 Hz, 2H, Ar-H), 8.65 (s, 1H, NH), 9.40 (s, 1H, NH); ^{13}C NMR (100 MHz, DMSO-d_6): δ=17.01, 20.93, 26.42, 36.59, 36.91, 54.84, 109.63, 111.20, 112.33, 119.48, 122.74, 127.87, 128.39, 134.50, 135.45, 139.49, 148.72, 151.70, 167.57, 193.95; ^{15}N NMR (40.55 MHz, DMSO-d_6) δ= 124.2, 134.4; HRMS of [$C_{25}H_{27}N_3O_2$+Na^+] (m/z): 424.1998; Calcd.: 424.2001.

6.3 Results and Discussion

6.3.1 XRD analysis

Fig. 1 illustrates the X-ray diffraction pattern of 2.5 wt% Fe_2O_3-ZrO_2 with diffraction peaks 2θ from 10° to 80°. The major peaks placed at 2θ = 24.8°, 28.6°, 31.9°, 34.7°, 41.3°, 50.3° and 55.4° agree with peaks for ZrO_2 (JCPDS 37-1484). The Fe_2O_3 peaks were shown in the XRD diffractogram at 2θ = 35.5°, 45.3°, 54.2°, 57.1°, 59.6° and 62.7° (JCPDS 39-1346). The diffraction peaks confirm the polycrystalline nature of the material. Based on the Scherrer equation, average crystallite size (10 .23 nm) was calculated from the maximum intensity diffraction peak.

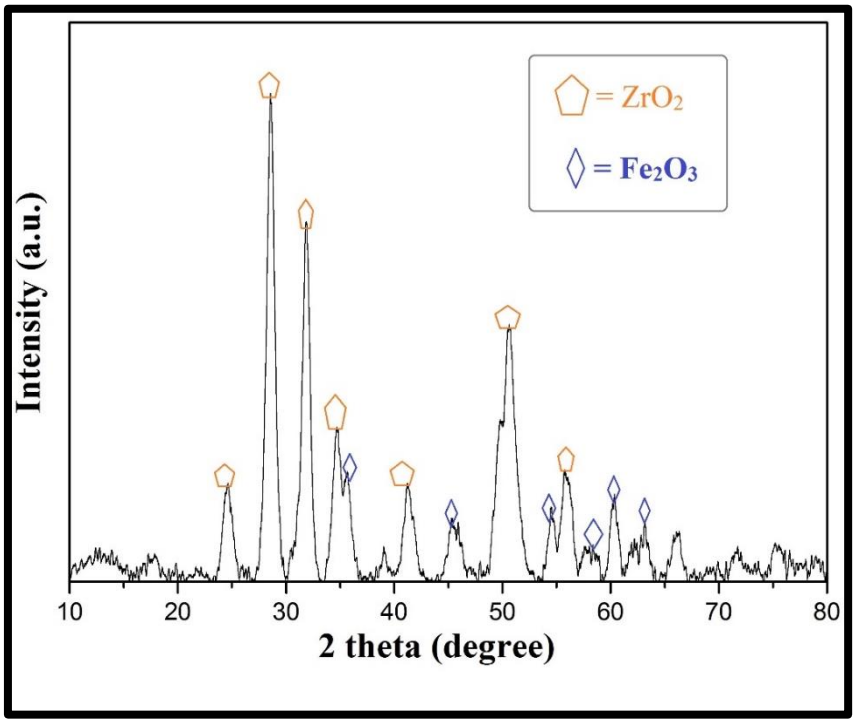

Fig. 1 Powder X-ray diffractogram of 2.5% Fe_2O_3-ZrO_2 catalyst.

6.3.2 TEM analysis

Fig. 2a illustrates the surface morphology of 2.5% Fe_2O_3/ZrO_2 catalyst material by TEM analysis. The image displayed a uniform distribution of iron on the surface of the zirconia support, with an average particle size 8.5 nm showed in **Fig. 2b**. The magnified particles exhibited irregular oval shapes. The even dispersion of iron oxide on the surface of support was confirmed by the darker parts on the image.

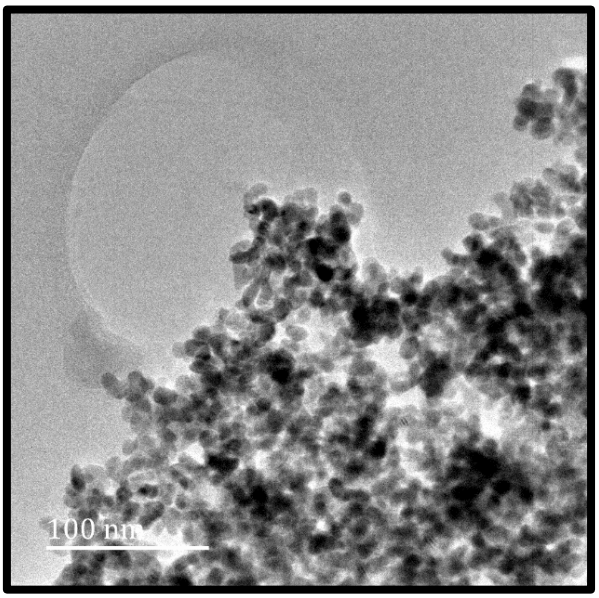

Fig. 2a TEM micrograph of 2.5% Fe_2O_3/ZrO_2 catalyst.

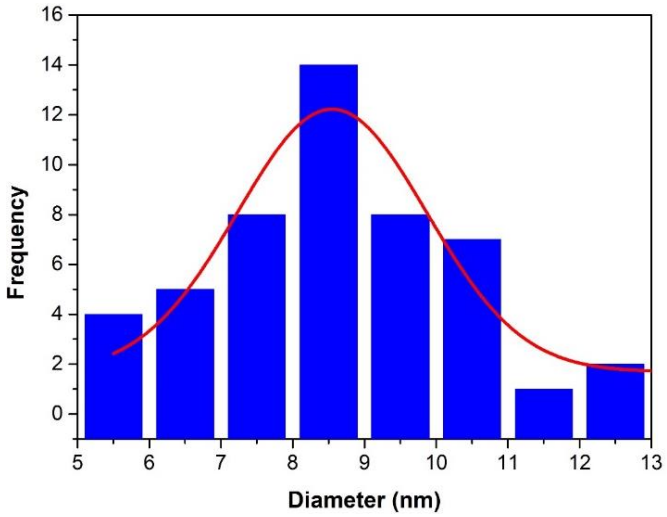

Fig. 2b Particle size distribution of Fe_2O_3/ZrO_2.

6.3.3 SEM analysis

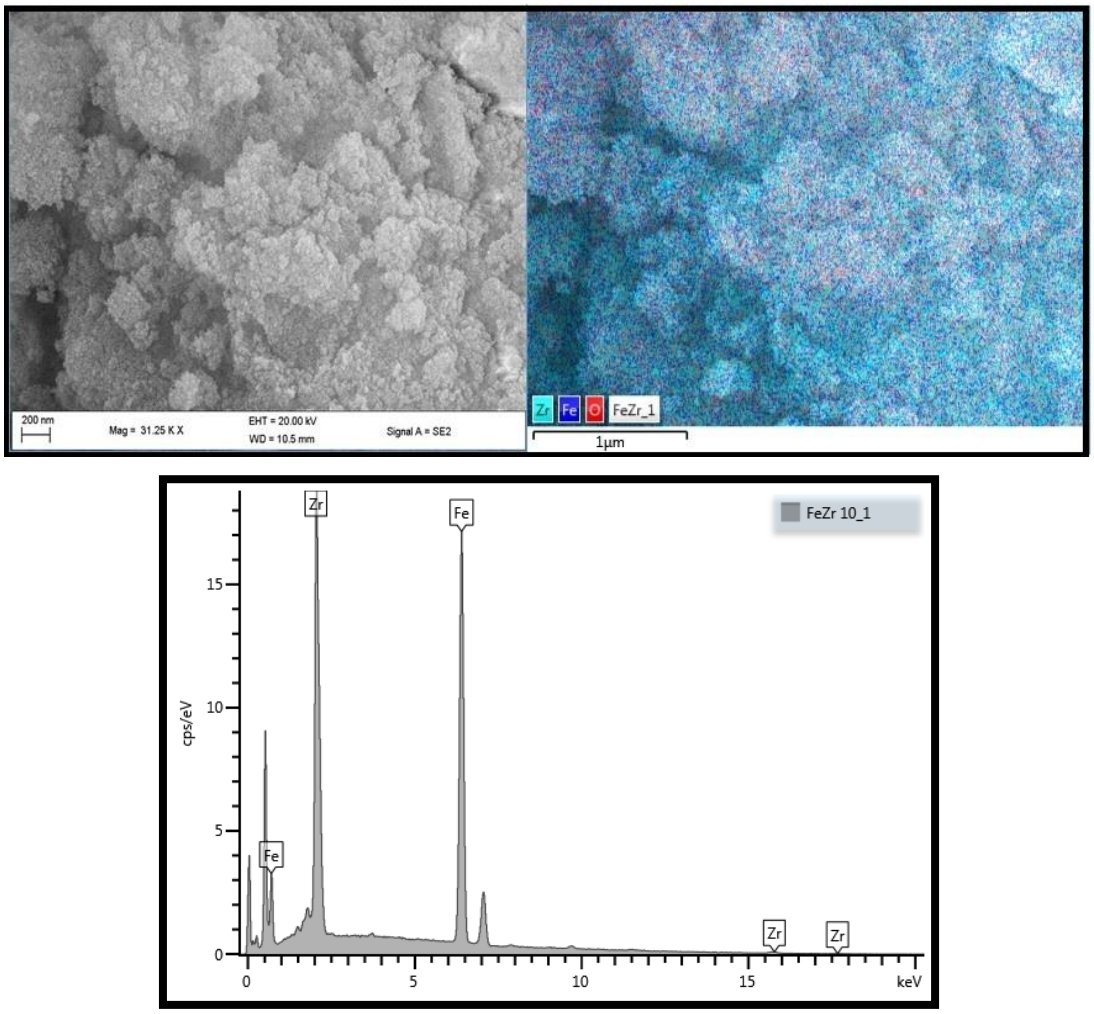

Fig. 3 SEM micrograph, EDS mapping and EDS spectra of the 2.5% Fe_2O_3/ZrO_2 catalyst.

Fig. 3 shows the SEM image of a 2.5% Fe_2O_3/ZrO_2 material. A number of irregular white shaped particles on the monograph suggests a homogeneous distribution of iron oxide on the ZrO_2 surface, which was further supported by SEM–EDS mapping, The EDS spectra demonstrated that the prepared catalyst composed of Fe, Zr and O elements, as well as ICP elemental analysis (2.13 wt% Fe). Moreover, the catalyst morphology from the SEM images illustrated the crystallinity and homogeneity of the sample.

6.3.4 BET surface area analysis

Fig.4 illustrates the Brunauer–Emmett–Teller (BET) analysis of 2.5% Fe_2O_3/ZrO_2, by adsorption–desorption of N2 at 77 K to characterise its surface area. With an H2 hysteresis loop showing a type-IV adsorption isotherm, the surface area of the material was found to be 84.34 m2/g, and the P/Po ratio was in the range of 0.63–0.98, which is > 0.25. This confirms 2.5%

Fe_2O_3/ZrO_2 as a mesoporous material, and average pore size and average pore volume were 8.92 nm and 0.25 cm3/gm, respectively.

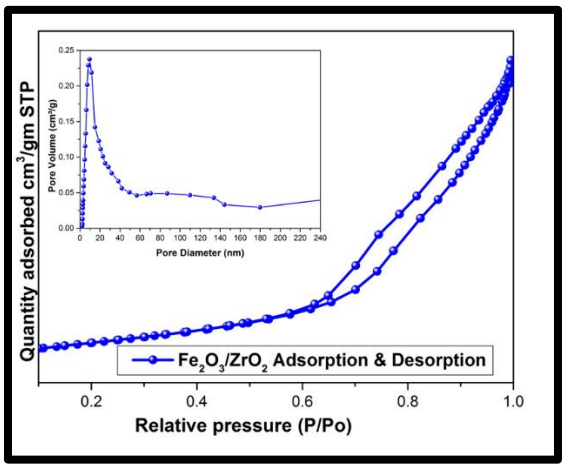

Fig. 4 N_2 adsorption-desorption isotherms of 2.5% Fe_2O_3/ZrO_2 catalyst.

6.3.5 Pyridine IR analysis

The surface-active sites are identified by adsorbing the pyridine as a probe on the prepared material. Mainly, pyridine adsorbed on the surface in two different ways: (a) pyridine can act as a Lewis base and coordinate with the electrophilic Lewis acidic sites present on the surface; (b) pyridine can act as a Brønsted base and coordinate and forms a pyridinium ion produced by the transfer of a proton from the surface hydroxyl group (Brønsted acid sites) to the pyridine molecule. The ex situ pyridine adsorbed FT-IR [43] spectra of Fe_2O_3/ZrO_2 is depicted in Fig. 5. The main feature was a broad band in the range 1550–1400 cm^{-1}. The spectrum showed a peak at 1448 cm^{-1} which corresponds to Lewis acidic sites. The peak at 1487 cm^{-1} was attributed to Brønsted and Lewis acidic sites, and the peak at 1548 cm−1 corresponds to Brønsted acidic sites. Overall, it illustrated the Lewis acidic nature of the prepared catalyst.

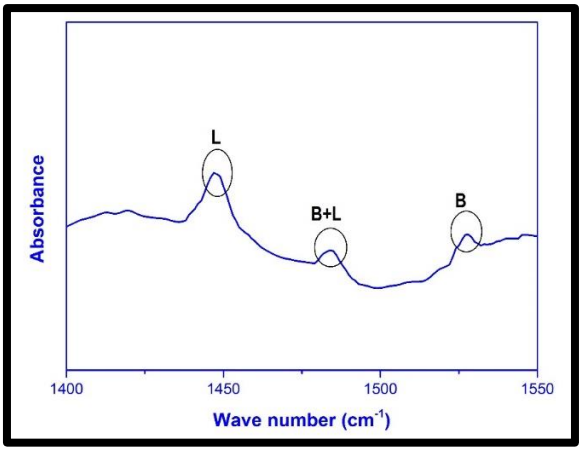

Fig. 5 Pyridine IR spectra of 2.5% Fe_2O_3/ZrO_2 catalyst; L = Lewis acidic sites; B + L Brønsted and Lewis acidic sites and B = Brønsted acidic sites.

6.3.6 Reaction optimization

The trial reaction was performed using 3-hydroxy benzaldehyde **(1a)**, 1,3-cyclohexanedione **(2)**, acetoacetanilide **(3)** and ammonium acetate **(4).** For optimisation of the reaction conditions, the effect of different solvents, catalysts and temperature was examined. Reaction progress was monitored by TLC. Only trace amounts of product were afforded when the reaction was performed under catalyst-free conditions, both under RT and reflux conditions (Table 1, entries 1 and 2). Various commercially available acidic catalysts like acetic acid, $FeCl_3$ and p-toluenesulphonic acid (PTSA) in EtOH at RT for 9 h gave 29–49% yield only (Table 1, entries 3–5). Use of ionic liquids, like $(Bmim)BF_4$ or l-proline, failed to give any satisfactory yield of desired product (10–16%, Table 1, entries 6 and 7). Use of various organic and inorganic base catalysts, like TEA, pyridine, DABCO, NaOH and K_2CO_3, studied at RT could yield only 19–32% product (Table 1, entries 8–12). With our interest in heterogeneous catalysts, the activity of different metal oxides like Al_2O_3, SiO_2, and ZrO_2 was examined, which gave satisfactory to good yields (54–79%) in 3 h at RT (Table 1, entries 13–15). Based on the encouraging results with zirconia as catalyst (yield 79%, Table 1, entry 14), we further explored its effectiveness in combination with different metals. Different materials like 2.5 wt % of CuO/ZrO_2, MnO_2/ZrO_2 and Fe_2O_3/ZrO_2 were examined as catalysts, and all afforded good overall yields of (80–98%) in EtOH at RT (Table 1, entries 16–18). 2.5% Fe_2O_3/ZrO_2 catalyst offered an excellent yield (98%) compared with the other mixed oxides assessed. Hence, the effect of different percentage loading of Fe_2O_3 on ZrO_2 (1% and 5%) as catalysts was investigated under similar conditions. 1% Fe_2O_3/ZrO_2 catalyst (Table 1, entry 19) gave 90% yield in 40 min, whereas 5% loading showed a slight decrease in the yield relative to 2.5%

loading, from 98 to 94% for the same reaction times. The lower yield with 1% Fe_2O_3/ZrO_2 was due to the lower number of active sites, whereas with 5% Fe_2O_3/ZrO_2 loading, the lower yield was presumably due to oligomerization of Fe_2O_3 on the surface of ZrO_2. Higher efficacy with 2.5% Fe loaded material could be attributed to the homogeneous distribution and exposing of iron oxide active sites on the surface of zirconia. The 2.5% Fe_2O_3/ZrO_2 catalytic system was therefore subsequently used to synthesise all the other 1,4-dihydropyridine derivatives in the series.

Table 1 Effect of catalysts on the synthesis of **5a** *

Entry	Catalyst	Condition	Time (h)	Yield (%) #
1	--	RT	11	10
2	--	Reflux	11	18
3	AcOH	RT	9.0	41
4	$FeCl_3$	RT	9.0	49
5	PTSA	RT	9.0	29
6	$(Bmim)BF_4$	RT	8.0	10
7	L-proline	RT	7.0	16
8	TEA	RT	8.0	19
9	Pyridine	RT	4.5	24
10	DABCO	RT	4.5	32
11	NaOH	RT	4.5	22
12	K_2CO_3	RT	4.5	30
13	Al_2O_3	RT	3.0	54
14	SiO_2	RT	3.0	62
15	ZrO_2	RT	3.0	79
16	2.5% CuO/ZrO_2	RT	1.5	84
17	2.5% MnO_2/ZrO_2	RT	1.0	80
18	2.5% Fe_2O_3/ZrO_2	RT	0.33	98
19	1% Fe_2O_3/ZrO_2	RT	0.66	90
20	5% Fe_2O_3/ZrO_2	RT	0.33	94

* Reaction conditions: 3-hydroxy benzaldehyde (1 mmol), 1,3-cyclohexanedione (1 mmol), and acetoacetanilide (1 mmol), ammonium acetate (1 mmol) and solvent (5 mL) were stirred at RT.
# Isolated yields.
-- No catalyst.

The effect of solvent medium was investigated, with a focus on reaction yields (Table 2). Non-polar solvents facilitated no reaction, possibly due to the poor solvent–solid interactions (Table 2, entries 1 and 2). Polar aprotic solvents such as tetrahydrofuran (THF) and dimethyl formamide (DMF) and polar protic solvents like MeOH, EtOH and H_2O showed low yields (Table 2, entries 3 and 4), and with protic solvents (H_2O, MeOH and EtOH), reasonable yields

were obtained (Table 2,entries 5, 6 and 7). EtOH proved to be the ideal solvent for the reaction. Moreover, it has better acceptability as green solvent over MeOH.

Table 2 Optimization of various solvent condition for the model reaction*

Entry	Solvent	Time(h)	Yield (%)
1	*n*-hexane	1.6	--
2	Toluene	1.6	--
3	THF	1.0	15
4	DMF	1.0	18
5	H_2O	1.0	64
6	MeOH	0.66	83
7	EtOH	0.33	98

*Reaction conditions: 3-hydroxy benzaldehyde (1 mmol), 1,3-cyclohexanedione (1 mmol), and acetoacetanilide (1 mmol), ammonium acetate (1 mmol) and solvent (5 mL) were stirred at room temperature.

DMF= Dimethyl formamide; THF= Tetrahydrofuran; H_2O= Water; CH_3OH= Methanol; C_2H_5OH= Ethanol.

-- No product.

The effect of the amount of 2.5% Fe_2O_3/ZrO_2 used on the yield and reaction time was further examined (Table 3). With increase in the amount of catalyst used from 15 up to 45 mg, the reaction yield steadily improved from 65 to 98% with concurrent reduction in reaction time. A further increase of catalyst amount (45–65 mg) registered no improvement in yield or reaction time. Thus, 45 mg of 2.5% Fe_2O_3/ZrO_2 catalyst was taken as the optimum amount for the chosen reaction conditions.

Table 3 Optimization of various amounts of 2.5% Fe_2O_3/ZrO_2 for the model reaction*

Entry	**Catalyst (mg)**	**Yield (%)**	**Time (h)**
1	15	65	0.83
2	25	73	0.58
3	35	90	0.33
4	45	98	0.33
5	55	98	0.33
6	65	98	0.33

* Reaction conditions: 3-hydroxy benzaldehyde (1 mmol), 1,3-cyclohexanedione (1 mmol), and acetoacetanilide (1 mmol), ammonium acetate (1 mmol) and solvent (5 mL) were stirred at room temperature.

To further broaden the utility of the optimized protocol, reactions were conducted using different substituted aldehydes to synthesize their respective 1,4 dihydropyridine derivatives. Reaction with ten different aldehydes with varied substituents all gave excellent yields (92–98%**, 5a–j)**. Thus, 2.5% Fe_2O_3/ZrO_2 proved to be an excellent material to catalyze the facile one-pot synthesis of targeted 1,4 dihydropyridine scaffolds at RT in ethanol with a short reaction time of 20 min (Table 4). The nature of the substituents on the phenyl ring showed significant effect on the reaction yields. It was due to less functional group tolerance towards the reaction. In all reactions, the halogen substitution at the para position gave higher yields compared to at the ortho position. In summary, the aldehydes with electron-donating groups at the ortho position offered higher yields compared to the halogen groups. It also showed that the catalyst system works well with both electron-donating and electron-withdrawing groups on the phenyl ring of the aldehydes. The single crystal structure of *5j* is shown in Fig. 6.

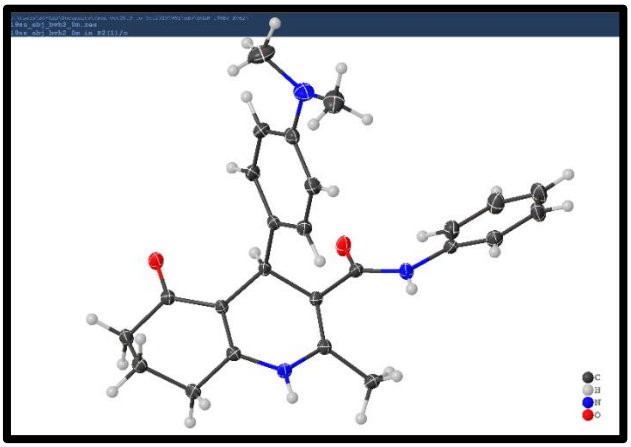

Fig. 6 Crystal structure of **5 j** (CCDC no.1903627).

Table 4 Synthesis of novel functionalized pyridine derivatives by 2.5% Fe_2O_3/ZrO_2 catalyst*

Entry	R	Product	Mp °C	Yield* (%)
1	3-OH	5a	185-187	98
2	2-OMe	5b	193-195	96
3	4-OMe	5c	190-192	93
4	2-Cl	5d	210-212	92
5	4-Br	5e	206-208	94
6	2-Br	5f	213-215	93
7	4-F	5g	200-202	96
8	2,5-OMe	5h	220-222	98
9	3,4-OMe	5i	225-227	97
10	4-$N(CH_3)_2$	5j	218-220	93

* Reaction conditions: arylaldehyde (1 mmol), 1,3-cyclohexanedione (1 mmol), and aceto acetanilide (1 mmol), ammonium acetate (1 mmol) and solvent (5 mL) were stirred at room temperature. R = substituted benzaldehydes. * = Isolated yields.

The identity of each reaction product was confirmed by ^{1}H NMR and ^{13}C NMR analysis (Figs. 7, 9 and 10). For example, for **5a**, the characteristic singlets at δ = 2.03, 4.90, 8.74, 9.50 and 9.11 indicate the –CH_3, –CH, two –NH protons and –OH proton, respectively. The heteronuclear multiple-bond correlation (HMBC) interactions are unambiguous proof to substantiate the formation of **5a**. In Fig. 8, the proton in the region of δ = 4.90 was assigned to the –CH proton in the 1,4-dihydropyridine ring, further confirmed by the HMBC interaction with carbon atoms at δ = 108.92, 111.02, 118.05, 134.52, 148.47, 152.36, 167.50 and 194.10. The proton in the region of δ = 8.74 was assigned to the nitrogen proton in the dihydropyridine ring, further endorsed by its HMBC interaction with carbon atoms at δ = 16.97, 26.44 and 152.36. The nitrogen in the acetoacetanilide appeared in the region of δ = 9.50 with the specific HMBC interactions at δ = 119.59, 139.37 and 167.50. The –OH proton was assigned to δ = 9.11, which was further confirmed by the HMBC interactions at δ = 112.67, 114.37 and 157.00. The carbon resonances at δ = 37.63, 108.92, 111.02, 148.47 and 152.36 were indicative of the 1,4-dihydropyridine ring, whereas the prominent signal at δ = 194.10 is attributed to the carbonyl group of cyclohexanone. The carbonyl group in the acetoacetanilide resonates at 167.50. The HRMS showed the *m/z* 397.1546 $[C_{23}H_{22}N_2O_3 + Na]+$, which corresponded well with the theoretical value for **5a**, based on its formulae (Figs. 8, 9 and 10).

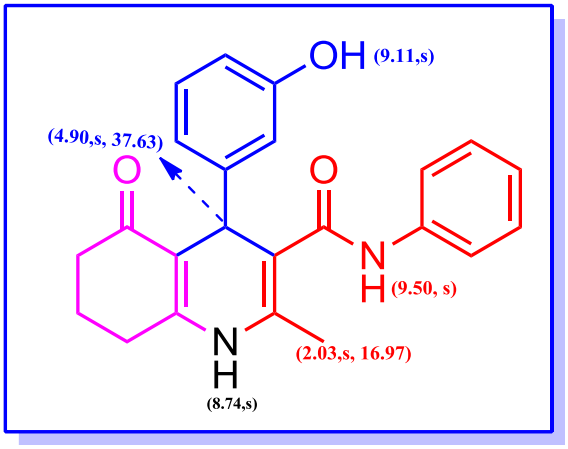

Fig. 7 Characteristic ^{1}H and ^{13}C NMR signals of compound **5a**

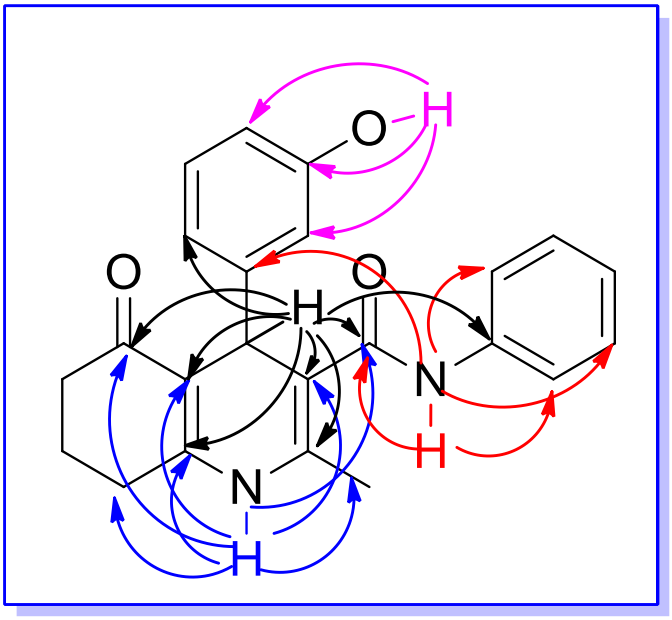

Fig. 8 Selected HMBC interactions of –CH, –NH & -OH Protons of **5a**

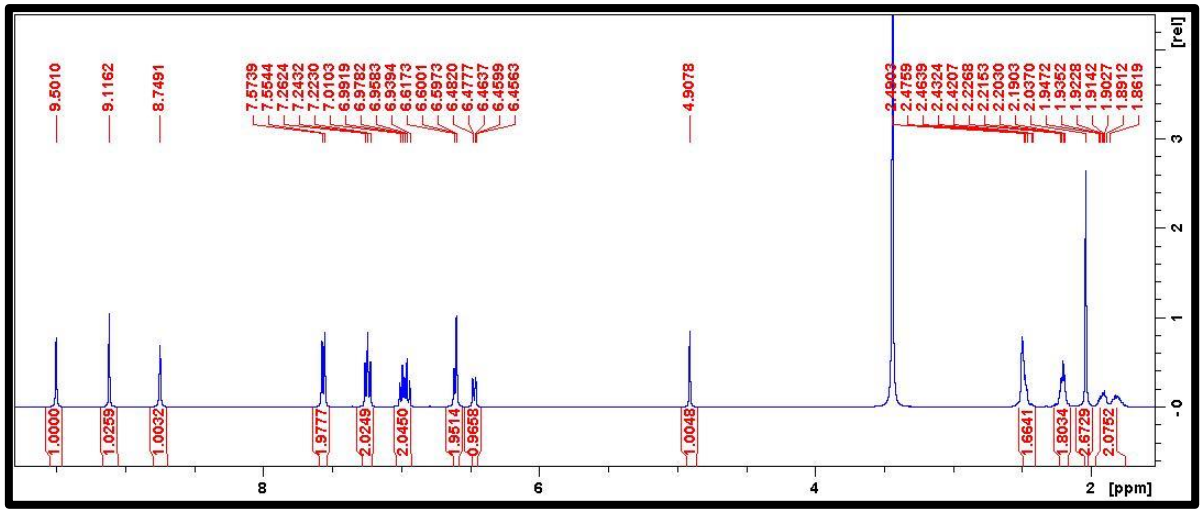

Fig. 9 ^{1}H NMR spectra of compound **5a**

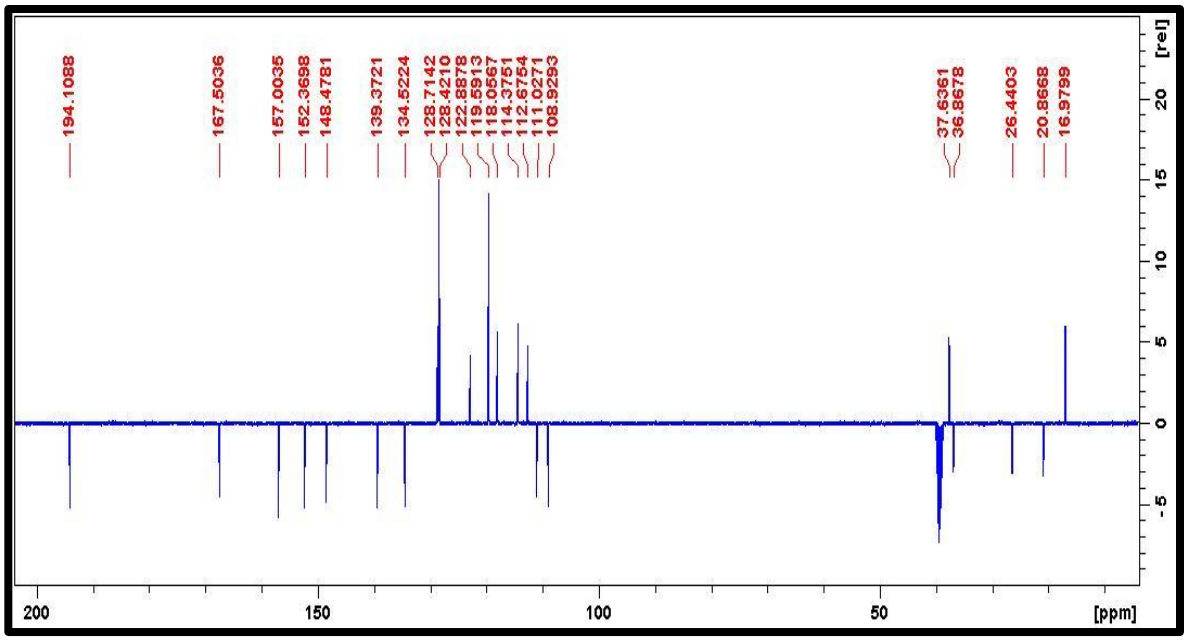

Fig. 10 ^{13}C NMR spectra of compound **5a**

6.3.7 Mechanism of the reaction

From the above results, a proposed mechanism is shown in Scheme 2 from the previous reports[44], [45]. The Lewis acidic sites present on the surface of the catalyst will facilitate the overall reaction. Initially, a Knoevenagel condensation product was formed by the coordination of Lewis acidic sites with the carbonyl oxygen affording a carbocation intermediate **(a)**, and

then the interaction of active methylene group of the acetoacetanilide with the intermediate **(a)**. Next, the intermediate will dissociate from the surface of the catalyst and obtain a proton from the EtOH, affording the intermediate **(b)**. Subsequently an intramolecular dehydration generates the key intermediate **(c)**, further condensation of the intermediate with **(2)** finally produce the target molecules **(5a-j)**. **Table 5** summarize a comparison of other catalysts with the prepared Fe_2O_3/ZrO_2 on the title reaction.

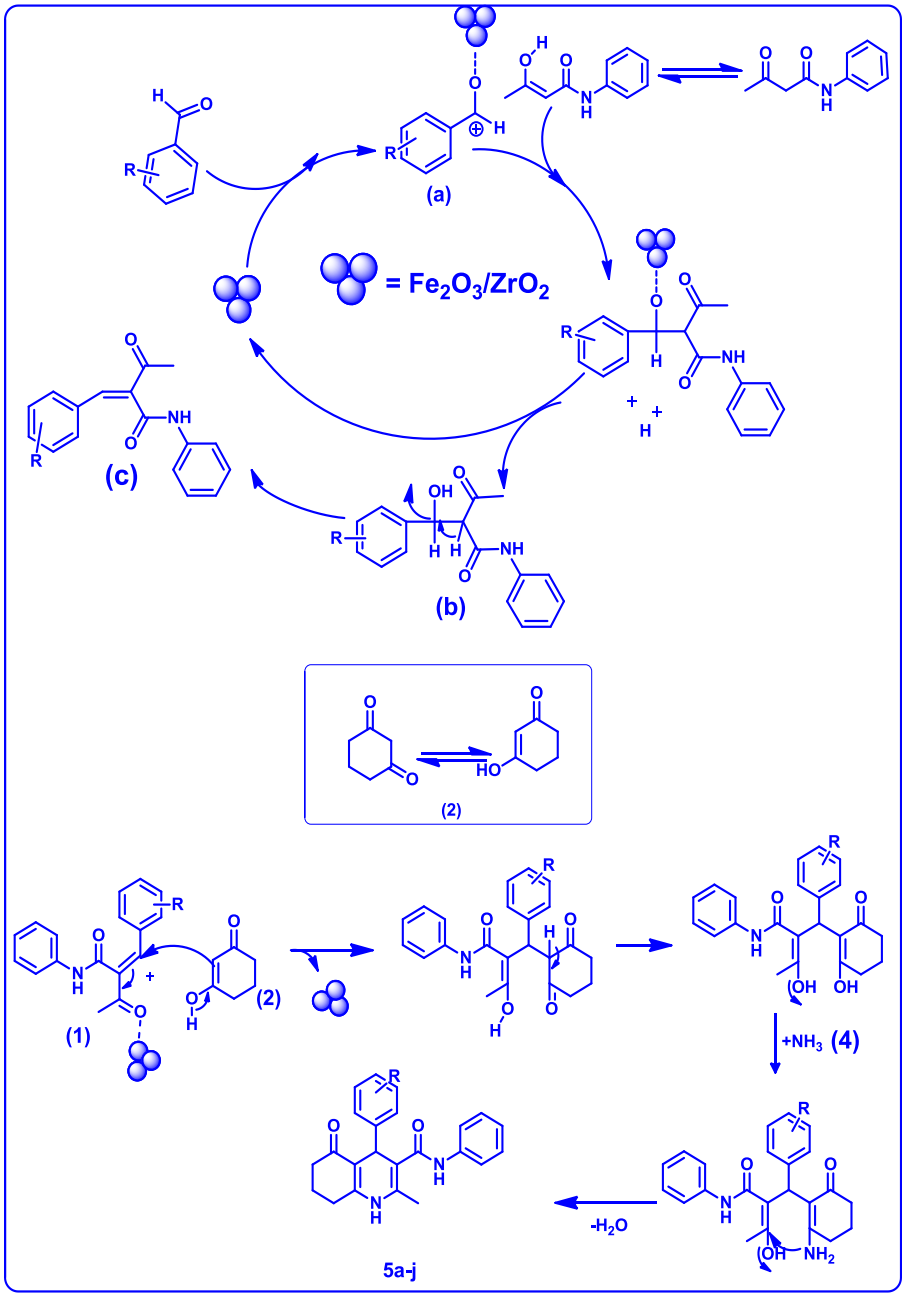

Scheme 2 Proposed reaction mechanism for the formation of 1,4-dihydropyridine derivatives.

Table 5 Comparison table with various other catalysts to synthesis 1,4-dihydropyridine derivatives.

Catalyst [Ref]	Solvent	Reaction Temp.	Reaction Time	Yield (%)
$M^{II}Zr_4(PO_4)_6$[31]	EtOH	Reflux	30-45 min	82-93
Zirconocene bis(perfluorobutanesulfonate)[32]	solvent-free conditions	80 °C	2-3h	86-96
Sulfated polyborate[33]	solvent free conditions	90 °C	15-40 min	85-95
Silica functionalized sulfonic acid coated with ionic liquid[34]	solvent-free conditions	60 °C	5-50 min	80-95
Chitosan supported oxo-vanadium[35]	Solvent-free	130 °C	55-75 min	53-88
Sulfated boric acid nanoparticles[36]	EtOH	60 °C	30-60 min	86-98
DBU[37]	EtOH	RT	2.5-3 h	80-94 %
Nicotinic acid[38]	Solvent-free	80 °C	2-7 min	87-96
γ-Fe_2O_3/Cu@cellulose [39]	Solvent-free	RT	9-30 min	80-98
SBA-15@AMPD-Co [40]	Solvent-free	100 °C	35-90 min	90-97
Fe_3O_4@D-NH-$(CH_2)_4$-SO_3H [41]	EtOH	Reflux	40 min	86-90
Cu-Adenine@boehmite [42]	EtOH	Reflux	20-120 min	89-97

6.4 Reusability of catalyst

After the reaction, the used material of the Fe_2O_3/ZrO_2 catalyst was separated by filtration and washed with EtOH solvent. It was then dried at 120 °C for 3 h and was recycled up to six successive cycles without loss of catalytic activity. The decrease in the catalytic activity after the 6 successive cycles observed may be due to the accumulation of impurities on the pores of catalyst surface, which deactivate the catalytic activity. This may the main reason and there may be partial loss of active material during the reaction process. **Fig.10** shows the Recycling study of 2.5% Fe_2O_3/ZrO_2 catalyst.

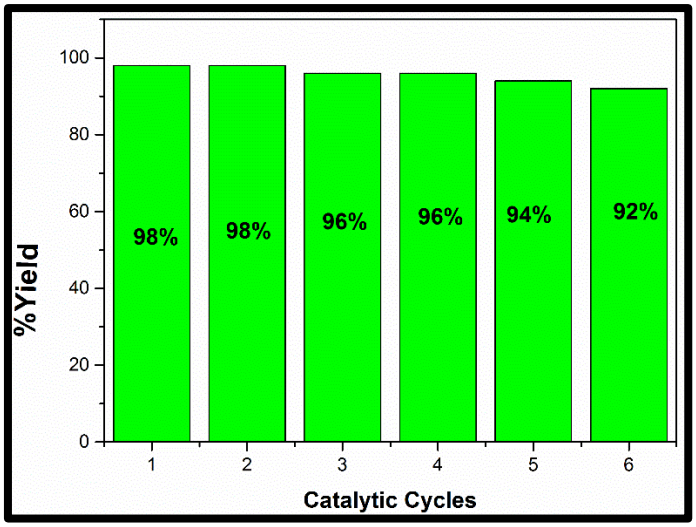

Fig.10 Recycling study of 2.5% Fe_2O_3/ZrO_2 catalyst for the synthesis of 1,4-dihydropyridine 5a.

6.5 Conclusion

We have developed a robust green protocol at RT using green ethanol solvent for the synthesis of novel 1,4-dihydropyridine derivatives by using Fe_2O_3/ZrO_2 as catalyst, employing earth-abundant and inexpensive Fe as active material. The main advantage of this protocol is shorter reaction time, simple work-up procedure, reusable catalyst material and most importantly excellent yields making this protocol practical for the synthesis.

6.6 Supplementary Information

The CCDC number 1903627 contains the information regarding the supplementary crystallographic data. These data can be obtained free of charge via www.ccdc.cam.ac.uk/conts/retrieving.html or [from the Cambridge Crystallographic Data Center (CCDC), 12 Union Road, Cambridge CB21 EZ, UK; Fax: +44(0)1223-336,003; E-18 mail:deposit@ccdc.cam.ac.uk]. Structure factor table is available from the authors.

6.7 Acknowledgements

The authors are thankful to the National Research Foundation of South Africa, and University of KwaZulu-Natal, Durban, for financial support and research facilities.

6.8 References

1. B.H. Rotstein, S. Zaretsky, V. Rai, A.K. Yudin, Chem. Rev. **114**, 8323 (2014)

2. A. Domling, W. Wang, K. Wang, Chem. Rev. **112**, 3083 (2012)

3. S.V.H.S. Bhaskaruni, S. Maddila, K.K. Gangu, S.B. Jonnalagadda, Arab. J. Chem. (2017). https ://doi.org/10.1016/j.arabj c.2017.09.016

4. R.A. Sheldon, Chem. Soc. Rev. **41**, 1437 (2012)

5. R. Pagadala, S. Maddila, S. Rana, S.B. Jonnalagadda, RSC Adv. **4**, 6602 (2014)

6. S.H.S. Bhaskaruni, S. Maddila, W.E. van Zyl, S.B. Jonnalagadda, RSC Adv. **8**, 16336 (2018)

7. C.J. Védrine, Catal. **7**, 341 (2017)

8. S.V.H.S. Bhaskaruni, K.K. Gangu, S. Maddila, S.B. Jonnalagadda, Chem. Rec. (2018). https ://doi.org/10.1002/tcr.20180 0077

9. V. Menon, V. Popa, C. Contescu, J.A. Schwarz, Rev. Roum. Chim. **43**, 393–397 (1998)

10. S. Kouva, K. Honkala, L. Lefferts, J. Kanervo, Catal. Sci. Technol. **5**, 3473 (2015)

11. Y. Zhao, W. Li, M. Zhang, K. Tao, Catal. Commun. **3**, 239 (2002)

12. V. Kozell, T. Giannoni, M. Nocchetti, R. Vivani, O. Piermatti, L. Vaccaro, Catal. **7**, 186 (2017)

13. M. Sharbatdaran, F. Farzaneh, M.M. Larijani, J. Mol. Catal. A Chem. **382**, 79 (2014)

14. T. Okachi, N. Murai, M. Onaka, Org. Lett. **5**, 85 (2003)

15. M.B. Gawande, R.K. Pandey, R.V. Jayaram, Catal. Sci. Technol. **2**, 1113 (2012)

16. S.V.H.S. Bhaskaruni, S. Maddila, W.E. van Zyl, S.B. Jonnalagadda, Catal. Commun. **100**, 24 (2017)

17. I. Bauer, H.-J. Knölker, Chem. Rev. **115**, 3170 (2015)

18. J.I. Padrón, V.S. Martín, in *Iron Catalysis-Fundamentals and Applications*, ed. by B. Plietker (Springer, Berlin, 2011), pp. 1–26

19. B. Åkermark, M.P.T. Sjögren, Adv. Synth. Catal. **349**, 2641 (2007)

20. R.N. Naumov, M. Itazaki, M. Kamitani, H. Nakazawa, J. Am. Chem. Soc. **134**, 804 (2012)

21. N.S. Shaikh, K. Junge, M. Beller, Org. Lett. **9**, 5429 (2007)

22. A. Guđmundsson, K.P.J. Gustafson, B.K. Mai, B. Yang, F. Himo, J.-E. Bäckvall, ACS Catal. **8**, 12 (2018)

23. C. Cassani, G. Bergonzini, C.-J. Wallentin, ACS Catal. **6**, 1640 (2016)

24. J. Hu, V.V. Galvita, H. Poelman, C. Detavernier, G.B. Marin, J. CO_2 Util. **17**, 20 (2017)

25. K.-S. Kang, C.-H. Kim, K.-K. Bae, W.-C. Cho, S.-U. Jeong, Y.-J. Lee, C.-S. Park, Chem. Eng. Res. Des. **92**, 2584 (2014)

26. J.-P. Wan, Y. Liu, RSC Adv. **2**, 9763 (2012)

27. M.M. Khan, R. Yousuf, S. Khan, Shafiullah, RSC Adv. **5**, 57883 (2015)
28. M.M. Khan, S. Khan, Saigal, S. Iqbal, RSC Adv. **6**, 42045 (2016)
29. R.N. Goto, L.M. Sobral, L.O. Sousa, C.B. Garcia, N.P. Lopes, J. Marín-Prida, E. Ochoa-Rodríguez, Y. Verdecia-Reyes, G.L. Pardo-Andreu, C. Curti, A.M. Leopoldino, Eur. J. Pharmacol. **819**, 198 (2018)
30. N.C. Desai, A.R. Trivedi, H.C. Somani, K.A. Bhatt, Chem. Biol. Drug Des. **86**, 370 (2014)
31. J. Safaei-Ghomi, H. Shahbazi-Alavi, A. Ziarati, Res. Chem. Intermed. **43**, 91 (2017)
32. J. Wang, N. Li, R. Qiu, X. Zhang, X. Xu, S.-F. Yin, J. Organomet. Chem. **785**, 61 (2015)
33. D.S. Rekunge, C.K. Khatri, G.U. Chaturbhuj, Tetrahedron Lett. **58**, 1240 (2017)
34. P. Sharma, M. Gupta, Green Chem. **17**, 1100 (2015)
35. M. Safaiee, B. Ebrahimghasri, M.A. Zolfigol, S. Baghery, A. Khoshnood, D.A. Alonso, N. J. Chem. **42**, 12539 (2018)
36. K. Azizi, J. Azarnia, M. Karimi, E. Yazdani, A. Heydari, Synlett **27**, 1810 (2016)
37. M.M. Khan, Saigal, S. Khan, S. Shareef, M. Danish, Chem. Sel. **3**, 6830 (2018)
38. J. Davarpanah, M. Ghahremani, O. Najafi, J. Mol. Struct. **1177**, 525 (2019)
39. A. Maleki, V. Eskandarpour, J. Rahimi, N. Hamidi, Carbohydr. Polym. **208**, 251 (2019)
40. A. Ghorbani-Choghamarani, M. Mohammadi, T. Tamoradi, M. Ghadermazi, Polyhedron **158**, 25 (2019)
41. B. Maleki, O. Reiser, E. Esmaeilnezhad, H.J. Choi, Polyhedron **162**, 129 (2019)
42. A. Ghorbani-Choghamarani, P. Moradi, B. Tahmasbi, Polyhedron **163**, 98 (2019)
43. S. Bhaskaruni, S. Maddila, W. van Zyl, S. Jonnalagadda, Mol. **23**, 1648 (2018)
44. R. Kumar, N.H. Andhare, A. Shard, Richa, A.K. Sinha, RSC Adv. **4**, 19111 (2014)
45. Q. Li, X. Wang, Y. Yu, Y. Chen, L. Dai, Tetrahedron **72**, 8358 (2016)

6.9 Supplementary information

6.9.1. Catalyst instrumentation details

Employing a Bruker D8 Advance instrument (Cu K radiation source with a wave length of 1.5406 Å), the X-ray diffraction data related the structural phases of the catalyst were acquired. Using a JEOL JEM-1010 electron microscope and JEOL JSM-6100 microscope, the TEM and SEM analysis data was recorded. iTEM software was used analyse the TEM data and images. Employing the X-ray analyser (energy-dispersive), EDX-analysis on the SEM images was conducted.

6.9.2. Experimental Section

All chemicals and reagents required for the reaction were of analytical grade and were used without any further purification. Bruker AMX 400 MHz NMR spectrometer was used to record the ^{1}H NMR, ^{13}C NMR and ^{15}N NMR spectral values. High-resolution mass data were obtained using a Bruker micro TOF-Q II ESI instrument operating at ambient temperature. The DMSO-d6 solution was utilized for this while TMS served as the internal standard. TMS was further used as an internal standard for reporting the all chemical shifts in δ (ppm). Purity of all the reaction products was confirmed by TLC using aluminium plates coated with silica gel (Merck Kieselgel 60 F_{254}). Infrared (IR) spectra were recorded on a Perkin Elmer Precisely equipped with a Universal ATR sampling accessory using a diamond crystal. The powdered material was placed on the crystal and a force of 120 psi was applied to ensure proper contact between the material and the crystal.The spectra were analyzed using Spectrum 100 software. Before recording the IR spectra, pyridine was adsorbed by placing a drop of pyridine on 10 mg of the sample followed by evacuation in air for 1 h at room temperature to remove reversibly adsorbed pyridine on the surface of the catalyst.

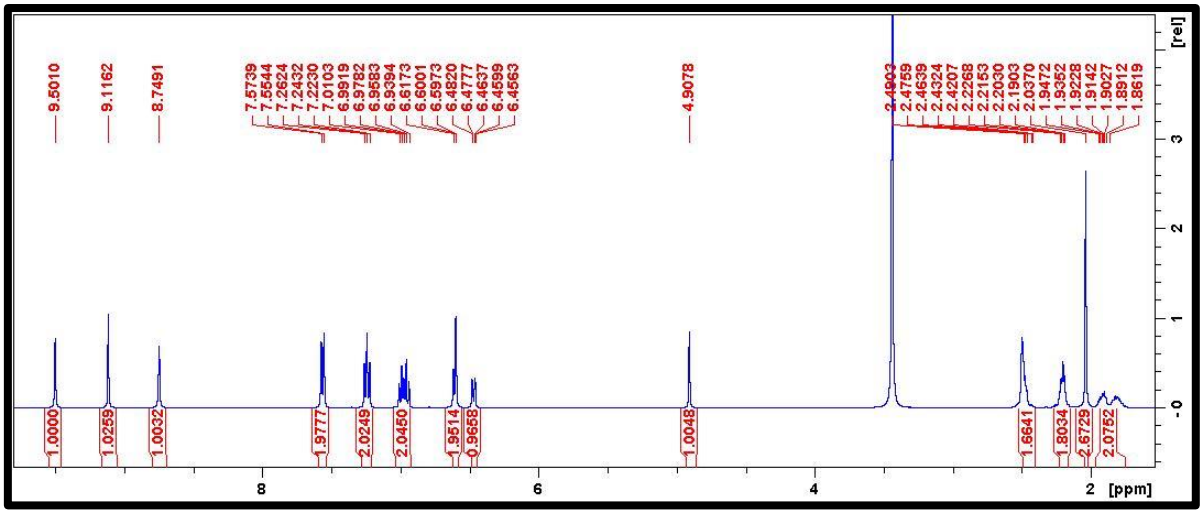

^{1}H NMR spectra of compound **5a**

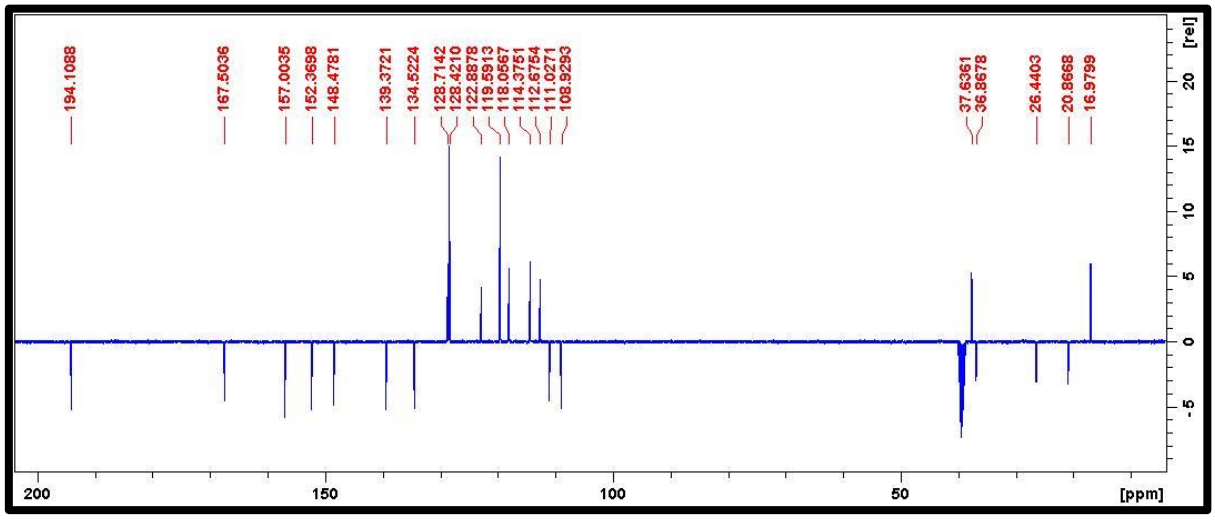

^{13}C NMR spectra of compound **5a**

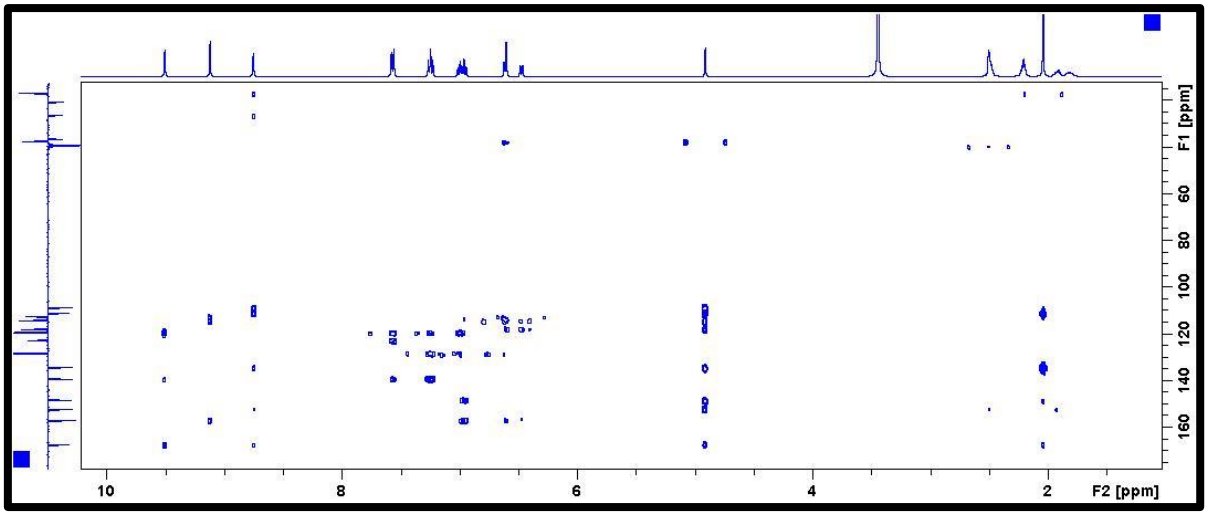

HMBC spectra of compound **5a**

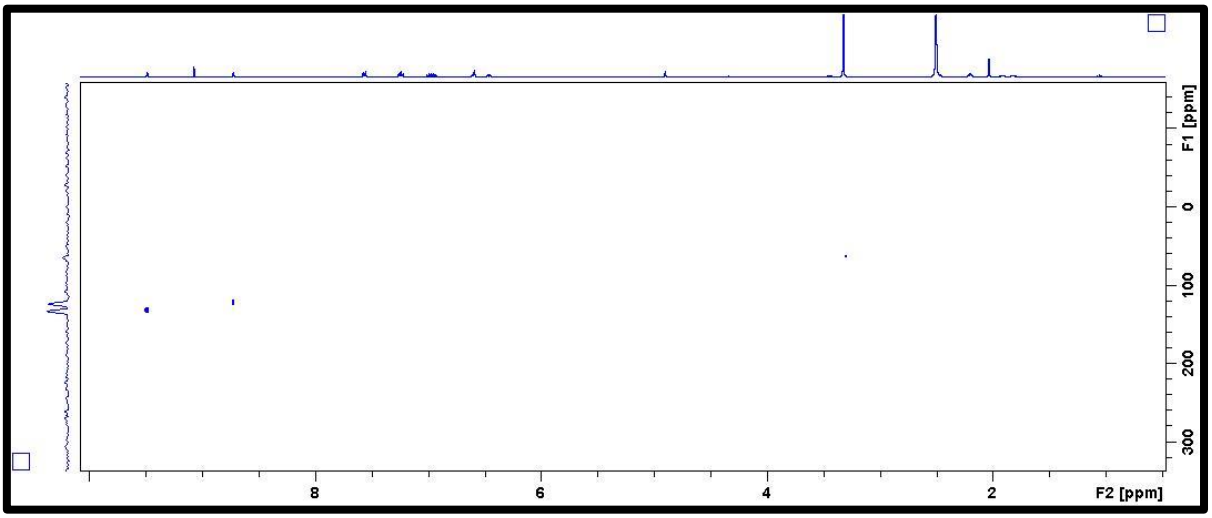

^{15}N NMR spectra of compound **5a**

Elemental Composition Report **Page 1**

Single Mass Analysis
Tolerance = 5.0 PPM / DBE: min = -1.5, max = 100.0
Element prediction: Off
Number of isotope peaks used for i-FIT = 2

Monoisotopic Mass, Even Electron Ions
15 formula(e) evaluated with 1 results within limits (up to 20 closest results for each mass)
Elements Used:
C: 20-35 H: 20-25 N: 0-5 O: 0-5 Na: 1-1
9T-12 5 (0.135) Cm (1:61)
TOF MS ES+

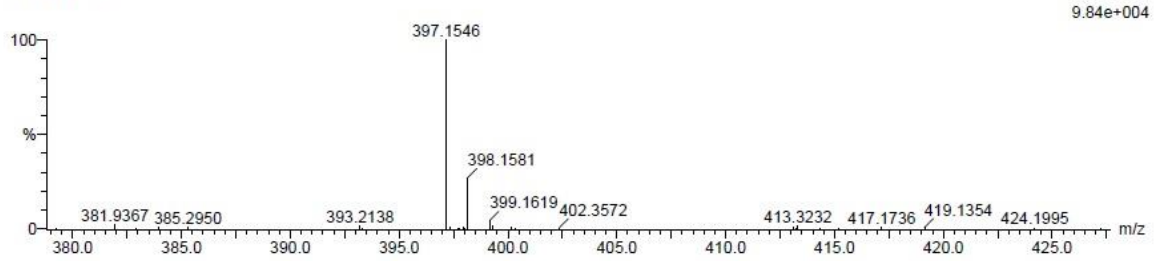

Minimum:				-1.5			
Maximum:		5.0	5.0	100.0			
Mass	Calc. Mass	mDa	PPM	DBE	i-FIT	i-FIT (Norm)	Formula
397.1546	397.1528	1.8	4.5	13.5	70.6	0.0	C23 H22 N2 O3 Na

HRMS spectra of compound **5a**

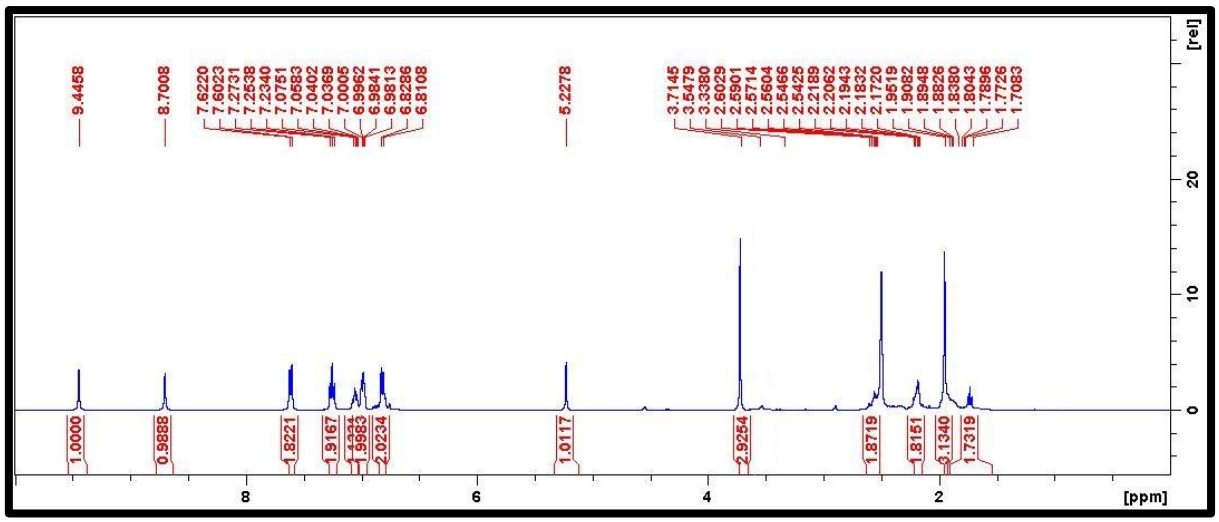

^{1}H NMR spectra of compound **5b**

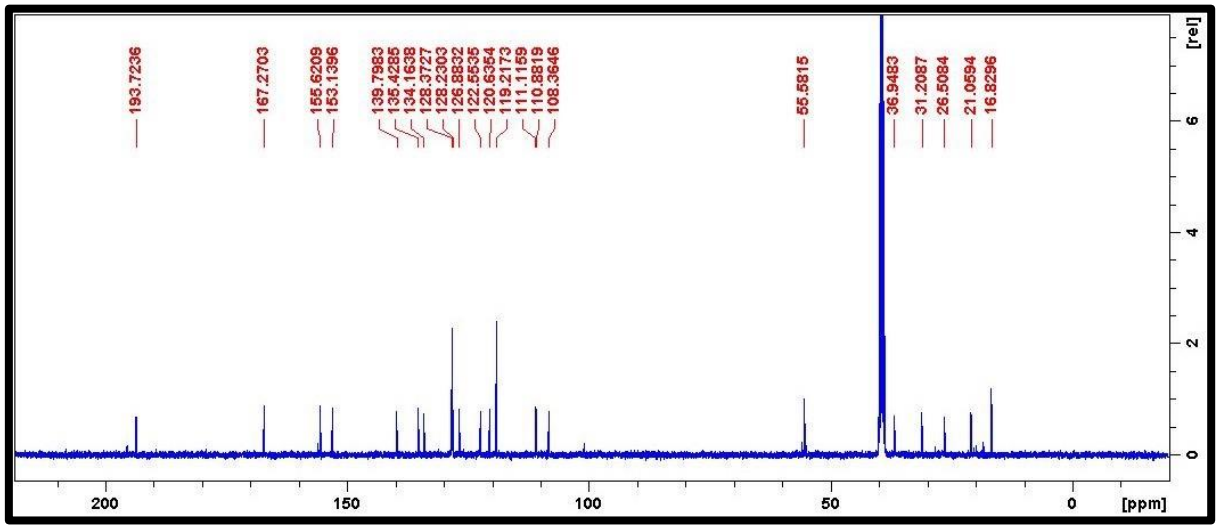

^{13}C NMR spectra of compound **5b**

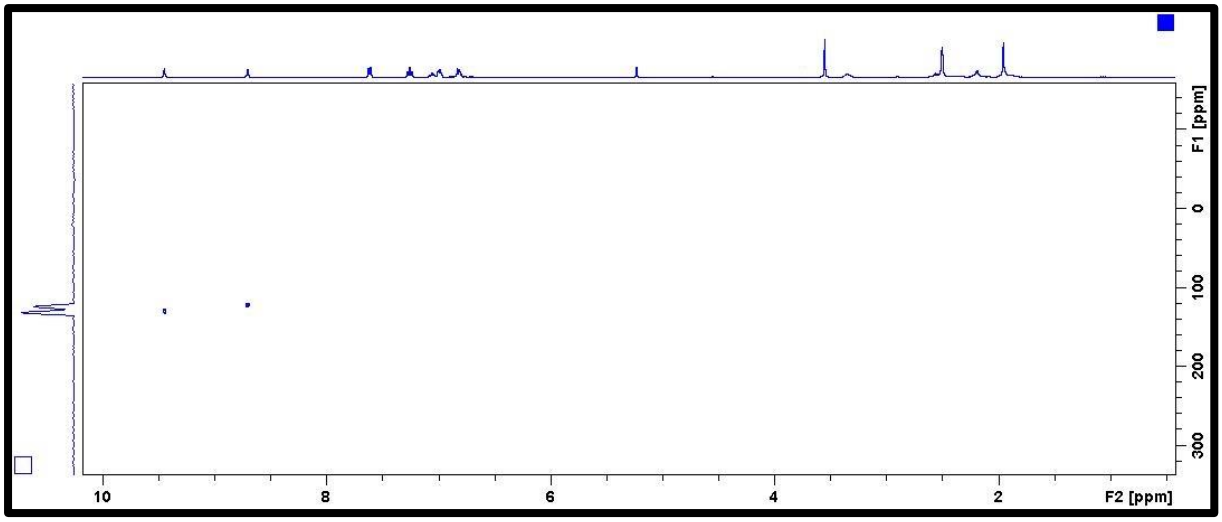

^{15}N NMR spectra of compound **5b**

Elemental Composition Report **Page 1**

Single Mass Analysis
Tolerance = 5.0 PPM / DBE: min = -1.5, max = 50.0
Element prediction: Off
Number of isotope peaks used for i-FIT = 2

Monoisotopic Mass, Even Electron Ions
26 formula(e) evaluated with 1 results within limits (up to 20 best isotopic matches for each mass)
Elements Used:
C: 20-25 H: 20-25 N: 0-5 O: 1-5 Na: 1-1
9T-1 54 (1.787) Cm (1:61)
TOF MS ES-

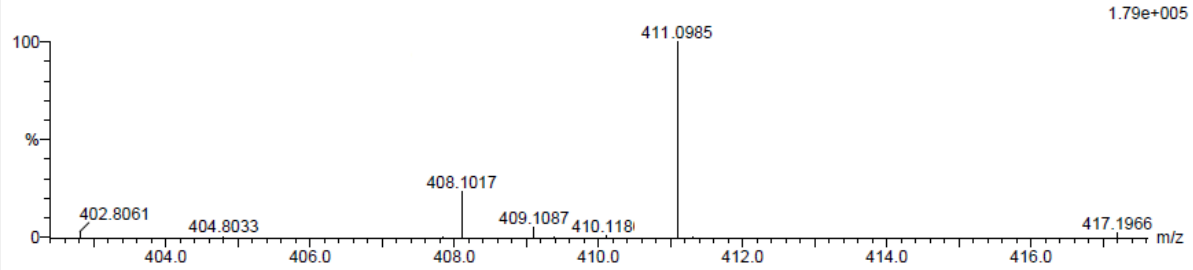

Minimum:				-1.5			
Maximum:		5.0	5.0	50.0			
Mass	Calc. Mass	mDa	PPM	DBE	i-FIT	i-FIT (Norm)	Formula
411.0985	411.0983	0.2	0.5	13.5	37.8	0.0	C24 H24 N2 O3 Na

HRMS spectra of compound **5b**

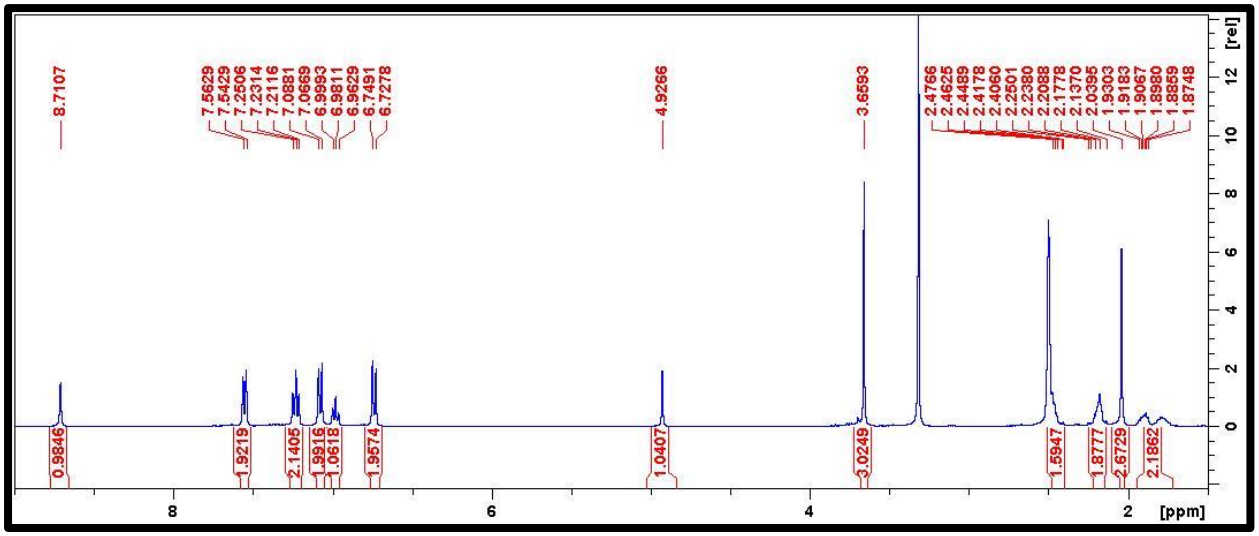

^{1}H NMR spectra of compound **5c**

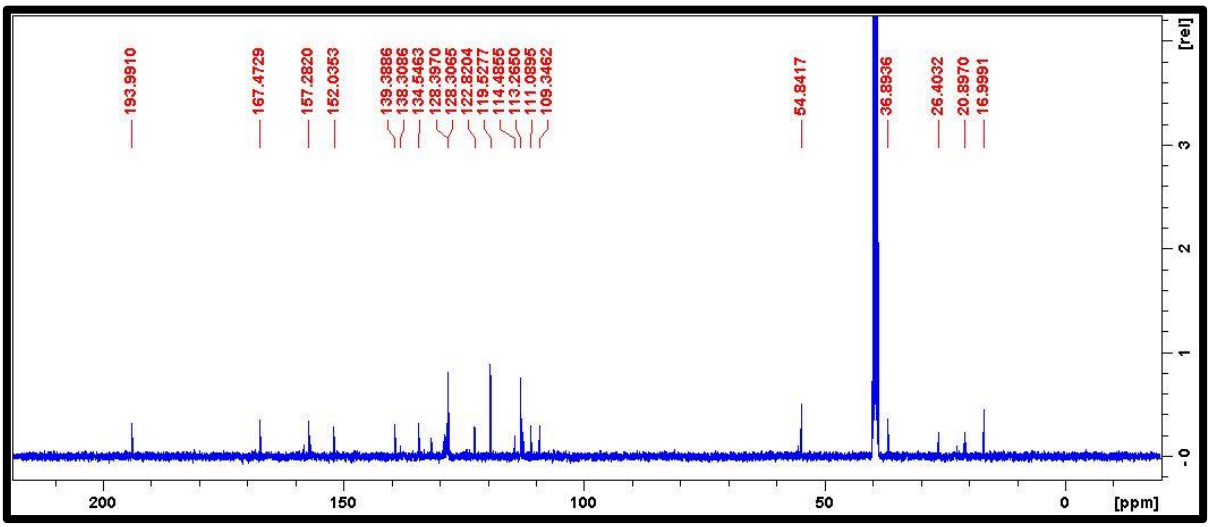

^{13}C NMR spectra of compound **5c**

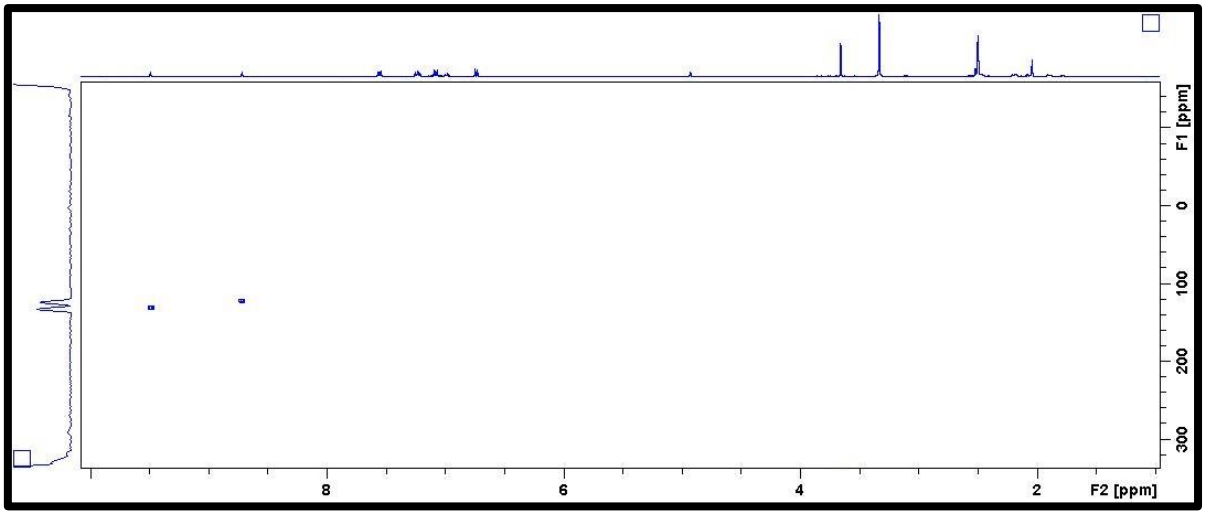

^{15}N NMR spectra of compound **5c**

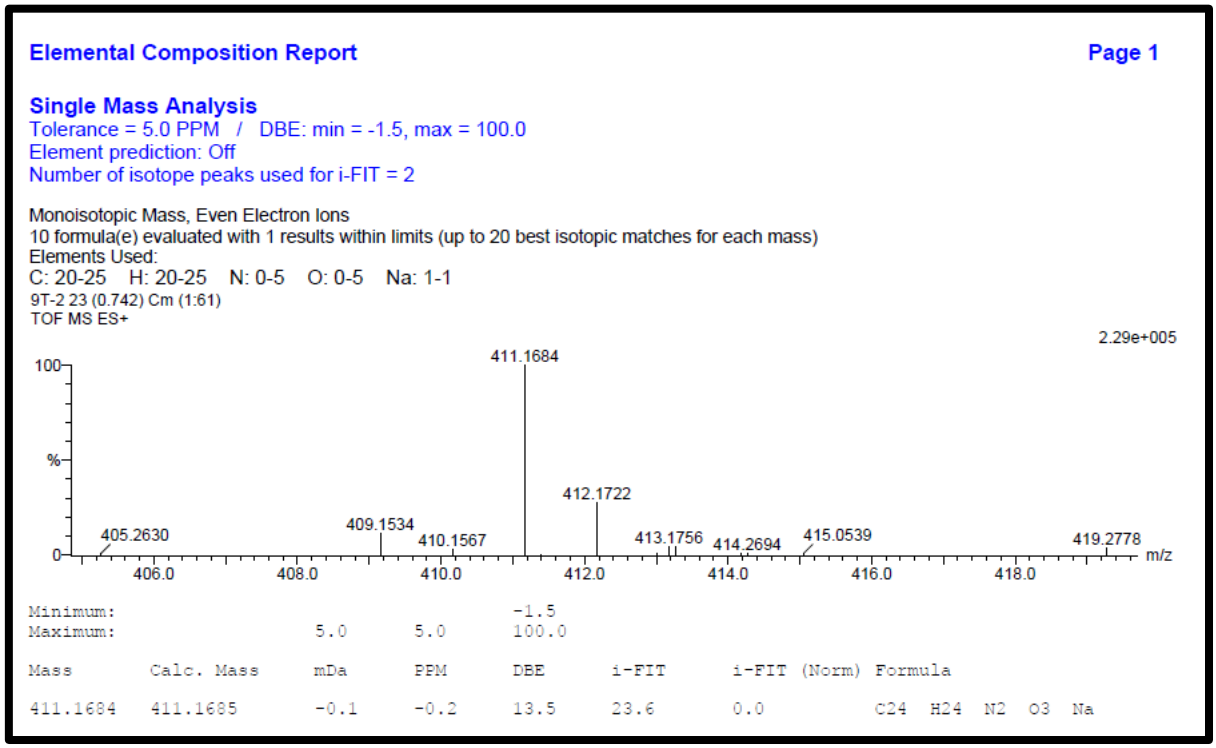

Elemental Composition Report **Page 1**

Single Mass Analysis
Tolerance = 5.0 PPM / DBE: min = -1.5, max = 100.0
Element prediction: Off
Number of isotope peaks used for i-FIT = 2

Monoisotopic Mass, Even Electron Ions
10 formula(e) evaluated with 1 results within limits (up to 20 best isotopic matches for each mass)
Elements Used:
C: 20-25 H: 20-25 N: 0-5 O: 0-5 Na: 1-1
9T-2 23 (0.742) Cm (1:61)
TOF MS ES+

2.29e+005

Minimum:				-1.5			
Maximum:		5.0	5.0	100.0			
Mass	Calc. Mass	mDa	PPM	DBE	i-FIT	i-FIT (Norm)	Formula
411.1684	411.1685	-0.1	-0.2	13.5	23.6	0.0	C24 H24 N2 O3 Na

HRMS spectra of compound **5c**

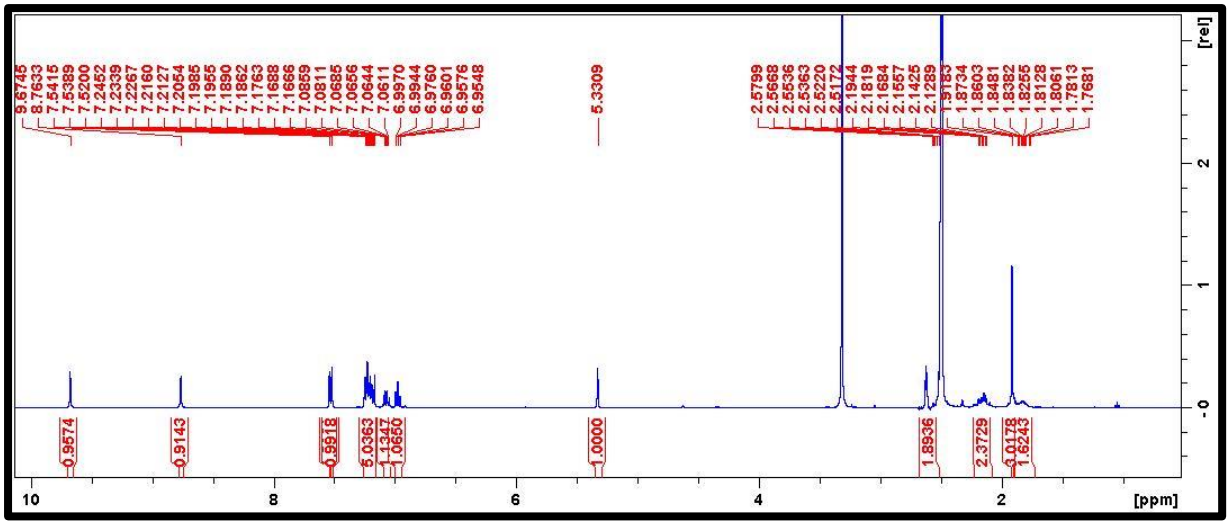

^{1}H NMR spectra of compound **5d**

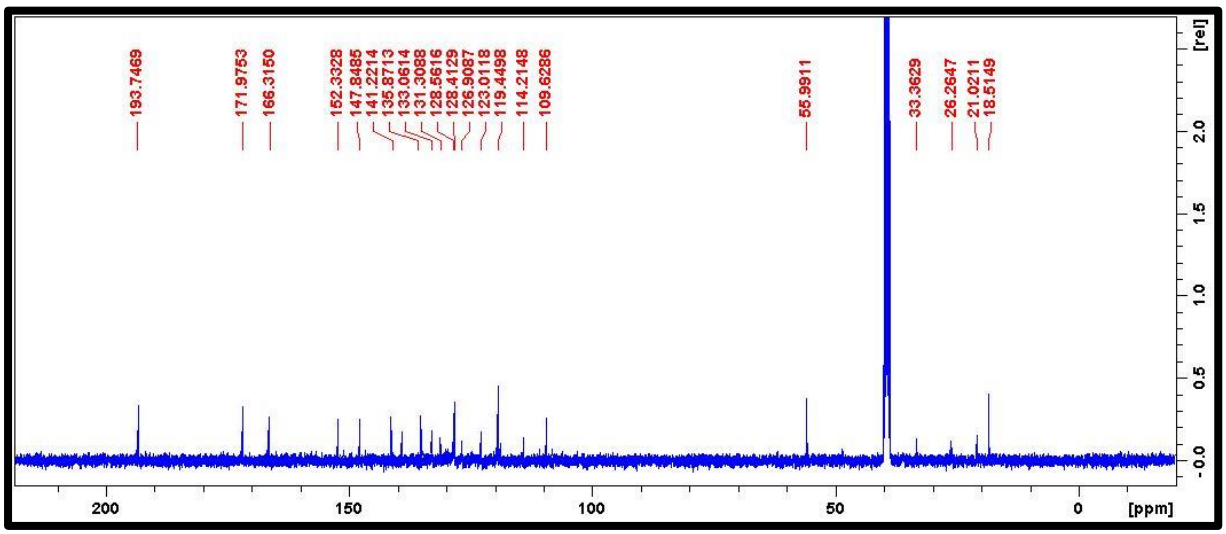

^{1}H NMR spectra of compound **5d**

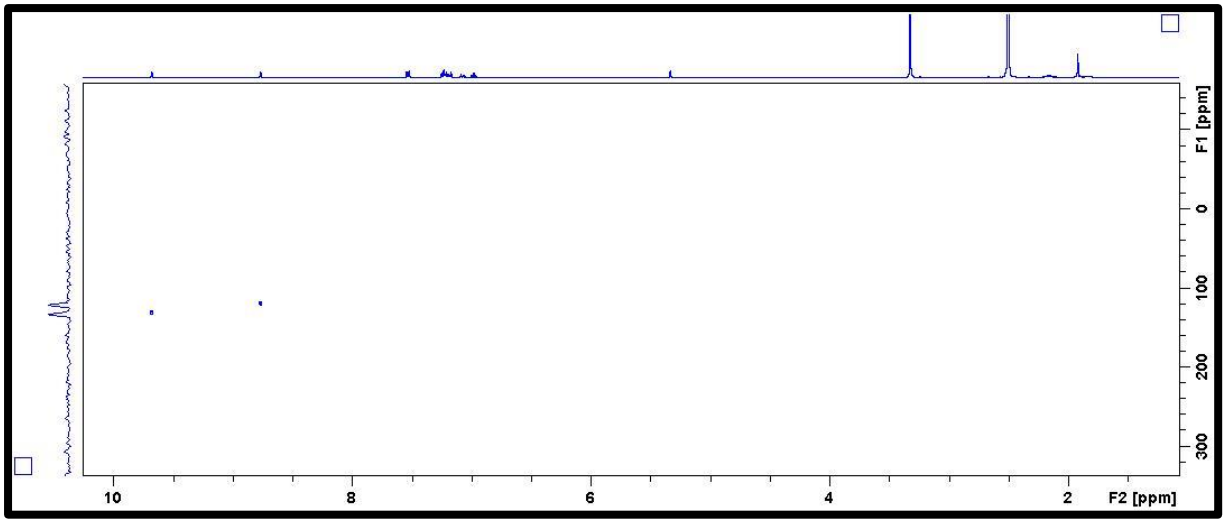

^{1}H NMR spectra of compound **5d**

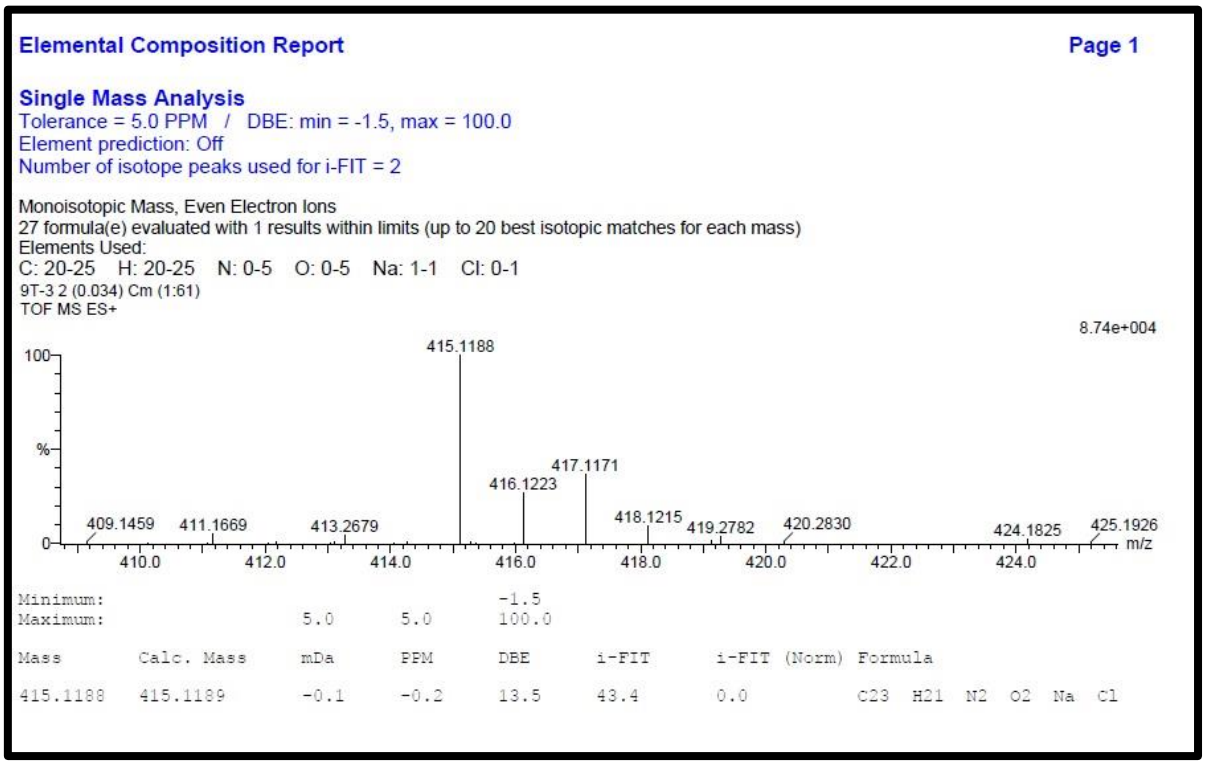

Elemental Composition Report Page 1

Single Mass Analysis
Tolerance = 5.0 PPM / DBE: min = -1.5, max = 100.0
Element prediction: Off
Number of isotope peaks used for i-FIT = 2

Monoisotopic Mass, Even Electron Ions
27 formula(e) evaluated with 1 results within limits (up to 20 best isotopic matches for each mass)
Elements Used:
C: 20-25 H: 20-25 N: 0-5 O: 0-5 Na: 1-1 Cl: 0-1
9T-3 2 (0.034) Cm (1:61)
TOF MS ES+

8.74e+004

Minimum:				-1.5			
Maximum:		5.0	5.0	100.0			
Mass	Calc. Mass	mDa	PPM	DBE	i-FIT	i-FIT (Norm)	Formula
415.1188	415.1189	-0.1	-0.2	13.5	43.4	0.0	C23 H21 N2 O2 Na Cl

^{1}H NMR spectra of compound **5d**

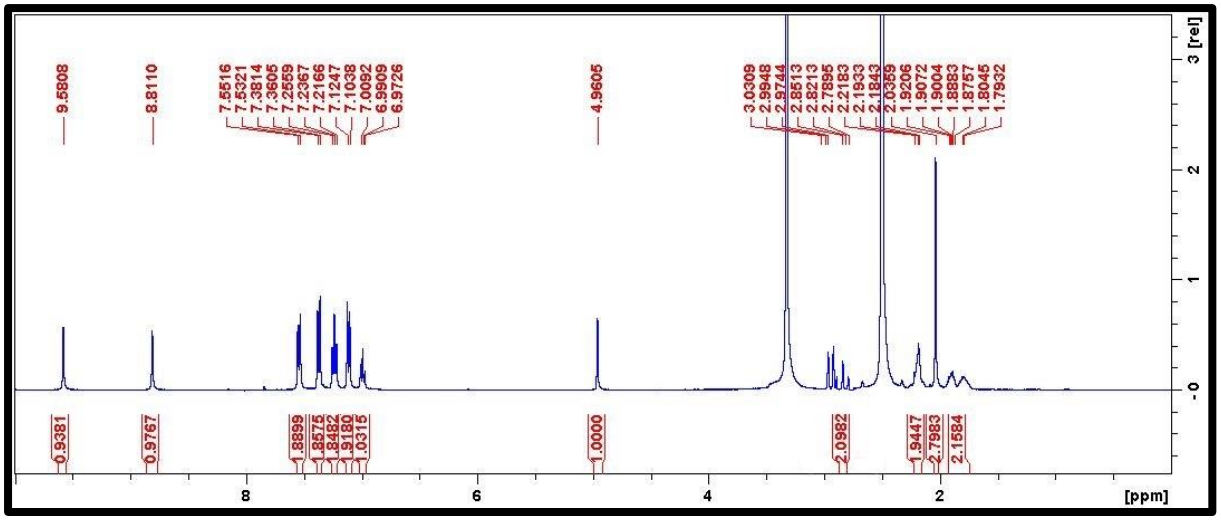

^{1}H NMR spectra of compound **5e**

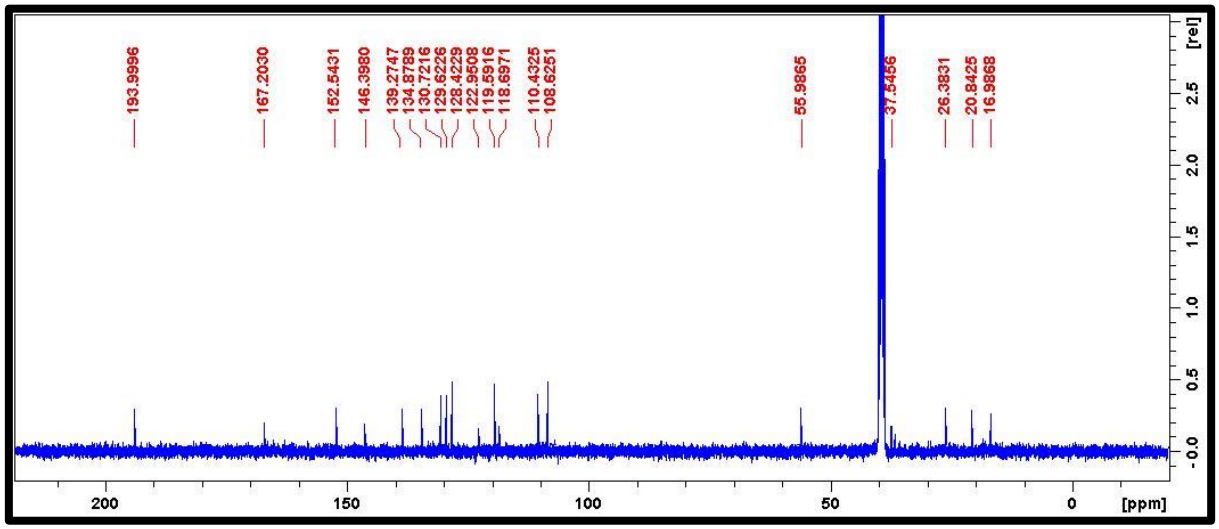

^{13}C NMR spectra of compound **5e**

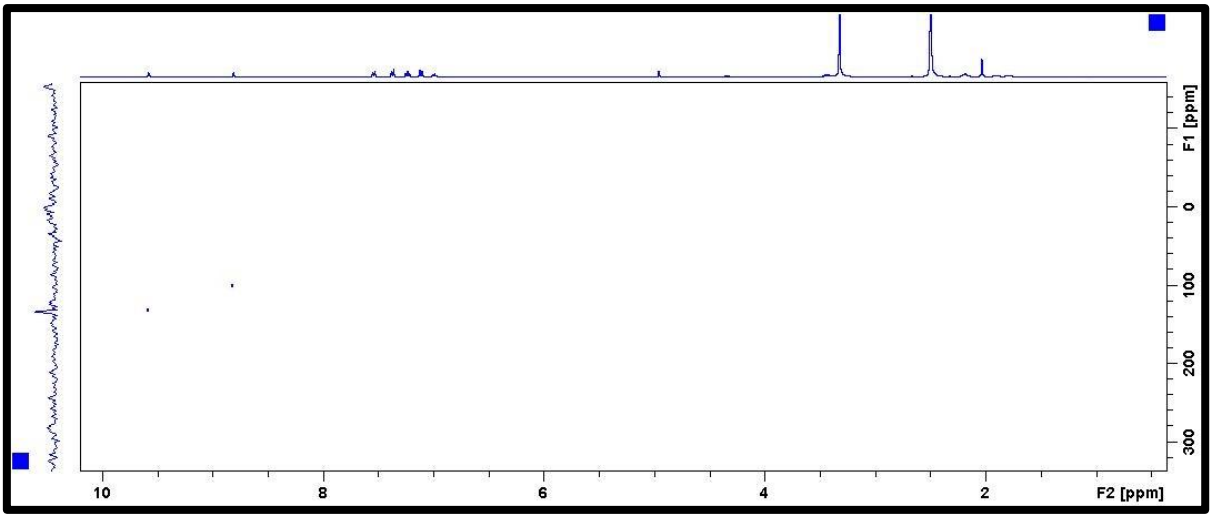

^{15}N NMR spectra of compound **5e**

Elemental Composition Report **Page 1**

Single Mass Analysis
Tolerance = 5.0 PPM / DBE: min = -1.5, max = 100.0
Element prediction: Off
Number of isotope peaks used for i-FIT = 2

Monoisotopic Mass, Even Electron Ions
29 formula(e) evaluated with 1 results within limits (up to 20 best isotopic matches for each mass)
Elements Used:
C: 20-25 H: 20-25 N: 0-5 O: 0-5 Na: 1-1 Br: 0-1

9T-4 57 (1.889) Cm (1:61)
TOF MS ES+

4.53e+005

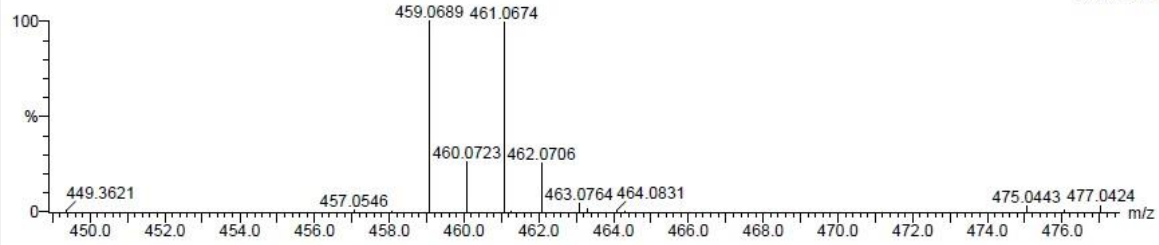

Minimum:				-1.5			
Maximum:		5.0	5.0	100.0			
Mass	Calc. Mass	mDa	PPM	DBE	i-FIT	i-FIT (Norm)	Formula
459.0689	459.0684	0.5	1.1	13.5	13.6	0.0	C23 H21 N2 O2 Na Br

HRMS spectra of compound **5e**

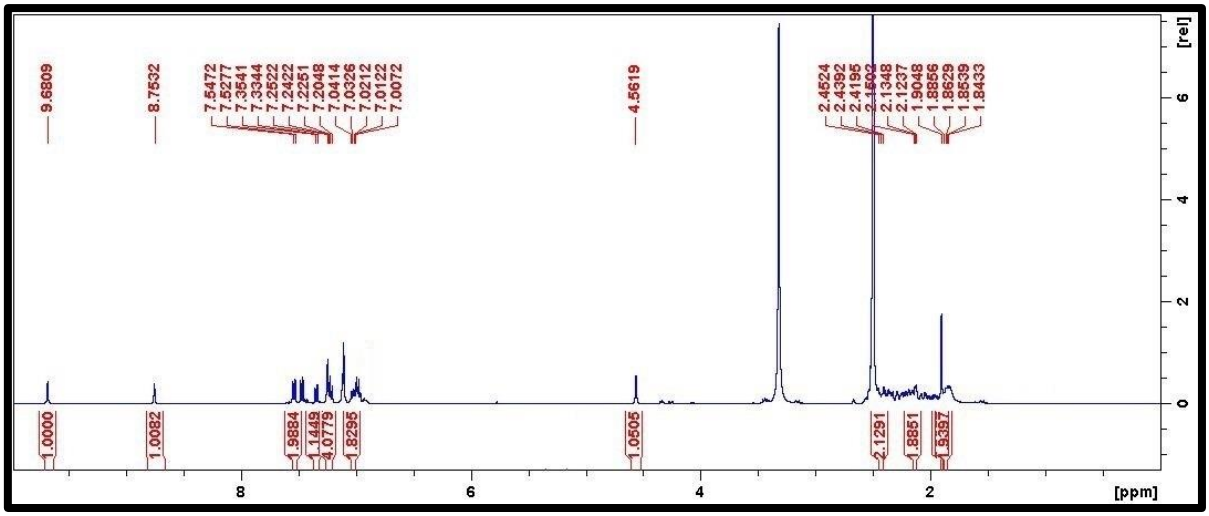

^{1}H NMR spectra of compound **5f**

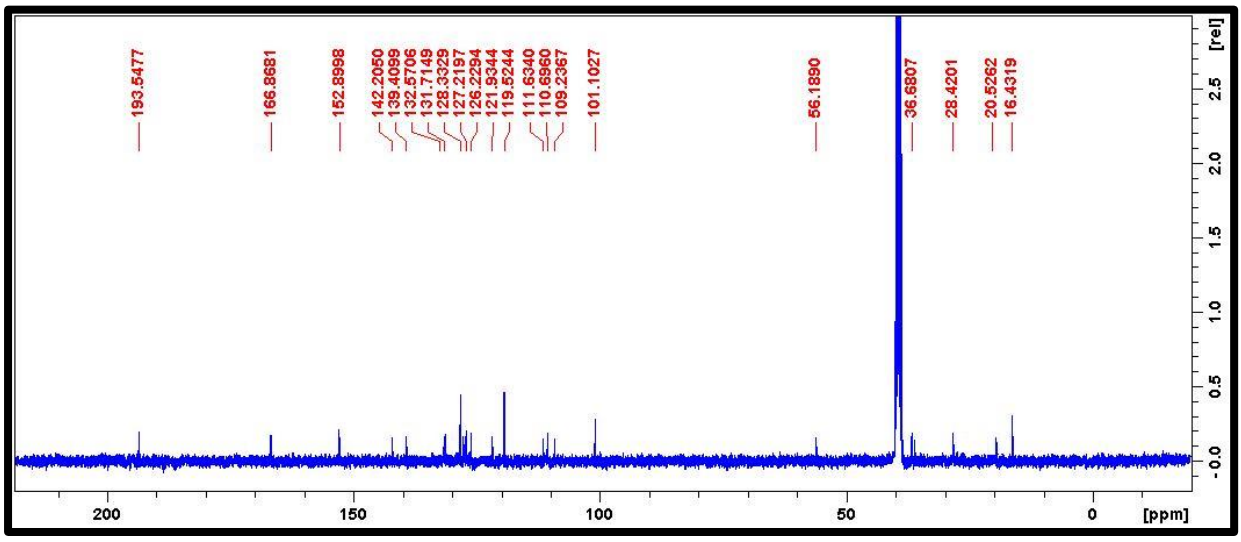

^{13}C NMR spectra of compound **5f**

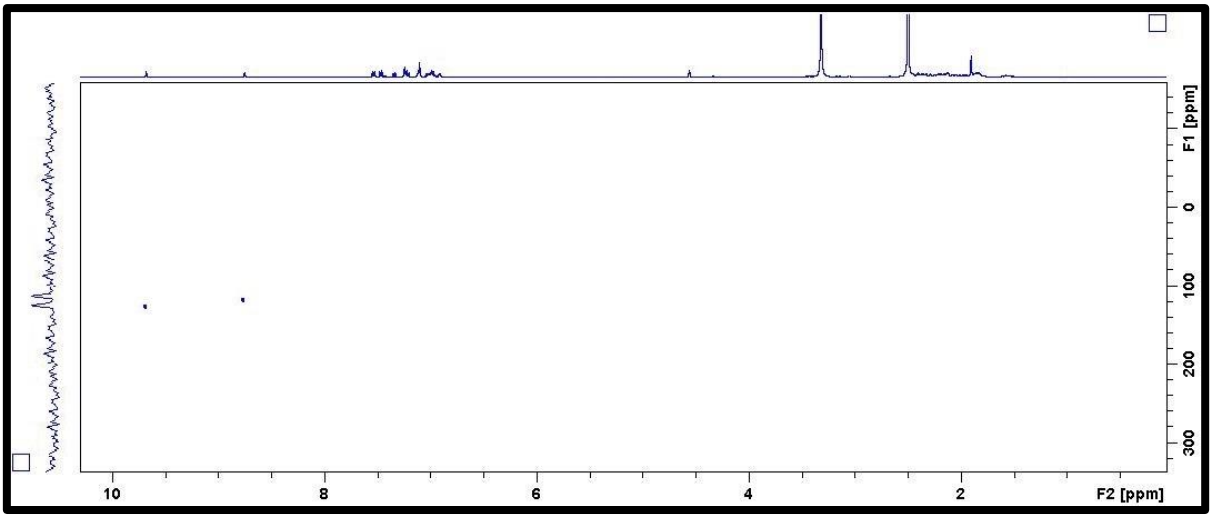

^{15}N NMR spectra of compound **5f**

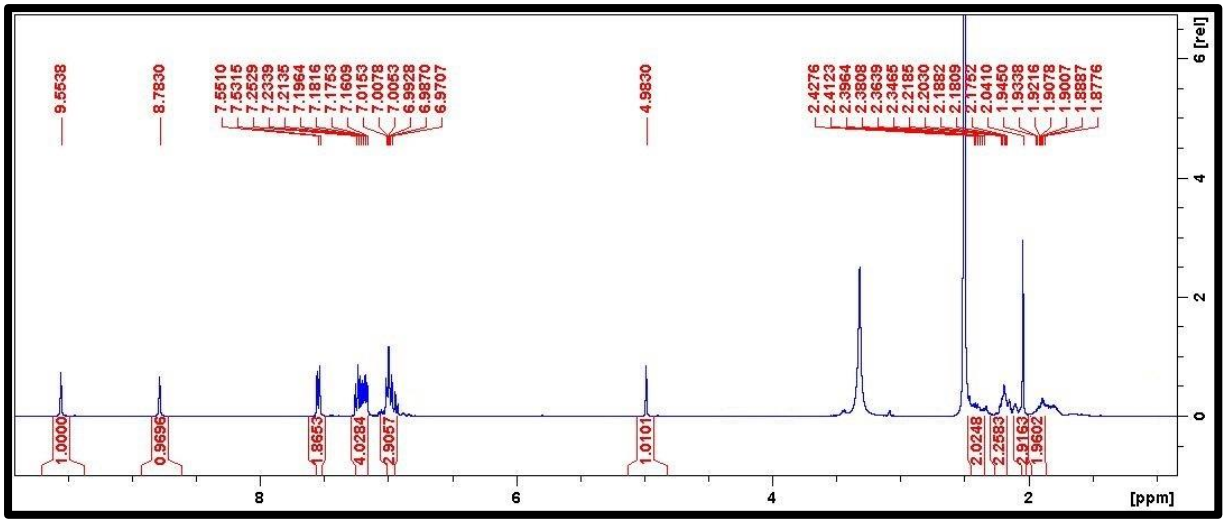

^{1}H NMR spectra of compound **5g**

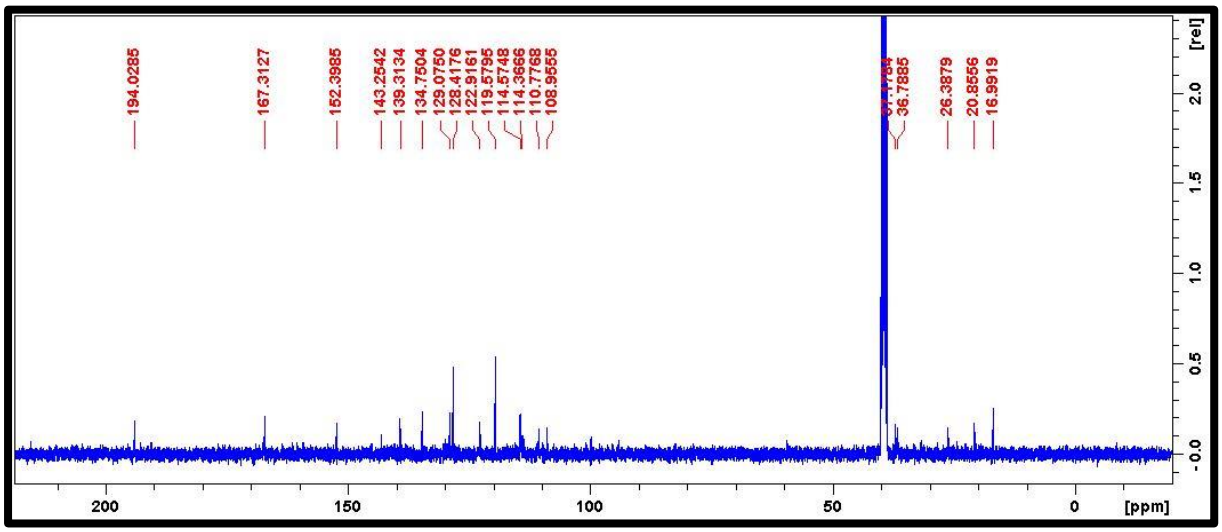

^{13}C NMR spectra of compound **5g**

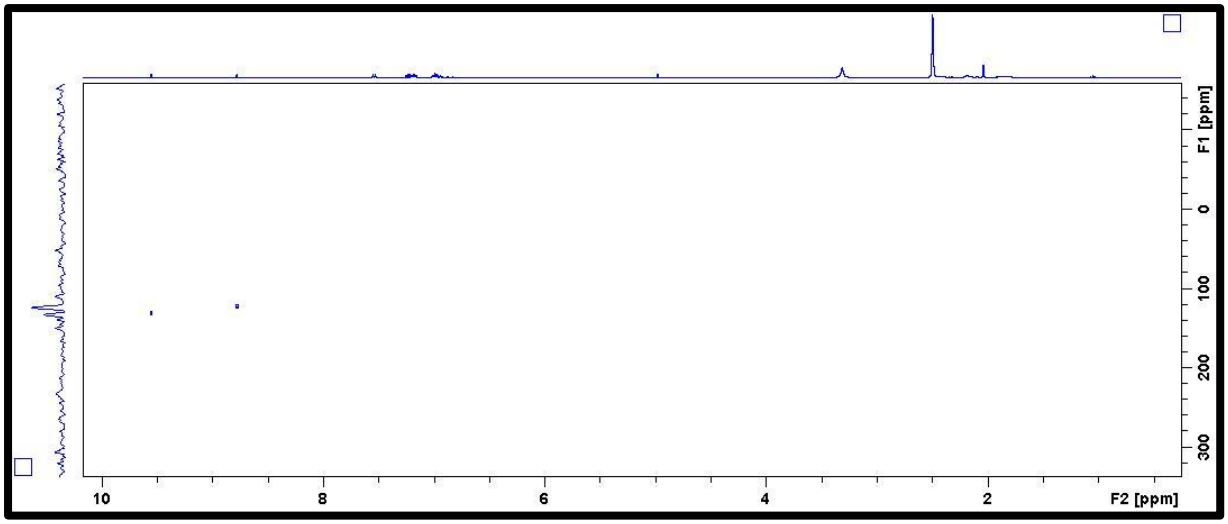

^{15}N NMR spectra of compound **5g**

Elemental Composition Report **Page 1**

Single Mass Analysis
Tolerance = 5.0 PPM / DBE: min = -1.5, max = 100.0
Element prediction: Off
Number of isotope peaks used for i-FIT = 2

Monoisotopic Mass, Even Electron Ions
26 formula(e) evaluated with 1 results within limits (up to 20 best isotopic matches for each mass)
Elements Used:
C: 20-25 H: 20-25 N: 0-5 O: 0-5 F: 0-1 Na: 1-1
9T-7 2 (0.034) Cm (1:61)
TOF MS ES+

1.09e+006

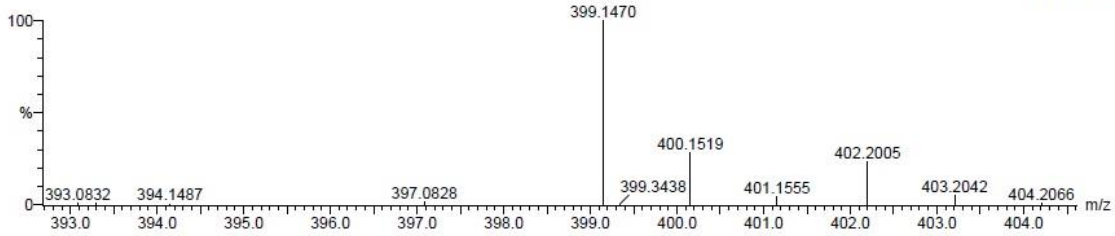

Minimum:				-1.5			
Maximum:		5.0	5.0	100.0			
Mass	Calc. Mass	mDa	PPM	DBE	i-FIT	i-FIT (Norm)	Formula
399.1470	399.1485	-1.5	-3.8	13.5	37.0	0.0	C23 H21 N2 O2 F Na

HRMS spectra of compound **5g**

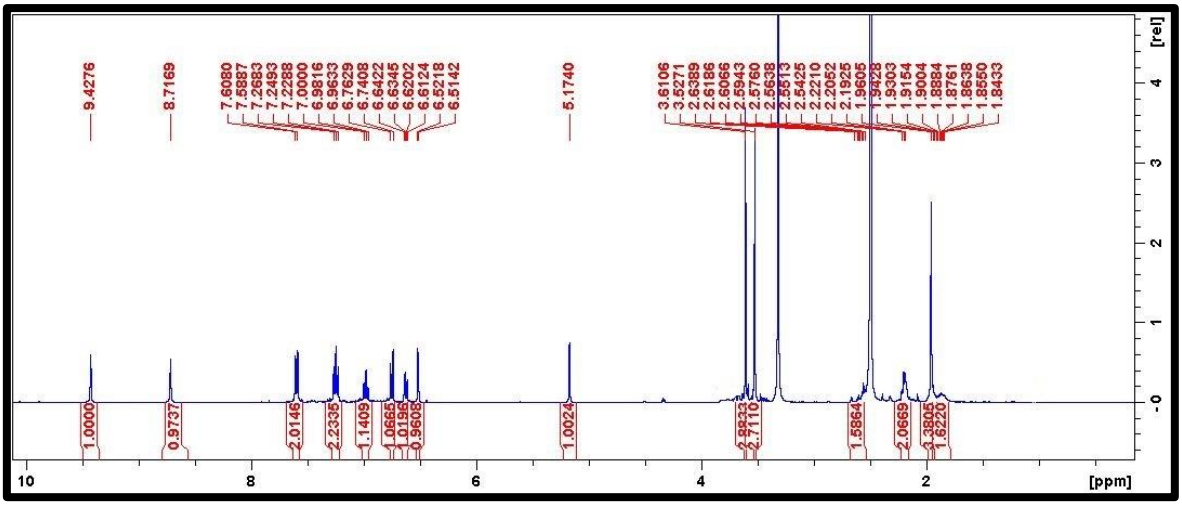

^{1}H NMR spectra of compound **5h**

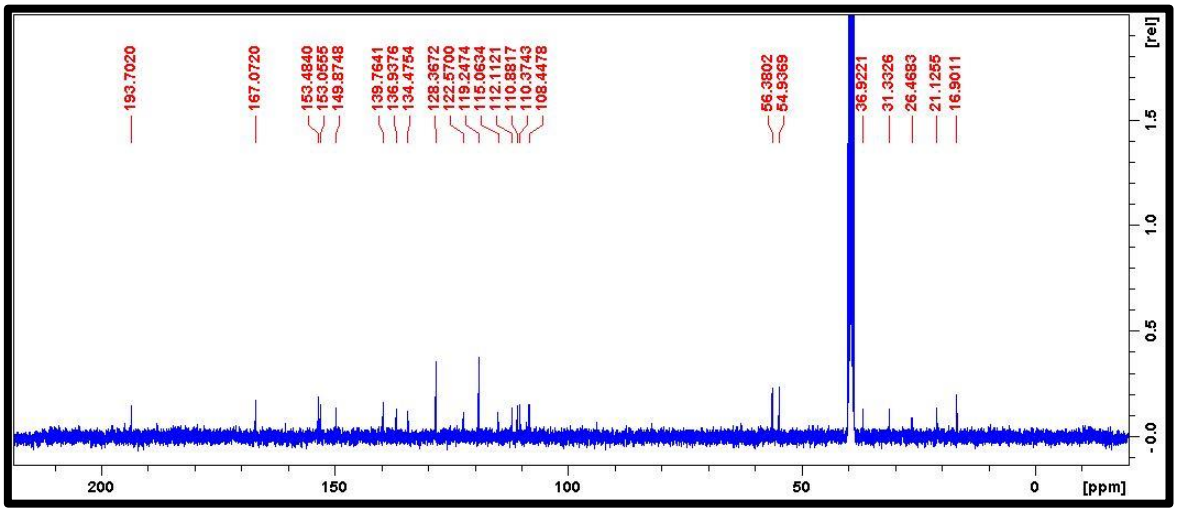

^{13}C NMR spectra of compound **5h**

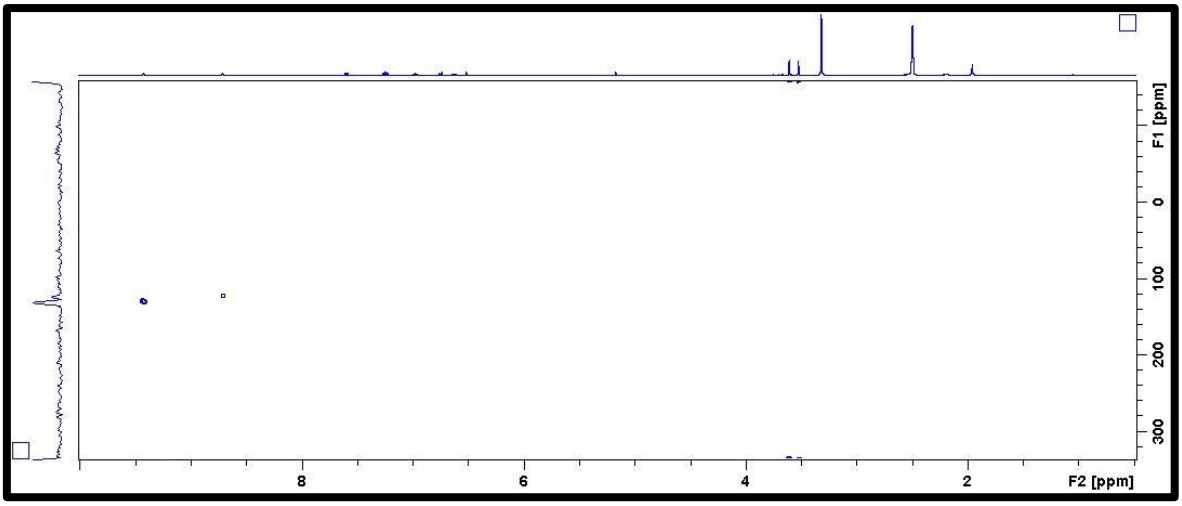

^{15}N NMR spectra of compound **5h**

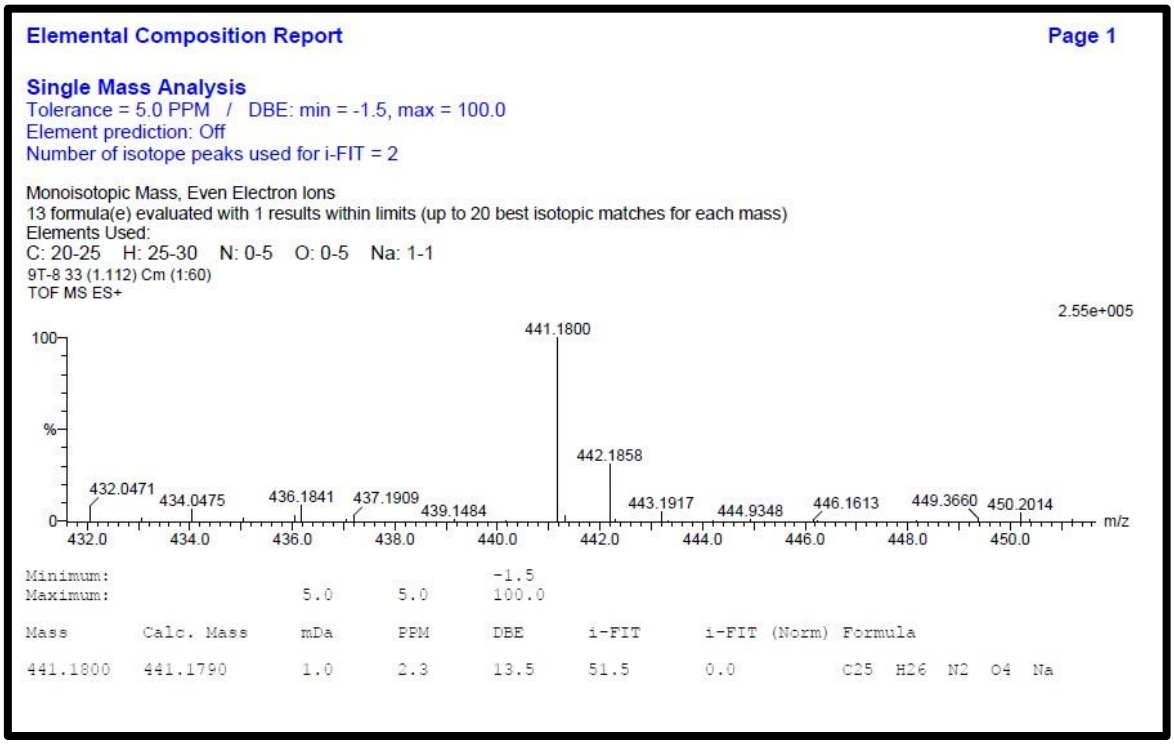

HRMS spectra of compound **5h**

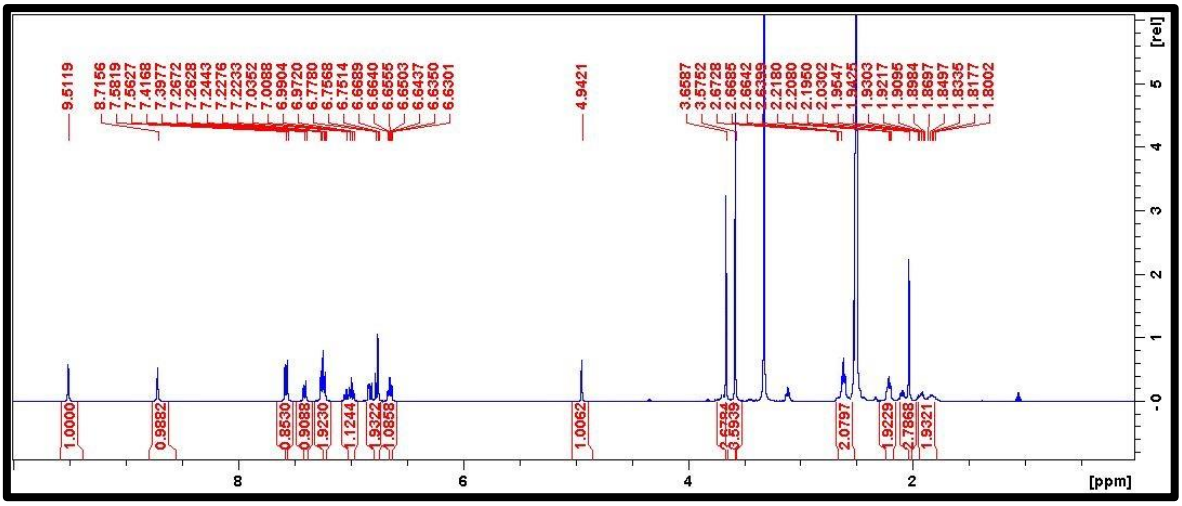

^{1}H NMR spectra of compound **5i**

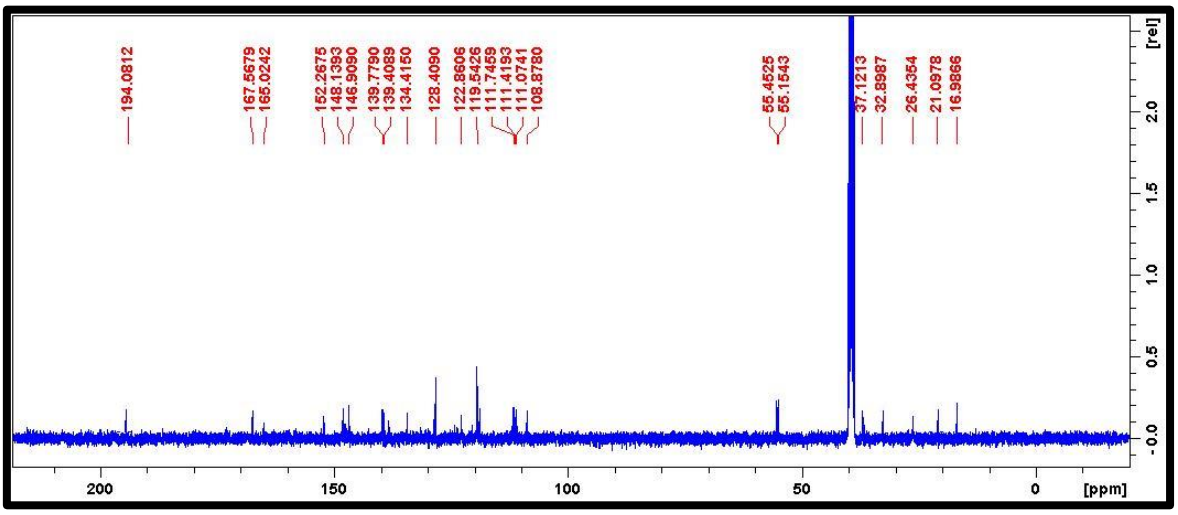

^{13}C NMR spectra of compound **5i**

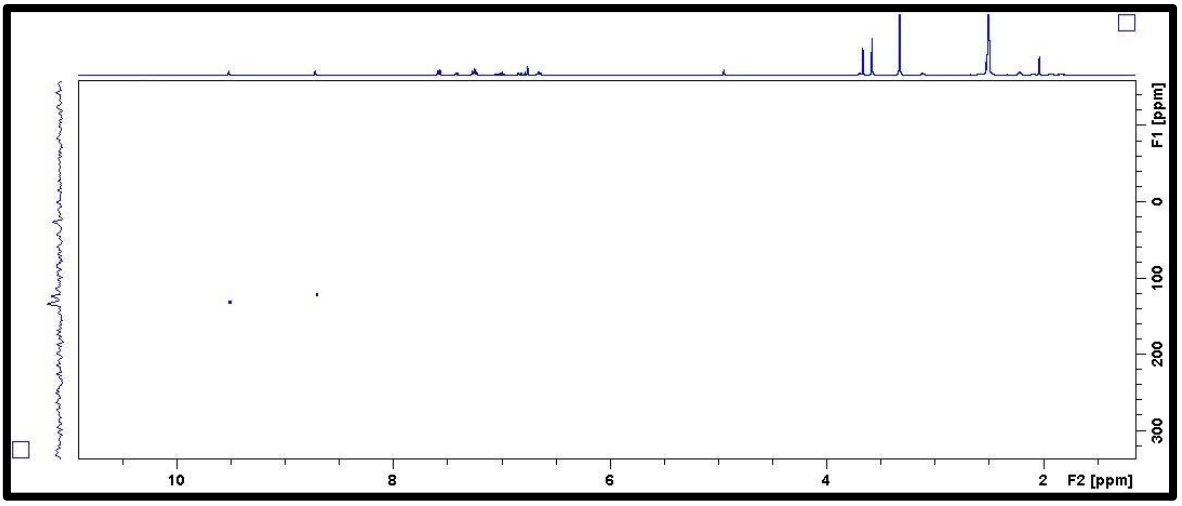

^{15}N NMR spectra of compound **5i**

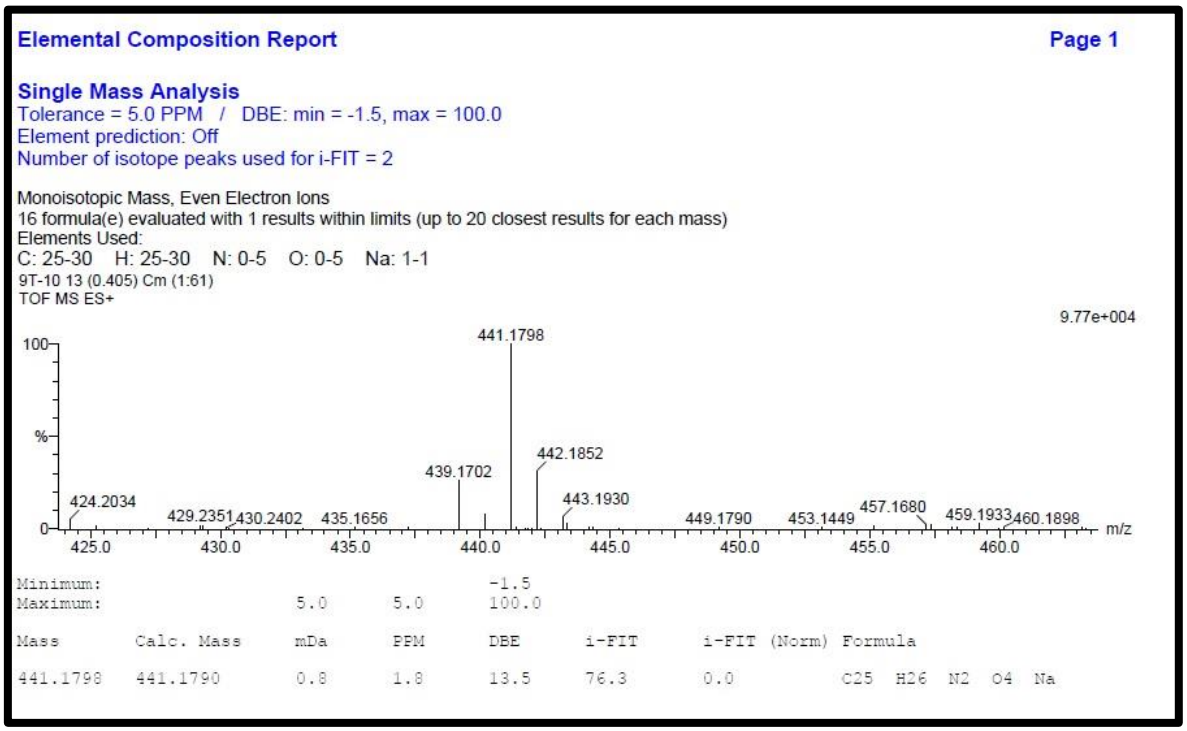

HRMS spectra of compound **5i**

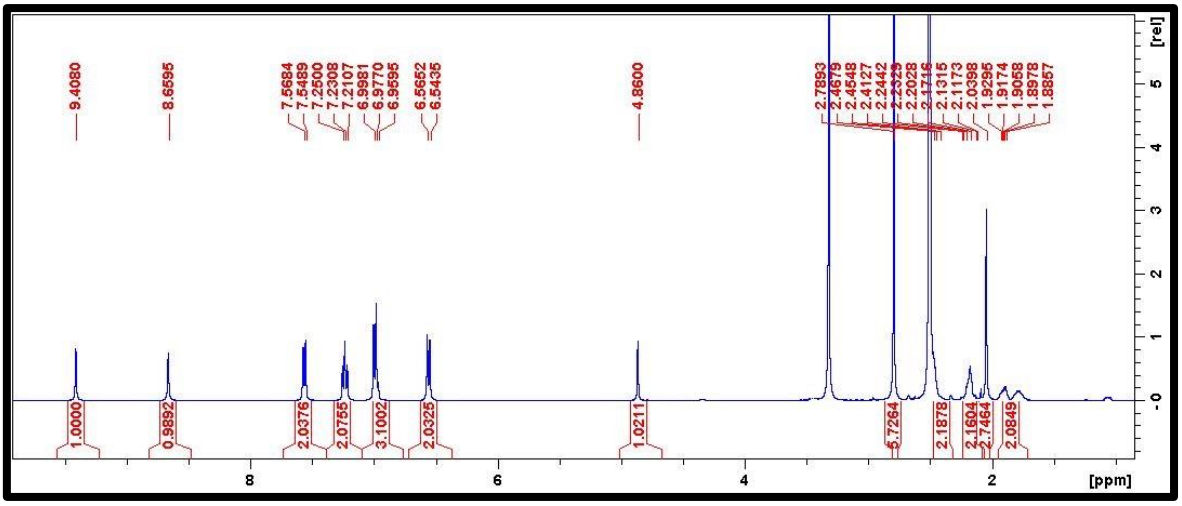

^{1}H NMR spectra of compound **5j**

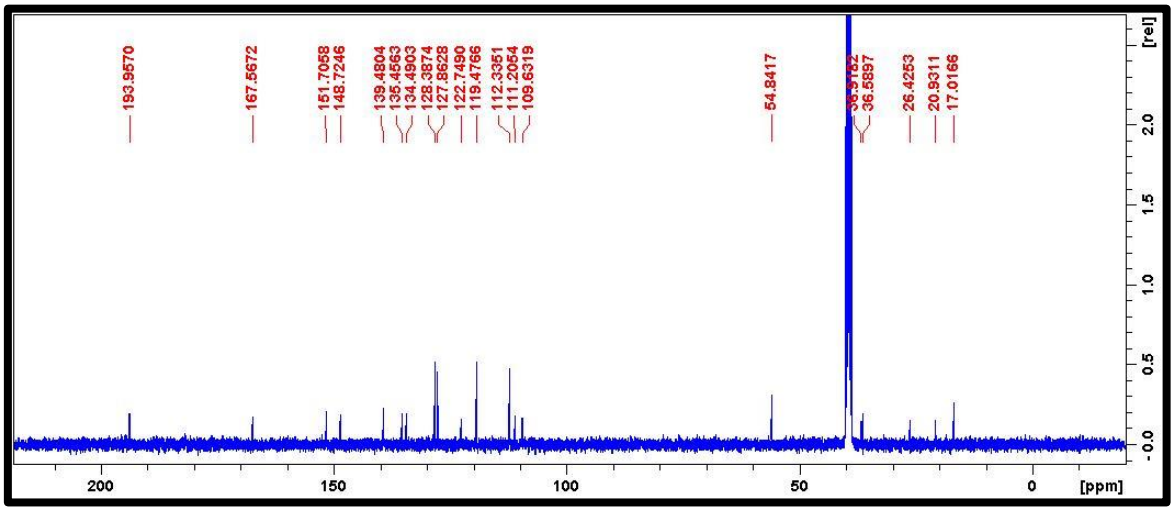

^{13}C NMR spectra of compound **5j**

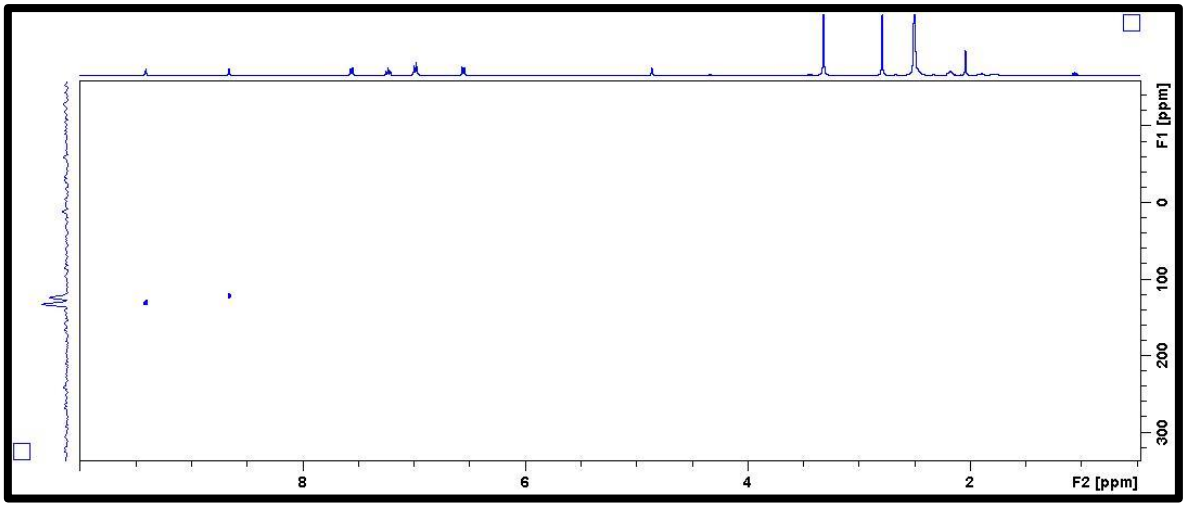

^{15}N NMR spectra of compound **5j**

Elemental Composition Report **Page 1**

Single Mass Analysis
Tolerance = 5.0 PPM / DBE: min = -1.5, max = 100.0
Element prediction: Off
Number of isotope peaks used for i-FIT = 2

Monoisotopic Mass, Even Electron Ions
13 formula(e) evaluated with 1 results within limits (up to 20 closest results for each mass)
Elements Used:
C: 20-25 H: 25-30 N: 0-5 O: 0-5 Na: 1-1
9T-14 50 (1.652) Cm (1:61)
TOF MS ES+
1.19e+005

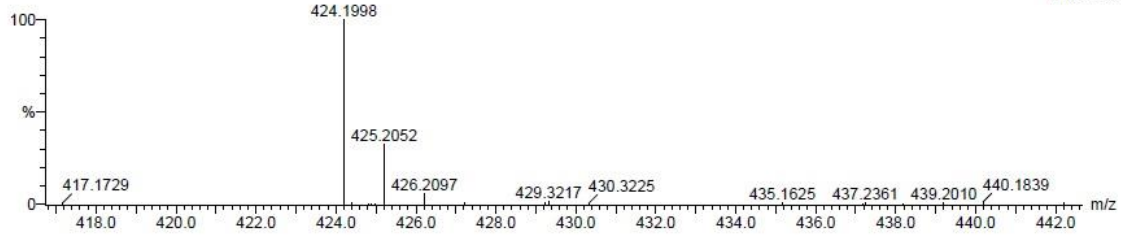

Minimum:				-1.5			
Maximum:		5.0	5.0	100.0			
Mass	Calc. Mass	mDa	PPM	DBE	i-FIT	i-FIT (Norm)	Formula
424.1998	424.2001	-0.3	-0.7	13.5	67.5	0.0	C25 H27 N3 O2 Na

HRMS spectra of compound **5j**

Crystal data:

Identification code	5j
Empirical formula	$C_{25}H_{27}N_3O_2$
Formula weight	401.49
Temperature/K	99.99
Crystal system	monoclinic
Space group	$P2_1/c$
a/Å	10.9896(2)
b/Å	17.8516(3)
c/Å	11.6313(2)
α/°	90
β/°	115.0000(10)
γ/°	90
Volume/Å^3	2068.06(6)
Z	4
ρ_{calc}g/cm^3	1.290
μ/mm^{-1}	0.083
F(000)	856.0
Crystal size/mm^3	0.34 × 0.26 × 0.17
Radiation	MoKα (λ = 0.71073)
2Θ range for data collection/°	4.09 to 56.608
Index ranges	$-14 \leq h \leq 13$, $-23 \leq k \leq 23$, $-10 \leq l \leq 15$
Reflections collected	27824
Independent reflections	5136 [R_{int} = 0.0309, R_{sigma} = 0.0349]
Data/restraints/parameters	5136/0/274
Goodness-of-fit on F^2	1.033
Final R indexes [I>=2σ (I)]	R_1 = 0.0434, wR_2 = 0.1017
Final R indexes [all data]	R_1 = 0.0655, wR_2 = 0.1132
Largest diff. peak/hole / e Å^{-3}	0.37/-0.28

.

Chapter 7

A Four-Component fusion protocol with NiO/ ZrO_2 as robust recyclable catalyst for novel 1,4-dihydropyridines

Sandeep V.H.S. Bhaskaruni, Suresh Maddila, Werner E. van Zyl and Sreekantha B. Jonnalagadda*

*School of Chemistry & Physics, University of KwaZulu-Natal, Westville Campus, Chiltern Hills, Durban-4000, South Africa

*Corresponding Author: Prof. Sreekantha B. Jonnalagadda
School of Chemistry & Physics,
University of KwaZulu-Natal,
Durban 4000, South Africa.
Tel.: +27 31 2607325,
Fax: +27 31 2603091
E-mail address: jonnalagaddas@ukzn.ac.za

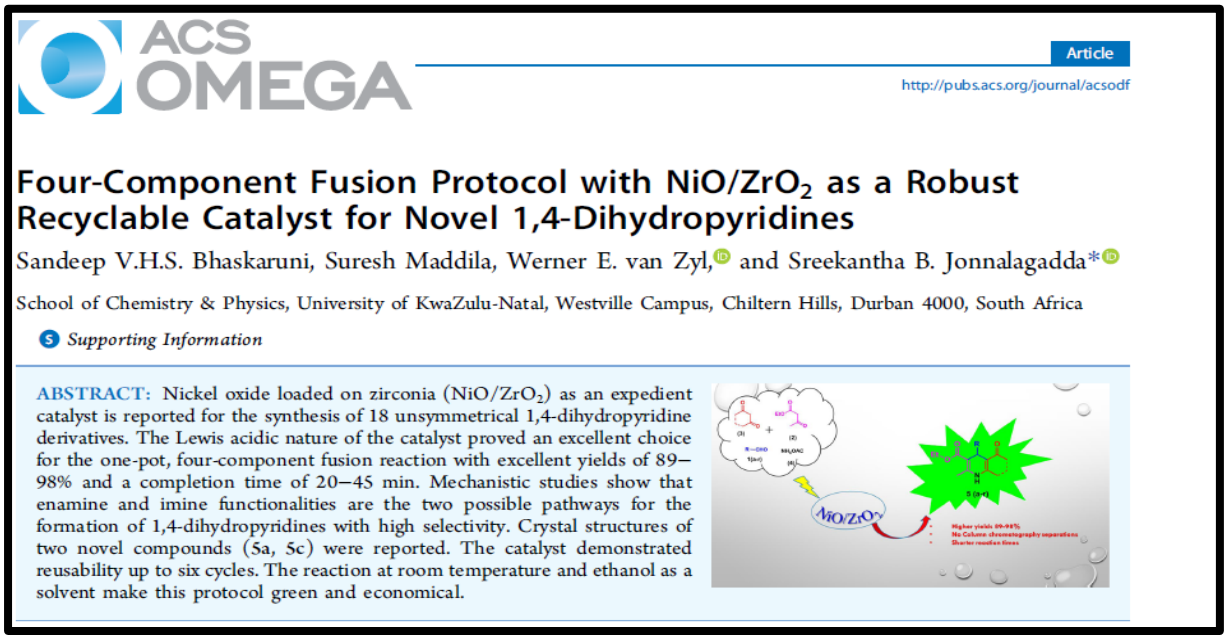

ACS OMEGA

Article

http://pubs.acs.org/journal/acsodf

Four-Component Fusion Protocol with NiO/ZrO_2 as a Robust Recyclable Catalyst for Novel 1,4-Dihydropyridines

Sandeep V.H.S. Bhaskaruni, Suresh Maddila, Werner E. van Zyl, and Sreekantha B. Jonnalagadda*

School of Chemistry & Physics, University of KwaZulu-Natal, Westville Campus, Chiltern Hills, Durban 4000, South Africa

Supporting Information

ABSTRACT: Nickel oxide loaded on zirconia (NiO/ZrO_2) as an expedient catalyst is reported for the synthesis of 18 unsymmetrical 1,4-dihydropyridine derivatives. The Lewis acidic nature of the catalyst proved an excellent choice for the one-pot, four-component fusion reaction with excellent yields of 89−98% and a completion time of 20−45 min. Mechanistic studies show that enamine and imine functionalities are the two possible pathways for the formation of 1,4-dihydropyridines with high selectivity. Crystal structures of two novel compounds (5a, 5c) were reported. The catalyst demonstrated reusability up to six cycles. The reaction at room temperature and ethanol as a solvent make this protocol green and economical.

This chapter is accepted in the journal **ACS OMEGA**, and has been structured according to the journal's format.

Chapter 7

A Four-Component fusion protocol with NiO/ ZrO_2 as robust recyclable catalyst for novel 1,4-dihydropyridines

Sandeep V.H.S. Bhaskaruni, Suresh Maddila, Werner E. van Zyl and Sreekantha B. Jonnalagadda*

*School of Chemistry & Physics, University of KwaZulu-Natal, Westville Campus, Chiltern Hills, Durban-4000, South Africa

*Corresponding Author: Prof. Sreekantha B. Jonnalagadda
School of Chemistry & Physics,
University of KwaZulu-Natal,
Durban 4000, South Africa.
Tel.: +27 31 2607325,
Fax: +27 31 2603091
E-mail address: jonnalagaddas@ukzn.ac.za

Abstract

Nickel oxide loaded on zirconia (NiO/ZrO_2) as an expedient catalyst is reported for the synthesis of 18 unsymmetrical 1,4-dihydropyridine derivatives. The Lewis acidic nature of the catalyst proved an excellent choice for the one-pot, 4-component fusion reaction with excellent yields of 89-98% and completed in 20-45 minutes. Mechanistic studies show that enamine and imine functionality are the two possible pathways for the formation of 1,4-dihydropyridines with high selectivity. Crystal structures of two novel compounds (**5a, 5c**) were reported. Catalyst demonstrated reusability up to 6 cycles. Reaction at room temperature (RT) and ethanol as solvent make this protocol green and economical.

Keywords: 1,4 dihydropyridine, NiO/ZrO_2, 4-component reaction, Hantzsch dihydropyridine, mixed metal oxide.

7.1 Introduction

Catalysts play a crucial role in facilitating product selectivity and decreasing the activation energy of the reactions.[1] Although homogeneous catalysts show better efficiency in chemo- and regioselectivity and their reaction mechanisms are better understood, their recovery from the reaction mixture is often difficult and involves several neutralization procedures.[2] To overcome these drawbacks, heterogeneous catalysts are more chosen in organic synthesis. Because of their surface-to-volume ratio, the amount of heterogeneous catalyst required for the transformation is reduced, enabling the transformation to become both efficient and economical, and it is easy to separate from the reaction medium.[3] In this context, mixed metal oxides as heterogeneous catalysts contributed significantly to organic synthesis because of their tuneable characteristics of the versatile surface sites.[4] The synergy between active metal and support typically dictates the catalytic properties of the material.[5] In this context, nickel has been used both as a homogeneous and heterogeneous catalyst in many organic transformations like C−C bond formations, reductive eliminations including C−N and C−O bond formation reactions, and cross-coupling reactions.[6] Zirconia has attracted more interest than other support materials because of its higher tolerance toward corrosion and high temperatures,[7] as demonstrated by the use of ZrO_2 in the heat shield of space shuttles. Moreover, zirconia gained importance as a catalyst due to its surface properties by possessing both acidic and basic sites. The surface properties can be modified by loading/doping with suitable metals.[8,9] Based on these advantages, we prepared materials with different loadings of Ni on ZrO_2 support and investigated their efficacy as a reusable catalyst for selective organic transformation. Previous reports demonstrated the use of NiO/ZrO_2 as a catalyst for simple conversions such as oxidative dehydrogenation[10] and C−S cross-coupling reactions.[11]This is the first report of using NiO/ZrO_2 as a catalyst in a multicomponent, one-pot reaction system.

Multicomponent reactions (MCRs) are important synthetic tools with the ability to craft complex organic molecules with high atom economy. An MCR is an ecofriendly means to synthesize libraries of biologically important scaffolds.[12]Among the heterocyclic compounds, N-heterocyclic scaffolds in general acquired more prominence in the medicinal and pharmaceutical chemistry. In particular, 1,4-dihydropyridines (1,4-DHPs) are scaffolds of biological importance [13] as antimicrobial,[14] anti-tubercular, [15] anticancer,[16] anticoagulant,[17] neuroprotector,[18] antioxidant,[19] L/T-type calcium channel blocking,[20] AChE inhibiting, [21] and bone anabolic agents.[22] 1,4-DHPs were first reported by Hantzsch in 1882 via the multicomponent reaction of aromatic aldehyde, β-ketoester, and ammonia as nitrogen sources.

[23] Well-known commercial drugs like felodipine, diludine, and nifedipine constitute 1,4-DHPs as the core moiety (Figure 1).

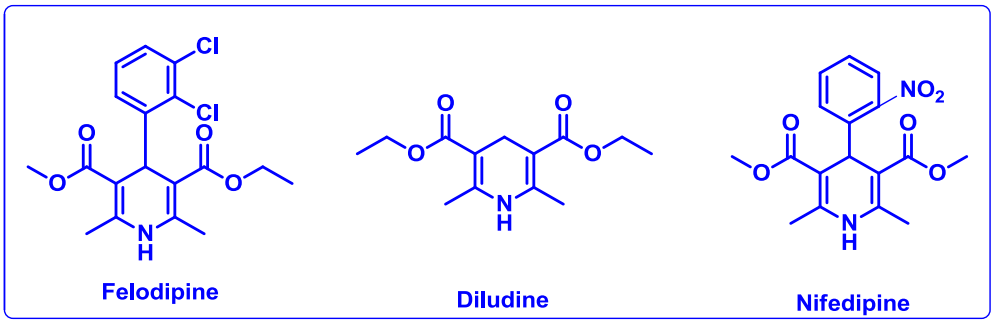

Fig.1 Structures of commercially available 1,4-dihydropyridine drugs.

Due to the vast biological and synthetic importance of 1,4-DHP derivatives, several protocols have been reported via a one-pot strategy and employing different catalysts like nano-tungsten trioxide-supported sulfonic acid (n-WSA),[24]sulfated boric acid nanoparticles,[25] chitosan-supported copper(II)sulfate,[26] Fe_3O_4@SiO_2@Si-$(CH_2)_3$@melamine-picolineimine@SO_3H, [27] sulfated polyborate,[28] Fe_3O_4/KCC-1/BPAT,[29] chitosan-supported vanadium oxo,[30] magnetic guanidinylated chitosan,[31] nano-ZrO_2-SO_3H (n-ZrSA),[32] $Gd(OTf)_3$,[33] nicotinic acid,[34] γ-Fe_2O_3/Cu@cellulose,[35] SBA-15@AMPD-Co,[36] sulfamic acid,[19] Fe_3O_4@D-NH-$(CH_2)_4$-SO_3H,[37] Cu-adenine@boehmite,[38] hydromagnesite,[39] $Cu(OTf)_2$,[40] ascorbic acid,[41] NS-C_4(DABCO-$SO_3H)_2$·4Cl,[42] CBr_4,[43] and aminated CNTs.[14] Many of these methods either suffer from usage of reflux conditions, lower yields, or long reaction times.

We report for the first time NiO/ZrO_2 as a reusable catalyst in a one-pot four-component fusion reaction for the synthesis of novel 1,4-dihydropyridine derivatives at room temperature. We also report significant advances into the proposed mechansm based on the reaction intermediates, including a single-crystal structure.

7.2 Experimental Section

7.2.1 Catalyst preparation

A series of nickel oxide-loaded zirconia (NiO/ZrO_2) catalysts with different weight percentages (1, 2.5, and 5 wt %) of Ni were prepared by the wet impregnation method. A mixture of zirconium oxide (ZrO_2, 2 g, Alfa Aesar) and appropriate amount (wt %) of nickel sulfate ($NiSO_4·6H_2O$, Alfa Aesar) in 60 mL of deionized water was stirred for 7 h at room temperature. The resultant slurry was filtered under vacuum and dried at 100 °C for 6 h, followed by

calcination at 450 °C for 6 h in the presence of air, to obtain different weight percents of NiO/ZrO_2. Instrumentation details are included in the Supporting Information.

7.2.2 General method for the synthesis of series of 1,4-dihydropyridine derivatives (5a-r)

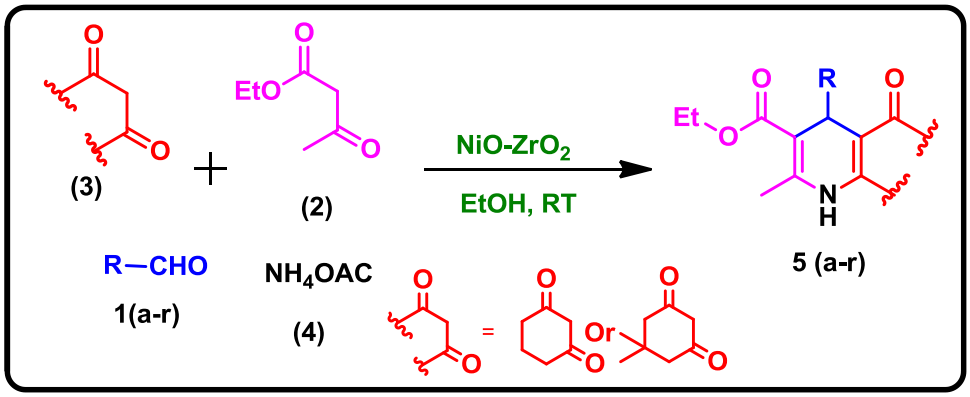

Scheme 1 Synthesis of novel 1,4-dihydropyridines.

1,4-Dihydropyridine Derivatives (5a-r). For the synthesis of a series of 1,4-dihydropyridine derivatives, the reaction was performed in a 25 mL round-bottom flask containing 5 mL of EtOH as a solvent. To these equimolar quantities of substituted aldehyde (1), ethyl acetoacetate (2), 1,3-cyclohexadione (3) and ammonium acetate (4) was added 30 mg of NiO/ZrO_2 and stirred at room temperature (RT) (Scheme 3). TLC was used to monitor the progress of the reaction at regular time intervals. After completion of the reaction, the catalyst was filtered by adding excess ethanol. The solvent was then evaporated, and the pure product was afforded by recrystallization from EtOH. The details and spectra are given in the Supplementary Information.

Ethyl 2-methyl-5-oxo-4-(2,3,4-trimethoxyphenyl)-1,4,5,6,7,8-hexahydroquinoline-3-carboxylate (5a) : The compound was obtained as described in the general procedure using 2,3,4-trimethoxybenzaldehyde (1 mmol;100 mg), ethyl acetoacetate (1 mmol; 57.14 mg), 1,3-cyclohexadione (1 mmol; 66.32 mg), ammonium acetate (1 mmol; 39.28 mg) in 98 % yield as a yellow solid (200.51 mg): mp. = 211-213 ^{o}C; ^{1}H NMR (400 MHz, DMSO): δ= 1.13 (t, *J*= 7.12 Hz, 3H, CH_3), 1.66-1.91 (m, 2H, CH_2), 2.09-2.16 (m, 2H, CH_2), 2.19 (s, 3H, CH_3), 2.46 (t, *J*= 4.8 Hz, 2H, CH_2), 3.68 (s, 3H, OCH_3), 3.71 (s, 3H, OCH_3), 3.77 (s, 3H, OCH_3), 3.90-3.96 (m, 2H, CH_2), 4.99 (s, 1H, CH), 6.60 (d, *J* = 7.72 Hz,1H, Ar-H), 6.78 (d, *J* = 8.68 Hz, 1H, Ar-H), 8.99 (s, 1H, NH) ; ^{13}C NMR (100 MHz, DMSO): 14.02, 18.04, 20.75, 26.29, 32.40, 36.79, 55.59, 58.78, 59.87, 60.09, 103.90, 106.89,

110.54, 124.53, 133.19, 141.42, 143.42, 151.41, 151.53, 167.29, 194.25; ^{15}N NMR (40.55 MHz, DMSO) δ= 129.8 ; HRMS of [$C_{22}H_{27}NO_6$-H^+] (m/z): 400.1770; Calcd.: 400.1760.

Ethyl 4-(2-bromophenyl)-2-methyl-5-oxo-1,4,5,6,7,8-hexahydroquinoline-3-carboxylate (5b) : 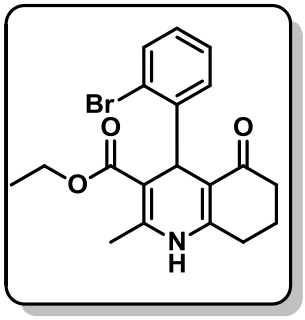

The compound was obtained as described in the general procedure using 2-bromobenzaldehyde (1 mmol; 100 mg), ethyl acetoacetate (1 mmol; 60.6 mg), 1,3-cyclohexadione (1 mmol; 70.33 mg), ammonium acetate (1 mmol; 41.66 mg) in 93 % yield as a yellow solid (196.16 mg): mp. = 197-199 ^oC; ^{1}H NMR (400 MHz, DMSO-d_6): δ= 1.07 (t, *J*= 7.08 Hz, 3H, CH_3), 1.67-1.86 (m, 2H, CH_2), 2.06-2.17 (m, 2H, CH_2), 2.22 (s, 3H, CH_3), 2.45 (t, *J*= 8.88 Hz, 2H, CH_2), 3.90-3.98 (m, 2H, CH_2), 5.15 (s, 1H, CH), 6.95-6.99 (m, 1H, Ar-H), 7.19-7.26 (m, 2H, Ar-H), 7.38 (d, *J*= 7.8 Hz,1H, Ar-H), 9.13 (s, 1H, NH) ; ^{13}C NMR (100 MHz, DMSO-d_6): 14.19, 18.10, 20.69, 26.23, 36.77, 37.00, 58.87, 103.71, 111.03, 122.30, 127.47, 131.54, 132.22, 144.50, 147.18, 151.50, 166.81, 194.11; ^{15}N NMR (40.55 MHz, DMSO-d_6) δ= 129.6 ;HRMS of [$C_{19}H_{20}NO_3Br$+Na^+] (m/z): 412.0530; Calcd.: 412.0524.

Ethyl 2-methyl-5-oxo-4-(o-tolyl)-1,4,5,6,7,8-hexahydroquinoline-3-carboxylate (5c) : The 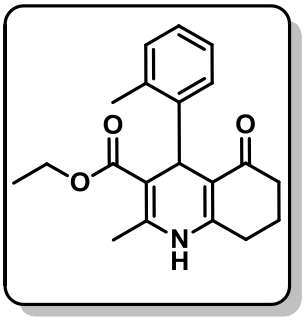

compound was obtained as described in the general procedure using o-Tolualdehyde (1 mmol; 100 mg), ethyl acetoacetate (1 mmol; 93.32 mg), 1,3-cyclohexadione (1 mmol; 108.31 mg), ammonium acetate (1 mmol; 64.15 mg) in 97 % yield as a yellow solid (262.70 mg): mp. = 191-193 ^oC; ^{1}H NMR (400 MHz, DMSO-d_6): δ= 1.07 (t, *J*= 7.08 Hz, 3H, CH_3), 1.61-1.90 (m, 2H, CH_2), 2.08 (S, 3H, -CH_3), 2.11-2.23 (m, 2H, CH_2), 2.27 (s, 3H, CH_3), 2.46 (t, *J*= 4.96 Hz, 2H, CH_2), 2.59 (s, 3H, CH_3), 3.91-3.97 (m, 2H, CH_2), 4.93 (s, 1H, CH), 6.91-6.93 (m, 2H, Ar-H), 6.99-7.03 (m, 1H, Ar-H), 7.09 (d, *J*= 7.52 Hz,1H, Ar-H), 9.06 (s, 1H, NH) ; ^{13}C NMR (100 MHz, DMSO-d_6): 14.09, 18.28, 20.64, 26.22, 30.60, 32.29, 36.70, 37.06, 105.21, 112.65, 125.52, 126.04, 128.59, 129.13, 134.80, 144.22, 147.87, 151.22, 167.11, 194.91; ^{15}N NMR (40.55 MHz, DMSO-d_6) δ= 129.1 ;HRMS of [$C_{20}H_{23}NO_3$-H^+] (m/z): 324.1595; Calcd.: 324.1600.

Ethyl 2-methyl-5-oxo-4-(2,4,5-trimethoxyphenyl)-1,4,5,6,7,8-hexahydroquinoline-3-carboxylate(5d): The compound was obtained as described in the general procedure using

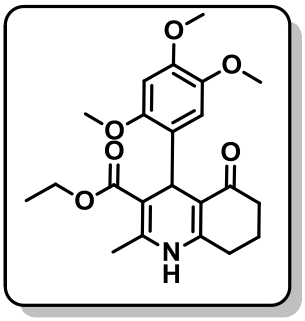

2,4,5-trimethoxybenzaldehyde (1 mmol;100 mg), ethyl acetoacetate (1 mmol;57.14 mg), 1,3-cyclohexadione (1 mmol; 66.32 mg), ammonium acetate (1 mmol; 39.28 mg) in 96 % yield as a yellow solid (196.41 mg): mp. = 214-218 ^{o}C; ^{1}H NMR (400 MHz, DMSO-d_6): δ= 1.19 (t, J= 7.12 Hz, 3H, CH_3), 1.72-1.96 (m, 2H, CH_2), 2.17-2.20 (m, 2H, CH_2), 2.23 (s, 3H, CH_3), 2.48-2.51 (m, 2H, CH_2), 3.68 (s, 3H, OCH_3), 3.72 (s, 3H, OCH_3), 3.76 (s, 3H, OCH_3), 3.96-4.03 (m, 2H, CH_2), 4.97 (s, 1H, CH), 6.59 (s,1H, Ar-H), 6.70 (s, 1H, Ar-H), 9.04 (s, 1H, NH) ; ^{13}C NMR (100 MHz, DMSO-d_6): 14.15, 17.85, 20.19, 26.22, 30.61, 32.75, 36.83, 55.67, 56.38, 56.59, 58.74, 99.38, 103.08, 109.74, 115.60, 127.39, 142.0, 143.52, 147.89, 151.68, 152.13, 167.42, 194.35; ^{15}N NMR (40.55 MHz, DMSO-d_6) δ= 130.7; HRMS of [$C_{22}H_{27}NO_6$-H^+] (m/z): 400.1767; Calcd.: 400.1760.

Ethyl 2-methyl-5-oxo-4-(2,4,6-trimethoxyphenyl)-1,4,5,6,7,8-hexahydroquinoline-3-carboxylate (5e) : The compound was obtained as described in the general procedure using

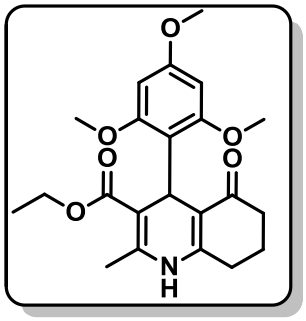

2,4,6-trimethoxybenzaldehyde (1 mmol;100 mg), ethyl acetoacetate (1 mmol;57.14 mg), 1,3-cyclohexadione (1 mmol; 66.32 mg), ammonium acetate (1 mmol; 39.28 mg) in 95 % yield as a yellow solid (194.37 mg): mp. = 206-208 ^{o}C; ^{1}H NMR (400 MHz, DMSO-d_6): δ= 1.04 (t, J= 7.12 Hz, 3H, CH_3), 1.59-1.84 (m, 2H, CH_2), 2.01-2.08 (m, 2H, CH_2), 2.13 (s, 3H, CH_3), 2.35 (t, J= 5.88 Hz, 2H, CH_2), 3.68 (s, 9H, 3 X OCH_3), 3.79-3.90 (m, 2H, CH_2), 5.33 (s, 1H, CH), 6.07 (s,2H, Ar-H), 8.81 (s, 1H, NH) ; ^{13}C NMR (100 MHz, DMSO-d_6): 14.00, 18.09, 20.90, 26.36, 37.09, 54.83, 55.98, 58.32, 101.67, 109.61, 117.02, 144.20, 151.64, 158.60, 159.30, 167.70, 193.75; ^{15}N NMR (40.55 MHz, DMSO-d_6) δ= 131.9 ;HRMS of [$C_{22}H_{27}NO_6$+Na^+] (m/z): 424.1742; Calcd.: 424.1736.

Ethyl 4-(2-methoxyphenyl)-2-methyl-5-oxo-1,4,5,6,7,8-hexahydroquinoline-3-carboxylate

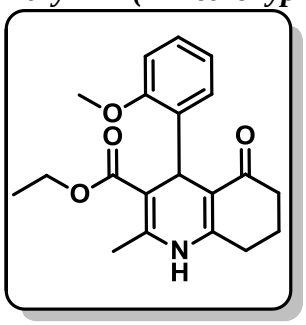

(5f): The compound was obtained as described in the general procedure using 2-methoxybenzaldehyde (1 mmol;100 mg), ethyl acetoacetate (1 mmol; 82.35 mg), 1,3-cyclohexadione (1 mmol; 95.58mg), ammonium acetate (1 mmol; 56.61mg) in 98 % yield as a yellow solid (245.73 mg): mp. = 188-190 ^{o}C; ^{1}H NMR (400 MHz, DMSO-d_6): δ= 1.11 (t, *J*= 7.08 Hz, 3H, CH_3), 1.67-1.91 (m, 2H, CH_2), 2.06-2.13 (m, 2H, CH_2), 2.16 (s, 3H, CH_3), 2.43-2.47 (m, 2H, CH_2), 3.69 (s, 3H, OCH_3), 3.90-3.96 (m, 2H, CH_2), 5.07 (s, 1H, CH), 6.75-6.77 (m, 1H, Ar-H), 6.82 (t, *J*= 708 Hz, 1H, Ar-H), 7.02-7.06 (m, 2H, Ar-H), 8.99 (s, 1H, NH) ; ^{13}C NMR (100 MHz, $CDCl_3$): 14.26, 19.16, 21.08, 27.19, 35.58, 37.11, 55.14, 59.80, 106.09, 113.19, 113.28, 128.92, 139.86, 143.51, 150.59, 157.80, 167.67, 196.22 ; ^{15}N NMR (40.55 MHz, DMSO-d_6) δ= 131.3. HRMS of [$C_{20}H_{23}NO_4$+Na^+] (m/z): 364.1527; Calcd.: 364.1525.

Ethyl 4-(3-bromophenyl)-2-methyl-5-oxo-1,4,5,6,7,8-hexahydroquinoline-3-carboxylate

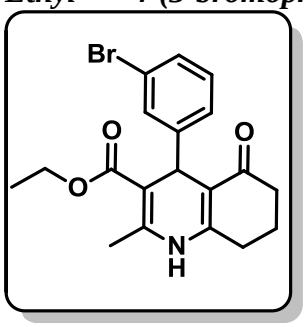

(5g): The compound was obtained as described in the general procedure using 3-bromo benzaldehyde (1 mmol; 100 mg), ethyl acetoacetate (1 mmol; 60.60mg), 1,3-cyclohexadione (1 mmol; 70.33mg), ammonium acetate (1 mmol; 41.66mg) in 94 % yield as a yellow solid (198.27 mg): mp. = 192-194 ^{o}C; ^{1}H NMR (400 MHz, DMSO-d_6): δ= 1.12 (t, *J*= 7.12 Hz, 3H, CH_3), 1.74-1.93 (m, 2H, CH_2), 2.14-2.22 (m, 2H, CH_2), 2.29 (s, 3H, CH_3), 2.36-2.48 (m, 2H, CH_2), 3.95-4.01 (m, 2H, CH_2), 4.87 (s, 1H, CH), 7.14-7.17 (m, 2H, Ar-H), 7.27 (t, *J*= 8.01 Hz, 2H, Ar-H), 9.21 (s, 1H, NH) ; ^{13}C NMR (100 MHz, DMSO-d_6): 14.56, 18.73, 21.23, 26.55, 36.32, 37.08, 59.63, 103.35, 111.01, 121.54, 126.95, 129.04, 130.72, 146.00, 150.87, 152.24, 167.10, 195.21; ^{15}N NMR (40.55 MHz, DMSO-d_6) δ= 131.3.

Ethyl 2-methyl-5-oxo-4-(pyridin-3-yl)-1,4,5,6,7,8-hexahydroquinoline-3-carboxylate (5h):

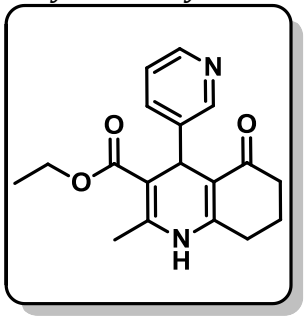

The compound was obtained as described in the general procedure using pyridine-3-carboxyaldehyde (1 mmol; 100mg), ethyl acetoacetate (1 mmol; 104.68mg), 1,3-cyclohexadione (1 mmol; 121.50 mg), ammonium acetate (1 mmol; 71.96 mg) in 95 % yield as a yellow solid (277.04 mg): mp. = 224-226 ^{o}C ; ^{1}H NMR (400 MHz, DMSO-d_6): δ= 1.09 (t, *J*= 7.08 Hz, 3H, CH_3), 1.68-1.92 (m, 2H, CH_2), 2.12-2.26 (m, 2H, CH_2), 2.29 (s, 3H, CH_3), 2.42-2.48 (m, 2H, CH_2), 3.94-3.98 (m, 2H,

CH_2), 4.87 (s, 1H, CH), 7.20-7.23 (m, 1H, Ar-H), 7.46-7.49 (m, 1H, Ar-H), 8.27-8.28 (m, 1H, Ar-H), 8.36 (d, *J*= 1.64 Hz, 1H, Ar-H), 9.22 (s, 1H, NH); ^{13}C NMR (100 MHz, DMSO-d_6): 14.05, 18.21, 20.74, 26.02, 33.88, 36.53, 59.11, 102.55, 110.32, 123.30, 134.79, 142.90, 145.74, 146.83, 148.84, 151.80, 166.50, 194.60; ^{15}N NMR (40.55 MHz, DMSO-d_6) δ= 131.3 ;HRMS of [$C_{18}H_{20}N_2O_3$-H^+] (m/z): 311.1385 ; Calcd.: 311.1396.

Ethyl 4-(3-hydroxy-4-methoxyphenyl)-2-methyl-5-oxo-1,4,5,6,7,8-hexahydroquinoline-3-carboxylate (5i) : 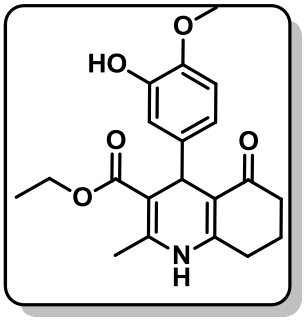

The compound was obtained as described in the general procedure using 3-hydroxy-4-methoxybenzaldehyde (1 mmol; 100 mg), ethyl acetoacetate (1 mmol; 73.69mg), 1,3-cyclohexadione (1 mmol; 85.53 mg), ammonium acetate (1 mmol; 50.66 mg) in 95 % yield as a yellow solid (223.15 mg): mp. = 204-206 ^{o}C ; ^{1}H NMR (400 MHz, $CDCl_3$): δ= 1.22 (t, *J*= 7.08 Hz, 3H, CH_3), 1.86-2.02 (m, 2H, CH_2), 2.25-2.32 (m, 2H, CH_2), 2.34 (s, 3H, CH_3), 2.38-2.42 (m, 2H, CH_2), 3.81 (s, 3H, -OCH_3), 4.05-4.11 (m, 2H, CH_2), 5.01 (s, 1H, CH), 5.76 (s, 1H, -OH), 6.43 (s, 1H, NH), 6.69 (d, *J*= 8.28 Hz, 1H, Ar-H), 6.82-6.88 (m, 2H, Ar-H); ^{13}C NMR (100 MHz, $CDCl_3$):14.25, 19.30, 21.03, 27.35, 35.77, 37.06, 55.85, 59.81, 106.04, 110.02, 113.27, 113.93, 119.90, 140.75, 143.30, 144.94, 145.22, 149.92, 167.60, 195.98; ^{15}N NMR (40.55 MHz, $CDCl_3$) δ= 127.7 ;HRMS of [$C_{20}H_{23}N_2O_5$+Na^+] (m/z): 380.1479; Calcd.: 380.1474.

Ethyl 2-methyl-5-oxo-4-(pyridin-4-yl)-1,4,5,6,7,8-hexahydroquinoline-3-carboxylate (5j): 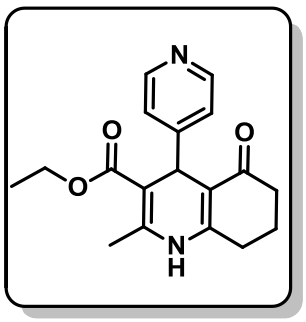

The compound was obtained as described in the general procedure using pyridine-4-carboxyaldehyde (1 mmol; 100 mg), ethyl acetoacetate (1 mmol; 104.68 mg), 1,3-cyclohexadione (1 mmol; 121.50 mg), ammonium acetate (1 mmol; 71.96 mg) in 93 % yield as a yellow solid (271.21 mg): mp. = 216-218 ^{o}C ; ^{1}H NMR (400 MHz, DMSO-d_6): δ= 1.10 (t, *J*= 7.08 Hz, 3H, CH_3), 1.74-1.92 (m, 2H, CH_2), 2.14-2.27 (m, 2H, CH_2), 2.30 (s, 3H, CH_3), 2.35-2.43 (m, 2H, CH_2), 3.95-4.00 (m, 2H, CH_2), 4.90 (s, 1H, CH), 7.12 (d, *J* = 5.32 Hz, 2H, Ar-H), 8.38 (d, *J* = 3.68 Hz, 2H, Ar-H), 9.26 (s, 1H, NH); ^{13}C NMR (100 MHz, DMSO-d_6): 14.05, 18.23, 20.68, 26.05, 35.49, 36.53, 59.18, 101.88, 109.79, 122.70, 146.10, 149.13, 149.24, 149.75, 152.10, 155.51, 166.48, 194.62; ^{15}N NMR (40.55 MHz, DMSO-d_6) δ= 133.0 ;HRMS of [$C_{18}H_{20}N_2O_3$-H^+] (m/z): 311.1391 ; Calcd.: 311.1396.

Ethyl 4-(3,4-dimethoxyphenyl)-2-methyl-5-oxo-1,4,5,6,7,8-hexahydroquinoline-3-carboxylate (5k) : 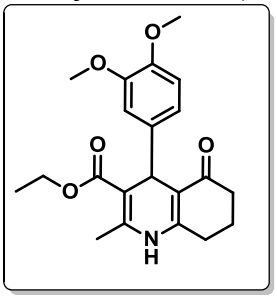
The compound was obtained as described in the general procedure using 3,4-dimethoxybenzaldehyde (1 mmol;100 mg), ethyl acetoacetate (1 mmol; 67.47 mg), 1,3-cyclohexadione (1 mmol; 78.31 mg), ammonium acetate (1 mmol; 46.38 mg) in 94 % yield as a yellow solid (209.96 mg): mp. = 191-193 ^{o}C; ^{1}H NMR (400 MHz,$CDCl_3$): δ= 1.20 (t, *J*= 7.12 Hz, 3H, CH_3), 1.73 (s, 1H, CH_2), 1.92-2.03 (m, 2H, CH_2), 2.27-2.37 (m, 2H,CH_2), 2.38 (s, 3H, CH_3), 2.42 (t, *J*= 6.8 Hz, 2H, CH_2), 3.80 (s, 3H, OCH_3), 3.85 (s, 3H, OCH_3), 4.05-4.10 (m, 2H, CH_2), 5.06 (s, 1H, CH), 6.33 (s, 1H, NH), 6.70-6.78 (m, 2H, Ar-H), 6.96 (d, *J* = 1.56 Hz, 1H, Ar-H); ^{13}C NMR (100 MHz, $CDCl_3$): 14.30, 19.30, 21.07, 27.41, 35.80, 37.10, 55.78, 55.84, 59.80, 106.04, 110.87, 112.05, 113.43, 119.59, 140.21, 143.23, 147.24, 148.27, 149.71, 167.56, 195.94; ^{15}N NMR (40.55 MHz, $CDCl_3$) δ= 127.60;HRMS of [$C_{21}H_{25}NO_5$+Na^+] (m/z): 394.1628 ; Calcd.: 394.1630.

Ethyl 4-(3-hydroxyphenyl)-2-methyl-5-oxo-1,4,5,6,7,8 hexahydroquinoline-3-carboxylate (5l) : 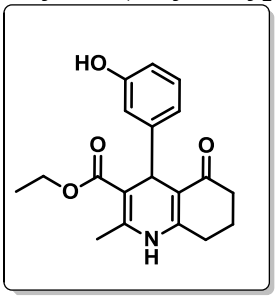
The compound was obtained as described in the general procedure using 3-Hydroxybenzaldehyde (1 mmol;100 mg), ethyl acetoacetate (1 mmol; 91.81 mg), 1,3-cyclohexadione (1 mmol; 106.56 mg), ammonium acetate (1 mmol; 63.11 mg) in 90 % yield as a yellow solid (241.10 mg): mp. = 230-232 ^{o}C; ^{1}H NMR (400 MHz, DMSO-d_6): δ= 1.20 (t, *J*= 7.08 Hz, 3H, CH_3), 1.79-1.99 (m, 2H, CH_2), 2.24-2.27 (m, 2H, CH_2), 2.23 (s, 3H, CH_3), 2.48-2.54 (m, 2H, CH_2), 4.02-4.07 (m, 2H, CH_2), 4.89 (s, 1H, CH), 6.52 (dd, *J*= 8Hz, 9.36 Hz, 1H, Ar-H), 6.63 (t, *J*=2.48 HZ, 2H, Ar-H), 7.00 (t, *J*= 7.96 Hz, 1H, Ar-H), 9.13 (s, 1H, -OH), 9.14 (s,1H, NH) ^{13}C NMR (100 MHz, DMSO-d_6): 14.14, 18.19, 20.75, 26.12, 35.24, 36.72, 58.99, 103.53, 110.95, 112.58, 114.39, 118.05, 128.57, 144.61, 149.01, 151.29, 156.85, 166.97, 194.61; ^{15}N NMR (40.55 MHz, DMSO-d_6) δ= 131.20.

Ethyl 4-(4-ethylphenyl)-2-methyl-5-oxo-1,4,5,6,7,8-hexahydroquinoline-3-carboxylate (5m) : 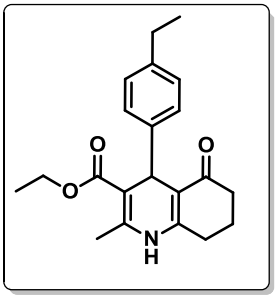
The compound was obtained as described in the general procedure using 4-Ethylbenzaldehyde (1 mmol;100 mg), ethyl acetoacetate (1 mmol; 83.56 mg), 1,3-cyclohexadione (1 mmol; 96.98 mg), ammonium acetate (1 mmol; 57.44 mg) in 96 % yield as a yellow solid (242.66 mg): mp. = 229-231 ^{o}C; ^{1}H NMR (400 MHz, DMSO-d_6): δ= 1.10-1.15 (m, 6H, CH_3), 1.74-1.92 (m, 2H, CH_2), 2.17-2.20 (m, 2H, CH_2), 2.27 (s, 3H,CH_3), 2.48 (t, *J*= 3.8 Hz, 4H, CH_3), 3.96-4.01 (m, 2H, CH_2), 4.87 (s, 1H, CH), 6.99-

7.06 (m, 4H, Ar-H), 9.08 (s, 1H , Ar-H); ^{13}C NMR (100 MHz, DMSO-d_6): 14.64, 16.03, 18.70, 21.29, 26.60, 28.19, 35.58, 37.21, 59.47, 104.20, 111.67, 127.67, 127.77, 141.37, 145.14, 145.61, 151.77, 167.44, 195.10; ^{15}N NMR (40.55 MHz, DMSO-d_6) δ= 132.1.

Ethyl 4-(4-(dimethylamino)phenyl)-2-methyl-5-oxo-1,4,5,6,7,8-hexahydroquinoline-3-carboxylate (5n) : 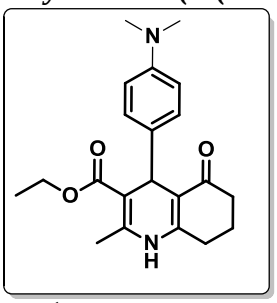

The compound was obtained as described in the general procedure using 4-(Dimethylamino)benzaldehyde (1 mmol;100 mg), ethyl acetoacetate (1 mmol; 75.15 mg), 1,3-cyclohexadione (1 mmol; 87.23 mg), ammonium acetate (1 mmol; 51.66 mg) in 95 % yield as a yellow solid (225.53 mg): mp. = 230-232 ^{o}C; ^{1}H NMR (400 MHz, DMSO-d_6): δ= 1.14 (t, *J*= 7.08 Hz, 3H, CH_3), 1.73-1.92 (m, 2H, CH_2), 2.12-2.19 (m, 2H, CH_2), 2.25 (s, 3H, CH_3), 2.47 (d, *J*= 5.04Hz, 2H, CH_2), 2.79 (s, 6H, 2XCH_3), 3.95-4.00 (m, 2H, CH_2), 4.77 (s, 1H, CH), 6.54 (d, *J*= 8.64 Hz, 9.36 Hz, 1H, Ar-H), 6.94 (t, *J* = 8.6 HZ, 2H, Ar-H), 9.01 (t, *J*= 7.96 Hz, 1H, Ar-H); ^{13}C NMR (100 MHz, DMSO-d_6): 14.18, 18.16, 20.84, 26.10, 34.27, 36.77, 40.29, 58.89, 104.14, 111.51, 112.56, 127.82, 136.16, 144.06, 148.68, 150.82, 167.10, 194.61 ; ^{15}N NMR (40.55 MHz, DMSO-d_6) δ= 131.0. HRMS of [$C_{21}H_{26}N_2O_3$+Na^+] (m/z): 377.1842; Calcd.: 377.1841.

Ethyl 4-(4-chlorophenyl)-2-methyl-5-oxo-1,4,5,6,7,8-hexahydroquinoline-3-carboxylate (5o) : 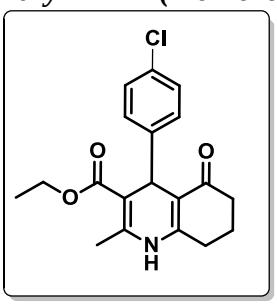

The compound was obtained as described in the general procedure using 4-Chlorobenzaldehyde (1 mmol;100 mg), ethyl acetoacetate (1 mmol; 79.77 mg), 1,3-cyclohexadione (1 mmol; 92.58 mg), ammonium acetate (1 mmol; 54.83 mg) in 92 % yield as a yellow solid (225.88 mg): mp. = 248-250 ^{o}C; ^{1}H NMR (400 MHz, $CDCl_3$): δ= 1.19 (t, *J*= 7.08 Hz, 3H, CH_3), 1.91-2.01 (m, 2H, CH_2), 2.31-2.37 (m, 2H, CH_2), 2.38 (s, 3H, CH_3), 2.41-2.45 (m, 2H, CH_2), 4.04-4.09 (m, 2H, CH_2), 5.07 (s, 1H, CH), 6.16 (s,1H, NH),7.17 (d, *J* = 8.44 Hz, 2H, Ar-H), 7.25-7.32 (m, 2H, Ar-H) 9.01 (t, *J*= 7.96 Hz, 1H, Ar-H); ^{13}C NMR (100 MHz, $CDCl_3$):14.20, 19.37, 21.01, 27.42, 36.09, 36.98, 59.91, 105.70, 113.13, 128.03, 129.44, 131.62, 143.56, 145.71, 149.80, 167.23, 195.76; ^{15}N NMR (40.55 MHz, $CDCl_3$) δ= 126.8; HRMS of [$C_{19}H_{20}N_2O_3Cl$+Na^+] (m/z): 368.1030 ; Calcd.: 368.1029.

Ethyl 2-methyl-5-oxo-4-propyl-1,4,5,6,7,8-hexahydroquinoline-3-carboxylate (5p) : The compound was obtained as described in the general procedure using n-butraldehyde (1 mmol;100 mg), ethyl acetoacetate (1 mmol; 155.49 mg), 1,3-cyclohexadione (1 mmol; 180.47

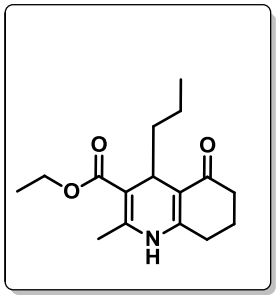

mg), ammonium acetate (1 mmol; 106.89 mg) in 89 % yield as a yellow solid (359.38 mg): mp. = 178-180 ^{o}C; ^{1}H NMR (400 MHz, DMSO-d_6): δ= 0.76 (t, *J*= 6.68 Hz, 3H, CH_3), 1.74-1.92 (m, 2H, CH_2), 1.02-1.08 (m, 2H, CH_2), 1.09-1.16 (m, 2H, CH_2), 1.19 (t, *J*= 7.08 Hz, 3H, CH_3), 1.79-1.91 (m, 2H, CH_2), 2.13-2.18 (m, 1 H, CH_2), 2.20 (s, 3H,CH_3), 2.23-2.28 (m, 1H, CH_2), 2.37-2.43 (m, 2H, CH_2), 3.81 (t, *J*= 4.4 Hz,1H, CH), 4.01-4.12 (m, 2H, CH_2), 8.91 (s, 1H, NH); ^{13}C NMR (100 MHz, DMSO-d_6): 14.75, 17.95, 18.61, 21.44, 26.34, 26.62, 26.77, 31.14, 37.30, 59.35, 103.44, 110.72, 145.87, 152.77, 167.74, 195.54 ; ^{15}N NMR (40.55 MHz, DMSO-d_6) δ= 132.7.

Ethyl 2,7,7-trimethyl-5-oxo-4-(2,3,4-trimethoxyphenyl)-1,4,5,6,7,8-hexahydroquinoline-3-carboxylate (5q) : The compound was obtained as described in the general procedure using 2,3,4-trimethoxybenzaldehyde (1 mmol;100 mg), ethyl acetoacetate (1 mmol; 57.14 mg), 5,5-Dimethyl-1,3-cyclohexanedione (1 mmol; 71.43 mg), ammonium acetate (1 mmol; 39.28 mg) in 96 % yield as a yellow solid (210.0 mg): mp. = 208-210 ^{o}C; ^{1}H NMR (400 MHz, DMSO-d_6): δ= 0.88 (s, 3H, CH_3), 1.00 (s, 3H, CH_3), 1.13 (t, *J*= 7.08 Hz, 3H, CH_3), 1.91-2.14 (m, 2H, CH_2), 2.20 (s, 3H, CH_3), 2.27-2.40 (m, 2H, CH2), 3.65 (s, 3H, OCH_3), 3.70 (s, 3H, OCH_3), 3.79 (s, 3H, OCH_3), 3.89-3.96 (m, 2H, CH_2), 4.97 (s, 1H, CH), 6.59 (d, *J* = 8.68 Hz,1H, Ar-H), 6.80 (d, *J* = 8.64 Hz, 1H, Ar-H), 8.93 (s, 1H, NH) ; ^{13}C NMR (100 MHz, DMSO-d_6): 14.51, 18.64, 26.91, 29.61, 32.48, 32.91, 50.85, 56.03, 59.31, 60.29, 60.60, 61.00, 104.38, 107.24, 109.92, 125.11, 133.62, 141.92, 143.96, 150.33, 151.87, 151.98, 167.80, 194.50; ^{15}N NMR (40.55 MHz, DMSO-d_6) δ= 130.3.

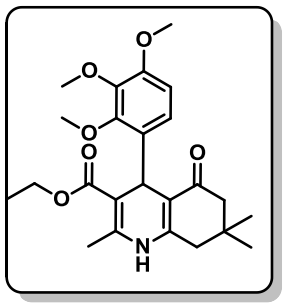

Ethyl 2,7,7-trimethyl-5-oxo-4-(2,4,5-trimethoxyphenyl)-1,4,5,6,7,8-hexahydroquinoline-3-carboxylate (5r) : The compound was obtained as described in the general procedure using 2,4,5-trimethoxybenzaldehyde (1 mmol; 100 mg), ethyl acetoacetate (1 mmol; 57.14 mg), 5,5-Dimethyl-1,3-cyclohexanedione (1 mmol; 71.43 mg), ammonium acetate (1 mmol; 39.28 mg) in 97 % yield as a yellow solid (212.19 mg): mp. = 218-220 ^{o}C; ^{1}H NMR (400 MHz, DMSO-d_6): δ= 0.86 (s, 3H, CH_3), 1.00 (s, 3H, CH_3), 1.14 (t, *J*= 7.12 Hz, 3H, CH_3), 1.88-2.14 (m, 2H, CH_2), 2.19 (s, 3H, CH_3), 2.25-2.41 (m, 2H, CH_2), 3.62 (s, 3H, OCH_3), 3.68 (s, 3H, OCH_3), 3.71 (s, 3H, OCH_3), 3.91-3.95 (m, 2H, CH_2), 4.92 (s, 1H, CH), 6.12 (s, 1H, Ar-H), 6.68 (s, 1H, Ar-H), 8.94 (s, 1H, NH) ; ^{13}C NMR (100 MHz, DMSO-d_6): 14.64, 18.49, 26.56, 29.84, 32.44, 33.13, 50.85, 56.06, 56.67, 56.80, 59.23,

103.40, 109.23, 116.25, 127.47, 142.25, 144.43, 148.32, 150.27, 152.28, 167.84, 194.46 ; ^{15}N NMR (40.55 MHz, DMSO-d_6) δ= 130.1.

7.3 Results and Discussion

7.3.1 XRD analysis

Figure 2 shows the X-ray diffraction pattern of 2.5 wt % NiO−ZrO2 and the diffraction peaks (2 theta) from 0 to 80°. The major diffraction peaks at 2θ of 24.5, 27.8, 31.3, 35.4, 40.5, 50.3, 54.4, 55.6, 57.8, 59.9, 65.4, and 71.2° for ZrO_2 are correlated with the inter-national standard file (JCPDS 37-1484). The NiO peaks are displayed in the XRD diffractogram at 2θ = 37.2, 45.3, 62.8, 71.3, and 75.5° were further matched with the standard file (JCPDS 47-1049). The diffraction pattern revealed the poly-crystalline nature of the prepared catalytic material.

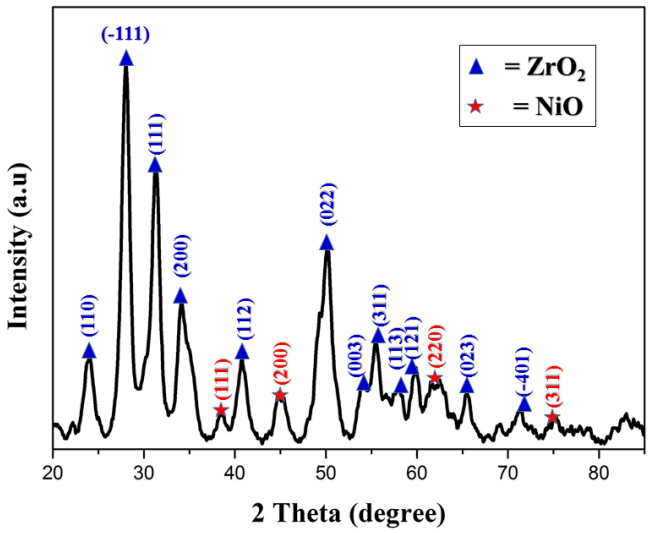

Figure 2. Powder X-ray diffractogram of 2.5% NiO-ZrO_2 catalyst.

7.3.2 TEM analysis

The TEM investigation was performed to explore the catalyst morphology. Figure 3 illustrates a distinctive TEM image NiO/ZrO_2 (2.5 wt %). The image indicated an irregular cubic morphology with nominal agglomeration of NiO. It was further observed that the black irregular-shaped nickel oxide particles are evenly distributed on the surface of oval-shaped zirconia particles, which may improve catalytic activity.

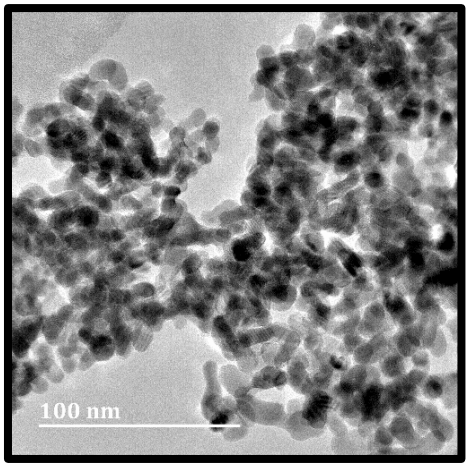

Fig. 3 TEM micrograph of 2.5% NiO-ZrO_2 catalyst.

7.3.3 SEM analysis

The surface morphology of 2.5 wt % NiO/ZrO_2 was assessed by SEM, which is shown in Figure 4. Figure 4a shows the irregular round particles aggregated on the surface of ZrO_2. The surface was further analyzed by mapping and energy-dispersive X-ray spectroscopy (EDS) (Figure 4b,c), which show the even distribution of Ni on the surface of zirconia.

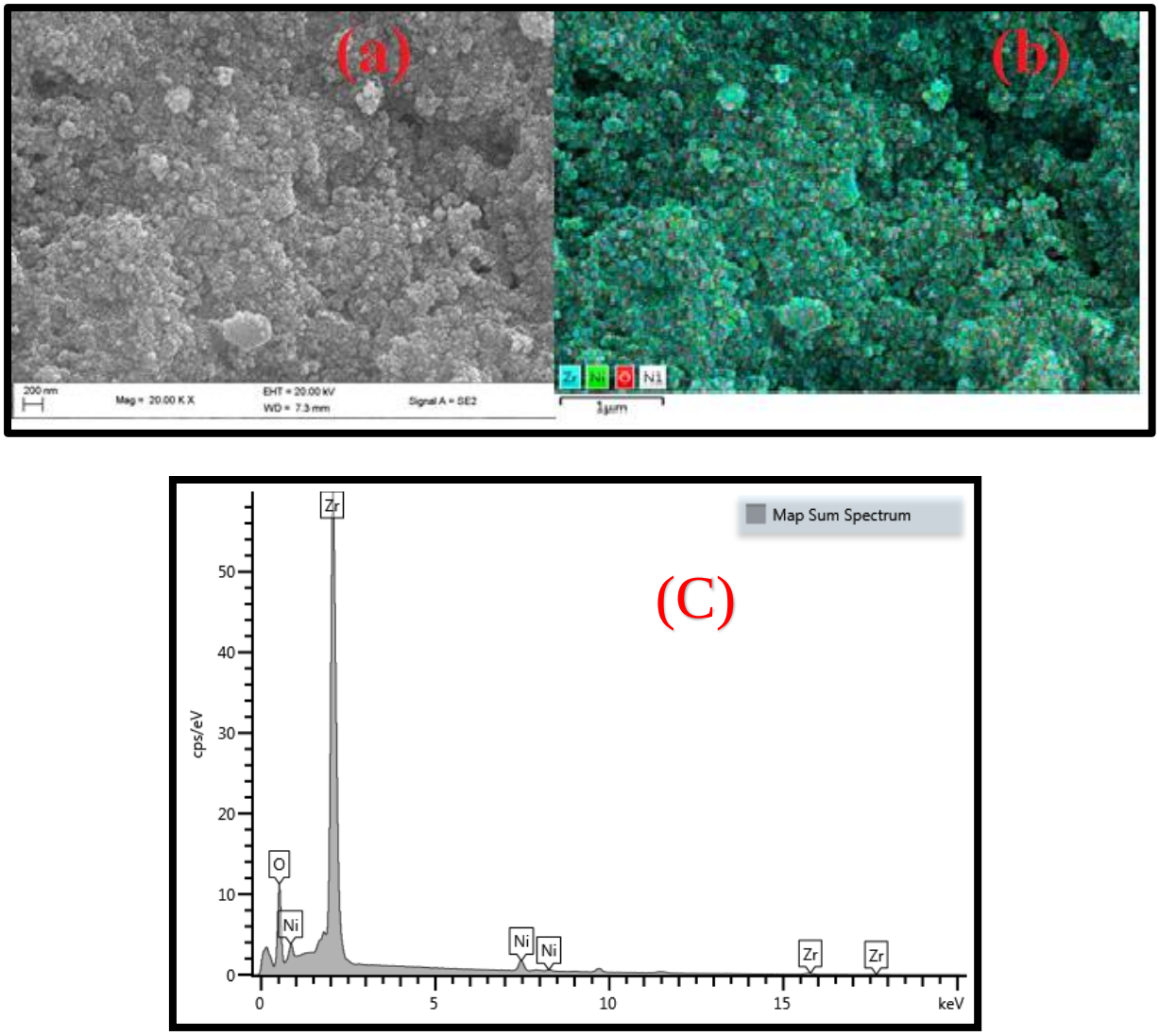

Fig. 4 (a) SEM micrograph (b) Mapping (c) EDS spectra of 2.5% NiO/ZrO_2 catalyst.

7.3.4 BET surface area analysis

The 2.5 wt % NiO/ZrO_2 N_2 adsorption−desorption isotherm illustrated in Figure 5 shows a type-IV adsorption isotherm with a hysteresis loop of H_2, which is a characteristic of a mesoporous material (p/po range of 0.67−0.98). The surface area is 76.35 $m^2\ g^{-1}$ with a pore volume of 0.29 $cm^3\ g^{-1}$ and a pore size 12.14 nm.

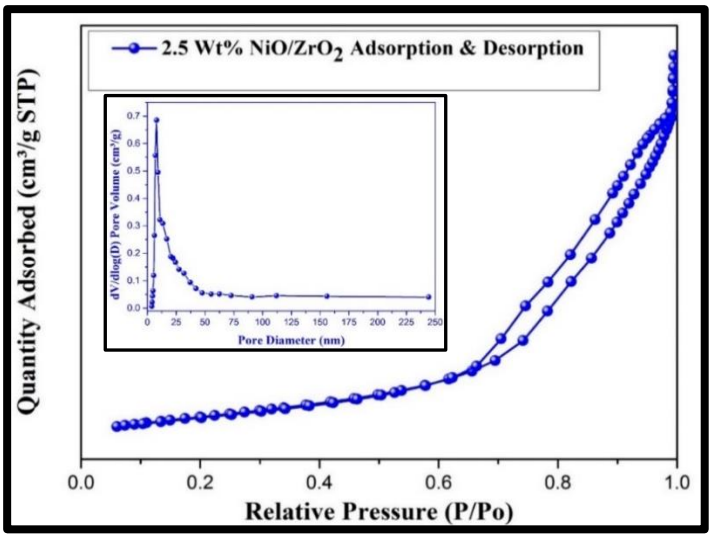

Fig. 5 N_2 adsorption-desorption isotherms of 2.5% NiO/ZrO_2 catalyst.

7.3.5 Pyridine IR

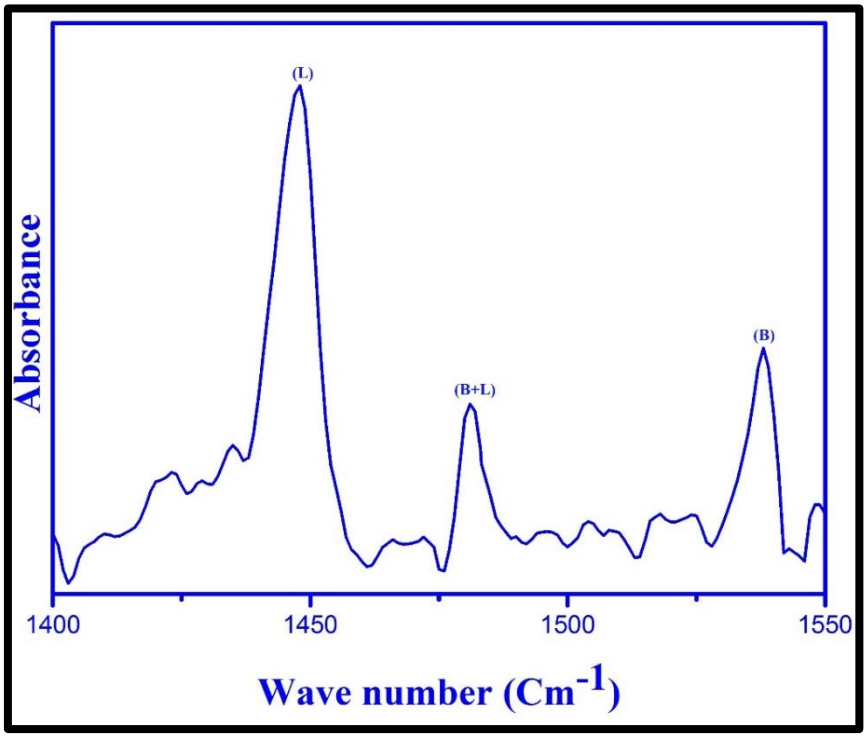

Fig. 6 Pyridine FT-IR spectra of 2.5% NiO/ZrO_2 catalyst. L = Lewis acidic sites; B + L = Brønsted and Lewis acidic sites; B = Brønsted acidic sites.

The nature of the surface active sites was examined by ex-situ Pyridine IR.[44] Pyridine is widely used as a probe to characterize the surface acidity of the materials. Pyridine as a base interacts with Brønsted acid sites and through H^+ transfer lead to the formation of pyridinium ion. Pyridine can act as a Lewis base, and it is capable to donate a pair of electrons toward the

electrophilic Lewis acidic sites. Such characteristic bands are perceived in the range of 1550−1400 cm^{-1}. Based on this, the characteristic peak at 1448 cm^{-1} corresponds to the Lewis acidic sites with bands at 1481 and 1531 cm^{-1} that correspond to the Lewis + Brønsted and Brønsted acidic sites, respectively. Figure 6 confirms that the catalyst possesses prominent Lewis acidic sites, which could facilitate its catalytic activity.

7.3.6 Reaction optimization

The catalytic efficiency of prepared NiO/ZrO_2 toward the title multicomponent reaction was evaluated. The reaction was performed by taking four components, 2,3,4-OMe benzaldehyde (1a), ethyl acetoacetate (2) cyclohexanone (3), and ammonium acetate (4) in the same molar ratio (Scheme 1). In separate studies, the effects of various catalysts, the amount of catalyst, and role of solvents were examined. Initially, the reaction was studied under neat conditions at room temperature and reflux up to 8 h. Only a trace amount of product was obtained. Next, the effect of different homogeneous catalysts and organic or inorganic bases such as triethyl amine (TEA), pyridine, DABCO, NaOH, and K_2CO_3 were explored on the title reaction at room temperature (RT) conditions (5−7 h) and low yields were observed (Table 1, entries 3−7). Further studies with various acidic catalysts such as AcOH, $FeCl_3$, PTSA, and TFA, moderate yields were obtained in 4−6 h (Table 1, entries 8−11). Different heterogeneous metal oxides like SiO_2, ZrO_2, and Al_2O_3 (normally used as support materials) were explored under the same reaction conditions. SiO_2 gave 53% yield, Al_2O_3 gave 60% in 3.5−4 h time, ZrO2 gave a higher yield of 68% in 2 h time, and NiO gave 65% in 2.5 h time (Table 1, entries 12−15). Considering the interesting results from NiO and ZrO_2, to identify the efficient catalyst, the scope of various ZrO_2-based mixed oxide catalysts, 2.5 wt % CuO/ZrO_2, CeO_2/ZrO_2, and NiO/ZrO_2 (Table 1, entries 16−18) were investigated. An impressive yield of 98% was observed with 2.5% NiO/ZrO_2 in a relatively short time of 20 min compared to 73% in 60 min with 2.5% CuO/ZrO_2 (Table 1, entry 16) and 81% yield in 45 min (Table 1, entry 17) with 2.5% CeO_2/ZrO_2. While using 1% NiO/ZrO_2 catalyst yielded 91% product in 30 min under similar conditions (Table 1, entry 19), 5% NiO/ZrO_2 led to slight decreased yield (94%) in 25 min (Table 1, entry 20). Therefore, 2.5% NiO/ZrO_2 was the preferred catalyst for further studies. The higher catalytic activity may be due to the even distribution of the active material on the surface of the support and availability of more optimally active NiO sites in combination with ZrO_2, which help in speeding up the rate of reaction selectively compared to 1 and 5% catalyst. For the 1% NiO/ZrO_2 catalyst loading, the particles are small and have a high surface area but

less number of active sites compared to the 2.5% NiO/ZrO_2, whereas for 5% NiO/ZrO_2 loading, the nickel particles are visibly larger and hence have a smaller surface area, thus slightly lower yield when compared to the 2.5% NiO/ZrO_2. Hence, 2.5%NiO/ZrO_2 acts as a good promoter for the present transformation.

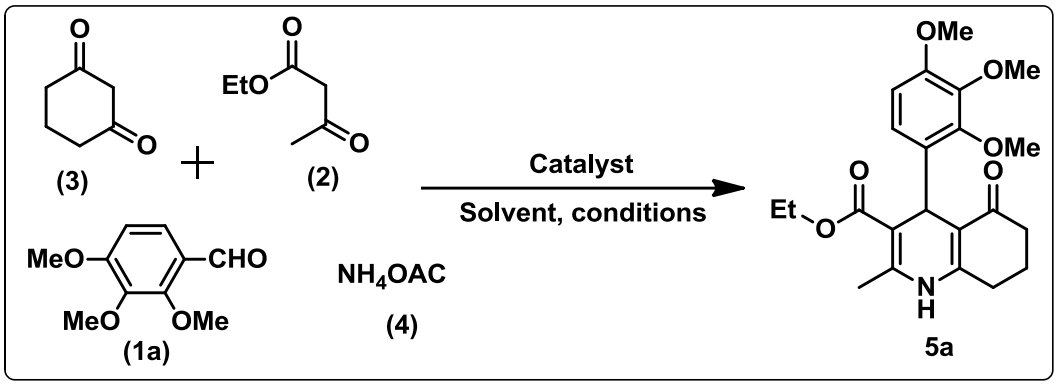

Scheme 2 Optimisation reaction conditions for 5a synthesis.

Table 1: Effect of different catalysts on the synthesis of 5a[a].

Entry	Catalyst	Solvent	Condition	Time (h)	Yield (%)[b]
1	–	–	RT	8	12
2	–	–	Reflux	8	17
3	TEA[c]	EtOH	RT	5.0	30
4	Pyridine[c]	EtOH	RT	7.0	27
5	DABCO[c]	EtOH	RT	5.0	25
6	NaOH[c]	EtOH	RT	6.0	33
7	K_2CO_3[c]	EtOH	RT	6.0	29
8	AcOH[c]	EtOH	RT	5.5	36
9	$FeCl_3$[c]	EtOH	RT	5.0	38
10	PTSA[c]	EtOH	RT	6.0	45
11	TFA[c]	EtOH	RT	4.0	40
12	SiO_2[d]	EtOH	RT	4.0	53
13	ZrO_2 [d]	EtOH	RT	2.0	68
14	Al_2O_3[d]	EtOH	RT	3.5	60
15	2.5%CuO/ZrO_2 [e]	EtOH	RT	1.0	73
16	2.5%CeO_2/ZrO_2[e]	EtOH	RT	0.75	81
17	2.5% NiO/ZrO_2 [e]	EtOH	RT	0.33	98
18	1% NiO/ZrO_2 [e]	EtOH	RT	0.50	91
19	5% NiO/ZrO_2 [e]	EtOH	RT	0.41	94

[a]Reaction conditions: 2,3,4-trimethoxybenzaldehyde (1 mmol) (1), Ethyl acetoacetate (1 mmol) (2), and 1,3-Cyclohexadione (1 mmol) (3) and Ammonium acetate (1 mmol) (4), 5 mL solvent were stirred at RT. [b] Isolated yields. – No catalyst. [c] = 100 mg catalyst. [d] = 60 mg catalyst. [e] = 30 mg catalyst.

To further optimize the conditions, we examined the role of the solvent in the organic conversion employing different nonpolar and polar solvents (Table 2). In the presence of nonpolar solvents like n-hexane and toluene at RT, no product was identified even after 4 h possibly due to the poor solubility of the reactants. Among the polar solvents such as DMF, THF, MeCN, EtOH, and MeOH, the highest yields were observed with EtOH.

Table 2: Role of different solvent in the synthesis of 5a[a]

Entry	Solvent[b]	Time (h)	Yield (%)
1	*n*-hexane	4.0	–
2	toluene	4.0	–
3	DMF	1.3	19
4	THF	1.1	24
5	MeCN	1.0	31
6	CH_3OH	0.75	76
7	C_2H_5OH	0.33	98

[a]Reaction conditions: 2,3,4-trimethoxybenzaldehyde (1 mmol) (1), Ethyl acetoacetate (1 mmol) (2), and 1,3-Cyclohexanedione (1 mmol) (3) and Ammonium acetate (1 mmol) (4), 5 mL solvent were stirred at RT. [b]DMF= Dimethyl formamide; THF= Tetrahydrofuran; MeCN=Acetonitrile; CH_3OH= Methanol; C_2H_5OH= Ethanol.–No product.

Next, the required amount of catalyst for the reaction was optimized. Results are summarized in Table 3 and show that the yields of products increased with the increase in amount of catalyst from 10 to 30 mg. There was no increase in the yield with >30 mg. To broaden the viability and scope of the method,the optimized conditions were employed to synthesize 18 substituted 1,4-dihydropyridines using different substituted aldehydes, different active methylene groups up on that 12 are novel derivatives. All of the 18 derivatives gave excellent yields in a relatively short time of ≈45 min, and the results are summarized in Figure 7. The structures of all synthesized compounds were confirmed by ^{1}H NMR, ^{13}C NMR, and ^{15}N spectroscopy and high-resolution mass spectrometry (HRMS) analyses. The single-crystal X-ray structures of 5a and 5c are shown in Figures 8 and 9, respectively. Table 4 shows the crystal data, and further information is incorporated in the supporting Information.

Table 3: Optimization of amount of 2.5 % NiO/ZrO_2 catalyst on the synthesis of 5a[a]

Entry	Catalyst (mg)	Time (h)	Yield (%)
1	10	0.83	74
2	20	0.5	85
3	30	0.33	98
4	40	0.33	98
5	50	0.33	97
6	60	0.33	97

[a]Reaction conditions: 2,3,4-trimethoxybenzaldehyde (1 mmol) (1), Ethyl acetoacetate (1 mmol) (2), and 1,3-Cyclohexadione (1 mmol) (3) and Ammonium acetate (1 mmol) (4), 5 mL EtOH were stirred at RT.

Figure 7. Library synthesis of novel unsymmetrical 1,4-dihydropyridine derivatives *

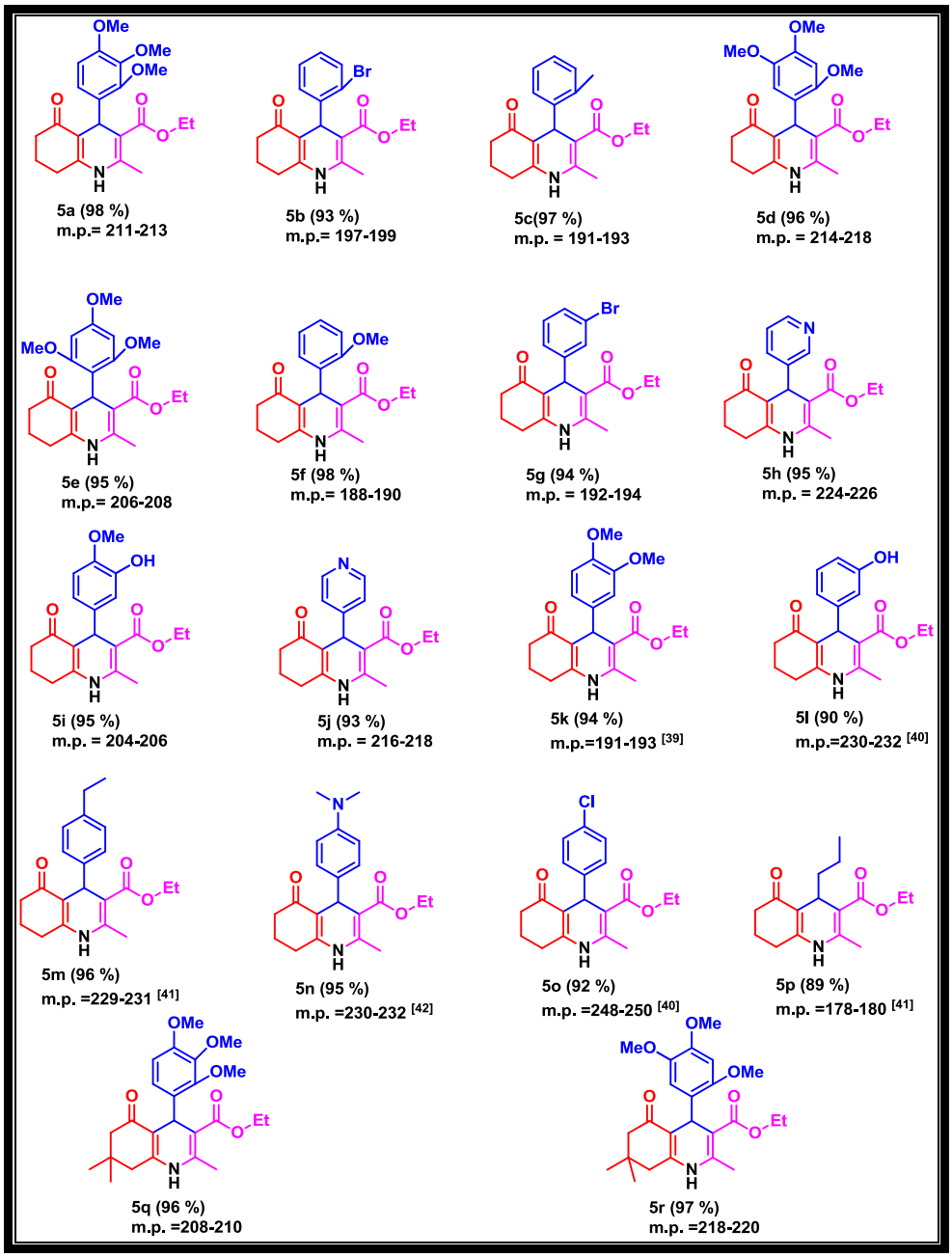

* Reaction conditions: Substituted aldehydes (1 mmol) (1), Ethyl acetoacetate (1 mmol) (2), and 1,3-Cyclohexadione/ 5,5-dimethyl-1,3-cyclohexanedione (1 mmol) (3) and Ammonium acetate (1 mmol) (4), 5 mL Ethanol, 2.5% NiO/ZrO_2 (30 mg) catalyst stirred at RT; Melting point (m.p.) in ^oC.

Crystal Data:

$C_{22}H_{27}NO_6$ (*M* =401.44g/mol): orthorhombic, space group $Pna2_1$ (no. 33), *a* = 14.6836(6) Å, *b* = 8.4477(3) Å, *c* = 15.5290(6) Å, *V* = 1926.26(13) $Å^3$, *Z* = 4, *T* = 100.0 K, μ(MoKα) = 0.101 mm^{-1}, *Dcalc* = 1.384 g/cm^3, 13133 reflections measured (5.246° ≤ 2Θ ≤

56.7°), 4622 unique (R_{int} = 0.0196, R_{sigma} = 0.0237) which were used in all calculations. The final R_1 was 0.0312 (I > 2σ(I)) and wR_2 was 0.0796 (all data).

$C_{20}H_{23}NO_3$ (M =325.39 g/mol): triclinic, space group P-1 (no. 2), a = 7.29920(10) Å, b = 9.58180(10) Å, c = 12.3976(2) Å, α = 83.9450(10)°, β = 86.8650(10)°, γ = 71.9730(10)°, V = 819.69(2) Å3, Z = 2, T = 100.0 K, μ(MoKα) = 0.088 mm-1, Dcalc = 1.318 g/cm3, 26777 reflections measured (3.304° ≤ 2Θ ≤ 57.038°), 4083 unique (Rint = 0.0179, Rsigma = 0.0131) which were used in all calculations. The final R1 was 0.0365 (I > 2σ(I)) and wR2 was 0.1008 (all data).

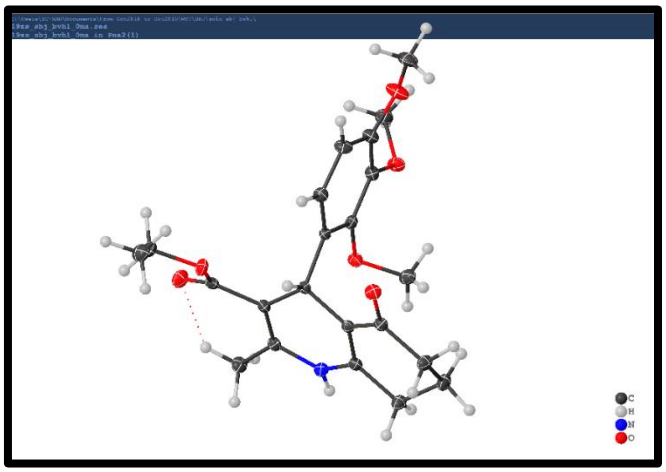

Fig. 8 Single-crystal X-ray structure of **5a.**

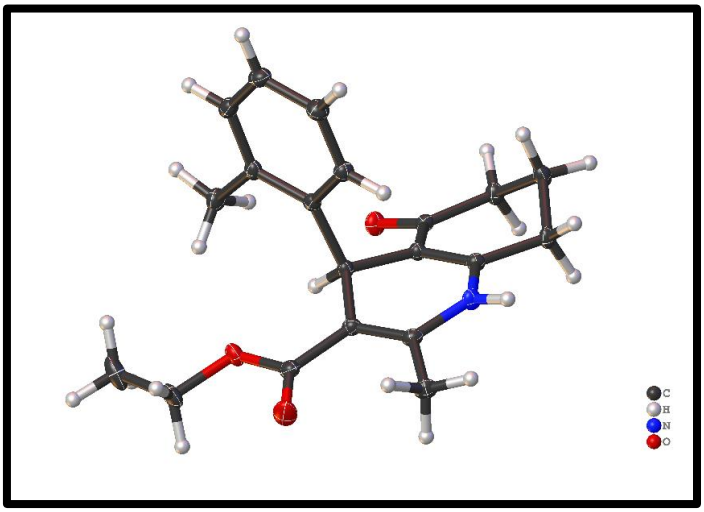

Fig. 9 Single-crystal X-ray structure of **5c**.

Table 4: Single crystal data of **5a** and **5c**

Identification code	**5a**	**5c**
Empirical formula	$C_{22}H_{27}NO_6$	$C_{20}H_{23}NO_3$
Formula weight	401.44	325.39
Temperature/K	100.0	100.0
Crystal system	orthorhombic	triclinic
Space group	$Pna2_1$	P-1
a/Å	14.6836(6)	7.29920(10)
b/Å	8.4477(3)	9.58180(10)
c/Å	15.5290(6)	12.3976(2)
α/°	90	83.9450(10)
β/°	90	86.8650(10)
γ/°	90	71.9730(10)
Volume/$Å^3$	1926.26(13)	819.69(2)
Z	4	2
$\rho_{calc}g/cm^3$	1.384	1.318
μ/mm^{-1}	0.101	0.088
F(000)	856.0	348.0
Crystal size/mm^3	0.38 × 0.24 × 0.16	0.31 × 0.23 × 0.12
Radiation	MoKα (λ = 0.71073)	MoKα (λ = 0.71073)
2Θ range for data collection/°	5.246 to 56.7	3.304 to 57.038
Index ranges	$-19 \le h \le 15$, $-11 \le k \le 11$, $-20 \le l \le 20$	$-9 \le h \le 9$, $-12 \le k \le 12$, $-16 \le l \le 16$
Reflections collected	13133	26777
Independent reflections	4622 [R_{int} = 0.0196, R_{sigma} = 0.0237]	4083 [R_{int} = 0.0179, R_{sigma} = 0.0131]
Data/restraints/parameters	4622/1/267	4083/0/220
Goodness-of-fit on F^2	1.024	1.048
Final R indexes [I>=2σ(I)]	R_1 = 0.0312, wR_2 = 0.0772	R_1 = 0.0365, wR_2 = 0.0972
Final R indexes [all data]	R_1 = 0.0345, wR_2 = 0.0796	R_1 = 0.0408, wR_2 = 0.1008
Largest diff. peak/hole / e $Å^{-3}$	0.29/-0.21	0.40/-0.19

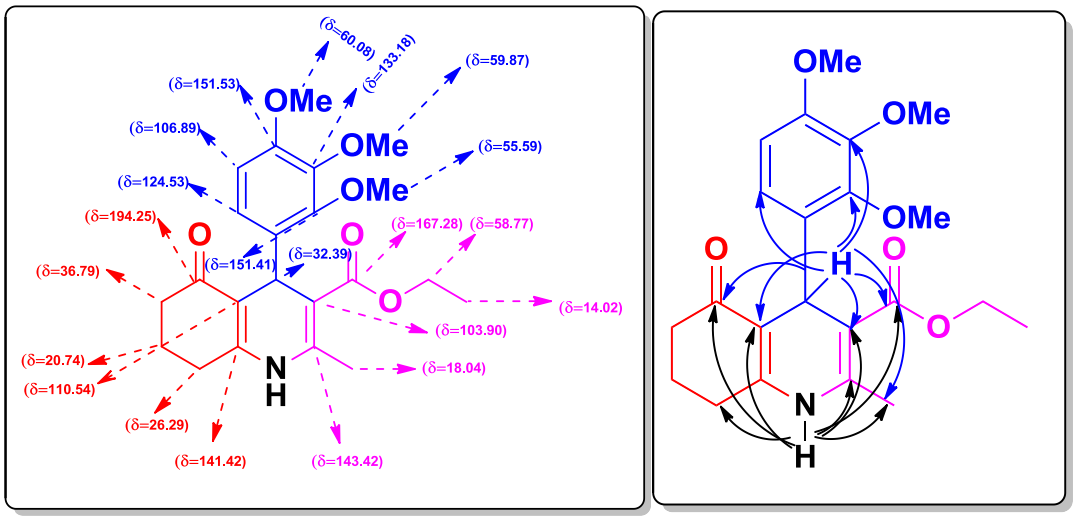

Fig. 10 ^{13}C chemical shifts, selected HMBC interactions of –CH, –NH protons of **5a.**

The heteronuclear multiple bond correlation (HMBC) interactions of trial reaction 5a are shown in Figure 10. In the 1H NMR spectra, the distinguishing singlet peaks at δ = 2.18, 3.67, 3.70, 3.77, 4.98, and 8.99 indicate the presence of −CH_3, −OCH_3, −CH, and −NH protons. The selected HMBC interactions of 5a are a definite proof for the product formation. The −CH proton in the 1,4-dihydropyridine ring was assigned to the peak at δ = 4.98, and it further interacted with carbon atoms at δ = 18.04, 103.90, 110.54, 124.53, 133.18, 151.41, 167.28, and 194.25. The singlet peak at δ = 8.99 was attributed to the −NH proton in the dihydropyridine ring, which further interacts with the carbon atoms at δ = 18.04, 26.29, 110.54, 103.90, 143.42, 167.28, and 194.25. The HRMS showed the m/z = 400.1770 [$C_{22}H_{27}NO_6$-H^{+}], which corresponds well with the theoretical value for 5a.

7.4 Insight into the mechanism

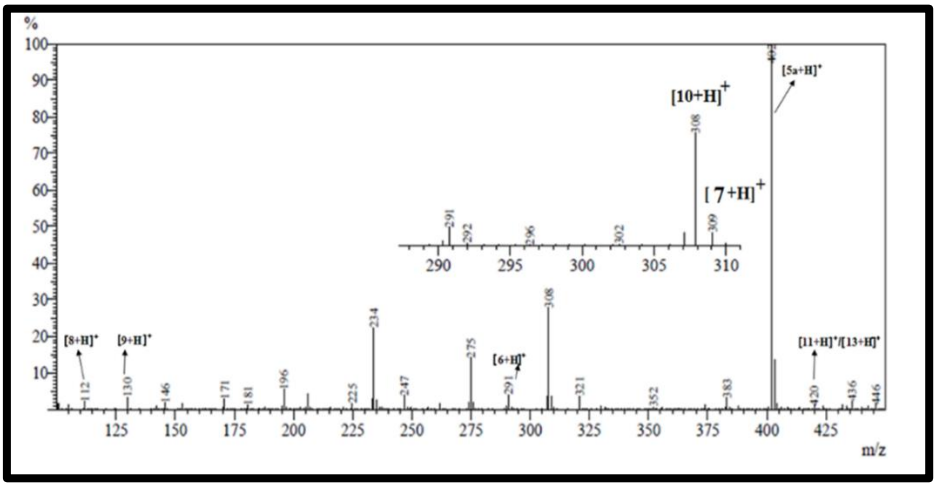

Fig. 11 LC-MS spectra of reaction mixture with compound **5a**

To examine the mechanism of the present reaction, an attempt was made to identify the reaction intermediates by analyzing the reaction mixture after 10 min (Figure 11). Characterization relied on liquid chromatography−mass spectrometry (LC−MS) studies and was based on peaks identified at 112 and 130 corresponding to the presence of enamine, the peak at 309 corresponding to imine, and the peak at 291 to the existence of a Knoevenagel condensation transient intermediate. Based on experimental observations, the generation of the final product is proposed to occur through two pathways: (i) by enamine and (ii) by imine, which is supported by the literature reports.[45,46] In the proposed scheme, the key intermediates in the reaction are designated as (6), (7), (8), and (9). It is assumed that for the formation of a knoevenagel intermediate[47] between 2,3,4-OMe benzaldehyde (1) and 1,3-cyclohexanedione (2), Lewis acidic sites present on the surface plays a key role, which can activate the carbonyl group of aldehyde and make it electrophilic to form an inter mediate (a) and then react with nucleophilic 1,3-cyclo-hexanedione (2), which further will dissociate from the catalyst surface by taking a proton from the solvent ethanol to give the intermediate (b) and to give (6) upon further dehydration. Similarly, (7) is also formed by the same procedure with the reaction of ethyl acetoacetate through the intermediate (c). Furthermore, ammonium acetate (4) acts as a nitrogen source to further dissociate to ammonia (4a). The enamine intermediates (8) and (9) are formed by the reaction of ammonia (4a) with (2) and (3) on the catalyst surface. Enamine (8) possibly reacts with (7) and undergoes Michael addition to give the key structure (11). The ring closure of (11) leads to the formation intermediate (12), which undergoes dehydration, finally yielding the stable product, 5a. Similarly, the enamine (9) upon reaction with (6) gives (13) via Michael addition and subsequent ring closure generates intermediate (14), which upon dehydration offers 5a. The enamine (9) reacts with (1) to give an imine intermediate (10), which further reacts with (2) to give (13). Further ring closure provides the intermediate (14) followed by dehydration, which gives 5a (Scheme 2). The comparative catalytic efficiency of the 2.5% NiO/ZrO_2 with other reported catalysts is given in Table 5.

Moreover, green metrics calculation given in supporting information. For the proposed method, the calculated atom economy and atom efficiency ranges from 74.1 to 83.2%, which are below 100% due to the loss of three H_2O molecules and one acetate ion as by products, and E factors ranging from 0.26 to 0.44 g/g are also validated and indicate the good green credential of the present protocol. The other green metrics are shown in supporting Information.

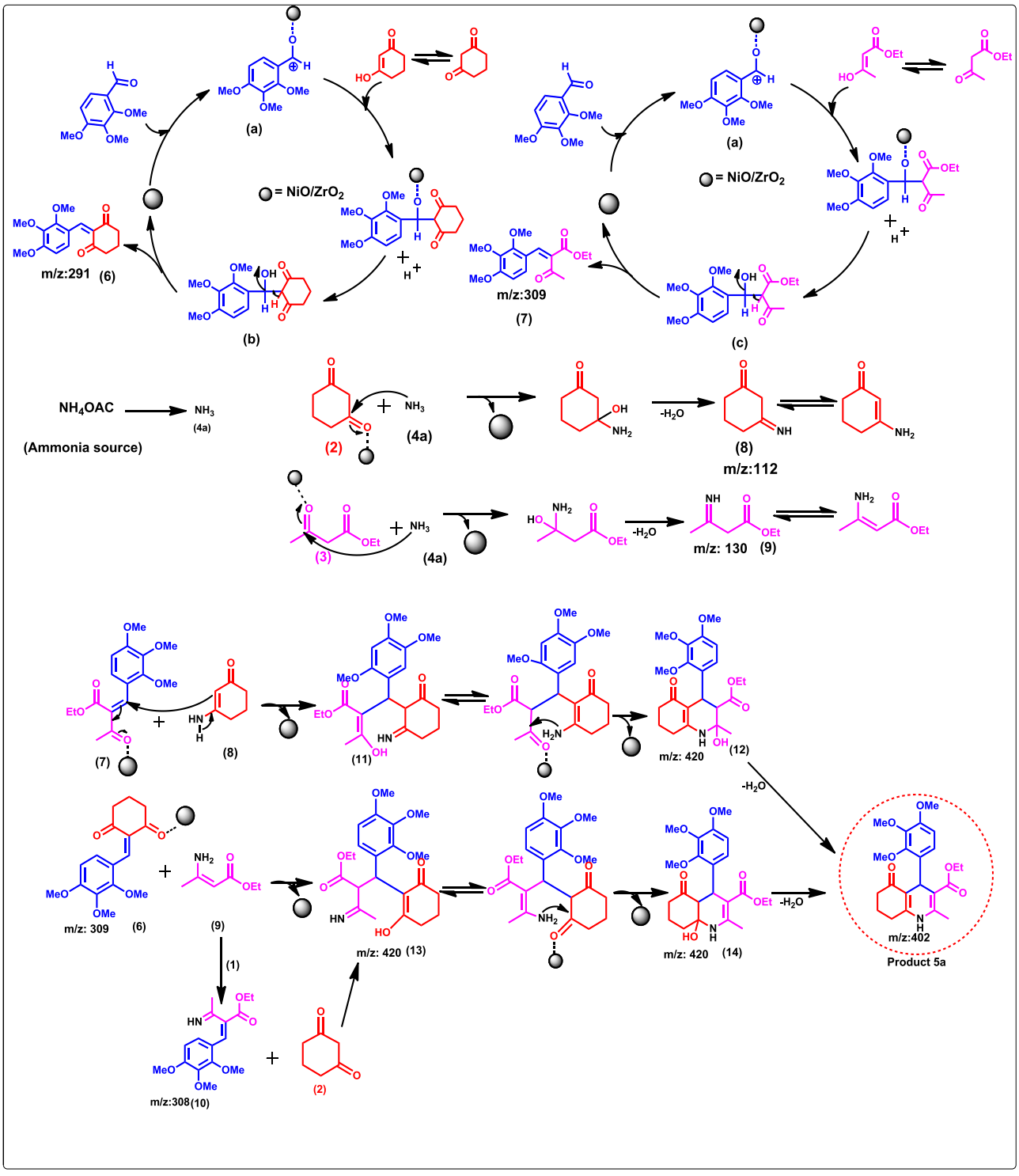

Scheme 3 Formation of unsymmetrical 1,4-DHPs **5a** in the presence of NiO/ZrO_2 catalyst.

Table 5: Comparison of present work with previous reports

Catalyst [Ref]	Solvent	Reaction Condition	Time	Yield (%)
Sulfamic acid[19]	MeOH	Reflux	24 h	47-92
γ-Fe_2O_3/Cu@cellulose[35]	Solvent-free	RT	9-30 min	80-98
SBA-15@AMPD-Co[36]	Solvent-free	100 °C	35-90 min	90-97
Fe_3O_4@D-NH-$(CH_2)_4$-SO_3H [37]	EtOH	Reflux	40 min	86-90
Cu-Adenine@boehmite[38]	EtOH	Reflux	20-120 min	89-97
Nano-tungsten trioxide-supported sulfonic acid (n-WSA)[24]	Solvent-free	100 °C	10-25 min	86-98
Sulfated boric acid nanoparticles[25]	EtOH	60 °C	20-60 min	86-98
Chitosan supported copper(II) sulfate (CSCS)[26]	EtOH	Reflux	20-87 min	80-97
Fe_3O_4@SiO_2@Si-$(CH_2)_3$@melamine-picolineimine@SO_3H[27]	Solvent-free	60 °C	4-11 min	48-90
Sulfated polyborate[28]	Solvent-free	90 °C	15-35 min	85-95
Fe_3O_4/KCC-1/BPAT[29]	Water	Reflux	4h	79-88
Chitosan supported vanadium oxo[30]	Solvent-free	85 °C	20-55 min	81-94
Magnetic guanidinylated chitosan[31]	EtOH	Reflux	15 min	82-89
Nano-ZrO_2-SO_3H (n-ZrSA)[32]	Solvent-free	80 °C	35-65 min	84-93
$Gd(OTf)_3$[33]	EtOH	RT	5-6 h	82-89
nicotinic acid[34]	Solvent-free	80 °C	2-7 min	87-96
Hydromagnesite[39]	Water	90 °C	20-45 min	80-98
$Cu(OTf)_2$[40]	EtOH	100 °C	15 min	81-98
Ascorbic acid[41]	Solvent-free	80 °C	1.5-4.5 h	70-96
NS-C_4(DABCO-$SO_3H)_2)\cdot 4Cl$[42]	Solvent-free	100 °C	8-50 min	80-100
CBr_4[43]	EtOH	RT	3-6 h	70-98

Aminated CNTs [14]	EtOH	Reflux	3-6 h	80-96
2.5%NiO/ZrO_2 (Present work)	EtOH	RT	20-45 min	89-98%

7.5 Reusability of catalyst

To examine the catalyst stability, recyclability experiments were conducted. After every run, the catalyst was recovered from the reaction mixture, washed with ethanol, and dried at 120 °C for 2 h. For the first six cycles, the catalyst proved efficient and the activity was retained with no loss. Afterward, the material catalytic activity decreased in the seventh cycle (Figure 12). To examine the heterogeneity of the used 2.5% NiO/ZrO_2 catalyst, a hot filtration method was employed for the synthesis of 5a. Twelve minutes after the start of the reaction, the catalyst was removed from the reaction mixture through centrifugation and the remaining reaction mixture was kept under the same stirred condition to monitor the reaction progress. Even after 60 min, no reaction or increase in the product yield was observed (Figure 13). From the above result, it shows that the catalyst leaching is very low. Furthermore, the catalyst after the reaction was analyzed by XRD and TEM given in supporting information. The XRD pattern of the reused material is much similar to that of the fresh one; furthermore, from the TEM image of the reused catalyst, there is as much similar to that of the fresh one, which indicates that there is no such erosion of the active material from the support, which shows the presence of the heterogeneous nature of material.

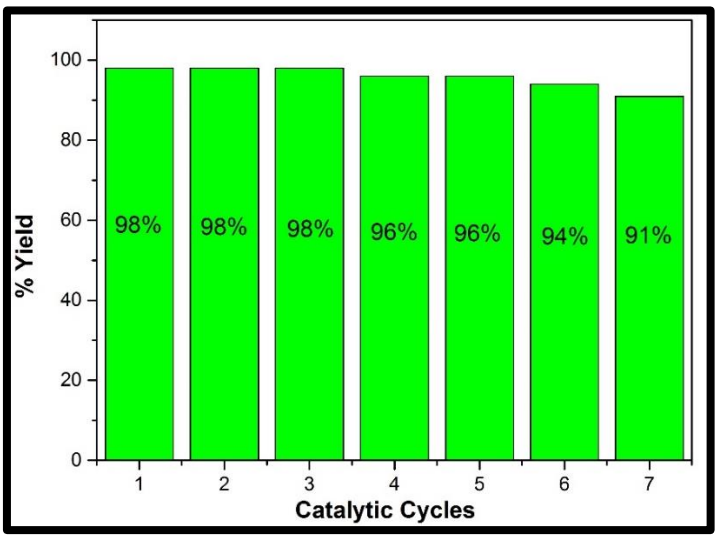

Fig. 12. Recycling study of 2.5% NiO/ZrO_2 catalyst for the synthesis of 1,4-dihydropyridine **5a**

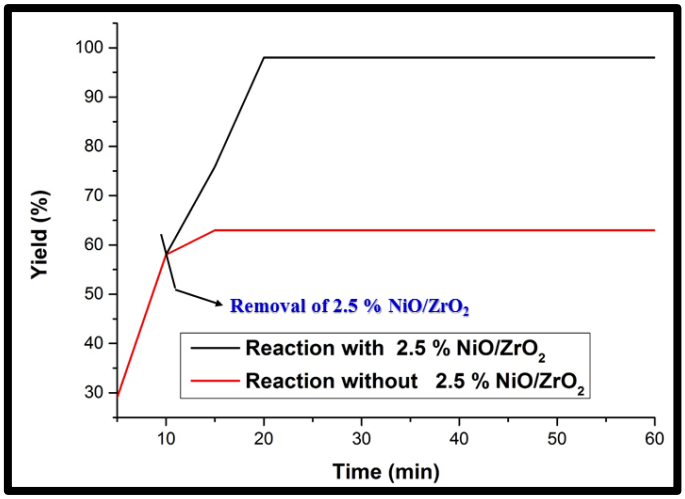

Figure 13. Hot filtration test results of 2.5 % NiO/ZrO_2 catalyst for **5a**.Reaction conditions: 2,3,4-trimethoxybenzaldehyde (1 mmol) (1), Ethyl acetoacetate (1 mmol) (2), and 1,3-Cyclohexadione (1 mmol) (3) and Ammonium acetate (1 mmol) (4), 5 mL EtOH were stirred at RT.

7.6 Conclusions

We introduced NiO/ZrO_2 as an efficient and cost-effective catalyst for the synthesis of 12 novel 1,4-dihydropyridine derivatives in a four-component, one-pot strategy. This method proved effective toward the reaction of aromatic, heteroaromatic, and aliphatic aldehydes obtained with high yields. ESI-MS/MS studies are conducted, and insights into the mechanism of the reaction are proposed, which revealed that1,4-DHPs mainly follow the enamine and imine pathways.We anticipate that this catalytic system will find further applications in both academic and industrial fields, and the prepared series of 1,4-DHPs may provide potential biological activity in the area of pharmaceutical sector.

7.7 Supplementary Information

The CCDC number 1903627, 1889376 contains the information regarding the supplementary crystallographic data. These data can be obtained free of charge via www.ccdc.cam.ac.uk/conts/retrieving.html or [from the Cambridge Crystallographic Data Center (CCDC), 12 Union Road, Cambridge CB21 EZ, UK; Fax: +44(0)1223-336,003; E-18 mail:deposit@ccdc.cam.ac.uk]. Structure factor table is available from the authors.

7.8 Acknowledgements

The authors are thankful to the School of Chemistry and Physics, University of KwaZulu-Natal, Durban for the research and other facilities.

7.9. Refrences

1 S. Dang, H. Yang, P. Gao, H. Wang, X. Li, W. Wei and Y. Sun, *Catal. Today*, 2019, **330**, 61–75.

2 L. Liu and A. Corma, *Chem. Rev.*, 2018, **118**, 4981–5079.

3 H. Ceri, P. Daniele and T. Giulia, *R. Soc. Open Sci.*, 2019, **5**, 171315.

4 C. J. Védrine, *Catal.* , 2017, 7.

5 S. V. H. S. Bhaskaruni, K. K. Gangu, S. Maddila and S. B. Jonnalagadda, *Chem. Rec.*, , DOI:10.1002/tcr.201800077.

6 V. P. Ananikov, *ACS Catal.*, 2015, **5**, 1964–1971.

7 A. Peters, F. Nouroozi, D. Richter, M. Lutecki and R. Gläser, *ChemCatChem*, 2011, **3**, 598–606.

8 Y. Zhao, W. Li, M. Zhang and K. Tao, *Catal. Commun.*, 2002, **3**, 239–245.

9 S. Kouva, K. Honkala, L. Lefferts and J. Kanervo, *Catal. Sci. Technol.*, 2015, **5**, 3473–3490.

10 K. Fukudome, A. Kanno, N. Ikenaga, T. Miyake and T. Suzuki, *Catal. Lett.*, 2011, **141**, 68–77.

11 N. Pal and A. Bhaumik, *Dalt. Trans.*, 2012, **41**, 9161–9169.

12 S. Brauch, S. S. van Berkel and B. Westermann, *Chem. Soc. Rev.*, 2013, **42**, 4948–4962.

13 N. Edraki, A. R. Mehdipour, M. Khoshneviszadeh and R. Miri, *Drug Discov. Today*, 2009, **14**, 1058–1066.

14 R. Mahinpour, L. Moradi, Z. Zahraei and N. Pahlevanzadeh, *J. Saudi Chem. Soc.*, 2018, **22**, 876–885.

15 N. C. Desai, A. R. Trivedi, H. C. Somani and K. A. Bhatt, *Chem. Biol. Drug Des.*, 2014, **86**, 370–377.

16 R. N. Goto, L. M. Sobral, L. O. Sousa, C. B. Garcia, N. P. Lopes, J. Marín-Prida, E. Ochoa-Rodríguez, Y. Verdecia-Reyes, G. L. Pardo-Andreu, C. Curti and A. M. Leopoldino, *Eur. J. Pharmacol.*, 2018, **819**, 198–206.

17 A. Ahamed, I. A. Arif, M. Mateen, R. Surendra Kumar and A. Idhayadhulla, *Saudi J. Biol. Sci.*, 2018, **25**, 1227–1235.

18 A. Leoni, M. Frosini, A. Locatelli, M. Micucci, C. Carotenuto, M. Durante, S. Cosconati and R. Budriesi, *Eur. J. Med. Chem.*, 2019, **169**, 89–102.

19 D. da Costa Cabrera, E. Santa-Helena, H. P. Leal, R. R. de Moura, L. E. M. Nery, C. A. N. Gonçalves, D. Russowsky and M. G. Montes D'Oca, *Bioorg. Chem.*, 2019, **84**, 1–16.

20 D. Schaller, M. G. Gündüz, F. X. Zhang, G. W. Zamponi and G. Wolber, *Eur. J. Med. Chem.*, 2018, **155**, 1–12.

21 R. Azzouz, L. Peauger, V. Gembus, M.-L. Ţînţaş, J. Sopková-de Oliveira Santos, C. Papamicaël and V. Levacher, *Eur. J. Med. Chem.*, 2018, **145**, 165–190.

22 R. K. Modukuri, D. Choudhary, S. Gupta, K. B. Rao, S. Adhikary, T. Sharma, M. I. Siddiqi, R. Trivedi and K. V Sashidhara, *Bioorg. Med. Chem.*, 2017, **25**, 6450–6466.

23 A. Hantzsch, *Justus Liebigs Ann. Chem.*, 1882, **215**, 1–82.

24 M. Bitaraf, A. Amoozadeh and S. Otokesh, *J. Chinese Chem. Soc.*, 2016, **63**, 336–344.

25 K. Azizi, J. Azarnia, M. Karimi, E. Yazdani and A. Heydari, *Synlett*, 2016, **27**, 1810–1813.

26 M. G. Dekamin, E. Kazemi, Z. Karimi, M. Mohammadalipoor and M. R. Naimi-Jamal, *Int. J. Biol. Macromol.*, 2016, **93**, 767–774.

27 A. Khazaei, N. Sarmasti and J. Yousefi Seyf, *J. Mol. Liq.*, 2018, **262**, 484–494.

28 D. S. Rekunge, C. K. Khatri and G. U. Chaturbhuj, *Tetrahedron Lett.*, 2017, **58**, 1240–1244.

29 S. M. Sadeghzadeh, *RSC Adv.*, 2016, **6**, 99586–99594.

30 M. Safaiee, B. Ebrahimghasri, M. A. Zolfigol, S. Baghery, A. Khoshnood and D. A. Alonso, *New J. Chem.*, 2018, **42**, 12539–12548.

31 A. Maleki, R. Firouzi-Haji and Z. Hajizadeh, *Int. J. Biol. Macromol.*, 2018, **116**, 320–326.

32 A. Amoozadeh, S. Rahmani, M. Bitaraf, F. B. Abadi and E. Tabrizian, *New J. Chem.*, 2016, **40**, 770–780.

33 S. Sheik Mansoor, K. Aswin, K. Logaiya and S. P. N. Sudhan, *Arab. J. Chem.*, 2017, **10**, S546–S553.

34 J. Davarpanah, M. Ghahremani and O. Najafi, *J. Mol. Struct.*, 2019, **1177**, 525–535.

35 A. Maleki, V. Eskandarpour, J. Rahimi and N. Hamidi, *Carbohydr. Polym.*, 2019, **208**, 251–260.

36 A. Ghorbani-Choghamarani, M. Mohammadi, T. Tamoradi and M. Ghadermazi, *Polyhedron*, 2019, **158**, 25–35.

37 B. Maleki, O. Reiser, E. Esmaeilnezhad and H. J. Choi, *Polyhedron*, 2019, **162**, 129–141.

38 A. Ghorbani-Choghamarani, P. Moradi and B. Tahmasbi, *Polyhedron*, 2019, **163**, 98–107.

39 U. C. Rajesh, S. Manohar and D. S. Rawat, *Adv. Synth. Catal.*, 2013, **355**, 3170–3178.

40 K. K. Pasunooti, C. Nixon Jensen, H. Chai, M. L. Leow, D.-W. Zhang and X.-W. Liu, *J. Comb. Chem.*, 2010, **12**, 577–581.

41 I. Sehout, R. Boulcina, B. Boumoud, T. Boumoud and A. Debache, *Synth. Commun.*, 2017, **47**, 1185–1191.

42 O. Goli-Jolodar, F. Shirini and M. Seddighi, *RSC Adv.*, 2016, **6**, 26026–26037.

43 J. Wu, W.-Z. Wang and W. Sun, *Chinese J. Chem.*, 2007, **25**, 1072–1075.

44 S. Bhaskaruni, S. Maddila, W. van Zyl and S. Jonnalagadda, *Mol.* ,2018, 23.

45 A. R. Katritzky, D. L. Ostercamp and T. I. Yousaf, *Tetrahedron*, 1986, **42**, 5729–5738.

46 V. G. Santos, M. N. Godoi, T. Regiani, F. H. S. Gama, M. B. Coelho, R. O. M. A. de Souza, M. N. Eberlin and S. J. Garden, *Chem. – A Eur. J.*, 2014, **20**, 12808–12816.

47 Q. Li, X. Wang, Y. Yu, Y. Chen and L. Dai, *Tetrahedron*, 2016, **72**, 8358–8363.

7.10. Supplementary information

7.10.1. Catalyst instrumentation details

Employing a Bruker D8 Advance instrument (Cu K radiation source with a wave length of 1.5406 Å), the X-ray diffraction data related the structural phases of the catalyst were acquired. Using a JEOL JEM-1010 electron microscope and JEOL JSM-6100 microscope, the TEM and SEM analysis data was recorded. iTEM software was used analyse the TEM data and images. Employing the X-ray analyser (energy-dispersive), EDX-analysis on the SEM images was conducted.

7.10.2. Experimental Section

All chemicals and reagents required for the reaction were of analytical grade and were used without any further purification. Bruker AMX 400 MHz NMR spectrometer was used to record the ^{1}H NMR, ^{13}C NMR and ^{15}N NMR spectral values. High-resolution mass data were obtained using a Bruker micro TOF-Q II ESI instrument operating at ambient temperature. The DMSO-d6 and $CDCl_3{-}d_6$ solution was utilized for this while TMS served as the internal standard. TMS was further used as an internal standard for reporting the all chemical shifts in δ (ppm). Purity of all the reaction products was confirmed by TLC using aluminium plates coated with silica gel (Merck Kieselgel 60 F_{254}). Infrared (IR) spectra were recorded on a Perkin Elmer Precisely equipped with a Universal ATR sampling accessory using a diamond crystal. The powdered material was placed on the crystal and a force of 120 psi was applied to ensure proper contact between the material and the crystal.The spectra were analyzed using Spectrum 100 software. Before recording the IR spectra, pyridine was adsorbed by placing a drop of pyridine on 10 mg of the sample followed by evacuation in air for 1 h at room temperature to remove reversibly adsorbed pyridine on the surface of the catalyst.

Single crystals of **$C_{22}H_{27}NO_6$ (5a)** were **[The material was recrystallized from DMSO by slow evaporation]**. A suitable crystal was selected and **[The crystal was mounted on a MITIGEN holder in paratone oil]** on a '**Bruker APEX-II CCD**' diffractometer. The crystal was kept at 100.0 K during data collection. Using Olex2 [1], the structure was solved with the ShelXS [2] structure solution program using Direct Methods and refined with the ShelXL [3] refinement package using Least Squares minimisation.

Single crystals of **$C_{20}H_{23}NO_3$ (5c)** were **[The material was recrystallized from DMSO by slow evaporation]**. A suitable crystal was selected and **[The crystal was mounted on a MITIGEN holder in paratone oil]** on a '**Bruker APEX-II CCD**' diffractometer. The

crystal was kept at 100.0 K during data collection. Using Olex2 [1], the structure was solved with the ShelXS [2] structure solution program using Direct Methods and refined with the ShelXL [3] refinement package using Least Squares minimisation.

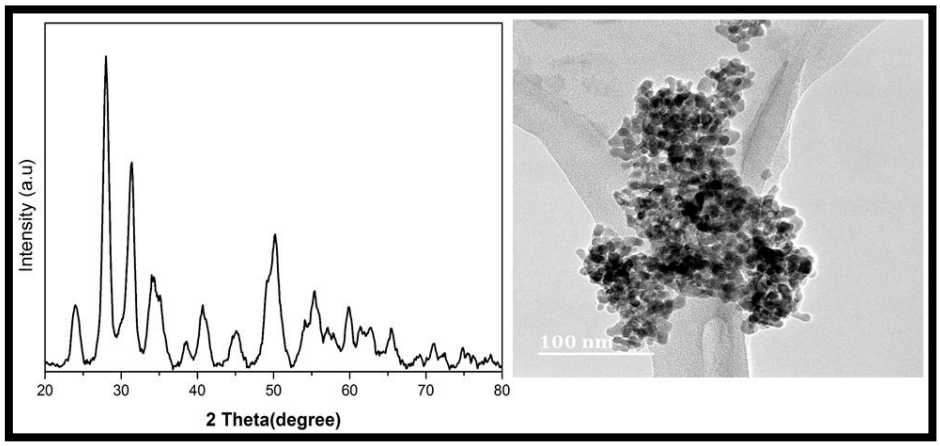

Figure S1. XRD and TEM images of reused used 2.5 % NiO/ZrO_2 (after 6 cycles).

Crystal Data:

$C_{22}H_{27}NO_6$ (*M* =401.44g/mol): orthorhombic, space group $Pna2_1$ (no. 33), *a* = 14.6836(6) Å, *b* = 8.4477(3) Å, *c* = 15.5290(6) Å, *V* = 1926.26(13) $Å^3$, *Z* = 4, *T* = 100.0 K, μ(MoKα) = 0.101 mm^{-1}, *Dcalc* = 1.384 g/cm^3, 13133 reflections measured (5.246° ≤ 2Θ ≤ 56.7°), 4622 unique (R_{int} = 0.0196, R_{sigma} = 0.0237) which were used in all calculations. The final R_1 was 0.0312 (I > 2σ(I)) and wR_2 was 0.0796 (all data).

$C_{20}H_{23}NO_3$ (M =325.39 g/mol): triclinic, space group P-1 (no. 2), a = 7.29920(10) Å, b = 9.58180(10) Å, c = 12.3976(2) Å, α = 83.9450(10)°, β = 86.8650(10)°, γ = 71.9730(10)°, V = 819.69(2) Å3, Z = 2, T = 100.0 K, μ(MoKα) = 0.088 mm-1, Dcalc = 1.318 g/cm3, 26777 reflections measured (3.304° ≤ 2Θ ≤ 57.038°), 4083 unique (Rint = 0.0179, Rsigma = 0.0131) which were used in all calculations. The final R1 was 0.0365 (I > 2σ(I)) and wR2 was 0.1008 (all data).

General procedure for the synthesis of 5(a-j) derivatives:

For the synthesis of series of 1,4-dihydropyridine derivatives, reaction was performed in a 25 mL round bottom flask containing 5 mL of EtOH as a solvent. To this equi-molar quantities of aldehyde, ethyl acetoacetate, ammonium acetate and 1,3 cyclohexadione are added together with 30 mg of NiO/ZrO_2 and stirred at room temperature (RT). TLC was used to monitor the progress of reaction in regular time intervals. After the completion of reaction, the catalyst was filtered by adding extra ethanol. Then, the solvent was evaporated and the pure product was afforded by recrystallization from EtOH.

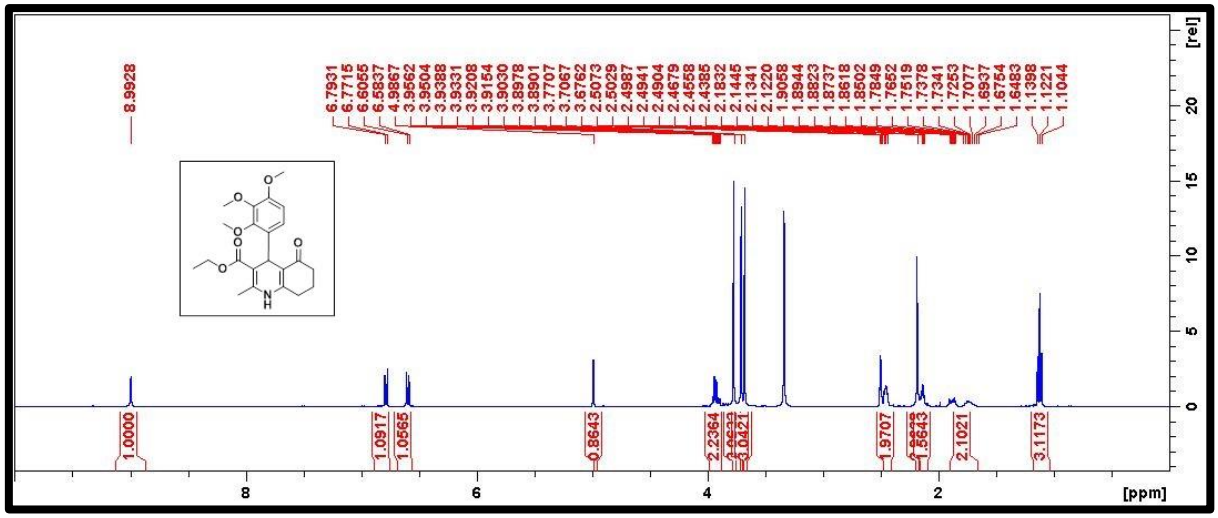

^{1}H NMR spectra of compound **5a** (400 MHz, DMSO)

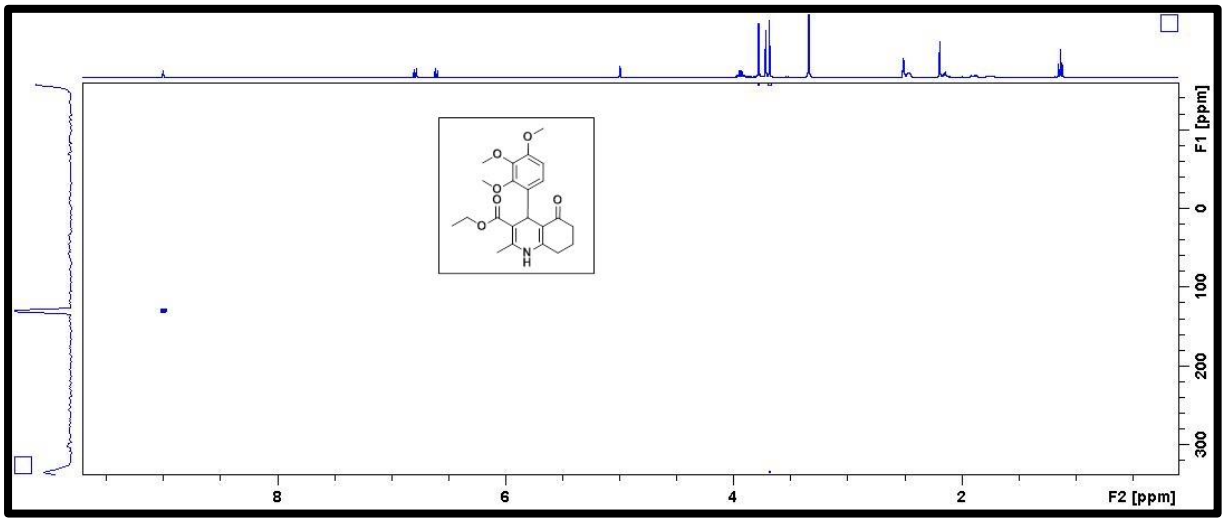

^{15}N NMR spectra of compound **5a** (40.55 MHz, DMSO)

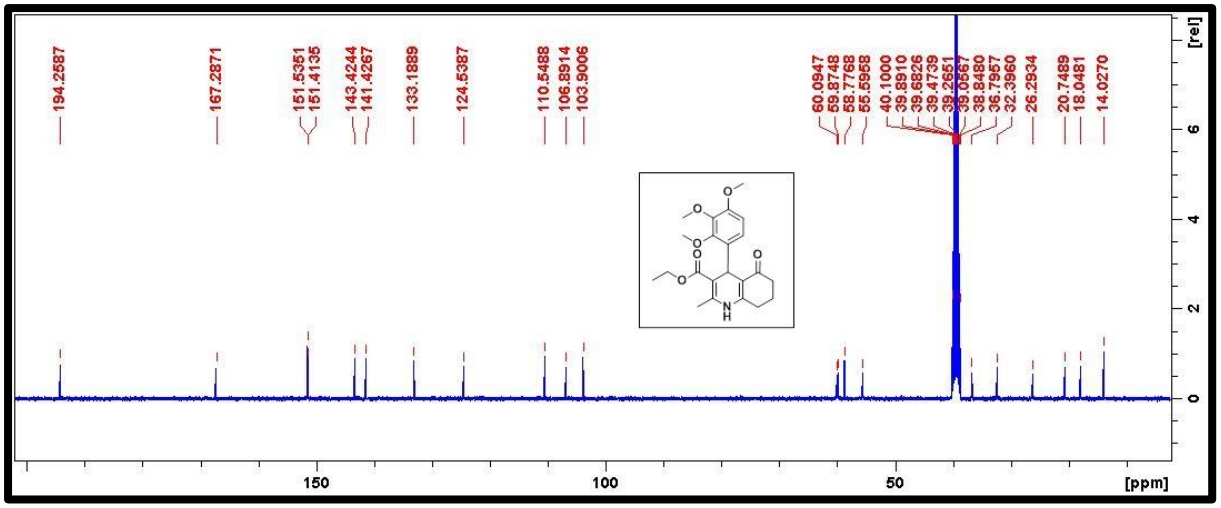

^{13}C NMR spectra of compound **5a** (100 MHz, DMSO)

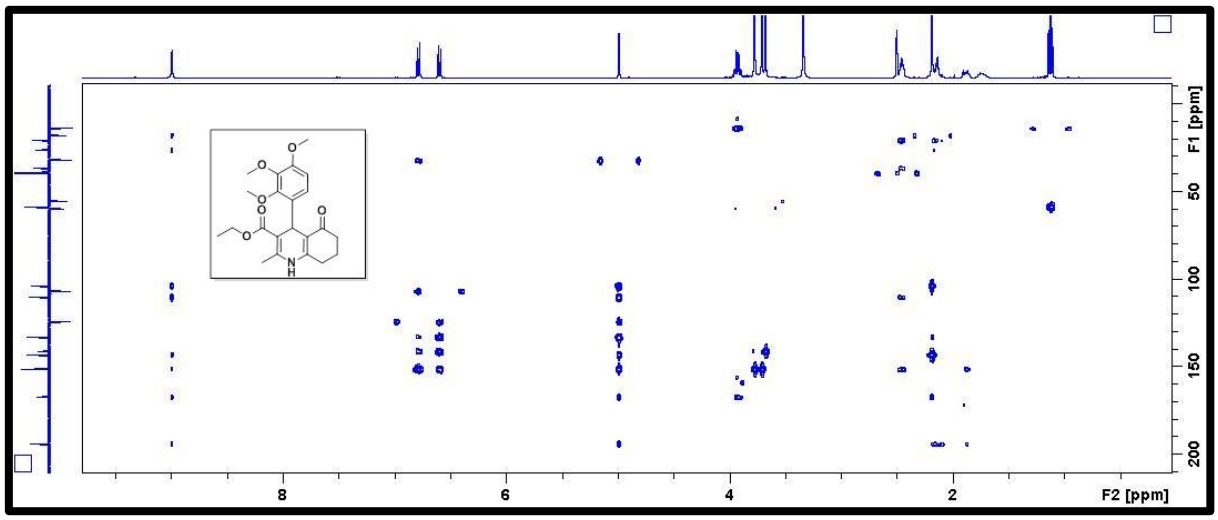

HMBC spectra of compound **5a**

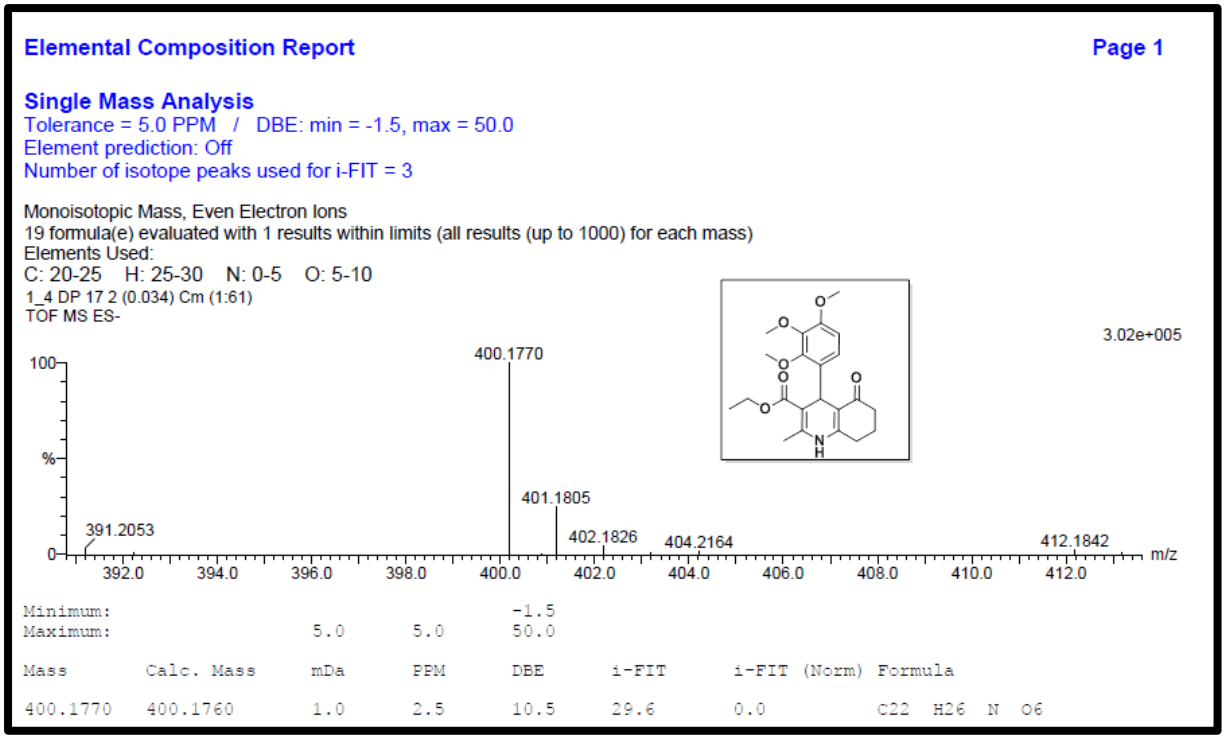

HRMS spectra of compound **5a**

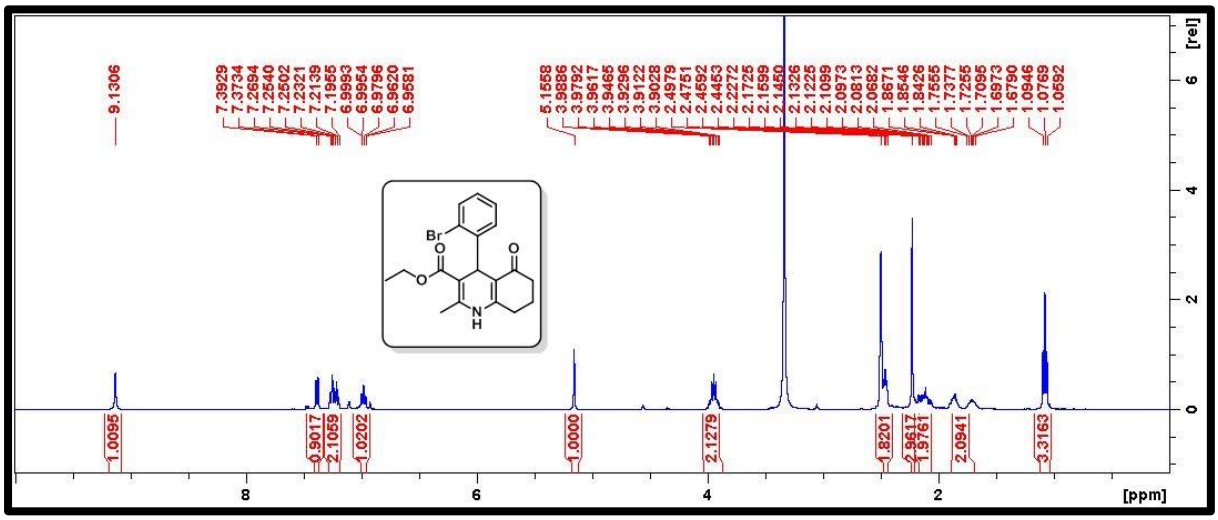

^{1}H NMR spectra of compound **5b** (400 MHz, DMSO)

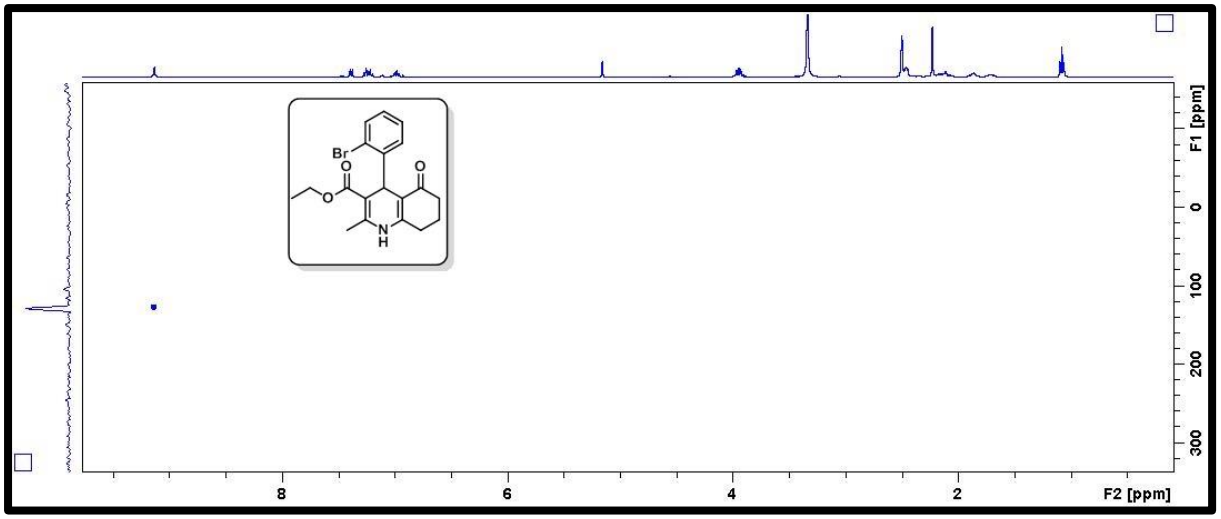

^{15}N NMR spectra of compound **5b** (40.55 MHz, DMSO)

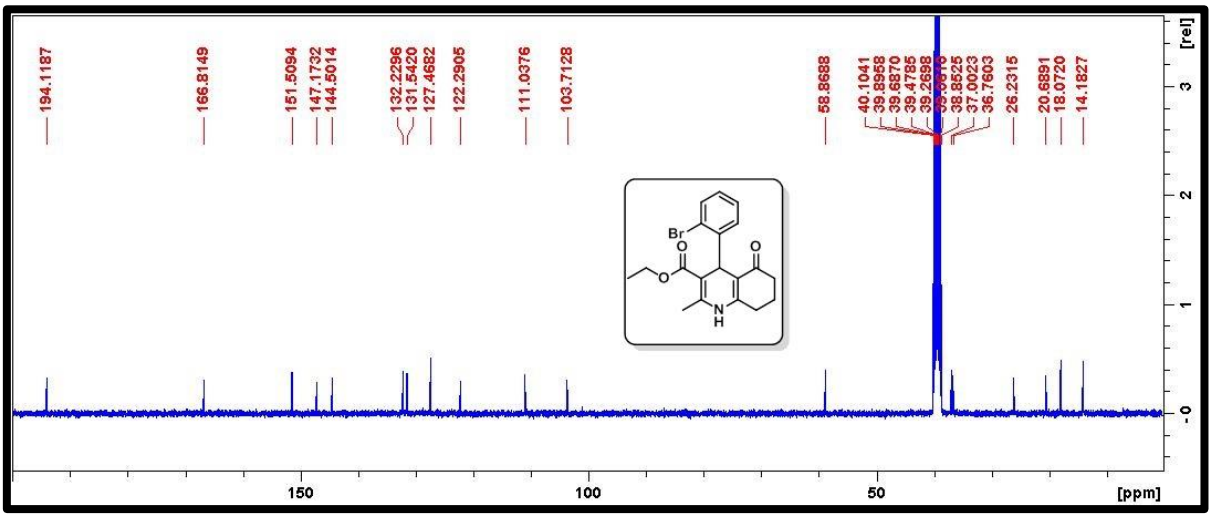

^{13}C NMR spectra of compound **5b** (100 MHz, DMSO)

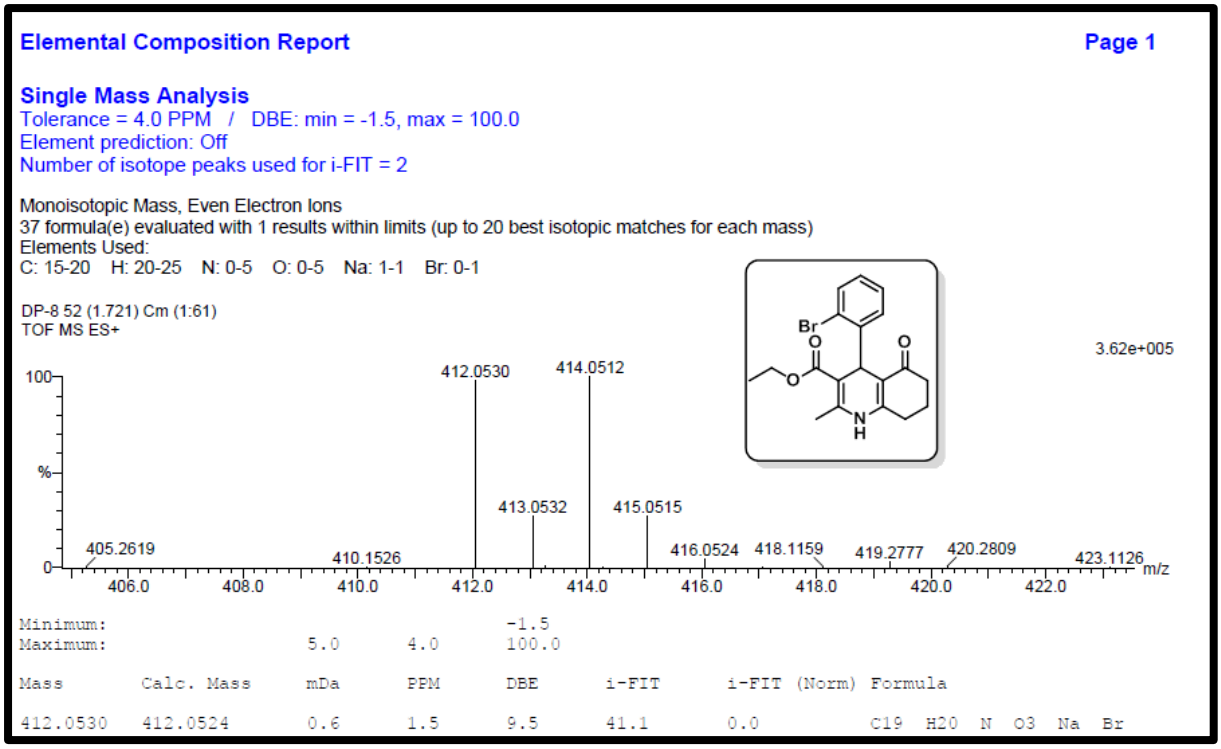

HRMS spectra of compound **5b**

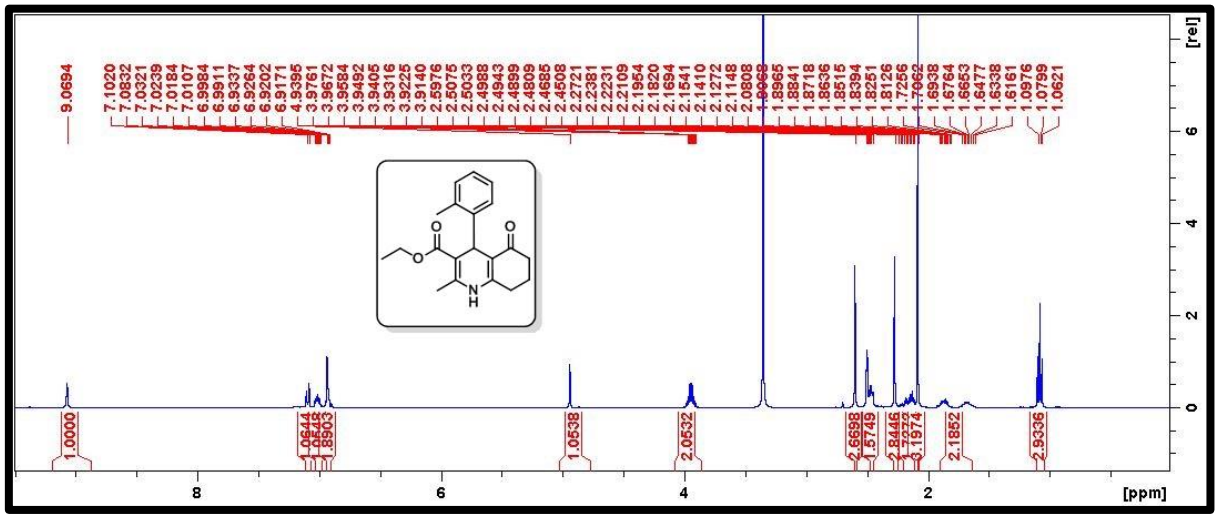

^{1}H NMR spectra of compound **5c** (400 MHz, DMSO)

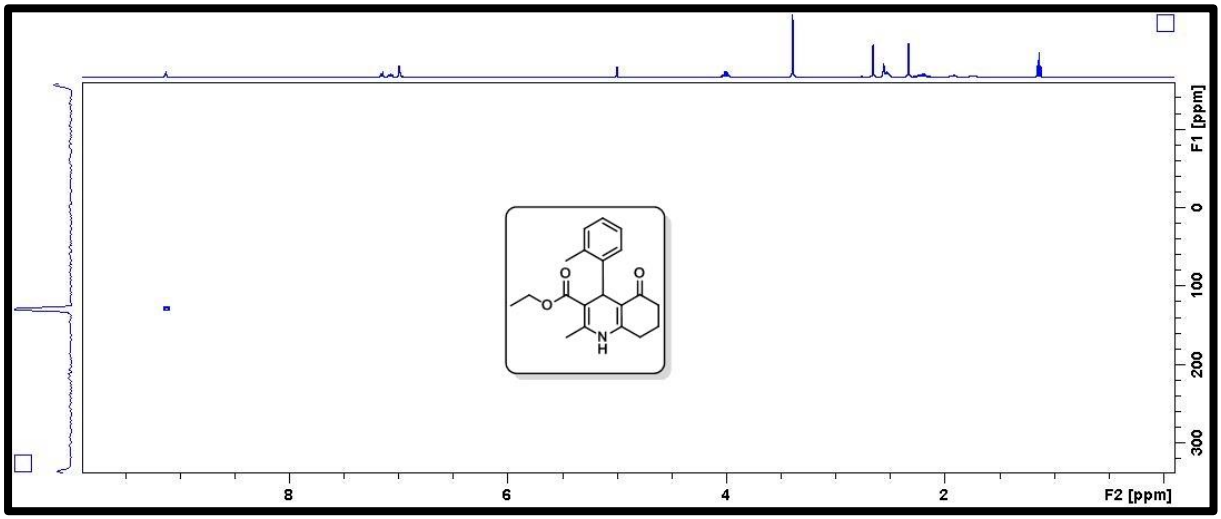

^{15}N NMR spectra of compound **5c** (40.55 MHz, DMSO)

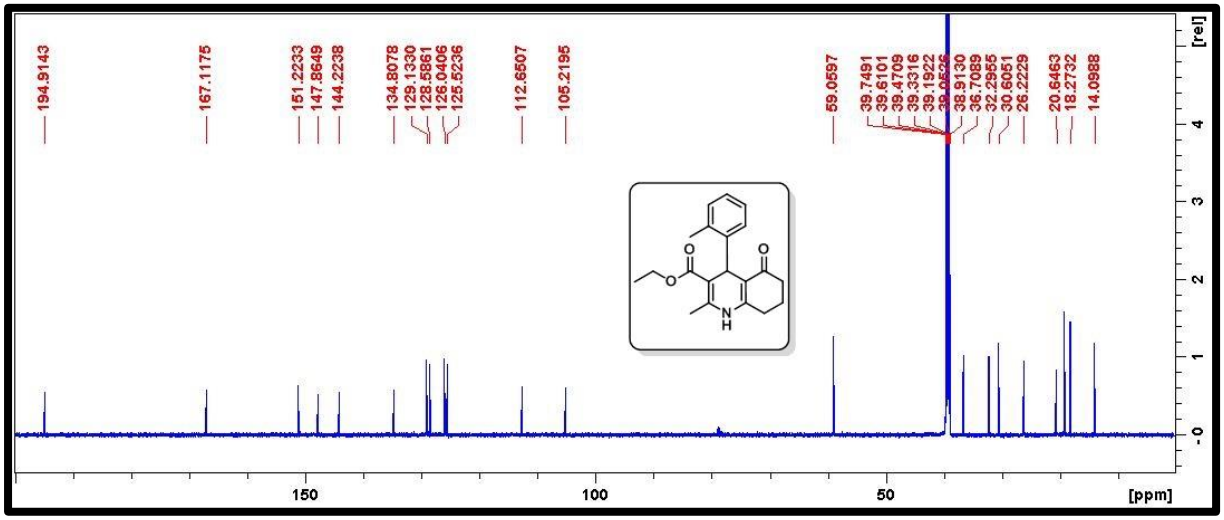

^{13}C NMR spectra of compound **5c** (100 MHz, DMSO)

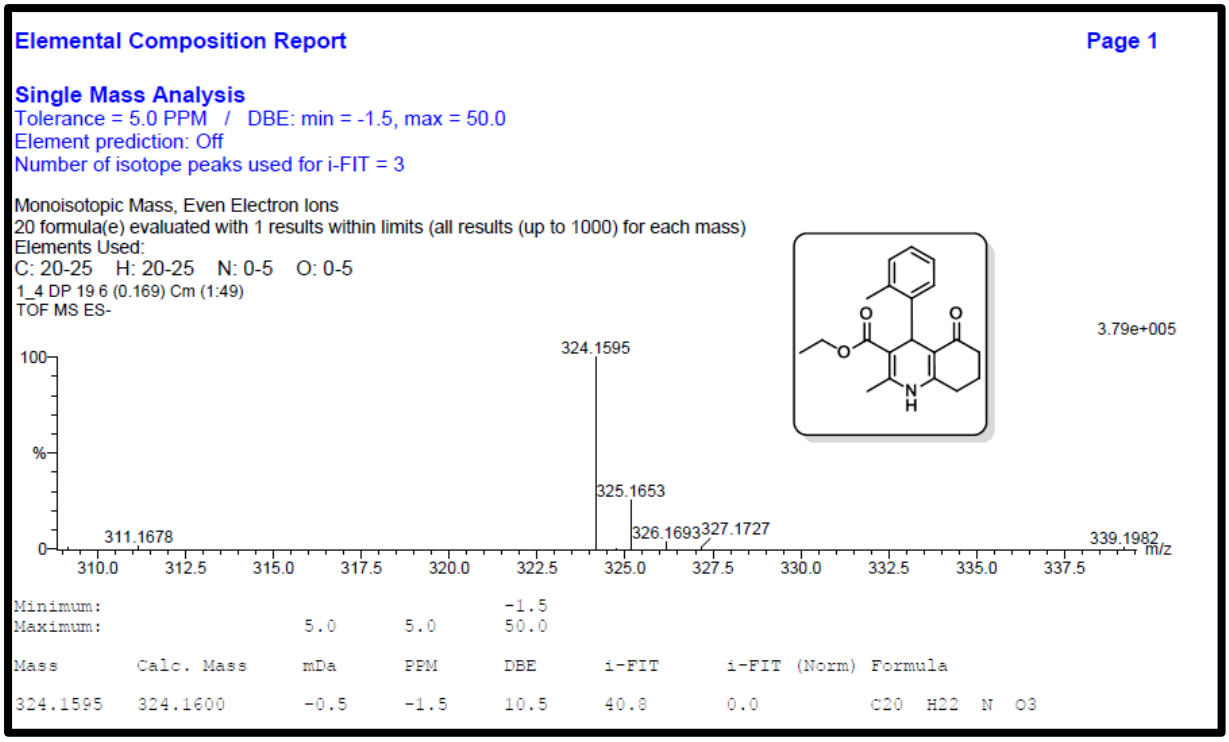

HRMS spectra of compound **5c**

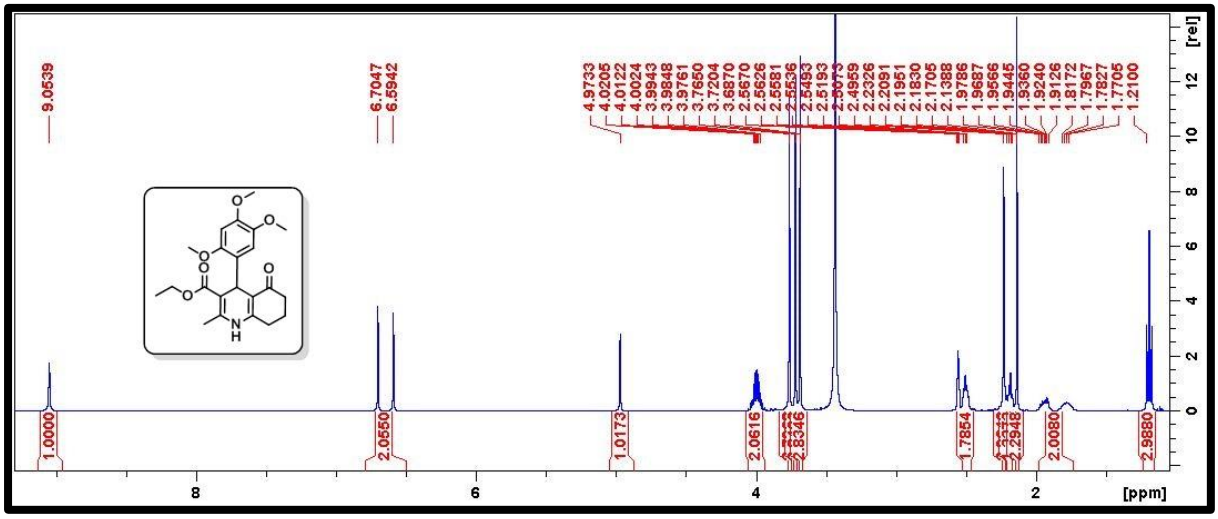

^{1}H NMR spectra of compound **5d** (400 MHz, DMSO)

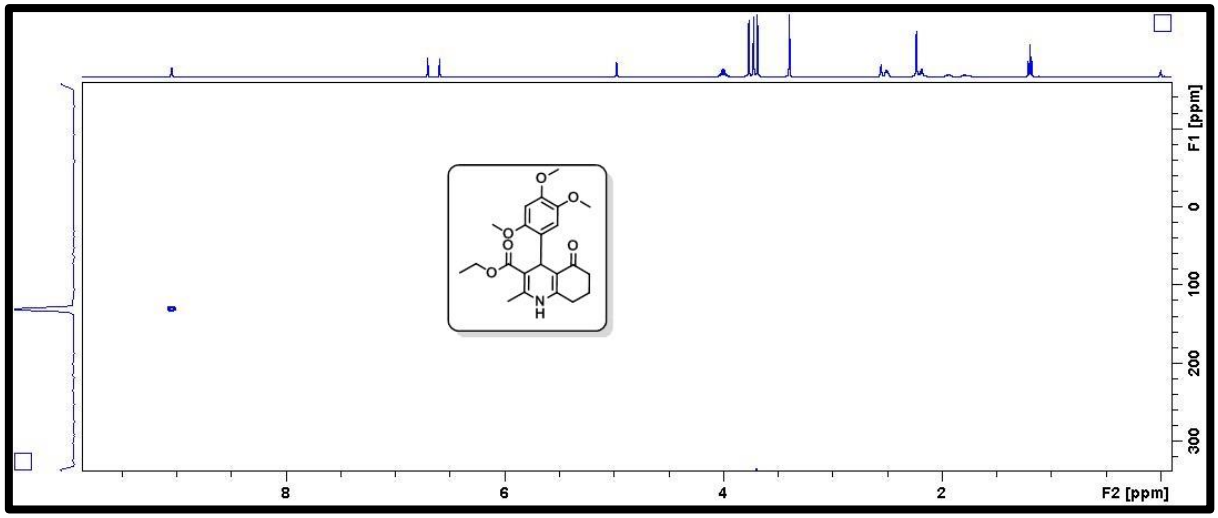

^{15}N NMR spectra of compound **5d** (40.55 MHz, DMSO)

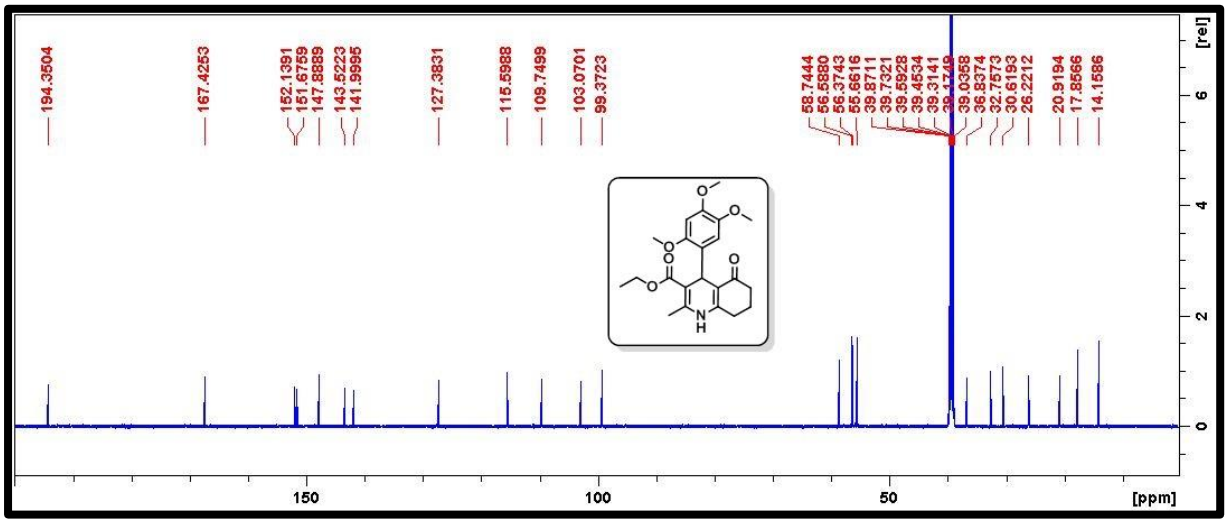

^{13}C NMR spectra of compound **5d** (100 MHz, DMSO)

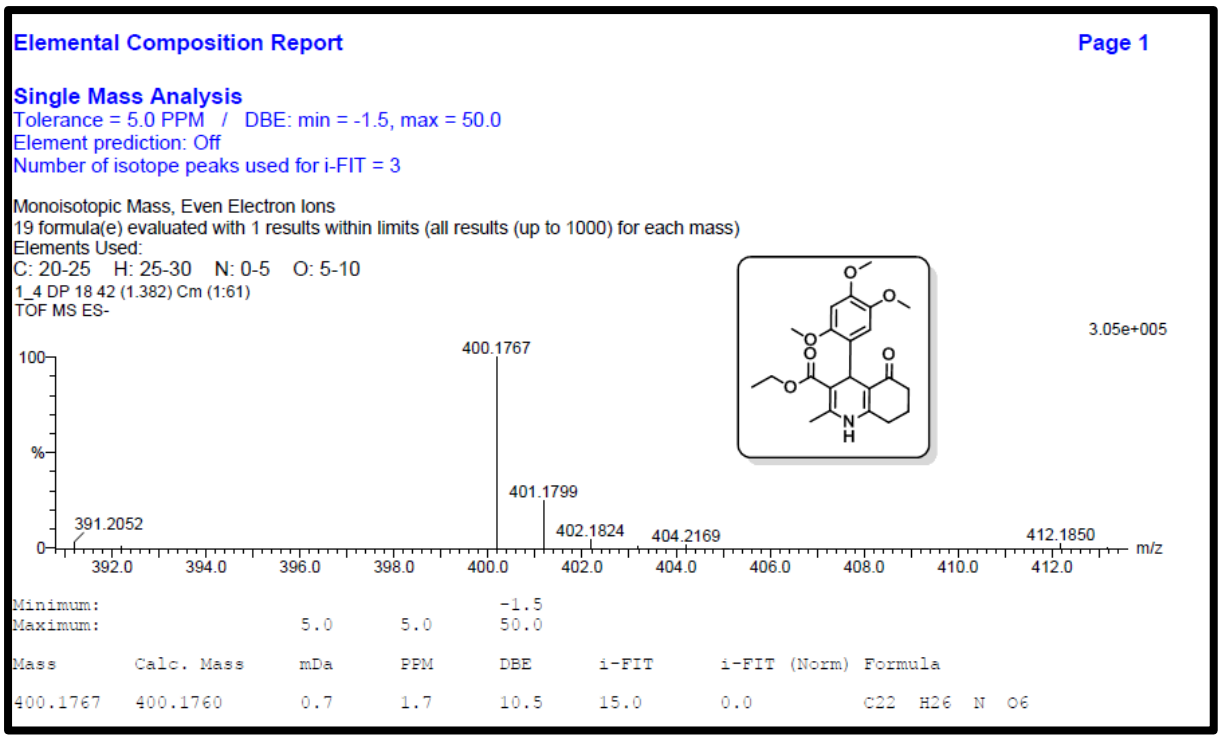

HRMS spectra of compound **5d**

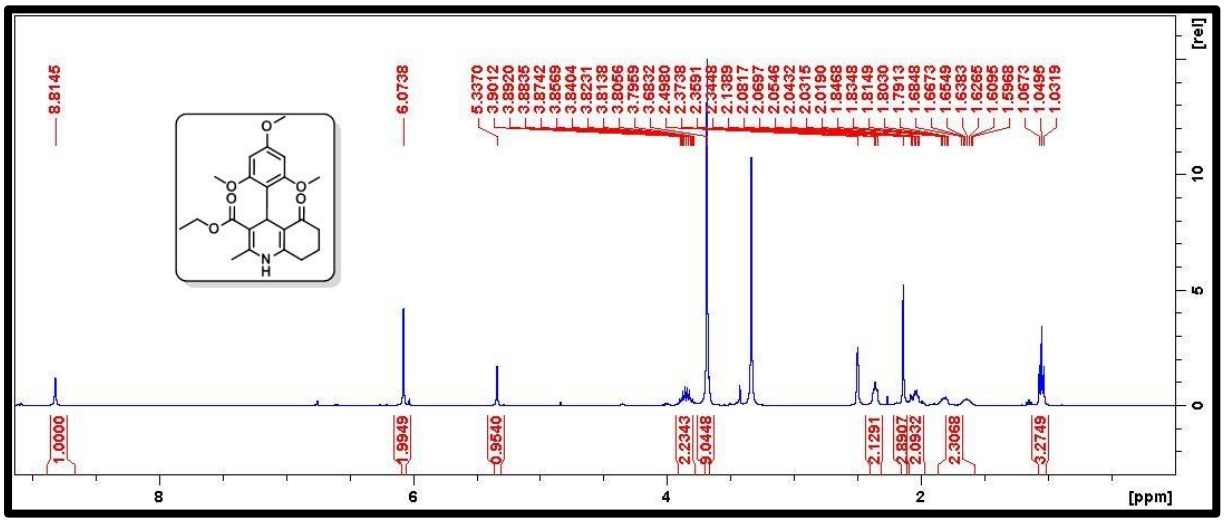

^{1}H NMR spectra of compound **5e** (400 MHz, DMSO)

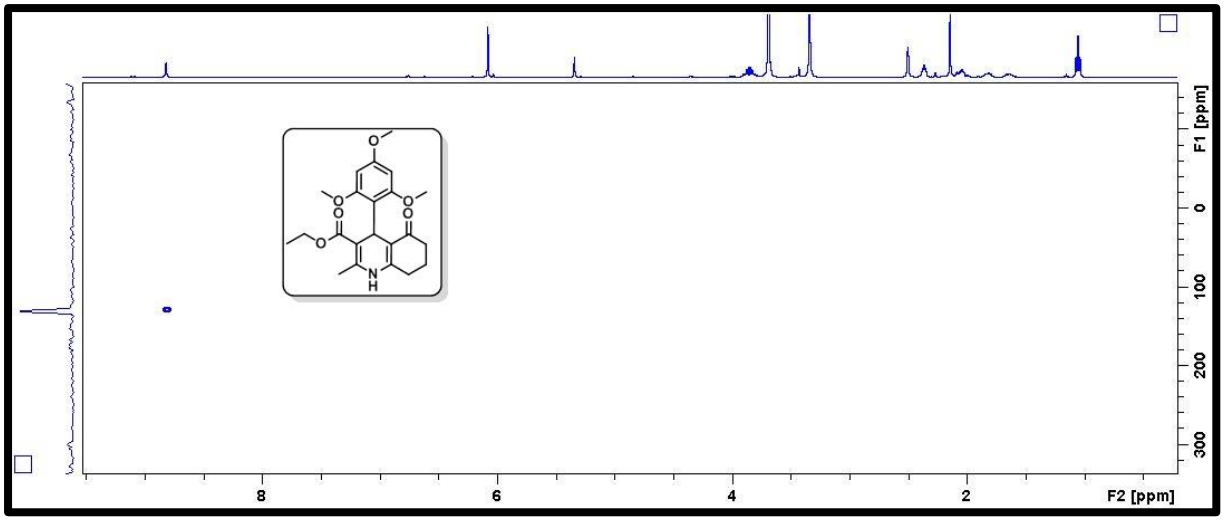

^{15}N NMR spectra of compound **5e** (40.55 MHz, DMSO)

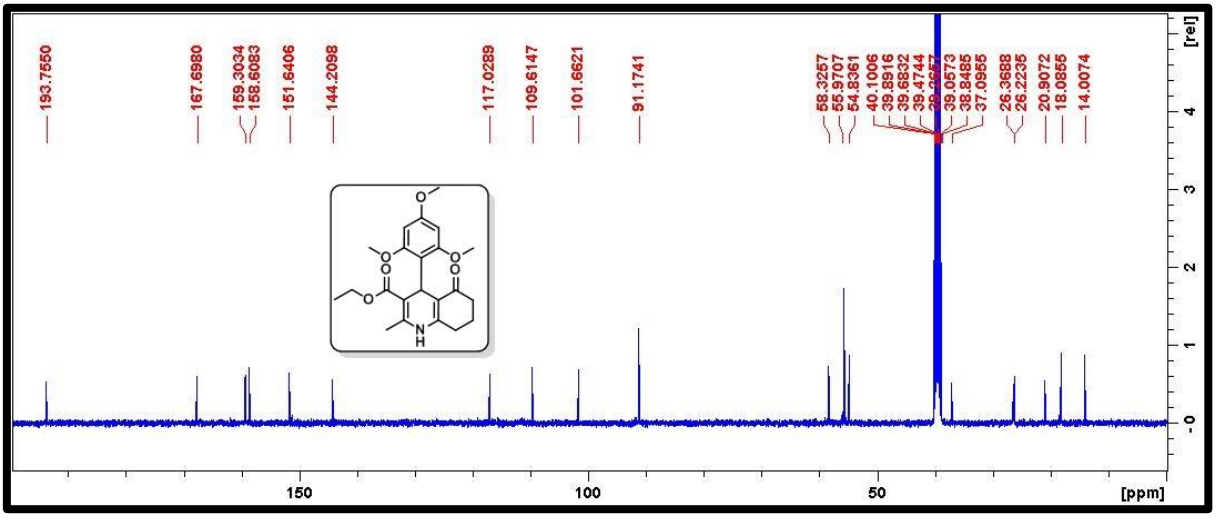

^{13}C NMR spectra of compound **5e** (100 MHz, DMSO)

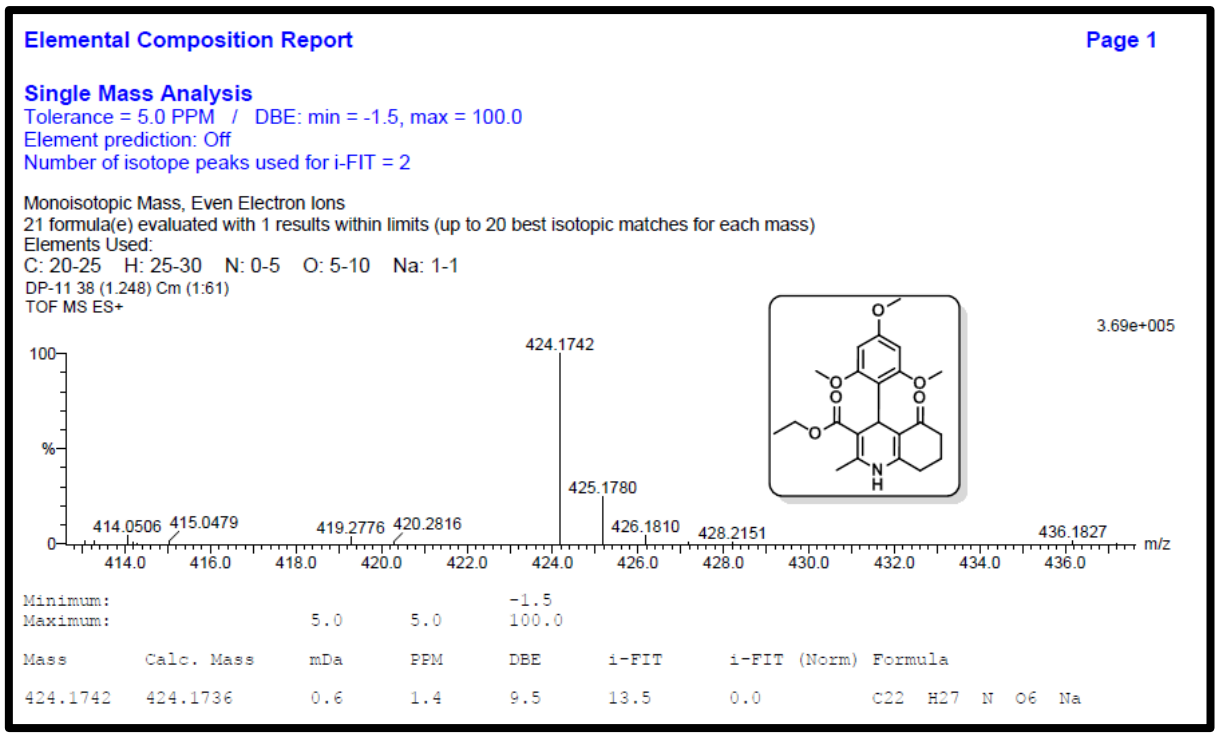

HRMS spectra of compound **5e**

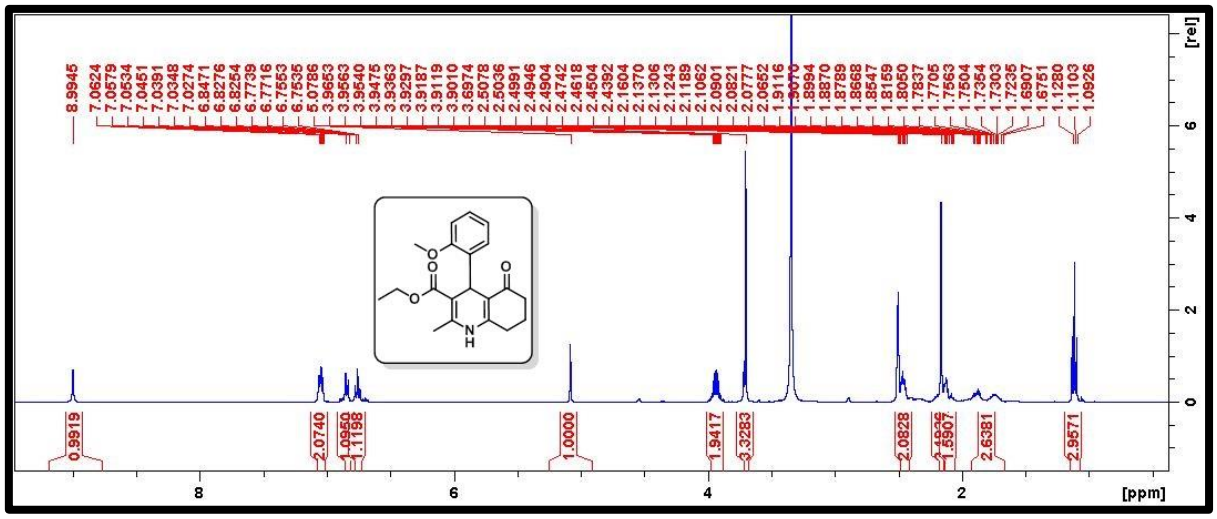

^{1}H NMR spectra of compound **5f** (400 MHz, DMSO)

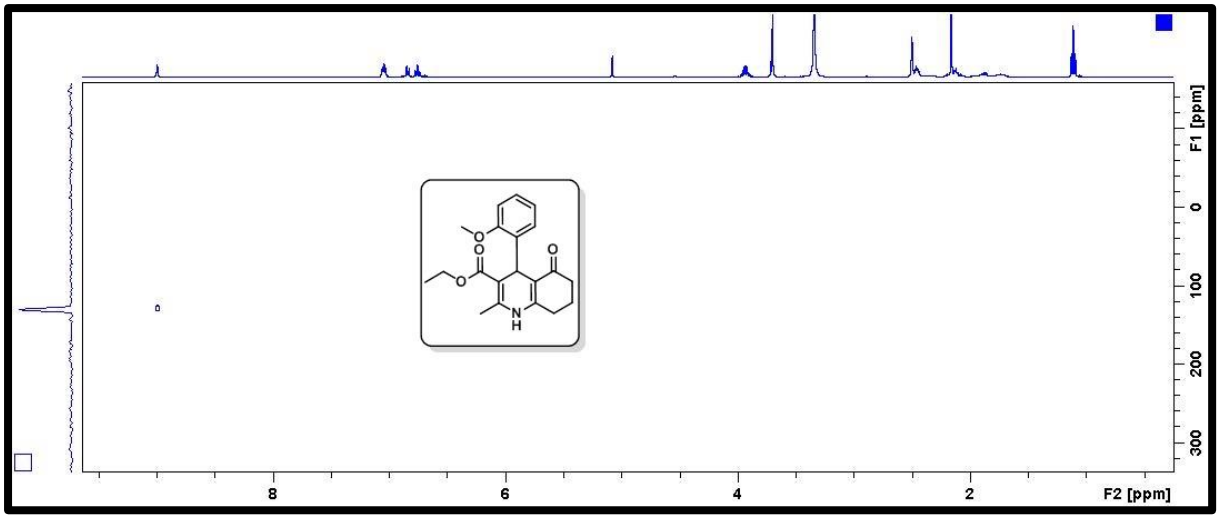

^{15}N NMR spectra of compound **5f** (40.55 MHz, DMSO)

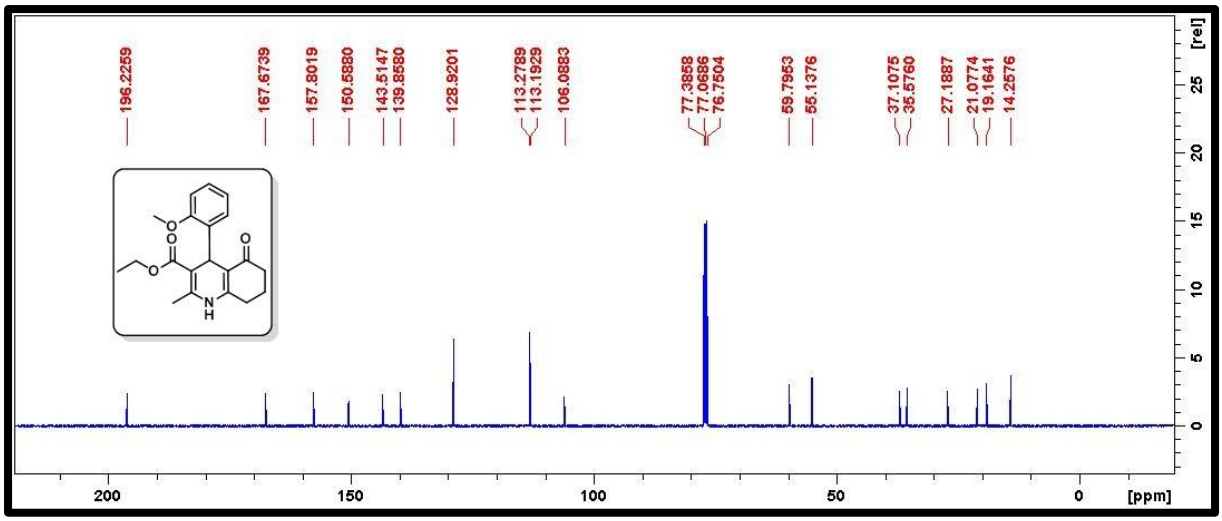

^{13}C NMR spectra of compound **5f** (100 MHz, $CDCl_3$)

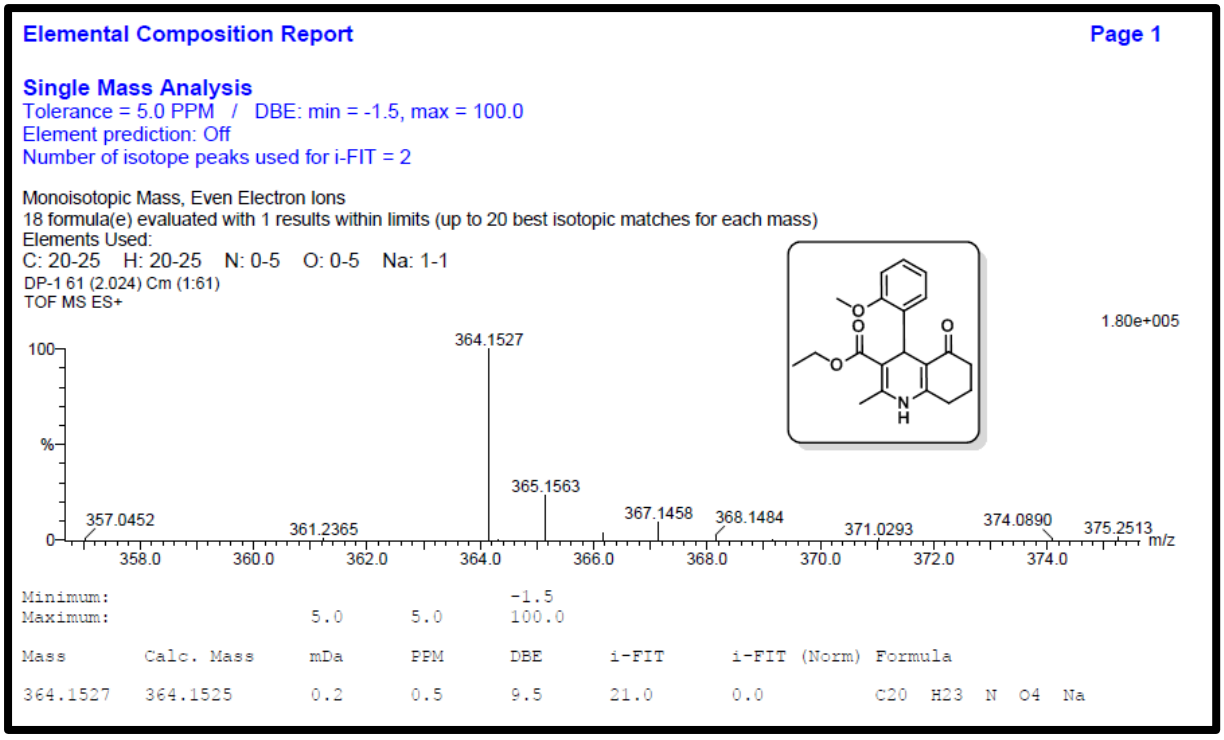

HRMS spectra of compound **5f**

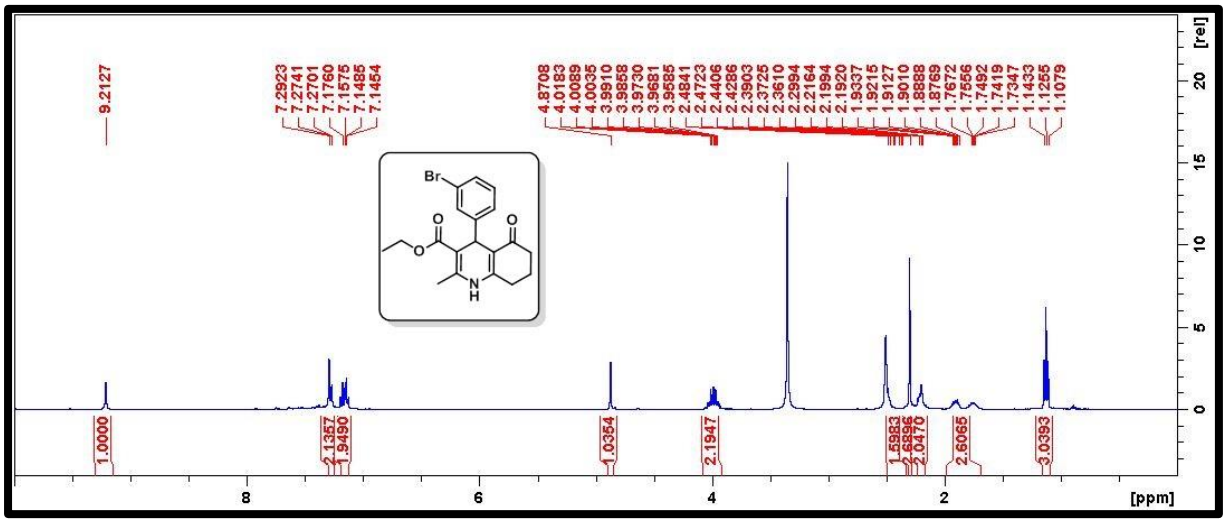

^{1}H NMR spectra of compound **5g** (400 MHz, DMSO)

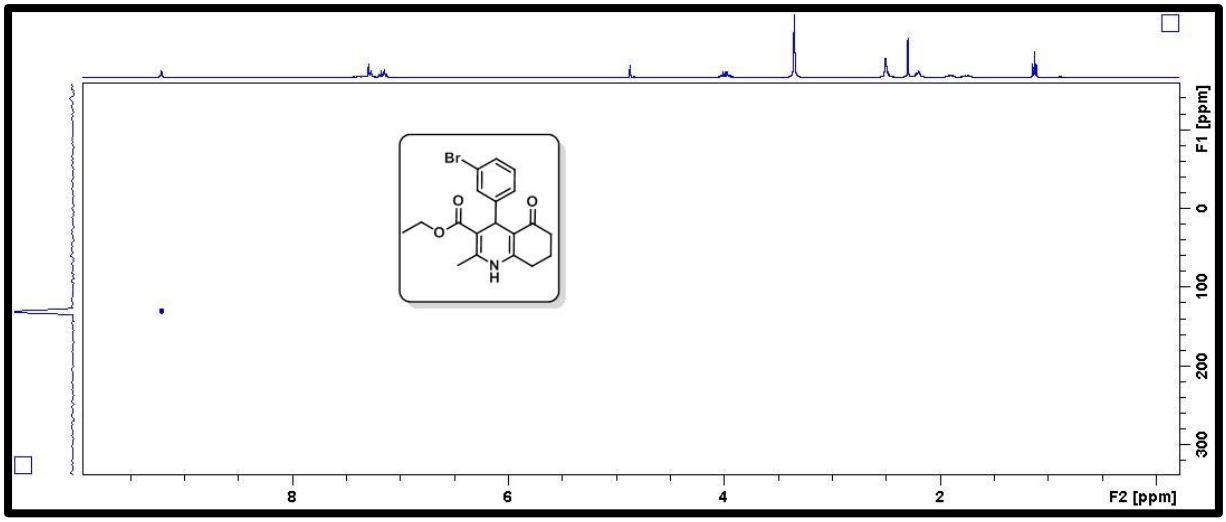

^{15}N NMR spectra of compound **5g** (40.55 MHz, DMSO)

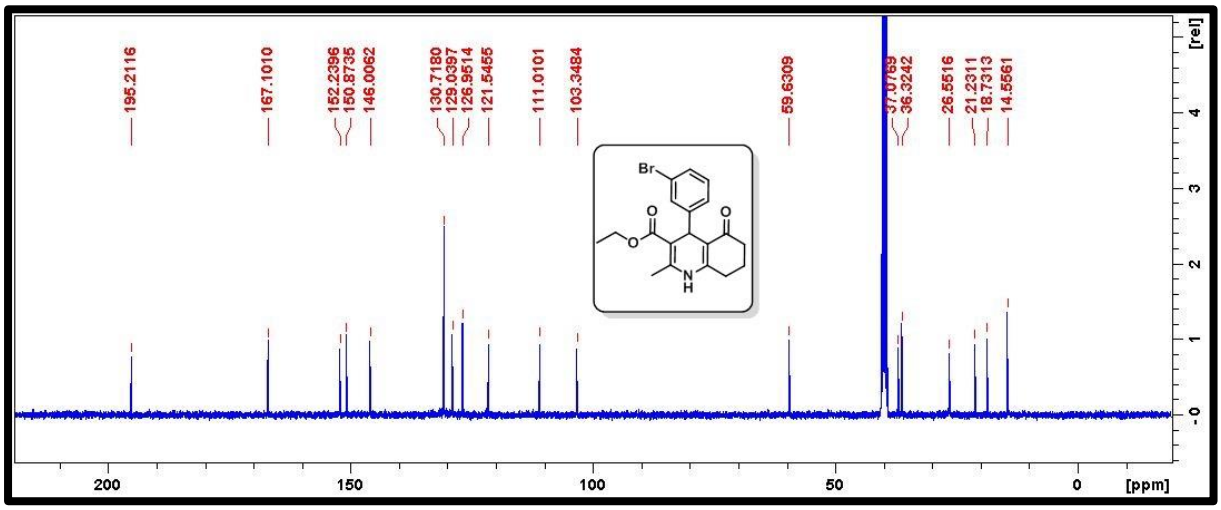

^{13}C NMR spectra of compound **5g** (100 MHz, DMSO)

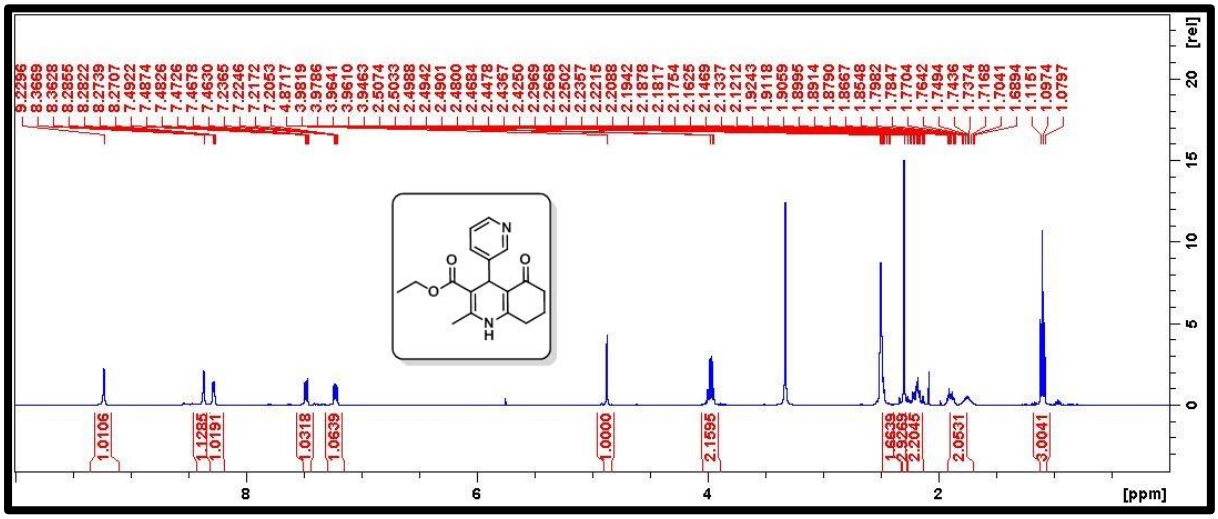

^{1}H NMR spectra of compound **5h** (400 MHz, DMSO)

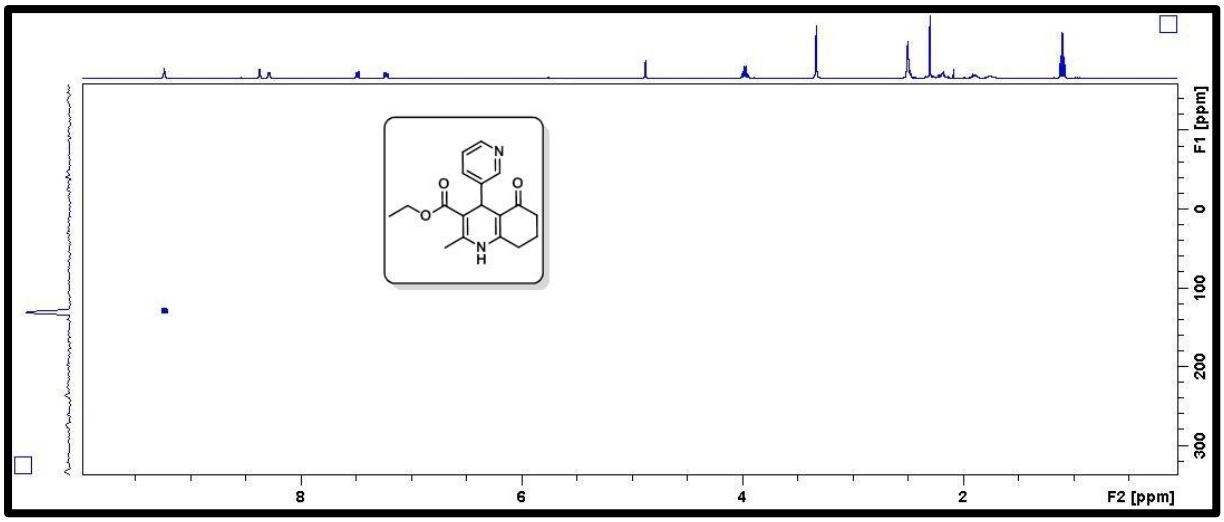

^{15}N NMR spectra of compound **5h** (40.55 MHz, DMSO)

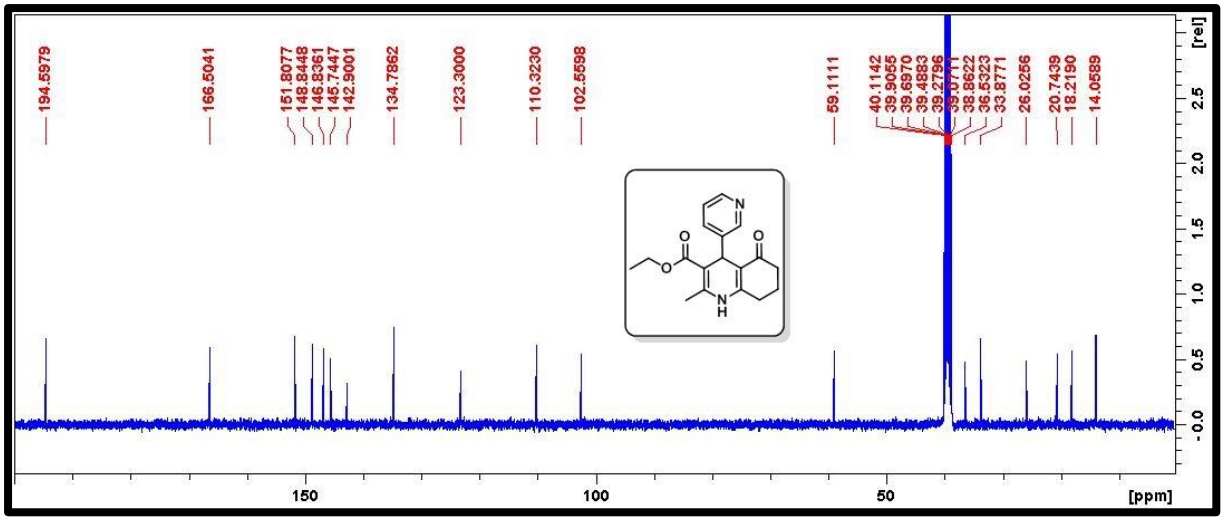

^{13}C NMR spectra of compound **5h** (100 MHz, DMSO)

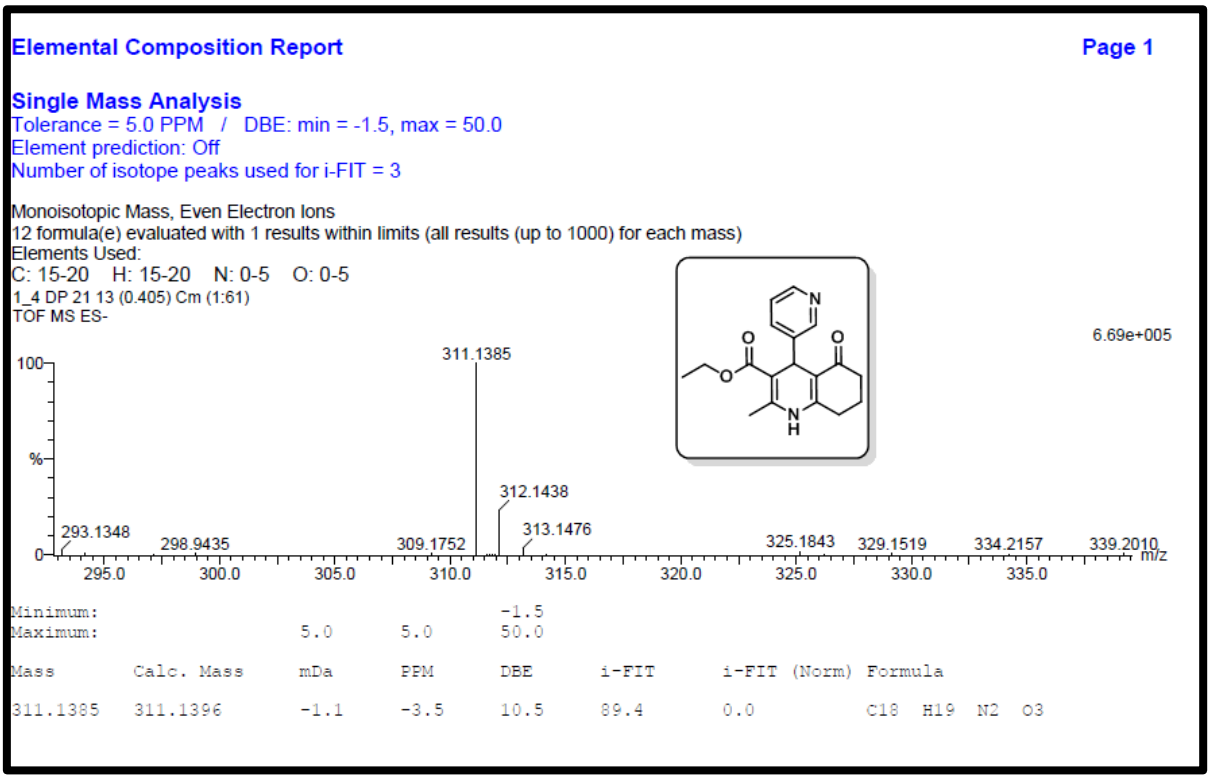

HRMS spectra of compound **5h**

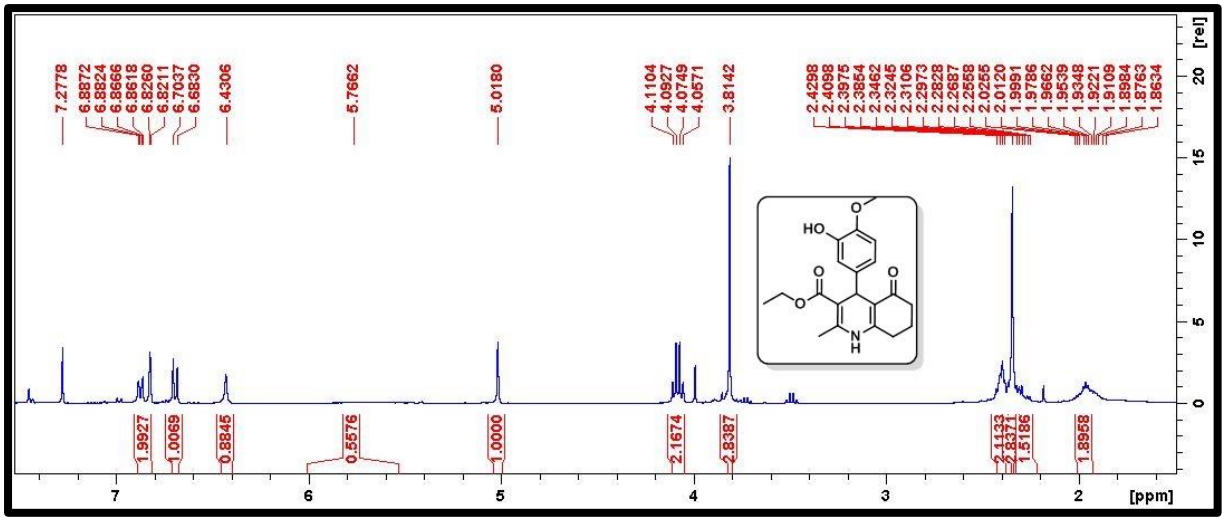

^{1}H NMR spectra of compound **5i** (400 MHz, $CDCl_3$)

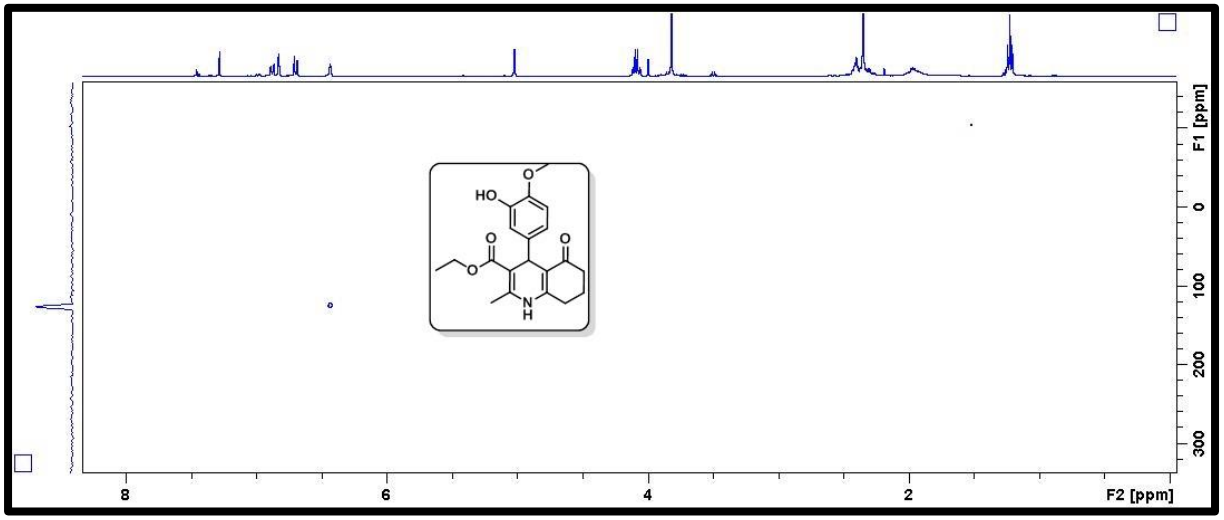

^{15}N NMR spectra of compound **5i** (40.55 MHz, $CDCl_3$)

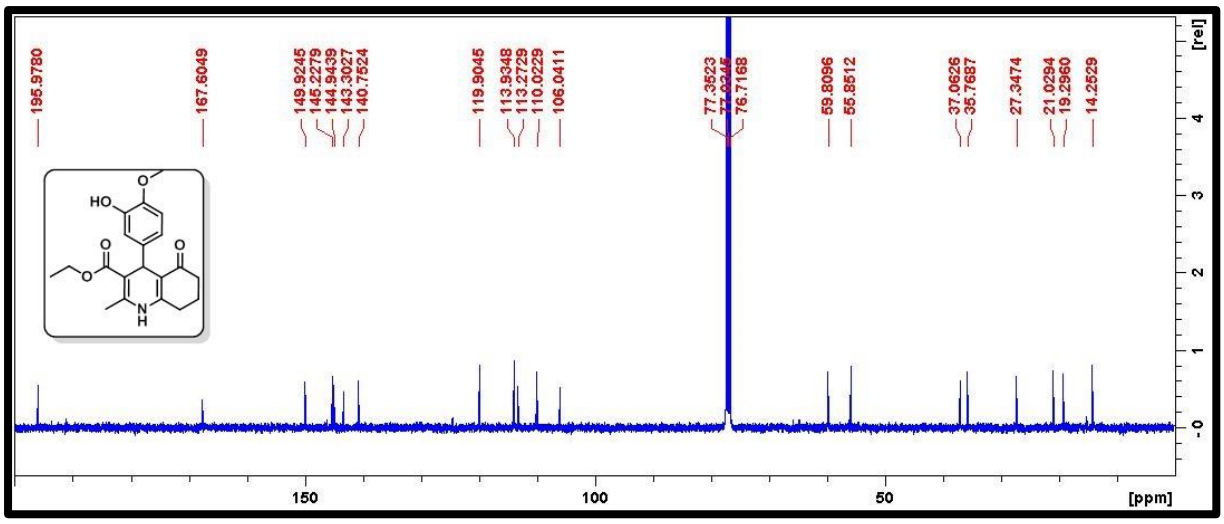

^{13}C NMR spectra of compound **5i** (100 MHz, $CDCl_3$)

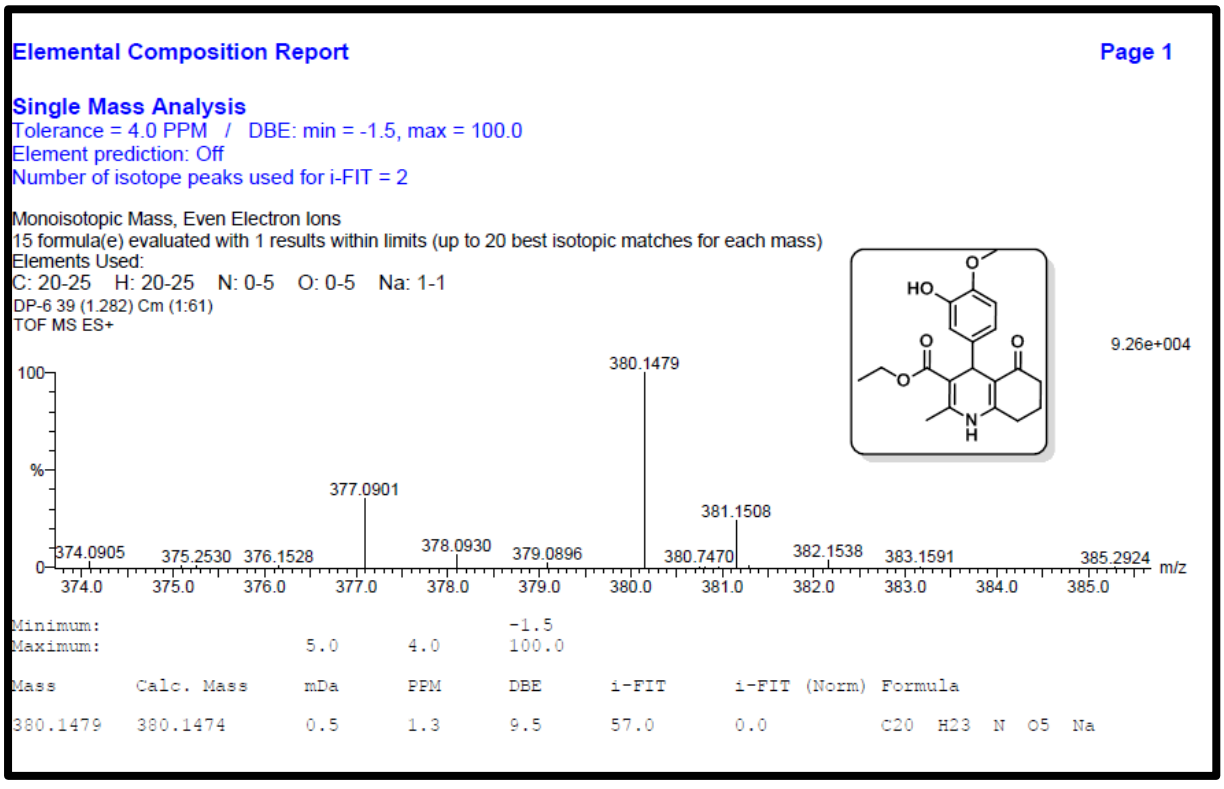

HRMS spectra of compound **5i**

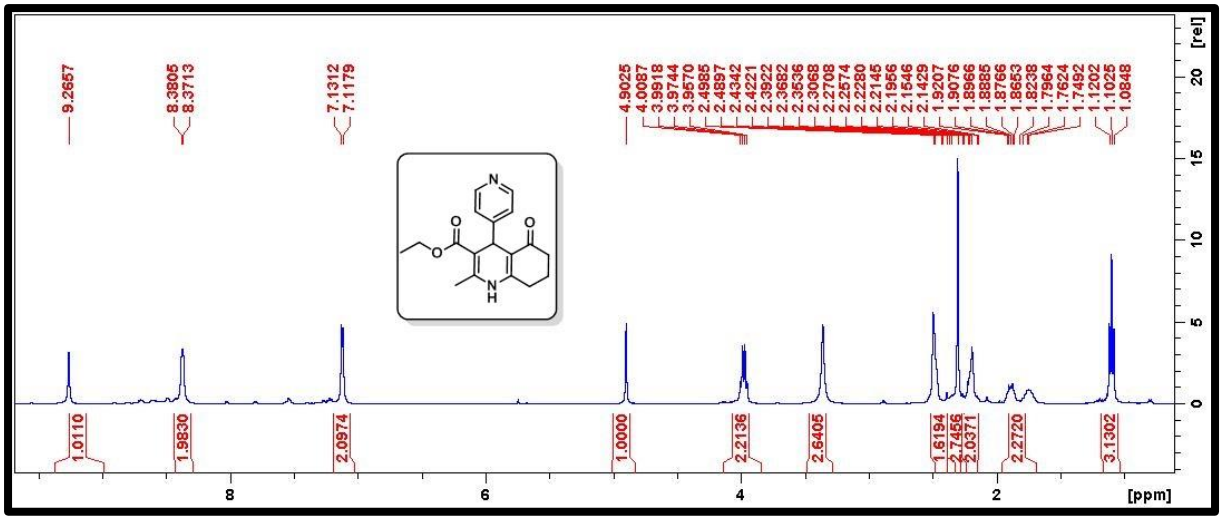

^{1}H NMR spectra of compound **5j** (400 MHz, DMSO)

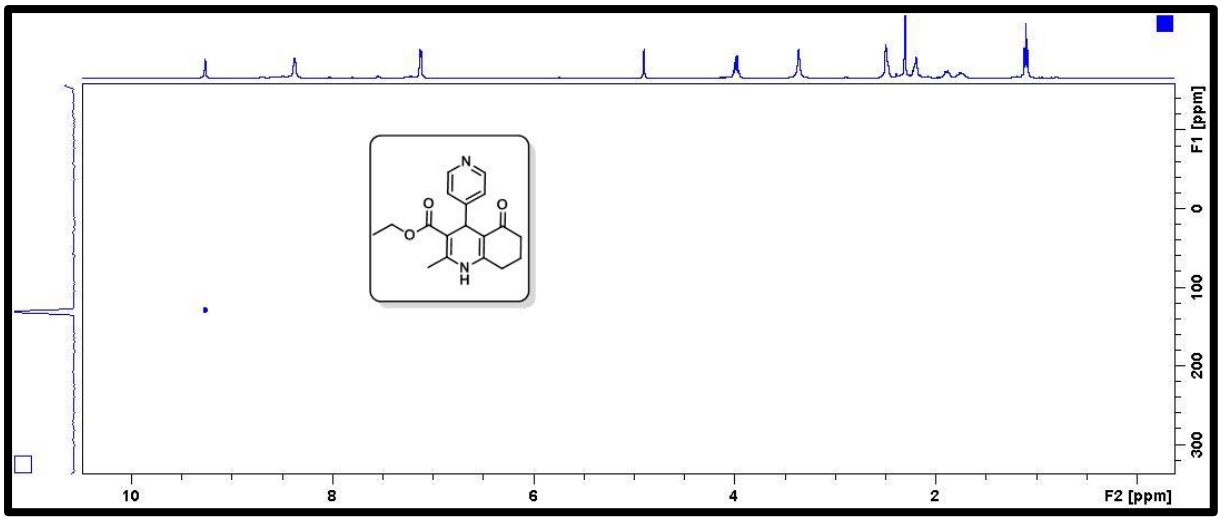

^{15}N NMR spectra of compound **5j** (40.55 MHz, DMSO)

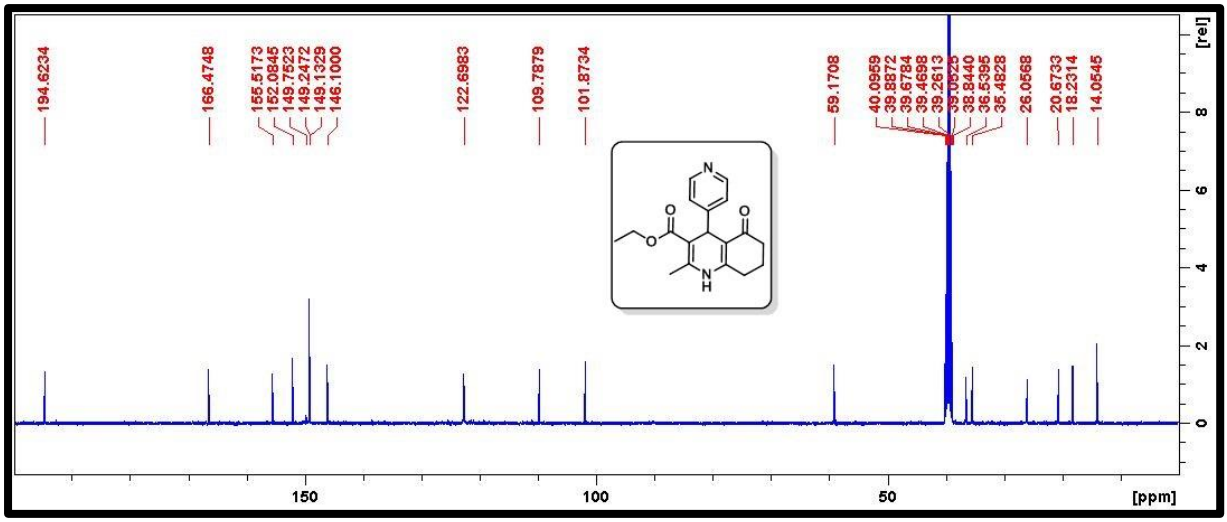

^{13}C NMR spectra of compound **5j** (100 MHz, DMSO)

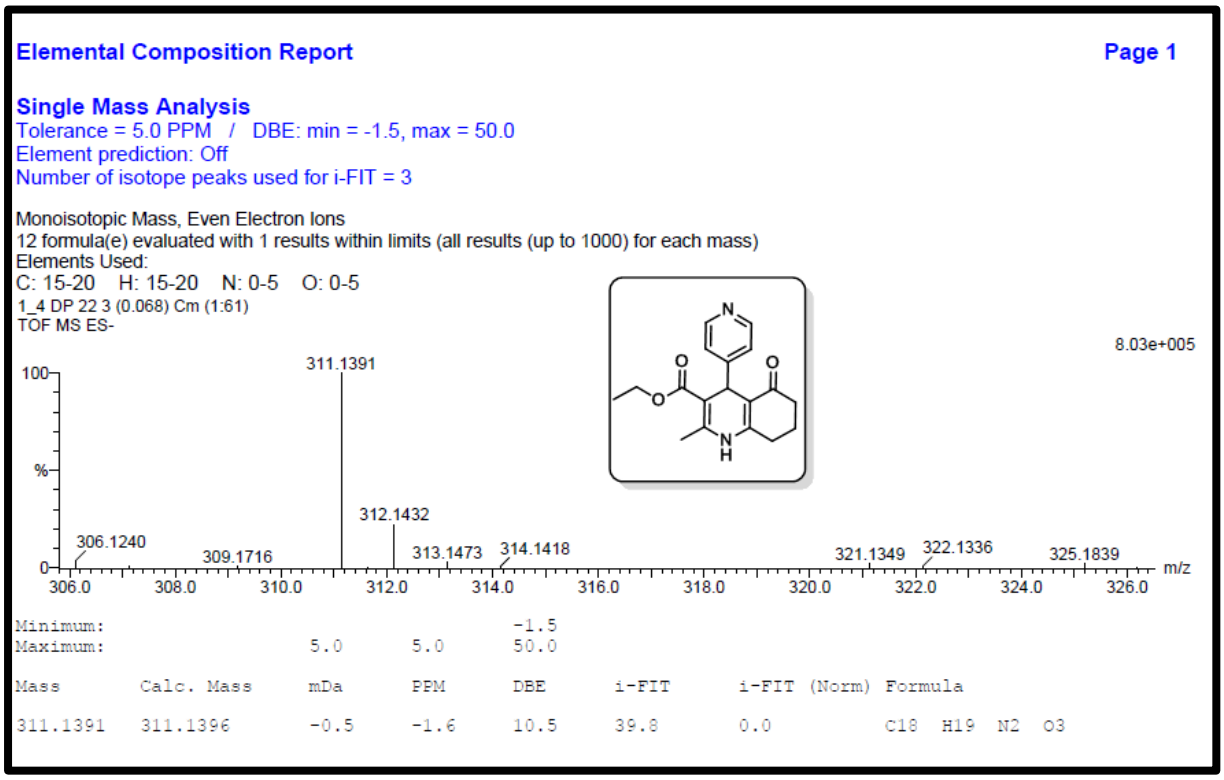

HRMS spectra of compound **5j**

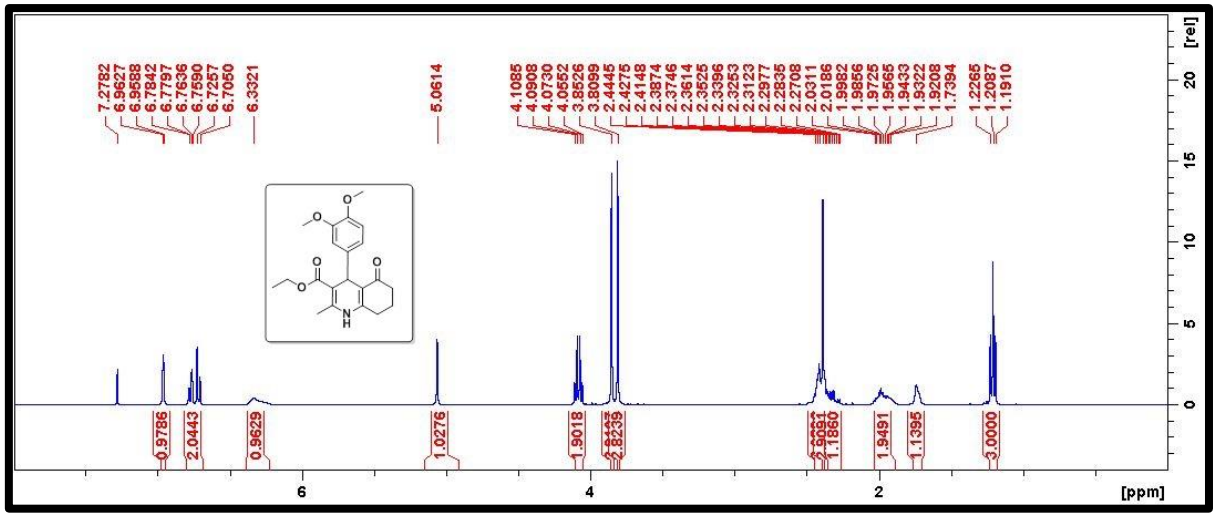

^{1}H NMR spectra of compound **5k** (400 MHz, $CDCl_3$)

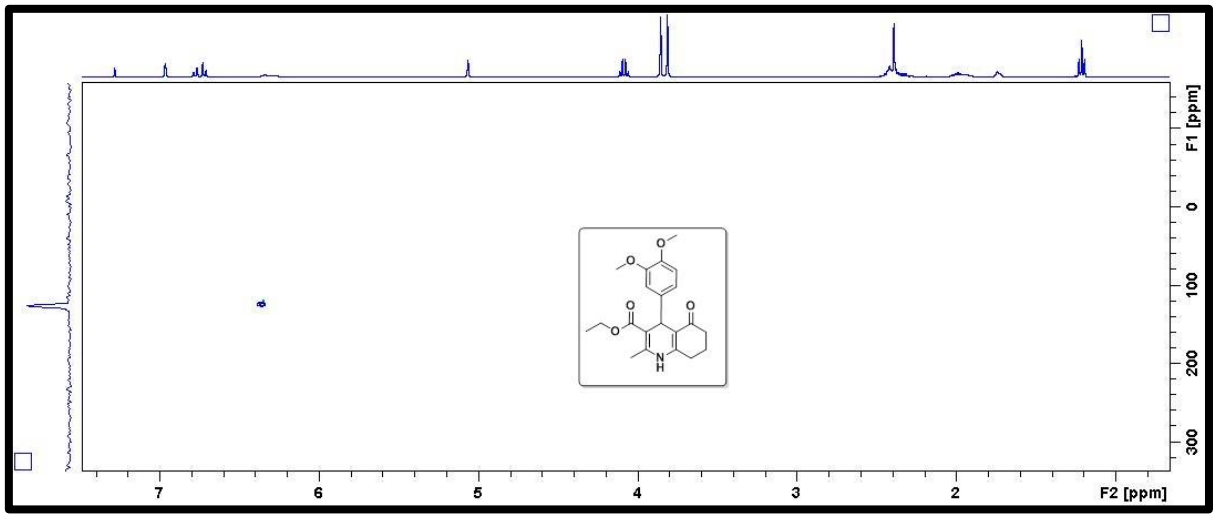

^{15}N NMR spectra of compound **5k** (40.55 MHz, $CDCl_3$)

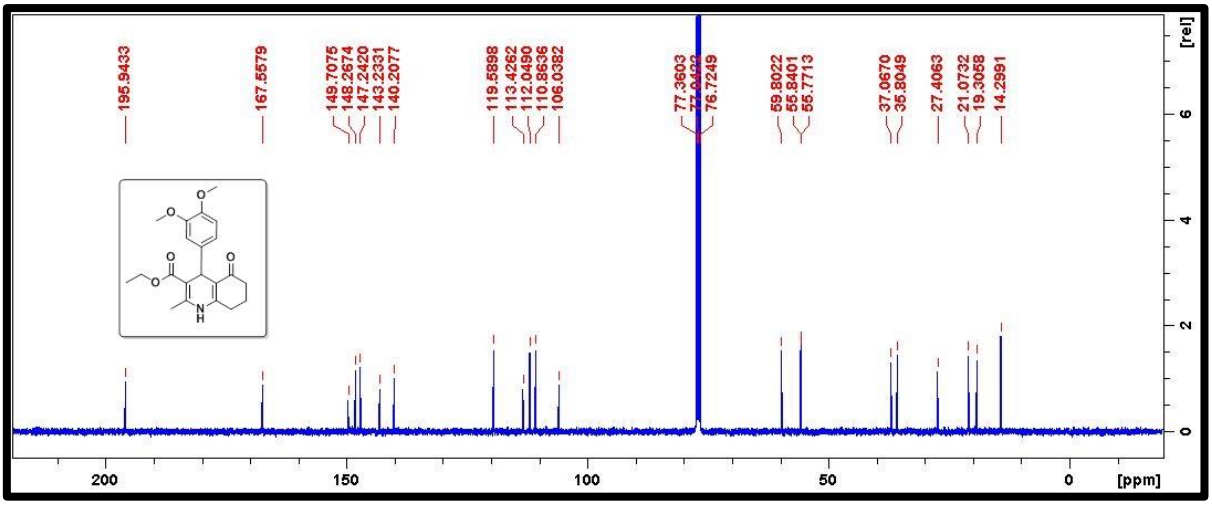

^{13}C NMR spectra of compound **5k** (100 MHz, $CDCl_3$)

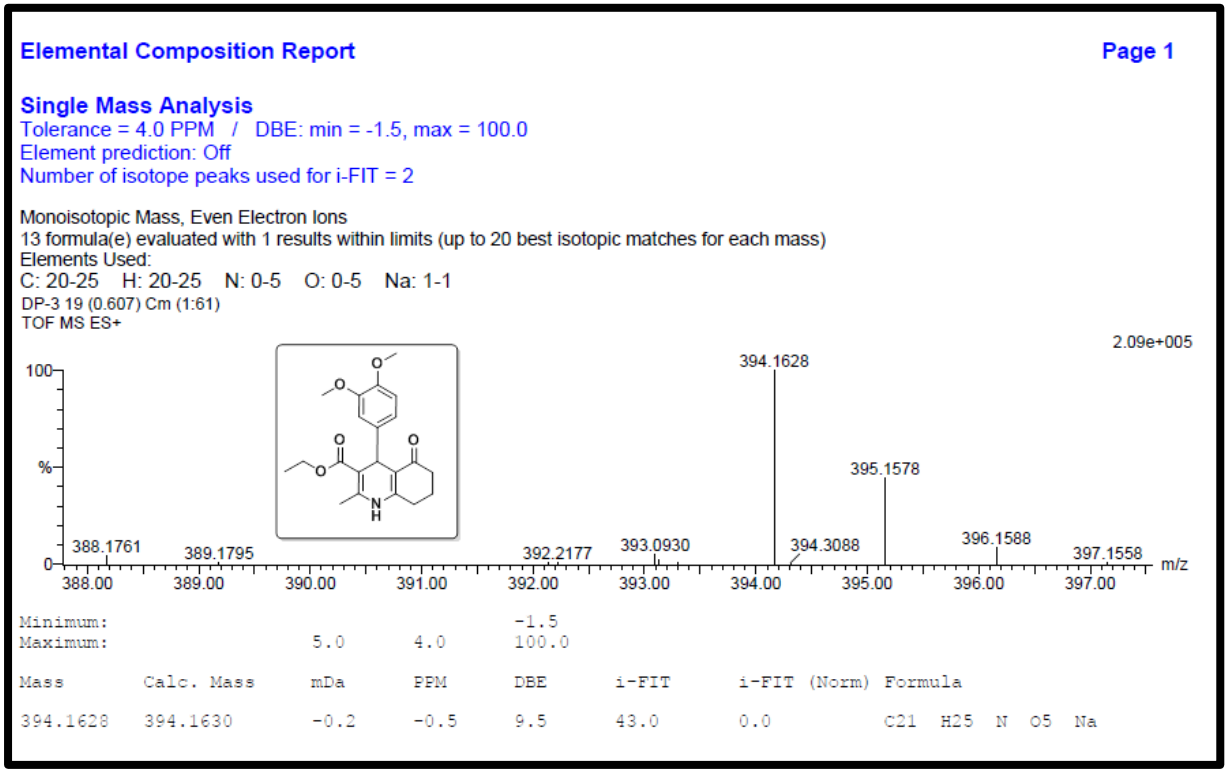

HRMS spectra of compound **5k**

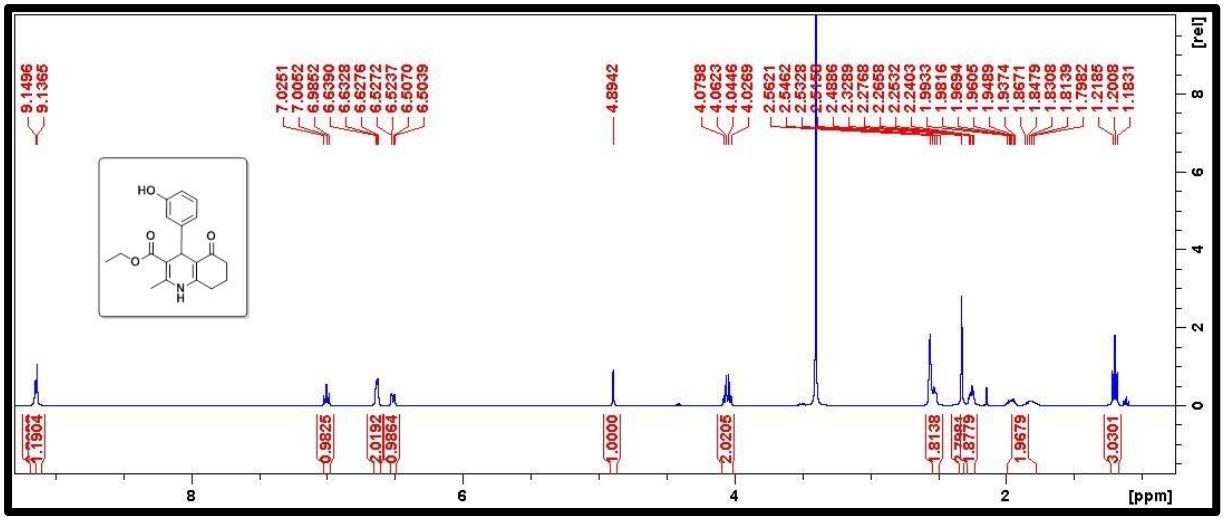

^{1}H NMR spectra of compound **5l** (400 MHz, DMSO)

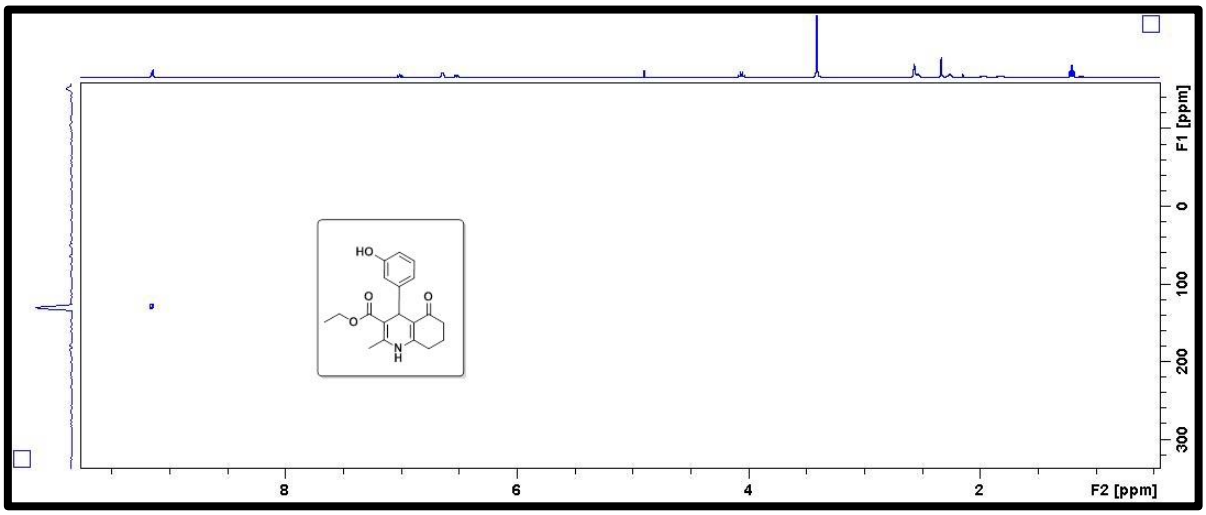

^{15}N NMR spectra of compound **5l** (40.55 MHz, DMSO)

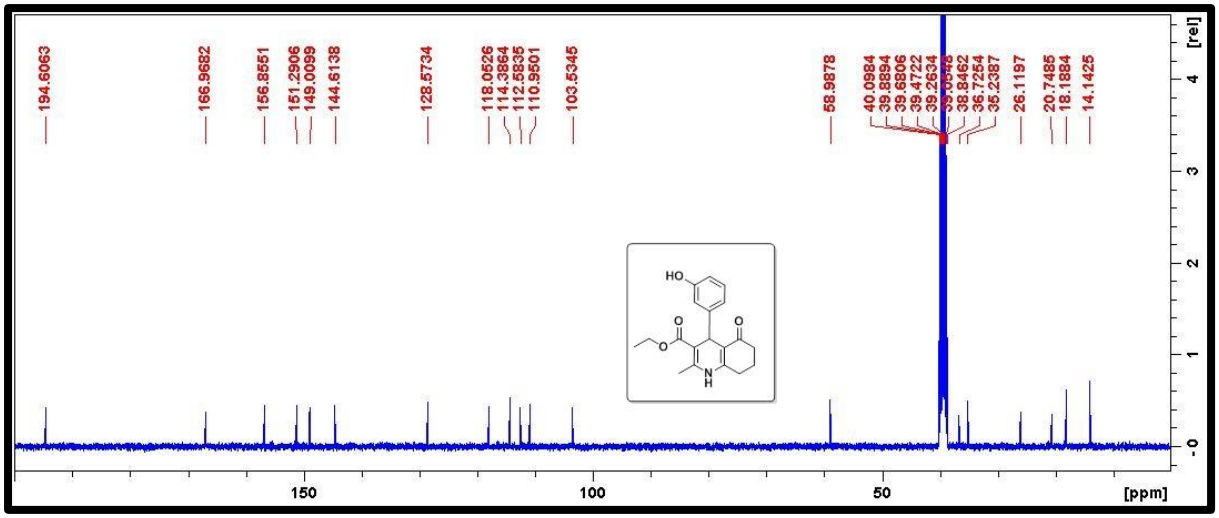

^{13}C NMR spectra of compound **5l** (100 MHz, DMSO)

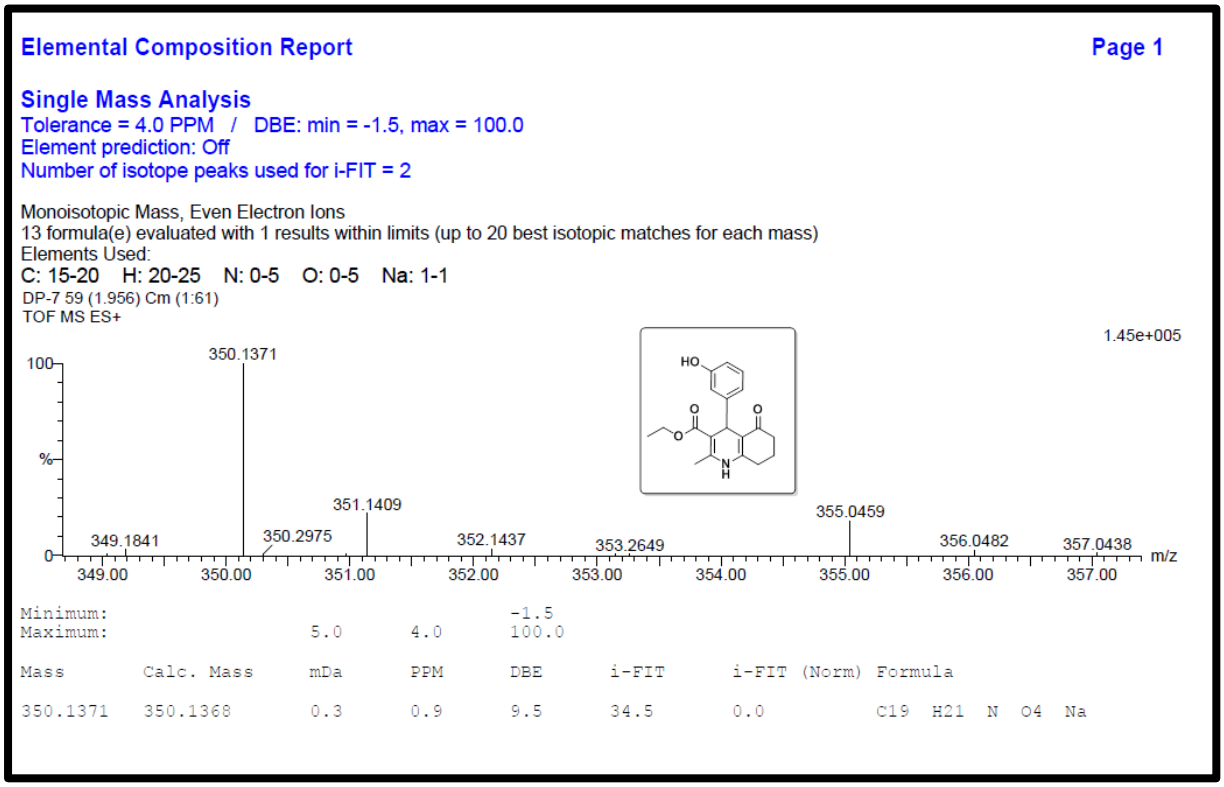

HRMS spectra of compound **5l**

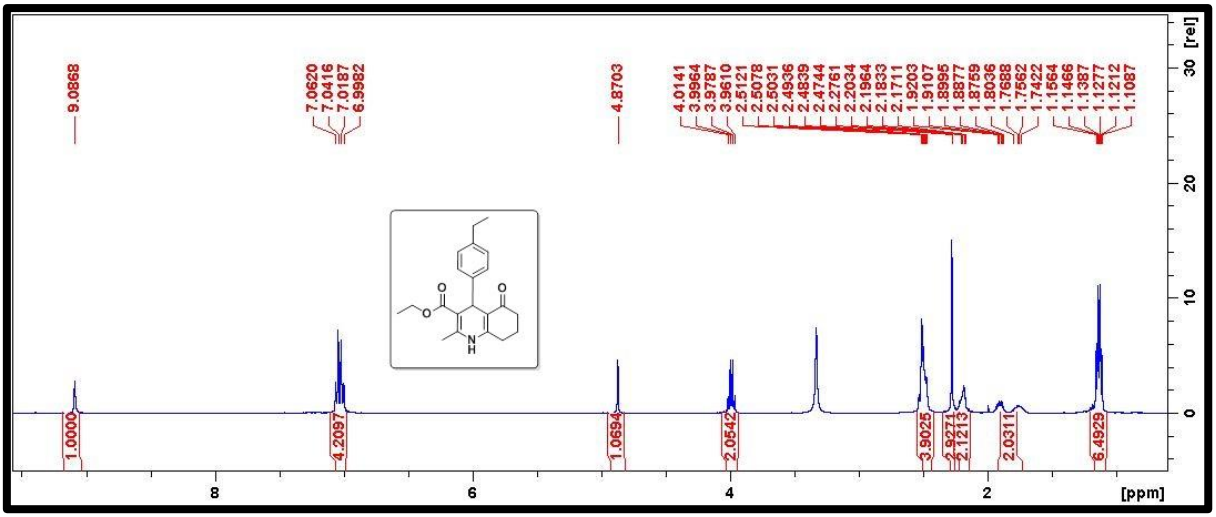

^{1}H NMR spectra of compound **5m** (400 MHz, DMSO)

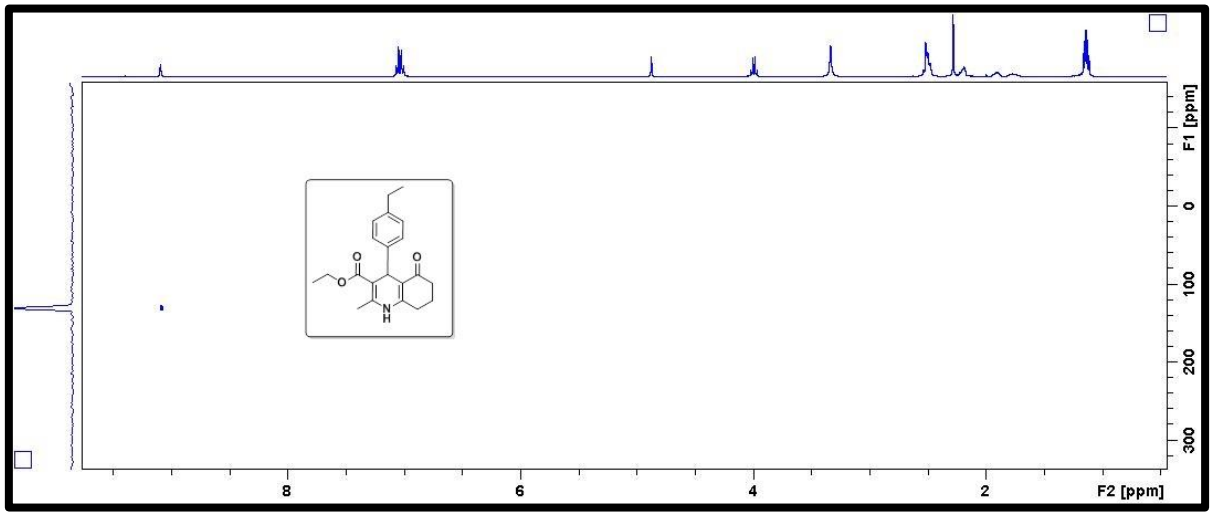

^{15}N NMR spectra of compound **5m** (40.55 MHz, DMSO)

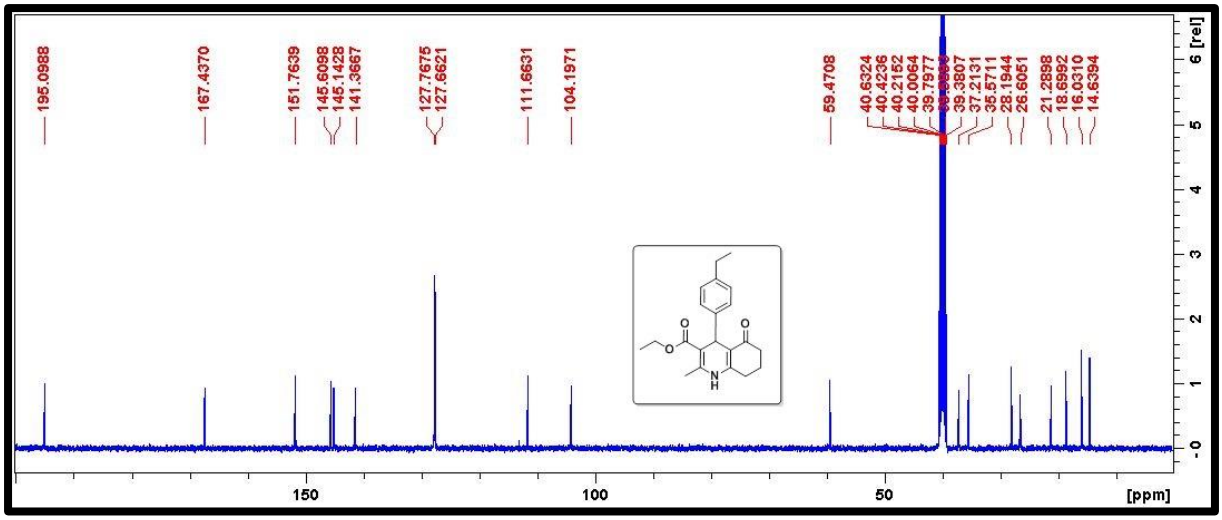

^{13}C NMR spectra of compound **5m** (100 MHz, DMSO)

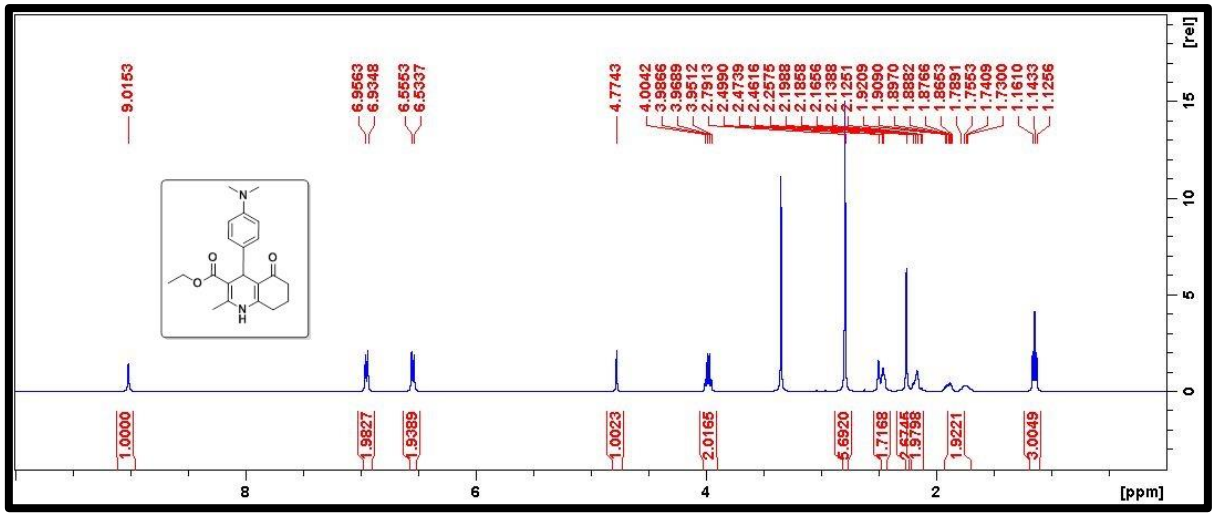

^{1}H NMR spectra of compound **5n** (400 MHz, DMSO)

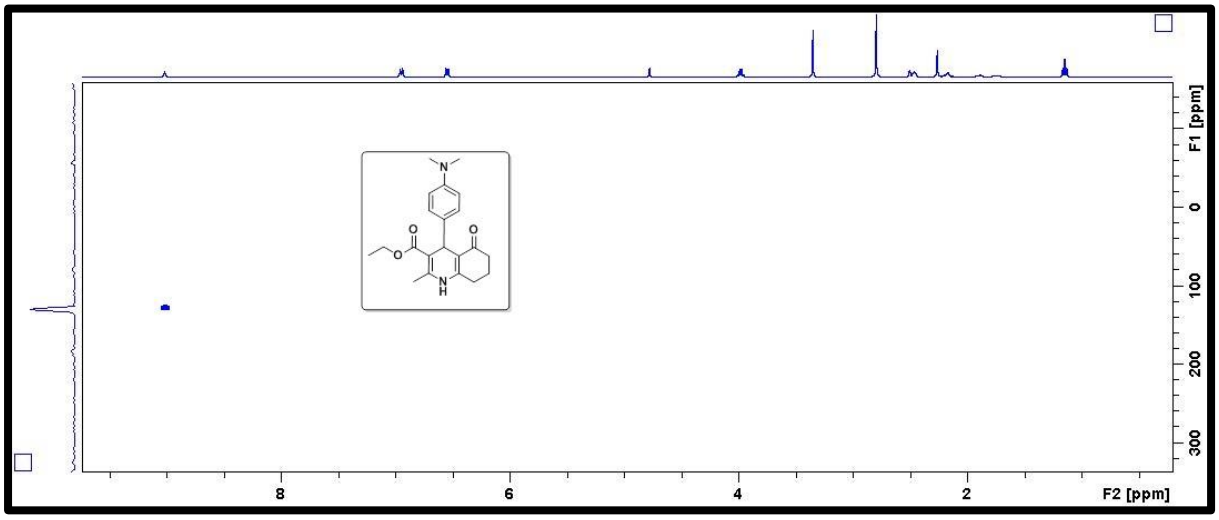

^{15}N NMR spectra of compound **5n** (40.55 MHz, DMSO)

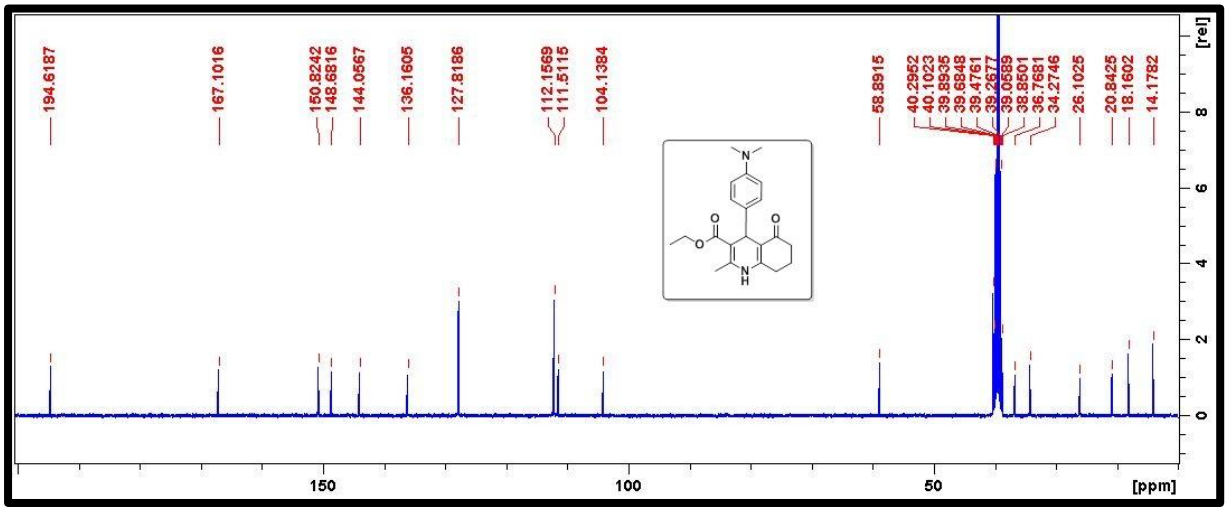

^{13}C NMR spectra of compound **5n** (100 MHz, DMSO)

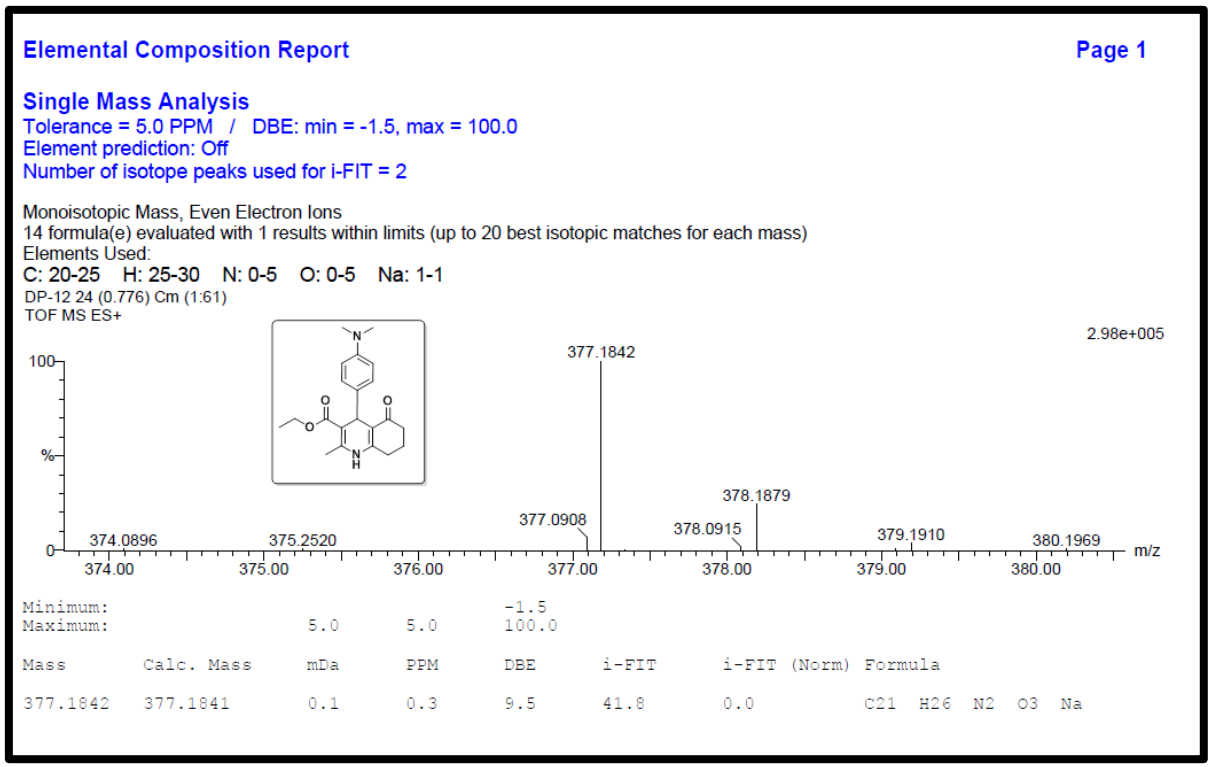

HRMS spectra of compound **5n**

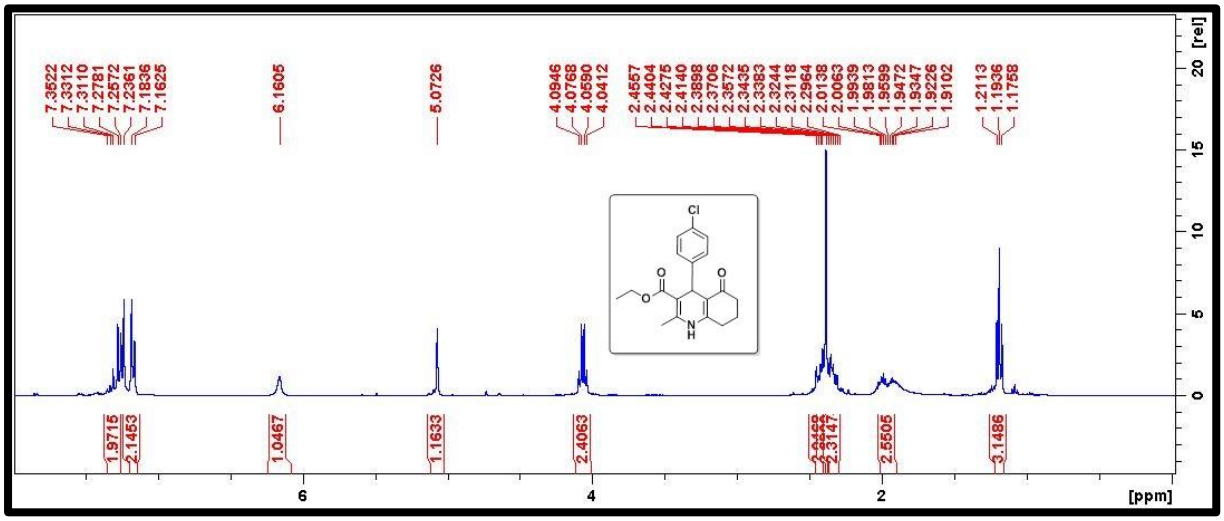

^{1}H NMR spectra of compound **5o** (400 MHz, $CDCl_3$)

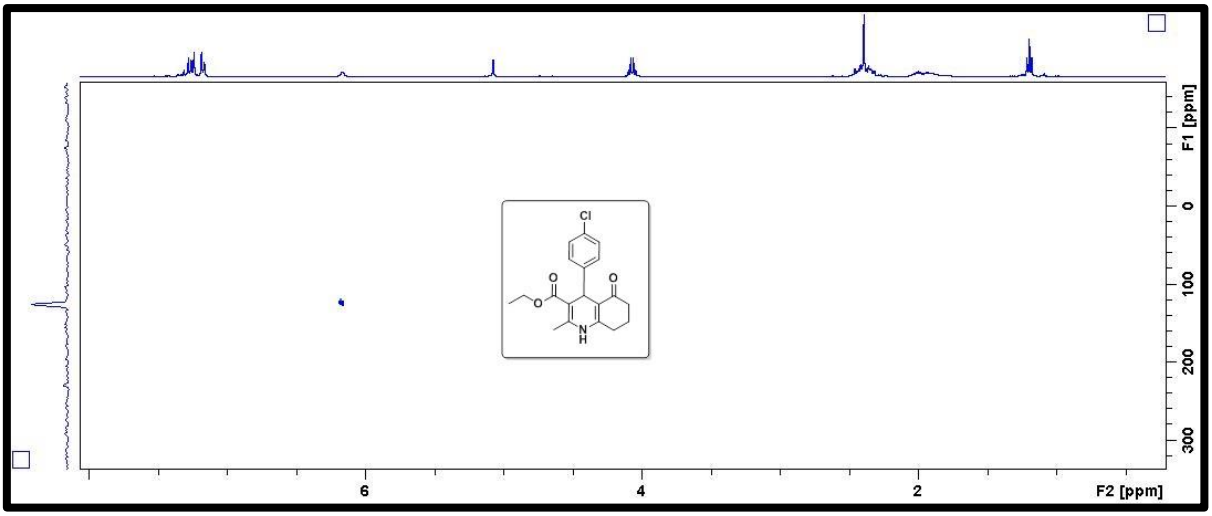

^{15}N NMR spectra of compound **5o** (40.55 MHz, $CDCl_3$)

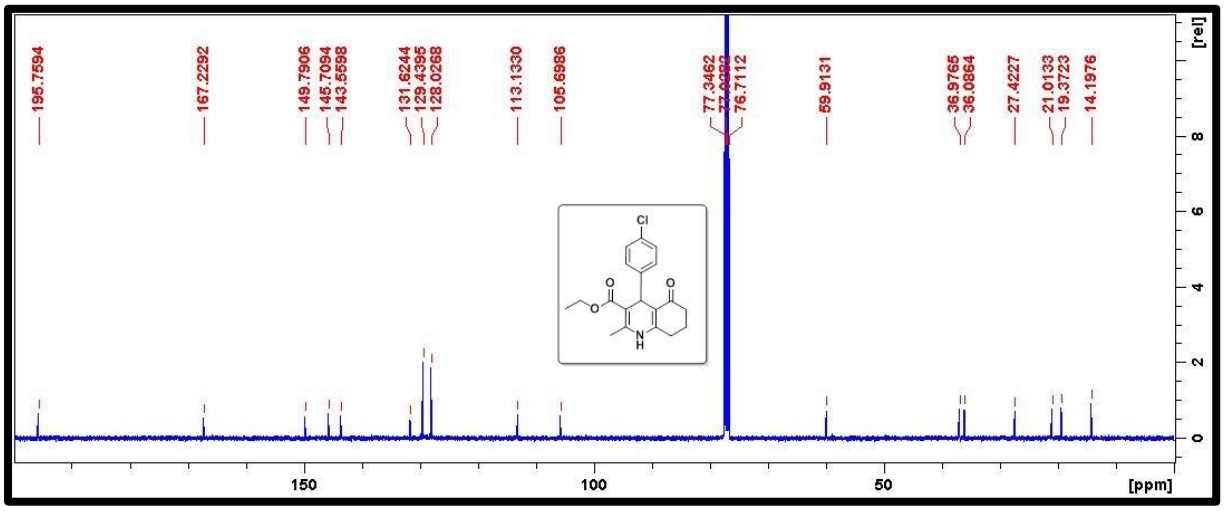

^{13}C NMR spectra of compound **5o** (100 MHz, $CDCl_3$)

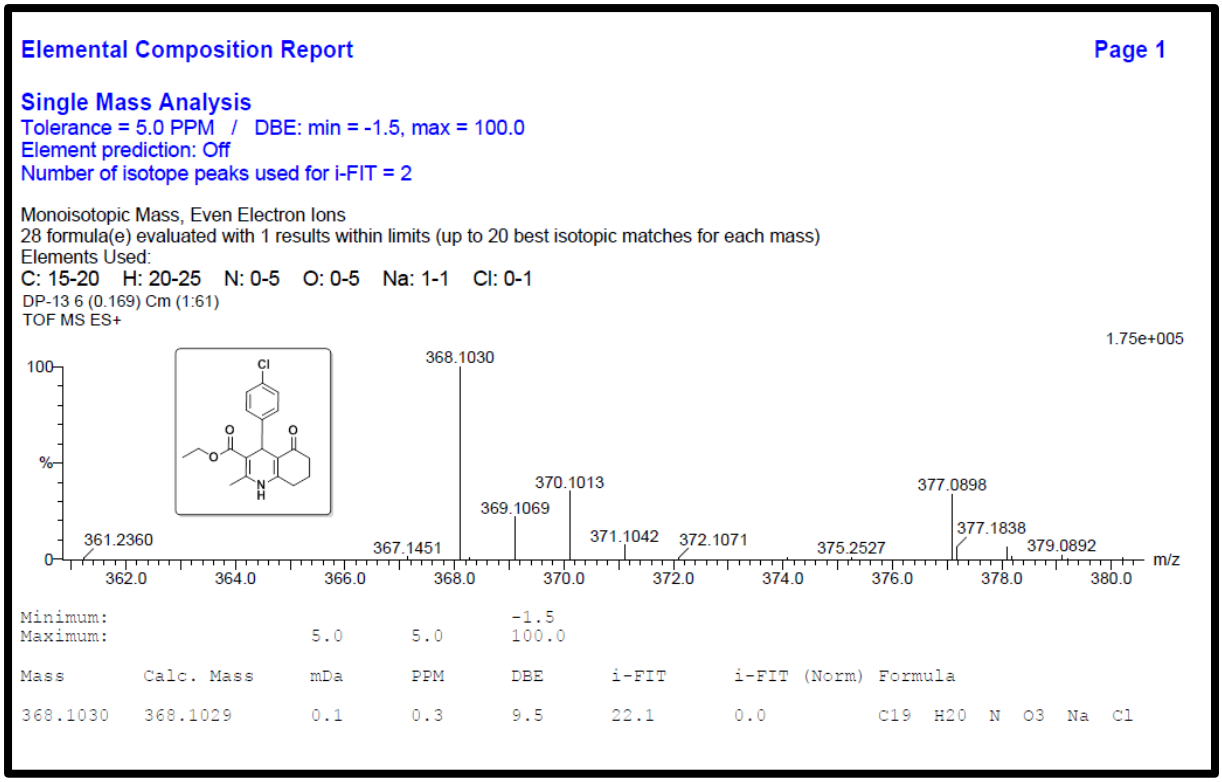

Elemental Composition Report Page 1

Single Mass Analysis
Tolerance = 5.0 PPM / DBE: min = -1.5, max = 100.0
Element prediction: Off
Number of isotope peaks used for i-FIT = 2

Monoisotopic Mass, Even Electron Ions
28 formula(e) evaluated with 1 results within limits (up to 20 best isotopic matches for each mass)
Elements Used:
C: 15-20 H: 20-25 N: 0-5 O: 0-5 Na: 1-1 Cl: 0-1
DP-13 6 (0.169) Cm (1:61)
TOF MS ES+

1.75e+005

Minimum:				-1.5			
Maximum:		5.0	5.0	100.0			
Mass	Calc. Mass	mDa	PPM	DBE	i-FIT	i-FIT (Norm)	Formula
368.1030	368.1029	0.1	0.3	9.5	22.1	0.0	C19 H20 N O3 Na Cl

HRMS spectra of compound **5o**

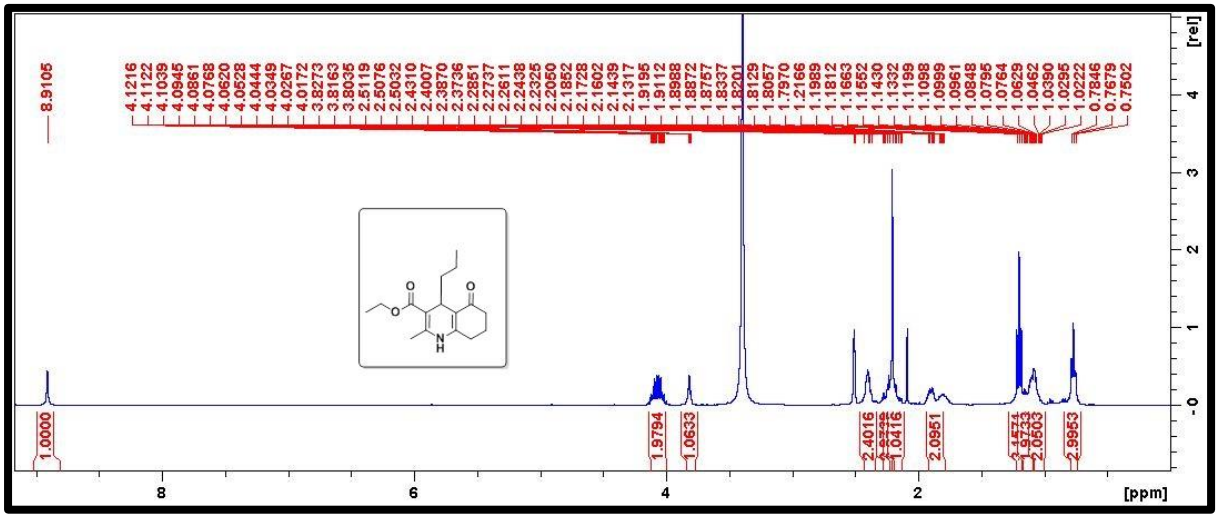

^{1}H NMR spectra of compound **5p** (400 MHz, DMSO)

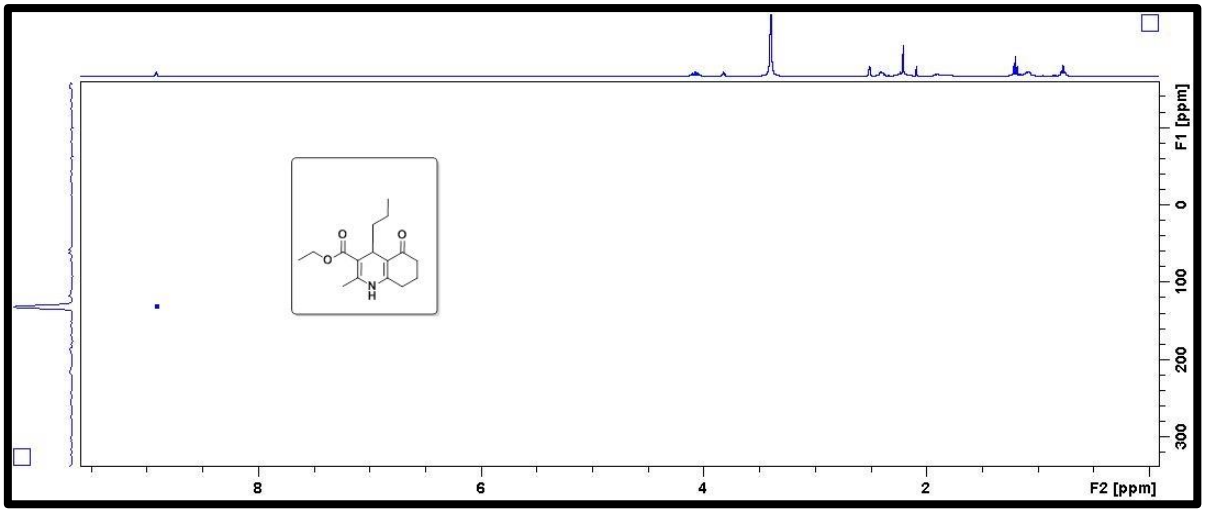

^{15}N NMR spectra of compound **5p** (40.55 MHz, DMSO)

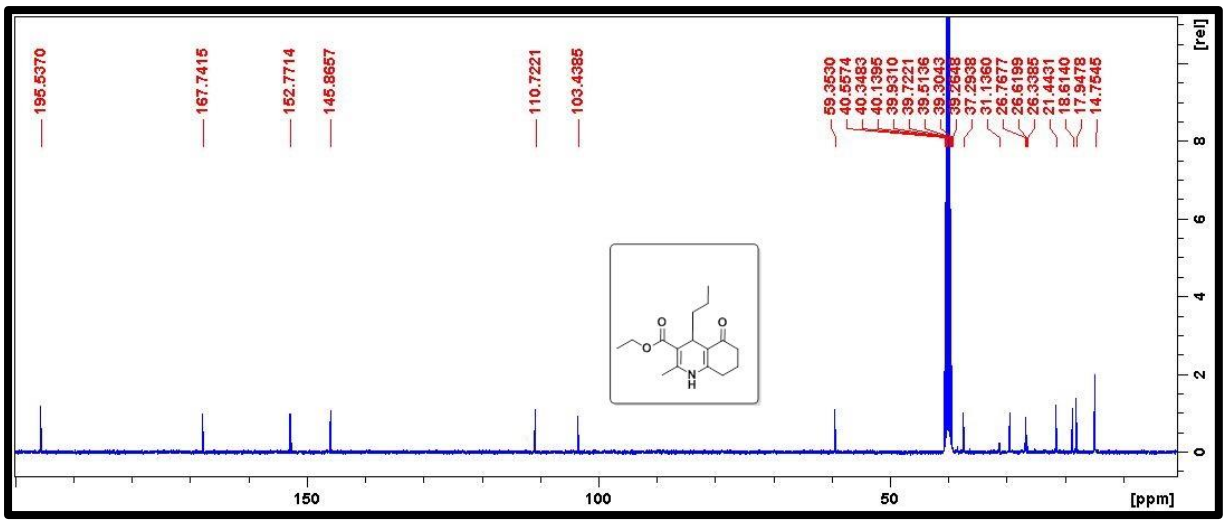

^{15}N NMR spectra of compound **5p** (100 MHz, DMSO)

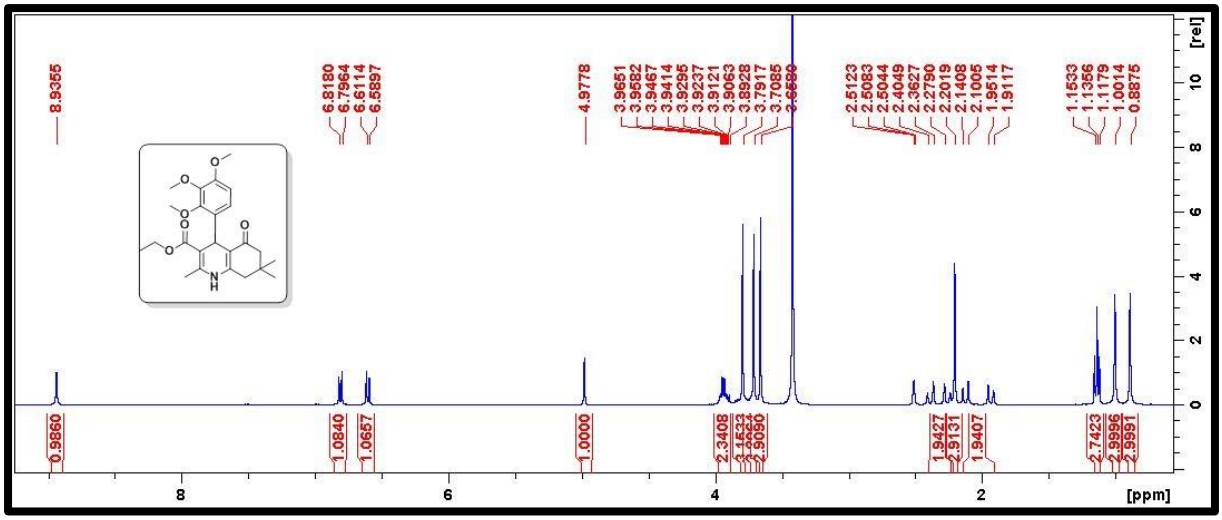

^{1}H NMR spectra of compound **5q** (400 MHz, DMSO)

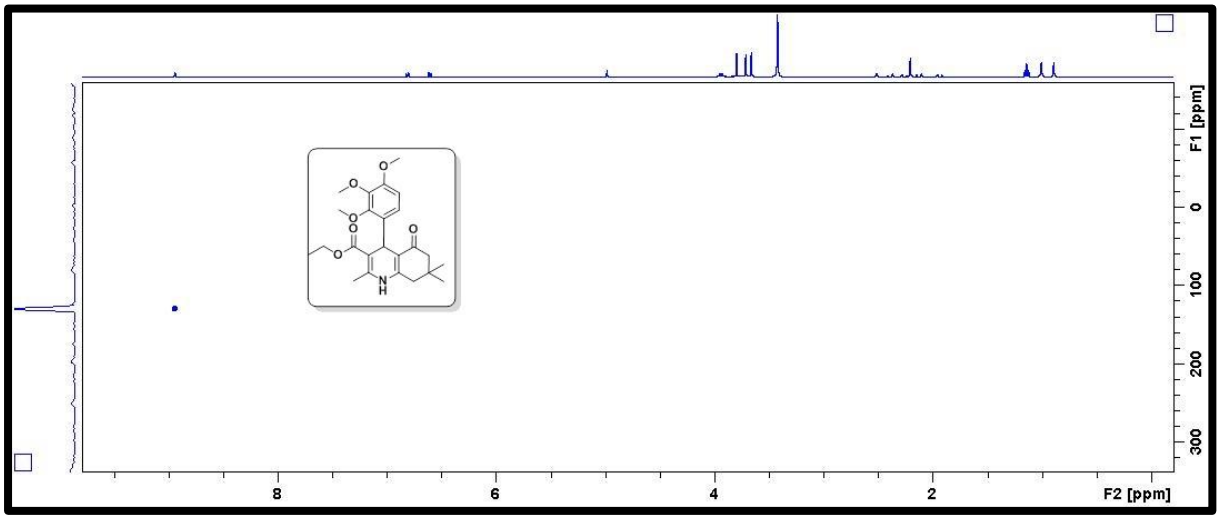

^{15}N NMR spectra of compound **5q** (40.55 MHz, DMSO)

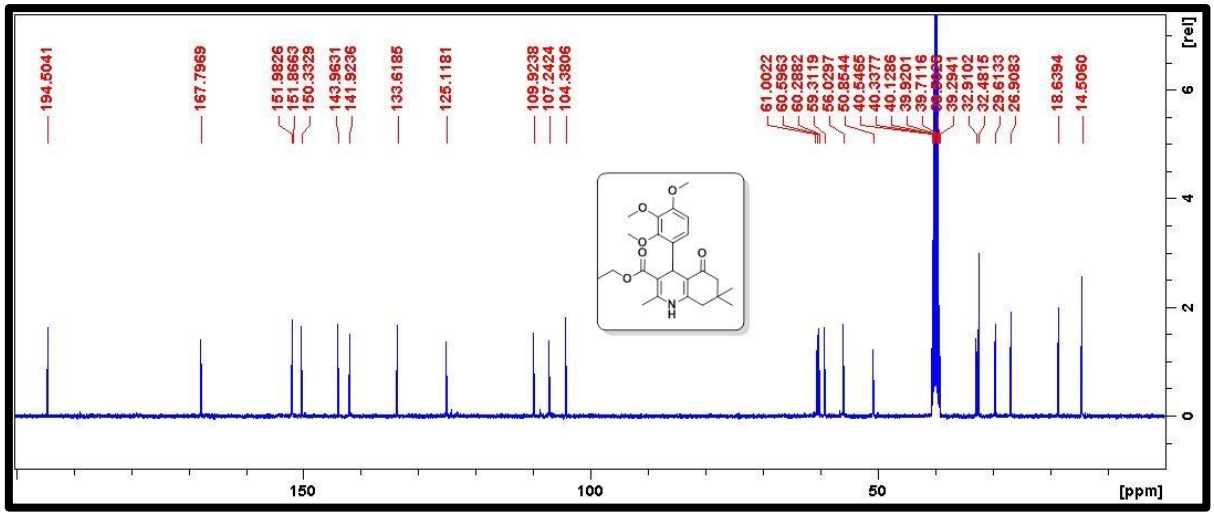

^{13}C NMR spectra of compound **5q** (100 MHz, DMSO)

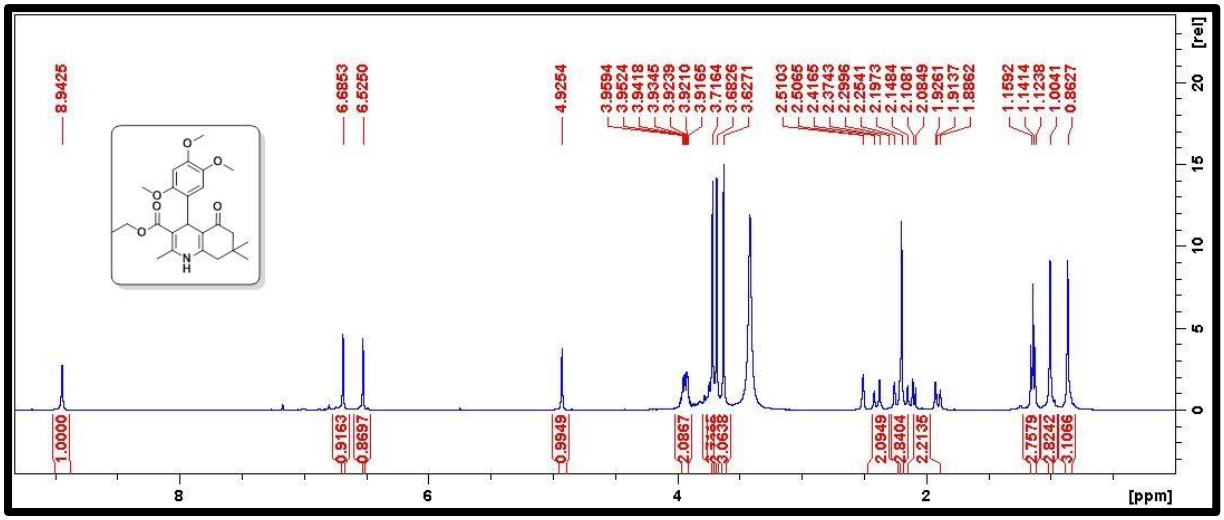

^{1}H NMR spectra of compound **5r** (400 MHz, DMSO)

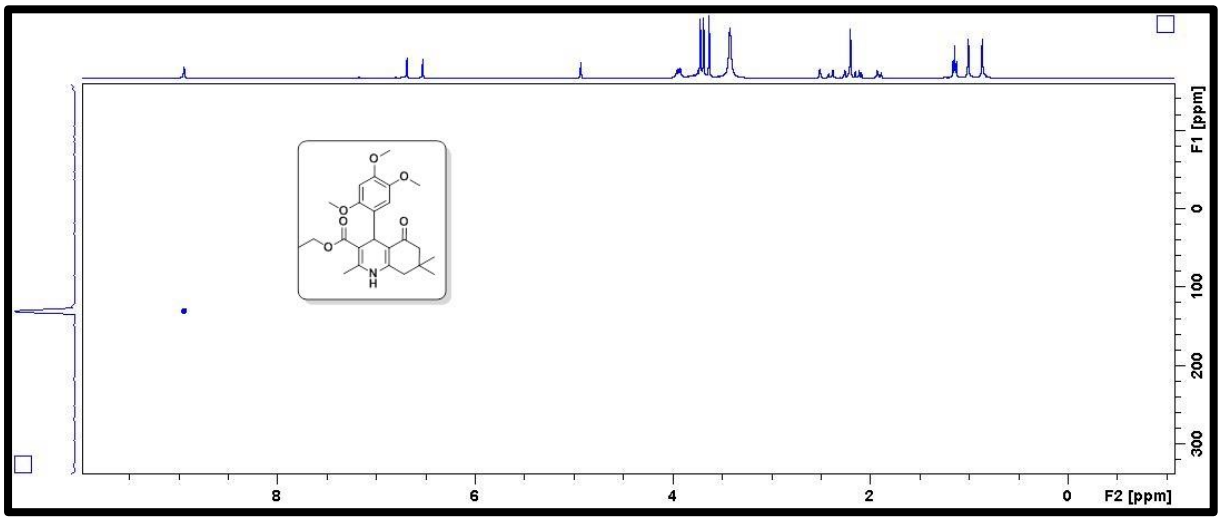

^{15}N NMR spectra of compound **5r** (40.55 MHz, DMSO)

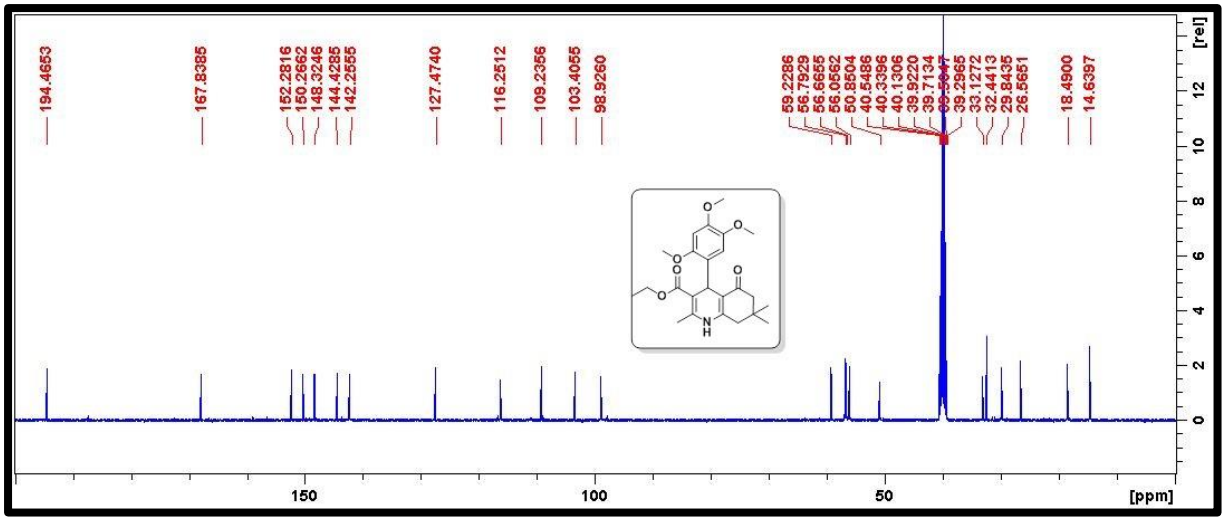

^{13}C NMR spectra of compound **5r** (100 MHz, DMSO)

Table S1. Green metrics (EMY, AE, AEF, RME, OE, and E-factor) for compounds (**5a-r**)

S.No	Products	Yield (%)	EMY (%)	AE (%)	AEF (%)	RME (%)	OE (%)	E-factor (g/g)[a]	TON[b]
1	**5a**	98	76.309	77.867	76.309	76.309	98	0.310	3.307
2	**5b**	93	71.961	77.378	71.961	71.961	93	0.389	3.328
3	**5c**	97	71.817	74.039	71.817	71.817	97	0.392	5.346
4	**5d**	96	74.752	77.867	74.752	74.752	96	0.337	3.240
5	**5e**	95	73.973	77.867	73.973	73.973	95	0.351	3.206
6	**5f**	98	73.451	74.951	73.451	73.451	98	0.361	4.766
7	**5g**	94	72.735	77.378	72.735	72.735	94	0.374	3.364
8	**5h**	95	69.582	73.245	69.582	69.582	95	0.437	5.873
9	**5i**	93	68.118	73.245	68.118	68.118	93	0.468	5.750
10	**5j**	95	72.010	75.801	72.010	72.010	95	0.388	4.134
11	**5k**	89	66.201	74.383	66.201	66.201	89	0.510	8.173
12	**5l**	94	71.861	76.448	71.861	71.861	94	0.391	3.746
13	**5m**	90	66.694	74.105	66.694	66.694	90	0.499	4.880
14	**5n**	96	71.795	74.787	71.795	71.795	96	0.392	4.738
15	**5o**	95	71.814	75.595	71.815	71.814	95	0.392	4.217
16	**5p**	92	69.035	75.039	69.035	69.035	92	0.448	4.433
17	**5q**	96	78.396	83.253	79.923	78.396	94	0.275	3.240
18	**5r**	97	79.212	83.253	80.755	80.755	95	0.262	3.273

[a] Lower is the value, better greener is the process.

[b] TON= Number of moles of products/Number of moles of catalyst.

References:

1. Sheldrick, G.M., A short history of ShelX, *Acta Cryst.*, (2008), **A64**, 339-341.

2. O.V. Dolomanov and L.J. Bourhis and R.J. Gildea and J.A.K. Howard and H. Puschmann, Olex2: A complete structure solution, refinement and analysis program, *J. Appl. Cryst.*, (2009), **42**, 339-341.

3. Sheldrick, G.M., Crystal structure refinement with ShelXL, *Acta Cryst.*, (2015), **C27**, 3-8.

Chapter 8

Conclusion

The thesis describes the effectiveness of mixed transition-metal oxide catalysts and green solvents at room temperature (RT) to accomplish synthesis of some important *N*-heterocyclic scaffolds in excellent yields in short reaction times.

Chapter one, describes the general literature review, about green chemistry and different types of MCRs. Detailed description about heterogeneous catalytic applications towards the synthesis of various N-heterocyclic scaffolds under greener conditions. Heterogeneous catalysts using Ru, V, Bi, Ag, Fe, Ni and Zr with their unique properties are described and applications in organic synthesis is summarised. Heterocyclic compound more specifically literature about multi substituted pyridine derivatives, pyrano pyrazole derivatives and pyrimidine derivatives were given.

Chapter two describes MCR protocol for synthesis of ten novel 1,4-dihydropyridine derivatives under RT conditions. This protocol involved condensation of selected aromatic aldehyde, 5,5-dimethyl-1,3-cyclohexanedione, acetoacetanilide and ammonium acetate in the presence of 60 mg 2.5 wt % V_2O_5/ZrO_2 catalyst. The 1,4-dihydropyridine derivative formation occurred through Knoevenagel condensation and subsequent Michael addition. Product formation was confirmed by several spectral analyses. In the presence of various homogeneous inorganic and organic acidic catalysts no product has obtained even after 8h, but ionic liquids gave 9-12 % yields in 6-6.5 h time. The organic and inorganic basic catalysts gave 19-36 % yields in 4.5-6 h. Further catalytic activity of different metal oxides like SiO_2, TiO_2 and ZrO_2 were studied. Promising results were obtained with ZrO_2 because of higher surface area and the amphoteric nature of the oxide compared to other classical support materials. Of the 1-5% loading of vanadia on ZrO_2 , 2.5 % V_2O_5/ZrO_2 proved superior with 96 % yield in 20 min, because of the even distribution of vanadia particles on the zirconia surface, making it an ideal promoter for the formation of 1,4-dihydropyridine, derivatives. 2.5% of V_2O_5/ZrO_2 catalyst was reusable for up to five catalytic cycles.

Chapter three describes synthesis of eleven novel halopyridine derivatives under rt conditions by taking an equimolar mixture of benzaldehydes, malononitrile, diethyl acetylenedicarboxylate and 3-chloro-4-fluoroaniline in presence of 30 mg of 2 wt % RuO_2/ZrO_2 catalyst. From the pyridine-IR experiment it confirms that the surface of RuO_2/ZrO_2 covers with Lewis acidic sited, which accelerates the reaction, initially Knoevenagel condensation

between benzaldehyde and malononitrile group to give Knoevenagel adduct, further Michael addition between the previously formed Knoevenagel adduct and 1,3-dipole intermediate compound formed from diethyl acetylenedicarboxylate and 3-chloro-4-fluoroaniline. Formation of product was confirmed by several spectral techniques. 2% RuO_2/ZrO_2 catalyst showed 96% yields in 10 min due to the more crystalline nature for the catalytic activity and also equal distribution of acidic sites compared to 1% and 4% loadings. The lower yields with 1% loading due to the insufficient active sites, whereas with 4% loading oligomerisation of ruthenia particles took place on the surface, which decreased its efficiency. The 2% loading recorded highest catalytic activity due to uniform distribution of active species on the support. Additionally, the presence of higher surface area, smaller particle size, equal distribution of ruthenia on the support surface and the synergetic effect between ruthenia-zirconia facilitated the reaction in shorter period of time and was reusable up to six cycles.

Chapter four describes the synthesis of eleven 2,4-dihydropyrano[2,3-c]pyrazole-3-carboxylate derivatives under Rt condition by taking an equimolar mixture of aromatic aldehydes, malononitrile, hydrazine hydrate and diethyl acetylenedicarboxylate in presence of 30 mg 2.5 wt % Bi_2O_3/ZrO_2 catalyst. In the pyridine IR analysis, a promising band at bands at 1449 cm^{-1} shows the presence of Lewis acidic character of surface active sites. The mechanism of 2,4-dihydropyrano[2,3-c]pyrazole-3-carboxylate formation taken place through Knoevenagel condensation between aromatic aldehyde and malononitrile which are catalysed by the Lewis acidic sites of Bi_2O_3/ZrO_2. Further, Michael addition between the Knoevenagel adduct and ethyl 5-oxo-2,5-dihydro-1H-pyrazole-3-carboxylate took place during the reaction between diethyl acetylenedicarboxylate and hydrazine hydrate. Product formation was confirmed by several spectral techniques. In the presence of different homogeneous acidic and basic compounds and ionic liquids as catalysts, the reaction yields were 6-41 % in 9.5 h time. Various metal supported metal oxides like 2.5 % CuO/ZrO_2, MnO_2/ZrO_2, and Bi_2O_3/ZrO_2 gave good yields, of which 2.5% Bi_2O_3/ZrO_2 gave excellent yields (91-98%) within 15 min time. From the TEM-particle size analysis, the average particle size was 8.54 nm, which is a characteristic of equal distribution of active material on the zirconia. The 2.5% Bi_2O_3/ZrO_2 showed good catalytic activity and was reusable up to six cycles. Compared to other MMOs because the special character of bismuth that possess poor shielding effects of 4f-electrons. The surface active sites of the bismuth correlates with the amphoteric nature of zirconia and provides necessary active sites to decrease the activation energy between the reactants, which facilitates the reaction in good yields.

Chapter five describes the synthesis of eleven indenopyrimidine derivatives at room temperature by taking an equimolar mixture of aromatic aldehydes, indane-1,3-dione, and guanidinium hydrochloride in the presence of 60 mg of 2.5 % Ag_2O/ZrO_2 catalyst. The mechanism of indenopyrimidine formation occurred through Knoevenagel condensation reaction between the aromatic aldehyde and indane-1,3-dione which were catalysed by the Lewis acidic sites on the surface of the Ag_2O/ZrO_2. Further Michael addition between the Knoevenagel adduct and guanidinium hydrochloride took place. The homogeneous catalysts gave good yields of up to 50 %, but the reaction took longer time and needed column separations. 2.5 % Ag_2O/ZrO_2 catalyst showed the highest yields (96%) within 15 min. The Lewis acidic nature of silver loaded on zirconia facilities the reactions by providing the active sites, which can attack the carbonyl carbon to give the carbocation. It further reacted with the active methylene group to give the Knoevenagel adduct. Further, Michael addition and intramolecular cyclisation yielded final product. From the TEM micrographs of the three loadings of Ag on ZrO_2, it was found that 1 % had less dispersion of silver on the surface, whereas in 5 % silver agglomerated on the surface, preventing the contribution of active sites in the reaction. The surface of 2.5% loaded catalyst was evenly dispersed by the Ag, which made it an ideal catalytic material to accelerate the reaction by providing more synergetic active sites. The prepared 2.5 % Ag_2O/ZrO_2 is reusable up to six catalytic cycles.

Chapter six describes the multicomponent synthesis of ten new 1,4-dihydropyridine derivatives under Rt condition by employing an equimolar mixture of aromatic aldehydes, 1,3-cyclohexanedione, acetoacetanilide and ammonium acetate in presence of 45 mg of 2.5 wt % Fe_2O_3/ZrO_2 catalyst. The formation of 1,4-dihydropyridine derivative took place through Knoevenagel condensation and subsequent Michael addition. Product formation was confirmed by several spectral analysis. An overall 92-98% yield was obtained with 2.5 % Fe_2O_3/ZrO_2 in 20 min. The even dispersion of active metal facilitated the fast Knoevenagel-Michael addition reactions, by the strong Lewis acidic sites. The single crystal structure of the -4N $(CH_3)_2$ derivative was also elucidated. The 2.5 % Fe_2O_3/ZrO_2 showed the same efficacy up to six catalytic cycles

Chapter seven describes the multicomponent synthesis of eighteen 1,4-dihydropyridine derivatives prepared at rt by taking an equimolar mixture of aromatic aldehydes, 1,3-cyclohexanedione, ethylacetoacetate and ammonium acetate in the presence of 30 mg 2.5 wt% NiO/ZrO_2 catalyst. An attempt was made to understand the mechanism of the 1,4-dihydropyridine formation. 2.5% NiO/ZrO_2 showed good activity in only 20 min with high

yields of 98% compared to other materials due to equal dispersion of active nickel on the surface of zirconia. Additionally, it was identified that the product formation mainly takes place through enamine and imine pathways. At first Knoevenagel condensation occurs at Lewis acidic sites present on the surface which activates the carbonyl group of the aldehyde, forming a carbocation, which is electrophilic in nature. The intermediate carbocation reacting with the active methylene groups of 1,3-cyclohexanedione and ethylacetoacetate forms the Knoevenagel condensation intermediate. On the other hand, enamine intermediates formed by the reaction between ammonium acetate and cyclohexanedione or ethylacetoacetate, followed by the Michael addition with Knoevenagel product, giving the targeted dihydropyridine derivative through intramolecular cyclisation. The single-crystal X-ray structures of two novel molecules were also reported. The 2.5 % NiO/ZrO_2 showed its efficacy up to six catalytic cycles.

The rationale of choosing and designing of a catalyst is based on the available literature. For example, the use of RuO_2/ZrO_2 in the formation of functionalized halopyridine derivatives, presence of strong Lewis acidic nature of Ru played a key role to form a knoevenagel adduct and further the ring formation by Michael addition. In the synthesis of 1,4-dihydropyridine derivatives, knoevenagel adduct between a benzaldehyde and active methylene group like ethyl acetoacetate need milder acidic sites compared to ruthenia. RuO_2/ZrO_2 could work, but other catalysts with less acidic surface sites compared to ruthenia could do better. Where as with Bismuth, Lewis acidic nature is due to the poor shielding of the 4 f-orbital electrons, which allows bismuth to accept electron pair quickly, the poor shielding of the 4 f-orbital electrons makes the catalys an electron pair acceptor which activates aromatic aldehydes and the hydrazine quickly, makes an efficient catalyst for the synthesis of 2,4-dihydropyrano[2,3-c] pyrazole-3-carboxylate derivatives in a shorter period. Vanadium oxide, Iron oxide and Nickel oxide supported on the surface of zirconia serves as the best lewis acidic catalyst for activation of molecules with 1,3 di-carbonyl group by attacking the high electron density sites, capable of the formation of C-C bonds by providing milder surface active sites which palyed a key role in the formation of functionalized dihydropyridine derivatives.

Future work

- To investigate the biological activity of the new synthesized compounds.
- To broaden the scope of this protocols by using different hetero aromatic aldehydes and other active methylene groups.

- To investigate the photocatalytic activity of prepared catalyst materials for other potential applications